IEEE POWER ENGINEERING SOCIETY

Please address reply to:
Mr. G. S. Haralampu
New England Electric System
25 Research Drive
Westborough, MA 01581

November 13, 1979

DOCKET NUMBER PROPOSED RULE PR - misc. Notice - Reg. Guide

Secretary of the Commission
Docketing and Service Branch
U.S. Nuclear Regulatory Commission
Washington, DC 02555

D-1

Gentlemen:

SUBJECT: Draft Regulatory Guide on "Lightning Protection for Nuclear Power Plants," dated August 1979, Task RS 705-4

An Ad Hoc Working Group (3.4.13) composed of members of the Surge Protective Devices Committee (SPD) and the Nuclear Power Engineering Committee (NPEC) of the Institute of Electrical and Electronics Engineers (IEEE), and the American National Standards Institute C62 (ANSI C62) has reviewed the draft Regulatory Guide on "Lightning Protection for Nuclear Power Plants" dated August 1979, Task RS 705-4 (Guide). An extension of time for comments on this Guide from the SPD Committee to November 23, 1979, was granted by Mr. E. C. Wenzinger, Chief of Reactor Systems Standards Branch, in his letter dated September 7, 1979, to Mr. W. R. Ossman, Chairman of the Ad Hoc Working Group.

The attached comments are submitted with the intent of improving the technical content of the draft Regulatory Guide. In particular, the comments discuss lightning theory to the extent it applies to lightning stroke current magnitudes, lightning protective systems, and lightning stroke currents bypassing the protective shielding. The discussions and comments are based on the assumption that the nuclear power plant and associated substation are shielded from lightning.

For clarification and convenience we have proposed in the attachment the rewording of several sections of the draft Guide. References are included to support the technical aspects of our comments.

90004001

Acknowledged by card... dh 11/30

8001030106

The technical basis of our discussion also applies to the draft "Value/Impact Statement." Since specific comments were not made on individual sections of the "Statement," it should not be interpreted as concurrence.

Very truly yours,

G. S. Haralampu

G. S. Haralampu, Chairman
Surge Protective Devices Committee - IEEE

J. L. Koepfinger, Chairman
C62 Committee - ANSI

J. T. Boettger by R. E. Allen V.C. NPEC

J. T. Boettger, Chairman
Nuclear Power Engineering Committee - IEEE

cc: C. L. Wagner, Chairman, Technical Operations Department
Power Engineering Society - IEEE

90004002

Discussion and Comments on Draft Regulatory Guide
Task RS 705-4, August, 1979 on
Lightning Protection for Nuclear Power Plants

by the

Ad Hoc Working Group (3.4.13) on
Lightning Protection for Nuclear Power Plants

Ad Hoc Working Group composed of members of the:

Surge Protective Devices Committee -
Institute of Electrical and Electronics Engineers

Nuclear Power Engineering Committee -
Institute of Electrical and Electronics Engineers

C62 Committee -
American National Standard Institute

1.0 Section B - Page 3 of the Guide

1.1 Line 12 - Replace the words "frequency of lightning surges" with the words "frequency of lightning strokes"

This better describes the event and agrees with the definitions in the IEEE Dictionary.

1.2 Line 14 - Replace the words "design basis discharge surge" with the words "design basis stroke"

This better describes the design basis.

1.3 Line 17 - Replace the words "lightning-induced surges" with the words "lightning caused surges"

The surges being discussed are not induced

1.4 Line 18 - Replace the words "Lightning surges" with the words "Lightning strokes"

Same comment as above

1.5 Line 19 - Complete the sentence with the words "at a lower frequency of occurrence"

This clarifies the intent.

90004003

1.6 Discussion for paragraph beginning with line 29

Mention is made in this paragraph of the sensitivity of solid state logic systems to transient voltages generated externally to a plant. This thought is commingled with the application of surge protection to the power transformers supplying the station auxiliary power. By this action one would be led to believe that the application of surge protection to the power transformer would prevent failures of sensitive equipment.

Surge protection applied to protect transformers or switchgear insulation does not necessarily reduce surges sufficiently to protect sensitive solid state equipment. This equipment may need its own protective system. This position is supported by work which is being carried out by the IEEE Surge Protective Devices Working Group No. 3.3.6, Low Voltage Surge Protective Devices. This Working Group is producing a Standard titled "Application Guide for Low Voltage Surge Protective Devices (600 Volts or less)," IEEE Standards Project 769.

1.7 Suggested rewording starting with line 34 and continuing on page 4 of the Guide through line 10

"For example, power to redundant on-site safety related electric distribution systems is typically supplied from the off-site transmission system through a minimum of two power transformers to provide redundancy.

"In any of these transformers, there is a very low probability that a primary to secondary insulation failure would occur for any reason. If this type of failure does occur, it could impress the primary voltage onto the secondary windings. To avoid a "design basis event common mode failure" affecting the redundant safety systems, surge arresters or other protective devices shall be applied on the transformer secondary winding system.

"If calculations indicate that the arresters located on the high voltage winding of the transformer adequately protect the insulation of the transformer low voltage winding system, surge arresters are not required on this system. Calculations are treated in the IEEE Tutorial Course Text 79EHO 144-6 PWR on Surge Protection in Power Systems.

"Additionally, a lightning caused surge entering the high voltage side of the transformer can propagate to the low voltage circuit through capacitive and magnetic coupling of the transformer. Arresters located on the transformer primary winding will provide secondary winding protection.

"Any of the above surges entering from the high voltage side of the transformer are not expected to damage any of the power plant safety related systems. These systems are low voltage systems at least two transformations from the off-site high voltage transformer."

1.8 Discussion

A lightning strike to one line feeding one of the off-site transformers or a direct hit to the transformer will not disable the plant.

The NRC Regulatory Guide 1.6 entitled "Independence Between Redundant Standby Power Sources and Between Their Distribution Systems" endorses IEEE Standard 308-74, entitled "Criteria for Class IE Electric Systems for Nuclear Power Generation Station." These documents state that a minimum of two off-site independent systems have to be available to feed any class IE equipment and that in addition, each system shall have an on-site power source such as diesel power. Therefore, the failure of any off-site transformer should not affect the safe shutdown of a nuclear power plant.

In addition, a lightning surge entering the transformer primary is not expected to reach the low voltage circuits since the impedance between the transformer primary and class IE equipment is high and the surge will have dissipated before reaching the low voltage systems (600 Volt and below).

A direct hit on the lightning protective systems on the plant site will cause the ground potential to rise. It is possible that solid state electronic devices important to safety, will become stressed under this condition. To reduce the chance of damage, low voltage protective devices can be applied.

2.0 Page 4 of the Guide

2.1 Line 24 - Replace the words "lightning arresters" with the words "surge arresters."

The former term has been superceded.

2.2 Line 31 - Same comment as for 2.1.

3.0 Page 5 of the Guide

3.1 Line 10 - Same comment as for 2.1.

3.2 Lines 10-11 - Delete the last sentence of the paragraph: "This standard also was no ..."

We don't believe this sentence is pertinent here.

3.3 Lines 12-15 - Suggested rewording to include additional information which is pertinent:

"The statistical data on lightning stroke and arrester discharge characteristics relied upon for development of the above standards were collected in the 1940's. Continuing studies subsequently have verified and added to this data. The most recent studies have been documented by EPRI in the report EL-1140 and by DOE, as outlined in reference 34 of the Guide."

90004005

3.4 Section C-1

3.4.1 Discussion on the Wave Shape

It is recognized that in service, the discharge currents through surge arresters seldom, if ever, have an 8 x 20 microsecond wave shape. Data from field studies indicates that a greater percentage of the arrester discharge currents crest in less than 8 microseconds, and exceed 20 microseconds at half of the crest value on the wave tail.(11)

The use in Standards of the 8 x 20 microsecond wave shape is valid as a laboratory definer for the following reasons:

a. All laboratories are equipped with surge generators, and wave shaping parameters external to the surge generator, that readily produce the 8 x 20 wave shape for the range of discharge currents considered for insulation coordination.

b. The 8 x 20 microsecond arrester discharge current, in the current range considered for insulation coordination produces a voltage wave that approximates the 1.2 x 50 microsecond wave shape that is used to determine the withstand strength of insulation.

It is recommended that paragraph C-1 delete any reference to the wave shape of the stroke current. It erroneously implies that the discharge current through surge arresters is the same as the stroke current.

3.4.2 Discussion on the Design Basis

The Guide makes no distinction or difference in the terminology of stroke or stroke current, surge or surge current or discharge current. In the electrical power industry and among practitioners of surge protection, these have distinctly different meanings and relate to different functions and times in the mechanism of generating and protecting against a lightning stroke or switching surge. In the recommendations presented, this terminology has been clarified and used in its correct meaning.

The Draft Regulatory Guide assumes a finite probability that a 200,000 ampere lightning stroke can occur. It also assumes a finite probability that this 200,000 ampere stroke will contact a protected structure or system and will discharge the full value of this stroke current through a protecting arrester. It is submitted that the second assumption is unrealistic. In fact, lightning protective systems can be and are designed so that the maximum current of a lightning stroke which bypasses the protective shielding and terminates on a protected conductor is limited to a lesser value by design. This lesser value is an order of magnitude less than the possible maximum stroke current. Further, the design of surge and lightning protective systems involves the use of shielding systems, grounding systems, and capacitive coupling systems (as well as discrete protective components such as surge arresters and capacitors) to reduce, divert, attenuate, and dissipate the stroke and surge energy so that no element in the system is ever subjected to the full value of the incident stroke current. In designing the protective system, advantage is taken of the configuration, or ability to configure the protected system in order to improve the ability of the protected system to absorb or dissipate the lightning energy and thus render the protected system less vulnerable to damage.

These aspects of the design and application of lightning and surge protective systems have been excluded by the second assumption embodied in the present Draft Guide. The IEEE Surge Protective Devices Committee strongly urges NRC to recognize the impracticability of the second assumption, which would have a serious impact on the surge protective industry in developing a new class of arrester for the proposed 200,000 ampere discharge current, which is over three times the present capability as demonstrated by tests. Such a high discharge current can be prevented by applying the arrester in an overall protective system which has been designed to limit the surge current applied to the arrester to a lower specified value than that of the stroke current.

In making this recommendation, the IEEE Surge Protective Devices Committee fully supports the recommendation in Section 2 of Attachment A to the Draft Regulatory Guide. This recommendation would limit the maximum lightning stroke current which can bypass the station protective shielding by design of the elevations and horizontal separations between shielding conductors and protected conductors. These relationships are controlled to limit the maximum striking distance (stroke attraction distance) of a protected conductor to about 150 feet. (33)

Control is achieved when, for any possible stroke leader tip location at greater than the specified striking distance (and therefore greater prospective stroke current), there is a protective shield conductor closer to the stroke leader tip than is the protected conductor. This can be visualized as a spherical ball with radius equal to the specified striking distance (recommended 150 feet) with stroke leader tip at the center, rolling across the ground and protected structures to occupy every possible position of a descending lightning stroke. Every point touching the sphere wherever it moves will be at specified striking distance and specified prospective stroke current. Every point outside the sphere will be at greater striking distance and greater prospective stroke current, but will be protected by preferential breakdown and stroke discharge to some point touching the sphere. If a smaller striking distance (and smaller prospective stroke current) is selected, this can be visualized as a smaller diameter sphere which can roll down between the shield conductors to touch the protected conductors if the radius is small enough.

The basic protective principle is based upon an electrogeometric model of lightning strikes to shielding and protected conductors which has been calibrated against many thousands of mile-years of performance of various transmission line designs. Good correlation has been obtained between actual and calculated predicted results. The theoretical basis starts with understanding the mechanism of the lightning stroke as it descends from a cloud charge (1) (2) (3) (4) (5) (6). Golde observed that the stroke is attracted at some point in the order of 100 meters from its terminus (7). Golde also observed that the attractive distance was shorter for low stroke currents, as was also noted by Franklin. He postulated that electric gradient under a stroke leader is a function of the charge in the leader channel which is in turn proportional to the amplitude of the stroke current. When the stroke leader tip approaches close enough to ground or a structure to develop a critical breakdown gradient of about 5 kV/cm, the stroke terminus is determined (8). Wagner developed a model for the stroke, and predicted stroke voltages, stroke currents and striking distances (9) (10). The model and predictions were verified by laboratory long gap breakdown and other experiments (9) (10) (12) (13) (14) (15).

Based on Wagner's model of strike distance and prospective stroke current, Brown developed the analytical electrogeometric model of lightning shielding (17). Both models were extensively verified in the late 1960's under the Pathfinder project which installed some 4600 lightning stroke recorders on 50 transmission lines (16) (18) (19) (20).

The electrogeometric analytical model has been extended and calibrated against actual performance by Brown to predict discharge currents, line flashovers (shielding failures), and backflashes (21) (22) (23), together with simplification of the analytical techniques (24). The application of this work to EHV transmission line performance has continued successfully (25) (26) (27).

Concurrently, there have been applications of the electrogeometric model of shielding to high voltage substations, based on the transmission line work and Sargent's analysis of strokes to tall structures and to open ground (28) (29) (30). Recently, the work on stations by Mousa (31) has shown the practicality of design to control stroke current to a bus under shielding failure conditions by limiting the maximum strike distance. Lee has shown a simplified graphical technique for design application (32).

There is some variation in the relationship between strike distance and prospective stroke current as reported by various investigators. However, subsequent to the early work by Golde and Wagner which was primarily based on theoretical deductions from stroke photographs, there is remarkable agreement among the five relationships in the literature which have been used in predicting transmission line performance. At 20,000 ampere prospective stroke current these have a striking distance range from 205 to 281 feet, with a mean of 235 feet and a sigma of 29 feet. At 150 foot striking distance they have a prospective stroke current range of 10,000 to 12,500 amperes with a mean of 11,000 amperes and a sigma of 1,100 amperes. A very conservative design with adequate margins can be achieved by coordinating insulation impulse withstand with a 20,000 ampere stroke reaching the protected conductor but designing the protective shielding for 150 foot maximum strike distance which would allow a probable maximum stroke to the protected structure of only 12,500 amperes.

It is recommended that the design basis event for lightning and surge protection in nuclear power plants be based on a 200,000 ampere lightning stroke reaching the lightning protective system and a lesser stroke, limited by design of that protective system (as described in Section 2 of Attachment A to the Draft Regulatory Guide) to 20,000 amperes reaching the protected structure or system. The insulation withstand capability of the protected system and the arrester discharge current capability would then be selected to protect properly, and survive without damage, whichever of these conditions produces the most severe surge stress.

By proper coordination and design of the protective and the protected systems, the system designer can control at each point in the system whichever of these design basis strokes will prevail. It is recommended that the changes proposed to accommodate this technical approach, which is the current state of the surge protective art, be adopted in the Guide.

3.4.3 Paragraph C-1, page 5

Based on the above discussions, we recommend that this paragraph be changed as follows:

"1. DESIGN BASIS LIGHTNING STROKE

The design basis for lightning and surge protection shall be either:

a. A lightning stroke current of 200,000 amperes reaching the lightning protective system; or

b. A lightning stroke of 20,000 amperes reaching the protected structure by shielding failure (limited by design of the shielding system) which may subsequently be discharged by a surge arrester."

3.5 Section C-2, pages 5 and 6 - Discussion for sections C-2.1, C-2.2, C-2.3, and C-2.4

Section 2.0, as now prepared, fails to recognize that the surge protection selected should be designed with two purposes:

1. It must provide an adequate protective margin for the insulation system it is to protect against various types of surges.

2. It must perform its protective function and then be capable of returning to normal (resealing) when the surge has been dissipated.

In Section C-2.1 the emphasis is placed upon the use of a surge arrester rated for 100% of normal line to line voltage. This emphasis fails to give recognition to the fact the modern transformer and insulation system for off-site power sources are designed to have insulation withstand levels which would not be adequately protected by a 100% rated arrester.

Section C-2.2 is an apparent attempt to acknowledge that certain systems can and must use less than 100% arresters to properly protect an insulation system. However, it presents an over-simplification of the application rules for surge arresters. The attempted simplification stated in Section C-2.2 relates to a rule for the acceptable application of a surge arrester rated 80% of the line-to-line voltage. If the statements given in Section C-2.3 are followed, there is no need for the inclusion of Section C-2.1 or C-2.2 in the Regulatory Guide.

Similarly, Section C-2.4 is unnecessary since ANSI C62.2 and the statement in Section C-2.3 provide adequate guidance for all instances of the application of surge protection for transformers and switchgear.

4.0 Page 6 of the Guide

4.1 Sections C2.5, C-2.6, and C-2.7

4.1.1 Discussion - See comments made in Section 1.8.

4.1.2 Suggested Rewording of Section C-2.5

"Surge arresters with a current discharge capability at least equal to the current to which they would be subjected by a design basis stroke if exposed to lightning should be installed only on windings of start-up and auxiliary transformers where the insulation withstand does not exceed by an accepted margin (per ANSI C62.2) the surge voltage at the winding terminal resulting from a design basis stroke. For redundant systems that do not share transformers, the discharge capability recommended in Section 7 of ANSI C62.1-1975 is acceptable."

4.1.3 Suggested Rewording of Section C-2.6

"Surge arresters with a current discharge capability at least equal to the current to which they would be subjected by a design basis stroke if exposed to lightning should be installed at the electrical switch-gear upstream of the feeder breaker connected to start-up and unit auxiliary transformers shared by redundant systems where the switchgear insulation withstand does not exceed by an accepted margin (per ANSI C62.2) the surge voltage at the switchgear bus resulting from a design basis stroke. For redundant systems that do not share transformers, the discharge capability recommended in Section 7 of ANSI C62.1-1975 is acceptable."

4.1.4 Section C-2.7

Since the design basis will limit the arrester discharge current to 20,000 amperes, there is no need to consider paralleling surge arresters. Section C-2.7 should therefore be deleted.

90004011

5.0 Page 7 of the Guide

5.1 Section C-2.9

We recommend that this section be deleted. As has been discussed in the revised Section C-1, "Design Basis Lightning Strokes," a surge arrester when applied to an adequately shielded power system will not be exposed to a discharge current of greater than 20,000 amperes.

We interpret the reference which is made in C-2.9 to ANSI C62.1-1975 (Section 7.5.1) to a durability design test for a surge arrester. Currently this test specifies an artificially high arrester discharge current of 65,000 amperes. This is used in the design test of the arrester to impress upon its internal parts, voltage stresses which are considerably in excess of those which it would experience in actual use. Thus, there is no real requirement for a 200,000 ampere durability test.

5.2 Section C-2.10

5.2.1 Line 3 of the paragraph

Delete the words "design basis" to clarify the sentence.

5.2.2 Lines 4-7 (Last Sentence)

Reword the sentence as follows to include the technical basis discussed in 3.4.2 above:

"However, for redundant systems important to safety which are electrically connected to these transformers, the surge voltage at each of the transformer terminals and for the discharge voltage of any surge arresters applied on these terminals when subjected to a discharge current of 20,000 amperes, shall be less than the transformer insulation withstand by an accepted margin per ANSI C62.2."

5.3 Section C-2.11

This entire section should be revised to include wording resulting from the following discussion:

Removal of surge arresters after a period of field service for retest does not fully accomplish the intended results. Testing at any interval without other monitoring means does not preclude the failure of an arrester within the interval between tests.

The removed arresters cannot be tested as specified in the Guide in accordance with all the performance test requirements of the Design Test section of the applicable arrester standard.

Because of the limitations of surge generators, and 60 Hertz power sources, the arrester units must be dismantled and reassembled into smaller prorated sections for a number of the tests. Noteworthy among these are the High-Current and Duty Cycle tests. It is well documented that a prorated section of an arrester can accurately represent, for a particular test, the characteristics of a complete arrester. If the testing of arresters removed from service is required, the testing of the parts of the larger unit as prorated sections must be an acceptable practice to the Nuclear Regulatory Commission. It must also be recognized that there is the possible consequnece of damaging the arrester during removal and rebuilding the components into the lesser rated prorated sections. The conversion of the larger unit into a number of prorated sections will also increase the cost of retesting.

It is recommended that an alternative approach be used to determine the condition of the surge arresters rather than the specified removal and test procedure. The arrester's condition can be periodically monitored while energized by suitable devices in series with the arrester. With these devices, reliable information about the arrester's condition can be obtained. Proper judgement of the data from these devices can also anticipate well in advance a potential failure of the arrester.

There are recording instruments, or devices, with reliable field service records that can provide the necessary data. Surge counters are used to record the number of times the arrester has operated. A Rogowski coil, around the ground lead of the arrester, that is coupled to a recorder can determine the magnitude and wave shape of the surge current through the arrester. A current milliammeter can determine the grading current through the arrester, and if suitably designed, can indicate the presence of conducting contaminant on the surface of the weather housing. A replica of the interrupting gap of the arrester can be connected into the circuit so that a judgement can be made of the condition of the arrester gaps. The voltage wave shape of the grading current through a noninductive resistor can be observed on an oscilloscope. The latter gives an indication of corona if present and the magnitude of the leakage current. The periodic recording of the data from such methods can be compared for indications of arrester change or severe duty. A judgement can then be made to remove the arrester. Inspection of the unit removed will serve as an indicator for refining the decision to remove, or leave in place, arresters with similar design and duty records.

6.0 Page 8 of the Guide

6.1 Section C-3.1

Change the words "Ground wires" to the words "Shield wires." (Accepted terminology)

6.2 Section C-3.2

We recommend rewording of this section to reflect the discussion in 3.4.2 above:

"Transmission line shielding should be designed to limit shielding failure stroke current contacting the conductors to no more than 20,000 amperes."

6.3 Section C-3.3

We recommend rewording for clarification and accuracy:

"The footing resistances to ground of the towers for a sufficient distance from the station should be designed low enough to minimize the probability of backflash of the line insulation."

6.4 Section C-4

6.4.1 We recommend title be changed to:

"LIGHTNING SHIELDING FOR PROTECTION OF STRUCTURES"

6.4.2 Section C-4.1

We recommend the addition of the following words at the beginning of the sentence:

"Lightning shielding, including shield wires or air terminals..."

6.4.3 Section C-4.2

We recommend the beginning of the sentence read as follows:

"The protective shielding system should be connected..."

6.4.4 Section C-4.3

We recommend rewording for technical accuracy as follows:

"Lightning protective shielding systems should be designed to limit the prospective stroke current of shielding failures (strokes contacting the protected structures) to no more than 20,000 amperes. A striking distance of 150 feet is recommended for conservative design."

7.0 Page 10 - Value/Impact Statement

Comments previously made for pages 3-7 of the guide also apply to this page.

8.0 Page 11 - Value/Impact Statement

8.1 Line 3

Change the words "The frequency of induced" to the words "The frequency of occurrence of direct lightning..." for clarification purposes.

8.2 Section b starting with Line 13

Discussion of 3.4.2 made previously applies here also. The parenthetical phrase on line 20 "(if the secondary is not properly grounded)" is not pertinent here. It makes no difference; the phrase should be deleted.

8.3 First sentence starting with Line 22

This sentence should be rewritten as follows: "Substantial effort has been expended to determine a conservative 'design basis stroke.' This work is actively continuing (Refs. 34 and 36-39)."

9.0 Page 12 - Value/Impact Statement

9.1 Line 1

Replace the word "ground" with the word "shield." This is an accepted terminology.

9.2 Line 4

Replace the word "Conventional" with the words "Protective shielding and lightning rods..."

9.3 Paragraphs c and d starting with Line 8

Replace with the following:

"Installation of surge arresters to adequately protect switch-yards and substation equipment in accordance with good engineering practice and existing standards."

9.4 Line 12

This line should read as follows:

"Installation of low voltage surge protectors on..."

10.0 Page 13 - Value/Impact Statement

Section 1.3.1 - Fourth Paragraph

Replace the words "surge characteristics" with the words "lightning stroke characteristics," and the words "surge amplitudes" with the words "lightning stroke amplitudes." In addition, the end of the first sentence should read "... and frequency of occurrence."

The equipment insulation tolerance to voltage surges is defined in several ANSI and IEEE Standards and Guides. The NRC should identify areas needing attention. The IEEE Technical Committees may be willing to provide the technical expertise.

11.0 General Comments on the Value/Impact Statement

All our discussions and comments on the Guide are also applicable to the Value/Impact Statement. Proper correlation should be made.

REFERENCES

(1) B. F. J. Schonland and H. Coll[illegible]s, "Progressive Lightning," Proc., Royal Soc. London, Vol. 143, pp. 654-74, 1934.

(2) B. F. J. Schonland, D. J. Malan and H. Collens, "Progressive Lightning II," Proc. Royal Soc. London, Series A, Vol. 152, pp. 595-625, 1935.

(3) D. J. Malan and H. Collens, "Progressive Lightning III, The Fine Structure of the Return Stroke," Proc. Royal Soc. London, Vol. 162, pp. 175-203, 1937.

(4) B. F. J. Schonland, D. B. Hodges and H. Collens, "Progressive Lightning V, A Comparison of Photographic and Electrical Studies of the Discharge Process," Proc., Royal Soc. London, Vol. 166, p. 56, 1938.

(5) I. S. Stekolnikov, "The Nature of the Long Spark," Izdatel'sivo Akademii Nauk USSR, pp. 1-272, 1960. English trans. available from Foreign Tech. Div., Air Force Systems Command, Wright-Patterson AFB, Ohio.

(6) C. F. Wagner and A. R. Hileman, "The Lightning Stroke II," AIEE Trans., Pt. III (Power Apparatus and Systems), Vol. 80, pp. 622-42, Oct. 1961.

(7) R. H. Golde, "The Attractive Effect of a Lightning Conductor," J.I.E.E., Vol. 9, p. 212, 1963.

(8) R. H. Golde, "The Lightning Conductor," J. Franklin Inst., Vol. 283, pp. 451-477, June 1967.

(9) C. F. Wagner, "Relations Between Stroke Current and Velocity of the Return Stroke," IEEE Trans. on Power Apparatus and [illegible]stems, pp. 609-17, 1963.

(10) C. F. Wagner, "The Lightning Stroke as Related to Transmission Line Performance," Parts I and II, Elec. Eng., May and June, 1963.

(11) K. Berger, R. B. Anderson, H. Kröninger, "Parameters of Lightning Flashes," CIGRE Committee 33, Electra No. 41

(12) C. F. Wagner, A. R. Hileman, "Mechanism of Breakdown of Laboratory Gaps," AIEE Transactions, pt. III (Power Apparatus and Systems), Vol. 80, pp. 604-22, October 1961.

(13) C. F. Wagner, A. R. Hileman, "Surge Impedance and Its Application to the Lightning Stroke," Ibid., pp. 1011-22, 1961 ([illegible]eb. 1962 section).

(14) C. F. Wagner, C. M. Lane, C. M. Lear, "Arc Drop During Transition From Spark Discharge to Arc," AIEE Transactions, pt. III (Power Apparatus and Systems), Vol. 77, pp. 242-47, June 1958.

(15) C. F. Wagner, "Lightning and Transmission Lines," J. Franklin Inst., Vol. 283, No. 6, June 1967

REFERENCES

(16) H. R. Armstrong and E. R. Whitehead, "A lightning stroke pathfinder," IEEE Trans. Power Apparatus and Systems, Vol. 83, pp. 1223-1227, December 1964.

(17) G. W. Brown, "The Electrogeometry of Shielding Against Lightning," Ph.D. dissertation, Illinois Institute of Technology, Chicago, Ill., 1967.

(18) H. R. Armstrong and E. R. Whitehead, "Field and Analytical Studies of Transmission Line Shielding," IEEE Trans. Power Apparatus and Systems, Vol. PAS-87, pp. 270-281, January 1968.

(19) Gordon W. Brown, Member, IEEE, and Edwin R. Whitehead, Fellow, IEEE, "Field and Analytical Studies of Transmission Line Shielding: Part II," IEEE Transactions on Power Apparatus and Systems, Vol. PAS-88, No. 5, pp. 617-626, May 1969.

(20) E. R. Whitehead, "Final Report on Edison Electric Institute Research Project No. RP-50, Mechanism of Lightning Flashover on Transmission Lines," No. 72-900, EEI, 90 Park Ave., New York, NY 10017, (1972).

(21) Gordon W. Brown and Steven Thunander, "Frequency of Distribution Arrester Discharge Currents Due to Direct Storkes," IEEE Transactions on Power Apparatus and Systems, Vol. PAS-95, No. 5, pp. 1571-1578, September/October 1976.

(22) Gordon W. Brown, "Lightning Performance II Updating Backflash Calculations," IEEE Transactions on Power Apparatus and Systems, Vol. PAS-97, No. 1, pp. 39-52, January/February 1978.

(23) Gordon W. Brown, "Joint Frequency Distributions of Stroke Current Rates of Rise and Crest Magnitude to Transmission Lines," IEEE Transactions on Power Apparatus and Systems, Vol. PAS-97, No. 1, pp. 53-58, January/February 1978.

(24) Gordon W. Brown, "Lightning Performance - I Shielding Failures Simplified," IEEE Transactions on Power Apparatus and Systems, Vol. PAS-97, No. 1, pp. 33-38, January/Feburary 1978.

(25) D. W. Gilman and E. R. Whitehead, "The Mechanism of Lightning Flashover on High-Voltage and Extra-High-Voltage Transmission Lines," Electra No. 27, pp. 65-96, March 1973.

(26) E. R. Whitehead, "CIGRE Survey of the Lightning Performance of Extra-High-Voltage Transmission Lines," Electra, 33, pp. 63-89, (1974).

(27) E. R. Whitehead, "Analytical Speculations on Improved Electrogeometric Models of the Lightning Flash and Transmission Line Environment, with Addendum and Appendix. IWD 12 and 12a SC33, WG 33.01, (1976)

REFERENCES

(28) M. A. Sargent, "The Frequency Distribution of Current Magnitudes of Lightning Strokes to Tall Structures," IEEE Trans. PAS-91, No. 5, pp. 2224-2229, September/October 1972.

(29) M. A. Sargent, "Monte Carlo Simulation of the Lightning Performance of Overhead Shielding Networks of High-Voltage Stations," IEEE Trans., Vol. PAS-91, No. 4, pp. 1651-1656, July/August 1972.

(30) H. Linck, "Shielding of Modern Substations Against Direct Lightning Strokes," IEEE Transactions on Power Apparatus and Systems, Vol. PAS-94, No. 5, pp. 1674-1679, September/October 1975.

(31) Abdul M. Mousa, "Shielding of High-Voltage and Extra-High-Voltage Substations," IEEE Transactions on Power Apparatus and Systems, Vol. PAS-95, No. 41, pp. 1303-1310, July/August 1976.

(32) Ralph H. Lee, "Protection Zone for Buildings Against Lightning Strokes Using Transmission Line Protection Practice," IEEE Transactions on Industry Applications, Vol. 1A-14, No. 6, pp. 465-470, November/December 1978.

(33) Ralph H. Lee, "Lightning Protection of Buildings," IEEE Transactions on Industry Applications, Vol. 1A-15, No. 3, pp. 236-240, May/June 1979.

rod-to-plane gap upon application of a 60-cycle voltage or an impulse having a slow front and long tail. The higher value of 160 kv per foot or 5,300 volts per cm represents the characteristic of a rod-rod gap to which a negative potential is applied. It would be interesting if data pertaining to a rod plane gap were obtained in a range of 400 inches for which the applied voltage is a negative slow-front wave. These data could be compared directly with the low gradient of 1,800 volts per cm obtained with a positive wave. Fig. 14 of reference 1 of Mr. Hagenguth's discussion provides some information concerning rod-rod gaps which indicates linearity up to 180 inches and a gradient of about 5,000 volts per cm.

The question raised by Mr. Hagenguth betrays that we were not sufficiently clear in the general exposition of the paper. We tried to convey that sparkover of the gap occurs in two phases, first the development of the space charge (corona discharge), and second, the development of the channel (high conducting arc plasma). Only the first phase develops below critical voltage. Above critical voltage both occur in sequence.

Regarding the development of the space charge, Park and Cones stated that "An analysis of a large number of records obtained with slowly rising surges indicated that the peak current was approximately proportional to the actual value of voltage at the instant the discharge started." Therefore, in an ambient of low free electron concentration and with the application of a steep voltage wave, the crest value of the voltage wave is attained before triggering occurs. But if the concentration of free electrons is high, triggering may occur on the rising portion of the wave with a corresponding reduction in crest value of the current. It is to be presumed that a corresponding lengthening of the current wave would ensue. According to our theory of breakdown, the substantial development of the space charge is a precedent to the development of channel. The current required to develop the space charge is small in comparison with the short-circuit current of the surge generator when ultimate breakdown occurs. Therefore, when the current shunt is adjusted to read the short-circuit current, the space charge current is swamped by the channel formation currents even in the early stages of the channel formation and its presence is not apparent.

In reply to the comment made in the last paragraph of Mr. Hagenguth's discussion, it does not appear that a glow discharge or pilot leader without some sort of conducting core (channel) would possess sufficient conductivity in the form of a cylinder 10,000 or 20,000 feet in length and 100 feet in diameter, to supply the current required to provide the progressing corona discharge (space charge) in front of the leader. Furthermore, if the leader consisted of only such a glow discharge, the gradient per unit length must be approximately 7,000 volts per cm. The drop alone in such leader of 20,000 feet length would be 5×10^9 volts. This would require a deposition of charge along the stroke channel that increases linearly with height. The resultant current at the earth, as the return stroke tapped these charges progressively, would result in a current at the earth that would increase progressively with time up to about 100 μsec and in magnitude would be many times the recorded values. Thus we are of the opinion that a conducting core must exist within the leader.

POOR ORIGINAL

REF. 6

The Lightning Stroke—II

C. F. WAGNER
FELLOW AIEE

A. R. HILEMAN
MEMBER AIEE

IN A PREVIOUS PAPER,[1] similarly titled, the authors undertook to synthesize certain characteristics of the lightning stroke by applying and extrapolating the results of laboratory experiments. They were supported in this effort by data concerning the transient characteristics of arcs[2] and the properties of corona within cylindrical shells. A companion paper[3] in this issue, discusses the properties of laboratory-produced sparks and the present paper applies this information, together with additional data concerning natural lightning, to a more detailed consideration of the lightning stroke. A new mechanism of the leader steps is presented. Also, a theory of the very important events that occur during the early stages of the return stroke is elucidated.

General Description of the Stroke

Before discussing the various phases of the stroke, a general description of the stroke without detailed substantiation will be presented. The hypothesis pictures the leader as composed of two parts: a very thin good conducting core, which will be called the channel, preceded and surrounded by a negative space charge which will be called the corona sheath. The diameter of the channel is only about 2 mm (millimeters) and its drop about 50 or 60 volts per cm (centimeters). It has characteristics of an arc plasma with very high temperatures and may be highly luminous. The diameter of the corona envelope may be about 100 feet and may extend about 150 feet in front of the channel. The internal gradient of the corona sheath lies between 5,000 and 10,000 volts per cm. It has characteristics of a glow or corona discharge; its temperature is low; it is pierced by streamers; and considerable difficulty is sometimes experienced in photographing it.

As the channel of the leader of the first component of a stroke reaches a particular point it is momentarily arrested and streamers forge ahead into virgin air. These streamers form the corona sheath and as they proceed distribute a space charge that has characteristics similar to a corona discharge and to the space charge associated with the formative stage of the breakdown of long gaps. As the space charge develops, the potential difference across the corona sheath has an increasing effect in restraining the progress of the discharge. But, before the charge can become fully effective in checking the further progress of the streamers, conditions just in advance of the tip of the channel become conducive to the initiation of a channel or arc plasma at this point. This new channel in reality merely constitutes a further extension of the leader channel. Each new channel spurt starts with a relatively low velocity that follows a curve with time that is strongly concave upward. This continues until the channel catches up with the boundary of the corona sheath. The channel cannot progress into virgin air in the form of a highly conducting plasma and, therefore, ceases. In the meantime the corona streamers continue to progress from the new tip of the channel and the whole process is repeated. The photographic studies of Schonland[4] and his associates reveal this rapid extension of the channel as a short step of very high brilliance. And with respect to the development of the channel (which they term streamers) they say, "Definite evidence that the streamers [channels] travel downward is, however, afforded by the broadening of the upper part of their tracks."

According to Schonland, the lengths of the steps vary between 10 and 80 meters with a modal value of about 50 meters or

Paper 61-488, recommended by the AIEE Transmission and Distribution Committee and approved by the AIEE Technical Operations Department for presentation at the AIEE South East-South Central District Meeting, New Orleans, La., April 5-7, 1961. Manuscript submitted January 9, 1961; made available for printing March 3, 1961.

C. F. WAGNER and A. R. HILEMAN are both with Westinghouse Electric Corporation, East Pittsburgh, Pa.

90004020

150 feet. The corona sheath advances with an average velocity of between 1.5 × 10^7 and 8.0×10^7 cm per sec (second) or between 0.0005c and 0.0025c, where c is the velocity of light. The time required to develop the corona sheath before it is again overtaken by the channel, usually ranges from 30 to 90 μsec (microseconds), and the velocity of the step exceeds 5×10^9 cm per sec or 0.16c. However, more recent measurements of electric fields next to the earth,[5-7] indicate that as the earth is approached the time intervals between steps become smaller and attain a value of 13 μsec. Schonland and his associates[4,8-10] reported uncompleted leaders which ceased to develop before reaching the earth. They also found that the intervals between steps and the length of the steps sometimes remained constant during a considerable portion of the leader path.

While the foregoing description applies to the more common cloud-initiated stroke, a similar phenomenon occurs with earth-initiated strokes. Hagenguth and Anderson[11] presented a photograph of a stroke that was initiated from the 1,275-foot Empire State Building. It exhibited very pronounced steps that occurred at intervals of approximately 25 μsec. The explanation for the formation of steps must, therefore, be independent of polarity except in degree.

The step process of the lightning stroke, is, in some respects, simpler than laboratory-produced discharges. The formation of the space charge in the case of the stepped stroke always emanates from an arc plasma constituting a copious supply of free electrons. There is, therefore, no statistical time lag during which the initiation of the discharge awaits the propitious positioning of a free electron. The process is not complicated by the necessity of considering the development of streamers from an opposing electrode until the leader nears the earth.

Analysis of the Stepped Leader

Potential and Charge Distribution

As a preliminary step in the discussion of the nature of the step mechanism, it will be necessary to establish the stroke potential and the general nature of the charge distributed along the leader. Since the potential of the channel is assumed to be the same along its entire length, then the sum of the drop across the corona sheath and the drop from the corona sheath to ground must be the same at any point. To determine this potential some assumption must be made with regard to the distribution of charge across the lateral sections of the corona sheath. Since the charge at the very tip constitutes such a small proportion of the total charge, it cannot have a very great influence upon the potential of the conducting channel lying on the axis of the downward leader. For the moment consideration will be limited to the essentially cylindrical portion of the leader. It is shown in the companion paper that in laboratory discharges, just prior to breakdown, one function of the space charge appeared to be to equalize the electric gradient so that the uniform gradient equalled the average gradient.

In a cylindrically symmetrical space charge, that distribution which leads to a uniform radial field is one for which the density varies inversely as the radius. Thus

$$q = \frac{A_c}{r} \text{ in coulombs per cm}^3 \qquad (1)$$

where r is the radial distance from the axis and A_c is a constant that represents the charge density at 1 cm. It is also true that if the charge extends to radius r_o with E_r the radial field in volts per cm, q_o the total charge in coulombs per cm length of the channel, and V_{or} the total radial potential drop, then

$$r_o = \frac{18\times 10^{11}}{E_r} q_o \text{ in cm} \qquad (2)$$

and

$$V_{or} = 18\times 10^{11} q_o \text{ in volts} \qquad (3)$$

Such may be the distribution of charge around the wire of a wire-plane electrode just prior to breakdown.

Since the leader tip is always in a state of incipient breakdown it is not unreasonable to assume that after the tip of the channel has passed a particular point the distribution still remains somewhat the same. Furthermore, at breakdown the gradient for a negative electrode is about

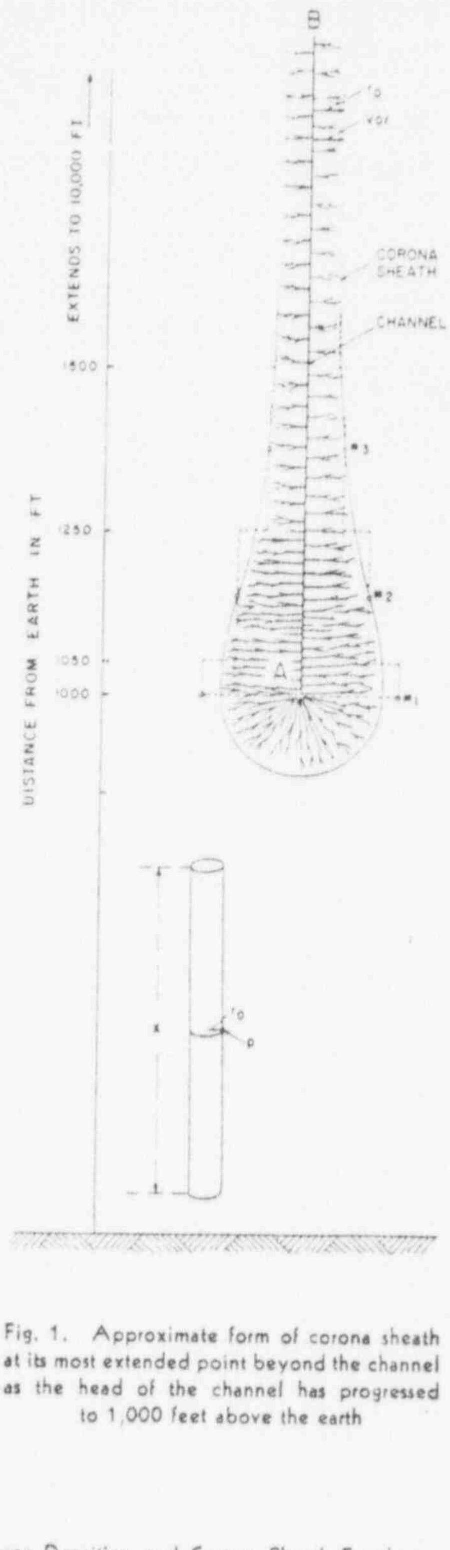

Fig. 1. Approximate form of corona sheath at its most extended point beyond the channel as the head of the channel has progressed to 1,000 feet above the earth

POOR ORIGINAL

Table I. Determination of Leader Potential, Charge Densities, and Corona Sheath Envelope for Fig. 1

Row	Due to Charge Density in This Section	Contribution to Potential at These Points × 10^6 Volts				
		1	2	3	4	5
a	1	4.8	4.7	1.7	0.4	0.0
b	2	9.2	16.6	9.1	1.3	0.0
c	3	3.2	6.0	18.0	1.3	0.14
d	4	4.5	6.0	10.5	32.4	0.91
e	5	2.2	2.5	3.2	6.6	43.20
f	V_r in 10^6 volts	23.8	35.8	42.4	42.0	44.32
g	q_o in 10^{-5} coulombs/cm	17.8	11.8	6.8	5.6	5.0
h	r in feet	150	100	57	47	42
i	v_{or} in × 10^6 volts	32.0	21.3	12.2	10.1	9.0
j	V in × 10^6 volts	55.8	57.1	54.6	52.1	53.2

90004021

9,000 volts per cm, and since no branches of the stroke are initiated from behind the tip, a somewhat smaller gradient of 7,000 volts per cm may be assumed to exist there. Therefore, if in any section q_0 is assumed then from equations 2 and 3, r_0 and V_{or} are determined.

An instant in the progress of the leader will be chosen, shown in Fig. 1, at which the channel is just about to begin another spurt in its advance. The corona sheath along the channel and in advance of it is fully developed for that particular step. Only that part of the vertical path below an altitude of 10,000 feet is considered. While there may be other collecting paths within the cloud it is assumed that they have no effect upon the phenomenon occurring at the tip. It has been shown by Schonland, Hodges, and Collens[10] that the total charge on the first leader when it is fully extended is about 60% of the charge in the section of the cloud originally tapped by it. Calculations indicate that such a proportionate part of the charge in the cloud, because of its distance, has a negligible effect upon the phenomenon occurring at the tip. The tip of the channel is assumed at this instant to be 1,000 feet above the earth. The leader is assumed to be divided into five cylindrical sections with a hemispherical dome at the base. The four bottom cylindrical sections and the hemispherical dome are shown in Fig. 1. The bottom cylindrical section is 50 feet long and the others in succession are 200, 250, 1,500, and 7,000 feet respectively. An infinitely small diameter, perfectly conducting core or channel is assumed to extend from point A up through the column.

In Table I, the results of a cut-and-try computation to determine the charge distribution and the potential of the core are shown. The charge densities in the five sections are shown in row g. Row h gives the corresponding radii of the sheaths and row i the corona sheath potential drops.

The inset of Fig. 1 shows one of the elemental cylinders into which the corona sheath is divided. To determine the potential of a point p on the surface of the sheath midway along the cylinder, the volume charge can be assumed to be concentrated along the axis of the cylinder. The potential of this point due to the charge on the cylinder is then, from Fig. 34 of reference 12,

$$\psi = 9\times 10^{11} q_0 \frac{x+\sqrt{r_s^2+x^2}}{r_s} \text{ in volts} \qquad (4)$$

where q_0 is the charge in coulombs per cm. By similar expressions given in reference 12, the potential of point p due to the charge on the other elemental cylinders can be obtained. This also applies to the negative image charges. Rows a to e thus show the contributions to the potentials at the mid-points of the five sections due to the charges in themselves and the other four sections. Row f is the sum of the individual contributions. Adding the internal potential drops given in row i to these values gives the potentials in row j which represent the potentials of the points on the channel just opposite the mid-points. These should be equal in order to satisfy the condition that all points on the channel have the same potential. Thus, for this condition, the potential of the channel is about 55×10^6 volts. In addition to the charges in the cylinders, an approximately hemispherical bowl of charge at the end of the leader, must be included in the computations. The total charge within a sphere whose charge density varies as A/r is just 1/2 of the total charge within a cylinder whose length is equal to its diameter and whose density is A/r. On this basis it can be estimated that, in this case, the contribution of this charge to the potential at point 1 would just about be equal to the contribution of the charge in element 1, which is 4.8×10^6 volts. This would require a slight modification in the charge densities and the radii of Table I. With these computations as a background, the curved shape shown in Fig. 1 was drawn as being representative of the form of the charge volume surrounding the channel in which the internal field is 7,000 volts per cm. This is only an approximate result but since the theory, proposed here, is not critically dependent upon the shape and distribution of the space charge it was deemed sufficiently accurate for the purpose at hand. The average density of charge over the bottom 500 feet is about 9×10^{-6} coulombs per cm. If this charge is drained to earth as a wave of current at a constant velocity of 30% that of light, then in accordance with equation 1 of reference 1, the discharge would develop a current of 80,000 amperes or at a velocity of 10%, 27,000 amperes. Schonland[13] arrived at a value of charge density of 8×10^{-6} coulombs per cm from entirely different considerations, such as the modal values of charge lowered in a complete stroke, the number of components in a stroke and the length of the stroke. More will be said of the development of the actual current to ground.

It is of interest to observe that for this case the potential of the channel falls within the range of 10^7 to 10^8 volts accepted by the majority of the workers in this field.

Ahead of the channel tip the space charge density and the electric field are probably more intense than in a radial direction behind the front. The electric field ahead of the channel approaches the critical value of about 9,000 volts per cm at which the channel extension again commences.

Time for Space Charge Formation and Velocity of Its Formation

Very little information is available from laboratory data upon which to base these quantities. In reference 3, it was shown that from the Park and Cones data[14] on sphere-to-plate gaps, with the sphere negative, for an 11.5-cm gap the time for the corona current to reach zero was 0.3 μsec. This corresponds to an effective velocity of charge formation of 0.0006 c. With the sphere positive the velocity was 0.0013 c. The Hagenguth, Rohlfs, and Degnan[15] data for a 200-inch rod-rod gap with the anode grounded gave a time of formation of 9 μsec, which corresponds to a velocity of 0.0009 c.

Schonland's modal value of 150-foot steps indicates a time of formation of the negative space charge of 50 μsec. Since the average need travel only half the distance, this corresponds to an average velocity of formation of

$$\frac{150\times 30.48}{2\times 50\times 10^{-6}} = 4.5\times 10^7 \text{ cm per sec} \qquad (5)$$

$$= 0.0015c$$

For the positively projected steps[11] from the Empire State Building, cited earlier, a 50-foot step, with a time of formation of 25 μsec, gives a velocity of formation of

$$\frac{50\times 30.48}{2\times 25\times 10^{-6}} = 3\times 10^7 \text{ cm per sec} \qquad (6)$$

$$= 0.001c$$

The lightning and laboratory data compare favorably. Not all of the step interval time can be attributed to the formation of the space charge as a portion is also required for the formation of the channel.

Velocity of Channel

So far the comparison of the characteristics of the step of natural lightning with those of laboratory-produced sparks have shown gratifying agreement. However, when one compares the velocity with which the channel advances, the agreement ceases. It was mentioned in reference 3 that in the Park and Cones experiments[14] the head of the positive channel starts with an initial velocity of 4×10^6 cm per sec or 0.00013 c and increases gradually at first and then more rapidly,

90004022

attaining a terminal velocity of about 10^8 cm per sec or 0.003 c. The negative channel seems to travel with a greater but unknown velocity. Since similar thermal processes must be involved the velocity of both polarities should be of the same order of magnitude. Schonland[13] states that the steps of the downward leader complete their passage in 1 μsec, which for the 150-foot step to which he was referring, involves a velocity of

$$\frac{150 \times 30.48}{10^{-6}} = 4.5 \times 10^9 \text{ cm per sec} = 0.15\,c \tag{7}$$

This is a serious discrepancy but as the analysis proceeds it will be explained satisfactorily.

Development of Channel Currents

Fig. 1 shows the column of the lightning discharge at an instant when the space charge in advance of the arrested channel has reached its point of greatest advance. Conditions just in advance of the tip, point A, of the channel are at this instant propitious for a further advance of the channel. It seems as though these conditions are related to a certain combination of high charge density and field. It certainly involves the same relations as the transition from a glow discharge to a high conducting arc plasma, for this is the essence of the phenomenon involved. This is essentially thermal in nature and involves considerations of high energy concentration. The conditions conducive to this transition are not well understood. In the companion paper it is indicated that when the anode is far removed from the cathode, the critical gradient at which a space charge develops into an arc plasma at the cathode is in the order of 9,000 volts per cm. Fig. 2 shows another view of the tip of the leader. The density of the dots is intended to be suggestive of the charge density. From this condition it may be assumed that the conducting channel extends itself from position A to position C and as it extends into the space charge it quickly attains a low voltage drop. Justification for this statement is provided by Higham and Meek,[16] who demonstrated that for currents in the range of 60 to 500 amperes that rose to crest in 1/4 μsec, the drop reduces to 150 volts per cm in 1/2 μsec. This drop is small in comparison with the electric field of the space charge, which had been assumed to be 9,000 volts per cm. The high initial drop may still be significant in its effect upon the phenomenon. However, for the moment assume that the drop along the channel extension is zero.

The projected channel as it advances forms a pencil of zero electric field along a line where previously the gradient had been constant at about 9,000 volts per cm. If the extension of the channel into the space charge is very rapid and if it is assumed that the surrounding space charge cannot change rapidly, to achieve the condition of zero gradient parallel to the axis of the extended channel, charges must be induced in this part of the channel that produce a gradient parallel to the channel that is just equal and opposite to that of the field before being disturbed by the projection of the channel. To form an idea of the charges and currents in the extension, two conditions should be assumed. First, that no current is fed into the extension from A, that is, that the extension from A consists of an elongating conductor insulated from the main channel at A. Second, that this connection is closed and that the channel and its extension are perfectly conducting.

For the first case, the problem is the determination of the charge distribution along a cylindrical conductor whose length is large with respect to its diameter, whose total charge is zero, and whose electric gradient along the surface of the conductor parallel to the axis is known. Assuming a step whose length is 150 feet, whose gradient is 9,000 volts per cm, and whose radius is 0.01 foot, or 3 mm, an approximately triangular charge distribution results, as shown in Fig. 3(A), whose density at the leading tip is -1.5×10^{-6} coulombs per cm and at the trailing tip of $+1.5 \times 10^{-6}$ coulombs per cm. The resulting density is not sensitive to variations in radius; thus, decreasing the radius to 0.005 foot increases the density about 10% and increasing the radius to 0.03 foot decreases the density about 12%. As the head assumes intermediate positions in its travel, the distributions continue to be approximately triangular at any instant.

In justification of the diameters of the channel extensions used here, reference is made again to the work of Higham and Meek,[16] which shows that the diameter of a 500-ampere arc grows from 1 mm at 1/4 μsec, to 2 mm at 1 μsec, and 4 mm at 6 μsec. This curve is reproduced in Fig. 4 of reference 2.

Current must flow within the channel extension to achieve such charge redistribution. If the tip of the extension moves with constant velocity then, as it reaches a certain point, the current rises suddenly at that point and remains constant until the channel has reached its maximum extension. These relations are shown in Fig. 3(B) for an assumed travel time of the head of 1 μsec with a velocity of 0.15 c. While this may not be the actual travel time, it does correspond to the time indicated by Schonland. In any case, it can be used later as a basis for reference. At the very tip the current reaches a maximum value of 7,000 amperes. At any point the product of current and duration of the flow is constant.

Now consider the case in which the extension is connected to the channel at A as shown in Fig. 4. While the extension is traveling downward, the disturbing influence of the sudden propagation of the downward step is also felt in the conducting leader behind point A. The velocity with which a disturbance travels along the arc plasma appears to be dependent upon the previous intensity of ionization of the plasma, as is evidenced by the velocity of propagation of dart leaders and return strokes. In this case assume that the disturbance travels up the channel at a velocity of 50% that of light. Thus, during 1 μsec while the channel is moving downward 150 foot from A to C, the influenced portion of the channel is the 500 foot above A. Let it be assumed that the radii of the leaders on both sides of

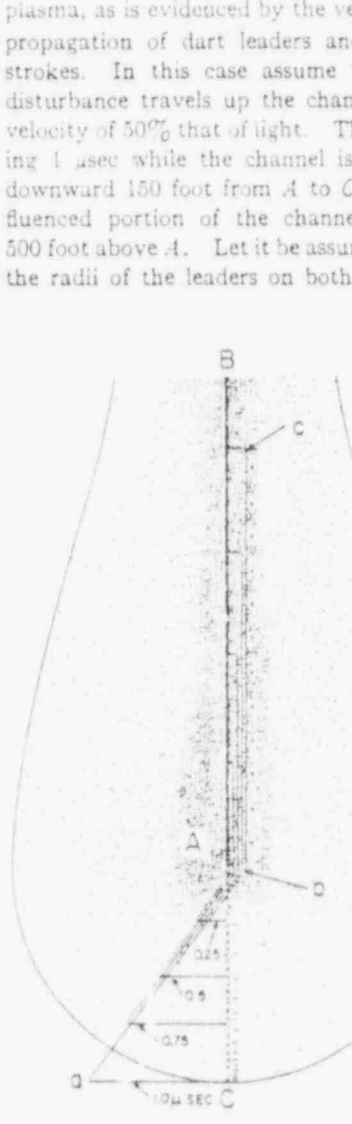

Fig. 2. Tip of the downward leader of the first component of a stroke, showing the approximate distribution of charge within the corona sheath and the charges that must be induced in the channel extension and in the channel above the channel tip, for several positions of the channel extension, assuming that the channel extension occurs rapidly

90004023

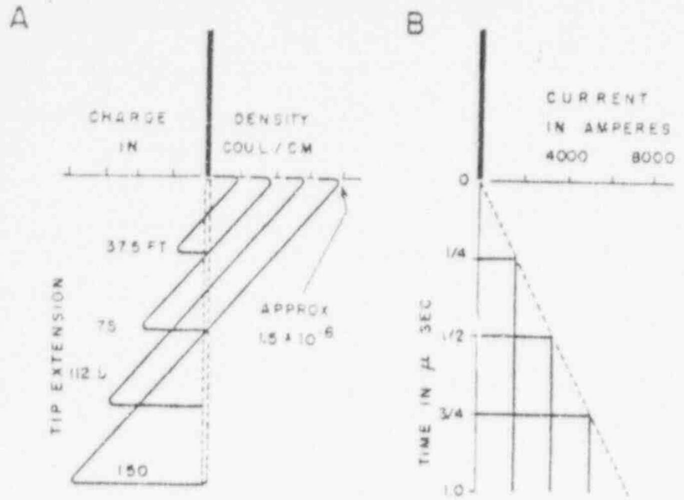

Fig. 3. Charge and current distribution in the channel extension assuming that no charge is drawn from the channel behind its tip during the interval that the extension is taking place

A are 0.01 foot, or 3 mm. For the moment assume that this movement is so rapid that the space charge contributing to the field cannot change in intensity in the immediate space surrounding these lengths. In this case the charges induced on these lengths are approximated by the solution of the electrostatic problem, for which the potential from A downward increases linearly to $150\times30.48\times9{,}000$ or 41×10^6 volts at C and upward from A the potential is the same as that at A. The average potential of the 650-foot length must shift subject to the condition that the total charge is zero. Fig. 4(A) shows such a distribution of potential. The determination of charge density, in terms of known potentials, is rather difficult without recourse to a digital computer, but the inverse of determining potentials, in terms of charge densities, is relatively simple. In Fig. 4(B) the dotted lines show an assumed charge distribution of the nature expected in this case. The solid lines show the corresponding potentials. It is found that the potential distribution approximates in shape the one under consideration. From this solution the desired charge distribution produced by the known potential is given in Fig. 4(C).

This curve of charge density is replotted in Fig. 2 by the curve *abc*. Other curves for one fourth, one half, and three fourths of the travel distances are also shown in Fig. 2 and in Fig. 4(C). The currents resulting from these charge distributions are shown in Fig. 4(D). For these assumptions the maximum current is about 12,000 amperes.

The actual condition for rapid advances of the channel probably lies between these two cases. They will be greatly enhanced by the characteristics that influence the transition from a glow to an arc and also by the transient characteristics of an arc as the current tends to increase rapidly. In Fig. 11 of reference 2, it is shown, that for an impulse current wave that rises linearly from zero to 10,000 amperes in 1/4 μsec the voltage drop at 1/4 μsec is 3,200 volts per inch or 1,250 volts per cm. For shorter instants, with the same rate of rise, the drop is even higher. This is merely indicative of the voltage drops that may occur with very rapid changes in current. Because of the rapid velocity of propagation above point A, the reference point in Fig. 4, and the longer distances involved above A, it is likely that the arc drop will also influence this portion of the circuit and offer additional impedance to the flow of current downward from A. Actually, the arc drop tends to suppress the charges in both circuits to some extent, because whatever drop does occur reduces the need for additional charge to annul the electric field existent before the development of the leader.

The criterion that determined the magnitude of the induced charges was that the electric field parallel to the channel extension produced by there charges is equal and opposite to the field into which it is projected. This results in a zero electric field parallel to the axis of the extension. No such cancellation exists for the radial field along the extension of the channel or for points in front of the extension. If, for example, the charge density attains a value of 1.5×10^{-4} coulombs per cm that is indicated in Fig. 3, the electric field 4 mm to the side or 2 mm in front of the tip would reach the following fantastic value; see equation 5 of Fig. 5 of reference 1:

$$E_r = \frac{9\times10^{11}}{a} q_s = \frac{9\times10^{11}\times1.5\times10^{-4}}{0.4} \quad (8)$$

$$= 3.40\times10^{8} \text{ volts per cm}$$

This merely means that in the attempt to maintain a low axial field, charges of great value develop which in turn produce profuse ionization in the space surrounding the channel. This is merely another form of corona or glow discharge. The radius of the corona sheath would expand to about 10 times 2 mm, or 2 meters. But this would not vitiate the argument concerning the axial gradient. As the corona expands into the original space charge, equalization of charge density results which in turn decreases the field originally responsible for the ejection of the channel. In this manner the charge density below A in Fig. 2 is gradually transformed into a charge volume density

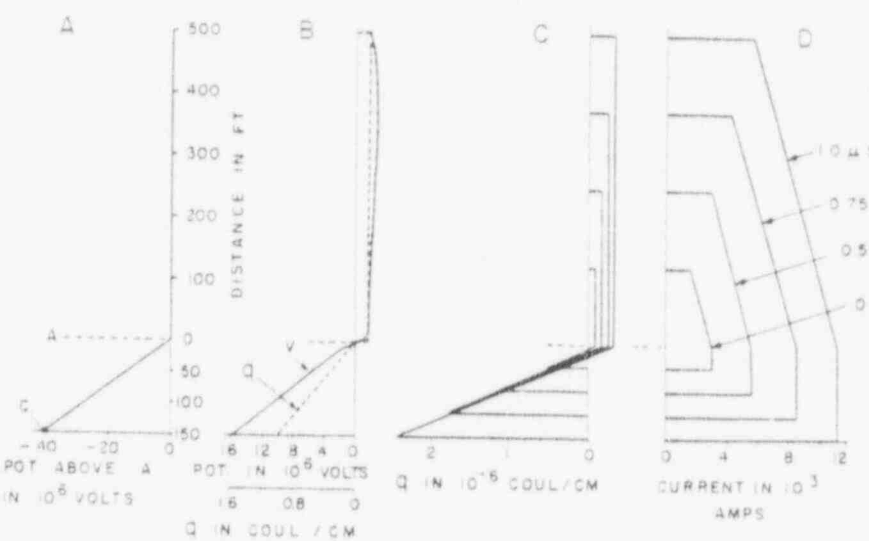

Fig. 4. Nature of charge and current distribution induced in the extension and the channel during a rapid extension of the channel when the total induced charge in the extension is drawn from the channel behind the tip

90004024

Fig. 5. Measurements of electric fields next to earth at points remote from the stroke[6,7]

A—Replot of cathode-ray oscillogram that illustrates relative magnitude of fields produced by steps and by return stroke of first component of a stroke

B—Actual record that shows that as earth is approached the field produced by the steps just ahead of the return stroke become smaller and of shorter duration

C—Replot of a typical section of the field record taken from the early life of the leader

resembling that above point A. The intense field ahead of the tip just mentioned probably supplies the explanation for the high velocity with which the leaders in the steps of lightning advance.

The currents described so far illustrate the assumed phenomenon that the travel time of the channel extension is 1 μsec. In considering the case in which an open circuit was used at A of Fig. 2, it is evident that this assumption is incorrect, for some current must certainly flow from above this point. In considering the other case current would cease below A after a time of 1 μsec, but would continue to flow above A because, after a current wave is once established, it should continue to flow until its energy is absorbed by losses. Evidence to support the condition of Fig. 4 is offered by the photographs of Schonland, that show that not only the step and a short distance behind it is highly luminous, but also that a fine trace of much fainter luminescence exists behind the tip of each step. This suggests that current such as illustrated by Fig. 4 is also being supplied from a long length of the channel. If the channel development time is 5 μsec instead of 1 μsec, the currents involved would be correspondingly smaller.

In laboratory-produced sparks, as the tips of the channels approach each other the gradient between them becomes larger and larger. This condition does not exist in natural lightning because the two terminals may be separated by enormous distances and the movement of the length of one step would not make any appreciable change in gradient from this consideration alone. Therefore, the induced charge in the channel extension becomes an important element not only in explaining the movement itself but in explaining the high velocities that may be attained.

But, while the photographic evidence of Schonland supports some sort of activity such as just outlined, there still remains the statement by Schonland that only 1 μsec is required to travel the length of the step. This contradicts laboratory data which show that channels start at a low velocity and increase rapidly. So before drawing definite conclusions, consideration will be given to additional evidence. This evidence is discussed subsequently when the electric fields, next to earth at points remote from the stroke, are examined.

Positive Polarity Steps

The experiments of Park and Cones[14] manifest the same external characteristics for the formation of both positive and negative space charges. Therefore, assuming that steps result from the same interplay of the space charges and the channels, the negative channel formation should be similar in character to the positive channel formation. Furthermore, since the channel formation and characteristics are essentially thermal phenomena involving the absorption and the loss of energy, one would expect the characteristics to be similar for both polarities.

Electric Field Measurements Next to the Earth

In the past this information has been analyzed in terms of the electric couple of the charges comprising the strokes.[5-7,17,18] More recently Wagner[19] has interpreted these measurements in terms of waves of charge and has concentrated on those phases of concern to the transmission engineer. A definite limitation of some of these data has been the resolution of the time sweeps and the time constant of the measuring circuit. Time resolutions of 1 μsec have been difficult to attain. In recent work of this nature

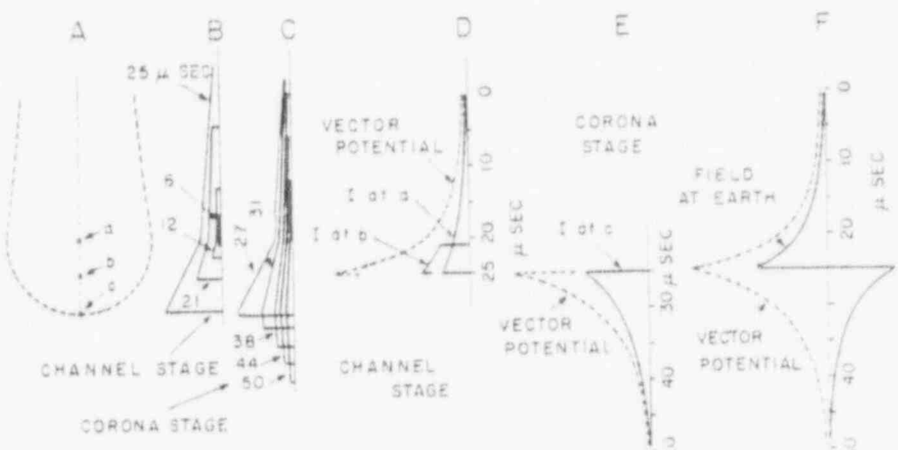

Fig. 6. Interplay of current supplying the corona sheath with current in the channel extension of a step that leads to the development of an electric field at the earth at a point remote from the stroke of a character similar to measured values

90004025

Clarence and Malan have utilized an amplifier with a high amplification and a frequency response up to 300 kc. Kitagawa and Kobayashi[20] state that their recording equipment can measure a rise time of about 1 μsec and that the time resolution of the time sweep is less than 10^{-6} sec.

Fig. 5(A), which is a replot by Kitagawa and Kobayashi[8] of one of their records, shows the electric field about 10 miles from a stroke. The field produced by the first return stroke is indicated by the first large sudden change, the *R* change. The small pips preceding the *R* change are stated by the authors to be about 50 μsec apart; they approach 20, then 13, μsec during the time just preceding the *R* change and are due to the steps in the first leader.

Fig. 5(B) is an oscillogram which was obtained by Kitagawa and Brook[7] in New Mexico. The nature of the field measurements preceding the *R* change is shown in more detail. Fig. 5(C) is another replot of a very early portion of Fig. 5(B) by the present authors and is intended only to indicate the general nature of the field produced by the steps. The rapid changes in Figs. 5(A) and 5(B) are faithful measurements but might be distorted slightly by limitations in response. The dropping portion of the large *R* change, is definitely affected by the time constant of the low-cut filter used in the recording apparatus and should not be used to draw conclusions. Clarence and Malan[8] observed similar field changes just preceding the return stroke and state that they consist of a "train of steep and predominantly positive pulses following each other at 5- to 10-μsec intervals."

As a result of field measurements Schonland[13] was led to conclude very early that the current in the steps is less than 10% of the current in the main return stroke. This conclusion was verified by later work and is discussed in more detail by Wagner.[19] But aside from the magnitude of the ground gradient measurements, the shape of the records leads to important conclusions.

Mechanism of Propagation

Fig. 6 represents an effort to show qualitatively the sequential mechanism of the step. Fundamentally it is based upon the observed facts that for laboratory gaps the formative current[3] of the space charge starts at a high value and decreases somewhat exponentially with time and that the current[3] supplying the channel during its development stage starts at a low value and increases almost as a positive exponential with time. In Fig. 6(A) the tip of the channel is shown just as the corona space charge is developed to its maximum position and the channel is about to start its development from *a* to *c*. All references to time are referred to this instant as zero. Fig. 6(B) shows the currents within the newly developed channel and also for points above *a* at different instants which start small and increase with time. At 25 μsec the head of the channel reaches the boundary of the space charge and must stop its progress. At this instant the character of the discharge changes suddenly from a channel extension to a corona discharge. A counter gradient builds up inside the corona sheath through the development of the space charge and the current begins to decrease. The manner of change is indicated in Fig. 6(C) at different instants. The solved lines in Figs. 6(D) and 6(E) show the time variation of the current at specific points.

A knowledge of the vector potential of the current is necessary to determine the electric field at the ground at a point remote from the stroke. This is proportional to the integral of the product of the current and the distance through which it is operative divided by the distance to to the point of observation. Since the distance to the point of observation is substantially constant for all of the points in the step, one need only consider the area under the curves of Figs. 6(B) and 6(C). The dotted lines in Figs. 6(D) and 6(E) represent these quantities as a function of time. These are also shown by the dotted lines in Fig. 6(F).

Except for the slow propagation of an average charge to replenish the charge in older steps and to supply part of the charge in the new step, the rapid changes in charge involve equal positive and negative values of charge. In other words, the process is largely one of rapid redistributions of charge rather than a translation of a charge. Such redistributions do not contribute to the development of an electric field at the observation point. Thus, the only contributing factor is the time rate of change of the vector potential of current. The time differential of the dotted line of Fig. 6(F) is indicated by the solid line of Fig. 6(F). The field at the observation point is proportional to this quantity. The discontinuity arises from the fact that the slope of the vector potential changes signs rapidly as the discharge transforms from a channel to a corona discharge. It can be seen that this field is similar in general character to the electric fields depicted in Fig. 5(C). This interpretation of the phenomenon of the step results in an electric field to which the circuit of Kitagawa and Kobayashi[20] can respond faithfully, and for which the time resolution of their films is adequate.

The time interval during which the channel current has the higher currents is small in comparison with the total duration of the step, perhaps only several microseconds. But it does appear that the duration is longer than the 1 μsec referred to by Schonland. Perhaps the sharply rising portions of the current curves should be sharper than here indicated and that Schonland was able to record only a short interval of the very highest current with the photographic sensitivity of the film that he used. Perhaps also, the resolution of Schonland's film was not sufficiently fast. Malan,[21] in describing the type of equipment he and Schonland used in South Africa, states of the time resolution due to the velocity of the lens as "possible to measure intervals with an accuracy of a few microseconds."

The luminosity of the steps should give some idea of the current carried thereby. Incidentally Schonland[13] arrived at a value of 16,000 amperes, but concluded that the "luminosity of the step process is far too weak to make it likely that the step carries a current of this magnitude." The discussion just presented is not sufficiently precise to warrant an accurate estimate of the magnitude of the current. It does, however, offer a method suggesting how magnitudes in the order of several thousand amperes might occur. This is based upon decreasing the value of 12,000 amperes, discussed in the development of the channel formation, somewhat in proportion to a 5- or 10-μsec channel formation period instead of the 1 μsec assumed at that point.

Further, it was assumed that the charge and channel formation periods were about equal. The time of space charge formation increases with gap spacing but the time of channel formation is independent of gap spacing. This would tend to make the time of channel formation smaller than the time of space charge formation. It is difficult to assign a definite value for the ratio because the time of channel formation also decrease as the overvoltage increases.

The detailed oscillogram in Fig. 5(B) clearly shows that the early stages of the downward leader are much more variable than the later stages. Just prior to the *R* change, while periods of the steps are still discernible and, as stated by Kitagawa and Kobayashi, have reduced to 13 μsec, the magnitude of field changes are

90004026

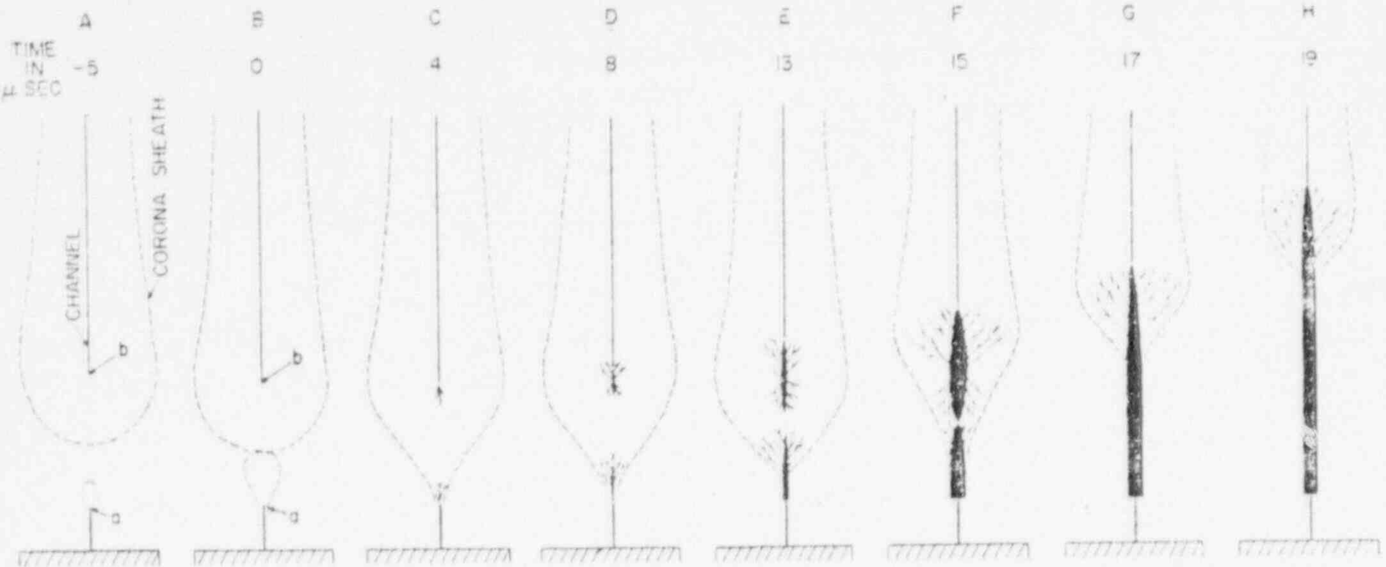

Fig. 7. Stages in the development of an upward channel

negligible in comparison with the R change. Norinder and Stoffregen[18] also comment on the fact that in some of their measurements of ground gradients "there is a calm period before the beginning of the main discharge." The step phenomenon is only an incidental preliminary setting the stage for the great incident culminating in the main stroke.

The long periods of the steps during the beginning of the leader formation may be occasioned by the limitations in the charge accumulating ability of that portion of the discharge within the cloud, or stated differently, by limitations of the leader's ability to maintain its potential as its capacitance is increased with fixed charge. As the length of the leader increases, the reservoir constituting the source of the charge for the next step is greater and constitutes a more reliable voltage source.

It is significant that so few photographs are available showing steps in the latter stage of the leader development just before striking the earth. Only two or three such photographs are available and these indicate small steps. On the other hand, negative evidence is available from the work of Berger, who has photographed the last stages of the leader at a very close range of less than 1,000 feet and with the exception of two photographs has not been able to discern the presence of steps. Three explanations suggested themselves to Berger: (1) the photographic sensitivity of his films was not sufficiently great to penetrate the intervening atmospheric conditions; (2) the Plexiglas drum (2 mm thick) through which the light must pass may have absorbed the light from the steps, and (3) the steps and current variations in the leader were so small that the light appeared as a continuous beam. The third possibility is probably correct, particularly in view of the evidence afforded by the ground gradient measurements.

Current in Corona Sheath

It is possible to estimate the magnitude of current in the leader steps by an extrapolation of the measured laboratory currents. In reference 3 the current pip for a 6-foot rod-rod gap, for a positive impulse voltage of 860,000 volts (90% of critical) was estimated as 25 amperes. Now apply these data to a lightning stroke in which the voltage across the space charge in its most extended position is about 30,000,000 volts. To get an idea of the current that might be expected in a stroke to form the corona sheath at each step, simply prorate these voltages. This results in a current peak of $30,000,000/860,000\times25$, or 880 amperes. Park and Cones[14] observed that the current pips vary over considerable limits for a given condition. Taking this factor into consideration, and prorating the data of Park and Cones (sphere-plate gap) and that of Hagenguth, Rohlf, and Degnan[15] (horizontal rod-rod gap), it may be concluded that the current in the steps of the strokes may be in the order of 1,000 or 2,000 amperes. Although these extrapolations are quite large, they indicate that the lightning stroke channel currents necessary to develop the corona are of a relatively modest value compared to the return stroke current.

The work of Park and Cones demonstrates most clearly that the development of the corona space charge is entirely independent of and a precursor to the subsequent channel development, although the channel may begin before the space charge is fully developed. That this work was conclusive probably can be attributed to three conditions: (1) the use of a 0.07×100-μsec wave that rose so rapidly that it could be regarded as a rectangular wave; (2) the choice of a sphere instead of a sharp rod; and (3) the control of the free electrons and ions in the gap. In most cases the voltage rose to full value and for some gap spacings the air next to the gap was stressed to as high as 150,000 volts per cm before a free electron or ion was positioned to trigger the gap. When a slower wave that rose to crest in 1 μsec was used the results became erratic and the crest of the corona current pip was approximately proportional to the voltage at which triggering occurred. It would be expected then, that with a copious supply of free electrons the current peak would be relatively low and spread out over considerable time. This condition must have presented itself in the experiments conducted by Saxe and Meek and possibly others in which the current in a pointed electrode over a flat plane failed to exhibit the magnitude of current peaks of Park and Cones when the applied voltage rose to crest in about 2 μsec.

But the magnitude of the peak corona current is also dependent upon the ratio of the time to crest of the applied voltage to the time required to develop the space charge. For a lightning stroke step length of 150 feet a time of about 25 to 50 μsec is required to develop the corona sheath ahead of the channel tip. There-

90004027

fore, a gradual rise in potential of the point from which the corona emanates in, say, 5 μsec would not have much effect upon the peak value of the corona current passing through this point, because during this time the back voltage developed by the space charge would not have sufficient time to build up.

Development of Return Channel

Approaching the Earth

Fig. 7 is a simplified picture of the general processes that occur at successive instants as a stroke strikes a tall object such as a mast or a transmission line tower. Evidence has indicated that as the leader approaches the earth the steps become shorter in length and time. In order to discuss what occurs at and near the earth, the steps will be assumed to be so small that the channel and its associated corona sheath propagates with a constant velocity of 1 foot per μsec, which is approximately what Schonland observed as the average velocity of the downward leader. While specific numerical values are ascribed to the various stages, it should be realized that the actual values vary over the wide limits characteristic of lightning phenomenon. The mast is indicated as being 100 feet tall and the width of the heavy lines is intended to convey an impression of the current flowing at the instant. It is assumed that the potential of the channel, indicated by the full line on the axis of the corona sheath, is 50,000,000 volts with respect to the earth.

Fig. 7(A) shows the position of the channel at an instant where the tip, b, is still about 400 feet above the earth. It is surrounded by its negative corona sheath. When even more remote than this a corona discharge begins to develop from the tower and at this instant has already developed sizable proportions. From this position the channel and its corona sheath continue their progress to earth and when they attain the position shown in Fig. 7(B), in which the tip is 275 feet above the tower, a channel begins to develop from a.

This distance is determined when the average gradient between a and b attains a value of about 6,000 volts per cm, the critical value at which breakdown occurs. Thus

$$\frac{50,000,000}{6,000 \times 30.48} \approx 275 \text{ feet} \quad (9)$$

This instant will be designated as the reference point for time. Prior to this profuse corona had existed at a but the channel had not begun to develop until this instant. Four microseconds later, as shown in Fig. 7(C), the channel from both a and b has progressed to the points indicated. In 7(D) further progress has been made and the current has grown significantly. At the same time the current feeding the downward moving channel of the last step draws current from the old low-current channel feeding this last step from above. As was explained in the discussion of the step process the propagation of this current is slower than the speed of light; it is limited primarily by the speed with which the arc path can accommodate itself to the higher conductivity and the speed with which it can draw the charge from the space charge. Corresponding fingers of the channel must extend into the space charge above the last step to collect the appropriate current. And so the progress continues through (E) and (F), the instant at which contact is finally made between the main channels in the last step. Fig. 7(G) and (H) show later instants at which the head of the return channel has penetrated farther into the space charge and lowered a substantial portion of this charge to earth.

Note both the progress of the upward channel of the last step and the time intervals between the indicated positions which have been chosen to suggest increasingly higher and higher velocities of the upward channel. As the upward channel progresses, tentacle-like streamers reach outward and upward and tend to spread the positive charge over a greater area than that encompassed by the channel itself.

The current at the earth associated with the development of the corona sheath is small with respect to the current occurring during the channel formation stage. This statement is based upon laboratory tests. The surge impedance of the stroke does not differ greatly from the series resistance that is usually employed in high-voltage laboratory test circuits, so that the final reference currents should be proportional to the voltages in the two cases. Several sets of data, Park and Cones,[14] Hagenguth, Rohlfs, and Degnan,[15] and Wagner and Hileman,[3] indicate magnitudes of the first current pip (current that supplies the space charge) less than a few per cent of the final current. The tests of Park and Cones show that when the critical voltage is only slightly exceeded, even when the wave shape is almost rectangular, the current crest is very small. As the slope of the applied wave becomes slow, which should be the case as the electrodes move toward each other slowly, the first current pip is even smaller.

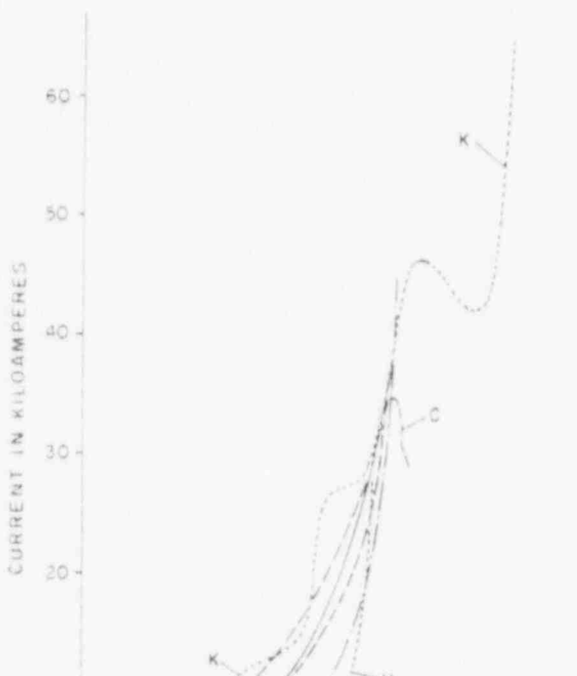

Fig. 8. Replot of the oscillograms of high stroke currents recorded by Berger,[22] translated with respect to time to pass through 40,000 amperes at the same instant

Fig. 9. Channel formation in an arrested discharge in a 6-foot rod-rod gap showing the outward formation of parallel channels

Current Curves

The most extensive oscillographic measurements of stroke currents are those made by Berger[22] in Switzerland which were collected on a 70-meter steel tower and mast mounted atop Mount San Salvatore. The measuring shunt was located at the base of the 18-meter mast. Berger has published 39 cathode-ray oscillograms taken from 1946 to 1954 of which the 14 that exceeded 40,000 amperes are reproduced in reference 19. Oscillograms B, C, H, I, J, and K from Fig. 5 of this reference are replotted in Fig. 8. They were intentionally translated with respect to time so a better idea of the extent to which they coordinate with each other could be seen. Oscillogram (B) is the most well-defined. The others, with the exception of (C) for which the zero of time was clearly indicated, were drawn so that they coincided with (B) around 30,000 amperes. They all indicate a variation with time that follows a somewhat positive exponential curve. Other available oscillograms of stroke currents are reproduced in Fig. 3 of reference 1. With the exception of the record obtained by means of a captive balloon, which is not characteristic of direct ground strokes, they all exhibit this same upward concave characteristic.

As shown in the companion paper[2] all of the gap currents for rod-rod gaps exhibit the same positive exponential characteristic with time. It also illustrates that the time lag of rod-rod gaps is the same expressed in microseconds for all gap spacings, and is only dependent on the fractional amount by which the critical voltage is exceeded. The times to crest of the currents from Fig. 8 do not differ greatly from the laboratory curves, despite the great difference in gap lengths, if the curve for comparison is one in which the critical voltage is exceeded only slightly.

Both the rate of current rise during the formative stage of the channel and the terminal or final values of the current are affected by the constants or impedances of the test circuits. It is shown in the companion paper that the current increases from zero along a concave upward curve until it is limited by the series resistance. The Berger oscillograms of the lightning stroke current show that similar forces must be active in limiting the flow of current to an essentially constant value after contact of the two channels has been established. These forces probably involve such factors as the speed with which the low-current channel of the downward leader can be converted to a highly conducting high-current channel and the velocity with which the positive corona head of the return streamer can propagate within the negative space charge cylinder that had been deposited by the head of the downward leader in its progress toward earth. A substantially constant velocity is attained and some of the factors determining this velocity will be discussed next.

Induced Charges and Velocity of Upward Streamer

Wagner and McCann[23] showed that as the upward leader propagates upward within the cylindrical volume charge deposited by the downward leader in its progress earthward, by virtue of the electrostatic relationship, a positive charge is drawn upward from the earth by induction. This charge may be viewed as neutralizing the negative charge of the downward leader. In the Appendix of reference 23 the following relation is derived expressing the proportion of charge so neutralized. This might be called the induction factor.

$$\frac{dq_u}{dQ_1} = \log \frac{R}{r_1} / \log \frac{R}{r_u} \qquad (10)$$

where dQ_1 is the charge in an elemental ring of radius r_1 in the downward corona sheath, dq_u is the induced positive charge in the upward channel produced by dQ_1, r_u is the radius of the upward channel, and R is the radius of a large concentric cylinder representing earth. The potential of the upward channel is the same as that of the large cylinder representing earth. The value of the neutralizing charge so computed is dependent upon the assumptions used. For the values assumed by Wagner and McCann the induced positive charge was about 70% of the negative charge. This same concept was later amplified by Wagner and Hileman.[1] Assuming R to be 500 feet, the radius of the arc channel to be 0.2 inch, and that the charge on the downward corona sheath was concentrated at a radius r_1 equal to 200 cm or 6.75 feet, they arrived at a value of 0.42. The factor used is thus dependent upon the mechanism by which the neutralization takes place. On further reflection it appears that the channel probably extends upward and outward as indicated in Fig. 7. This condition is illustrated by the last stages of the arrested discharge shown in Fig. 9, which shows the nature of the development of the channels of a vertical 6-foot rod-rod gap for which the voltage has been chopped by a parallel gap just prior to the union of the channels extending from both electrodes. This type of mechanism indicates that the radius of the upward channel r_u, of equation

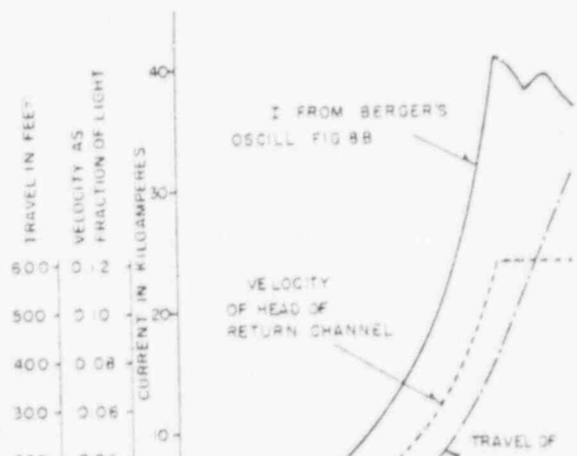

Fig. 10. Velocity-time curve computed to have a terminal velocity of 0.12 c and to be proportional to the current curve, Fig. 8(B). The corresponding distance curve is also shown

90004029

10, is much larger than previously thought and that an induction factor approaching unit might well be achieved.

Whether the actual mechanism of neutralization is of this character, involving a rapid movement of positive charges into a region adjacent to the negative charges, or whether the negative charges also move in toward the positive channels is not known. It is probably similar to that which occurs in the last stages of the laboratory-produced spark where high terminal velocities are produced.

A number of experimenters[2,10,14,24] have measured the progress of the tip of the channel as it moves across a laboratory gap and from these measurements have computed the velocity. They all show that the channel starts at a low velocity and increases rapidly with time. The result resembles the shape of the current-time curves.

Schonland, Malan, and Collens, discussing the velocities of the return streamers of lightning, state that the range of variation is from 2.0 to 14.4×10^9 cm/sec and the mean 5.2×10^9 cm/sec, while the value indicated as most frequent is 3.5×10^9 cm/sec or 0.12 c.

In the companion paper evidence is shown to indicate that the channel currents in rod-rod gaps bear the following relation to the instantaneous velocity:

$$i_c = 3.2 \times 10^{-6} V \tag{11}$$

where i_c is the current in amperes and V is the velocity in cm per sec. If the most frequent return velocity of 0.12 c is inserted in this equation then i_c becomes 11,500 amperes, which is gratifyingly close to the most frequent magnitude of stroke current of 14,000 amperes.

Or, viewed differently, if a rectangular wave of charge moves vertically from the earth at a constant velocity, vc, then the associated current is also a rectangular wave. If the return channel can be represented by such a wave, the implication is that the head of the wave on reaching any vertical section instantly annuls the portion of negative charge at that elevation.

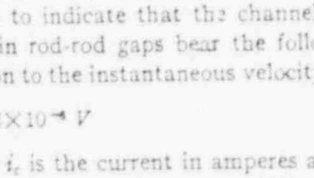

Fig. 11. Boys' camera photograph of stroke to ground

The following simple relation then exists between the charge per unit length and the current:

$$i = vcq_o \tag{12}$$

If, on the other hand, the charge at any section transfers inductively to the downward channel at a constant linear rate as a function of time, with the velocity remaining constant, the current also increases at a linear rate until the crest is attained. Thereafter, the same simple relation exists between the current and the linear charge density. If the head of the return channel moves upward with a velocity that is not constant, but increases progressively with time, the above simple relation between current and charge density continues to hold if the wave of charge remains truly rectangular. This condition also requires that the wave of current remains rectangular, that is, that it increases equally for all points behind the head of the wave, if it is accepted that the velocity of the heat of the current wave is similar in shape to the current-time wave. No accurate photographs of the first few hundred feet of travel of the return channel are available from which the velocity can be estimated. If it is assumed that the flat portions of the stroke currents, obtained by Berger,[22] arise from the induced charges rising up the column, after contact is made between the upward and downward channels, then it can be expected that the terminal velocity of the upward channel on contact must be (using the most frequent value) in the order of 12% that of light. Fig. 8(B), which is the most clearly defined of Berger's stroke currents, is replotted in Fig. 10. Assuming that the velocity is proportional to this curve and fixing the terminal velocity at 0.12 c, a velocity curve shown by the dotted line is obtained. Integrating this curve with time results in the dot-dash curve that gives the travel of the head. The distance traveled in the time required to attain constant velocity indicates the point above ground at which union with the downward channel occurs. This distance, about 400 feet, falls within the range of expectancy.

Evidence of Upward Leaders

Fig. 11 is a photographic reproduction of a sketch showing the lower end of a Boys' camera record obtained by Dr D. J. Malan and presented in a discussion of upward leaders by Dr. R. H. Golde.[26] The point x indicates where the downward leader terminated and was met by the upward channel from the earth. Its height is approximately 50 meters. The lengths of the last few steps before contact with the upward channel are clearly shown.

Tortuosity of Path

Schonland observed that successive steps do not generally follow the same direction. The tendency to maintain a straight line in the progress of the channel is not strong. Since the channel of each step starts from the center of high charge concentration, the direction taken by the channel would be highly sensitive to slight differences in density. There may be many simultaneous starts in different directions but only one finally dominates. The dominating one develops a lower impedance, and in the process of forging ahead decreases the electric field parallel to its path in its vicinity, and also the tangential components of field of the lagging channels so that less charge separation is required in them to neutralize the field in which they are advancing.

General Discussion

In laboratory gaps the space charge forms at a substantially constant velocity and thus the time of formation is proportional to the gap length. On the other hand, with gap lengths of at least 100 inches as shown in Fig. 10 of reference 3, the time to breakdown is substantially independent of gap length. These relations indicate that the time of space charge formation plays a more important part as the gap length increases and emphasize the role of the charge formation in the step mechanism of lightning.

The forcing electric field at the earth is applied slowly in steps as the downward leader approaches and then more rapidly as the tip of the last downward channel develops. In this way the positive charge at the earth has a somewhat longer time to develop than the space charge ahead of the downward channel as the latter can develop intensively only after the channel has completed another step to a new position. Or if the head of the downward channel moves at substantially constant velocity, as the ground gradient measurement of Kitagawa and Kobayashi and others indicate, then the space charge is continually being formed from an electrode that moves at the average velocity of about 1 foot per μsec. The space charge from the earth terminal is being formed from a stationary electrode. The current during this interval supplying the charge in the corona sheath is relatively small. The significant current only oc-

90004030

curs after the head of the upward channel has attained a high velocity, such as in excess of 0.02 c.

The presence of the steps in the downward leader should not be accepted as evidence that the space charge formation is completely halted at any point as might be the case when a definite impulse voltage is applied to a cylindrical conductor and the space charge develops to a definite region. Rather, it should be thought of as a continuing formation, and when the conditions at the terminal are favorable to the formation of a channel the progress of the channel is renewed. These two conditions merely merge into each other. A similar phenomenon is present in the leader of strokes subsequent to the first. These leaders had been thought to be continuous and propagate with a velocity of about 0.01 c. But the electric field measurements,[5] at points remote from the stroke, have demonstrated that they involve fast repeating processes with a period about 10 μsec.

The co-ordination between the various components of the stroke can be illustrated by a numerical example. Consider a stroke approaching the earth with a potential with respect to the earth of 50,000,000 volts. Assume that the average gradient of the space charge between the head of the downward channel and the earth necessary to initiate the channel from the earth is 6,000 volts per cm. As can be seen from equation 9 this determines the height of the downward channel at this instant as 275 feet. From Table I and Fig. 1, it can be estimated that the charge distribution along the stroke some distance back from the tip is about 5×10^{-6} coulombs per cm for a stroke potential of 50,000,000 volts. Now if it is assumed that the velocity of the head of the upward channel at and after contact is 0.12 c, then the stroke current at which it levels off is, from equation 12,

$$i = 0.12 \times 3 \times 10^{10} \times 5 \times 10^{-6}$$
$$= 18,000 \text{ amperes}$$

and if the velocity is 0.3 c, the stroke current is 45,000 amperes.

In the theory proposed here, it was assumed that the charge density varied inversely with the radius which results in a constant electric gradient. However, this assumption is not critical. It should be recalled that one role of this particular quantity is to indicate when the combination of field and charge density reaches such a critical value next to the arrested channel that the channel will again resume its progress. It might be that the actual distribution is not of the type assumed here but, whatever it is, the average field might constitute a measure of the conditions necessary for channel development. The space charge must be related to the total potential thereby produced as it is the quantity whose development retards the downward progress of a step. Also, it was seen to be a measure of the critical sparkover gradient. For this purpose an average gradient could be used with equal validity as a constant gradient. The other role of the charge distributed within the downward leader is the manner in which it affects the potential of the conducting channel comprising the core. But this is only one factor that affects the potential. The charge in other portions of the leader and the distance from the earth are also important. The field outside as well as inside the space charge determines the potential of the core. Thus considerable departure from the assumed charge distribution might be permissible without greatly affecting the potential.

Multiple Strokes

The fact that multiple lightning strokes take the same path to ground implies that the effects of the preceding component have not become fully dissipated by the time the charge-gathering mechanism within the cloud has attained sufficient potential to break down the weakened path. The usual explanation given for the subsequent strokes seeking the same path is that some remanent ionization in the path which offers some sort of directive effect still remains. McCann and Clark,[26] however, offer an alternate explanation by stating that the main return stroke current heats a small column of air to a very high temperature. Following completion of the stroke, the heated column diffuses into the surrounding air, but as it does so it forms a column with a larger and larger radius, whose density gradually approaches normal. Since the breakdown voltage decreases with decreasing density, the preceding path offers an easier path for the subsequent discharge.

But, regardless of the explanation, it is an observed fact that the velocity of propagation of the downward leader of components of a stroke subsequent to the first travel with a much higher velocity than the first component. These are called dart leaders. They are almost free of steps, although Kitagawa and Kobayashi[8] have seen indications of very-high-frequency steps in these discharges also. While the average velocity of propagation of the first component is about 0.001 c, the velocity of the dart leader is about 0.03 c. As the dart leader approaches the earth, there must still exist next to the earth a similar channel in which the same conditions exist as in the channel through which the dart had developed. Therefore, a similar dart leader should spring from the earth and meet the downward moving dart leader. If it is true, as with the conventional gap, that the current increases with the velocity of approach of the channels, then the current should have a steeper slope than the first component. In Fig. 10, for example, the current should tend to start from the value at which the velocity is 0.03 c, and the average rate of rise should be higher. The latter stages of the current curve should be similar in slope to the latter stages of the current of the first component.

Recently Berger[27] presented information concerning the waveshape of the currents in components, subsequent to the first, that were obtained on Mount San Salvatore. One chart shows the current in an 11-component stroke. The first component had the usual concave-upward shape and rose to 50,000 amperes in 9.0 μsec. The crests of the subsequent components were smaller but the rise time was less than 1 μsec. In conversation with one of the authors Berger stated that this information was limited by the tripping time of the cathode-ray oscillograph, and that the portion of the record prior to this was lost. These rates of rise are much faster than for the first component and may be significant in considerations affecting transmission line performance. Both the magnitudes of the subsequent components, and their times to half-value, were less than the first component. This information is still too meager to draw general conclusions.

Comparison With Other Theories

In a subject as complicated as lightning discharge it is difficult to determine who originated certain component aspects of the theory. The novelty of a complete theory resides rather in how the component characteristics are assembled and affect each other. Little attention has been given to the behavior of the stroke just before reaching the earth and the mechanism of the return stroke. Without attempting to cover the entire field, several theories that have received widespread attention will be described briefly.

Schonland[13] concludes that the charge advances downward as a cylindrical, weakly ionized body whose surface gradient is 30,000 volts per cm or somewhat less to account for the lower air densities at high altitudes. This pilot leader advances at a constant velocity. It is accompanied in steps by a highly ionized leader. The highly ionized leader cannot advance into the uncharged space ahead of the weakly ionized pilot. Suppose one considered an instant shortly after the leader has caught up to the pilot. They advance together in a field of about 30,000 volts per cm. But as the pilot advances the negative charge produces a negative gradient behind it that is directed in an opposite direction to that of the propelling field and eventually the net field drops below 6,000 volts per cm at a point behind it. At this point the advance of the leader ceases. This rapidly produces a positive space charge ahead of the arrested leader because electrons cannot be furnished to replenish the space charge. In the meantime, the pilot advances by virtue of its self-inductive property. With the development of the positive space charge, a gradient of 30,000 volts per cm is again quickly established and the thermally ionized channel again advances.

Komelkov,[28,29] on the other hand, assumes as do the present authors that the channel tip is fed by a thermally ionized channel having a drop of about 60 volts per cm and that a corona space charge having a gradient of between 6,000 and 10,000 volts per cm is produced ahead of and around it. The stoppage of the leader, according to Komelkov, is attributed to a decrease in the potential of the channel tip caused by the need to charge up the new section.

Bruce [30] attributes the step formation to the rapid transition from a glow discharge of high gradient to an arc discharge of low gradient when the low discharge current reaches the critical value of 1 ampere. He also postulates that as the arc has paused and starts on its new step a lateral flow of current to supply the glow occurs. The current at the tip increases as the length of the step increases until it reaches approximately 1 ampere.

Griscom[31] has proposed another theory with a highly conducting channel that feeds the tip. This theory is radically different from the others. His concept is that as the discharge advances a great bulbous volume of charge is formed at the end of the conducting channel many times greater in diameter than the cylindrical envelope of charge behind the tip. As the charge volume grows, it maintains a surface gradient of 30,000 volts per cm, although mention is made of a gradient within the space charge. The next step develops when, through chance, a protuberance is formed on the envelope of the bulbous space charge that may occur anywhere on its surface. This produces an unstable condition and, the new protuberance is enlarged, it draws its charge by means of a plasma that glows inward into the last bulbous tip.

The theory presented here is a combination of these theories. Cetain aspects are drawn from each and certain additions have been made. The small-diameter conducting core is similar to that premised by Komelkov, Griscom, and the authors in a previous paper. The shape of the corona sheath is somewhat like Komelkov's. All the theories accept that the gradient in the corona space charge is in the order of several thousand volts per cm, but only Schonland recognizes that the average value must exceed a certain critical value to encourage the development of the extension of the plasma channel. However, Schonland is somewhat vague as to the actual existence of such a plasma channel within the pilot leader. It is probable that the actual transition from the glow to the arc is of the nature proposed by Bruce but on a filamentary basis. Thus, the space charge in advance of the arrested channel is fed by a host of filaments or streamers and the current at the base of each one increases as its length increases. At some instant, current in one of these filaments reaches the critical value of 1 ampere and at this instant, an arc plasma begins to grow from this point. This may occur in several filaments almost simultaneously. But one of the filaments eventually prevails in its growth and because of its shielding effect upon the others robs them and eventually emerges as the new channel. The direction taken is determined by chance which would explain the forked character of the stroke path. This is similar to the explanation of Komelkov.

No doubt a temporary drop in potential of the tip of the channel as the new step is formed exists just as premised by Komelkov. But the authors feel that this has a secondary rather than a primary influence. The present theory differs from that of Griscom but agrees with that of the other three in the assumption that the extension of the conducting plasma begins from the tip of the last channel and grows toward the earth, rather than from some spot on the periphery of the corona sheath back to the conducting channel. The Griscom prestrike theory views the timing of the inception of the new step as a chance distortion occurring on the surface of the envelope, and the other theories view the phenomenon as more of the nature of a triggering phenomenon. The long periods of rather uniform steps would seem to favor the triggering viewpoint.

As was mentioned at the beginning of this paper, the real interest of the authors lies in studying the sequence of events as the stroke strikes the earth. Aside from the work of Bruce and Golde,[32] Griscom, and the authors, little has been done along this line. Golde[32] assumes that as the downward leader approaches the earth, corona streamers develop when a gradient of about 10,000 volts per cm is attained. The reduction from 30,000 volts per cm is taken to provide for minor irregularities such as grass, shrubs, etc. This he takes as the condition for determining where a stroke will strike. The authors believe that a corona sheath will develop much as Golde proposes. They do not feel, however, that the existence of the corona sheath at the earth is the controlling criterion. They feel that the significant factor is the instant at which the average gradient between the tip and a point on the earth, of about 5,500 or 6,000 volts per cm, is attained. At this point a conducting plasma is formed from the point on the earth which moves upward with accelerating velocity toward the slowly moving downward conducting plasma of the leader. Griscom's prestrike theory proposes that before the development of the currents of the return streamer a prestrike current, from which this theory derived its name, occurs at the earth whose magnitude is about that of the return stroke current and whose duration is about 1 μsec. During this microsecond, the current presumably rises from zero to the crest value and returns again to approximately zero before the current associated with the return stroke occurs.

Improvement of Line Performance

While the purpose of this paper is to analyze the lightning stroke characteristics with the aid of the available knowledge concerning the predischarge current of laboratory gaps, a knowledge of the latter suggests a modification of the manner in which the impulse characteristics of insulation are applied in the computation of the lightning characteristics of lines. It is not generally appreciated how important the predischarge currents of certain types of gaps might be.

Fig. 12 shows a ground wire attached to the top of a tower and a conductor suspended from a tower arm by means of an insulator string. It is assumed that the tower top, tower arm, and ground wire are all at the same potential with respect to ground which will be designated by e_g. Also

e_c = potential of conductor at the tower
i_g = current flowing in ground wire from each side
i_c = current flowing in conductor from each side
Z = surge impedance of ground wire and conductor, assumed to be the same
Z_m = mutual surge impedance between conductor and ground wire

Then by applying conventional wave theory equations

$$e_g = Zi_g + Z_m i_c \tag{13}$$

$$e_c = Z_m i_g + Zi_c \tag{14}$$

Eliminating i_g from these equations

$$e_c = \frac{Z_m}{Z} e_g + \frac{Z^2 - Z_m^2}{Z} i_c \tag{15}$$

and letting the coupling factor Z_m/Z be designated by K

$$e_c = Ke_g + (1-K^2)Zi_c \tag{16}$$

The voltage across the insulator string, e, is

$$e = e_g - e_c = (1-K)e_g - (1-K^2)Zi_c \tag{17}$$

$$= (1-K)e_g - (1-K^2)Zi/2 \tag{18}$$

where i is the predischarge current taken by the insulator string.

The first term is the component of voltage that is usually considered in line calculations, but the actual voltage across the insulator string is less than this by the drop through the line impedance $(1-K^2)Z_i/2$. This relation is true whether the computed value $(1-K)e_g$, neglecting the predischarge currents, is produced by the stroke currents in the tower and ground wires or by electrostatic induction from the charge in the stroke above the tower.

In reality, therefore, the significant voltage that should be used with the conventionally computed values for the insulator string is the laboratory-obtained voltage across the insulator string or other form of insulation plus $(1-K^2)Zi/2$. Tests have not been made on a bare string of insulators but suppose that for 18 5¾-inch insulators for a 4-μsec time lag the flashover voltage is about 2,000,000 volts, then if the predischarge current is about 300 amperes, $Z = 500$ ohms and $K = 0.3$

$$(1-K^2)Zi/2 = 68{,}000 \text{ volts} \tag{19}$$

or 3.9% of the flashover voltage.

But if steps are taken to amplify the predischarge currents, much greater effects can be obtained. Consider this same insulator string. Suppose that a triangular pipe-pipe gap such as described for Figs. 19 and 20 of reference 3 is used. For a breakdown at 4 μsec, a charging voltage of about 160 is required for the 6-foot gap. The predischarge current is about 600 amperes and for the voltage across the gap is about 1,000,000 volts. Comparing Figs. 19 and 20 of reference 3 it will be seen that the current is proportional to the gap spacing for the same overvoltage conditions. So, if the gap is increased to 12 feet the terminal voltage will be about 2,000,000 volts which matches the insulator string flashover voltage and the predischarge current will be about 1,200 amperes. The drop through the line impedance is then (0.91)(500)(1,200)/2 or 273,000 volts. This amounts to 13.6% of the insulator string voltage.

Conclusions

The authors have attempted in the light of laboratory data to determine what happens during the very complicated phenomenon of the lightning stroke. Because of the modest limitations of laboratory facilities, it is necessary to extrapolate a great deal to reach the grand scale of natural lightning. The following is a brief summary of the theory advanced in this paper.

1. The downward leader of the first component of the stroke consists of a central highly conducting arc plasma channel of about 2 mm in diameter which has a drop of about 60 volts per cm. The conducting arc plasma is surrounded by a negative space charge whose radial gradient is about 9,000 volts per cm. The radius is approximately 20–30 feet and depends upon the potential of the stroke.

2. The steps of the first component are formed by the alternate advance of the central channel and its surrounding corona sheath. If an instant at which the central channel has just reached a point of maximum progress in one of the steps is considered, the corona sheath advances beyond this point in front of the channel tip. Reasonable agreement is obtained by extrapolating, from laboratory data, the time of formation of corona pulses of gaps to the time of formation of the increment of the corona sheath. When in the progress of the development of the corona sheath, the energy concentration at the tip of the arrested channel reaches a critical value or possibly when individual corona streamers reach a certain critical current, the progress of the channel is again resumed. The high speed of the progress of the channel step is explained by the high charges induced in its tip, because it constitutes an extending pencil of high conductivity that pierces the relatively stable space charge of the corona sheath. This phenomenon is repeated as the leader head travels from the cloud to the earth. The currents in the steps are small in comparison with the currents in the return stroke.

3. From independent measurements of electric fields next to the earth at points remote from the stroke, it has been shown that the frequency of the impulses produced by the steps becomes smaller as the earth is approached; they diminish from about 50 to 100 μsec at the cloud to about 13 μsec near the earth. One might assume that the step lengths are correspondingly reduced. This deduction is reinforced by several photographic records that show steps of short lengths just prior to reaching the earth.

4. As an approximation, it might be assumed that the downward leader, as it approaches the earth, moves with a constant velocity without steps. When a certain point in its progress is reached the electric gradient on objects projecting from the earth exceeds a value of 30,000 volts per cm and corona streamers begin to form at the earth. These streamers continue to grow and a corona sheath is formed about these objects. As such they are not important but the space charge associated with them has an equalizing effect upon the field between the advancing channel and the earth. The current at the earth associated with the formation of the corona sheath is small with respect to the current in the return stroke. Only when the advancing channel has reached a point where the gradient between the channel tip and the earth, or projecting objects, reaches an average value of 6,000 volts per cm does an arc plasma form from the object upon the earth. Prior to this instant the entire tower top of a transmission line tower might be enshrouded in corona without serious consequences. Thereafter, the current at the earth increases at an ever increasing rate forming a concave upward curve with time until the maximum value is attained. At this point the channel tends to flatten off.

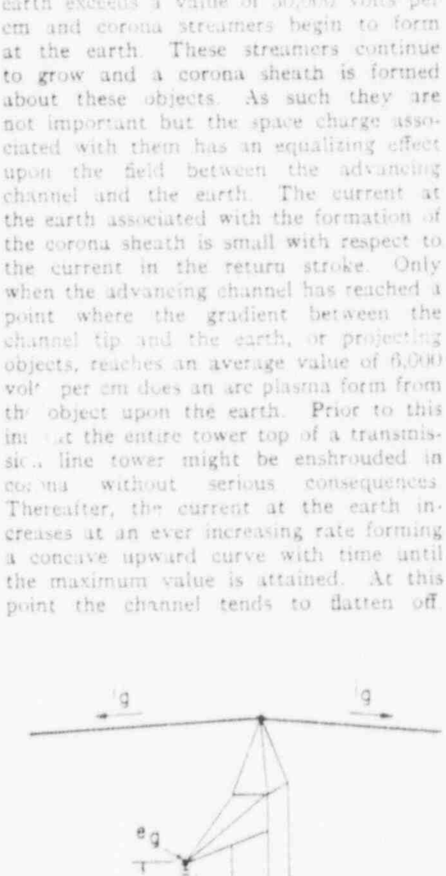

Fig. 12. Diagrammatic sketch of tower with ground wire and conductor showing nomenclature used

90004033

The velocity of the tip of the downward channel is approximately 1/10 of 1% that of light or 1 foot per μsec so that it might be viewed as an electrode at a constant potential of several tens of millions of volts progressing toward a flat opposing electrode or a projecting rod. As this occurs the gap length is decreased slowly. Thus, in referring to laboratory data for guidance concerning the phenomenon, one must look to the current that results when an impulse voltage that will just cause breakdown is applied to a gap. In these cases it is found that the current increases at an ever-increasing rate and extrapolating from laboratory dimensions one finds an acceptable agreement in the duration of the rising portion of the current. Again, arguing from laboratory results which show a corresponding increase in velocity of the tip as the current increases, one might conclude that a corresponding increase in velocity of the return channel also occurs. The limiting value of the velocity is that of the observed head of the brightly luminous return stroke which is in the order of 10-30% of the velocity of light. This value is attained as the current becomes constant and is limited by the potential of the stroke divided by its surge impedance. The voltage drop caused by the channel formation current being drawn through the surge impedance of the stroke slows the velocity with which the final channels approach each other and consequently lengthens the rise time of the current at the earth.

5. For components of the stroke after the first, the leader from the cloud advances at a relatively high velocity (3% that of light). Since the same condition, that gave rise to the high velocity of the downward lead, exists in the channel next to the earth, it is reasonable to suppose that the return channel of components subsequent to the first likewise develops at a more rapid rate than the return channel for the first component. In consequence, as observed by Berger, the rise time of the current at the earth of components subsequent to the first is much smaller than that of the first component.

6. A method has been presented for including the effects of the predischarge currents of the insulator string into the computation of the lightning performance of transmission lines. In this connection it will be observed that a knowledge of the volt-time characteristic, alone, of a gap may be quite inadequate to apply a protective gap or to predict the performance of a string of insulators with its grading ring. The channel currents must also be known. Adjacent objects such as the tower structure will affect these currents.

References

1. The Lightning Stroke, C. F. Wagner, A. R. Hileman. *AIEE Transactions*, pt. III (*Power Apparatus and Systems*), vol. 77, June 1958, pp. 229-42.

2. Arc Drop from Spark Discharge to Arc, C. F. Wagner, C. M. Lane, C. M. Lear. *Ibid.*, pp. 242-47.

3. Mechanism of Breakdown of Laboratory Gaps, C. F. Wagner, A. R. Hileman. *Ibid.* (see pp. 604-22 of this issue).

4. Progressive Lightning—II, B. F. J. Schonland, D. J. Malan, F. Collens. *Proceedings*, Royal Society of London, London, England, series A, vol. 152, 1935, pp. 595-625.

5. Preliminary Discharge Processes in Lightning Flashes to Ground, N. D. Clarence, D. J. Malan. *Quarterly Journal*, Royal Meteorological Society, London, England, vol. 83, no. 356, Apr. 1957, pp. 161-71.

6. Field-Changes and Variations of Luminosity Due to Lightning Flashes, N. Kitagawa, M. Kobayashi. "Recent Advances in Atmospheric Electricity" (book), Pergamon Press, Inc., New York, N. Y., 1958, pp. 485-501.

7. A Comparison of Intercloud and Cloud-to-Ground Lightning Discharges, N. Kitagawa, M. Brook. *Journal of Geophysical Research*, Washington, D. C., vol. 64, 1960, pp. 1189-1201.

8. Progressive Lightning, B. F. J. Schonland, H. Collens. *Proceedings*, Royal Society of London, vol. 143, 1934, pp. 654-74.

9. Progressive Lightning III—The Fine Structure of the Return Stroke, D. J. Malan, H. Collens. *Ibid.*, vol. 162, 1937, pp. 175-203.

10. Progressive Lightning V—A Comparison of Photographic and Electrical Studies of the Discharge Process, B. F. J. Schonland, D. B. Hodges, H. Collens. *Ibid.*, vol. 166, 1938, p. 56.

11. Lightning to the Empire State Building—Part III, J. H. Hagenguth, J. G. Anderson. *AIEE Transactions*, pt. III (*Power Apparatus and Systems*), vol. 71, Aug. 1952, pp. 641-49.

12. A New Approach to the Lightning Performance of Transmissions Lines, C. F. Wagner. *Ibid.*, vol. 75, Dec. 1956, pp. 1233-56.

13. The Pilot Streamer in Lightning and the Long Spark, B. F. J. Schonland. *Proceedings*, Royal Society of London, vol. 220, 1953, pp. 25-38.

14. Surge Voltage Breakdown of Air in a Non-uniform Field, J. H. Park, H. N. Cones. *Journal of Research*, National Bureau of Standards, Washington, D. C., vol. 56, no. 4, Apr. 1956, pp. 201-24.

15. Sixty-Cycle and Impulse Sparkover of Large Gap Spacings, J. H. Hagenguth, A. F. Rohlfs, W. J. Degnan. *AIEE Transactions*, pt. III (*Power Apparatus and Systems*), vol. 71, Jan. 1952, pp. 455-60.

16. Voltage Gradients in Long Gaseous Channels, J. B. Higham, J. M. Meek. *Proceedings*, Physical Society of London, London, England, vol. 63, pt. 9, Sept. 1950.

17. Thunderstorms—The Electric Field Variations Radiated from Lightning Discharges, H. Norinder. *Extract*, report of the second meeting of the Joint Commission of Radio-Meteorology, Aug. 16-18, 1951.

18. The Nature and Variation of Atmospherics Caused by Lightning Discharges, H. Norinder, W. Stoffregen. *Arkiv för Matematik, Astronomi Och Fysik*, Stockholm, Sweden, vol. 33*A*, no. 16, 1946, pp. 1-44.

19. Determination of the Wave Front of Lightning Stroke Currents from Field Measurements, C. F. Wagner. *AIEE Transactions*, pt. III (*Power Apparatus and Systems*), vol. 79, Oct. 1960, pp. 581-89.

20. Recording Apparatuses for Use in Studies of Field Change Due to Lightning Discharge, M. Kobayashi, N. Kitagawa. *Meteorology and Geophysics*, Tokyo, Japan, vol. VIII, no. 1, 1957, pp. 102-06.

21. Lightning, D. J. Malan. *Endeavour*, London, England, vol. XVIII, no. 70, pp. 61-69.

22. Measuring Equipment and Results of Lightning Research During 1947-1954 on Mount San Salvatore, K. Berger. *Bulletin*, Schweizerischen Elektrotechnischen Vereins, Zurich, Switzerland, vol. 46, nos. 5, 9, 1955.

23. Induced Voltage on Transmission Lines, C. F. Wagner, G. D. McCann. *AIEE Transactions*, vol. 61, 1942, pp. 916-30.

24. On Impulse Discharge Voltages Across High-Voltage Insulation as Related to the Shape of the Voltage Wave, A. A. Akopian, V. P. Larionov, A. S. Torosian. *Report no. 411*, CIGRE, Paris, France, 1954.

25. Occurrence of Upward Streamers in Lightning Discharges, R. H. Golde. *Nature*, London, England, vol. 160, Sept. 20, 1947, p. 395.

26. Dielectric-Recovery Characteristics of Large Air Gaps, G. D. McCann, J. J. Clark. *AIEE Transactions*, vol. 62, Jan. 1943, pp. 45-52.

27. *Discussion* by K. Berger of Report on the Work of the International Study Committee on Lightning and Surges (No. 8), H. Baatz. *Bulletin no. 314*, CIGRE, 1960.

28. Structure and Parameters of the Leader Discharge, V. S. Komelkov. *Bulletin*, Academy of Science, Moscow, USSR, Technical Sciences Section, no. 8, 1947, pp. 955-66.

29. The Development of Electric Discharge in Long Gaps, V. S. Komelkov. *Ibid.*, no. 6, 1950.

30. The Initiation of Long Electrical Discharges, C. E. R. Bruce. *Proceedings*, Royal Society of London, vol. 183, 1944, pp. 228-42.

31. The Prestrike Theory and Other Effects in the Lightning Stroke, S. B. Griscom. *AIEE Transactions*, III (*Power Apparatus and Systems*), vol. 77, Dec. 1958, pp. 919-33.

32. The Lightning Discharge, C. E. R. Bruce, R. H. Golde. *Journal*, Institution of Electrical Engineers, London, England, vol. 88, pt. III (*Power Engineering*), no. 6, Dec. 1941, pp. 487-505.

33. The Frequency of Occurrence and the Distribution of Lightning Flashes to Transmission Lines, R. H. Golde. *AIEE Transactions*, vol. 64, 1945, pp. 902-10.

90004034

Discussion

K. Berger (Association Suisse des Electriciens, Zurich, Switzerland): It is of extreme value that the authors undertook to draw a consistent picture of the lightning phenomenon on the basis of all available research work about lightning and in comparison with new measurements on breakdown of long laboratory gaps. This job facilitates the work of the power engineer who is unable to concern himself with the electrical details but who is interested in having a clear idea of the areas of greatest disturbance in his high-voltage transmission system. It also allows the specialist to have an over-all view of the lightning process so that he may discover real or apparent contradictions in the picture. The report is based on measured or observed figures and does not lose itself in unknown microphysical processes.

In the companion paper the authors have examined present information on breakdown of long gaps and added some new investigations. The presentation results in a two-part development of leader strokes which is composed of a constantly growing corona discharge with a large diameter of 10 to 20 meters and a very thin channel of 2 to 3 mm of φ that expands in very rapid steps of 10 to 100 meters. The authors compare velocity, mean gradients, and currents of artificial sparks, with those of leaders and they succeed in showing that there is a surprising parallelism or agreement.

The transition from corona to arc discharge of the leader is of special interest. The first current pip creates the space charge of rather constant gradient of about 6 kv/cm. When this growing corona space charge has reached a certain length, a highly conducting channel begins to form in the center of this charge. This channel stop- immediately and resumes later in the next step.

A solution should be found by the discharge specialists to explain the reason for the very fast transition of high field corona discharge to the low field of the channel or finally arc discharge. When comparing different theories the authors speak of the conceneration of energy and the heating of the fine channel or of a critical current, which according to Bruce, is approximately 1 ampere. In the classical opinion of Professor M. Töpler, who made investigations on impulse discharges in the beginning of this century at the University of Dresden, especially on *Lichtenberg* figures or *Gleitentladungen* on glass plates, it was found that the transition from glow discharge (corona discharge) to arc discharge (lightning channel) took place, when a certain electric charge has passed within a short time in a single corona streamer. This critical charge amounts to approximately 1 electrostatic unit.[1–4] According to Töpler, the lightning discharge is a gliding discharge like *Lichtenberg* figures, but is in space, instead of on a surface of insulator.

Another problem which has not been solved by the discharge physicists is why the freshly formed channel supplement stops immediately after formation of a certain length. The authors say that the channel cannot expand beyond the space charge. According to Töpler this is not true. He found that *Lichtenberg* figures expand far out of space charges and he states expressly that this is the case with lightning. According to Schonland, stoppage is caused by the field-creating action of the electric charges of the proceeding channel, which corresponds to the theories of Meek and Loeb on breakdown of sphere gaps.[4]

I have verified this effect on the basis of Figs. 3 and 6 of the authors' paper. Indeed the gradient of a 50-meter space charge of the densities mentioned in the paper results in a value of about 6 kv/cm existing in the corona space, and therefore can cancel it. The velocity of electrons are then decreased creating a plasma, which is just the prolongated channel. The only necessary condition to achieve this effect is that the supply of electrons from behind the tip of the channel is less rapid than the advance of electrons before the tip.

I found the comparison of the shape of current fronts of artificial sparks with the front of lightning currents of great interest. Indeed the concordance is astonishingly good. Furthermore, the explication of steeper current fronts in subsequent strokes, as observed on Mount San Salvatore, by the higher speed of the subsequent leaders is of much interest.

The authors stated that they attempted to present a picture of the very complicated phenomenon of the lightning stroke. I think they did this in a very clear and concise manner, not as physicists, but as engineers who are accustomed to making all the necessary observations and measurements. It is to be hoped that the yet unanswered basic physical problems will also be solved by discharge physicists.

REFERENCES

1. M. Topler. *Annalen der Physik*, Leipzig, Germany, vol. 65, pp. 873–876; vol. 66, pp. 660–675, pp. 1061–1080, 1898; vol. 19, pp. 191–209; vol. 21, pp. 193–222, 1906; vol. 22, pp. 119–128; vol. 23, pp. 867–874, 1907.

2. M. Topler. *Physikalische Zeitshrift*, Leipzig, Germany, vol. 8, pp. 186–187, pp. 743–748, 1907.

3. HANDWÖRTERBUCH DER NATURWISSENSCHAFTEN (book), M. Topler. Vol. 4, Verlag Fischer, Jena, Germany, 1913.

4. THE MECHANISM SPARK DISCHARGE IN AIR AT ATMOSPHERIC PRESSURE—I, Meek, Loeb. *Journal of Applied Physics*, New York, N. Y., June, 1940.

E. Beck (Consultant, Pittsburgh, Pa.): This paper presents a new study of the lightning stroke. It is assumed that the several recent papers on this subject have been motivated by the unexpected flashovers that have occurred on high-voltage lines on high towers with single shield wire. At the end of the present paper reference is made to that transmission line problem. In the transmission line problem it has seemed to us that the probability of direct hits on the tower conductors, so-called shielding failures, have not been emphasized sufficiently. They are not really shielding failures because the shielding is probably not good under the circumstances encountered.

In considering both the Wagner-Hileman theory, with the large corona envelope, and the Griscom theory, with a bulge of charge which progresses by successive bursts, the chances of stroke contact with a conductor seem to be significant although we are not able to back this up by calculation.

In the case of a high tower and with conductors oriented beyond the shield wire, what does the stroke think when the leader, corona envelope, or bulb has approached within about the tower height of the earth and reasonably close to the line? It sees the earth and it also sees the line conductors as well as the shield wire and tower, perhaps as a bulk. Corona or streamers emanate from all three, and the bursts from the Wagner-Hileman corona envelope or the Griscom bulb may go sideways. Photographs are extant showing almost right angle bends in a stroke. The stroke has to decide whether to hit the earth, the tower, the shield wire, or the line conductor. This decision may be the result of relative positions and some fortuitous factors. On a 345-kv system one of the conductors may be 280 to 300 kv below earth potential which is an added attraction for the stroke. What we are trying to say is that as the tower height increases, the shielding is less effective and direct hits are promoted by this and by the bias caused by the line potential. It is not our intention to argue against the proposed stroke theory and maintain that all of the unexpected flashovers are the result of direct hits to the line conductors, but it is our opinion that a high percentage of them are.

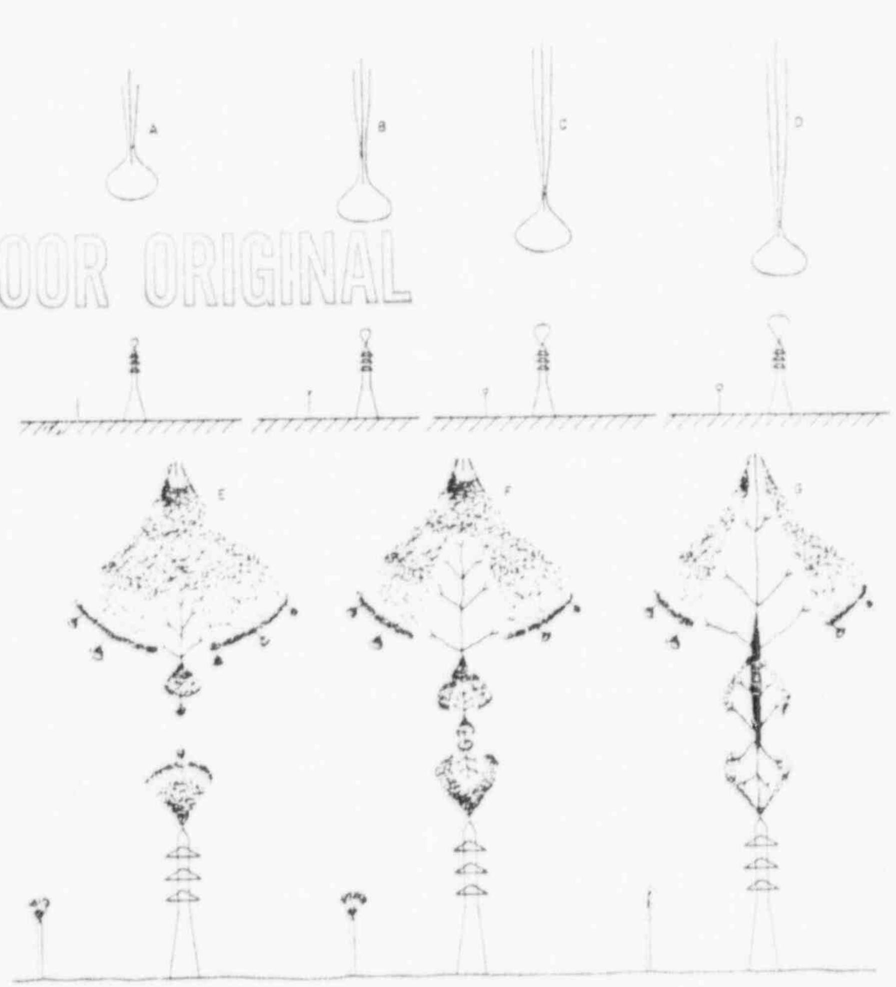

Fig. 13. Successive positions of leader head approaching a tower, A–D, and concept of prestrike discharge process of leader head, E–G

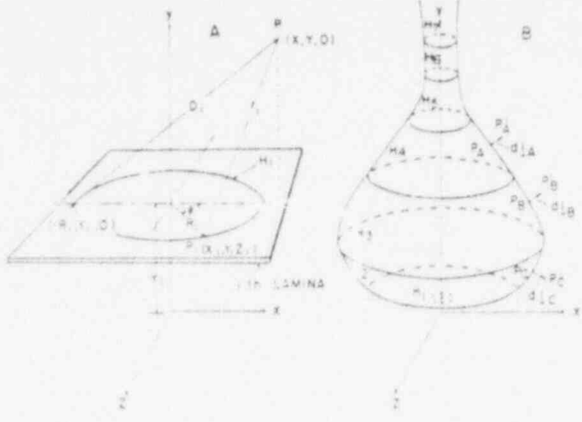

Fig. 14. (A) Geometric description of an elemental hoop of charge used in deriving equation 2, and (B) the general appearance of the space charge at the earthward extremity of a lightning leader head. Note: The x-z plane is about 300 meters above the earth's surface

S. B. Griscom (Westinghouse Electric Corporation, East Pittsburgh, Pa.): The authors have integrated many items of experimental data and theoretical arguments into a complete theory regarding the phenomena of natural lightning. In the section of their paper entitled "Comparison with Other Theories," they point out that their theory agrees with some, but disagrees with other, views expressed in these theories. The prestrike theory[1] written by this discusser was one examined by them. While agreeing with some elements of the prestrike theory, the authors differ regarding certain crucial points. This is a healthy and desirable attitude, for it is only by the expression of views and counterviews that the secrets of lightning eventually may be wrested from nature. I still firmly hold to the validity of the prestrike theory and its implications on the stroke mechanism, therefore, most of the comments brought out in this discussion refer to the differences in concepts.

To illustrate some of the areas of agreement and disagreement, Fig. 14 of reference 31 of the paper is reproduced here as Fig. 13 for comparison with the authors' Fig. 7. Agreement will be noted in that both figures show bulbous ends in the space charge volume surrounding the lower end of the leader core and the authors state elsewhere that they attribute over three times as much charge per unit length for the tip as for the leader proper. In their previous paper of the same title, the mathematical analysis and conclusions were entirely confined to uniformly distributed charges along geometrical lines.[2] Thus, they have adopted one of the components of the prestrike theory. Further points brought out originally in the prestrike paper, and used in the authors' paper, are:

1. The bulbous volumes of space charge at the lowermost end of the leader are pulling charges of opposite sign from grounded objects projecting upward.

2. There are capillarial spark traceries cavitating charges out of the leader head space charge [the discusser's stage (E) and the authors' stages (C) and (D)].

3. These spark traceries materialize into highly conducting plasma channels [discusser's stage (G) and authors' stage (E)].

4. Culmination finally takes place as shown in Fig. 20 of reference 31, not here reproduced, and stages (F) and (G) of the authors' Fig. 7.

One of the dissimilarities of viewpoints between the two figures is that the authors have assumed a volumetric distribution of space charge varying inversely with distance from the leader tip such as to produce a radial gradient of 7,000 volts per cm. The prestrike paper used 3,000 volts per cm. This is implicit from the term $-3 \times 10^6 R$ in equation 1 of reference 31, where R is in meters. Also, in describing their stepping mechanism they consider the plasma channel to grow from the leader core to the boundaries of the space charge, according to their Figs. 2, 3, and 4, whereas the prestrike theory calls for a cavitation of charge with a plasma channel finally making a junction with the leader core, whereupon a moderately heavy current of 12,000 amperes for the average case flows down that channel, forming the bright step and re-illuminating the pilot leader core upward of the junction point.

It is curious that the authors should show the same prestrike cavitation process in their Fig. 7 that the discusser showed in Fig. 13, but otherwise describe the stepping process as a plasma channel growth in the reverse direction, that is, from (A) to (C) in their Fig. 2. This they justify by quoting Schonland,[3] "Definite evidence that the streamers travel downward is, however, afforded by the broadening of the upward part of their tracks." However, Schonland was referring to the pilot leader, and not its extension, as evidenced by the fact that the foregoing quotation was taken from a section entitled "Velocity of Leader Streamers," and also from preceding and following context in the same paper. The following statement is made in the discusser's prestrike paper: "This analysis leads to the conclusion that the pilot leader trace and the bright step start simultaneously and at the same point in space, the former traveling upward, the latter downward."

It appears, therefore, that the authors and I agree that the stepping process is self-triggered at the lowermost tip of the leader and not at the cloud, and consequently we are both in disagreement with Schonland on this particular point. A further interesting quotation from Schonland is, "the tips of the streamers (the channel extensions in this instance) exhibit no distortion due to lens motion. . . ," which is another way of saying that he did not have sufficient resolving power to determine whether they traveled up or down.

It is not too difficult to explain Schonland's experimentally observed "broadening of the upward part of their (the pilot leader) tracks." When the step occurs, the newly formed channel demands charge, that is the flow of current. That this demand is violent and accompanied by a large increment of current is evidenced by the photographic brightness of the step, and the re-illumination of the pilot leader track. In engineering language, a short-duration high-magnitude pulse of current is drawn from the pilot leader core and the pulse travels up toward the cloud as a traveling wave. After a fashion, the pilot leader core acts like a transmission line with distributed L, C, and R elements. R is much higher per unit length than for a metallic conductor so there is considerable energy loss, causing re-illumination of the plasma channel in air, a spreading in time and space of the current pulse, and a reduction in current amplitude, as the pulse travels up the leader to the cloud, in its quest for charge replenishment. This fits in perfectly with Schonland's statement,[3] "Each bright step appears as a termination of a fainter streamer extending the whole way from the starting point of the discharge, such (fainter) streamers increasing in brightness and decreasing in width as their earthward ends are approached," accepting that Schonland was in error in assuming that the starting point is at the cloud end.

It is suggested that the authors' concept of the leader and its tip, or head, their Fig. 2, is more nearly what would be expected from a continuing corona discharge, except that with the latter, in still air, further charges with density varying as $1/r$ would extend beyond the authors' arbitrary boundary where the gradient was assumed to be 7,000 volts per cm. It would seem that in the violent stepping of the natural lightning leader the phenomenon would be a corona burst or impulse corona, where the charge displacement is rapid, producing loud crackling sounds when a conductor is suddenly overvolted. The charge is mostly concentrated in a shell outside of which the electric gradient averages 30,000 volts per cm or slightly less.

While the authors have now recognized that the charge on a leader cannot be regarded as constant per unit of length they still use line charges to compute potentials. This is shown by their equation 4, which applies to line charges. The procedure is to use zones of charge with the lineal density of charge increasing as the earthward tip of the leader is approached. The maximum ratio of line charge density used by them is 17.8/5 or 3.55 to 1.0. There can be no objection to the use of zonal variations in charge per unit length when the end use is to obtain the voltage contributions to locations remote from the leader. However, the line charge concept does not give the correct contour for the envelope of charge whether the charge is considered as mainly on the surface of the envelope as is my contention or varying inversely as the distance from the centerline according to the authors' concepts.

90004036

The following treatment for charges having rotational symmetry with respect to an axis is more rigorous, and permits the contour of a volume of charge to be determined to an accuracy dependent only upon the perseverance of the investigator. In such a volume of charge as illustrated in Fig. 14(B), let H_i in Fig. 14(A) be a circular hoop of charge, located in the ith lamina and parallel to the x-z plane. Let λ be the electronic charge density per unit of length of the hoop in coulombs per meter and other quantities as defined on Fig. 14(A). Then, the contribution to the potential in volts dV_i of a point P in the x-y plane due to an infinitesimal length of charge at P_i is

$$dV_i = \frac{9\times 10^9 \lambda R_i d\theta}{r_i} \qquad (20)$$

The potential contribution V_i in volts due to the entire hoop H_i is obtained as twice the integral of equation from $\theta=0$ to $\theta=\pi$. This is:

$$V_i = \frac{9\times 10^9 \times 4\lambda R_i}{D_i} \int_0^{\frac{\pi}{2}} \frac{d\phi}{\sqrt{1-k^2 \sin^2 \phi}} \qquad (21)$$

where

$$k^2 = \frac{4XR_i}{D_i^2} \text{ for } X>0$$

$$\phi = \theta/2$$

Equation 21 is a complete elliptic integral provided $0<k<1$, and may be evaluated by the use of standard published tables.

The total potential at any point P, Fig. 14(A), for any surface or volume of charge symmetrical about the y axis may be determined by summing up the contributions of as many hoops of charge as necessary to define the postulated space charge with respect to its contour and charge distribution. If the charge is mainly on the surface, then only one hoop per lamina is required. If the charge is volumetrically distributed, then several hoops per lamina may be used, with variable hoop charge densities λ_1, λ_2, etc. For a lightning leader, the effect of image charges in contributing to the potential of P must also be considered.

This method of obtaining potentials due to space charges is not nearly as time-consuming as might be anticipated. Trial-and-error procedures are necessary, as with the line charge method used by the authors, but convergence is rapid.

The authors arrive at 4.8×10^6 volts as the contribution of voltage at point 1, of their Fig. 1, due to the hemispherical bowl of charge below zone 1, whereas the more rigorous procedure given here shows a contribution of 8.0×10^6 volts. This difference does not tell the complete story, because it must be borne in mind that the proper contour for the corona envelope will not be obtained unless the computation procedures are correct. When the more rigorous treatment is used, it will be found that the form of the corona envelope shown by the authors' Fig. 1 does not adequately reveal the disproportionality between the charge in the bulbous leader head, and the channel charge immediately above.

In determining the contour of a leader head wherein the major portion of the charges is regarded as being on the bounding surface, the first approximations are directed toward obtaining an equipotential surface. This means finding, by trial and error, mutually consistent contours and hoop charge densities, λ of equation 21, such that the potentials at points P_A, P_B, P_C, etc., on Fig. 14(B) are essentially equal. Let P_A', P_B', P_C', etc., be points located by vectors normal to the surface such as $d\mathbf{1}_A$, $d\mathbf{1}_B$, $d\mathbf{1}_C$ chosen of convenient length.

Since

$$\nabla V \cdot d\mathbf{1} = dV \qquad (22)$$

then

$$dV/d\mathbf{1} = (V'-V)/d\mathbf{1} \qquad (23)$$

where V' is the scalar potential at a primed point and V is the scalar potential at the corresponding unprimed point.

If the gradient dV/dl given by equation 23 is not the desired value, then the hoop charges must be altered accordingly. It should be understood that the leader charges above H_i of Fig. 14(B) and the various image charges must be given due consideration in determinations of the potentials of all points. Line or point charges can be used when D_i is large compared with R_i, Fig. 14(A). In the idealized case, the desired surface field intensity is 30,000 volts per cm, but irregularities will cause the average gradient to be much less. Any points P_A, P_A', etc., of Fig. 14(B) must not be coincident with points on any hoop of charge, as the elliptic integral formulation is not valid for such cases. If it is desired that there be a small fall of potential from P_A to P_B to P_C, etc., then the vectors $d\mathbf{1}_A$, etc., can be inclined from the normal. For example, if a fall of 3,000 volts per cm is desired along the charge envelope and 30,000 volts per cm from P_A to P_B', etc., then $d\mathbf{1}_A$ can be directed downwardly about 6 degrees from the normal with satisfactory accuracy. It would seem that when the leader core has penetrated to C of the authors' Fig. 2, the electric field intensity at its tip would be enormous compared to what it was when located at A. In the prestrike theory a "virtual anode" cavitates charge from the leader head and this is a nonviolent process until it bores its way to the leader core. While the authors show this same cavitation process in Fig. 7 where the anode is a real one, they do not do so during the stepping process and this appears inconsistent.

They have endeavored to use the recordings of certain investigators of electric field intensity to support their version of the lightning discharge mechanism. I had examined similar data and concluded that while useful for certain purposes, this type of record was unsuited to determining the mechanism of the lightning stroke. In their section on electric field measurements next to the earth, the authors speak of electronic devices having "high amplification" and "sweep resolution" times of 10 μsec. High amplification appears to be the inverse of the requirements for field intensity measurements during thunderstorms. Some of the discusser's investigations[4] showed electric field intensities of the order of 100 kv per meter for nearby strokes. Fig. 15 is a typical record. Attention is called to the fact that most receiving-type triodes or pentodes will not accept more than 5 volts input without saturation. This is because they will draw grid current, or the plate current will fall to zero beyond these values of input voltage. In a multistage amplifier, which is necessary for high amplification, the last amplifier in the chain may saturate when the input is of the order of 1 millivolt. Assuming an antenna of 1 meter effective height, the ratio of field intensities indicated above is tremendous ($10^5/10^{-3}=10^8$). The term "low-cut filter" is unfamiliar to me, and a description would be appreciated. The wide excursion and slow return shown on Fig. 5 seems most likely to be due to the clipping and subsequent recovery of vacuum tube grids from a paralyzing pulse of voltage, with a complex interaction of interstage coupling capacitors and control grid leak resistances. I am dubious about the value of information concerning electric fields due to distant thunderstorms as recorded by vacuum tube or transistor circuitry. One need only contemplate that thunderstorms are area affairs, and flashes often occur almost simultaneously at several azimuths. Further, the initial leaders are multiple-branched, and the zigs and zags are randomly toward, away, or parallel to the recording station and variously polarized and reflected. All of this results in a conglomeration of pulses arriving at the recording station, and deductions as to time rates of change of leader current based on such records must be appraised with extreme caution. I have obtained more than 80 records of electric field changes due to thunderstorms at three measurement locations, more or less in a straight east-west line, spaced at 4-mile intervals. The threshold of gradient measurement was about 6,000 volts per meter and the upper limit about 100,000 volts per meter. It was found that during many thunderstorms, records were obtained at only one of the three recording locations. In other words, for this equipment, the maximum distance from a thundercloud which would produce a record was in the order of 4 miles. This seems to be a de-

Fig. 15. Klydonograph-type record of electric field change of about 100,000 volts per meter during thunderstorm

sirable attribute. The essential point here is that recording devices with sensitivities capable of showing field changes as low as 1 millivolt per meter may produce records, particularly at night, of atmospherics as much as 1,000 miles away, whereas devices having a range of say 6 to 100 kv per meter will most certainly only record local events.

The authors present Fig. 9 as though they regard it as the equivalent of a "snapshot" of that part of the electric discharge occurring during the interval between the application of voltage and the time of the voltage chop by a paralleling gap. Actually, such photographs are composites of the happenings while the voltage is rising, plus the events following the chop. Merrill and von Hippel[5] conclusively demonstrated that electronic charges propagated out from an electrode into a gas will rush back to the electrode when voltage is rapidly removed from it. They term the resultant *Lichtenberg*-type recordings as "backfigures." Park and Cones' Fig. 17[6] show identical results occurring three dimensionally during chops. The upward projection of charge from the negatively charged sphere is followed by the development of downwardly directed plasma channels from both the anode plate and from local concentrations of charge which had been deposited in the intervening air space as the voltage was rising. The direction of travel for each of these phenomena is unquestionable in view of the mass of evidence by many investigators that the travel direction of gaseous electric discharges is revealed by branches which diverge in the direction of travel. The foregoing is with respect to the small electrode as negative, as is the case with most lightning leaders. The process is slightly different when the small electrode is positive. It is of further interest to note that *A-A'* and *B-B'* in Fig. 18 of the same reference, show voltage chopping to result in an almost identical, but reversed displacement of charge as that which took place during the application of voltage. This near equality only exists for discharges where there are few or no plasma channels developed. The former condition approximates the charge and discharge of a lossless capacitor; the condition involving plasma channels is more like a leaky capacitor wherein a large part of the initially stored energy is dissipated in Joulean heat and is therefore not recoverable upon discharge.

The authors misunderstand one aspect of the prestrike theory in that they state "the charge volume grows, maintaining all the while a surface gradient of 30,000 volts per cm...." The paper does not make such a statement. It is only when the surface gradient drops to this value, or somewhat lower, that growth ceases or becomes very slow. Fig. 8 of the prestrike paper[1] plots charge propagation rates against gradient ratio (the number of times the surface gradient exceeds 30,000 volts per cm). During most of the growth of the leader head, the surface gradient greatly exceeds 30,000 volts per cm, the amount depending upon the interplay of equations 1 of the paper.

To clarify the leader stepping process of the prestrike, the following three sequences are regarded as constituting a step:

1. Space charge is propagated outward until the gradient at the boundary averages 30,000 volts per cm, or slightly less.

2. Because of a random protruding volume of space charge having a local surface gradient in excess of 30,000 volts per cm, plasma channels eat into the main volume, cavitating additional charge into the protruding charge volume.

3. The plasma channels finally eat their way to the tip of the leader core, whereupon, since the energy available to the plasma channels is now relatively unlimited, a heavy current flows down the channel extension, illuminating it brightly, and projecting another volume of space charge, at a lower elevation. Then a period of relative quiescence follows until another protuberance causes the sequence to repeat itself.

Wagner and Hileman's comments on this discussion, pro and con, should go a long way toward an understanding of this most fascinating and important subject.

I would like to repeat the appeal made in reference 1 for a standard terminology for use in describing the various phenomena of electric breakdown in gases. It may be that many of the disagreements between theories are due to misinterpretations of terms. In closing, I would like to acknowledge the assistance of D. L. Griscom for his helpful suggestions, and for his development of equation 21.

References

1. See reference 31 of the paper.

2. See reference 1 of the paper.

3. See reference 2 of the paper.

4. Scheme Shows High Electric Fields. S. B. Griscom. *Electrical World*, New York, N. Y., Apr. 10, 1961.

5. The Atom Physical Interpretation of Lichtenberg Figures and Their Application to the Study of Gas Discharge Phenomena. F. H. Merrill, A. von Hippel. *Journal of Applied Physics*, New York, N. Y., vol. 10, Dec. 1939.

6. See reference 14 of the paper.

C. F. Wagner and **A. R. Hileman:** We would like to thank Professor Berger for his complimentary comments, particularly with regard to his concurrence with the authors' engineering approach in their effort to correlate the stroke mechanism with laboratory measurements on long gaps. He has raised two very interesting points and it is hoped that further work on these subjects will remove much of the ignorance connected with these phases of the problem.

Mr. Beck has introduced an important point that worries the transmission engineer. While this paper is not concerned with the application of the theory of the stroke, certain characteristics of our mechanism are directly applicable to the problem of the shielding of conductors by overhead ground wires. This theory indicates, as is illustrated by equation 9, that the decisive point in the progress of the leader to earth as to whether the ground wire, the conductor, or some point on the earth, will be the ultimate stricken point, will not be reached before a distance of perhaps 100 to 300 feet from the stricken point is attained. This is a direct consequence of the theory presented in the paper. In conjunction with our associates we are working on this subject at the present time. As a result of work on the stroke mechanism we have not only modified our ideas concerning the current at the earth and the movement of the charges above the tower, but feel that a significant number of the unexplained line flashovers on the 345-kv lines must be due to shielding failures. And so we agree with Mr. Beck in emphasizing shielding failures as a possible source of trouble.

We agree wholeheartedly with Mr. Griscom in the desirability of the free expression of views and counterviews. We must admit that his further comments have not modified our own opinions regarding the physical processes involved in the lightning stroke. Mr. Griscom has listed four points and has preceded these with an additional one in which he implies that these characteristics of the discharge were original with the prestrike theory and that they were adopted from his previous paper on the subject. We have stated that it is difficult to determine the source of component aspects of this complicated phenomenon and in replying to Mr. Griscom's comments fully we should attempt to review all the literature bearing on these points. But in comparing our own publications with the prestrike paper we have the following comments.

It is not correct that in the previous paper (reference 1 of the current paper) that the analysis was "entirely confined to uniformly distributed charges along geometric lines." In Fig. 7, of the previous paper, the estimated vertical charge distribution in a leader is shown. It includes not only the end effect but also the effect of the voltage drop in the central channel feeding the charge. Laterally through the cross section of the leader it was recognized that the charge has a volume distribution. In this previous paper it was assumed that the boundary of the charge was such a surface as to possess a gradient due to the internal charge of 30,000 volts per cm. This is the same assumption used by Schonland and Griscom, and probably others. We recognized that an internal gradient must exist within such a volume and estimated this effect by simply assuming that the radius was half of the value so computed. But while it was recognized that the space charge was distributed over a volume, we never attached the same importance to its precise determination as does Griscom. While we have modified our own thinking from the assumption that there exists a field of 30,000 volts per cm around the periphery to the assumption of a volume distribution that varies inversely as the distance from the conducting core, we do not believe that either one can describe the boundary precisely. The actual physical processes are probably too complex to be satisfied by such simple assumptions.

With respect to Griscom's first point, reference need only be made to Fig. 10 of reference 1 of the paper to indicate the recognition of the production of corona space charge induced by the downward leader on various members of the tower. In addition, reference is made to Fig. 18, which shows the presence of the negative space charge in the downward directed leader and the positive space charge extend-

90004038

ing from the ground and also the development of the channel current. Since this previous paper was written we have modified our previous concept of how the channel develops from the space charge, but this has no relation to the point made by Mr Griscom. It has been known for a long time that space charge and upward channels develop from the ground as the leader approaches.

Griscom refers to "capillarial spark traceries" that cavitate out of the head space charge and the subsequent development of the channels. This language is somewhat vague and we do not fully understand the import of this phraseology. It is our understanding of Griscom's theory that the "cavitation" process begins from the bounding surface of the space charge and propagates into the space charge. This concept is entirely different from that proposed by us in that we believe that the extension of the channel develops from the tip of the conducting core of the leader and in the final step from the tower top also. With this understanding of the meaning of "cavitational" process, none of the processes described in Fig. 7 of the paper is a "cavitational" process, but are simply the development of channels emanating from relatively good conducting electrodes from the leader core for the downward development and from the mast for the upward moving channel. In reference 1 we described the process of charge collection by the return stroke as a sort of counter corona effect.

Mr. Griscom objects to our use of a line charge to compute the potential when the charge is in reality a volumetric distribution. With spherical distribution, the potential at any point is independent of the manner in which the charge is distributed within the radius of the point under consideration. This is true for infinitely long cylindrical distributions. It is also true for the potential of the midpoint of the surface of a cylinder of finite length as long as the length is several times the radius of the cylinder. The total charge can be regarded as distributed along the axis. This assumption is valid to axial lengths down to several times the radius. The range of validity of the use of this expression is dependent upon the actual charge distribution. For a charge distribution that varies inversely as the radius it is valid for much shorter cylinders than for a charge concentrated on the surface. Considering the present state of the knowledge regarding the charge distribution we feel that our use of this expression, in this manner, is justified.

We wish to congratulate Mr. Griscom on his development of the expression for the potential at a point due to a uniform distribution of charge around a loop. It is a convenient expression in a practical form.

He then computes the contribution to the potential at point *l* in Fig. 1 of the paper, and states that the more rigorous procedure gives 8.0×10^6 volts instead of 4.8×10^6 volts obtained by us. This difference is less than 10% of the total potential and while it might affect the shape of the space charge in the head of the leader it would not significantly affect the potential of the leader core. Any tendency to increase the radius would be partially compensated for by the increase in the internal drop. We do not feel that the assumptions warrant a statement of accuracy within 10% nor that the exact shape of the leader head is a significant factor. In our opinion, the significant factor is the average gradient between the leader core and earth prior to the last step.

But while the space charge distribution is under discussion, we might mention that we have been unable to determine the reason for choosing the particular value of 3,000 volts per cm for the gradient within the space charge used by Griscom in the prestrike theory. It is hidden within the mathematical expressions and no mention made in the text of how this particular number was derived.

Furthermore, we would like to comment on some aspects of Mr Griscom's computation of the contour of the space charge envelope at the instant of maximum development. As stated by him in the paragraph of his discussion preceding equation 22, the first approximations are directed toward obtaining an equipotential surface. Now let it be assumed that the leader head shown in Fig. 6 of his prestrike paper is such a surface. Further, let it be assumed, as an approximation, that the external surface gradient is normal to the surface and equal to 30,000 volts per cm and that the internal surface gradient is also normal to the surface and equal to 3,000 volts per cm. Now if a small cylinder is thought to be situated in such a way that one of the flat surfaces lies inside and the other outside of the contour surface, the surface integral of the normal component of field, around this cylinder, is equal to 4π times the surface charge density. This specifies the charge density distributed on the envelope which is constant over the entire surface. But such a constant surface charge distribution upon the contour of Fig. 6 of the prestrike paper bears no resemblance to the type of charge density depicted in Fig. 13(A) of the same paper.

In Fig. 15 of his discussion, Mr Griscom shows a dramatic *Lichtenberg* figure obtained by an instrument located on top of a building approximately within 2 miles of a lightning stroke. He states that this record represents an electric field intensity of the order of 100 kv per meter. This is not surprising as it is known that corona discharges occur from objects close to strokes and for a corona discharge to occur the field intensity must exceed 30,000 volts per cm. Furthermore, this record was obtained on the roof of all building which in itself enhances the magnitude of the observed field as contrasted with what would have occurred on level ground. Until the method of application of data of this nature is given one cannot comment upon the value of such records.

Mr. Griscom questions the suitability of electric field intensity measurements for the determination of the mechanism of the lightning stroke. Based upon the papers of Brook and Kitagawa, and supported by correspondence and personal conversations of one of the authors with these gentlemen, we have great confidence in such measurements for studying the mechanism of the stroke. The following comments concerning the accuracy of these observations are based in part on these personal contacts. The equipment being used by Brook and Kitagawa in New Mexico has a flat response out to a minimum of 5 mc. Since the film is run continuously, a compromise between film speed and resolution had to be made. In the interest of economy in the use of film, a resolving power of the records of a minimum of 10 μsec was chosen. However, this limitation does not affect the accuracy of the recorded instantaneous values of the field intensities. We have in our possession a record obtained from Dr. Brook in which the maximum deflection of the *R* change was held within the scale of the oscilloscope. This record provides a direct comparison between the magnitude of the field intensity produced by the steps and that produced by the *R* change which confirms the statement that the former are small in comparison with the latter. While the equipment used formerly by Dr. Kitagawa did not possess the high response of the present equipment, the oscillograms of the new equipment show essentially the same results without such defects as overshoot, etc.

Due to language difficulty the "low-cut filter" mentioned in Dr. Kitagawa's paper refers to a high-pass filter. The overshoot which can be seen on Dr. Kitagawa's old records is not caused by recovery from a parallelizing pulse of voltage. Depending upon the input time constant, the overshoot is more or less dependent upon the duration of the pulse. Dr. Kitagawa, in Japan, used a 300-microsecond time constant. In New Mexico Doctors Kitagawa and Brook used a 70-μsec time constant. Such overshoots are not significant. The system itself, antennas, amplifiers, etc., was checked by simulating a uniform field above the antenna with a plate several inches above the antenna and to which approximately 100-volt square waves were applied. The linearity of the equipment was excellent. An 80-decibel attenuator was located between the antenna and the preamplifier-cathode follower. This was adjustable and the setting was determined by the distance of the storm. This equipment has been in use and was developed, to its present degree of accuracy, after 5 years of questioning similar in nature to that mentioned by Mr. Griscom.

Mr. Griscom is in error in his statement that thunderstorms, at least in New Mexico where these observations were being made, are large-area affairs. They were isolated and located by observers in all directions while the recordings were being made. Their computations show that the probability of overlapping of successive strokes is very low. Perhaps the best evidence, according to Dr. Brook, of the existence of these pulses and their identification with a single lightning stroke comes from their correlation of actual stepped leader photographs with the stepped leader electric field change. Such one-to-one correlations are very convincing.

We appreciate that under certain conditions an arrested discharge cannot be regarded as a "snapshot" of the electric discharge at the instant of chopping. This is particularly true for applied voltages just below the critical value. But for applied voltages just above critical after the channels have had an opportunity to develop, the bright channels of high luminosity do represent the progress of

90004039

the discharge at that instant. This has been verified in reference 24. We concur with the discusser that to a large extent the current that flows prior to the development of channels is largely capacitative. However, the formation of the channels is essentially a thermal effect. This is discussed in the paper.

We acknowledge the error in interpreting the Griscom prestrike theory with respect to the growth of the space charge volume. We should have stated that only after the volume has developed to its maximum extent is the surface gradient equal to 30,000 volts per cm. We also appreciate the succinct statements that described the leader stepping process. But these statements seem strangely at variance with Fig. 13 of Mr. Griscom's prestrike paper. Fig. 13(F) shows the last stage of the development of a new step. At this instant a new space charge has just been completed [compare (F) with (A)] and still there is no heavy current in the core of the leader above *a*. The text accompanying this figure would lead one to believe that the charge for the new leader head in (F) had been drawn largely from the old leader head and not as stated in his discussion from the tip of the leader core. The leader core above *a* is not indicated by a heavy line as the line between *a* and *c* is indicated and if most of the charge transport consists of the transfer of the charge from the old head to the new head why in Fig. 13 of his prestrike paper should the contact of the channels propagating upward from *c* with the tip of the channel core at *a* constitute a triggering action? If Mr. Griscom is correct in showing in Fig. 13(F) that most of the current flow is from *a* to *c* then in this case there would be nothing critical about the instant at which contact is made at *a*.

Mr. Griscom's discussion is concerned almost entirely with the mechanism of the leader. It is our opinion that the difference in the current to the earth predicted by the prestrike theory and that predicted by the theory of the authors is of greater importance. According to the prestrike theory the main discharge current should be preceded by a short-duration current pip of magnitude about equal to the maximum value of the main discharge. The records of ground gradient measurements remote from the stroke fail to reveal a current of this magnitude. If it were present a pip of great magnitude should appear prior to the *E* change described in Fig. 5. No such pips have been observed.

Furthermore, the existence of such a prestrike current, a term from which the theory derives its name, should constitute a natural trigger for oscillograph measurements of current such as made by Berger. Berger has discovered no such currents but his tripping has been somewhat slow so that it is possible that he may have missed measurement of such current if it did exist. But the circuit is certainly not so slow that such a prestrike current would have constituted a natural tripping device for his oscillograph. Almost every record would have appeared as a perfect record. However, such was not the case. Berger actually lost much of the early portion of the record; a situation which we understand is being corrected. It will be interesting to observe the results of future measurements to determine the nature of the lightning fronts.

In conclusion, we wish to emphasize the need for further theoretical studies and field measurements to clarify many of the points. The engineeer, the physicist, and the meteorologist can all contribute in their particular fields to this problem. We do hope that in this paper and the companion paper we have added to the knowledge and explanation of the stroke mechanism and the breakdown process of the sparkover of gaps.

The Role of Grounding Cells and Similar Devices in the Effective Cathodic Protection of Lead-Sheathed Power Cables of Substation Exit Systems

SIDNEY E. TROUARD
MEMBER AIEE

MARTIN J. MAIER
ASSOCIATE MEMBER AIEE

The Anomaly Involved in the Cathodic Protection of Power Cable Sheaths

ORDINARILY, in the cathodic protection of such conventional underground structures as pipe lines, tank bottoms, etc., to economize in the use of direct current and thereby to minimize problems of cathodic protection coordination, the structures to be protected are well coated. A determined effort is made to keep these structures electrically free of deliberate or accidental contact with such low resistance to ground structures as electric neutral systems, shield wires, or other bare underground structures such as water mains, metallic sewers, drains, culverts or casings, steel reinforcing mats of buildings, etc. For example, consider a well-coated steel gas main whose resistance to ground is in the general order of magnitude of 100 ohms. The open circuit potential of this main to a copper sulfate electrode would generally be in the order of −0.600 volt. To achieve a change of potential of the main of 0.25 volt, and thereby bring the potential to −0.85 volt to a copper sulfate reference electrode, which is generally considered as the minimum criterion of full cathodic protection of ferrous structures, it is necessary to cause a direct current of only 2.5 milliamperes to collect electrolytically on the main. This could easily be furnished by an inexpensive buried galvanic anode of zinc tied to the main. If, however, this well-coated gas main were allowed to make accidental electric contact with a bare buried water pipe system, whose resistance to earth was in the order of 0.1 ohm, then the resistance to earth of the combined systems would be somewhat less than 0.1 ohm. The current required to achieve −0.85 volt would be in excess of 2.5 amperes, most of which would collect on the bare system, and would be entirely beyond the capability of the galvanic anode to supply. The result would be that the effectiveness of the cathodic protection on the coated steel gas main would be completely nullified and corrosion could be expected to occur on the steel gas main at flaws or holidays in the pipe coating. For this reason, every effort is made to maintain a reasonably high resistance to earth of the main to be protected. However, for one very cogent reason, cathodic protection of underground power cable sheaths is not quite so simple, even if the lead sheaths are jacketed with a highly dielectric material such as extruded polyethylene.

There is one problem indigenous to the cathodic protection of pipe-type cables and lead-sheathed power cables which is ordinarily not encountered in protecting other underground structures. For reasons of cathodic protection, the sheath

Paper 61-737, recommended by the AIEE Insulated Conductors Committee and approved by the AIEE Technical Operations Department for presentation at the AIEE Summer General Meeting, Ithaca, N. Y., June 18–23, 1961. Manuscript submitted March 16, 1961; made available for printing April 19, 1961.

SIDNEY E. TROUARD and MARTIN J. MAIER are both of the New Orleans Public Service Inc., New Orleans, La.

REF 8

Special Issue

Journal
of The Franklin Institute

DEVOTED TO SCIENCE AND THE MECHANIC ARTS

Volume 283, Number 6 *June 1967*

The Lightning Conductor

by R. H. GOLDE

The Electrical Research Association
Leatherhead, Surrey, England

Introduction

In his "Grammar of Science," Karl Pearson (1) writes "Disciplined imagination has been at the bottom of all great scientific discoveries. All great scientists have, in a certain sense, been great artists; the man with no imagination may collect facts but he cannot make great discoveries."

Disciplined imagination: this is indeed the attribute which seems best to explain the outstanding success achieved in little more than a decade's work which Benjamin Franklin, the printer and diplomatist, could devote to scientific enquiry. Yet, within that brief period, he clarified the nature of the lightning discharge and gave mankind the means for protecting our buildings against one of the most destructive forces of nature.

In the earlier issue of this Journal devoted to the question of lightning protection, Schonland (2) examined the development of Franklin's lightning rod, and Cohen (3) devoted a fascinating paper to the prejudice which followed its introduction. The interested reader is strongly advised to study these two authoritative publications of which the writer makes free use to trace the history of some aspects of the action of the lightning conductor and to examine the same questions in the light of modern knowledge.

Theoretical Considerations

The Function of a Lightning Conductor

It is a manifestation of human weakness that a prejudice once acquired tends to be retained even in the face of overwhelming factual evidence contradicting the basis on which it was founded. In the realm of science a prejudice may be termed a misconception. Such a misconception which has persisted for over two hundred years and which is still widespread is the belief that a lightning conductor has the ability, or indeed the purpose, of dissipating silently the electric charge in a thundercloud thus preventing the "protected" building being struck.

How did this conception originate and why has it persisted for over two centuries? Briefly stated, Franklin was led to solving the mystery of the lightning discharge by recognizing and stressing its similarity with the electric spark which could be produced and studied in the laboratory. In his experiments he found that a conducting body which was insulated from earth and which had been charged to a high voltage from Leyden jars could be silently discharged over distances to several inches by a pointed metallic conductor which was connected to earth. It was this observation which led him to suggest (4) that an earthed pointed lightning conductor might discharge a thundercloud and thus "prevent a stroke."

However, in the same letter written in 1755, *viz.* two years after the publication in Poor Richard's Almanac, he remarked: "I have mentioned in several of my letters, and except once, always in the *alternative, viz.* that pointed rods erected on buildings, and communicating with the moist earth, would either *prevent* a stroke, or, if not prevented, would *conduct* it, so that the building should suffer no damage."

Franklin continues to complain that, while the first alternative was only "part of the use" of a lightning conductor, the second alternative, which was proven beyond any doubt as soon as lightning conductors had been fitted to buildings in America and Europe, "seems to be totally forgotten." This concise statement clearly summarizes Franklin's views on the action of a lightning conductor.[1]

Franklin's warning and complaint were, however, soon forgotten. Following the highly personal controversy waged by the Abbé Nollet, and possibly stimulated by it, the installation of lightning conductors made rapid progress in France. This development was guided by several authoritative statements issued by the French Academy of Sciences during the period 1823 to 1867.

[1] In a further statement in 1760, while still emphasizing the preventing action of a lightning rod, he refers to the "second and principal intention of the rods . . ., *viz.* that of *conducting* the lightning" (see (4), p. 379).

Little attention ap
action of the ligh
aspects of the desi
question of the sp
had given little th

In England, th
the political clima
any suggestion w
result, the instal
Britain and scient
able time. Howev
several learned 1
received from th
porated in a hea
the time. Guided
dual function of a
the unfortunate
which was still se
(6).

Let us then c
modern knowled
field of a thunde
today. The time
has been frequ
proportional
field of 200
a vert
by a
flash
ductors wou
lightning flash.
manner must t
one function—t
and then to disc

As has been
stroke over ope
progresses from
cloud charge is
of which remain

[2] In common w
flash, is understo
tially the same d
of a downward lea

Little attention appears to have been paid in these publications to the mode of action of the lightning conductor; instead emphasis was placed on practical aspects of the design and installation of protective systems and on the important question of the space protected by a lightning rod, a question to which Franklin had given little thought and to which further reference will be made later.

In England, the introduction of the lightning rod was initially bedevilled by the political climate of the time, strengthened by King George III's loathing of any suggestion which originated from the rebellious American "colonies." As a result, the installation of lightning conductors progressed rather slowly in Britain and scientific discussions on its function did not develop for a considerable time. However, in 1878 a "Lightning Rod Conference" was convened by several learned British societies and their deliberations, including opinions received from the United States and several European countries, were incorporated in a heavily documented report (5) which received wide publicity at the time. Guided by the opinion of the many experts who were consulted, the dual function of a lightning rod was again stressed, thus contributing greatly to the unfortunate persistence in the belief of a preventive action, a possibility which was still seriously advocated by so eminent a scientist as Sir Oliver Lodge (6).

Let us then consider the function of a lightning conductor in the light of modern knowledge. That an earthed conductor when subjected to the electric field of a thundercloud discharges a current into the atmosphere is well known today. The time variation of the magnitude of this "point discharge current" has been frequently recorded (7). Its crest value is, as a first approximation, proportional to the magnitude of the electric gradient. In an average electric field of 200 volts/centimeter under a thundercloud the current flowing through a vertical conductor 50 feet high is about 5 microamperes. The charge dissipated by an average lightning flash[2] is about 30 coulombs and, if the average rate of flashing is taken to be two flashes per minute, it follows that 6,000 such conductors would be required over an area of, say, half a square mile to prevent one lightning flash. The practical possibility of lightning conductors acting in this manner must thus be discounted, and it is clear that a lightning rod has only the one function—to intercept a lightning discharge before it can strike a structure and then to discharge the lightning current harmlessly to earth.

As has been established by the work of Schonland (8), the normal lightning stroke over open ground develops in the form of a leader discharge which progresses from the cloud towards the ground. During this phase some of the cloud charge is deposited along the gradually extending leader channel, the tip of which remains at a potential with respect to earth which is only slightly lower

[2] In common with normal practice, a lightning flash or, more precisely, a multiple-stroke flash, is understood to denote the sequence of several individual lightning strokes along essentially the same discharge channel. A lightning stroke should be understood as the sequence of a downward leader followed by an upward return stroke.

than that of the cloud charge from which it developed. The magnitude of this potential can be inferred from physical reasoning, but the writer prefers to think in terms of the charge (**9**) on the leader channel which can be deduced directly from recordings of electrostatic field changes during the leader process and from oscillographic records of lightning currents. Charges from a fraction of a coulomb to about ten coulombs, with an average of about one coulomb, can thus be shown to be associated with the lower part of the channel of an individual lightning stroke.

The distribution of the charge along the leader channel must be affected by the position of branches which occur in the great majority of the leaders of the first component strokes and by the electrostatic field between the thundercloud and the leader channel and earth. As the tip of the leader moves towards the ground, the charge density near the leader tip must increase at a faster rate than the charge density in the upper parts of the channel. However, the effect of this non-uniform charge distribution can be neglected when determining the electrostatic field changes during the progression of the leader discharge.

Calculation (**10**) shows that, on the simplifying assumption of a vertical unbranched leader channel carrying 1 coulomb and of a plane ground surface, the electric field below the leader varies according to Fig. 1(a). As indicated, the field gradient is highest vertically below the leader and falls off rapidly in all directions with increasing distance. Figure 1(b) shows how the field increases as the height of the leader tip above ground decreases.

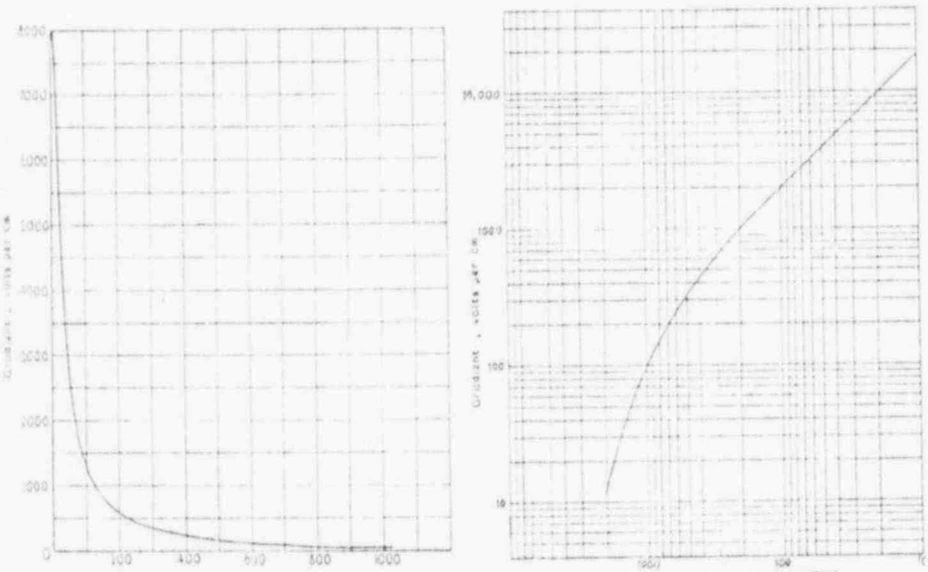

(a) (b)

Fig. 1. Electric gradient below leader channel: (a) as function of horizontal distance; (b) as function of leader tip above ground.

During the period considered so far, the current which flows between the ground and the thundercloud constitutes a displacement current to which are superimposed the point discharge currents which flow through all conducting objects on the ground, such as buildings, trees, bushes, or even grass blades. Further reference to these currents is made later. At this stage, consideration must be given to that instant when these upward flowing currents are concentrated to such an extent into one, or possibly several points, that the current through that point assumes the régime of an electric arc which, just as the leader channel itself, becomes self-propagating under the influence of the high electric field to which it owes its initiation.

The Long Spark Discharge

Franklin had already emphasized the similarity between the lightning discharge and the electric spark but, because of the high speeds of propagation involved, improved knowledge of the laboratory spark had to wait until very high voltages became available to produce long sparks and until fast rotating cameras and other devices had been developed which permitted the progress of the spark discharge to be recorded both photographically and oscillographically. The lightning current has a unidirectional wave shape which rises from zero to its crest value in a few microseconds and decays more slowly to zero within several tens or a few hundred microseconds. In the laboratory this wave shape was reproduced by impulse generators and the results of applying such voltages to long spark gaps were deemed by the writer (11) and others to represent, on a reduced scale, the development of the lightning discharge at the instant when the tip of the leader had approached the ground, or a lightning conductor, to within "striking distance," a term which will be defined more precisely later.

This method of approach is not quite correct, as can be shown by considering the rate of increase with time of the voltage to ground of the tip of the leader stroke. This rate can be expressed (11) by

$$de/dt = 1.8 \times 10^7 \, q \, \frac{\epsilon^{-\beta vt}}{vt^2} \text{ volts per cm.} \times \text{sec.} \qquad (1)$$

where q = the charge on the leader channel (1 coulomb for a stroke of average intensity)

β = a constant (10^{-3})

v = velocity of propagation of leader stroke (1.5×10^{7} cm./sec.)

vt = height of tip of leader above ground at time t.

With the above average values and for vt = 100 m. the rate of voltage rise is seen to be 24 kV/microsecond. This, then, is the order of magnitude at which the voltage applied to a long spark gap should increase if the mechanism of the last stages of a lightning stroke is to be studied. Assuming such a laboratory investigation to be carried out at, say, 2 MV, the test voltage should reach its crest value in about 85 microseconds, and not in about 1 microsecond as in the standard impulse with which most laboratory tests on long sparks have been performed.

A unidirectional voltage which rises to its crest in several tens or hundreds of microseconds is called a long-fronted impulse voltage in contrast to the fast impulse voltage which rises to its crest in about 1 microsecond and the wave shape of which has been standardized internationally to represent the voltage which is impressed on an overhead line conductor as the result of a direct lightning stroke to that conductor. Long-fronted impulse voltages have assumed increased importance in recent years since they can be used conveniently to study problems arising in the insulation co-ordination of e.h.v. lines due to switching operations in electrical transmission systems.

A substantial amount of information has become available recently on the breakdown characteristics of long air gaps (**12**) under long-fronted impulse voltages. These have been shown to be much more complex than the characteristics of the same gaps under short-fronted impulse voltages. Again, while the physical mechanism of breakdown of long gaps under short-fronted impulses is now reasonably well understood (**13**), corresponding knowledge relating to long-fronted impulses is still rather rudimentary. However, from some work reported by Stekolnikov (**14**) it can be concluded that, so far as the initiation of this breakdown is concerned (and this is the aspect in which we are here interested), there is no basic difference between its mechanism under short and long-fronted impulse voltages.

Breakdown of a long air gap under a steep-fronted impulse voltage is initiated almost invariably at the high-voltage electrode. In the case of a high-voltage rod electrode, breakdown starts by formation of corona which then leads to the development of a leader channel. The great majority of natural lightning discharges carry negative charges from the cloud to ground. They may therefore be simulated in the laboratory by negative high-voltage rod electrodes, the ground being represented by an earthed plane electrode. In such a negative rod-plane arrangement the negative initial corona and the subsequent leader spark cover almost the whole gap distance before an upward corona discharge and a counter spark are initiated from the earthed plane. As these two leader sparks meet, a return spark equivalent to the return stroke in the lightning discharge develops and the applied voltage collapses.

From Stekolnikov's work it appears that, if the same gap arrangement is subjected to slowly rising impulse voltages, the foregoing mechanism may be complicated by the development, after the initial corona stage and the development of a short leader spark from the high-voltage rod electrode, of a mid-gap breakdown process which progresses simultaneously and in opposite directions towards the high-voltage leader channel and the earthed plane. The occurrence of an upward spark discharge from the plane appears to be similar to that under the influence of a steep-fronted impulse.

If, now, a rod electrode is mounted vertically on the earthed plane, converting the rod–plane into a rod–rod configuration, the initial occurrence of

FIG. 2. Lightning stroke to chimney pot showing meeting point between downward leader and upward streamer.

corona and of a leader discharge at the negative high-voltage electrode subjected to a steep-fronted impulse voltage is unchanged. However, after a brief time interval or even simultaneously with the onset of the high-voltage corona, corona also develops from the tip of the earthed rod electrode, and the two pre-discharges from the high-voltage electrode and from the earthed point meet somewhere in the mid-region of the gap.

No similar information is available on the mechanism of breakdown of a rod-rod gap under slowly rising impulse voltages. Until such information becomes available, it must be assumed that the basic mechanism is unchanged as in the case of the rod-plane electrode system.

The Final Stage of a Lightning Stroke to Ground

Having thus formed a picture of the breakdown of a long air gap, it seems legitimate to assume that the final stage in the development of a lightning stroke to earth or to an earthed object is determined by the same phenomena, thus reverting once again to Franklin's argument about the similarity between the lightning discharge and the electric spark. Photographic evidence to support this argument is difficult to obtain[3] mainly because of the remote possibility of securing a photograph with a rotating camera of a close lightning discharge and because of the high speeds of propagation over short lengths of such a discharge. The writer is all the more happy to reproduce the still photograph (Fig. 2) of a close discharge kindly placed at his disposal by Mr. Vesanterä.

The photograph shows the lower end of a lightning discharge to the chimney pot of a building in Helsinki taken at a distance of about 215 feet. The discharge must clearly have been of low severity as indicated by the small amount of halation on the original photographic negative and by the absence of damage to the chimney pot apart from an accumulation of soot. Over most of its length the photograph shows the luminous core of the lightning channel, but near the centre this channel is clearly divided into four distinct parts. From an analogy of similar photographs of long spark discharges it is suggested that it is this point at which the downward moving leader stroke is met by the short upward leader discharge from the chimney pot.

A few other photographs have been published showing the occurrence of upward streamers from objects about to be struck[4] so that it may be accepted that a lightning leader stroke progresses in the form of a self-propagating discharge from a charge center in the cloud towards ground until the gradient at a point on the ground surface has increased sufficiently to cause an upward streamer of the type shown in Fig. 2, to be initiated. The question then arises as to the critical value of this gradient.

Reasons have been given to show that the gradient at the ground surface below a downcoming lightning leader stroke increases at a rate which is similar to that occurring in an impulse voltage which rises to its crest within a period of a few tens to a hundred microseconds. The breakdown voltages of long air gaps under such long-fronted impulse voltages have been determined experimentally during the last few years. A critical examination (12) of the results obtained by different investigators shows that, while average breakdown voltages and their statistical deviation can be established for positive impulse voltages, the available data for negative impulses are too meager and too inconsistent to permit any generalization.

The reason for this polarity effect is the much higher negative, as compared with the positive, breakdown voltage as a result of which an impulse generator producing a long-fronted voltage of 2 MV is capable of causing a breakdown of up to 6 meters (20 feet) under positive impulses, but only up to 3 meters (10

[3] Prof. Berger's companion paper (page 478) brilliantly shows how these difficulties have been overcome.

[4] See, for instance, Fig. 6, page 564, in the companion paper by Wagner.

feet) under negative impulses. This observation leads to the interesting conclusion that, in the rare case of a positive lightning discharge, the distance over which a lightning conductor would exert an attractive effect on a downcoming leader stroke would be greater than for a negative stroke.

TABLE I. *50 Per Cent Switching-Impulse Breakdown Gradients of Long Spark Gaps* kV/cm,

Configuration	Polarity	Distance in meters					Ref.
		1	2	3	4	5	
Rod-rod	−	6.7	6.5	5.9			(15)
Rod-rod	−	8.0	7.2				(16)
Rod-rod	−		7.0		6.0		(18)
Rod-plane	−	10.1	7.4	6.4			(15)
Rod-plane	−		9.0				(16)
Rod-plane	−	11.3	9.0				(17)
Rod-plane	−		8.4	7.3			(18)
Rod-rod	+	6.9	5.2	4.5	4.0	3.6	(12)
Rod-plane	+	4.5	3.7	3.3	3.0	2.8	(12)

In the upper part of Table I the 50 per cent breakdown voltages are collected together which have been obtained by different authors with negative impulse voltages rising to their crest within 100 to 200 microseconds. Dividing these voltages by the breakdown distances produces the values listed and these can be regarded as the critical gradients capable of producing gap breakdown in 50 per cent of all voltage applications. The information contained in this table can be summarized as follows for breakdown distances from 1 to 4 meters.

For rod-rod gaps the critical breakdown gradient decreases only little with increasing distance and for gaps of the order of 4 meters a value of about 6 kV/cm. can be accepted as representative. For rod-plane gaps, the critical breakdown gradient decreases with increasing distance and, for 3 meters, reaches a figure of about 7 kV/cm.

Positive lightning flashes constitute only about 20 per cent of all earth discharges in temperate regions and even less in tropical regions. The corresponding information on the critical breakdown gradient of long gaps under positive long-fronted impulse voltages is added to Table I. The values quoted constitute averages of a fairly large body of experimental data. It appears that, both for rod-rod and rod-plane gaps, the critical breakdown gradient continues to decrease with increasing distances within the range investigated and that the difference between these two configurations is greater than for negative polarity.

When applying these experimental data to the natural lightning discharge, several factors ought to be considered. First and foremost, any quantitative extrapolation from the scale of laboratory tests on gaps measuring a few meters to the scale of the lightning discharge must always be subject to certain mental reservations. Fortunately, an uncertainty with respect to the critical breakdown gradient within the fairly narrow limits involved can be shown (**10**) not seriously to affect the conclusions reached.

The second major consideration involves the geometrical representation of a lightning discharge to ground by a rod-plane configuration and of a lightning discharge to a lightning rod by a rod-rod arrangement. Considering first the lightning leader channel, its tip is surrounded by a corona envelope and the same occurs at a high-voltage rod electrode so that, electrostatically speaking, the two arrangements can be regarded as similar.

There is little objection to representing a single vertical lightning rod by an earthed rod electrode. On the other hand, open ground cannot, strictly speaking, be represented by a plane electrode. The earth's surface is normally covered by small growth, grass blades or stones and every such projection is capable of producing a point discharge, as beautifully demonstrated by Schonland's measurement of the point discharge current produced by a small tree. Similarly laboratory investigations of long rod-plane gaps have shown that, particularly for a positive plane which corresponds to the normal condition of a negative lightning discharge, roughness of the earth's plane or slight projections materially affect the breakdown mechanism so as to make it more similar to that of the rod-rod arrangement.

A third point worth noting is that the present discussion is confined to the case of a vertical unbranched leader channel. Most lightning discharges deviate by a greater or lesser degree from the vertical and both this fact and the occurrence of long branches from the main leader channel must cause a distortion of the electric field about a lightning conductor. The same applies if the lightning conductor is not placed on a uniform plane but on a building or on sloping ground. These factors must clearly affect the results to be derived from laboratory investigations of the type considered here.

Air pressure and rain fortunately exert only a very slight effect on the breakdown voltages of long air gaps.

From the foregoing considerations it can be concluded that, as a first approximation, it is legitimate to visualize the normal natural lightning leader stroke as a self-propagating discharge which progresses towards ground guided by the local field distribution in front of the leader tip but unaffected by any features on the ground until the critical breakdown strength of the remaining distance from ground is reached. When this stage has been reached, an upward streamer discharge is initiated and the leader stroke is diverted towards it.

The only condition in which the "normal" lightning discharge discussed

here is modified ari
State Building or of
tory on Mount San
of a downward lead
that the leader st
ductor leading to
In the present conte

The Striking Dist

In order to deter
upward discharge is
ture, it appears reas
that the critical bre
the ground configur
negative lightning c
With these values th
upward streamer is
The results of this e

As indicated by t

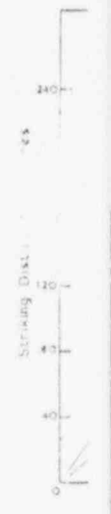

FIG. 3. Str

poin on the ground
nology which was sig
is a function of the

* At the present stat
which a "tall" structure
the reader is referred to

here is modified arises in the case of a structure of the height of the Empire State Building or of such tall towers as used in Berger's (19) lightning observatory on Mount San Salvatore. For structures of such height,[5] the normal process of a downward leader stroke followed by an upward return stroke is reversed in that the leader stroke is frequently initiated at the tip of the tall lightning conductor leading to an upward leader stroke followed by a pseudo-return stroke. In the present context this type of discharge will not be considered any further.

The Striking Distance of a Lightning Stroke

In order to determine the height above ground of the leader tip at which an upward discharge is liable to occur from the ground or from an earthed structure, it appears reasonable to suggest, on the basis of the data given in Table I, that the critical breakdown gradient is, as a first approximation, independent of the ground configuration and that its value is of the order of 5 kV/cm. for the negative lightning discharge and 3 kV/cm. for the positive lightning stroke. With these values the height of the tip of the leader can be calculated when an upward streamer is liable to be initiated from ground or from an earthed object. The results of this calculation are shown in Fig. 3.

As indicated by the curves in Fig. 3, the height of the leader tip at which the

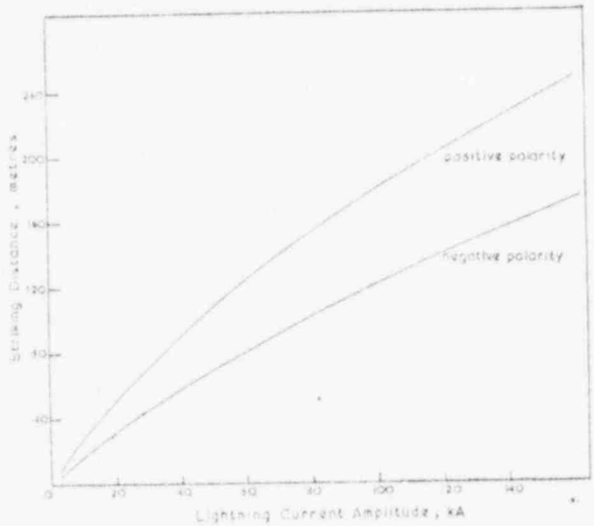

Fig. 3. Striking distances of negative and positive lightning strokes.

point on the ground to be struck is determined or, to use the descriptive terminology which was significantly already used by Franklin, the "striking distance" is a function of the intensity of the ensuing lightning stroke. This conclusion is

[5] At the present state of knowledge no indication can be given of the conditions under which a "tall" structure is capable of causing upward leader strokes to develop. However, the reader is referred to Berger's companion paper in which this question is discussed.

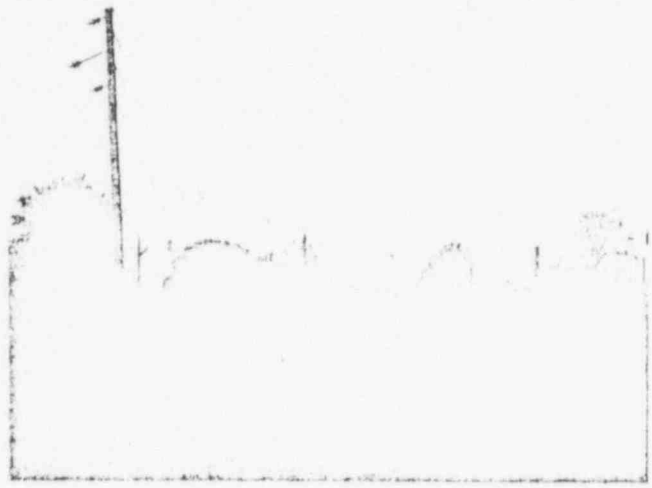

FIG. 4. Lightning stroke to chimney.

pretty obvious if we consider that the electric gradient under a leader channel is a function of the charge on the leader channel (as shown by Eq. 1) and that this in turn is proportional to the amplitude of the current in the return stroke to which it gives rise. This striking distance is greater for the less frequent positive stroke than for the normal negative lightning discharge. While this distance may amount to 200 m or slightly more for the rare, very intense lightning flashes, it amounts to no more than about 30 meters for an average negative lightning stroke of 20 kA.

Reverting to the photograph shown in Fig. 2, the height above the chimney struck of the subdivision in the lightning channel is about 9 m and if it is deduced from evidence provided by the long laboratory spark discharge that this meeting point of the downward and upward discharges occurs at a height of about 60 per cent of the total striking distance, this latter may be estimated to have been about 15 m. From Fig. 3 this would indicate a lightning current of about 9 kA, *viz.* a weak discharge, a conclusion which had already been reached from other evidence.

Figure 4 shows a lightning strike to an 85-foot high factory chimney or, to be more precise, as can be clearly seen with the aid of a magnifying glass from the

original photograph
track of the lightni
at which the down
charge from the
"striking dist
above and belo
was not much more
of moderate intensit
other photographs
strokes are availabl
indicated in Fig. 3.

Several research
calculating the stri
the scope of this pa
investigations.

The Attractive Ra
and the Space Pro

The striking dist
tip of the leader ch
struck is determine
by the geometrical
a stroke to open
also indicate
stroke an
the strok
"the attr
conductor attrac
constant but which

Once again it is
Franklin. In a lette
"The distance at w
suddenly, striking th
so highly charged, is
sions and form of th
This distance, what
striking distance, as
will be made."

The problem of
further question of th
Here a clear distinct
vertical lightning ro
by such a conductor,

original photographic negative, to its lightning conductor. The sharp bend in the track of the lightning channel can, in this case, be taken to constitute the point at which the downcoming leader stroke was first attracted by the upward discharge from the lightning conductor so that this distance would signify the "striking distance." Having regard to the similar light intensities of the track above and below the knee point, it can be deduced that the striking distance was not much more than about 30 meters, thus once again indicating a stroke of moderate intensity, as also suggested by the small amount of halation. Many other photographs showing similar, sudden changes in the tracks of lightning strokes are available supporting the order of magnitude of the striking distances indicated in Fig. 3.

Several research workers (**20**–**22**) have followed the author's approach in calculating the striking distances of lightning strokes. However, it is beyond the scope of this paper to discuss the varying assumptions or results of these investigations.

The Attractive Range of a Lightning Conductor and the Space Protected by it

The striking distances plotted in Fig. 3 were calculated as the height of the tip of the leader channel above ground at the instant when the point to be struck is determined. If, as argued earlier, this striking distance is unaffected by the geometrical configuration of the earth electrode, *viz.* if it is the same for a stroke to open ground as for a stroke to a vertical lightning conductor, then it also indicates the maximum horizontal distance between the tip of a leader stroke and a lightning conductor over which the latter is capable of attracting the stroke to itself. This distance may be called "the attractive distance" or "the attractive range." It thus follows from Fig. 3 that a single vertical lightning conductor attracts to itself lightning strokes over a distance which is not a constant but which increases with increasing intensity of the lightning discharge.

Once again it is interesting to note that this idea had already occurred to Franklin. In a letter written in September 1767 from Paris he states (**23**): "The distance at which a body charged with this fluid will discharge itself suddenly, striking through the air into another body that is not charged, or not so highly charged, is different according to the quantity of the fluid, the dimensions and form of the bodies themselves, and the state of the air between them. This distance, whatever it happens to be between any two bodies, is called their *striking distance*, as till they come within that distance of each other, no strike will be made."

The problem of the attractive range of a lightning conductor raises the further question of the space over which such a conductor will protect a building. Here a clear distinction needs to be made between the attractive range of a vertical lightning rod which has been discussed so far and the space protected by such a conductor, a distinction which is frequently overlooked. The *attractive*

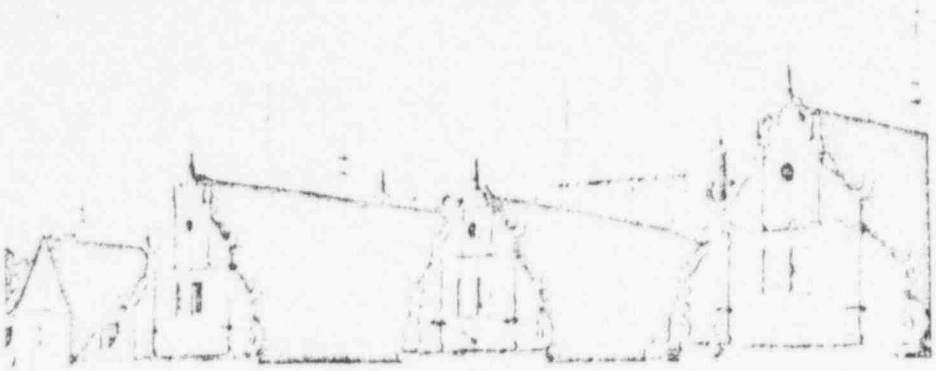

FIG. 5. Tall lightning rods on German castle.

range of a lightning rod describes the distance over which a single vertical lightning rod of given height standing on an undisturbed plane can be expected to attract a lightning leader stroke to itself. The *space protected* by such a conductor, on the other hand, should define the space over which a lightning conductor erected on a building of given dimensions can be relied upon to protect the building from being struck.

In a thunderstorm the surface of such a building is wet and, just like the surface of a tree, is capable of carrying currents which may be sufficient to support point discharges from corners of the roof structure. To what extent this effect can reduce the range over which a lightning conductor is capable of diverting a lightning leader stroke to itself is unknown. Fortunately, this question is of minor practical importance since modern lightning protection insists on fitting lightning conductors along ridges or parapets of roofs so that all prominent corners are effectively protected.

In existing publications, the essential difference between the attractive range and the space protected seems to have been widely overlooked and it is on this understanding that historical views about the space protected by a lightning conductor may now be examined. Beyond the statement just quoted, Franklin[6] does not seem to have made any pronouncement on this topic. The statement itself appears to have been completely overlooked by later investigators, and the first reference to the protective range of a lightning conductor

[6] Indirect evidence on Franklin's view regarding the space protected by a vertical lightning rod may be deduced from the famous case of the powder magazine at Purfleet (**24**), the lightning protection of which was designed by a committee of four scientists, one of whom was Franklin. A corner of this building was damaged by lightning. The ratio of the horizontal distance between this point and the lightning rod and the height of the tip of the rod above the point struck was 1.63 to 1, so that this "protective ratio" was apparently regarded as adequate by Franklin. It may be noted that once again the slight damage indicates a comparatively weak lightning discharge.

seems to occur in the
of Sciences (**25**) whic

In that edition,
lightning conductor
space about it, the ra
son (**26**), "the acqui
its results the erecti
buildings so as to inc
As an interested obs
exemplified by Fig. 5,
was undoubtedly ju
French Academy of
vital importance of f
protected by a lightni

In subsequent ed
attractive distance t
from 2 to 1.75 and i
Preece (**27**) it was f
the 19th century on

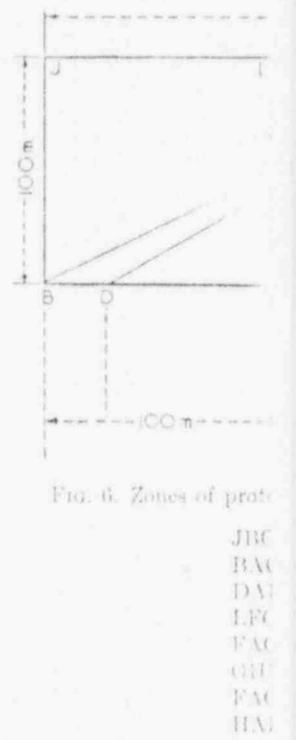

FIG. 6. Zones of prot

JBC
BAC
DAI
LFC
FAC
GH
FAC
HAI

seems to occur in the "Instructions sur les Paratonnerres" of the French Academy of Sciences (**25**) which were first issued in 1823.

In that edition, which was presented by Gay-Lussac, it was stated "A lightning conductor protects effectively against a lightning stroke a circular space about it, the radius of which is twice its height." As stated by R. Anderson (**26**), "the acquiescence in this supposed absolute formula had for one of its results the erection of monstrously huge rods made to tower high above buildings so as to increase the field of protection to the largest possible extent." As an interested observer can still notice on the continent of Europe and as exemplified by Fig. 5, Anderson's complaint about monstrously high conductors was undoubtedly justified. Yet, be this as it may, great credit accrues to the French Academy of Sciences for having first drawn official attention to the vital importance of formulating acceptable rules on the space which is effectively protected by a lightning rod.

In subsequent editions of the *French Instructions* the original ratio of the attractive distance to the height of a vertical lightning conductor was reduced from 2 to 1.75 and in the first British pronouncement on this subject made by Preece (**27**) it was further reduced to unity. The various suggestions made in the 19th century on this important ratio are illustrated in Fig. 6.

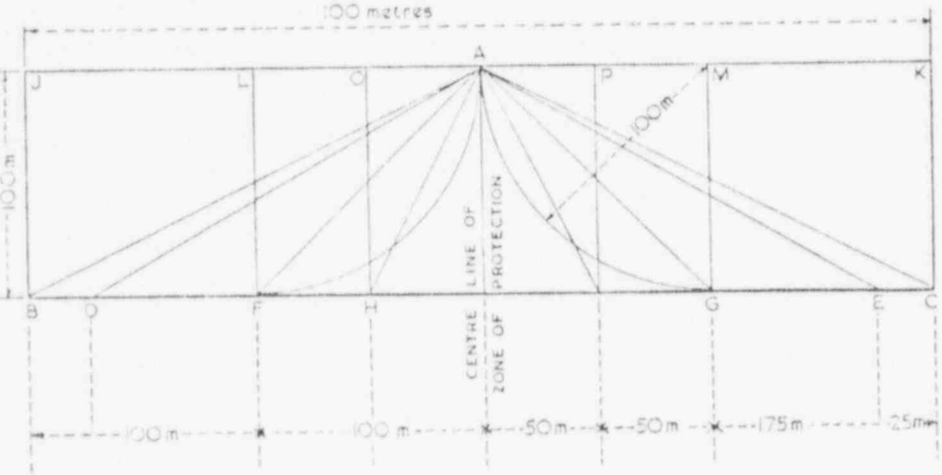

FIG. 6. Zones of protection by vertical lightning rod (after O. J. Lodge) (**6**).

JBCK	cylinder	Gay Lussac 1823
BAC	cone	De Fonveille 1874
DAE	cone	Paris Commission 1875
LFGM	cylinder	Chapman 1875
FAG	cone	Adams 1881
OHIP	cylinder	hypothesis
FAG	special cone	Preece 1881
HAI	cone	Melsens

Credit is frequently given to Walter (28) for making the first attempt at determining the protective range of a lightning conductor by collecting factual information on points struck by lightning in the immediate vicinity of church steeples equipped with lightning conductors. This overlooks the fact that about fifty years earlier a scientist such as Oliver Lodge (6) or a practicing engineer like R. Anderson (26) had already drawn attention to many instances where lightning had struck a building within the "protected" zone suggested by various authorities and had reached the conclusion that, to speak of a fixed space of protection, was "inadmissible."

However, once again all this earlier work was forgotten when the introduction of the high-voltage impulse generator made it possible to apply to a variety of test objects very high voltages which were believed to simulate the wave shape of that produced by a lightning stroke. This development initiated the period of laboratory model tests to determine experimentally the attractive range of a lightning conductor, thus reverting unconsciously to the unhappy Benjamin Wilson (29) who opposed the Franklin lightning rod and who tried to prove his point by tests carried out with an enormous battery of Leyden jars in the Pantheon, a large building in London's Oxford Street.

F. W. Peek (30), who was the first to undertake systematic model tests, found that the attractive range depended on the height above a ground plane of the high-voltage electrode chosen to represent the height of the thundercloud. Taking this height as a thousand feet, he found a "protective ratio" which varied between 2 and 4. Peek's reputation was such that this figure was incorporated in the 1932 edition of a U.S. Code (31) in which it was retained until 1945 when it was replaced by a ratio of unity for important cases and of up to 2 for less important cases.

Once it had been established that a lightning leader stroke is "unaware" of any feature on the ground until it has come within striking distance, model tests were carried out with the high-voltage electrode simulating the tip of the leader channel at a height above the ground plane which was gradually reduced to the height of the grounded rod electrode simulating the lightning conductor. Many such test series have since been performed (32) and the results have been applied to determining the attractive effect exerted by a lightning conductor.

Even with this latest refinement, there exist in the author's view several objections against the acceptance of results from model tests to a quantitative determination of the attractive range of a lightning conductor although they can be of considerable value for comparative investigations (33), such as the shielding effect of a ground wire with respect to the phase conductors of a transmission system. Apart from the rate of voltage rise which should in the future be used for such tests and which has been discussed earlier, the following major objections may be advanced:

1) If it is accept
function of the elect
tractive effect of a l
along the leader ch
difficult to see how

2) The breakdo
greatly affected by t
clearly established b
this also applies to
writer is at present u
a definite effective in

3) Having regar
impulse tests on long
tests have frequently
fication can be found
by a positive rod ele

To summarize, th
the author to the co
right in claiming th
lightning conductor
range of a lightnin
pending primarily
Fig. 3 are acce
attracted
even th
part of a
initiating an upw

Practical Aspects

A lightning cond
ductors, the down c
be briefly examined.

The Roof Cond

Franklin's public
was made in Poor Ri
(34), Franklin sugge
eight feet above the
states: "If the house
and a middling wire

In assessing Fran
must be remembered

1) If it is accepted that the striking distance of a lightning discharge is a function of the electric gradient between its tip and the ground, then the attractive effect of a lightning conductor must vary with the charge deposited along the leader channel and thus with the intensity of the discharge. It is difficult to see how this feature can be simulated in a laboratory test.

2) The breakdown mechanism of a long spark gap in the laboratory is greatly affected by the series resistance in the discharge circuit. This has been clearly established by tests with fast-rising impulse voltages. To what extent this also applies to the more slowly rising impulse voltages suggested by the writer is at present unknown. On the other hand, it is debatable to what extent a definite effective impedance can be attributed to a lightning leader channel.

3) Having regard to the very high negative impulse voltages required for impulse tests on long spark gaps and the great dispersion of the results, model tests have frequently been made with positive impulse voltages and no justification can be found for trying to represent the normal negative leader stroke by a positive rod electrode.

To summarize, then, the physical considerations outlined in this paper lead the author to the conclusion that Oliver Lodge and Richard Anderson were right in claiming that acceptance of a fixed value for the area protected by a lightning conductor is unjustified. Expressed more positively, the attractive range of a lightning conductor should be regarded as a statistical quantity depending primarily on the severity of the lightning stroke. If the curves given in Fig. 3 are accepted as a guide, a lightning stroke of average intensity would be attracted over a distance of about twice the height of the conductor. However, even this distance might be reduced by an unknown amount if any unprotected part of a building was of such a shape and in such a position as to be capable of initiating an upward streamer discharge.

Practical Aspects of the Lightning Protection of Structures

A lightning conductor system comprises three main parts, the roof conductors, the down conductors and the earthing arrangement; these will now be briefly examined.

The Roof Conductor System

Franklin's public introduction of the lightning conductor, it will be recalled, was made in Poor Richard's Almanac for 1753. In this briefest of specifications (34), Franklin suggests to provide "a small iron rod" which "may be six or eight feet above the highest point of the building." A few sentences later he states: "If the house or barn be long, there may be a rod or point at each end and a middling wire along the ridge from one to the other."

In assessing Franklin's ideas about the lightning protection of structures, it must be remembered that he was largely concerned with small dwellings and agricultural buildings, many of them made of wood, which were, and still are, frequently destroyed by fires started by lightning. However, even within this restricted range, he already recommended the two most important parts of the roof conductor system, *viz.* one or more vertical finials and a horizontal roof conductor.

Although Franklin took a keen interest in all cases of lightning strokes to buildings which had been protected by his lightning rods, and although he utilized the experience so gained in discussing such problems as the necessary cross section of a lightning conductor or the risk of side flashing, the experience assembled during his lifetime was severely limited. It is, therefore, all the more noteworthy that already in the first instruction for the protection of a "long" building he suggested that lightning conductors be installed "at each end" of the building.

As the knowledge of the value of the lightning conductor spread across the world but before modern specifications for the lightning protection of structures had been drawn up, the construction of protective systems deviated from Franklin's original suggestions in several respects. Let us first consider the "lightning rod" or finial. Franklin had suggested to give this the form of a "brass wire the size of a common knitting needle sharpened to a fine point."

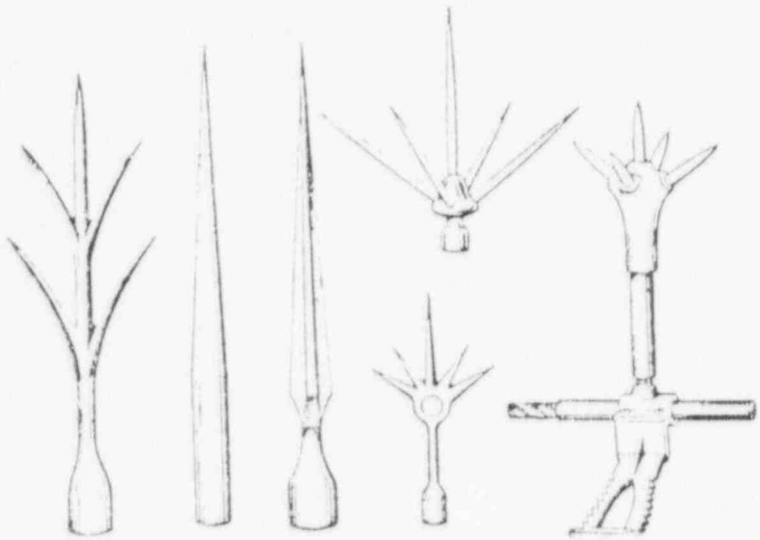

Fig. 7. Air terminals (after U. S. Code) (**31**).

He was clearly led to this suggestion by his observation that a pointed earthed conductor is more effective in discharging a charged body than a rounded or blunt conductor. We now know that, so far as lightning is concerned, this argument is invalid, but it led to the widespread adoption of many picturesque but quite useless designs in which a sharply pointed rod was surrounded by a multiplicity of spikes giving it occasionally the outline of an angry porcupine. Some blame for the preservation of these features must be placed on the report

produced by the L
earlier, a lightning
occurrence of a ligh
this construction
shown by the
ternatively, a
conductors for bui
latest edition of ano

As suggested ear
attract to itself eve
the companion pape

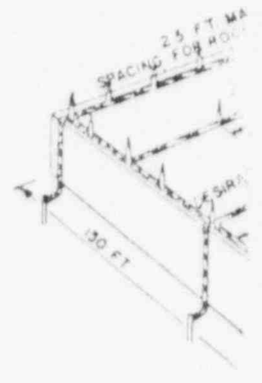

Fig. 8. Lightning prot

90004058

produced by the London Lightning Rod Conference in which, as mentioned earlier, a lightning rod was still credited with the function of preventing the occurrence of a lightning discharge. On the other hand, nowhere it seems has this construction been preserved longer than in the United States (**31**), as shown by the shapes of finials recommended as late as 1952 (see Fig. 7). Alternatively, a multiplicity of short finials superimposed on horizontal roof conductors for buildings of large ground surface is still recommended in the latest edition of another American Code (**35**) (see Fig. 8).

As suggested earlier, a lightning rod cannot be relied upon with certainty to attract to itself every lightning stroke of low severity. (Figure 40 [p. 505] of the companion paper by Berger shows a direct lightning stroke into one of the

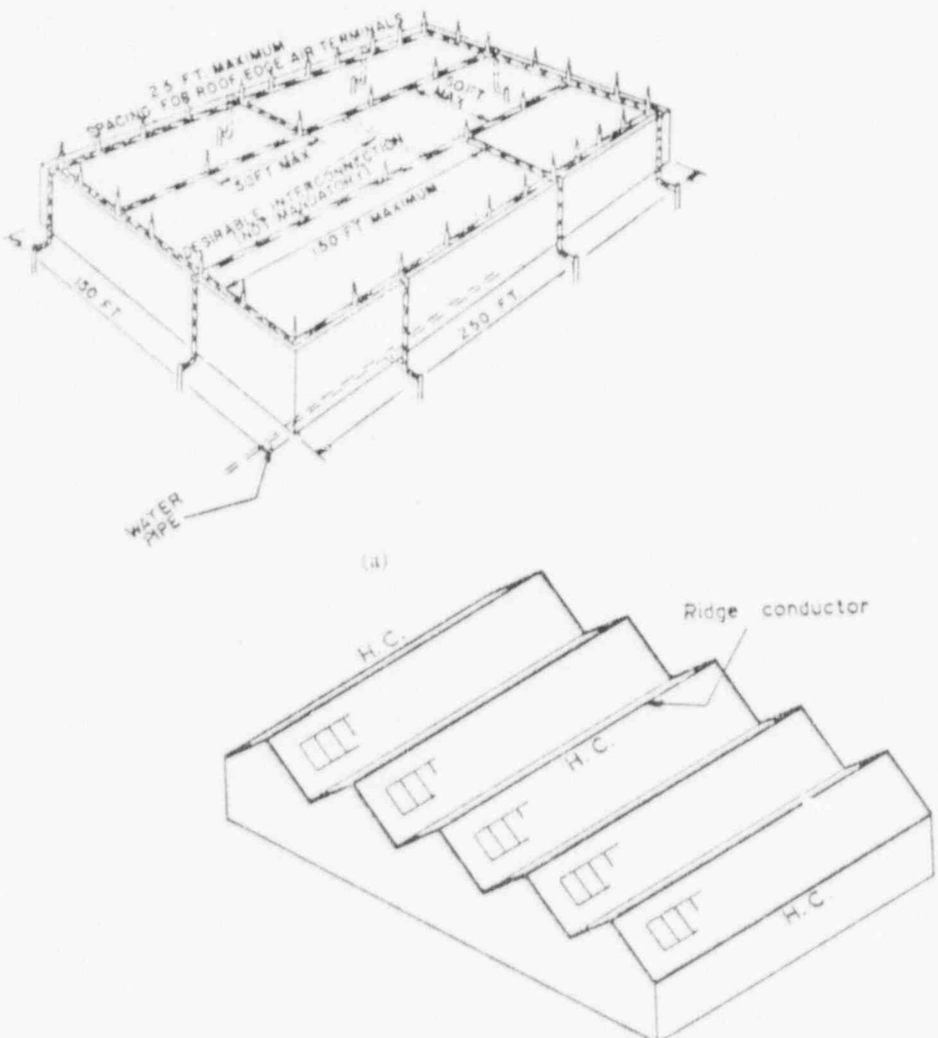

FIG. 8. Lightning protection of large roof: (a) after U. S. Code (**35**), (b) after British Code (**38**).

tall masts installed on Mount San Salvatore, and similar "failures" of a tall lightning conductor invariably to attract to itself every lighting stroke have been reported from the Eiffel Tower and the Empire State Building.)

Attention has already been drawn to the possibility of, say, a sharp corner of a roof structure causing a point discharge and giving rise to an upward streamer which then attracts a lightning leader stroke to the structure, bypassing the lightning rod. To avoid this risk most modern *Recommendations* state that the roofs of buildings be fitted with a ridge conductor running along the whole length of a gabled roof (Franklin's "middling wire") or along the parapets or edges of flat roofs. For roofs of large dimensions, these conductors laid along the perimeter are supplemented by additional horizontal tapes providing a mesh of prescribed dimensions. Typical recommendations for the width of such a mesh are listed in Table II.

TABLE II. *Dimensions of Roof Conductor Mesh*

		Maximum recommended distance between conductors (in meters)	
Country	Ref.	Ordinary structures	Danger structures
Switzerland	(36)	15	
Germany	(37)	20	10
Britain	(38)	18 (60 feet)	7.5 to 3.0 (25 to 10 feet) according to degree of risk
U. S.	(35)	50	(with additional finials)

Following the foregoing considerations to their logical conclusions, some modern *Codes* have dispensed altogether with the provision of vertical finials for roof structures. This development is based on the argument that under the influence of the strong electric fields discussed earlier, the shape of the conductor designed to intercept a lightning discharge is immaterial, a conclusion which is supported by the breakdown voltages of long sparks under long-fronted impulse voltages. Thus, in the latest British Code (38), the provision of an array of vertical lightning rods is recommended only for small danger structures while even for tall chimneys the provision of a ring conductor installed along the edge of the top of the structure is deemed to provide adequate protection. Neither in the Swiss (36) nor in the German (37) specifications are vertical finials mentioned at all. The only form of construction which runs counter to this development is the so-called *radio-active lightning conductor* for which it is claimed that a single vertical conductor can protect a building of large surface area. Further reference to this device is made later.

For explosive stores or other similar small structures it may be imperative to prevent a lightning current contacting any part of the structure surface. In

such a case the roof c
wires suspended from
as to exclude the pos
building. This schem
electrical transmissi

It is interesting
successfully by Szpor
quite different reaso
quently they have t
destroyed every year
impossible to provid
based on normal rule
inspected in later ye
Szpor thus suggested
lightning protective
scheme consists of a
suspended from two
and extending in bo
sufficient lengths at
earthing.

Down Conducto

Once a lightnin
it is the function
earth electrod
for a buil
conductor
down conductors
this is unacceptable
shafts.

However, for ma
tall structu , such
conductors are requ
crete buildings, the
system provided it
and lower ends. Sin
pense with separate
bond the upper ends
have it connected to

In effect, this sch
which goes beyond
James Clerk Maxw

such a case the roof conductor system is best replaced by a system of catenary wires suspended from tall towers arranged around the structure and so designed as to exclude the possibility of side flashing from the protective system to the building. This scheme is based on the same principle as the protection of an electrical transmission line by an overhead ground wire.

It is interesting to note in passing that the same principle has been adapted successfully by Szpor (**39**) for the protection of small farmhouses in Poland for quite different reasons. As a rule these buildings are made of wood and frequently they have thatched roofs. A large number of these farmsteads are destroyed every year by fire started by lightning and it proved economically impossible to provide all these structures with effective lightning protection based on normal rules and dimensions and to have these installations regularly inspected in later years to ensure that they remained in a satisfactory state. Szpor thus suggested a scheme which enabled the farmer to install his own lightning protective system and to do so at a minimal cost. Essentially his scheme consists of a galvanized iron wire of 10 mm² (0.016 sq. in.) cross section suspended from two wooden uprights installed at the two ends of the roof ridge and extending in both directions under a sloping angle down to ground level, sufficient lengths at either end being buried in the ground to provide effective earthing.

Down Conductors

Once a lightning stroke has been intercepted by the roof conductor system, it is the function of the down conductors to transfer the lightning current to the earth electrodes. For a small building a single down conductor is adequate, but for a building of large ground surface and for a tall structure several down conductors are required if side flashing to internal metal is to be avoided. Such down conductors may be installed on the outer surface of the building or, where this is unacceptable for aesthetic reasons, along internal walls or certain service shafts.

However, for many modern industrial or flat buildings as well as for many tall structures, such as water towers, cooling towers etc., no separate down conductors are required. Thus, for steel-framed structures and reinforced concrete buildings, the internal metal can be utilized as part of the protective system provided it gives a direct metallic connection between its uppermost and lower ends. Similarly, buildings with continuous curtain walling can dispense with separate down conductors. All that is necessary in such cases is to bond the upper ends of the metal framework to a roof conductor system and to have it connected to an efficient earthing system.

In effect, this scheme leads to the only important lightning protective system which goes beyond Franklin's original ideas. This scheme, first suggested by James Clerk Maxwell (**40**) and now applied to many small structures of ex-

90004061

treme explosive hazard, utilizes the conception of the so-called *Faraday cage* to avoid the occurrence of any potential difference within the protected building so as to make the building, in Maxwell's own words, "a closed conducting vessel."[7] It is the development of such a potential difference between the lightning conductor system and internal metal, earthed or otherwise, which has given rise to the great majority of alleged failures of the protective system and which brought Franklin's system into early unjustified disrepute.

The risk of side flashing can be overcome by efficient multiple bonding to the down conductors of any extended metal fixtures or services in or on the building. With increasing building height such bonding must be done both at the highest and lowest points of any extended metal components. This also stresses the need for careful record keeping and periodic checking to ensure that any alterations to service pip s and other metal fixtures have not interfered adversely with the efficacy of an originally sound arrangement.

Much uninformed criticism has been voiced against the use of a right-angle bend in a down conductor or its connection with a roof conductor. The bending forces arising at such a point are usually too low to affect a conductor of usual cross section and risks of side flashing are negligible unless the conductor is bent back so as to form a long but narrow re-entrant loop.

Earthing System

Franklin was well aware of the importance of a good earth connection for a lightning rod. Already in Poor Richard's Almanac does he recommend (**34**) that the lightning conductor be "of such a length that at one end being three or four feet in the moist ground." In later publications and letters he reverts repeatedly to this subject. Thus, in a letter dated February 20th 1762, in which he comments on an account of the successful discharge of a lightning flash to the house of a Mr. West in Philadelphia, he remarks (**41**):

> "There is one circumstance, *viz.* that the lightning was seen to diffuse itself from the foot of the rod over the wet pavement, which seems, I think, to indicate, that the earth under the pavement was very dry, and that the rod should have been sunk deeper, till it came to earth moister, and therefore apter to receive and dissipate the electric fluid."

Inadequate earthing of lightning conductors led to many failures in early installations with the result that this matter was given special attention by the French Academy of Sciences whose series of Recommendations have been mentioned before. A low earthing resistance may be required for two reasons.

[7] For the same reason, persons in an all-metal car or aeroplane are immune from electric shock. Maxwell, incidentally, was also the first person to draw attention to the fact that a lightning conductor would attract more flashes than would have occurred to the same spot had it not been fitted.

Firstly, apart from the in
conductor, the ohmic volt
side flashing and secondly
rect function of the eart
many fatal accidents to h

Buried plates which h
present time have the dr
which is liable to drying
between plate and surro
which compress the soil a
be used because of the ro
are effective, particularly
their initial surge impeda

Bonding of the earth
metal services such as e
method not only assists
protective system but it
ground. Such bonding m
tion, but means are avail

The Protective Ran

Information on th
lightning conductor
structures is c

Country
U. S.
Britain
Poland
South Africa

R = radius of protect
brackets have been derived

still to exist in national
ment in which the stati
ductor is stressed and
cannot be expected to
surprise since the auth

so-called *Faraday cage* to
in the protected building
ds, "a closed conducting
erence between the light-
or otherwise, which has
he protective system and
disrepute.

ient multiple bonding to
or services in or on the
ng must be done both at
l components. This also
iodic checking to ensure
tures have not interfered
gement.

t the use of a right-angle
conductor. The bending
fect a conductor of usual
less the conductor is bent

d earth connection for a
es he recommend (**34**)
: one end being three or
nd letters he reverts re-
ary 20th 1762, in which
e of a lightning flash to
1):

ng was seen to diffuse
, which seems, I think,
very dry, and that the
moister, and therefore

many failures in early
special attention by the
mendations have been
equired for two reasons.

he are immune from electric
attention to the fact that a
occurred to the same spot

Firstly, apart from the inductive voltage drop which arises across a long down conductor, the ohmic voltage drop in the earth electrode determines the risk of side flashing and secondly the potential drop across the ground surface is a direct function of the earthing resistance. The resulting voltages have led to many fatal accidents to human beings and to quadrupeds.

Buried plates which have been widely used for earthing purposes up to the present time have the drawback that they have to be placed in made-up soil which is liable to drying out so that, in the course of time, the area of contact between plate and surrounding soil may be materially reduced. Driven rods which compress the soil are therefore much to be preferred. When these cannot be used because of the rocky nature of the ground, horizontal buried conductors are effective, particularly if they are arranged in star formation so as to reduce their initial surge impedance.

Bonding of the earthing system of the lightning conductor to all buried metal services such as electric cables, gas or water pipes is imperative. This method not only assists in securing a low overall earthing resistance for the protective system but it also prevents the risk of a long arc discharge in the ground. Such bonding may tend to interfere with systems of cathodic protection, but means are available to overcome these difficulties.

The Protective Range

Information on the protective range or protective angle attributed to a lightning conductor in several modern national Codes for the protection of structures is collected together in Table III. Considerable differences are seen

TABLE III. *Protective Ranges (or Angles)* Adopted in National Recommendations

Country	Ref.	Ordinary structures		Danger structures	
		R/H	α	R/H	α
U.S.	(**31**)	2:1		1:1	(45°)
Britain	(**38**)	(1:1)	45°	(0.58:1)	30°
Poland	(**42**)	1.5:1			
South Africa	(**43**)	(1:1)	45°		

R = radius of protected circular base. H = height of lightning conductor. Figures in brackets have been derived for purposes of comparison.

still to exist in national recommendations. The British Code is the only document in which the statistical aspect of the attractive range of a lightning conductor is stressed and in which it is stated that a single lightning conductor cannot be expected to provide complete protection. This fact need not cause surprise since the author must admit at having exerted a certain influence in the deliberations of the drafting committee. On the other hand, it is noteworthy that the Swiss recommendations make no reference whatsoever to this subject.

Despite existing differences, all national Codes agree in ascribing to any lightning protective system a limited range of effectiveness. Completely different claims are made for protective systems employing radio-active materials incorporated at the tip of a conventional vertical lightning rod. The suggestion to use radio-active materials for various aspects of lightning protection is by no means novel, but claims have been made in recent years to the effect that a single rod of normal height, if fitted with a radio-active tip, is capable of protecting an entire building of large horizontal dimensions.

In order to test the efficacy of a radio-active lightning conductor, Müller-Hillebrand (44) erected four of these devices in accordance with the supplier's instructions and, at distances of between 31 and 53.4 meters, he erected a conventional lightning rod of the same height as the radio-active conductor. He

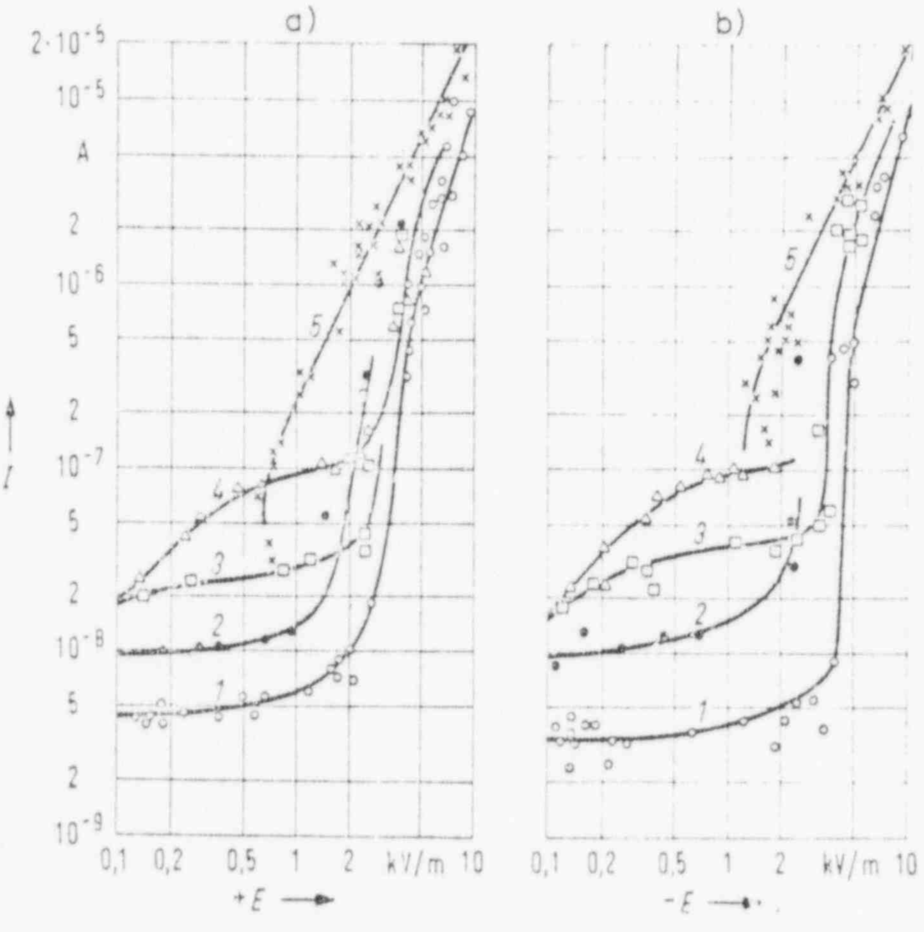

FIG. 9. Variation of emission current with electric gradient: (a) positive gradient; (b) negative gradient; 1,2,3,4—radio-active lightning conductor, 5—normal lightning conductor.

then recorded the
under thunderstorm
these investigations
gradients (distant
point discharge
currents of the
moves closer and
Hillebrand conclude

Thus, if it is adm
lightning conductor
conductor must be
tional conductor of

The only nation
active lightning co
provision of radio
worthy effect. The
scientific investigat
natural ionization o
active material." Th
are known by which
conductor.

Conclusions

The mode of
lished. Its
contact a
current l
metal can be ove
of side flashing is
protective system.
resistance is the rod
the point of earthin
essential between t
buried metal pipes

Apart from chu
roof conductors wh
roof structure. Inte
conductors. For bui
tinuous curtain wal
structural metal is
conductor system.

then recorded the point discharge currents produced by the two conductors under thunderstorm conditions in Switzerland and in Sweden. The results of these investigations are summarized in Fig. 9. The curves show that, for small gradients (distant thunderstorms), the normal rod produces no measurable point discharge current whereas the radio-active lightning conductor discharges currents of the order of a fraction of a microampere. However, as a thunderstorm moves closer and the gradient increases, the curves begin to merge. Müller-Hillebrand concludes that this result is in full accord with theoretical prediction.

Thus, if it is admitted that the current discharged into the atmosphere by a lightning conductor is indicative of its attractive action, a radio-active lightning conductor must be taken to provide the same degree of protection as a conventional conductor of the same height above ground.

The only national Code which appears to make specific reference to radio-active lightning conductors is that issued in Germany (37). It states "The provision of radio-active material on lightning rods cannot produce a noteworthy effect. The additional ionization created by them lies, according to scientific investigations, several orders of magnitude below that caused by natural ionization of a lightning rod in a thunderstorm field with no radio-active material." The British Code (38) merely indicates that no artificial means are known by which to increase the range of attraction afforded by a lightning conductor.

Conclusions

The mode of action of a lightning conductor is now reasonably well established. Its sole purpose is to intercept a lightning discharge before this can contact any point of the building to be protected and to discharge the lightning current harmlessly to ground. The risk of side flashing to internal or external metal can be overcome by bonding and, if this is efficiently carried out, the risk of side flashing is unaffected by the magnitude of the earthing resistance of the protective system. Under such conditions the main advantage of a low earthing resistance is the reduction of the potential drop across the ground surface about the point of earthing. In order to avoid side flashing in the ground, bonding is essential between the lightning protective earth electrode and any adjacent buried metal pipes or cables.

Apart from church steeples, vertical finials can be replaced by horizontal roof conductors which should be so arranged as to cover all sharp edges of the roof structure. Internally arranged down conductors are as effective as external conductors. For buildings with steel frames, continuous reinforcement or continuous curtain walling, down conductors can be dispensed with, provided the structural metal is effectively earthed and, where advisable, connected to a roof conductor system.

The space protected by a lightning conductor is still subject to further investigation although there are strong reasons to believe that the distance over which a lightning conductor is capable of attracting a lightning discharge is a statistical quantity related to the intensity of the lightning stroke.

In conclusion, the author wishes once more to pay homage to the genius of Benjamin Franklin whose lightning conductor system required only minor additions or modifications since its first enunciation in 1753. Truly, he was overmodest in writing (45) in 1762: "Indeed, in the construction of an instrument so new, and of which we could have so little experience, it is rather lucky that we should at first be so near the truth as we seem to be, and commit so few errors."

Bibliography

(1) K. Pearson, "The Grammar of Science," London, Adam & Charles Black, 1911.

(2) B. F. Schonland, "The Work of Benjamin Franklin on Thunderstorms and the Development of the Lightning Rod," *Jour. Frank. Inst.*, Vol. 253, p. 375, 1952.

(3) I. B. Cohen, "Prejudice against the Introduction of Lightning Rods," *Jour. Frank. Inst.*, Vol. 253, p. 393, 1952.

(4) I. B. Cohen, "Benjamin Franklin's Experiments," Harvard University Press, Cambridge, Mass., 1941, letter to M. D'Allibard, of June 29th 1755.

(5) G. J. Symons (editor), "Lightning Rod Conference," E. & F. N. Spon, London and New York, 1882.

(6) Oliver J. Lodge, "Lightning Conductors and Lightning Guards," London, Whittaker & Co., 1892.

(7) J. Alan Chalmers, "Atmospheric Electricity," Pergamon Press, London, Paris, New York, 1957.

(8) B. F. J. Schonland, "The Lightning Discharge," Handbook of Physics, Vol. XXII, Berlin, New York, Springer, 1956.

(9) C. E. R. Bruce and R. H. Golde, "The Lightning Discharge," *J.I.E.E.*, Vol. 88, Pt. II, p. 487, 1941. C. E. R. Bruce, "The Initiation of Long Electrical Discharges," *Proc. Roy. Soc.*, Vol. 183, p. 228, 1944.

(10) R. H. Golde, "The Frequency of Occurrence and the Distribution of Lightning Flashes to Transmission Lines," *Trans. A.I.E.E.*, Vol. 64, p. 902, 1945.

(11) R. H. Golde, "The Attractive Effect of a Lightning Conductor," *J.I.E.E.*, Vol. 9, p. 212, 1963.

(12) A. M. Thomas, "The Switching-Surge Strength of Insulating Arrangements for Systems Operating at Voltages Above 100 kV," *E.R.A.* Report No. 5080, Leatherhead, 1966.

(13) T. E. Allibone, "Mechanism of the Electrical Breakdown of Large Gaps in Air," *CIGRE* Report No. 328, Appendix I, 1964.

(14) I. S. Stekolnikov and A. V. Shkilev, "Investigation of the Mechanism of the Negative Spark," *Nauk SSSR*, Vol. 151, p. 1085, 1963.

(15) R. C. Hughes and W. J. Roberts, "The Effect of Wave Front Duration on the Impulse Flashover of Air Gaps," *Proc. I.E.E.*, Vol. 112, p. 198, 1965.

(16) T. Udo, "Switching Surge and Impulse Sparkover Characteristics of Long Gap Spacings and Long Insulator Strings," *I.E.E.E.*, paper No. TP-65-164.

(17) E. W. Boehne and G. Carrara, "On the E.H.V. Switching Surge Insulation Strength of Line and Station Insulating Air Spaces," *C.I.G.R.E.*, paper No. 415, 1964.

(18) L. Paris, "Influence of Air Gap Characteristics on Line to Ground Switching Surge Strength," *A.I.E.E.E.*, Paper 31, pp. 66-121, 1966.

(19) K. Berger and E. Vogelsanger, "Photografische Blitzuntersuchungen der Jahre 1955–1965 auf dem Monte San Salvatore," *Bull. A.S.E.*, 57, p. 599, 1966.

(20) T. Horvath, "Eine n... schlägen," *Elektrie*, V...

(21) F. Schwab, "Berech... *A.S.E.*, Vol. 56, p. 67...

(22) R. Davis, "Lightning...

(23) See Ref. (4), Letter N...

(24) B. Wilson, "Report o... p. 239, 1778.

(25) "Instructions sur les...

(26) R. Anderson, "Lightn...

(27) W. H. Preece, "On th... p. 427, 1880.

(28) ... Walter, "Von wo... *Physik*, Vol. 18, p. 10...

(29) B. Wilson, "On the...

(30) F. W. Peek, "Dielectr... Hill Book Co., Inc., 1...

(31) U. S. Department of ... 1932, 1937, 1945, 195...

(32) P. G. Provoost, "Th... No. 314, Appendix II...

(33) C. F. Wagner, G. D... *Trans. A.I.E.E.*, Vol...

(34) See Ref. (4), p. 129.

(35) National Fire Protect...

(36) Association Suisse de... tion contre la foudre,...

(37) Ausschuss für Blitzs... Berlin, 1963.

(38) British Standards In... don, 1965.

(39) S. Szpor, "Paratonn... p. 263, 1959.

(40) J. Clerk M... port, London...

(41) See Ref. (4), p. ...

(42) Wydawnictwa Norm... Warsaw, 1959.

(43) South African Burea... Against Lightning," ...

(44) D. Müller-Hillebrand... durch Raumladungen...

(45) See Ref. (4), p. 373.

90004066

(20) T. Horvath, "Eine neue Methode zur Ermittlung der Wahrscheinlichkeit von Blitzeinschlagen," *Elektrie*, Vol. 17, p. 216, 1963.
(21) F. Schwab, "Berechnung der Schutzwirkung von Blitzableitern und Türmen," *Bull. A.S.E.*, Vol. 56, p. 678, 1965.
(22) R. Davis, "Lightning Flashovers on the British Grid," *Proc. I.E.E.*, Vol. 110, p. 969, 1963.
(23) See Ref. (**4**), Letter XXIV, Paris, p. 389, Sept. 1767.
(24) B. Wilson, "Report on Lightning Accident at Purfleet," *Phil. Trans. Roy. Soc.*, Vol. 68, p. 239, 1778.
(25) "Instructions sur les Paratonnerres," Académie Royale des Sciences, Paris, 1823.
(26) R. Anderson, "Lightning Conductors," E. & F. N. Spon, London, New York, 1879.
(27) W. H. Preece, "On the Space Protected by a Lightning Conductor," *Phil. Mag.*, Vol. 10, p. 427, 1880.
(28) B. Walter, "Von wo ab steuert der Blitz auf seine Einschlagstelle zu?", *Z. für Techn. Physik*, Vol. 18, p. 105, 1937.
(29) B. Wilson, "On the Termination of Conductors," *Phil. Trans.*, Vol. 68, p. 999, 1778.
(30) F. W. Peek, "Dielectric Phenomena in High-Voltage Engineering," New York, McGraw-Hill Book Co., Inc., 1929.
(31) U. S. Department of Commerce, "Code for Protection Against Lightning," Wash., D. C., 1932, 1937, 1945, 1952.
(32) P. G. Provoost, "The Shielding Effect of Overhead Earth Wires," *C.I.G.R.E.*, paper No. 314, Appendix II, 1960.
(33) C. F. Wagner, G. D. McCann, G. L. MacLane, "Shielding of Transmission Lines," *Trans. A.I.E.E.*, Vol. 60, p. 313, 1941.
(34) See Ref. (**4**), p. 129.
(35) National Fire Protection Association, "Lightning Code 1965," Boston, Mass.
(36) Association Suisse des Electriciens, "Recommandations pour les installations de protection contre la foudre," Zurich, 1959.
(37) Ausschuss für Blitzableiterbau e.V. (ABB), "Allgemeine Blitzschutz-Bestimmungen," Berlin, 1963.
(38) British Standards Institution, "The Protection of Structures Against Lightning," London, 1965.
(39) S. Szpor, "Paratonnerres ruraux de type léger," *Revue Générale de l'Electricité*, Vol. 68, p. 263, 1959.
(40) J. Clerk Maxwell, "On the Protection of Buildings from Lightning," British Assn. Report, London, 1877.
(41) See Ref. (**4**), p. 372.
(42) Wydawnictwa Normalizacyjne, "Ochrona Budowli od Wyladowan Atmosferycznych," Warsaw, 1959.
(43) South African Bureau of Standards, "Code of Practice for the Protection of Buildings Against Lightning," Pretoria, 1959.
(44) D. Müller-Hillebrand, "Beeinflussung der Blitzbahn durch radioaktive Strahlen und durch Raumladungen," *Elektrotechnische Zeitschrift*, A, Vol. 83, p. 152, 1962.
(45) See Ref. (**4**), p. 373.

REF. 9

The Relation Between Stroke Current and the Velocity of the Return Stroke

C. F. WAGNER
FELLOW IEEE

Summary: The velocity of the return stroke is an important element in estimating (1) the surge impedance of the return stroke, (2) the potential of the downward leader, and (3) the length of the last striking distance. The energy required to establish an arc plasma can be determined from laboratory tests. By equating this quantity to the energy required to retard the velocity of a traveling wave, the consequent velocity of the return stroke can be evaluated in terms of the stroke current.

In 1955 Lundholm[1,2] presented an interesting relation between the current in, and the velocity of, the head of the return stroke. Rusck[3] later reviewed Lundholm's derivation and, after modifying one of the constants, arrived at the following result:

$$v = 1\Big/\sqrt{1+\frac{5.0\times10^4}{I}} \qquad (1)$$

in which v is the velocity of the head of the return stroke expressed in terms of the velocity of that of light, and I is the stroke current in amperes (amp). This relation is shown in Fig. 1.

Fig. 2 shows the distribution of occurrence curve of the velocity of the return stroke determined by Wagner and McCann[4] (Fig. 20 of reference 4) as a result of their analysis of 19 records presented by Schonland, Malan, and Collens.[5] Fig. 2 also shows a replot of the frequency of occurrence of stroke currents as published by the AIEE Lightning and Insulator Subcommittee.[6] Rusck, accepting, a priori, that the velocity of propagation is a function of the stroke current, plotted the mutually connected points shown by the dotted line in Fig. 1. It can be seen that the relation between the two curves is remarkably good.

The derivation of the Lundholm expression is somewhat obscure in some respects as it is based upon an empirical relation of Toepler[7] which states that the resistance of the path of a discharge varies inversely as the charge that passes that point in the discharge path. It is the purpose of this paper to re-examine the relation between the stroke current and the velocity of the return stroke in terms more susceptible to physical interpretation and more readily determinable from laboratory tests.

Simplified Analysis

To develop the physical concepts, a number of simplifying assumptions will be made. Later these will be modified or eliminated by further discussion. These assumptions are as follows:

1. The return stroke can be viewed as a wave of positive charge (and current) whose head travels upward, neutralizing, as it progresses, the negative charge laid down by the downward leader. This wave moves upward from a plane surface, which in this paper will be assumed to be perfectly conducting. For the initial assumptions, however, the system of simultaneous waves, shown in Fig. 3(A), that moves outward from 0 and 0', will be premised. This is done primarily because this system, after the heads of the waves have progressed sufficiently, leads to a finite solution. All of the essential elements of the actual case reside in this one also.

2. All of the waves of current (and charge) of Fig. 3(A) are rectangular.

3. The waves travel with a constant velocity vc, where c is the velocity of light and v a numeric.

4. Each wave of charge q_0, in coulombs per centimeter (cm), has associated with it a wave of current i_s, in which

$$i_s = vcq_0 \qquad (2)$$

5. The arc plasma behind the heads of the waves has a constant radius a in centimeters; its resistivity is zero.

6. All of the current flows on the surface of the plasma; all of the charge resides on its surface.

7. In Fig. 21 of reference 8 it is shown that to bring a 6-foot spark discharge to high conductivity for currents between 1,000 and 2,000 amp requires an energy that is proportional to the final current of the discharge. This energy is approximately equal to 0.002 watt-second per centimeter per ampere. Verification of this value is given in the Appendix.

The properties of a system of waves such as the one shown in Fig. 3(A) have been discussed in connection with Fig. 12 of reference 9, in which it is shown that to establish, as has been premised, rectangular waves of charge and current which travel with a constant velocity of vc, series-forcing voltages, as shown in Fig. 3(B), must be inserted on both sides 0 and 0'. In addition, a retarding voltage must be inserted that is symmetrical with respect to the heads of the current waves. The paths of the waves are separated a distance D; it will be shown subsequently that this system of waves is approximately equivalent to the case in which, when D is made equal to twice the distance the head has traveled from the earth, a wave of charge rises vertically from the earth. Fig. 3(C) shows in more detail the total voltage, using 0 and 0' as reference points, that must be inserted progressively in series to bring about the propagation of rectangular current waves. These voltages are the integrals, from these reference points, of the electric field's longitudinal component, at a radius a from the axes of propagation. The

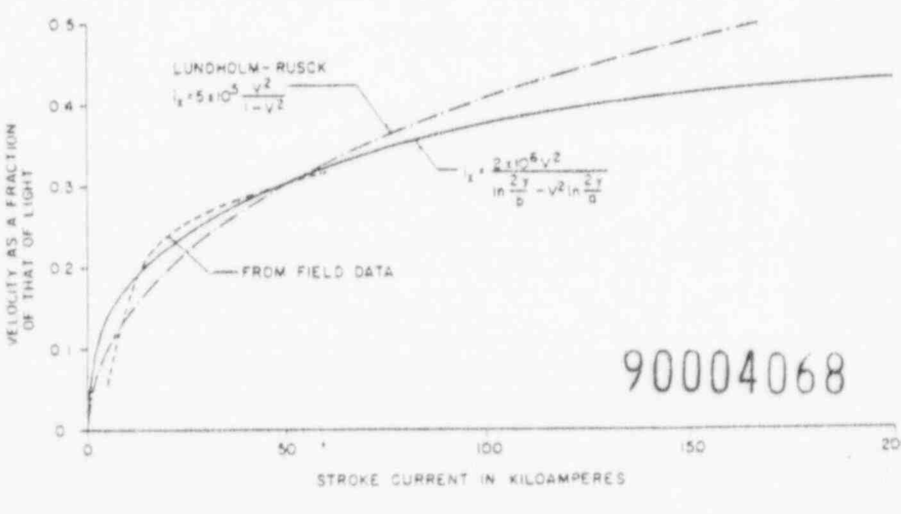

90004068

Fig. 1. Relations between stroke current and velocity of return stroke

Paper 62-1094, recommended by the AIEE Transmission and Distribution Committee and approved by the AIEE Technical Operations Department for presentation at the AIEE Summer General Meeting, Denver, Colo., June 17-22, 1962. Manuscript submitted March 21, 1962; made available for printing May 2, 1962.

C. F. WAGNER is with Westinghouse Electric Corporation, East Pittsburgh, Pa.

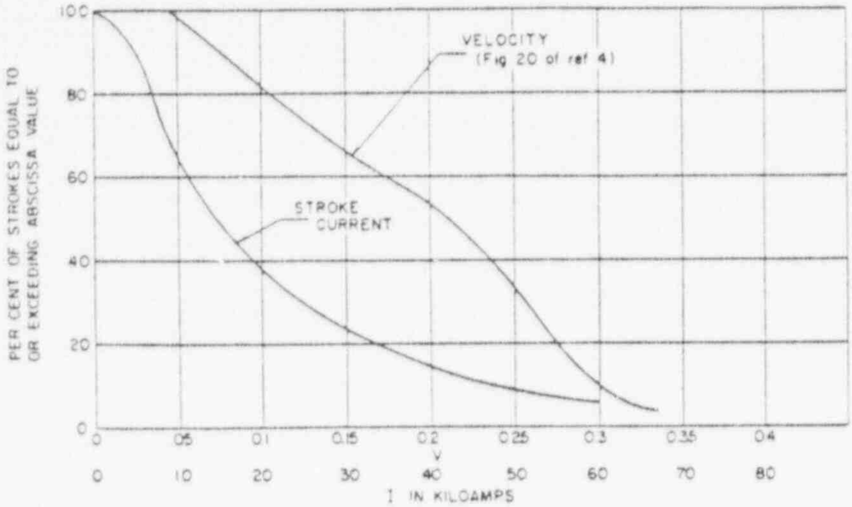

Fig. 2. Relation between frequency of occurrence of lightning strokes (AIEE curve) and velocity of return stroke

forcing voltage in each conductor, after a time slightly in excess of the travel time between the conductors, attains a constant value of

$$V = 60 i_z \frac{1}{v} \ln \frac{D}{a} \quad (3)$$

where D is the separation between the two parallel paths of waves. The retarding voltage V_r has two components: (a) that occasioned by the charge, which attains a limiting value of

$$V_c = -60 i_z \frac{1}{v} \ln \frac{D}{a} \quad (4)$$

and (b) that occasioned by the current, which attains a limiting value of

$$V_i = 60 i_z v \ln \frac{D}{a} \quad (5)$$

The retarding voltages are then the sum of these quantities:

$$V_r = 60 i_z \left(v - \frac{1}{v}\right) \ln \frac{D}{a} \quad (6)$$

Let it be assumed that the heads of the waves have progressed to a point where the forcing and retarding electromotive forces (emf's) do not overlap. If $v = 1$, the waves travel with the velocity of light; since the retardation voltage is zero and the voltage waves propagate with a vertical front, the forcing voltage is equal to $60 i_z \ln D/a$. For $i_z = 1.0$, this expression will be recognized as the conventional surge impedance. In addition to the longitudinal electric fields at radius a, from which the forcing and retarding voltages were derived, radial electric fields which arise from the charges q_0 also exist.

Before proceeding with the application of these relations, it is interesting to develop the energy relations involved. For $v = 1.0$, the power input into each conductor P_c is equal to $V i_z$. It can be shown that this power is expended in developing the magnetic energy per unit length P_{mc}, which is equal to $L i_z^2/2$, and the electrostatic energy associated with the radial field P_{ec}, which is equal to $CV^2/2$. These quantities are equal. Therefore, for $v = 1$,

$$P_c = P_{ec} + P_{mc} \quad (7)$$

and

$$P_{ec} = P_{mc} = P_c/2 \quad (8)$$

If $v \neq 1$, for the same forcing voltage an equal charge will be distributed along the conductors, but the current will be only v times as great as for $v = 1$. The surge impedance will be $1/v$ as great and the power input P will be

$$P = v P_c \quad (9)$$

The electrostatic energy will be distributed v times as fast as for $v = 1$ and, therefore,

$$P_e = v P_{ec} = \frac{v}{2} P_c \quad (10)$$

The magnetic energy per unit length will be v^2 times as great and will be distributed v times as fast. Therefore,

$$P_m = v^3 P_{mc} = \frac{v^3}{2} P_c \quad (11)$$

The power absorbed by the retardation effect is proportional to the instantaneous back emf and the current, but since the current exists only on the left-hand side of the retardation voltage, the power absorbed by this effect is

$$P_r = \frac{1}{2} V_r i_z \quad (12)$$

Remembering that for $v \neq 1$, i_z varies as v, then this quantity is proportional to

$$P_r = \frac{1}{2} v^2 \left(v - \frac{1}{v}\right) P_c \quad (13)$$

Equating the power input to the sum of the stored electrostatic power, the stored magnetic power, and the retardation power:

$$v P_c = \frac{v}{2} P_c + \frac{v^3}{2} P_c - \frac{v}{2}\left(v - \frac{1}{v}\right) v P_c \quad (14)$$

which is an identity and verifies the ultimate distribution of the power input.

Returning to the application of these relations to the immediate problem,

90004069

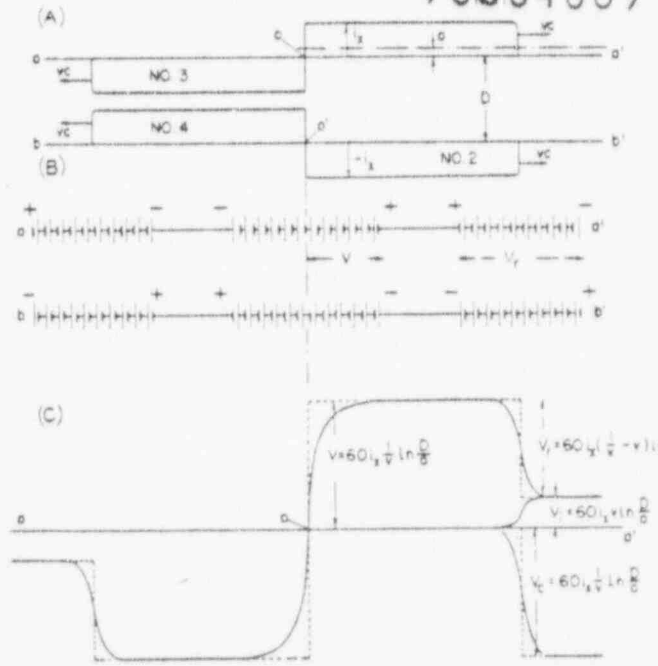

Fig. 3. Limiting values of voltages which produce a system of currents

A—System of simultaneous waves

B—Series - forcing voltages, inserted progressively in series, required to produce waves shown in (A)

C—Total voltage to be inserted

Fig. 4. Rectangular current rising from a plane of zero resistivity

A—Current wave

B — Longitudinal fields produced by current shown in (A)

C—Forcing voltage required to produce current shown in (A)

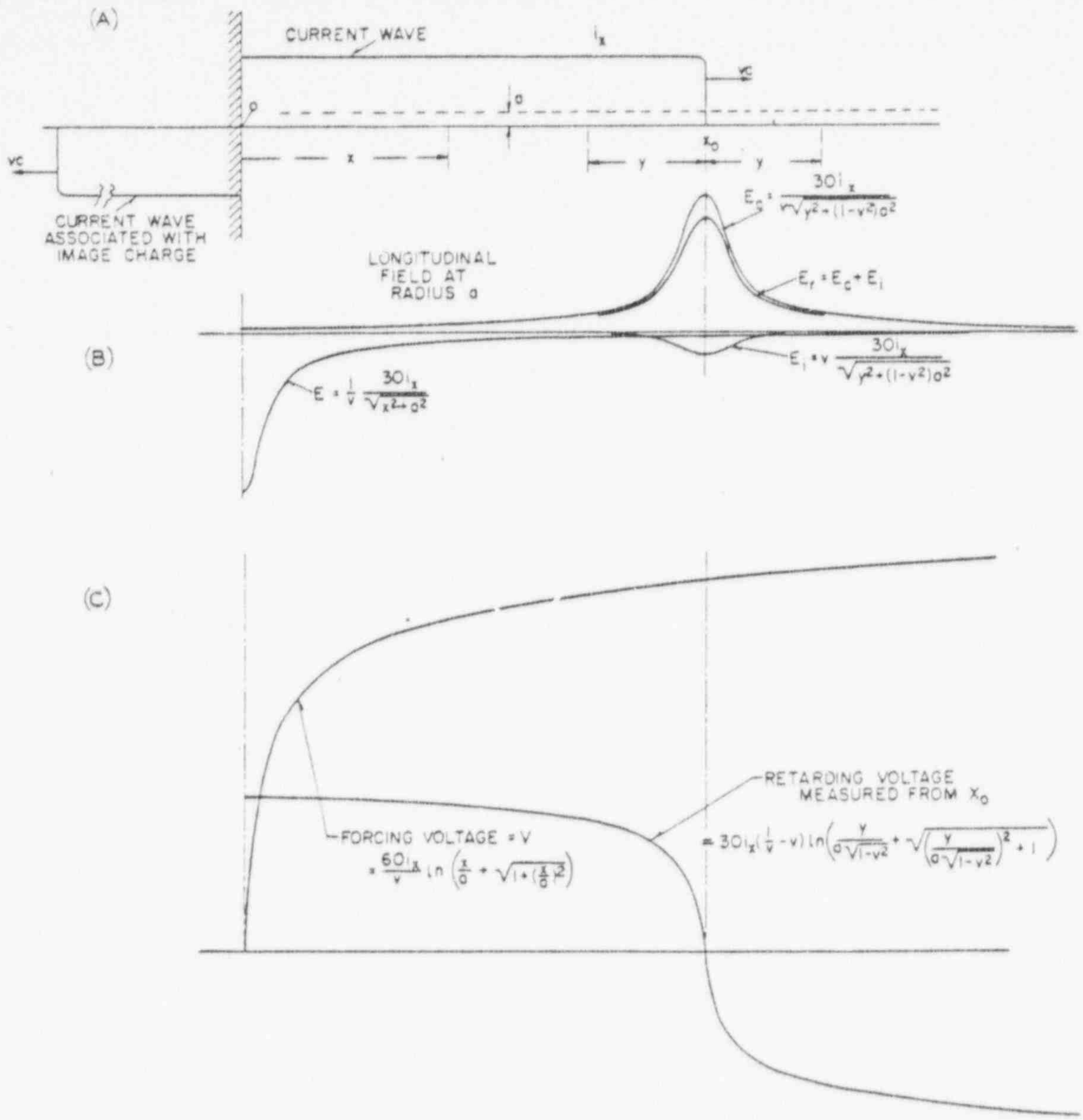

90004070

when V_r is inserted from equation 6 into equation 12,

$$P_r = -30\left(v-\frac{1}{v}\right)\ln\frac{D}{a}\, i_x^2 \text{ watts} \qquad (15)$$

which is the power that must be absorbed by the head of each wave so that the waves are retarded to a velocity v.

From assumption 7 it is revealed that the energy required to raise a spark to a conducting state within the time interval involved in the breakdown process of a rod-rod gap is 0.002 watt-second per centimeter per ampere. The power that must be absorbed by the head of the traveling wave, to bring it to a conductivity which will support the current of i_x amp, is proportional to the velocity. The power P_r can also be expressed, therefore, as

$$P_r = vc(0.002)i_x \qquad (16)$$

Equating equations 15 and 16

$$-30\left(v-\frac{1}{v}\right)\left(\ln\frac{D}{a}\right) i_x^2 = vc(0.002)i_x \qquad (17)$$

or

$$i_x = \frac{c(0.002)}{30\ln\frac{D}{a}}\,\frac{v^2}{1-v^2} \qquad (18)$$

and

$$v = 1\Big/\sqrt{\frac{c(0.002)}{30 i_x \ln\frac{D}{a}}+1} \qquad (19)$$

A certain similarity in the form of this equation and that of Lundholm-Rusck (equation 1) will be observed. The author does not wish to discuss at this point the numerical values of the parameters in this expression, except to state that a typical value of D would be about 600 feet, and of a, about 0.1 foot. For these values equation 19 becomes

$$v = 1\Big/\sqrt{\frac{2.3\times10^6}{i_x}+1} \qquad (20)$$

In the foregoing it was assumed that the effective radius at which the charge might be considered concentrated and the radius of the cylinder in which the current flows are identical. This is not true. The charge is concentrated at a much larger radius than that of the cylinder along which the current flows. When this is taken into consideration and the radius of the charge concentration is represented by the symbol b, then, as shown in reference 9, a in equation 4 should be replaced by b. Following this change through equations 6 and 15, it can be seen that equation 17 then becomes

$$30 i_x^2\left[\frac{1}{v}\ln\frac{D}{b} - v\ln\frac{D}{a}\right] = vc(0.002)i_x^2 \qquad (21)$$

and

$$i_z = \frac{v^2 c(0.002)}{30\left[\ln\frac{D}{b} - v^2 \ln\frac{D}{a}\right]} \qquad (22)$$

Representation of the Return Stroke by a Conductor Rising from the Earth

Up to this point, the stroke has been represented by waves of charge (and current) propagating along parallel paths. Actually, however, the downward leader distributes a negative charge that is approximately uniform along its entire length. The return streamer or stroke can be regarded as draining this charge to earth as its head moves upward, or as neutralizing the negative charge by an upward-moving positive charge. Therefore, the return stroke is represented more realistically by a wave of charge (and current) that rises vertically from a plane of infinite extent. Again, in order to state specific conditions and to obtain precise results for these assumptions, a rectangular wave of current will be premised that extends itself above a plane of zero resistivity with a constant velocity vc. The effect of the plane can be represented by replacing its presence by an image charge wave of opposite polarity and its associated current wave as shown in Fig. 4(A).

In passing, it should also be noted that this representation is not accurate. According to the author's viewpoint, the return-stroke channel current begins as a current that rises from the ground; simultaneously, a corresponding current begins to flow from the end of the downward leader toward ground, this current being supplied by a wave of current that progresses upward, draining as it does so the charge laid down by the downward leader in its progress toward the earth. But for the present discussion the return current will merely be assumed to rise from the earth.

For preliminary consideration, both the charge and the current will be assumed to be concentrated at radius a. As shown in reference 9, the current wave of Fig. 4(A) that flows to the right from 0 produces an electric field parallel to the path of propagation, given by the relations in Fig. 4(B), where a is the distance from the axis of propagation. The field E develops from 0 with the speed of light and, therefore, outdistances the head of the current wave. The field E_r travels with the head of the current wave and consists of two components: E_c, associated with the charge, and E_i, associated with the current. These fields are also circumscribed by the sphere that expands from 0 with the velocity of light. The image current to the left of 0 produces similar fields but, for large values of x_o, the instantaneous position of the head of the current wave, only that component of the field produced by the image current which expands from 0 and is equal to E is of importance.

The arc plasma that constitutes the return stroke has a very low drop (of the order of 60 volts per centimeter). The return stroke can then be conceived as a metallic conductor of essentially zero resistivity that extends itself vertically. The field along the surface of this conductor must then be zero. To produce the currents such as premised in Fig. 4(A), forcing fields equal and opposite to E and retarding fields equal and opposite to E_r must be assumed to be injected into the circuit. This can best be visualized by assuming that series voltages are inserted progressively in incremental quantities in series in the conductor, so that the integrated values of these fields are equal to these series voltages. The values of these voltages are indicated in Fig. 4(C).

It is difficult to generalize and to draw conclusions from these analytical expressions. A particular case is, therefore, chosen for numerical evaluation; this is given in Fig. 5. For this case v is taken as 0.3, a as 0.1 foot, and x_o as 1,000 feet. Of particular interest is curve D, which gives the voltage that must be inserted in series from the head of the current wave x_o for the wave to be slowed down to $v = 0.3$ and the current wave to be rectangular. This shows that for unit current a total voltage of 900 volts (the value of this curve for $x = 0$) is required. Thus, the power that must be absorbed in retarding the wave as determined from circuit conditions (that corresponding to equation 15) is

$$P_r = 900 i_z^2 \qquad (23)$$

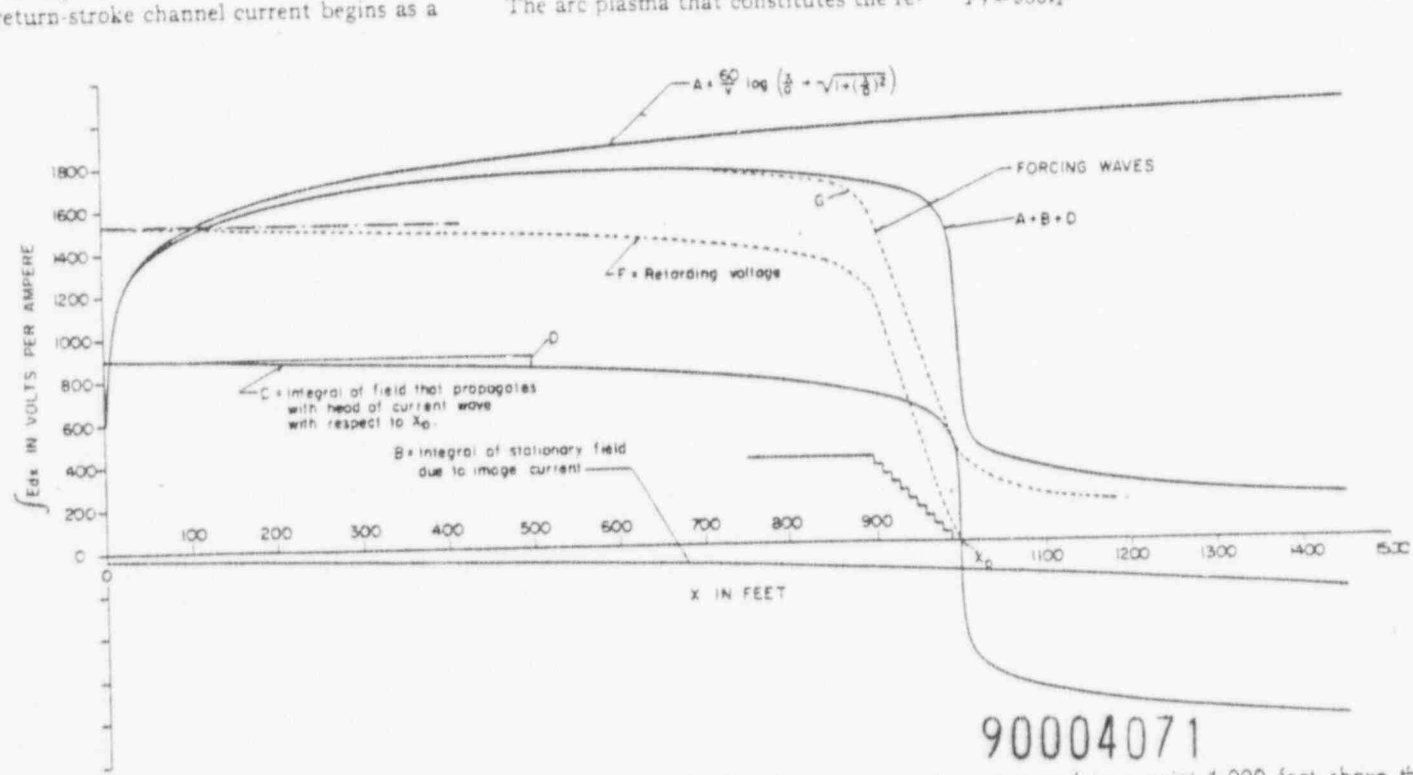

Fig. 5. Forcing and retarding voltages in the return stroke after the head of the current wave has progressed to a point 1,000 feet above the earth; a rectangular wave of current was assumed for the full-line computations and a current wave with a front of 100 feet was assumed for the dotted-line computations (assumed velocity of propagation, 30% that of light; radius, 0.1 foot)

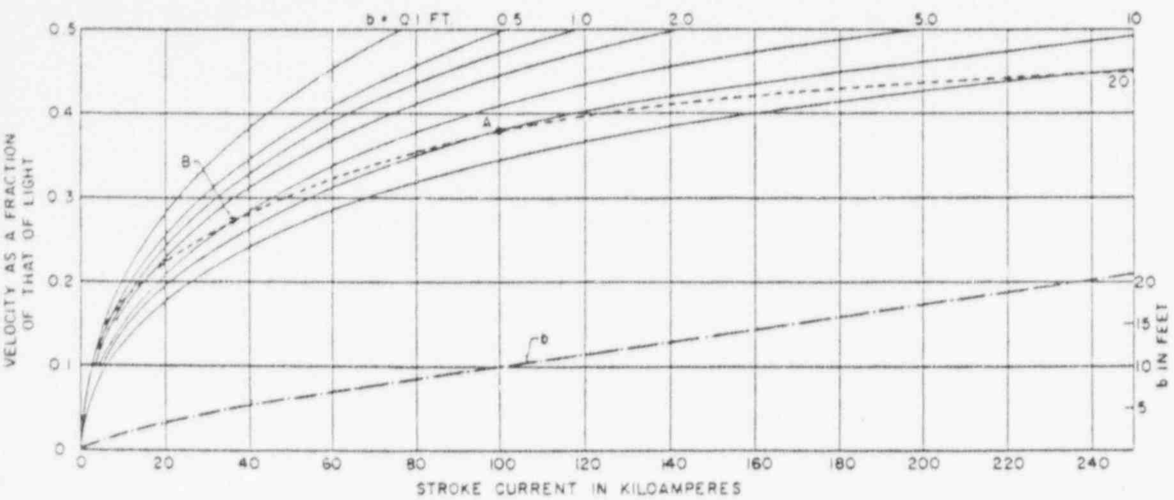

Fig. 6. Velocity-current curves computed from equation 30 for $y = 300$ feet, $a = 0.1$ foot, and different values of b

Equating this to the power determined by laboratory tests, as given in equation 16 for this particular value of v,

$$900 i_r^2 = (0.3)(3 \times 10^{10})(0.002) i_r \tag{24}$$

or

$i_r = 20{,}000$ amp

To determine the effect of the front of the current wave, the rectangular wave of unit amplitude was replaced by a stepped wave with ten steps of 0.1 amplitude each, as shown in Fig. 5. The corresponding forcing and retarding waves are indicated by the dotted lines. It will be seen first that the amplitude of the forcing wave, which corresponds to its surge impedance, is unaffected by the front of the wave. To determine the retarding effect it is necessary to evaluate the power rather than merely the voltage. For the case in which the current is rectangular, the current to the right of x_0 is zero, and to the left it is constant. The power absorbed at the head of the wave is then the product of this constant current and the series voltage indicated by curve D. Thus for unit current, if the wave is rectangular, the power that must be absorbed at this instant within 100 feet from the head is 690 watts; within 300 feet, 800 watts; and within 100 feet, 900 watts. But if the front is stepped, the current to the left of x_0 between x equals 900 feet and x equals 1,000 feet varies, and it is necessary to compute the voltage across each 10-foot interval, multiply by the corresponding current in each element, and integrate the products. This has been done; it was found that the power that must be absorbed between x equals 900 feet and x equals 1,000 feet is 554 watts for a crest current of unity. Adding to this the power that must be absorbed during the interval in which the current is constant, it is found that 794 watts must be absorbed within 300 feet of the head, and 904 watts within 1,000 feet of it. Thus it can be seen, as would be surmised, that the energy absorbed is dependent only upon the velocity, and is independent of the front.

From Fig. 4, it is shown that the retarding voltage for the rectangular wave is equal to

$$30 i_r \left(\frac{1}{v} - v\right) \ln \times \left[\frac{y}{a\sqrt{1-v^2}} + \sqrt{\left(\frac{y}{a\sqrt{1-v^2}}\right)^2 + 1}\right] \tag{25}$$

where y is the distance measured back from the head of the wave over which the field must be integrated. The energy that must be absorbed to reduce the velocity to v, then, is this expression multiplied by i_r. Equating this expression to P_r from equation 16,

$$30 i_r^2 \left(\frac{1}{v} - v\right) \ln \times \left[\frac{y}{a\sqrt{1-v^2}} + \sqrt{\left(\frac{y}{a\sqrt{1-v^2}}\right)^2 + 1}\right] = vc(0.002) i_r \tag{26}$$

$$i_r = \frac{v^2}{1-v^2} \times \frac{c(0.002)}{30 \ln\left[\frac{y}{a\sqrt{1-v^2}} + \sqrt{\left(\frac{y}{a\sqrt{1-v^2}}\right)^2 + 1}\right]} \tag{27}$$

For the present purposes, interest will be centered on values of y greater than 300 feet. In the discussion of arc characteristics in the Appendix, it is shown that the growth of the diameter of the arc requires considerable time and that, for the currents involved, the arc radius will be less than 0.1 foot. Therefore, unity under the radical can be neglected. Furthermore, y/a will be so large that $1 - v^2$ within the radical can be replaced by unity. With $c = 3 \times 10^{10}$, equation 27 then simplifies to

$$i_r = \frac{2 \times 10^6}{\ln\left(\frac{2y}{a}\right)} \frac{v^2}{1-v^2} \tag{28}$$

This is identical to equation 18 and demonstrates the similarity of the two circuits. For y/a equal to 3,000, this expression reduces to

$$i_r = 2.3 \times 10^5 \frac{v^2}{1-v^2} \tag{29}$$

If y/a is 30,000 instead of 3,000, i_r is only increased 26%.

Now if the difference in charge concentration at radius b and current concentration at radius a is taken into consideration and the same simplifications that led to equation 28 are included, the expression for stroke current becomes the same as equation 22 with D replaced by $2y$. Thus

$$i_r = \frac{v^2 c(0.002)}{30\left[\ln \frac{2y}{b} - v^2 \ln \frac{2y}{a}\right]} \tag{30}$$

The family of curves of Fig. 6 have been drawn from the above expression, with a equal to 0.1 foot (3.05 cm), D equal to 300 feet (91.4 meters), and different values of b. This particular value of D was chosen because it was estimated to be a reasonable value that would obtain over the entire range of currents as the stroke current attained its maximum value. Further, it has already been shown that the results are not critical with respect to the choice of D. Because of the factor v^2 for the term involving the quantity a, the choice of a is also not critical. The radius b is, however, critical. The distribution of the charge around the core of the downward leader is still controversial. Is the volume distribution uniform within a cylinder at whose surface the gradient is 30,000 volts per centimeter? Does almost all of the

90004072

charge reside near the surface of this cylinder? Or does the volume distribution vary inversely as the radius to produce gradient within the corona sheath?

Perhaps none of these conditions is correct. However, for the present situation, some assumption must be made. The author has made the assumption that b for the value corresponding to 100,000 amp is 10 feet. This establishes point A on the final curve depicting the relation between v and i_s. It will be assumed that b is proportional to q_0. From equation 2 it can be seen that b is also proportional to i_s/v. Therefore, to determine the point on the final curve for b equal to 5 feet, one must only draw a straight line through the origin whose slope is twice that of a straight line through A. In this way point B was obtained. By similar constructions, the dotted line shown in Fig. 6, which represents the relation between v and i_s and which incorporates the variation in b, was determined. This curve is replotted in Fig. 1 for comparison with the curve obtained by observation and the Lundholm-Rusck curve. The dot-dashed curve of Fig. 6 shows the corresponding values of b.

Fig. 7. (A) Gap voltage and (B) current for sparkover of a 9-foot rod–rod gap, together with (C) their replots and instantaneous power

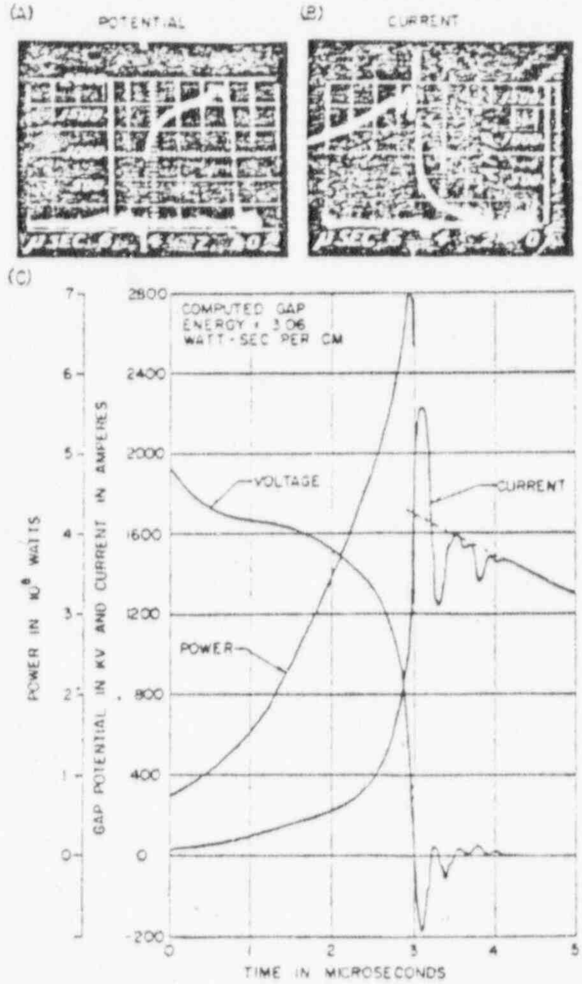

Relation Between Stroke Potential and Velocity of the Return Stroke

In Fig. 5 the series voltage V required to establish the current i_s is indicated. It can be approximated by the equation

$$V = 60 i_s \frac{1}{v} \ln \frac{2y}{b} \tag{31}$$

The radius for the charge concentration must be used in this expression. Inserting i_s from equation 30 into equation 31:

$$V = 1.2\times10^8 v \frac{1}{\left[1 - v^2 \ln \frac{2y}{a} \Big/ \ln \frac{2y}{b}\right]} \text{ in volts} \tag{32}$$

The main variable in this expression, except for v, is b. This factor can be estimated from the curve in Fig. 6 and V obtained as a function of current (or velocity). This procedure assumes a knowledge of the factor a, which has been taken as constant and equal to 0.1 foot. But in actuality a varies with current as well as b. A more realistic assumption is to let b be the value given in Fig. 6 and let a vary linearly with i_s being 0.1 foot at 100,000 amp. When this is done it is found that V can be approximated very closely by the following expression:

$$V = 1.2\times10^8 \frac{v}{1-2.2v^2} \tag{33}$$

This indicates that the stroke potential is independent of the stroke current and is a function of the velocity only. In Table I the stroke potentials are indicated for different values of v; it can be seen that they are of the order of magnitude estimated by other investigators.

According to the stroke mechanism theory proposed by Wagner and Hileman,[10] the length of the final striking distance as the downward leader approaches the earth is equal to the stroke potential divided by the critical breakdown gradient, which is about 5,000 or 6,000 volts per centimeter. The smaller the final striking distance, the smaller the shielding angle must be to provide adequate shielding. Therefore, to be conservative, the value of 6,000 volts per centimeter is used and the final striking distance X_s becomes

$$X_s = 2\times10^4 \frac{v}{1-2.2v^2} \text{ cm} \tag{34}$$

$$X_s = 656 \frac{v}{1-2.2v^2} \text{ feet} \tag{35}$$

Table I also indicates the range of these values.

Table I

i_s, In Amperes	V, In 10^6 Volts	X_s, In Meters	X_s, In Feet
20,000	28.0	50	164
40,000	40.3	68	222
60,000	48.8	83	273
100,000	64.0	111	364
150,000	76.8	134	438
200,000	84.8	150	491

General Comments

In Fig. 5 the curve $A+B+D$ represents the voltages that must be inserted in series in incremental amounts at that instant so that the resulting propagated current wave will be of unit value and rectangular in shape. Previously these voltages were arbitrarily divided into two parts: (1) that from $x=o$ to the crest (1,760 volts) was regarded as the forcing voltage; and (2) that between the crest and 3,300 feet (about −1,600 volts) was regarded as the retarding voltage. So long as these net voltages are maintained the same for any two cases (but not necessarily constant with time in either case) the two current waves propagate with the same velocity.

90004073

The manner in which they are distributed will affect the wave shape of the current. In determining the retarding voltage in equation 25, the retarding field was integrated from $x=y$ back to $x=o$. It would have been more accurate to have integrated from $x=y$ back to the point at which the curve $A+B+D$ crests (or 700 feet). However, it was shown that because of the logarithmic nature of the function this limit is not critical.

While from a mathematical viewpoint it is immaterial whether the charge transported from the leader is regarded as a negative charge lowered to ground or as a positive charge rising to neutralize the negative charge, from a physical viewpoint further consideration must be given to the problem. If, as the author believes, the charge on the downward leader exists in the form of negative ions, the mobility of such ions is low enough to prohibit the explanation of the formation of the current as a flow of negative ions. The current must rather consist of a flow of positive charge drawn from the earth that neutralizes the negative ions. If the return stroke is viewed as a highly conducting extensible conductor that rises from the earth, this current must rise by induction. As shown in reference 16, the magnitude of the current that would flow in this case is determined by the relative radii of the return-stroke channel and the charge location. The more nearly equal these are, the more perfect the neutralization and the larger the current. It is probable that in its upward travel the return-stroke channel branches out to collect by induction a large portion of the ionic charge. The core of the return stroke does not increase from absolute zero, but from a value existing in the core of the downward leader at the instant in which the head of the return stroke reaches that particular section of the downward leader.

Regarding the downward leader as a conductor of equal potential along its entire length, the charge distributed in the charged column will be larger near the earth than at points at higher altitudes. This should result in a gradually decreasing current in the return stroke after its initial crest has been attained. Since the velocity of the head varies with the current, as indicated in Fig. 1, the velocity of the head as it rises should also decrease. Also, as mentioned previously, as the length of the return stroke increases, the voltage drop required to supply the thermal energy conducted and radiated to the surrounding air no longer remains negligible; it also contributes to slowing the velocity of the head of the return stroke. Furthermore, as the length of the return stroke lengthens, its surge impedance also increases, which tends to diminish the current. On the other hand, while the voltage drop along the downward leader is small and negligible during the initial stages of the return stroke, its integrated effect over the length of the downward leader results in a higher potential of the downward leader near the cloud than near the earth. Thus, as the return stroke approaches the cloud, the higher forcing potential tends to counteract somewhat the effects just enumerated.

Several of the parameters used in this study are not known precisely. They vary with time, but specific values still must be assigned to them. The author does not, therefore, claim a precision that does not exist. Fortunately, these parameters occur as longarithms and so they need not be known with great precision. The precision is sufficiently great to define the nature of the phenomenon. As more data become available, appropriate corrections can be made. More information is desirable concerning the simultaneous variation of the velocity of the return stroke and its current. And little information is known concerning the charge distribution within the corona sheath, not only during the first few microseconds (µsec) of formation, but for longer times during which other factors than those dominant during formation may be active.

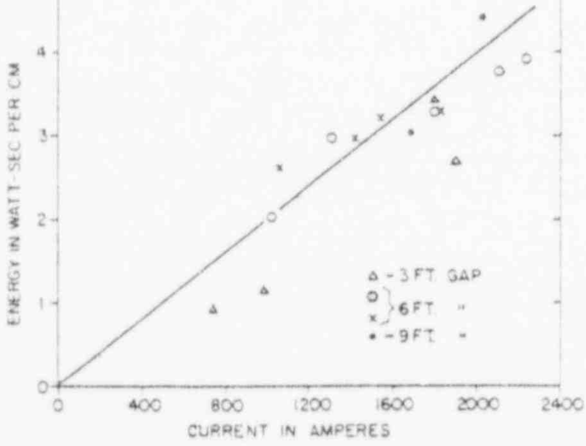

Fig. 8. Experimental evaluation of energy fed into rod-rod gaps of 3- to 9-foot spacings during sparkover as a function of the final current

Conclusions

While the lightning stroke has doubtless been idealized and simplified to a considerable degree in this analysis, a number of pertinent conclusions can be drawn within the purview of these limitations:

1. The general form of the modified equation relating the stroke current and the velocity of the return stroke, first suggested by Lundholm,[12] has been verified, using as a basis the energy required to establish a spark. The modified curve is shown in Fig. 1.

2. It is shown that the velocity of the return stroke is dependent only upon the energy necessary to make the arc conducting and not upon the rate of rise of the head of the current wave in the channel as it moves upward.

3. The potential of the downward leader as it nears the earth and the final striking distance are functions of the velocity of the return stroke and are given by the following relations:

$$V = 1.2 \times 10^{6} \frac{v}{1-2.2v^{2}} \qquad (33)$$

$$X_s = 656 \frac{v}{1-2.2v^{2}} \text{ feet} \qquad (35)$$

Appendix. Characteristics of Sparks and Arcs

Reference was made earlier to tests[8] in which, from the breakdown of spark gaps, the energy required to establish a given arc current was determined. These data were for rod-rod gaps 6 feet in length. While at the time that these tests were made tests on gaps of other lengths had been made, the energy had not been computed for the gaps of other lengths. Fig. 7 shows the form in which these data were collected and represents: (A) an oscillogram of the voltage across a 9-foot rod-rod gap of such a value as to produce complete breakdown in 3 µsec; (B) an oscillogram of the current through the gap; and (C) a replot of these two records, together with a computation of the instantaneous product or power. The total energy absorbed in the gap was found by integrating this curve, which was found equal to 3.06 watt-seconds per centimeter length of gap. The integration in this case was continued only to the first zero of voltage. The value of the current assigned to this test was the value obtained by extrapolating the smooth portion back to the instant at which the voltage became zero. This value was

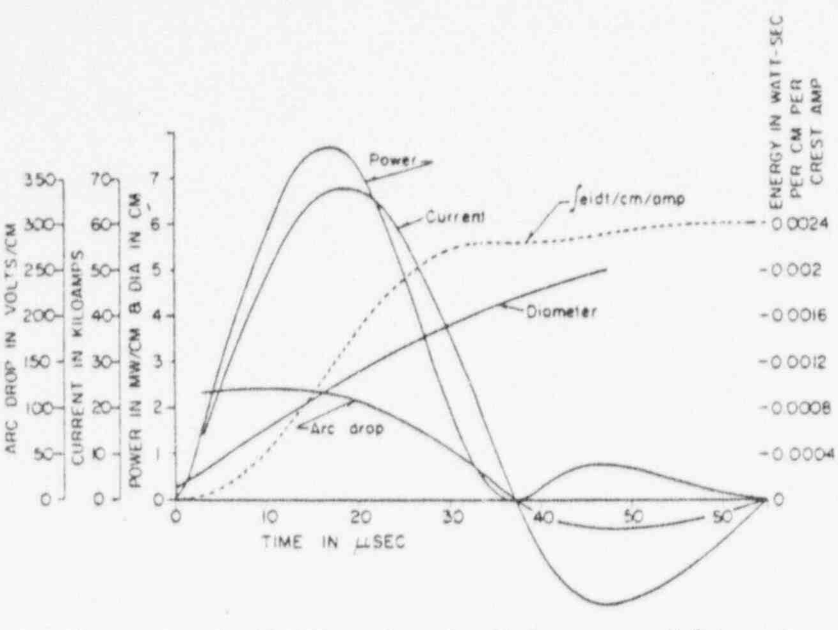

Fig. 9. Characteristics of a 68,000-amp damped oscillating current arc[11] that rose to crest in 19 μsec; length of gap, 51 cm

1,590 amp; therefore, the energy becomes equal for this case to 0.00192 watt-second per centimeter per ampere.

Fig. 8 gives the energy data for gaps 3, 6, and 9 feet in length. The data for the 6-foot gap are those given in reference 8. In drawing the mean, the data for the 9-foot gap were favored. The slope of the straight line is equal to 0.002 watt-second per centimeter per ampere. These data covered a current range up to 2,250 amp and channel formative times from 0.4 to 6.5 μsec.

While these tests indicate that the potential across the arc path drops almost immediately to zero, a drop of, for example, 60 volts per centimeter would be difficult to detect. A drop of this magnitude is equivalent for a duration of 1 μsec to 0.0005 watt-second per centimeter per ampere, or 2.5% of 0.002. For the purposes of this application, one is interested in only the first few microseconds after crest current is attained; therefore, this continuous contribution to the energy can be neglected. It can, however, be a contributing factor along with others in explaining the decrease in velocity as the head of the return stroke rises toward the cloud.

Consideration will now be given to other available data from which the energy input to bring an arc to a high conducting state can be determined. Norinder and Karsten,[11] by means of a combination of impulse generators, produced currents up to 102,000 amp through gaps of 25 and 51 cm. Fig. 9 gives their results for a current that rose to a crest of 68,000 amp in 19 μsec. The current, the arc drop, and the instantaneous power are in the form given by the observers. In this paper, the author integrated the power curve and divided by the crest current to provide the curve plotted by the dotted line. Fig. 10 shows similar information computed by the author from the data of Norinder and Karsten for different impulse currents. It is difficult to draw direct conclusions from these results, since the primary interest of this investigation lies approximately within the first 5 μsec. It can be concluded that the energy input per crest ampere increases with current. It is also clear that for long times the energy per ampere is well in excess of the value of 0.002, which again indicates that the velocity should decrease as the head of the return stroke approaches the cloud.

Wagner, Lane, and Lear[12] also measured the drop across high-current impulse arcs. The gaps they used were small (less than 2 inches) but the currents rose to crest in much shorter times. Fig. 11 shows some of their data reduced to energy input.

In judging these data it is necessary to bear in mind some of the very complicated properties of the arc. Mayr[13] showed that for a steady-state condition, the current distribution within the core of the arc falls off from the axis as a quadratic exponential function of the radius. Energy loss is by conduction, although radiation also plays a part. The arc core is surrounded by a sheath of air at high temperature, since at the core boundary the temperature is continuous. To determine the energy or "thermal content" that must be injected into the arc when the current rises slowly, the energy imparted to the surrounding air must be included. Yoon and Spindle,[14] in observations with an arc of 1 amp, obtained a thermal content of 0.0025 watt-second for air at atmospheric pressure and showed that for a stepped incremental increase (or decrease) the thermal content should vary exponentially with a time constant of 85 μsec. This slow phenomenon does not include the very rapid effect associated with impulse currents. Fig. 9 shows the growth of the diameter of the arc, as obtained by a photographic process by Norinder and Karsten. More recently Allen and Craggs,[15] photographing impulse currents that rose to a crest of 188 kiloamperes in 7.7 μsec, demonstrated that the initial velocity of expansion of the arc was $1.4-3.1\times10^{-6}$ cm per second, as compared to the velocity of sound of 0.34×10^{-6} cm per second. It seems reasonable to conclude that for the rapid changes of a few microseconds in duration, the surrounding air does not participate in the heating effect; however, it does participate for slower phenomena and phenomena of longer duration, such as when the arc path of the return stroke has lengthened as its head approaches the cloud, or during the dissipation time of the stroke between components.

From this brief and necessarily incomplete discussion of the arc, the additional information obtained from other than gap

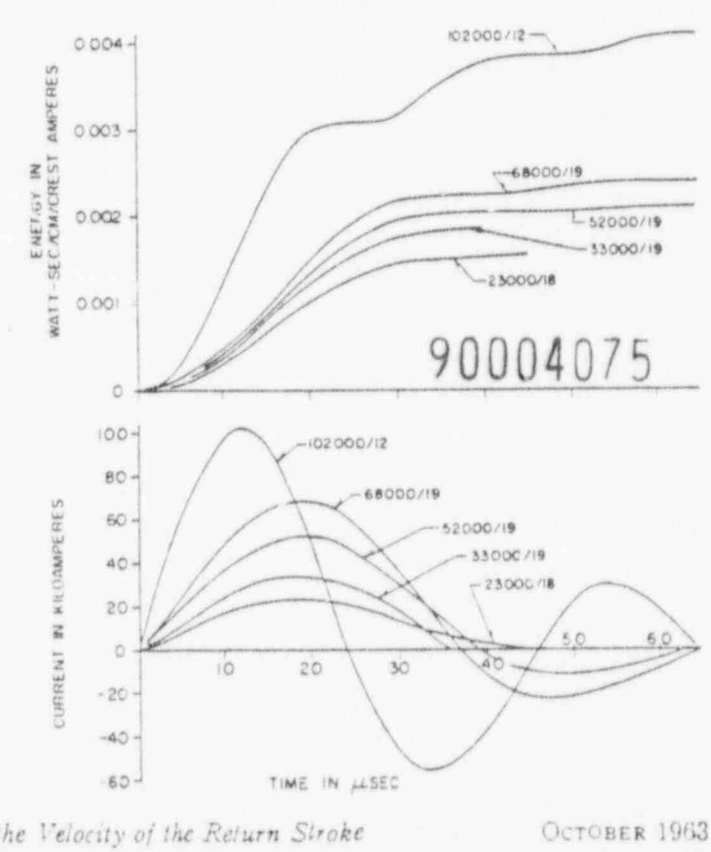

Fig. 10. Energy input into oscillatory current arcs

breakdowns, while not contributing to a more accurate evaluation of the energy to use in the velocity formula, does not contradict the value determined from the breakdown of long gaps.

References

1. INDUCED OVERVOLTAGES ON TRANSMISSION LINES AND THEIR BEARING ON THE LIGHTNING PERFORMANCE OF MEDIUM VOLTAGE NETWORKS, R. Lundholm. Duplic Göteborg, Gothenburg, Sweden, 1955.

2. INDUCED OVERVOLTAGE-SURGES ON TRANSMISSION LINES AND THEIR BEARING ON THE LIGHTNING PERFORMANCE AT MEDIUM VOLTAGE NETWORKS, R. Lundholm. *Transactions of Chalmers University of Technology*, Gothenburg, Sweden, vol. 188, 1957, pp. 1-17.

3. INDUCED LIGHTNING OVER-VOLTAGES ON POWER-TRANSMISSION LINES WITH SPECIAL REFERENCE TO THE OVER-VOLTAGE PROTECTION OF LOW-VOLTAGE NETWORKS, Sune Rusck. *Transactions of the Royal Institute of Technology*, Stockholm, Sweden, vol. 120, 1958.

4. INDUCED VOLTAGES ON TRANSMISSION LINES, C. F. Wagner, G. D. McCann. *AIEE Transactions*, vol. 61, 1942, pp. 916-29.

5. PROGRESSIVE LIGHTNING II, B. F. J. Schonland, D. J. Malan, H. Collens. *Proceedings of the Royal Society (London) A*, London, England, vol. 152, 1935, pp. 595-625.

6. A METHOD OF ESTIMATING LIGHTNING PERFORMANCE OF TRANSMISSION LINES, AIEE Committee Report. *AIEE Transactions*, vol. 69, pt. II, 1950, pp. 1187-96.

7. FUNKENKONSTANTE, ZÜNDFUNKEN AND WANDERWELLE, M. Toepler. *Archiv fuer Elektrotechnik*, Berlin, Germany, vol. 14, 1924, pp. 305-18; vol. 18, 1927, pp. 549-66.

8. MECHANISM OF BREAKDOWN OF LABORATORY GAPS, C. F. Wagner, A. R. Hileman. *AIEE Transactions* pt. III (*Power Apparatus and Systems*), vol. 80, Oct. 1961, pp. 604-22.

9. SURGE IMPEDANCE AND ITS APPLICATION TO THE LIGHTNING STROKE, C. F. Wagner, A. R. Hileman. *Ibid.*, 1961 (Feb. 1962 section), pp. 1011-22.

10. THE LIGHTNING STROKE—II, C. F. Wagner, A. R. Hileman. *Ibid.*, Oct. 1961, pp. 622-42.

11. EXPERIMENTAL INVESTIGATIONS OF RESISTANCE AND POWER WITHIN ARTIFICIAL LIGHTNING CURRENT PATHS, H. Norinder, O. Karsten. *Archiv for Matematik, Astronomi Och Fysik*, Sweden, vol. 36A, no. 16, pp. 1-48.

12. ARC DROP DURING TRANSITION FROM SPARK DISCHARGE TO ARC, C. F. Wagner, C. M. Lane, C. M. Lear. *AIEE Transactions*, pt. III (*Power Apparatus and Systems*), vol. 77, June 1958, pp. 242-47.

13. BEITRÄGE ZUR THEORIE DES STATISCHEN UND DES DYNAMISCHEN LICHTBOGEN, O. Mayr. *Archiv fuer Elektrotechnik*, vol. 37, no. 12, 1943, pp. 588-608.

14. A STUDY OF THE DYNAMIC RESPONSE OF ARCS IN VARIOUS GASES, K. H. Yoon, H. E. Spindle. *AIEE Transactions*, pt. III (*Power Apparatus and Systems*), vol. 77, 1958 (Feb. 1959 section), pp. 1634-42.

15. HIGH CURRENT SPARK CHANNELS, J. E. Allen, J. D. Craggs. *British Journal of Applied Physics*, London, England, vol. 5, 1954, pp. 446-53.

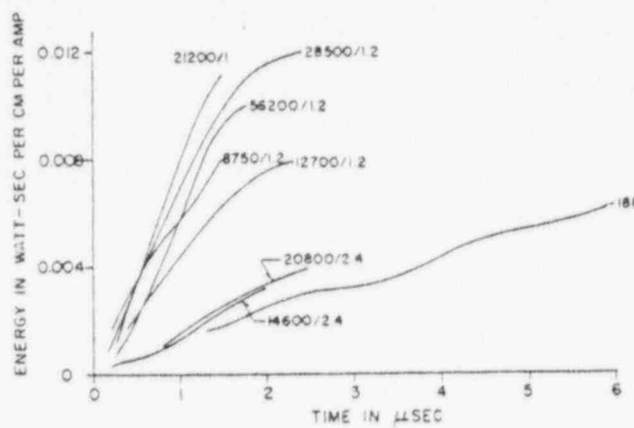

Fig. 11. Energy input into development of an oscillatory current arc (first number represents magnitude of first current crest; second number, time to first crest)

Discussion

J. H. Hagenguth (General Electric Company, Pittsfield, Mass.): Much of Dr. Wagner's theory of the lightning stroke is based on a leader mechanism;[1,2] he has postulated, "the downward leader consists of two parts, a very thin good-conducting core or channel, and a corona sheath that precedes and surrounds the channel."[1]

Photographic evidence, mostly by Schonland and his colleagues, does not indicate this. The corona sheath has not been photographed, but has been implied to be a so-called pilot leader. The photographs show that the conducting cores, which are not permanent, are formed and extinguished in a very short time and are reborn about every 50 μsec, each time progressing further toward the earth, possibly collecting positive ions produced during the progress of the invisible pilot leader and other positive debris in the corona sheath. I am not aware of a photograph that shows a continuous core of the downward leader. There is a photograph of an upward leader from the Empire State Building[3] with several portions where the core appears to be continuous. Possibly in this case the conditions postulated by Dr. Wagner existed. This one perhaps was the notable exception that proves the rule.

In connection with the relation between velocity of the return stroke and the stroke current, it would be interesting to know where the field data of Fig. 1 originated. Has it been possible to correlate Berger's data on this basis?

REFERENCES

1. RELATION BETWEEN STROKE CURRENT AND VELOCITY OF THE RETURN STROKE, C. F. Wagner. Thornton Butterworth, Ltd., London, England, 1962.

2. See reference 10 of the paper.

3. LIGHTNING TO THE EMPIRE STATE BUILDING—PART III, J. H. Hagenguth, J. G. Anderson. *AIEE Transactions*, pt. III (*Power Apparatus and Systems*), vol. 71, Aug. 1952, pp. 641-49.

C. F. Wagner: Mr. Hagenguth has raised a question concerning the evidence upon which I postulate that "the downward leader consists of two parts, a very thin good-conducting core or channel, and a corona sheath that precedes and surrounds the channel." There appears to be little doubt concerning the presence of a corona space charge. The only question must refer to the presence or absence of a good-conducting core. The head of the downward leader must be fed either through a channel consisting of a thin arc plasma whose voltage drop is about 60 volts per centimeter, or through a glow discharge. If the latter is true, the vertical voltage gradient must be of the order of several thousand volts per centimeter. If one assumes this gradient to be 5,000 volts per centimeter and assumes that the leader length is 5,000 feet (150,000 cm), the drop along the leader channel calculates to be 7.5×10^8 volts, quite beyond any modern estimates of the cloud potential. Furthermore, one would expect that the boundary of the resulting space charge (or corona) would have the form of an inverted cone of enormous radius near the cloud. This also is contrary to all modern thinking. The conducting cores to which Mr. Hagenguth refers are formed very quickly behind the steps, so quickly that their velocities approach the velocity of light. Such rapid development of good conductivity can only take place if the channel already consists of a good-conducting path. The fading away of luminosity merely reflects the reduction in current. Behind that part of the path which produces a trace on the photographic film there must exist a smaller current not sufficiently photographically sensitive that feeds the forward progress of the leader. In this region the current should be almost constant and of such low value that it does not record on the photographic film.

Mr. Hagenguth also inquires about the source of the field data in Fig. 1. I believe that the text explains this in detail. The original data consisted of the 19 photographic records of strokes obtained by Schonland, Malan, and Collens. Wagner and McCann then analyzed these data, from which the velocity curve in Fig. 2 was obtained. The stroke current curve of Fig. 2 is the AIEE curve. Then, assuming a single-valued relation between the stroke current and the velocity, the field data curve of Fig. 1 was obtained. To be more specific, any single value in Fig. 2 on the percentage ordinate will provide a single current value and a single velocity value, plotted as constituting one point in Fig. 1.

Subsequent to the preparation of this paper it came to the author's attention that Dr. Müller-Hillebrand had plotted similar curves between the velocity of the return streamer and the current.[1]

REFERENCE

90004076

1. THE PHYSICS OF THE LIGHTNING DISCHARGE, Müller-Hillebrand. *Electrotechnische Zeitschrift*, Braunschweig, Germany, vol. 82A, 1961, pp. 232-49.

C. F. WAGNER

REF. 10

POOR ORIGINAL

The lightning stroke as related to transmission-line performance

PART I

The mechanism of lightning-stroke formation is reviewed, with emphasis on those aspects of particular interest to the transmission-line engineer. The relation between the return-stroke current and the velocity of its head is shown to be a function of the speed with which energy can be fed into the return-stroke channel to achieve the necessary conductivity

Many problems of an engineering nature require an immediate solution, even though the fundamentals of the problem are still not completely understood. The engineer must do what he can with the available data and cannot wait for the physicist to provide, from theoretical considerations and laboratory observations, a more sophisticated understanding of the problem. A knowledge of the lightning stroke is of this nature. It has a profound influence upon the design of electric power transmission lines. This article emphasizes those aspects of the stroke that are of primary interest to the engineer and, in some respects, extrapolates the characteristics of the stroke from laboratory-scale models, without necessarily providing a detailed understanding of the physical nature of the phenomena involved.

Consistent with this approach, the meteorological and physical aspects of charge separation and other phenomena within the cloud will be bypassed. The discussion will begin with the assumption that the discharge is already established and on its course toward the earth. The vast majority of strokes are of negative polarity in that they lower a negative charge to earth. The stroke that eventually develops from the discharge may consist of only one or of many components. The average velocity[1] of the downward leaders is small, of the order of 0.001 *c*, where *c* is the velocity of light.

As the stroke approaches the earth or a projection from the earth, there is evidence[2,3] that a leader extends from the earth or from the projection to meet the downward leader. This is followed by a highly luminous return stroke that travels upward at a most frequent velocity of 0.12 *c*. The high current associated with the return stroke may reach a value of 100 kiloamperes or more. Its duration is approximately 150 microseconds.

After a variable time of about 0.01 to 0.1 second, a second component of the stroke may occur. The leader of this component does not possess the marked steps of the first component. The steps, if present at all, are short and rapid.[4] Because of the apparent absence of steps and their higher average velocity (0.01 *c*), these leaders are called "dart" leaders. The time to crest of the return current is shorter than the time to crest of the first component. The meager information available indicates, however, that the crest of the return component is smaller than for the first component. The second component may be followed by subsequent components that are similar to it.

Two other types of discharges exist. First, there are positive discharges that originate from the cloud. Berger's data[5] indicate that they are usually of very high value; one stroke reached a value in excess of 180,000 amperes. These positive discharges consist of only one component. Second, there are discharges that originate from the earth on tall objects, such as very tall buildings, masts, or mountains. These discharges have subsequent components of negative character that originate from the cloud in the form of dart leaders as in the case of the negative cloud-initiated stroke.

THE DOWNWARD LEADER

Although considerable controversy exists concerning the detailed explanation of downward-leader phenomena, there does seem to be general agreement that the leader consists of two parts: a thin core or channel of high conductivity, and a corona sheath or negative space charge that precedes and surrounds the channel.[7] It is impossible to specify

Part I of a two-part article, prepared originally for publication in German in a current issue of Elektrotechnische Zeitschrift. C. F. Wagner, Fellow IEEE, is a consulting engineer, Pittsburgh.

90004077

POOR ORIGINAL

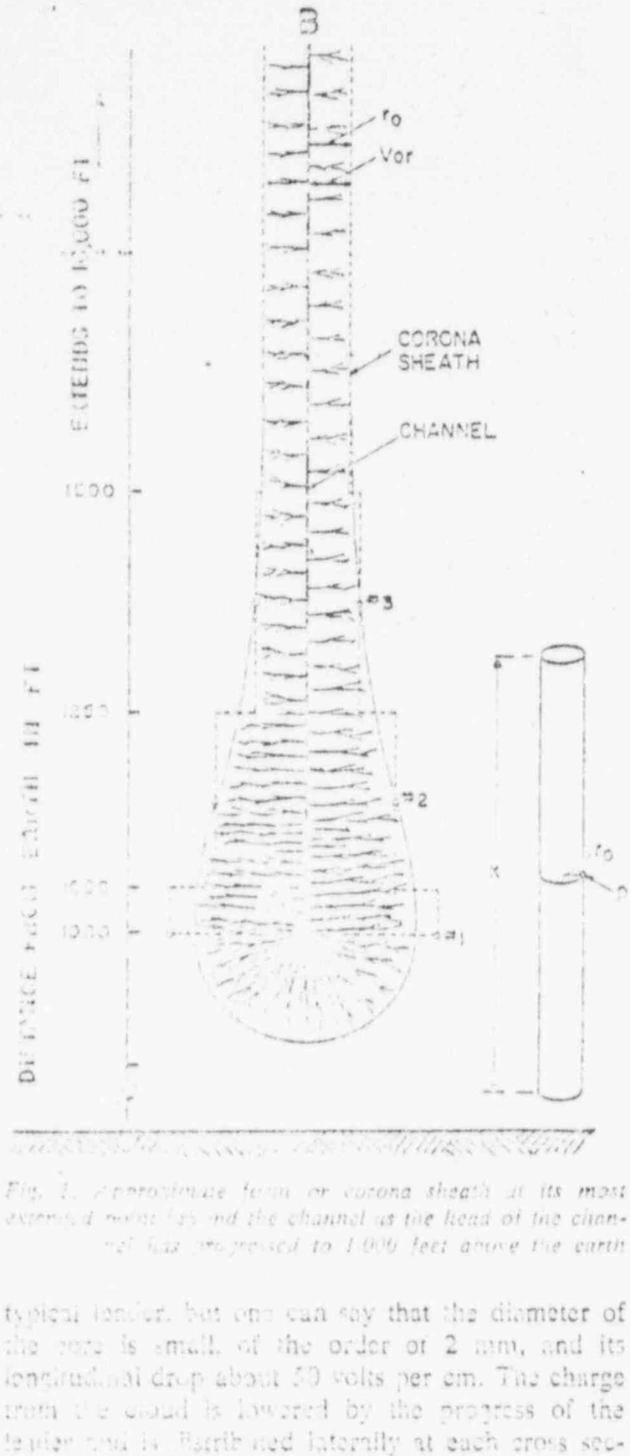

Fig. 1. Approximate form of corona sheath at its most extended point beyond the channel as the head of the channel has progressed to 1,000 feet above the earth

typical leader, but one can say that the diameter of the core is small, of the order of 2 mm, and its longitudinal drop about 50 volts per cm. The charge from the cloud is lowered by the progress of the leader and is distributed laterally at each cross section in the form of a corona space charge. The return stroke is formed by progressively tapping and lowering this distributed charge to earth as its tip reaches any particular lateral section. Thus, substantially the same charge is involved in the formation of the leader as is involved in feeding the high-valued return-stroke current. To form a conception of the order of magnitude of this distributed charge, consider a vertical stroke whose ultimate return-stroke current has a crest value of 50,000 amperes. Suppose further that the velocity of the tip of the return stroke is 0.3 c. The charge per unit length can then be derived from:

[illegible] (1)

where i is the current in amperes, v the velocity expressed as a fraction of that of light, and q is the charge in coulombs per cm. This expression then gives a value of 6×10^{-6} coulombs per cm. By similar reasoning, the leader current, if the average velocity of the downward leader be 0.001 c, is inversely proportional to the two velocities, or 170 amperes. Although the central conducting core has not actually been observed, only an arc plasma can provide the necessary conductivity. Higham and Meek[?] have shown that when an arc having a value between 50 and 1,000 amperes is suddenly established, the drop decreases from an initially high value to 100 volts per cm at 2 microseconds and a later stable value of 50 volts per cm in [illegible] microseconds. They also found that the diameter of a 150-ampere arc is about 2 mm.

For reasons given in reference 7, the writer and his associate, A. R. Hileman, have been prompted to assume that the charge distribution in the downward leader varies inversely as the radial distance from the channel core. Fig. 1, taken from that reference, shows the general shape of the corona space charge envelope with the tip of the channel located 1,000 feet from the earth and at an instant during the [illegible] process at which the space charge has attained its maximum extent before the reinitiation of the channel. Table I indicates elements in the computation, the leader having been divided into five sections for this purpose. The potential of the channel is shown to be about 53 × 10^6 volts. Row [illegible] the distribution of the charge along the length of the leader. The resistance drop in the channel was neglected because, in the writer's opinion, the assumptions did not warrant such accuracy. Other factors equally important affect the results, such as the vertical gradient produced by remaining charges within the cloud and the fact that with longer time of the leader, opportunity is given within the corona sheath behind the tip for migration of [illegible] so that the conditions approach a d-c corona distribution rather than an impulse distribution. Furthermore, as the head moves downward it leaves behind heavier ions that had already advanced radially to the maximum radius of the head.

As will be discussed later, the potential of the downward leader can also be estimated through a

Table I · Determination of leader potential, charge densities, and corona sheath envelope for Fig. 1

Row	Due to Charge Density in This Section	[illegible] 1	2	3	4	5
a	1	[illegible]	[illegible]	[illegible]	[illegible]	[illegible]
b	2	[illegible]	10.6	[illegible]	[illegible]	[illegible]
c	3	[illegible]	[illegible]	11.0	[illegible]	[illegible]
d	4	4.5	[illegible]	10.5	[illegible]	[illegible]
e	5	[illegible]	[illegible]	[illegible]	[illegible]	[illegible]
f	V_T in megavolts	[illegible]	[illegible]	[illegible]	[illegible]	[illegible]
g	q_0 in tenths of microcoulombs/cm	[illegible]	[illegible]	[illegible]	[illegible]	[illegible]
h	r in feet	[illegible]	[illegible]	[illegible]	[illegible]	[illegible]
i	Vor in megavolts	[illegible]	[illegible]	[illegible]	[illegible]	[illegible]
j	[illegible]	[illegible]	[illegible]	[illegible]	[illegible]	[illegible]

90004078

knowledge of the surge impedance of the return streamer.

According to the records of the electric field remote from the stroke, made by Kitagawa and Kobayashi[4] and also by Kitagawa and Brook,[5] the time interval between steps as the leader approaches the earth becomes shorter and shorter. While remote from the earth, the step interval is 50 microseconds; but this progressively decreases to 20 and finally 13 just before the earth is reached. It would be surmised that the lengths are correspondingly shorter but, to the writer's knowledge, good evidence of the stroke phenomenon near the earth is not available. Except for the discussion that follows immediately, the step phenomenon will be neglected, because it can have only a secondary effect upon the phenomenon occurring near the earth. Thus, as the leader approaches the earth, it will be assumed to approach at a constant rate.

However, before leaving the discussion of steps, one additional observation should be made. The steps, in the writer's opinion, result from the contrasting character of two attributes of the leader.[7] It was stated in connection with Fig. 1 that a corona space charge develops in advance of the arrested, highly conducting channel or core.

In the laboratory, when an impulse voltage too low to cause flashover is applied across a rod–plane gap, a charging current flows, but superposed upon the charging current is a short-time impulse corona current that rises very rapidly to crest and then decreases slowly to zero. The decay of the corona current may be attributed to the development of a corona space charge that finally inhibits further flow of current. This condition tends to occur in the case of the stroke leader; but before the stroke current is completely sealed off, the space-charge atmosphere in advance of the arrested (or almost arrested) channel becomes favorable for the development (or further advance) of the channel. This state has its analogy in the laboratory rod–plane gap when a voltage slightly in excess of the critical sparking voltage is applied. After the space charge development stage is almost completed, channels begin to form. The current supplying these channels increases at first slowly and then faster at an ever-increasing rate.

In each step the lightning channel extends in the form of a thin pencil of plasma and ceases when the tip has reached a point at which the space-charge conditions are no longer conducive to the further extension of the plasma. The space charge then continues its slower advance and the process is repeated. The average value of the channel current must be of the order of 100 or 200 amperes; its initial value is probably much less than this, and since the current tends to increase exponentially, the final value must be much greater—perhaps 1,000 amperes. The corona space charge is not photographically sensitive and the short time that the channel current is of large value creates the impression of very fast and halting steps.

POOR ORIGINAL

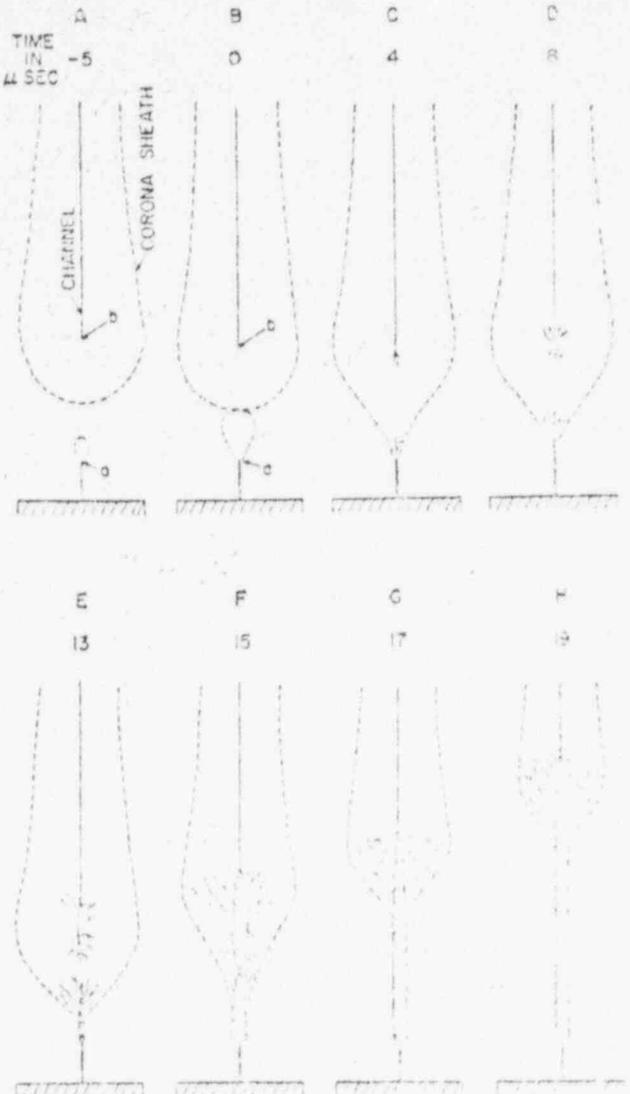

Fig. 2. Stages in the development of an upward channel

APPROACHING THE EARTH

Fig. 2 depicts the stages of the stroke as it nears the earth for the last step.[7] The channel of the leader is shown as a thin vertical line which in (A) has its tip at *b*. The potential of the channel will be taken as −50,000,000 volts and its velocity earthward is about one foot per microsecond. The leader is shown approaching a 100-foot mast. While specific numbers are ascribed to the various stages, it should be realized that the actual values vary over wide limits.

Fig. 2(A) shows the position of the channel at an instant at which the tip *b* is still 400 feet above the earth. It is surrounded by its negative corona sheath. When the channel is even more remote than this, a corona discharge begins to develop from the mast, and at this instant has already become stable. The discharges, which develop from the mast ...

90004079

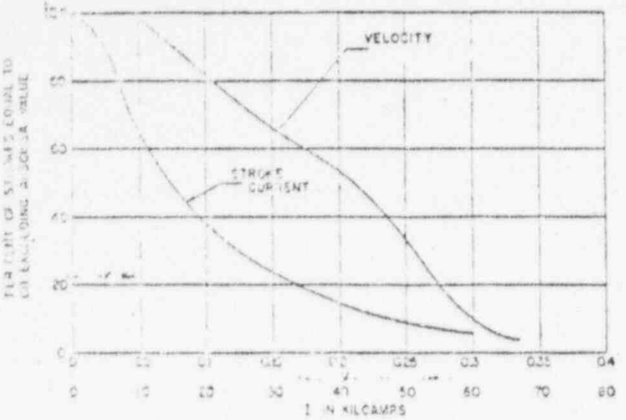

Fig. 3. Relation between frequency of occurrence of lightning strokes (AIEE curve) and velocity of return stroke

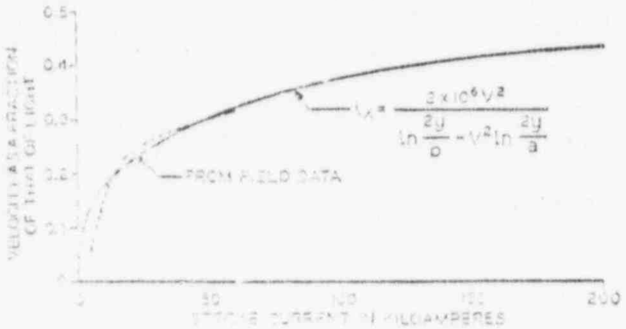

Fig. 4. Relations between stroke current and velocity of return stroke

POOR ORIGINAL

gradient exceeds the critical value of about 30,000 volts per cm, do not appear to be particularly important. They occur on any projection in the vicinity. The channel and its associated corona sheath continue their slow advance toward earth, and meanwhile the corona space charge above the mast also increases.

A critical point is reached in (B), at which the separation between *b* and the top of the mast in this case is 50,000,000/6,000 = 8,300 cm, or 270 feet. Laboratory tests with rod–rod gaps having long spacings indicate that when the average critical gradient of 6,000 volts per cm is exceeded, channels begin to form from both points. This is the instant at which the heavy return-stroke current begins to form, and is the reference point for time given at the top of Fig. 2. Four microseconds later, as shown in Fig. 2(C), the channels from both *a* and *b* have progressed to the points indicated. In 2(D), further progress has been made and the current has grown significantly. At the same time the current feeding the downward moving channel below *b* draws current from the old low-current channel above *b*.

The propagation of this current is slower than the speed of light; it is limited primarily by the speed with which the arc path can accommodate itself to the higher conductivity and the speed with which it can draw the charge from the corona space charge laid down by the leader. And so the progress continues through (E) and finally (F), the instant at which contact is made between the main channels. Fig. 2(G) and (H) show later instants at which the head of the return channel has penetrated farther into the space charge and lowered a further portion of this charge to earth. The magnitude of the current at the different points is suggested by the relative thickness of the lines.

Note also the progress of the upward channel, which is intended to suggest a higher and higher velocity until the last step is completely established, after which the velocity should be constant or decrease as the head of the return streamer advances toward the cloud. As the upward channel progresses, tentacle-like streamers reach outward and upward and tend to spread the positive charge over a greater area than that encompassed by the channel itself.

CREST CURRENT AND VELOCITY OF RETURN STROKE

Knowledge concerning the magnitude of the crest current of the lightning stroke is of an economical nature. Judging from the data concerning the percentage that exceed a particular value (which is usually termed the distribution curve), the knowledge is quite accurate—being based upon a large number of different studies over the past in many countries. But on the other hand, the stroke density (number of strokes per unit area of the earth) is only crudely known. It is based upon the number of storm days at the observer's location; a storm day being any day on which the observer has heard thunder during any of the intervals at which he conducts his other hourly routine observations. During the past few years very promising work has been undertaken, notably by E. T. Pierce, R. H. Golde, D. J. Malan and D. Müller-Hillebrand, in the development of an instrument that will count the number of strokes to ground. In spite of the admittedly crude measure in terms of storm days, this method has proved quite satisfactory in the past; but lightning investigators look forward with keen interest to the development of a satisfactory counter.

In Fig. 3 is plotted the current distribution curve developed by AIEE in 1950 after consideration of all known data available at that time. The velocity of the return stroke is of value in determining the physical phenomena associated with the return stroke. In Fig. 3 is shown the distribution-of-occurrence curve of this velocity as determined by Wagner and McCann (Fig. 20 of reference 11) as a result of their analysis of 19 records presented by Schönland, Malan, and Collens. A similar analysis was undertaken later by Müller-Hillebrand.

If we accept the fact that there exists a single-valued relation between stroke current and the velocity of the return stroke, then it is possible to obtain this relation by taking corresponding for any percentage of distribution. The result is shown by the dashed curve of Fig. 4.

The discussion[12] of what happens in the return stroke as it elongates from the earth can best be advanced by considering first the system of current waves shown in Fig. 5(A). These consist of four rectangular current waves that propagate with a constant velocity vc along the parallel lines aa' and bb', spaced a distance D. It is shown in references 12 and 13 that to establish and maintain a set of currents of this character, an emf equal to

$$V = 60i\,\frac{1}{v}\ln\frac{D}{a} \qquad (2)$$

must be inserted in each line on each side of o at a radius a and, in addition, a series retarding emf equal to

$$V_r = 60i\left(\frac{1}{v} - v\right)\ln\frac{D}{a} \qquad (3)$$

must also be inserted at a radius a at a point that moves progressively along the lines in phase with the heads of the current waves. This leaves a remanent series voltage equal to

$$V_s = 60iv\ln\frac{D}{a} \qquad (4)$$

that moves ahead of the current waves with the velocity of light. When $v = 1$, V_r reduces to zero and the remanent voltage V_s and voltage V become equal to the readily recognizable values usually associated with waves that travel with the velocity of light.

For practical purposes, the retarding voltage V_r can be regarded as concentrated at a point that travels with the head of the current wave. Between the origin o and the head of the wave, the longitudinal drop is zero. Similar relations apply when the current wave rises linearly from o with a sloping front. In this case the retarding voltage is spread out over the entire front of the current wave, and for the same final current has the same overall magnitude.

Tests on short arcs with currents up to tens of thousands of amperes indicate that after the crest current is reached, the drop across the arc decreases very quickly, in probably less than a microsecond, to about 1,000 volts per cm, and then more gradually to much smaller values. This sudden drop in voltage is demonstrated in Fig. 6, which shows the voltage across and the current through a 9-foot rod-rod gap when impulsed by a voltage sufficient to produce sparkover in 3 microseconds. The actual oscillograms are shown in (A) and (B) and their replots in (C). The accuracy of the voltage record is certainly sufficient to indicate a drop of 50 kv, which corresponds to a gradient of 200 volts per cm. And so it seems reasonable to assume that the gradient along the return stroke very quickly attains a value of 200 volts per cm, or less.

However, during the transition period while the arc path of the stroke is accommodating itself from the conductivity of a current of about 200 amperes, which is characteristic of the channel of the downward leader, to the conductivity of the 50,000 amperes or so of the return stroke, a very high transient voltage drop must occur. The diameter of the arc increases from about 2 mm to about 7 cm. During this period the arc must absorb an enormous amount of energy in increasing this volume of gas to the high-temperature characteristic of arc conduction. If the energy requirements derived from the traveling-wave relations are equated to the energy requirements obtained from laboratory tests on gaps, it is possible to develop a relation between the current in the return stroke and its velocity.[12]

Thus, from the circuit condition, it can be seen from Fig. 5(B) that the power absorbed in the battery occurs only during the period during which current flows (which accounts for the factor ½ in the equation) and is consequently

$$P_r = \frac{1}{2}V_r i = 30\left(v - \frac{1}{v}\right)\ln\frac{D}{a}\,i^2 \text{ watts} \qquad (5)$$

The energy input that will bring an arc to a particular degree of conductivity can be determined by measurement of the power input when a long rod-rod gap is broken down by the application of an impulse voltage. Fig. 6 shows the results of such a test. If the replots of voltage across the gap and current through the gap are multiplied and the product is integrated, an input of 5.06 watt-seconds per cm of gap is obtained. Current and voltage oscillograms indicate a sudden increase in current and a sudden decrease in voltage. This point of sudden change was taken as the instant at which the arc channels began to be developed. The small currents prior to this

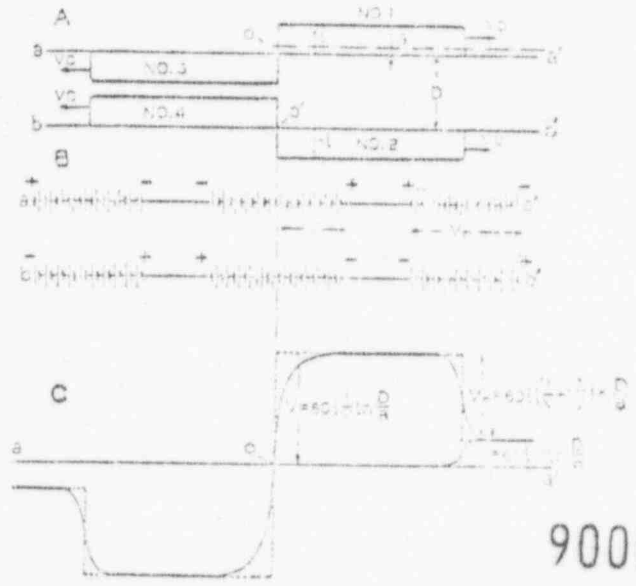

Fig. 5. Illustrating the limiting values of voltages shown in (C) that must be inserted progressively in the lines to maintain the system of currents shown in (A)

POOR ORIGINAL

90004081

for any percentage of distribution. The result is shown by the dashed curve of Fig. 4.

The discussion[14] of what happens in the return stroke as it elongates from the earth can best be advanced by considering first the system of current waves shown in Fig. 5(A). These consist of four rectangular current waves that propagate with a constant velocity v along the parallel lines aa' and bb' spaced a distance D. It is shown in references 12 and 13 that to establish and maintain a set of currents of this character, an emf equal to

$$V = 60i \frac{1}{v} \ln \frac{D}{a} \qquad (2)$$

must be inserted in each line on each side of o at a radius a and, in addition, a series retarding emf equal to

$$V_r = 60i\left(\frac{1}{v} - v\right) \ln \frac{D}{a} \qquad (3)$$

must also be inserted at a radius a at a point that moves progressively along the lines in phase with the heads of the current waves. This leaves a transverse voltage equal to

$$V = 60iv \ln \frac{D}{a} \qquad (4)$$

that travels ahead of the current waves with the velocity of light. When $v = 1$, V_r reduces to zero and the remaining voltage V_r and voltage V become equal to the readily recognizable values usually associated with waves that travel with the velocity of light.

For practical purposes, the retarding voltage V_r can be regarded as concentrated at a point that travels with the head of the current wave. Between the origin o and the head of the wave, the longitudinal drop is zero. Similar relations apply when the current wave rises linearly from o with a sloping front. In this case the retarding voltage is spread out over the entire front of the current wave, and for the same final current has the same overall magnitude.

Tests on short arcs with currents up to tens of thousands of amperes indicate that after the crest current is reached the drop across the arc decreases very quickly in probably less than a microsecond, to about 1,000 volts per cm. and then more gradually to much smaller values. This sudden drop in voltage is demonstrated in Fig. 6, which shows the voltage across and the current through a 9-foot rod-rod gap when impulsed by a voltage sufficient to produce sparkover in 3 microseconds. The actual oscillograms are shown in (A) and (B) and their product in (C). The accuracy of the voltage record is certainly sufficient to indicate a drop of 50 kv, which corresponds to a gradient of 200 volts per cm. And it seems reasonable to assume that the gradient in the return stroke very quickly attains a value of 200 volts per cm, or less.

However, during the transition period while the arc path of the stroke is accommodating itself from the conductivity of a current of about 200 amperes, which is characteristic of the channel of the downward leader, to the conductivity of the 20,000 amperes or so of the return stroke, a very high transient voltage drop must occur. The diameter of the arc increases from about 2 mm to about 7 cm. During this period the arc must absorb an enormous amount of energy in increasing this volume of gas to the high-temperature characteristic of arc conduction. If the energy requirements derived from the traveling-wave relations are equated to the energy requirements obtained from laboratory tests on gaps, it is possible to develop a relation between the current in the return stroke and its velocity.[15]

Thus, from the circuit condition, it can be seen from Fig. 5(B) that the power absorbed in the battery occurs only during the period during which current flows (which accounts for the factor ½ in the equation) and is consequently

$$P_r = \frac{1}{2} V_r i = 30\left(v - \frac{1}{v}\right) \ln \frac{D}{a} i^2 \text{ watts} \qquad (5)$$

The energy input that will bring an arc to a particular degree of conductivity can be determined by measurement of the power input when a long rod-rod gap is broken down by the application of an impulse voltage. Fig. 6 shows the results of such a test. If the records of voltage across the gap and current through the gap are multiplied and the product is integrated, an input of 5.06 watt-seconds per cm of gap is obtained. Current and voltage oscillograms indicate a sudden increase in current and a sudden decrease in voltage. This point of sudden change was taken as the instant at which the arc channels began to be developed. The small currents prior to this

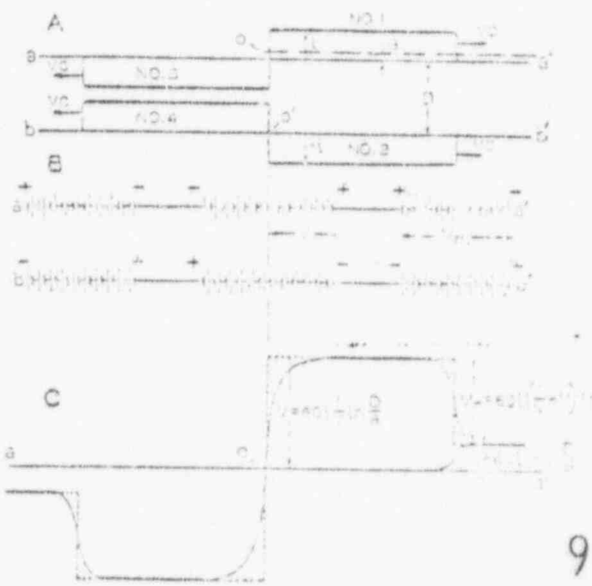

Fig. 5. Illustrating the limiting values of voltages ... (C) that must be inserted ... the system of currents ...

POOR ORIGINAL

instant were assumed to be associated with the development of the space charge. The current for this case was taken as 1,700 amperes; thus the energy becomes equal to 0.0018 watt-second per cm per ampere. Averaging the results of a large number of similar tests on 3-, 6-, and 9-foot rod–rod gaps gave a result equal to 0.0020 watt-second per cm per ampere. The actual power input into the arc of the return stroke must be proportional to its velocity in cm per sec, which is v times c times the current. Thus

$$P_r = vc(0.0020)\, i \text{ watts} \qquad (6)$$

Equating 5 and 6,

$$i = \frac{c(0.0020)}{30 \ln \dfrac{D}{a}} \frac{v^2}{1 - v^2} \qquad (7)$$

or

$$v = \frac{1}{\sqrt{\dfrac{c(0.0020)}{30 i \ln \dfrac{D}{a}} + 1}} \qquad (8)$$

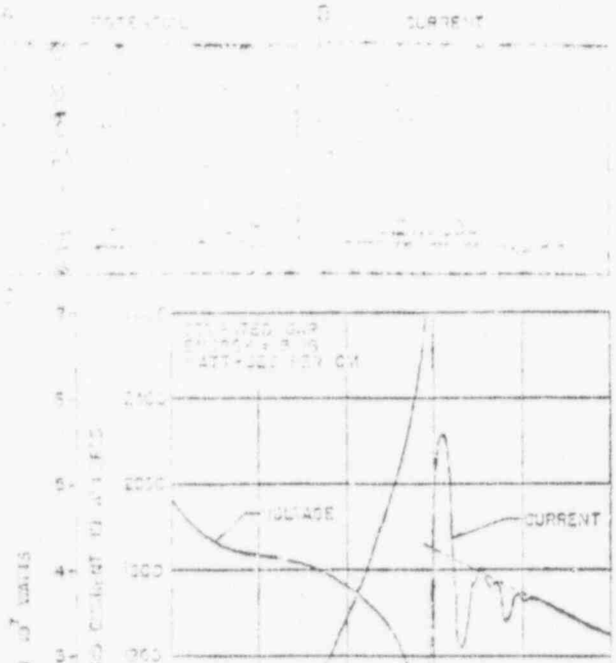

Fig. 5. Gap voltage (A) and current (B) for flashover of a [illegible] gap together with their product and instantaneous power in (C)

The foregoing assumption—that the effective radius at which the charge might be considered concentrated and the radius of the cylinder in which the current flows are identical—is erroneous. The charge is concentrated at a much larger radius b and the current at another point, such as a. Then, as shown in references 12 and 13, when this distinction is made, equation 7 becomes

$$i = \frac{v^2 c(0.0020)}{30\left[\ln \dfrac{D}{b} - v^2 \ln \dfrac{D}{a}\right]} \qquad (9)$$

In the interests of simpler presentation, the foregoing expression was developed for waves that travel parallel to each other, whereas in the actual case the wave travels upward from a flat plane. However, in reference 12 it is demonstrated that an expression identical to equation 9 results for this case if D is regarded as the instantaneous distance from earth that the tip of the return stroke has traveled.

To establish an analytical relation between i and v, the following parameters will be assumed. Because of the logarithmic manner in which D enters the expression, it is not critical with respect to this quantity, so D will be taken as 300 feet ([illegible] meters), representing the distance traveled by the time the stroke current reached maximum value. Because, also, of the factor v^2 ahead of the term involving a, the value of a is not critical and will be taken as 0.1 foot (3.05 cm), applying over the entire range of currents. The factor b is somewhat more critical, but actually very little precise information is available concerning the distribution of the charge around the downward leader. The assumption will be made that for a stroke whose resulting current is ultimately equal to 100,000 amperes, b will be made equal to 10 feet and for other values the radius will be proportional to the original charge. With these assumptions, the full-line curve of Fig. 4 is obtained. This curve can be compared with the curve for the field data.

Lundholm,[14] Rusck,[16] and later Müller-Hillebrand[9] derived similar expressions based upon the empirical relation of Toepler's[18] that states that the resistance of the path in a spark discharge varies inversely as the charge passing that point in the discharge path. Their results are given in the form of equation 8, in which a constant A replaces the quantity $c(0.0020)/30 \ln (D/a)$. If, again, $D = 300$ feet (91.4 meters) and $a = 0.1$ foot (3.05 cm), $A = 250,000$. This compares with the value 900,000 suggested by Lundholm; 500,000 by [illegible] and 200,000 for the first 5 microseconds of travel of the return stroke, and 500,000 for the mean [illegible] of development in the three-dimensional [illegible] suggested by Müller-Hillebrand.

CURRENT WAVE FRONT OF RETURN STROKE

Prior to the past few years, the writer [illegible] with other investigators in [illegible]

90004083

waveform of the current of the return stroke at the ground as the difference of two negative exponential curves, such as given by Bruce and Golde[17] in which the current rises rapidly at first, reaches a crest, and then decays slowly. For purposes of transmission-line computations this waveform was usually approximated by a linearly rising front to either 2 or 4 microseconds with a flat top. It was only after further contemplation of the results obtained by Berger[13] in his careful, patient, and painstaking investigation atop Mount San Salvatore, together with an effort to correlate these results with those obtained in the laboratory, that the writer and his associate, A. R. Hileman, became convinced that the waveshapes of all return stroke currents were concave upward to the crest value and then varied somewhat erratically, depending upon the complexities of branching.

Fig. 7 is a replot of the fronts of the larger currents reported by Berger[13] in 1955 from his results on Mount San Salvatore. Because of the gradual rise of the beginning of the fronts, the actual starts were not well defined. Therefore, the curves were translated so that they all passed through 40,000 amperes at the same instant. Fig. 8 shows a later series of oscillograms obtained by Berger[1] during 1959 and 1960.

Of importance in a discussion of this question is the evaluation of the surge impedance of the stroke. The downward leader in discharging into the final step between a and b of Fig. 2 offers an impedance to the rate at which this discharge can occur through the velocity at which the return stroke above the point b, as shown in Fig. 2(F), can propagate within the space charge laid down by the downward leader. This impedance is a function of the height of the tip of the return stroke and also its velocity. In reference 12 the following approximate expression is given for the potential of the stroke:

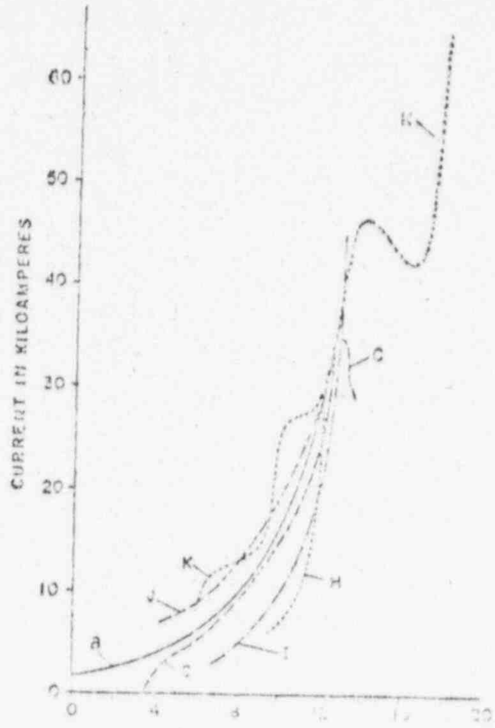

Fig. 7. Replot of the oscillograms of high stroke currents recorded by Berger,[13] translated with respect to time to pass through 40,000 amperes at the same instant.

$$V = 60\,I\,\frac{1}{v}\ln\frac{2D}{b} \qquad (10)$$

With I equal to unity, this expression can be used to evaluate the impedance. From Fig. 5 of the same reference, the following estimated values of v and b can be used to evaluate the impedance Z. Thus, if D be taken as 200 feet

I, amperes	50,000	10,000
D, feet	300	300
b, feet	6	2
v, a numeric	0.3	0.17
Z, ohms	920	2,000

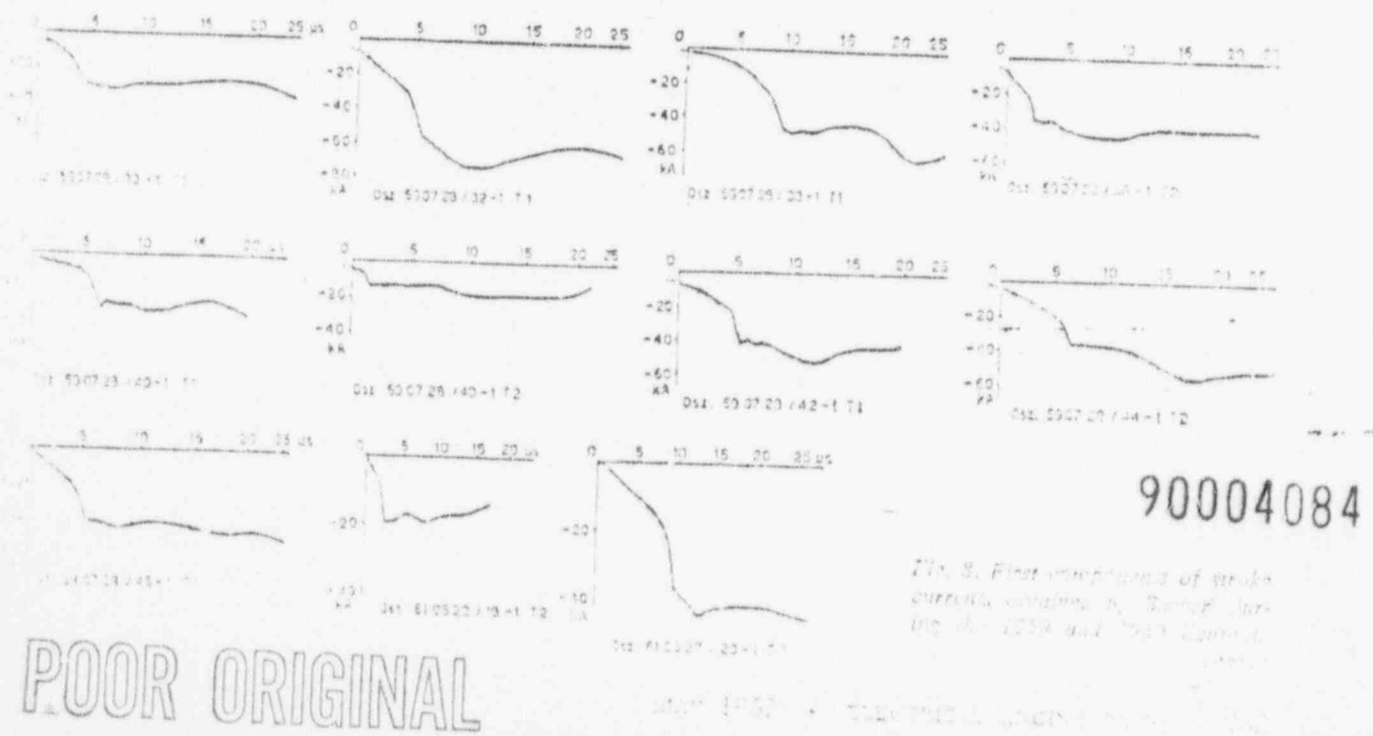

90004084

Fig. 8. First components of stroke currents obtained by Berger during the 1959 and 1960 ...

POOR ORIGINAL

The series impedance of the stroke is thus about 1,500 ohms.

It is shown in reference 20 that for rod–rod gaps between 20 inches (30.5 cm) and 100 inches (254 cm) in length, the time lag for the application of a 1.5x40-microsecond wave is independent of the gap length. This fact gives some justification for extrapolating from gaps of laboratory dimensions to those of natural lightning dimensions.

Fig. 9(B) shows the wavefront of the first component of current of lightning strokes. The letter designations on the curves refer to the corresponding curves of Fig. 7. The curves in Fig. 9(A) are computed curves[19] based upon: (1) an extension of the work of Akopian, Larionov, and Torosian[20] in which they demonstrated that for a 125-cm rod–rod gap, the velocity with which the channel tips from the two electrodes approach each other is proportional to the excess of the instantaneous gradient in the unbridged gap over the critical sparking gradient, which is independent of the gap length; and (2) the assumption, supported by tests, that the current taken by the gap is proportional to the velocity at which the channels approach each other. Figs. 9(C) and (D) show the results of actual tests, the former for rod–rod gaps and the latter for a rod–plane gap. In all cases, the current is plotted as a ratio of the final current, and time is plotted from the instant that crest current is reached.

It will be observed that all of the curves have the same general shape in that they are concave upward. Furthermore, the time scales are of the right order of magnitude. It thus appears that gap discharges observed in the laboratory can be applied directly to determine the nature of lightning phenomena. The excellent correlation between the observations in the laboratory and those on Mount San Salvatore provides confidence in the fact that, although the latter were obtained by means of a tall mast atop a high hill, they should be characteristic of similar phenomena on flat terrain as well.

COMPONENTS SUBSEQUENT TO THE FIRST

To this point, consideration has been given largely to the first component of a stroke. Of possible interest to the transmission engineer are the subsequent strokes. In Fig. 10 are shown a number of oscillograms for subsequent components, also obtained by Berger,[8] for the period 1959–61. Because of late tripping of the oscillograph, it was impossible to obtain the entire front for the 1959 records (identified by 59 in the first two digits of the numbers). But by subsequent calibration of the trip circuit, it was determined that the front must have been less than

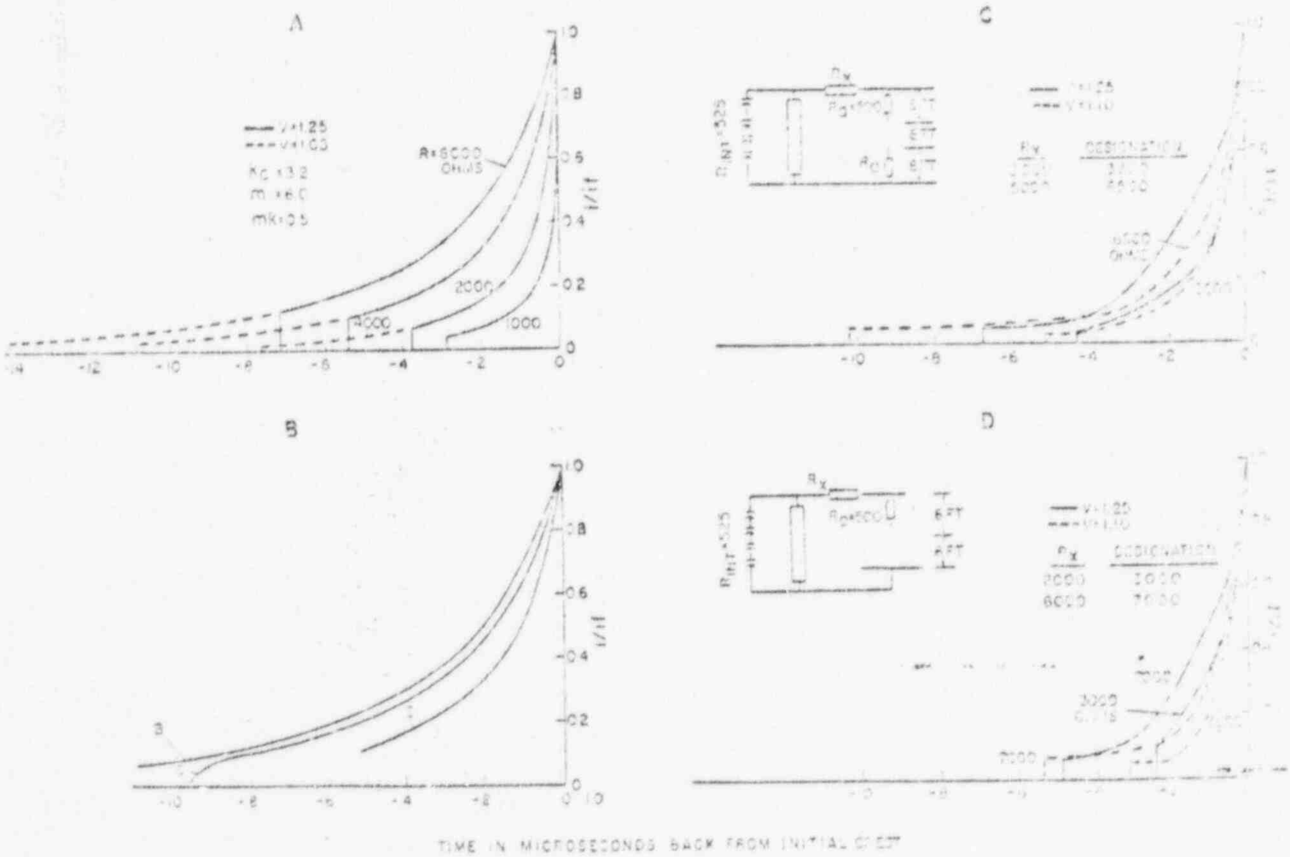

Fig. 9. Evaluation of return-stroke surge impedance from slope of return-stroke current wavefront. (A) Predischarge currents in rod–rod gaps, from computations. (B) Lightning-stroke currents measured by Berger. (C) [illegible] discharge currents in rod–rod gaps. (D) [illegible] charge currents in rod–plane gap. [illegible]

C. F. WAGNER

The lightning stroke as related to transmission-line performance

PART II

In the conclusion of this two-part article, the efficacy of ground wires in shielding the phase conductors is described in terms of the length of the striking distance of the downward leader. Upward concave return strokes, as well as repetitive strokes, have also been studied. The use of "pipe–pipe" gaps across insulator strings effectively improves the lightning performance of the line

It has long been accepted that the principal role of the ground wire is to intercept the stroke. Then, with sufficiently low tower-footing resistances, it has always been assumed that satisfactory transmission-line performance would be attained. However, with the introduction of extra-high-voltage transmission and its higher towers, unexplained outages developed, resulting in the need for a re-evaluation of methods of computing line performance and for a more detailed study of the stroke mechanism.

SHIELDING

Provoost[21] presented at Paris in 1960 an excellent résumé of the role of the ground wire in shielding the conductors. Supplementing this review the writer wishes to make the following additions to this rather complex problem.

Some of the earliest work was done on simulated models. It was recognized that precise similitude relations might not apply to reduced scale models. The Writer, McCann, and MacLane,[22] for example, in 1941 attempted to determine these relations by changing the model scale and by altering the relative cloud height. The theories of stroke propagation and spark breakdown that have been developed since that time would have provided reliable guidance on the proper cloud height or striking distances to use. Another approach to this problem is geometrical in nature, but its application is dependent upon setting up a criterion to determine the location of the lower tip of the downward leader at the instant at which the ultimate stroke termination—whether to the conductor, to the ground wire, or to the ground—becomes decisive. Golde,[23] assuming a particular charge condition of the leader, computed the electrostatic field strengths next to earth and assumed that the point to be struck is definitely chosen as soon as upward streamers develop from the earth or earthed objects. Strokes to earth were to be decisive when the computed gradient at the earth was 10 kv per cm. The writer followed another course[12] and computed the critical striking distance from a computation of the stroke potential and the critical breakdown gradient as determined from extrapolated laboratory tests. Young, Clayton, and Hileman[24] in a recent paper also adopted this approach in determining the location of the ground wire. Their analysis will be discussed in more detail later.

It would appear that the records of actual experience on the operation of transmission lines would provide the best measure of the protective angle. It is not always possible to determine precisely what faults are caused by lightning and when this fact is established it is not always possible to determine whether the particular failure was caused by a direct stroke to a conductor or by a back flash. To support the conclusions reached with models, the writer, Mc-

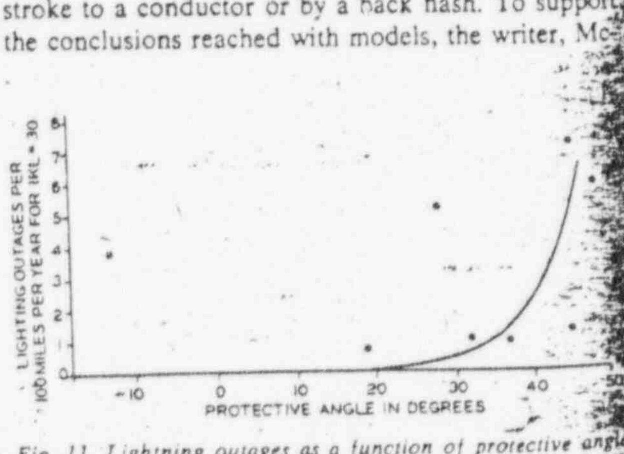

Fig. 11. Lightning outages as a function of protective angle for 110 to 165 kv, with average tower-footing resistances less than 10 ohms, as reported by AIEE committee 193

Part II of a two-part article, prepared originally for publication in German in a current issue of *Elektrotechnische Zeitschrift*.

C. F. Wagner, Fellow IEEE, is a consulting engineer, Pittsburgh, Pa.

90004086

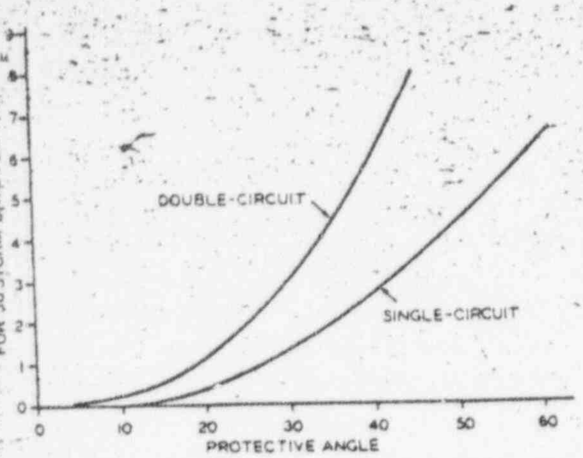

Fig. 12. Lightning faults as reported by W. Casson[25]

Cann, and MacLane[22] examined the data available in 1940 and published, among other curves, the one shown in Fig. 11. This curve was based upon the experience of a large number of lines in the voltage range between 110 and 165 kv, for which the average tower footing resistance was less than 10 ohms. In drawing the curve more weight was given to the points representing the larger circuit-years of experience. In 1959 Casson[25] presented the results of a survey questionnaire, which has now been extended and covers the performance of 180 circuits comprising 24,197 kilometers in the range above 225 kv. Fig. 12 is taken from this report. The breakdown into single-circuit and double-circuit experience shows the effect of the higher towers of the latter. In 1958 Burgsdorf[26] showed the same effect of the height of the line, but went further in that he computed the number of expected back flashes and, subtracting these from the actual flashovers, segregated the number of direct flashovers. This, of course, assumes an accuracy of back-flashover computation that may not be warranted in all cases. Kostenko, Polovoy, and Rosenfeld[27] extended this work to extra-high-voltage systems and found the following empirical relation to express the quantity ψ_{by}, which is defined as the ratio of strokes hitting the phase conductors to the total number of strokes hitting the line.

$$\log \psi_{by} = \frac{\alpha \sqrt{h_t}}{90} - 4 \qquad (11)$$

where

α = protective angle at the tower, degrees
h_t = ground wire height at the tower, meters

This function is plotted in Fig. 13 for three different heights. In the United States, experience indicates that the number of strokes to a line is about 100 per 100 miles per year. Taking this factor into consideration it is found that the curve in Fig. 11 agrees extremely well with the curve in Fig. 13 for $h = 30$ meters. The implication, of course, is that all of the outages for Fig. 11 were caused by shielding failures, which might well be the case because of the low tower-footing resistances.

These conditions of shielding are quite consistent with the picture of the stroke mechanism presented earlier in this article. As mentioned previously, the driving potential necessary to establish a rectangular wave of charge and current that moves vertically upward from the earth is given by equation 10, where y is the distance from earth to the head of the wave at any instant and b is the radius at which the charge can be regarded as concentrated. Inserting the value of i from equation 9 into this expression, then

$$V = 1.2 \times 10^8 v \frac{1}{\left[1 - v^2 \ln \frac{2y}{a} \Big/ \ln \frac{2y}{b}\right]} \text{ volts} \qquad (12)$$

The parameter a varies linearly with current and b almost linearly. If a be assumed equal to 0.1 foot and b 10 feet at 100,000 amperes, then equation 12 can be approximated by

$$V = 1.2 \times 10^8 \frac{v}{1 - 2.2 v^2} \qquad (13)$$

This equation indicates that the stroke potential is dependent upon v only. According to the stroke mechanism theory presented here, the length of the final striking distance as the downward leader approaches the earth is equal to the stroke potential divided by the critical breakdown gradient, which is about 5,000 or 6,000 volts per cm. The smaller the final striking distance, the smaller must the shielding angle be to provide adequate shielding. Therefore, to be conservative the value of 6,000 volts per cm is used and the final striking distance X_s becomes

$$X_s = 2 \times 10^4 \frac{v}{1 - 2.2 v^2} \text{ cm} \qquad (14)$$

$$= 656 \frac{v}{1 - 2.2 v^2} \text{ feet} \qquad (15)$$

This expression indicates that the last striking distance also is a function of v alone, or since v from

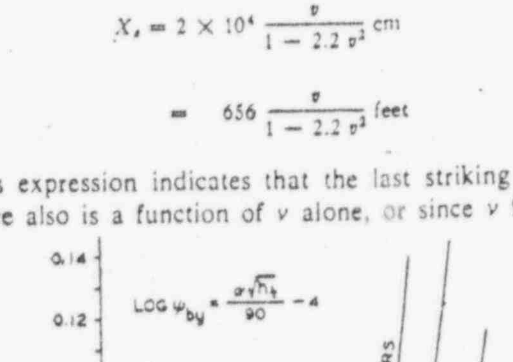

Fig. 13. Probability of shielding failures according to Kostenko, Polovoy, and Rosenfeld[27]

90004087

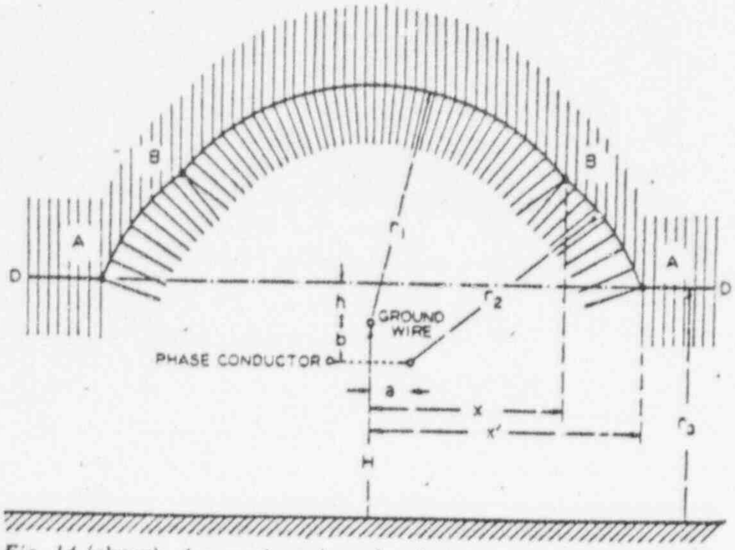

Fig. 14 (above). Assumption of stroke diversion according to Young, Clayton, and Hileman[24]

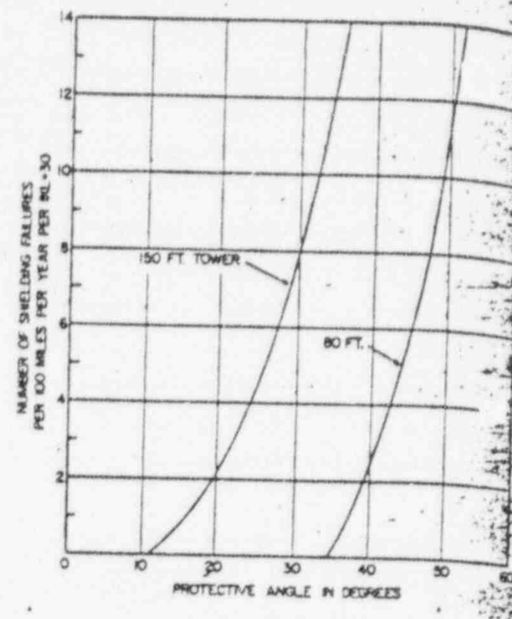

Fig. 15 (right) Shielding failures according to Young, Clayton, and Hileman, with fifteen 5¾-inch insulators; b = 15 feet

Fig. 4 is a single-valued function of the return stroke current, X_s is also a function of the current alone.

Table II gives both the stroke potential and the striking distance as determined by these relations. The stroke potentials are of the order usually associated with this quantity by other investigators in the field. From the fact that the striking distance can be of the same magnitude as tower heights, it can be surmised that the protective angle should be a function of the tower height.

The direction of propagation of a leader can be viewed as being influenced by two different effects. The first is the general directive field produced by the electrostatic field between the cloud and the earth, which determines the general path of propagation of the leader from the cloud to the earth. It is affected by the different cells of charge concentration within the cloud. In some cases this field will produce cloud-to-cloud discharges rather than cloud-to-earth discharges. It provides the general guidance of the discharge. The second effect is the more random field at the head of each step. This field is responsible for the sudden change in direction that sometimes occurs when a step is arrested and subsequently reinitiated.

If the earth plane were perfectly flat, one could assume that the stroke density would be uniform over the entire surface. In this case a projection from the earth of height *h* feet that is small in comparison

Table II · Stroke potentials and striking distances at various currents

I, amperes	V, megavolts	X_s, meters	X_s, feet
20,000	28.0	50	164
40,000	40.3	68	222
60,000	48.8	83	273
100,000	64.0	111	364
150,000	76.8	134	438
200,000	34.8	150	491

with the striking distance X_s would, as shown by Walter,[28] attract all the strokes within a radius *r* on the earth, so that

$$r = X_s\sqrt{2h/X_s}\ \text{feet} \quad (16)$$

or within an area, so that

$$A = 2\pi r^2 = 4\pi X_s h\ \text{square feet} \quad (17)$$

Thus a person 6 feet tall, if the striking distance is 300 feet, would attract all strokes within a radius of 60 feet.

If the assumption is maintained that the projection from the earth does not influence the stroke density, then as the height is increased all the strokes within a radius of X_s should be collected by the projection and a further increase should not increase the number. This conclusion does not agree with experience. A height is finally attained at which the attractive effect is increased either by simply altering the field or by the production of secondary effects, such as increased glow discharge currents as premised by Müller-Hillebrand.[9]

For the moment let us continue to assume that projections from the earth of the height of transmission-line towers do not affect the uniform stroke density. The degree of shielding can then be computed on a purely geometric basis.

In Fig. 14 the strokes between *B* and *B* would be attracted to the ground wire, between *A* and *B* on each side to the conductors, and between *D* and *A* on each side to the earth. Young *et al.*[24] attacked the problem on this basis. They first assumed the relation between *v* and *i* given in Fig. 4, computed the stroke potential in accordance with equation 15, and took the statistical distribution of current into consideration. They determined the number of shielding failures from operating experience, subtracting the computed number of back flashes, and then used

these
Becau
they c
distrib
curve
tween
justifi
used
values
earlier
have

Mü
ferenc
for the
more,
the ve
compu
assum
pheno
ward
in the
velocit
param
shown
failure
height
may b
sets of
secure
back fl

The
two ot
sented
countr
exposu
tion ir
attract
second
as dese
than in
This
value c
to be c

It w
tests o
of shiel
and no
of back

The
does no
the obs
manipu
that th
results
stroke
transm

1. T
a geon
striking

these data as a criterion of accuracy of the method. Because the results did not agree with this criterion, they compensated the assumption of uniform stroke distribution and other assumptions by modifying the curve in Fig. 4 to obtain satisfactory agreement between computations and experience. This appears justifiable on the basis that the values for velocity used in the production of this curve were average values over the entire return stroke path, whereas earlier values in the life of the return stroke should have been used.

Müller-Hillebrand[9] has shown a considerable difference between the average velocity and the velocity for the first 5 microseconds of return travel. Furthermore, a modification in one of the relations, such as the velocity–current curve, is justified because in the computation of the potential, the return stroke was assumed to rise directly from the earth, whereas the phenomenon is complicated by the simultaneous upward and downward approach of the heavy currents in the last step. Because these modifications of the velocity-current curve were the most convenient parameter to alter, Young *et al*[24] obtained the results shown in Fig. 15, in which the number of shielding failures are plotted as a function of the ground wire height at the tower and the protective angle. These may be compared with the curves of Fig. 13. Both sets of curves are, of course, based in part on data secured by assuming satisfactory ability to compute back flashes.

The paper, based upon model tests,[22] emphasized two other points that in the light of the theory presented here may be of importance. First, in hilly country, the down-slope side of the line offers greater exposure to lightning than does the same configuration in level terrain. This results from the lesser attraction of the earth to strokes on that side. And, second, in terrain of extremely high resistivity, such as desert country, the protective angle should be less than in terrain with low or moderate soil resistivity. This likewise results from the smaller protective value of the earth, because in effect the towers appear to be of greater height.

It would be highly desirable to make additional tests on transmission lines wherein the single factor of shielding failures is completely isolated from others and not dependent upon supplementary computations of back flashes.

The writer does not wish to imply a precision that does not exist, either with respect to a knowledge of the observations of the strokes or to the subsequent manipulation of their parameters. He does believe that the mechanism of the stroke as presented here results in a rationalization and coordination of the stroke with the shielding failure observations on transmission lines. It has been indicated that

1. The observed phenomenon can be explained on a geometric basis through the medium of the last striking distance.

2. The lengths of the last striking distance vary with the return stroke current, being smaller for smaller currents.

3. The lengths of these striking distances are to the order of 50 to 150 meters.

4. These lengths require that the protective angle for a 50-meter tower be less than for a 30-meter tower.

BACK FLASHES

Back flashes have traditionally been computed by assuming a current that rises linearly to a flat-topped crest value. Berger's waveshapes with their ever-increasing rate pose new questions regarding the adequacy of the linear-front assumption. In computing the probability of flashover of the insulators, only the front of the current wave and a few microseconds after crest current has been attained are of importance. However, to determine the destructive action upon protective devices the entire wave must be considered.

In the past only the effect of the current injected into the tower has been taken into consideration in computing flashovers. With the old assumption that the current rises directly from a stricken tower without the presence of an upward channel, Wagner and Hileman[29] showed that for a current front of two microseconds, the time–space change in charge in the stroke channel above the tower was sufficient to produce a voltage across the insulators of the same order as that produced by the current. But according to the theory presented in Fig. 2 the current develops by the formation of channel simultaneously from the lower tip of the leader and from the tower top. Fig. 16 represents a simple model[10] of the current and charge fluctuations for use in estimating the effect that the charge might have on the voltage across the insulator string. In (A) the

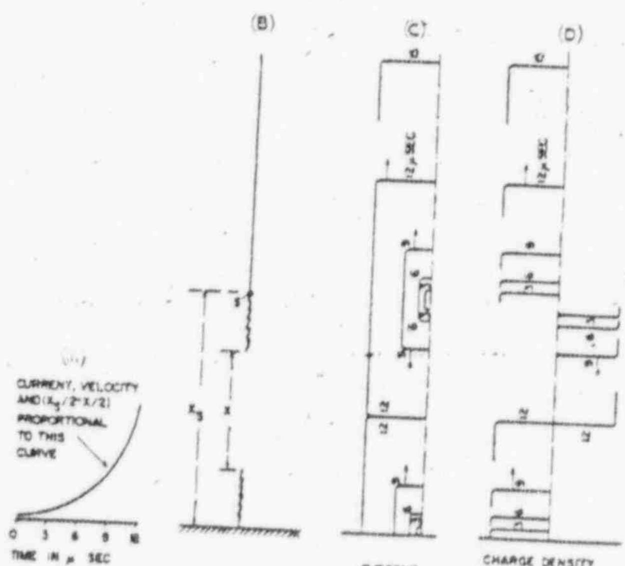

Fig. 16. Time and place variation of stroke current and charge just prior to and after impact with the earth

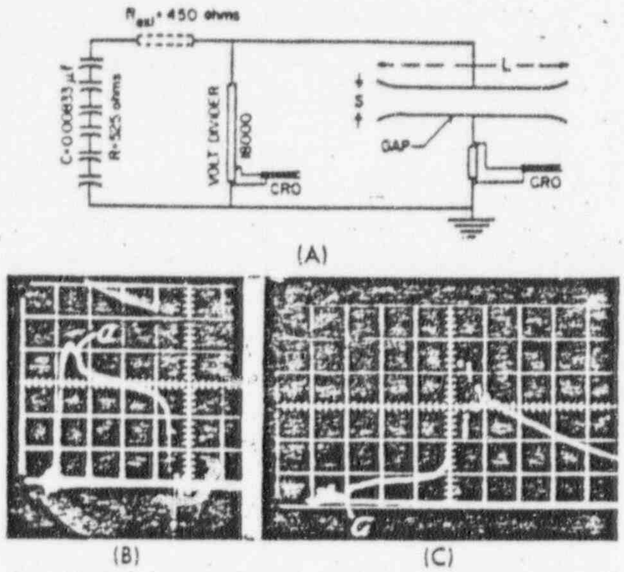

Fig. 17. (A) Surge-generator circuit. (B) Voltage and (C) current oscillograms for a gap having a length of 50 feet and spacing of 6 feet, with a series resistance of 975 ohms. Scale: 369 or 345 amperes per division, 2 microseconds per division

time variations of current, velocity, and the extension of the channels from the earth and from *s* in (B) are shown. In (C) and (D) are shown the corresponding special distributions at the instants marked on each curve. With these approximations it is possible to compute a preliminary estimate of the effect of the time–space change in charge above the tower. Qualitative considerations indicate that the effect is not as great as with the previous assumption of stroke characteristics.

REPETITIVE STROKES

It is still controversial as to whether a current of significant magnitude, measured in several amperes or tens of amperes, continues to flow in the path of the stroke between components. Berger's direct observations of current in the stroke at the earth[18] indicate a value of less than one ampere in the interval between components. This factor is of interest in shedding light on the reason for components subsequent to the first seek.. the same path. A continuous flow of current may n. be a necessary condition for such discrimination. Some authors have vaguely stated that the remanent ionization from the first component provides the guidance for the second component, but have not stated precisely how a greater concentration of ions in the previous path provides the preference factor. McCann and Clark[31] have suggested and given evidence that it is merely a thermal phenomenon. Time is required for the very hot gases comprising the arc plasma of the return stroke to diffuse into the surrounding cooler air. In this process the high-temperature core develops into a larger and larger cylinder of air that gradually drops in temperature. The density of the expanding cylinder is lower than the ambient atmosphere. Since a rarefied gas requires a lower breakdown voltage, it may be argued that this is the discriminative factor.

But regardless of the explanation, the second and subsequent strokes pass down the same path. It may superficially appear that, in a sense, the flashover path of a string of insulators is merely an extension of the stroke path to earth. This theory is not strictly true, however, because in the early stages of the discharge, the stroke current as it strikes the transmission line divides inversely as the surge impedances of the respective paths and only a small part may traverse the insulator string. And in the later stages the portion of the current that flows in the conductor in seeking a path to earth impinges upon the inductance of the transformer, whereas the portion that flows in the tower encounters only a very low impedance. Thus, it does not follow that the same condition prevails in the arc path across the flashed insulator string as prevails in the stroke path. It may be that during the interval between components the arc path across the insulator string has returned to its virgin state.

The effect of wind upon the stroke path of subsequent components is to impart a parallel displacement, which does not seem to affect the breakdown characteristics. A corresponding displacement of the channel of the arc that takes place across the insulator string would carry the terminals of the arc path away from the two ends of the insulator string and influence profoundly the breakdown characteristics of the string.

One would expect for the foregoing reasons that the factors tending to produce repetitive insulator flashovers are much less severe than those tending to produce repetitive strokes. And since the number of insulator string flashovers on high-voltage lines is only a small percentage of the total strokes to the line, it would be expected that the repetitive number of flashovers is very small indeed.

PREDISCHARGE CURRENTS

Although a discussion of the predischarge currents of gaps is not directly related to an engineering examination of the lightning stroke, no discussion of the lightning performance of a transmission line is complete without some reference to their influence. Predischarge currents are magnified in the case of two electrodes that are physically parallel. Wagner and Hileman[32] have applied the term "pipe-pipe gap" to such a gap, simply because their tests were made with pipes as the electrodes and because the term is descriptive.

Fig. 17(A) shows such a gap having a length and spacing *S*, both dimensions in feet. If an impulse voltage below its critical breakdown value is applied to such a gap, then only a relatively small current flows. This current is only sufficiently large to supp discharge. However, if an impulse voltage in excess of the critical value is applied as shown in Fig. 17(B), then at some instant such as *a* a large current flows, as shown by (C), until finally the short-circuit current of the surge generator flows. The increase in current results in an increase drop across the "damping resistance" of the surge generator and is reflected in the sudden drop in the gap voltage. It is found that the average value of the current increases as the "formative time" of the channels, a term which is defined as the interval between *a* and the instant of short circuit of the gap, decreases.

Fig. 18 serves to illustrate the general relations for a gap 50 feet in length having a spacing of 3 feet. The numbers on the curve represent the formative times. If a short-time impulse wave of a particular average voltage, but with duration of less than that given on the curve, is applied to the gap, then flashover will not result. It has also been found that for a particular formative time, the average voltage is substantially independent of the gap length and proportional to the gap spacing. Moveover, for a particular formative time, the average current is proportional to the gap length and to the gap spacing. It follows from these relations that the curve of Fig. 18 can be used to estimate the characteristics of a gap of any proportions.

To illustrate one application, consider how a gap of this nature connected across a string of suspension insulators of a transmission line can decrease the voltage that appears across the insulators when the transmission-line tower is struck by lightning. Suppose that the computed value of voltage that appears across the insulator string, neglecting predischarge currents, is the driving voltage E_t. This is the quantity that is usually taken as the tower-top potential times the quantity one minus the coupling factor. Also, for simplicity, let it be assumed that the waves are rectangular. Let it also be assumed that the full-wave critical flashover value of the insulator string under discussion is 625 kv. This particular value is chosen so that a pipe–pipe gap of spacing 3 feet and 50 feet in length, for which experimental data are available, can be assumed to be connected across the string. The solid line of Fig. 18 gives the relation between the average current through the gap and the average voltage across the gap.

The dots indicate the formative time, which, neglecting the time for the formation of the space charge, is approximately equal to the time to breakdown. If a voltage of 860 kv appears across the gap and insulator string, breakdown will occur in 2 microseconds. However, in the process of breaking down, an average predischarge or prebreakdown current of 2,700 amperes must flow for this time interval. The current must be drawn through some sort of surge impedance of the line. Actually, it flows through the conductor and returns through the parallel circuit consisting of the ground wire and earth. Since half the current flows from each side, the effective surge impedance will be about 150 ohms. The drop through this surge impedance is then 2,700 × 150 volts or 400 kv. This drop is spread out longitudinally along the transmission circuit. In other words, to produce a voltage of 860 kv across the insulator string, a driving voltage of 860 + 400 or 1,260 kv is actually required. This voltage E_t is plotted in Fig. 18 as the dashed line. An alternate method of comparison is to assume that the driving voltage E_t remains equal to 860 kv. Then, moving down along the E_t curve to 860 kv and then dropping vertically to the E_g curve, we find that the voltage across the insulator string and the gap is now 710 kv and the voltage can appear for a period of 2.9 microseconds before flashover occurs.

The inset of Fig. 1 shows the equivalent circuit, which can be set up very easily in the laboratory. The improvement resulting from the use of the pipe–pipe gap can be gauged by comparing the voltage E_g with the voltage E_t.

In the foregoing illustration, a line insulation of 625 kv was assumed. If, for example, a higher line insulation is involved, then the critical flashover value of the gap should be increased correspondingly—the equivalent of increasing the gap spacing. But the predischarge current for a specific formative time is proportional to the gap spacing. Since the surge impedance is substantially independent of the insulation level, the voltage drop through the surge impedance is proportionally higher than the assumed line insulation. It follows, therefore, that for a given length of pipe–pipe gap, the improvement is independent of the insulation level of the line. The ordinate of Fig. 18 can therefore be generalized to reflect this condition by adding the scale showing the ratio of the average gap voltage to the critical flashover of the gap. To the extent that the insulation level increases in proportion to the system voltage, it may

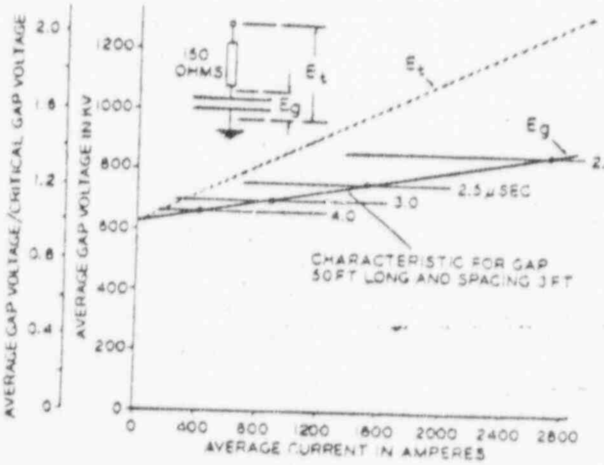

Fig. 18. Voltage–current characteristic of a pipe–pipe gap having a length of 50 feet and a spacing of 3 feet. Dashed line represents total voltage across the gap and a series resistance of 150 ohms

90004091

be concluded that for a given gap length the improvement is independent of the system voltage.

Because the predischarge current is proportional to the gap length, it follows that the improvement should be proportionately greater or less than that indicated in Fig. 18.

An additional characteristic of pipe–pipe gaps is of importance in their application. Tests have shown that their volt–ampere characteristic is unaffected by rain.

CONCLUSION

Transmission line insulation must satisfy three requirements. It must be able to withstand

1. The power-frequency voltage and some degree of contamination. Up to now this has not been a limiting condition and when and if it does become limiting, then doubtless additional research and development will be undertaken to provide a remedy.

2. Switching surges. In some cases at present, switching surges constitute the limiting condition. This limitation can be removed either by eliminating the high surges at their source or by controlling them by adequate lightning arresters. If the latter course is pursued, then it must be remembered that the control of switching surges can be attained by a relatively few number of installations. On the other hand, the provision for the power-frequency voltage or for lightning must be incorporated at every tower.

3. Voltages produced by lightning. Although in some cases lightning does not appear to be a limiting condition, when the necessary improvements are made to withstand normal power-frequency voltage and switching surges, lightning will then become a problem. A line with a phenomenally good operating performance from all causes should be regarded as an overbuilt line. As improvements are progressively made in system design, it becomes more and more imperative that the detailed reasons for the performance be better understood. And so the electrical industry is faced with the need for greater effort to collect information concerning lightning and to understand its effects.

The question of furthering such a policy lies with the managements of electric utilities, who are responsible for the operation of the systems, and, to a lesser extent, with the managements of the manufacturers who must supply the equipment for the systems. How much of the burden should the respective groups carry? What recognition should be given to those particular manufacturers who spend time and effort on system problems in which they have no direct interest? These are some of the questions that must be answered by the electric utility industry. There is great danger that because of the present profit squeeze some of these problems will go by default.

REFERENCES

21. Report on the Work of Study Committee No. 8 (Lightning and Surges). Appendix II. The Shielding Effect of Overhead Earth Wire. P. G. Provost. *Paper No. 314*, CIGRE, Paris, France, 1960.

22. Shielding of Transmission Lines. C. F. Wagner, G. D. McCann, G. L. MacLane. AIEE *Transactions*, vol. 60, 1941, pp. 313–28.

23. The Frequency of Occurrence and the Distribution of Lightning Flashes to Transmission Lines. R. H. Golde. *Ibid.*, vol. 64, 1945, pp. 902–10.

24. Shielding of Transmission Lines. F. S. Young, J. M. Clayton, A. R. Hileman. IEEE Paper 63-640, scheduled for publication in IEEE *Transactions*, pt. III (*Power Apparatus and Systems*), vol. 82, 1963.

25. Report on the Work of Study Committee No. 9 (Extra-High Voltage A-C Transmission). Appendix. Third Report on the Performance of EHV Lines Designed to Operate at Voltages above 225 Kv. W. Casson. *Report No 419*, CIGRE, 1962.

26. Lightning Protection of Overhead Transmission Lines and Operating Experience in the USSR. V. V. Burgsdorf. *Paper No. 326*, CIGRE, vol. III, 1958.

27. The Role of Lightning Strikes to the Conductors Bypassing the Ground Wires in the Protection of High-Voltage Class Lines. M. V. Kostenko, I. F. Polovoy, A. N. Rosenfeld. *Elektrichestvo*, Moscow, USSR, no. 4, 1961, pp. 20–26.

28. Uber Blitzschutz durch "Fernblitzableiter." B. Walter. *Zeitschrift fur technische Physik*, vol. 14, pp. 181–26.

29. A New Approach to the Calculation of the Lightning Performance of Transmission Lines III—A Simplified Method: Stroke to Tower. C. F. Wagner, A. R. Hileman. AIEE *Transactions*, pt. III (*Power Apparatus and Systems*), vol. 79, Oct. 1960, pp. 589–603.

30. The Lightning Stroke with Relation to Overhead Transmission Line. C. F. Wagner, in "Gas Discharges and the Electricity Supply Industry" (book). Butterworth's Scientific Publications, London, 1962.

31. Dielectric Recovery Characteristics of Large Air Gaps. G. D. McCann, J. J. Clark. AIEE *Transactions*, vol. 62, Jan. 1943, pp. 45–52.

32. Effect of Predischarge Currents upon Line Performance. C. F. Wagner, A. R. Hileman. AIEE Paper 62-1181, scheduled for publication in IEEE *Transactions*, pt. III (*Power Apparatus and Systems*), vol. 82, 1963.

J. W. K

Full-scale
that cover
and waves
Effects of
were inves
Estimated
justificatio

For years it h
increase, swit
come the dom
line and appa
switching surg
recent papers
Switching Sur
Distribution C
have the result
insulation been
de is to add
informed decis
line insulation
ing-surge duty.
cide whether le
entrance arrest
more economic
Although res
on many EHV
has shown that
high-speed reclo
erated by a rest

TEST METHOD

Test Environme
because (1) the
door laboratory
and (2) the equ
service. Outdoor

Essentially full text
Transmission and Di
IEEE Technical Ope
IEEE Winter Genera
1963. Scheduled for
Systems, 1963.

The author is gratefu
performed much of t
ticle is based.

J. W. Kalb. Fellow I
ton, Ohio.

Rep. 11

COMMUNICATIONS

PARAMÈTRES DES COUPS DE FOUDRE

par K. Berger, R.B. Anderson
et H. Kröninger
du Comité d'Etudes n° 33
(Surtensions et coordination de l'isolement)

Rapport publié à la demande
du Président du Comité
M. V. Palva

1. — Introduction.

Le Comité suisse des recherches en haute tension exploite depuis 1943 une station de mesure des phénomènes de foudre au Mont San Salvatore près de Lugano, Suisse. L'objet principal de ces mesures était l'enregistrement des formes de courant des coups de foudre qui frappent deux pylônes de télévision installés sur cette montagne. Des photographies de nuit ont été prises de coups de foudre se produisant dans le voisinage et l'on a également procédé plus récemment à des enregistrements du champ électrique au cours des orages. Des rapports décrivant l'installation de mesure et rendant compte des résultats obtenus ont été publiés en premier lieu par Berger en 1955 [1, 2], puis par Berger et Vogelsanger en 1965 [3] et à nouveau en 1966 [4]. En 1967 Berger a présenté l'un des cinq articles sur la foudre parus dans une édition spéciale du Journal du Franklin Institute [5].

Finalement, les résultats des mesures effectuées entre 1963 et 1971 ont été publiés par Berger en 1972 [6] et l'année suivante [7]. Au cours de l'année 1972, une partie des données recueillies pendant la période 1963-1971 a été analysée plus en détail; un ordinateur a été utilisé cette fois pour déterminer les courbes de fréquences cumulées, séparément pour les coups de foudre positifs, pour les premières composantes et pour les composantes suivantes des coups de foudre négatifs, ainsi que pour calculer les corrélations correspondantes. Le présent rapport présente des formes de courant de foudre et donne un résumé de tous les résultats obtenus.

2. — Paramètres des courants de foudre.

2.1. — *Définition des catégories.*

On a trouvé que l'ensemble des coups de foudre frappant les pylônes du Mont San Salvatore pouvait

PAPERS

PARAMETERS OF LIGHTNING FLASHES

by K. Berger, R.B. Anderson
and H. Kröninger
of Study Committee No. 33
(Overvoltages and Insulation Co-ordination)

Paper published at the request
of the Chairman of the Committee
Mr. V. Palva

1. — Introduction.

Ever since 1943 the Swiss high-voltage research committee has been maintaining a lightning measurement station on the Monte San Salvatore near Lugano, Switzerland. The main purpose of these measurements was to record current shapes of lightning flashes striking two television towers on the mountain. During the night photographs were taken of lightning flashes occurring in the vicinity, and more recently recordings of the electric field during a thunderstorm were also made. Reports on the measuring installation and the results obtained were published first by Berger in 1955 [1, 2], and later by Berger and Vogelsanger in 1965 [3] and again in 1966 [4]. In 1967 Berger contributed one of the five articles on lightning for a special edition of the Franklin Institute Journal [5].

Finally, the results of measurements between 1963 and 1971 were published by Berger in 1972 [6] and in the following year [7]. During 1972 some of the data collected over the period 1963-1971 were analyzed in more detail; this time a computer was used to determine cumulative distributions for positive strokes, and for negative first and subsequent strokes separately, and to calculate relevant correlations. Representative lightning current shapes and a summary of all results are given in this report.

2. — Parameters of lightning currents.

2.1. — Definitions of categories.

It has been found that the ensemble of lightning flashes striking the towers on Monte San Salvatore être groupé en catégories distinctes, comme il est indiqué ci-dessous.

- Coups de foudre
  - coups ascendants
    - coups positifs
    - coups négatifs
  - coups descendants
    - coups positifs
    - coups négatifs

Dans le présent rapport, la convention adoptée est que la polarité d'un coup de foudre est celle de la charge du nuage et elle peut facilement être identifiée d'après la polarité des courants mesurés. Les coups de foudre ascendants, qui constituent la majorité des coups au Mont San Salvatore, peuvent être identifiés par le fait qu'ils se ramifient vers le haut, quand une photographie du coup a été prise, ou, sinon, par la présence de courants de quelques centaines d'ampères se maintenant pendant des dizaines ou centaines de millisecondes et pouvant être suivis, soit immédiatement, soit après une brève interruption, d'une ou plusieurs impulsions de courant. D'autre part, les coups de foudre descendants se ramifient vers le bas et n'engendrent pas de courants de prédécharge de durée supérieure à quelques millisecondes.

Etant donné qu'on pense que les coups ascendants sont essentiellement associés à l'effet des pylônes de télévision installés sur le Mont San Salvatore, l'analyse présentée dans le rapport actuel traite uniquement des coups de foudre descendants, considérés comme plus représentatifs de la foudre naturelle. Toutefois, dans cette catégorie, un coup de foudre peut ne comporter qu'une seule impulsion de courant, ou, se composer au contraire d'une succession d'impulsions séparées par des intervalles de temps au cours desquels il ne s'écoule que peu ou pas de courant. On dit alors qu'il s'agit d'un coup de foudre multiple et, dans ce cas, la première impulsion présente des caractéristiques différant notablement de celles des impulsions suivantes, de sorte que lorsqu'on détermine les paramètres caractéristiques des impulsions composant les coups de foudre il est nécessaire de répartir celles-ci en deux catégories au moins, à savoir :

(a) première composante;

(b) composantes suivantes.

A la condition qu'il n'y ait pas d'autre facteur variable exerçant une influence significative sur le processus de la décharge de foudre, on devrait trouver, dans chacune de ces catégories de courants de coup de foudre, une population de courants homogène et l'on devrait pouvoir s'attendre à ce que l'ensemble des mesures fournisse des résultats uniformes, en dehors de différences mineures attribuables à des erreurs résiduelles. Ces résultats devraient donc présenter une répartition donnée (normale ou logonormale par exemple) autour de la moyenne de la population.

2.2. — *Choix des paramètres.*

La forme des coups de foudre et de leurs composantes peut être caractérisée par un petit nombre de

may be grouped into distinct categories as shown below :

- *Lightning flashes*
  - *upward flashes*
    - *positive flashes*
    - *negative flashes*
  - *downward flashes*
    - *positive flashes*
    - *negative flashes*

The convention adopted in this report is that the polarity of flashes is taken from the polarity of the charge in the cloud and is easily identified by the polarity of the measured currents. Upward flashes, which constitute the majority of the flashes at San Salvatore, may be identified by the upward branching of the flash if a photograph of the flash was taken or, failing this, by the continuing currents of a few hundred amps lasting tens or hundreds of milliseconds that may be followed immediately or after short current interruptions by one or several impulse currents. Downward flashes, on the other hand, branch downward and do not produce predischarge currents lasting more than a few milliseconds.

Since upward flashes are thought to be primarily associated with the effect of the television towers on Monte San Salvatore, the analysis presented in this report deals exclusively with downward flashes which are believed to be more representative of natural lightning. In this category, however, a flash may consist of only one current stroke or a succession of such strokes separated by intervals during which little, if any, current flows. The latter is termed a multiple stroke flash and in such a flash the first stroke displays characteristics which differ markedly from those of the following strokes, and thus when determining the characteristic parameters of lightning strokes, these should be separated into at least two separate categories, i.e.,

(a) first strokes, and

(b) following strokes.

Provided there are no further variable factors exercising a significant influence on the process of the lightning discharge, there should now, within these categories of lightning flash currents, be a homogeneous population of currents, and all measurements could be expected to yield uniform results apart from minor differences attributable to residual errors. These results should therefore follow some distribution (e.g. normal or lognormal) about the population mean.

2.2. — Selection of parameters.

The lightning flash and stroke current shape may be characterized by a few parameters, which are

90004094

paramètres, qui présentent également de l'intérêt lorsqu'on considère les dommages susceptibles d'être causés par un coup de foudre. Les paramètres mesurés sont les suivants :

(a) *Coup de foudre.*

(i) courant de crête — pic de courant le plus élevé du coup de foudre;

(ii) durée du coup de foudre — durée pendant laquelle il y a écoulement de courant ou, dans le cas d'un coup de foudre multiple, le temps qui s'écoule jusqu'à la fin de la dernière impulsion;

(iii) intervalles sans courant — intervalles de temps pendant lesquels il ne s'écoule aucun courant mesurable;

(iv) charge du coup de foudre — charge totale transportée par un coup de foudre.

(b) *Composantes d'un coup de foudre.*

(i) courant de crête — pic de courant le plus élevé d'une impulsion;

(ii) durée de front — intervalle de temps compris entre le point 2 kA du front et le premier pic;

(iii) durée de l'impulsion — intervalle de temps compris entre le point 2 kA du front et le point de la queue où l'amplitude du courant est tombée à 50 % de sa valeur de crête;

(iv) vitesse de montée maximale (raideur de front du courant) — tangente à plus forte pente du front d'une impulsion;

(v) charge du choc — charge électrique transportée par la partie variable de l'impulsion (le point de la queue de l'onde de courant à partir duquel la charge transportée n'a plus été considérée comme faisant partie de la « charge du choc » a été déterminé en examinant la forme du courant et il n'est donc pas défini de façon précise);

(vi) charge de l'impulsion — charge totale de l'impulsion, c'est-à-dire la charge du choc majorée de toute charge transportée par le courant continuant à s'écouler après la fin du choc;

(vii) énergie présumée de l'impulsion — énergie qui aurait été dissipée par le courant de l'impulsion s'écoulant à travers une résistance d'un ohm, c'est-à-dire $\int i^2 dt$ A^2s ou J/ohm. Cette définition fera l'objet d'une discussion ultérieure pour accord.

2.3. — *Répartition des variates.*

La répartition des mesures individuelles (variates) des paramètres dans leurs catégories respectives joue un rôle important de guide dans l'estimation des valeurs à escompter pour les mesures futures. Celles-ci peuvent être déduites, soit d'une connaissance préalable du processus physique engendrant un coup de foudre, soit la répartition même des échantillons recueillis. La prise en considération du processus physique, dans la mesure où nous comprenons bien ce dernier, ne fournit pas de raisons conduisant impérativement à admettre telle ou telle

also of interest when considering the possible damaging effect of a lightning stroke. The parameters which have been measured are the following :

(a) The lightning flash.

(i) peak current — the highest current peak in the flash;

(ii) flash duration — the length of time during which there is current flow or, in the case of a multiple stroke flash, until the completion of the last stroke;

(iii) no-current intervals — intervals between strokes of a flash during which no detectable current is flowing;

(iv) flash charge — the total charge transferred by a flash.

(b) Lightning strokes.

(i) peak current — the highest current peak in a stroke;

(ii) front duration — the time interval between the 2 kA point on the front and the first peak;

(iii) stroke duration — the time interval between the 2 kA point on the front and the point on the tail where the current amplitude has fallen to 50 % of its peak value;

(iv) maximum rate of rise (current steepness) — the steepest tangent on the front of a stroke;

(v) impulse charge — the electric charge transported by the rapidly changing part of the stroke (the point on the current tail after which the charge transported is no longer considered part of the "impulse charge" was determined by inspection of the shape and is therefore not precisely defined);

(vi) stroke charge — the total charge in the stroke, i.e. the impulse charge together with any charge transported by continuing current after the impulse;

(vii) prospective stroke energy — the energy which would be dissipated by the stroke current flowing through a one-ohm resistor, i.e. $\int i^2 dt$ A^2s or J/ohm. This definition is subject to further discussion and agreement.

2.3. — Distribution of variates.

The distribution of individual measurements (variates) of the parameters in their respective categories is an important guide as to the values expected to be found in future measurements. It may be inferred either from a foreknowledge of the physical process leading to the lightning discharge or from the sample distribution itself. Consideration of the physical process, as far as we understand it, does not provide compelling reasons to assume any particular distribution. The sample data itself must therefore provide the clue to which of the known dis-

répartition particulière. Ce sont donc les données elles-mêmes prises comme échantillons qui doivent servir à faire découvrir celle des répartitions connues qui peut s'adapter à elles avec un degré de confiance suffisant. Dans le passé, la répartition logarithmique a été généralement acceptée et des analyses antérieures [6] ont montré que la courbe des fréquences cumulées sur une base logarithmique s'apparente suffisamment avec les données dont on dispose, à un tracé rectiligne. La répartition logarithmique a donc été admise dans la présente analyse. Il faut toutefois prendre garde, dans les déductions qui en résultent, au fait qu'il peut très bien y avoir d'autres répartitions convenant aussi bien ou même mieux à ces données.

2.4. — *Résultats.*

Les figures 1 à 10 établies avec une base logarithmique, montrent les courbes des fréquences cumulées de dix des paramètres du courant de foudre. La ligne droite a été tracée en minimisant la somme des carrés des distances des points (également reliés entre eux par des lignes droites) et elle peut donc être utilisée pour obtenir la meilleure estimation possible de la moyenne et de l'écart-type σ des logarithmes des variates de la distribution de la population.

Cela implique que la fonction de densité de probabilité $w(x)$ ait la forme suivante :

tributions can be fitted to the data with a sufficient degree of confidence. Historically the logarithmic distribution has become generally accepted and past analyses [6] showed that cumulative distributions on a logarithmic base produce a reasonable fit of the data to a straight line. The logarithmic distribution has therefore also been assumed in this analysis. Caution should, however, be exercised when using the implications of this, since there may well be other distributions which fit the data just as well or better.

2.4. — Results.

Figures 1 to 10 show, on a logarithmic base, the cumulative distributions of, ten of the lightning current parameters. The straight line is the least squares fit to the points (which have also been connected by straight lines) and therefore may be used to obtain the best estimate of the mean μ and standard deviation σ of the logarithms of the variates in the population distribution.

The probability density function $w(x)$ is therefore implied to be :

$$w(x) = (1/x\sigma\sqrt{2}\,\pi)\exp\ \{(\log x - \mu)^2/2\sigma^2\} \quad (1)$$

et qu'elle soit donc complètement définie par les deux paramètres μ et σ.

Lorsqu'on compare les valeurs réelles aux valeurs données par la droite de régression, il est évident que des différences appréciables peuvent apparaître. Dans certains cas, en particulier lorsqu'il s'agit des parties extrêmes de la répartition, on pourrait également prendre en considération les valeurs réelles pour la prédétermination des fréquences d'occurrence de la variable.

Il n'a pas été tracé de courbe de répartition pour l'energie totale présumée du coup de foudre, étant donné que l'énergie des composantes consécutives à la première sont insignifiantes par rapport à celle de la première. Les résultats sont également présentés dans le tableau I, qui indique les valeurs correspondant, respectivement aux fréquences cumulées pour des niveaux de probabilité de 95 %, 50 % et 5 % (ces valeurs étant lues sur la droite de régression).

En ce qui concerne le tableau I, les valeurs des courants de crête de la foudre sont corroborées par les distributions de fréquence publiées par Popolansky [8], qui a trouvé une valeur médiane de 28 kA obtenue à partir de 624 valeurs de mesures de courant fiables effectuées sur des cheminées et des pylônes de grande hauteur, y compris 192 valeurs provenant des essais de K. Berger. Ce résultat incite à penser que les paramètres mesurés sur des coups de foudre descendants atteignant les pylônes de télévision de la montagne voisine de Lugano peuvent

and is fully defined by the parameters μ and σ.

When comparing actual values with values predicted by the regression line, it is clear that substantial differences may be found. In some cases, particularly where the extremes of the distributions are concerned, the actual values might also be considered when predicting frequencies of occurrence of the variable.

No distribution of total negative flash prospective energy has been drawn since the following stroke energies are insignificant when added to those of the first stroke. The results are also given in Table I showing the values for the cumulative distributions at the 95 %, 50 % and 5 % probability levels respectively. (As read off against the regression line).

Regarding Table I, corroboration of the values of peak lightning currents are shown in the distribution reported by Popolansky [8] who observes a median value of 28 kA obtained from 624 values of reliable current measurements made on tall chimneys and towers, including 192 values from Berger. This result tends to suggest that the measured parameters of downward flashes striking the television towers on the mountain in Lugano may be comparable with those of lightning striking tall structures in open country.

TABLEAU I – TABLE I

Paramètres typiques de la foudre.
Typical lightning parameters.

Fig. *No.*	N	Paramètre *Parameter*	Unité *Unit*	Pourcentage de cas dépassant la valeur indiquée dans le tableau *Per cent of cases exceeding tabulated value*		
				95 %	50 %	5 %
		Courant de crête *Peak current* (minimum 2 kA)				
1	101	premières composantes négatives et coups de foudre négatifs *negative first strokes and flashes*	kA	14	30	80
1	135	composantes suivantes négatives *negative following strokes*	kA	4,6	12	30
1	26	coups de foudre positifs (sans composantes suivantes) *positive flashes (no following strokes)*	kA	4,6	35	250
		Charge				
2	93	premières composantes négatives *negative first strokes*	C	1,1	5,2	24
2	122	composantes suivantes négatives *negative following strokes*	C	0,2	1,4	11
3	94	coups de foudre négatifs *negative flashes*	C	1,3	7,5	40
3	26	coups de foudre positifs *positive flashes*	C	20	80	350
		Charge du choc *Impulse charge*				
4	90	premières composantes négatives *negative first strokes*	C	1,1	4,5	20
4	117	composantes suivantes négatives *negatives following strokes*	C	0,22	0,95	4,0
4	25	coups de foudre positifs (une seule impulsion) *positive flashes (only one stroke)*	C	2,0	16	150
		Durée de front *Front duration*				
5	89	premières composantes négatives *negative first strokes*	µs	1,8	5,5	18
5	118	composantes suivantes négatives *negative following strokes*	µs	0,22	1,1	4,5
5	19	coups de foudre positifs *positive flashes*	µs	3,5	22	200

TABLEAU I (suite) — TABLE I (continued)

Fig. No.	N	Paramètre *Parameter*	Unité *Unit*	Pourcentage de cas dépassant la valeur indiquée dans le tableau *Per cent of cases exceeding tabulated value*		
				95 %	50 %	5 %
		di/dt maximal *Maximum di/dt*				
6	92	premières composantes négatives *negative first strokes*	kA/µs	5,5	12	32
6	122	composantes suivantes négatives et coups de foudre négatifs *negative following strokes and flashes*	kA/µs	12	40	120
6	21	coups de foudre positifs *positive flashes*	kA/µs	0,20	2,4	32
		Durée de l'impulsion *Stroke duration*				
7	90	premières composantes négatives *negative first strokes*	µs	30	75	200
7	115	composantes suivantes négatives *negative following strokes*	µs	6,5	32	140
7	16	coups de foudre positifs *positive flashes*	µs	25	230	2 000
		Intégrale (i^2dt) *Integral (i^2dt)*				
9	91	premières composantes négatives et coups de foudre négatifs *negative first strokes and flashes*	A^2s	$6,0 \times 10^3$	$5,5 \times 10^4$	$5,5 \times 10^5$
9	88	composantes suivantes négatives *negative following strokes*	A^2s	$5,5 \times 10^2$	$6,0 \times 10^3$	$5,2 \times 10^4$
9	26	coups de foudre positifs *positive flashes*	A^2s	$2,5 \times 10^4$	$6,5 \times 10^5$	$1,5 \times 10^7$
10	133	Intervalle de temps entre impulsions négatives *Time intervals between negative strokes*	ms	7	33	150
		Durée du coup de foudre *Flash duration*				
8	94	négatifs (y compris les coups de foudre à une seule impulsion) *negative (including single stroke flashes)*	ms	0,15	13	1 100
8	39	négatifs (non compris les coups de foudre à une seule impulsion) *negative (excluding single stroke flashes)*	ms	31	180	900
8	24	positifs *positive*	ms	14	85	500

90004098

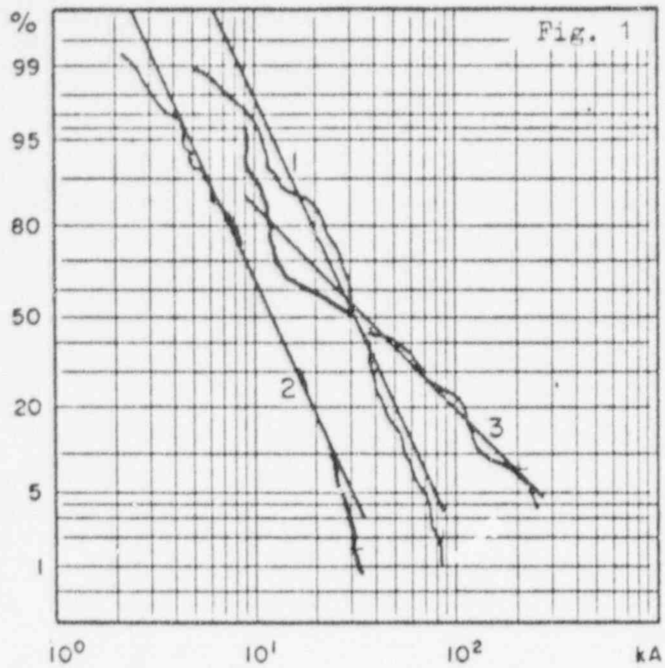

Figure 1

Courant de crête – I
(1) Premières impulsions négatives
(2) Impulsions suivantes négatives
(3) Impulsions positives ;

Peak current I
(1) Negative first strokes
(2) Negative following strokes
(3) Positive strokes

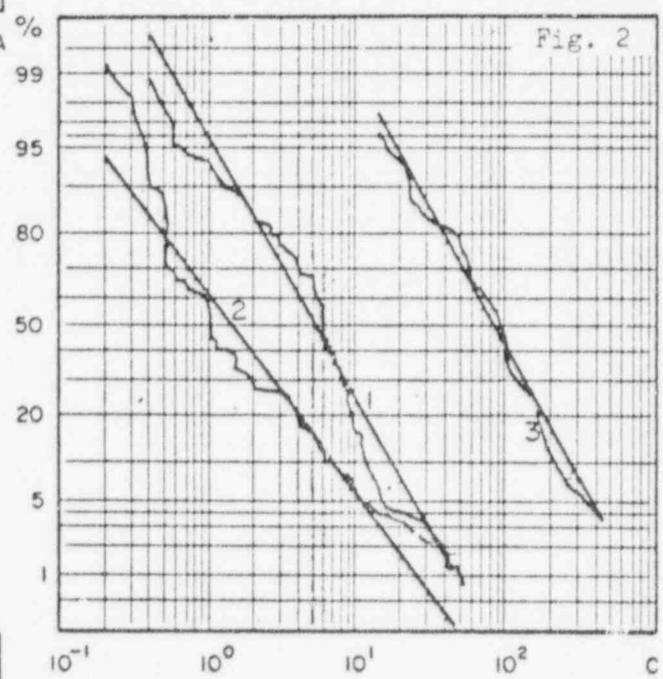

Figure 2

Charge de l'impulsion – Q (impulsion)
(1) Premières impulsions négatives
(2) Impulsions suivantes négatives
(3) Impulsions positives

Stroke charge – Q (stroke)
(1) Negative first strokes
(2) Negative following strokes
(3) Positive strokes

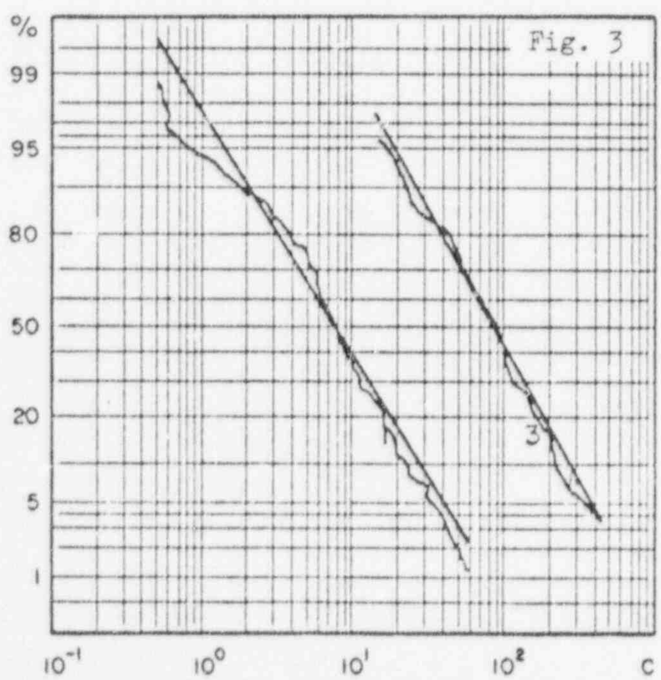

Figure 3

Charge du coup de foudre – Q (coup de foudre)
(1) Coups de foudre négatifs
(3) Coups de foudre positifs

Flash charge – Q (flash)
(1) Negative flashes
(3) Positive flashes

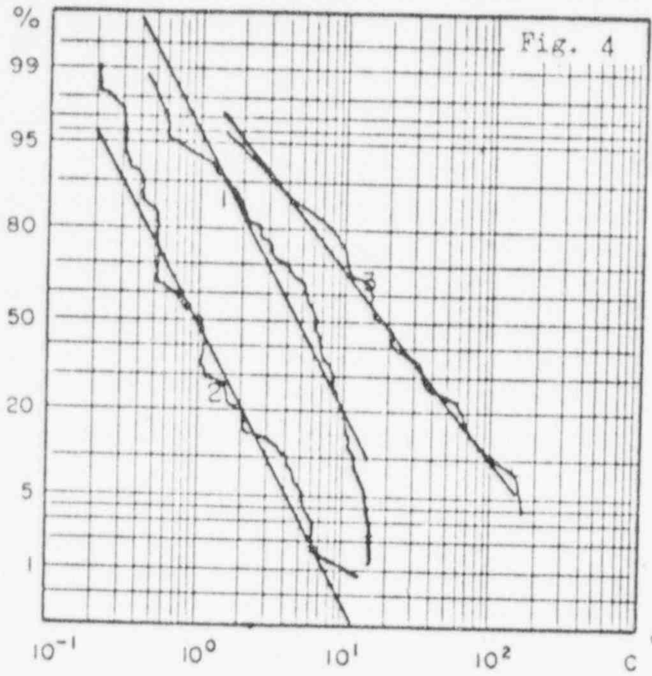

Figure 4

Charge du choc – Q (choc)
(1) Premières impulsions négatives
(2) Impulsions suivantes négatives
(3) Impulsions positives

Impulse charge Q (impulse)
(1) Negative first strokes
(2) Negative following strokes
(3) Positive strokes

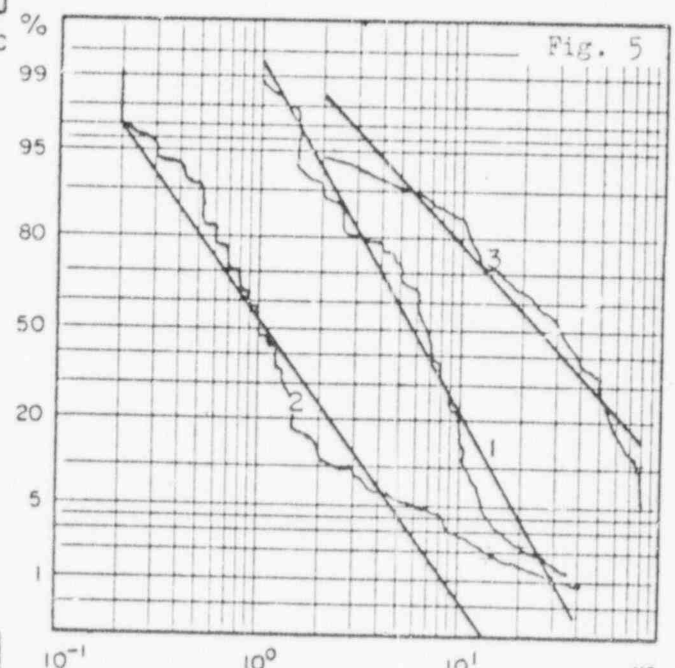

Figure 5

Durée de front – T (front)
(1) Premières impulsions négatives
(2) Impulsions suivantes négatives
(3) Impulsions positives

Front duration – T (front)
(1) Negative first strokes
(2) Negative following strokes
(3) Positive strokes

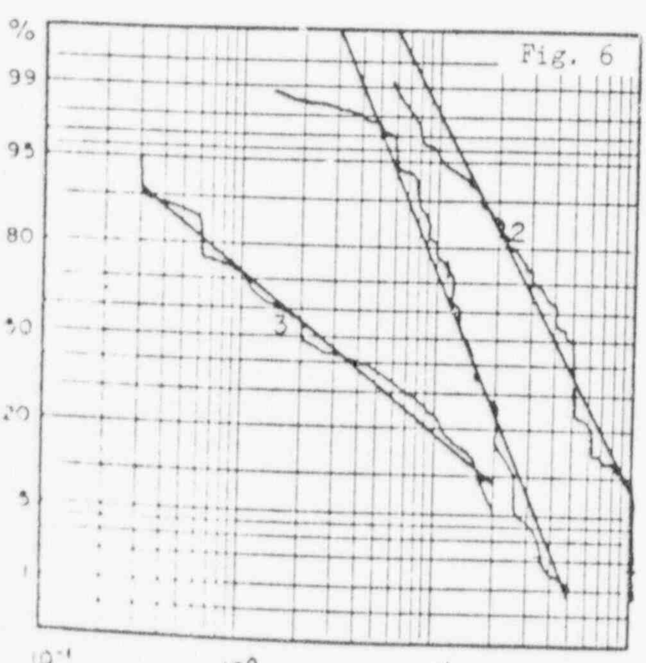

Figure 6

Vitesse de montée maximale du courant – di/dt (raideur de front du courant)
(1) Premières impulsions négatives
(2) Impulsions suivantes négatives
(3) Impulsions positives

Maximum rate of rise of current di/dt (current steepness)
(1) Negative first strokes
(2) Negative following strokes
(3) Positive strokes

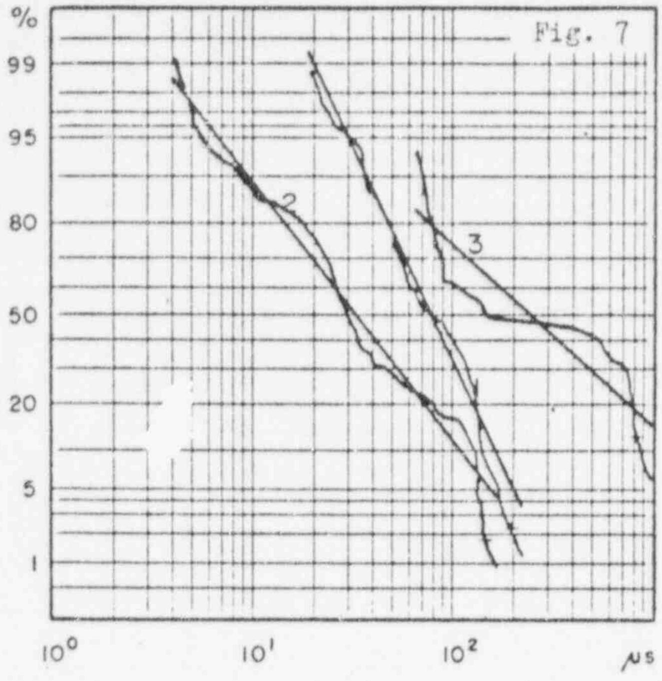

Figure 7

Durée de l'impulsion – T (queue)
(1) Premières impulsions négatives
(2) Impulsions suivantes négatives
(3) Impulsions positives

Stroke duration – T (tail)
(1) Negative first strokes
(2) Negative following strokes
(3) Positive strokes

POOR ORIGINAL

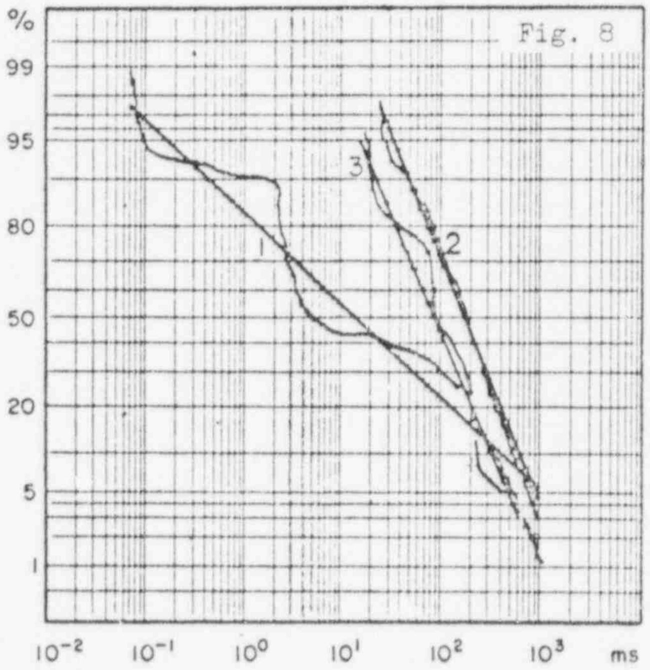

Figure 8

Durée du coup de foudre – T (coup de foudre)
(1) Coups de foudre négatifs y compris les coups de foudre simples.
(2) Coups de foudre négatifs non compris les coups de foudre simples.
(3) Coups de foudre positifs.

Flash duration T' (flash)
(1) Negative flashes including single strokes
(2) Negative flashes excluding single strokes
(3) Positive flashes

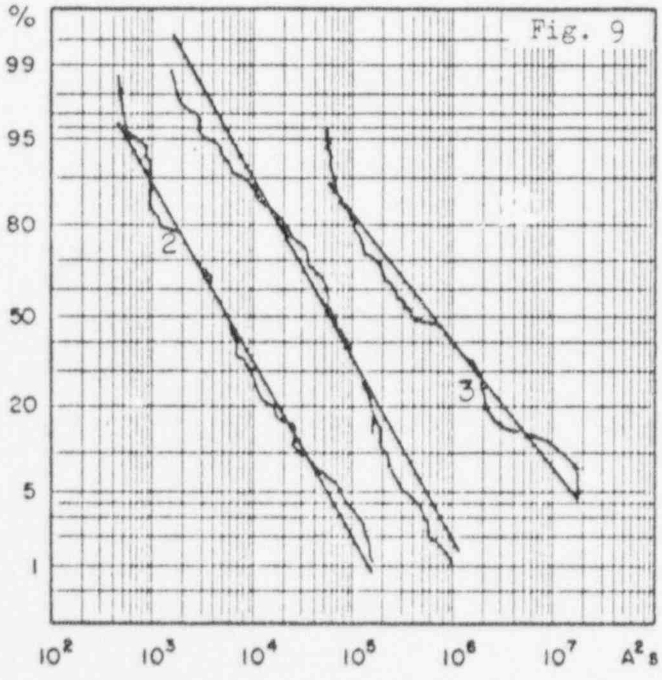

Figure 9

Energie présumée – $\int i^2 dt$
(1) Premières impulsions négatives
(2) Impulsions suivantes négatives
(3) Impulsions positives

Prospective energy – $\int i^2 dt$
(1) Negative first strokes
(2) Negative following strokes
(3) Positive strokes

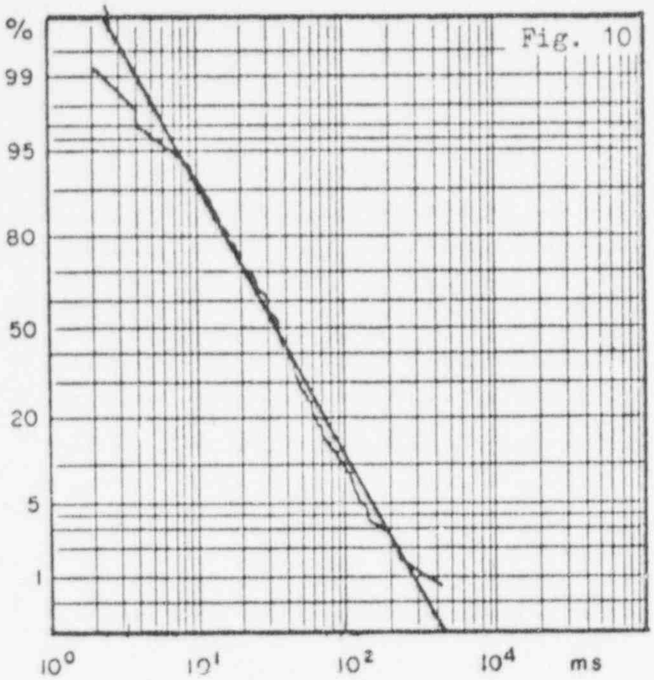

Figure 10

Intervalles sans courant entre impulsions négatives

No-current intervals between negative strokes

être comparables à ceux des coups de foudre atteignant des structures de grande hauteur en plaine.

3. — Corrélations entre les paramètres du courant de foudre.

On pourrait concevoir que des propriétés importantes de la décharge de foudre puissent être mises en lumière si certains des paramètres cités au paragraphe précédent étaient suffisamment corrélés. Si, par exemple, il existait une corrélation linéaire entre le courant de crête et la durée de front, on pourrait soupçonner l'existence d'une simple constante de temps, qui permettrait de calculer la vitesse de montée. Une simple analyse de régression considérant le courant de crête et les autres paramètres, puis séparément l'un après l'autre, a été effectuée autrefois [6] et ses résultats ont été présentés sous la forme de diagrammes de dispersion comportant aussi le tracé de la droite de régression. On a supposé une régression linéaire des logarithmes des variates, ce qui revient à dire qu'on a admis la relation $y = Ax^B$. Une représentation graphique de ce genre de régression est rassurante dans les premiers stades d'une analyse, mais, lorsqu'il s'agit seulement de faire l'essai d'une hypothèse de corrélation entre les paramètres ou entre les paramètres transformés il suffit de calculer le coefficient de corrélation et de vérifier sa validité à un niveau prédéterminé.

Les tableaux II, III et IV donnent les matrices des coefficients de corrélation calculés, respectivement pour les impulsions positives, pour les premières impulsions négatives et pour les impulsions suivantes négatives.

Les tableaux de coefficients de corrélation sont considérés, comme pouvant apporter une aide utile à la formulation d'un modèle de décharge de foudre.

3. — Correlation between lightning current parameters.

Important properties of the lightning discharge could conceivably be brought to light if some of the parameters mentioned in the previous sections were significantly correlated. If, for instance, the peak current and front duration were linearly correlated, a simple time constant to determine the rate of rise might be suspected. Simple regression analysis of peak current and other parameters, taken one at a time has been carried out before [6] and the results have been presented in the form of scatter diagrams showing also the linear regression line. Linear regression of the logarithms of the variates was assumed, i.e. the relationship $y = Ax^B$. Such a pictorial view of the regression is reassuring in the initial stages of an analysis but for the purpose of merely testing the hypothesis of correlation between the parameters, or transformed parameters, it is sufficient to compute the correlation coefficient and test its significance at a predetermined level.

Tables II, III and IV show the computed matrices of correlation coefficients in respect of positive strokes; negative first and negative following strokes.

The tables of correlation coefficients are considered to be useful as an aid to the formulation of a model on the lightning discharge. Some parameters,

Tableau II – Table II

Coefficients de corrélation entre les paramètres des premières impulsions positives (c'est-à-dire de coups de foudre positifs, car il n'y a pas de coups de foudre positifs multiples).

Correlation coefficients between parameters of positive first strokes. (or positive flashes, there being no positive multiple stroke flashes)

	Courant de crête *Peak current*	Durée de front *Front duration*	Vitesse de montée max. *Max. rate of rise*	Charge de choc *Impulse charge*	Energie *Energy*	Charge de l'impulsion *Stroke charge*	Durée de l'impulsion *Stroke duration*	Durée du coup de foudre *Flash duration*	charge du coup de foudre *Flash charge*
Courant de crête *Peak current*	1,00								
Durée de front *Front duration*	0,07	1,00							
Vitesse de montée max. *Max. rate of rise*	0,49	– 0,68	1,00						
Charge de choc *Impulse charge*	0,77	0,27	0,23	1,00					
Energie *Energy*	0,84	0,22	0,39	0,82	1,00				
Charge de l'impulsion *Stroke charge*	0,62	0,32	0,11	0,74	0,72	1,00			
Durée de l'impulsion *Stroke duration*	0,58	0,48	0,02	0,80	0,72	0,75	1,00		
Durée du coup de foudre *Flash duration*	0,33	0,112	– 0,15	0,24	0,17	0,64	0,24	1,00	
Charge du coup de foudre *Flash charge*	0,62	0,32	0 10	0,74	0,71	1,00	0,75	0,64	1,00

Les coefficients en caractères gras dépassent la valeur critique au niveau de signification de 5 %.
Coefficients in boldface exceed the critical value at the 5 % level of significance.
Degrés de liberté : 13.
Degrees of freedom : 13.

Certains des paramètres, tels que la charge de choc et la charge totale d'une impulsion, sont liés l'un à l'autre en vertu même de leur définition et il est évident qu'il existe entre eux une bonne corrélation. Néanmoins, l'existence ou l'absence de certaines autres corrélations peut fournir des indices significatifs quant au mécanisme probable de la décharge.

such as impulse charge and total stroke charge, are related as a result of their definition and a good correlation between them is self-evident. Nevertheless other correlations, or the lack of such, may provide significant pointers to the probable discharge mechanism.

4. — Formes typiques du courant de foudre.

4.1. — *Généralités.*

La constatation que les formes des premières impulsions positives, des premières impulsions négatives et des impulsions suivantes négatives sont nettement différentes, en ce qui concerne notamment les durées de front, nous a conduits à définir trois catégories d'impulsions. La bonne corrélation

4. — Typical lightning current shapes.

4.1. — General.

The observation that positive first stroke, negative first stroke and negative following stroke shapes are distinctly different, particularly in so far as the front durations are concerned, has led to the designation of three categories of strokes. Good correlation between parameters such as peak current,

TABLEAU III – TABLE III

Coefficients de corrélation entre les paramètres des premières impulsions négatives.
Correlation coefficients between parameters of negative first strokes.

	Courant de crête *Peak current*	Durée de front *Front duration*	Vitesse de montée max. *Max rate of rise*	Charge de choc *Impulse charge*	Energie *Energy*	Charge de l'impulsion *Stroke charge*	Durée de l'impulsion *Stroke duration*	Durée du coup de foudre *Flash duration*	charge du coup de foudre *Flash charge*
Courant de crête *Peak current*	1,00								
Durée de front *Front duration*	0,37	1,00							
Vitesse de montée max. *Max. rate of rise*	0,36	– 0,21	1,00						
Charge de choc *Impulse charge*	0,77	0,25	0,39	1,00					
Energie *Energy*	0,88	0,30	0,42	0,89	1,00				
Charge de l'impulsion *Stroke charge*	0,61	0,29	0,19	0,91	0,78	1,00			
Durée de l'impulsion *Stroke duration*	0,56	0,33	0,10	0,51	0,52	0,43	1,00		
Durée du coup de foudre *Flash duration*	0,08	0,25	– 0,02	0,14	0,10	0,23	0,11	1,00	
Charge du coup de foudre *Flash charge*	0,54	0,36	0,19	0,72	0,64	0,78	0,44	0,64	1,00

Les coefficients en caractères gras dépassent la valeur critique au niveau de signification de 5 %.
Coefficients in boldface exceed the critical value at the 5 % level of significance.
Degrés de liberté : 77
Degrees of freedom : 77

observée entre les paramètres tels que le courant de crête, la charge du choc et la durée de queue confirme que les formes de courant sont similaires dans chaque catégorie, ce qui incite à construire une forme typique pour chacune d'elles.

impulse charge and tail duration confirm that shapes within the categories are similar, and this suggests the construction of typical shapes for each of these categories.

4.2. — *Construction d'une forme de courant.*

4.2. — Constructing the shape.

Pour trouver une ordonnée $\bar{i}_k$ de la forme moyenne d'un courant d'impulsion de foudre, toutes les ordonnées i_k du point K des courbes enregistrées séparément ont été ajoutées et le résultat divisé par m, nombre des ordonnées mesurées.

On a donc :

To construct an ordinate $\bar{i}_k$ of the mean lightning stroke shape all ordinates i_k at point k on the separate curves have been added and the result divided by m, the number of ordinates.

Hence

$$\bar{i}_k = \frac{1}{m} \sum_{j=1}^{m} i_k \qquad (2)$$

où m est le nombre total de courbes utilisées pour la détermination de $\bar{i}_k$ au point k. Ce nombre est variable du fait de la différence des longueurs d'enregistrement, due aux techniques d'enregistrement et de chiffrage [3].

where m stands for the total number of curves contributing to $\bar{i}_k$ in the point k. The number varies as a result of different record lengths, caused by the recording and digitizing techniques [3].

Tableau IV – Table IV

Coefficients de corrélation entre les paramètres des impulsions suivantes négatives.
Correlation coefficients between parameters of negative following strokes.

	Courant de crête *Peak current*	Durée de front *Front duration*	Vitesse de montée max. *Max. rate of rise*	Charge de choc *Impulse charge*	Energie *Energy*	Charge de l'impulsion *Stroke charge*	Durée de l'impulsion *Stroke duration*
Courant de crête *Peak current*	1,00						
Durée de front *Front duration*	0,28	1,00					
Vitesse de montée max. *Max. rate of rise*	0,11	– 0,49	1,00				
Charge de choc *Impulse charge*	0,69	0,13	0,31	1,00			
Energie *Energy*	0,69	0,22	0,15	0,72	1,00		
Charge de l'impulsion *Stroke charge*	0,43	0,26	0,28	0,62	0,54	1,00	
Durée de l'impulsion *Stroke duration*	0,25	– 0,05	0,30	0,44	0,37	0,12	1,00

Les coefficients en caractères gras dépassent la valeur critique au niveau de signification de 5 %.
Coefficients in boldface exceed the critical value at the 5 % level of significance.
Degrés de liberté : 73
Degrees of freedom : 73

Avant de faire la somme puis la moyenne des ordonnées i_k, il est nécessaire de s'assurer que les courbes sont convenablement alignées, c'est-à-dire que les points i_{jk} de l'équation (2) correspondent au même stade du développement physique de la décharge de foudre. Le front raide des formes de courant est une caractéristique appropriée et facilement reconnaissable dans toutes les impulsions et c'est pourquoi les enregistrements ont été alignés en faisant coïncider les points d'amplitude 50 % de tous les fronts. Une technique différente, qui calcule la fonction d'intercorrélation entre les deux courbes et déplace l'une des courbes d'une quantité égale au retard au bout duquel la fonction a un maximum, a abouti à une forme moyenne presque identique, ce qui prouve la valeur de la première méthode (beaucoup plus simple que la seconde). De plus, toutes les courbes ont été ramenées à une même amplitude de crête prise comme unité avant de faire les moyennes.

Before summing and averaging the points i_k it is necessary to ascertain that the curves are properly aligned, i.e. the points i_{jk} in equation (2) should correspond to the same stage in the physical development of the lightning flash. The sharply rising front of the stroke shape is a suitable and easily recognisable feature in all strokes and the records were therefore aligned in such a way that the 50 % amplitude points on the fronts coincided. A different technique, which computes the cross-correlation function between two curves and shifts one curve by an amount equal to the lag at which the function shows a maximum, produced an almost identical mean shape, proving the merit of the first (much more simple) method. In addition, all curves were converted to a unit peak amplitude before averaging.

(a) *Premières impulsions positives.*

Bien que les impulsions positives soient caractérisées par des charges plus élevées et des fronts moins raides que leurs correspondantes négatives, elles n'ont pas entre elles suffisamment de caractéristiques communes pour permettre d'obtenir une forme de courant moyenne acceptable. C'est peut-être dû aussi en partie au petit nombre de coups de foudre positifs enregistrés dans la période considérée. C'est pourquoi nous nous sommes contentés de

(a) Positive first strokes.

Although positive strokes are characterized by greater charges and slower fronts than their negative counterparts, they do not have enough common features to produce an acceptable mean current shape. This may also be due partly to the small number of positive strokes which were recorded in the period. A selection of 4 of the most typical of 21 recorded curves is therefore shown in Figure 11.

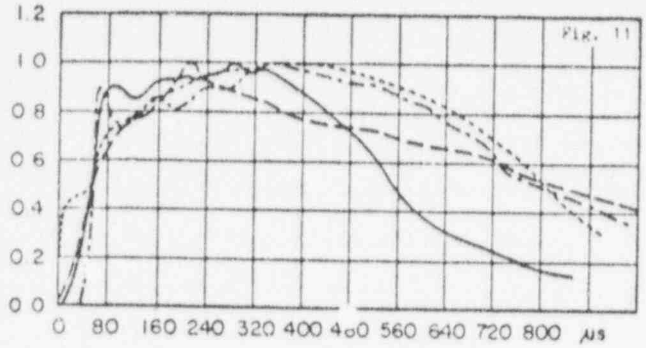

Figure 11

Formes de courant typiques – Impulsions positives

Typical current shapes – positive strokes

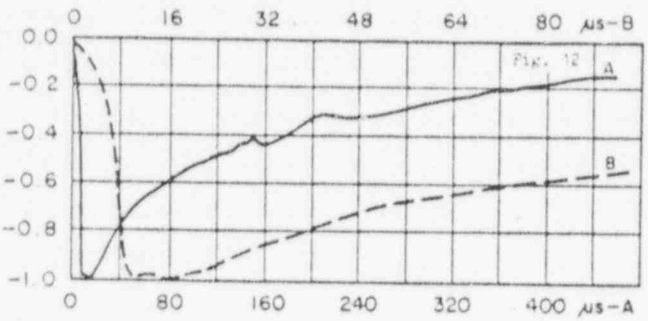

Figure 12

Forme de courant moyenne Premières impulsions négatives
A – échelle des temps inférieure B – échelle des temps supérieure

Mean current shape Negative first strokes
A – lower time scale B – upper time scale

reproduire sur la figure 11 un choix de 4 des courbes les plus typiques parmi les 21 courbes enregistrées.

(b) *Forme des premières impulsions négatives.*

La figure 12 montre la moyenne des formes de premières impulsions de courant négatives, tracée avec deux échelles de temps différentes (A et B). Dans la zone de 120 à 160 µs, le nombre de courbes utilisées pour la détermination de la courbe passe de 88 (enregistrements courts et longs) à 10 (enregistrements longs seulement), ce qui explique l'ondulation qu'on constate dans cette zone. Un autre défaut de précision, inhérent à la technique d'enregistrement employée à l'origine [3], se produit dans le voisinage de 200 µs et il est très probable qu'il est ici aussi une source d'erreurs résiduelles.

(b) Negative first stroke shape.

Figure 12 shows the mean negative first stroke current shapes on two different time scales (A and B). In the region between 120-160 µsec. the number of curves contributing to the mean curve changes from 88 (short and long recordings) to 10 (only long recordings) which explains the ripple in this area. A further inaccuracy, inherent in the original recording technique [3], occurs at around 200 µsec., most likely also contributing to residual errors here.

(c) *Forme des impulsions suivantes négatives.*

La figure 13 montre la moyenne de 76 formes d'impulsions suivantes négatives, tracées ici aussi avec deux échelles des temps (A et B). Un trait particulièrement frappant de ces courbes est la modification assez brutale de pente de la queue au bout d'environ 5 µs, suivie d'une décroissance lente

(c) Negative following stroke shape.

Figure 13 shows the mean of 76 negative following stroke shapes, again on two time scales (A and B). A striking feature of these curves is the rather abrupt change in slope of the tail after about 5 µsec. and the subsequent slowly decaying tail. Errors due to the same recording technique referred to above can

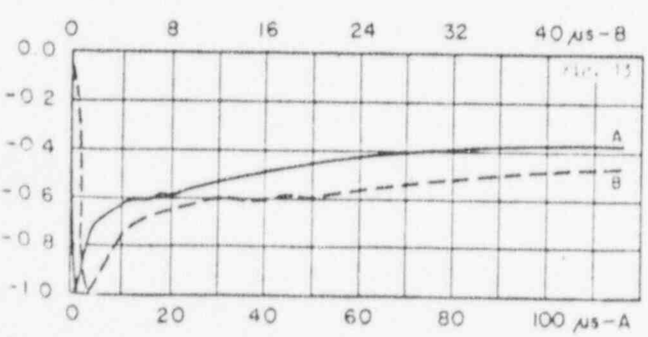

Figure 13

Forme de courant moyenne Impulsions suivantes négatives
A – échelle des temps inférieure B – échelle des temps supérieure

Mean current shape Negative following strokes
A – Lower time scale B – upper time scale

de la queue. Des erreurs dues à la même technique d'enregistrement, auxquelles il a été fait allusion plus haut, peuvent être tenues responsables de l'ondulation observée aux environs de 20 µs. Au delà de 50 µs après le début, le tracé devient incertain, car dans la plupart des enregistrements originaux, les amplitudes des courants à l'échelle adoptée sont très faibles et ne peuvent être lues avec précision.

be held responsible for the ripple at approximately 20 µsec. After about 50 µsec. from the start, accuracy deteriorates since the current amplitudes in most of the original records were very low on the scale and could not be accurately resolved.

5. — Remerciements.

Les auteurs remercient la Fondation suisse pour l'aide qu'elle leur a généreusement apportée pour l'exécution de leurs travaux au Mont San Salvatore et sans laquelle ils n'auraient pas été en mesure de recueillir ces données. Ils expriment également leurs remerciements au Conseil de la recherche scientifique et industrielle d'Afrique du Sud pour le financement des travaux de H. Kröninger, qui a participé pendant un an à l'analyse des données.

5. — Acknowledgements.

The authors thank the Swiss Foundation for their generous support of the work on Monte San Salvatore, without which these data could not have been compiled. Thanks are also due to the Council for Scientific and Industrial Research of South Africa for financing the work of H. Kröninger who assisted in the analysis of the data over the period of one year.

Bibliographie — References

[1] K. BERGER – "Die Messeinrichtung für die Blitzforschung auf dem Monte San Salvatore". Bull. SEV, n°5, 1955, pp. 193-232.

[2] K. BERGER – "Resultate der Blitzmessungen der Jahre 1947-1954 auf dem Monte San Salvatore". Bull. SEV., n°9, 1955, pp. 405-456.

[3] K. BERGER et E. VOGELSANGER – "Messungen und Resultate der Blitzforschung der Jahre 1955-1963 auf dem Monte San Salvatore". Bull. SEV., Bd. 56 (1965), n°1, pp. 2-22.

[4] K. BERGER et E. VOGELSANGER – "Photographische Blitzuntersuchen der Jahre 1955-1965 auf dem Monte San Salvatore". Bull. SEV., Bd 57 (1966), n°13, pp. 599-620.

[5] K. BERGER – "Novel observations on lightning discharges : results of research on Mount San Salvatore". Journal of the Franklin Institute, vol. 283, n°6, june 1967.

[6] K. BERGER – "Methoden und Resultate der Blitzforschung auf dem Monte San Salvatore bei lugano in den Jahren 1963-1971". Bull. SEV., Bd. 63 (1972), n°24, pp. 1403-1422.

[7] K. BERGER – "Oszillographische Messungen des Feldverlaufs in der Nähe des Blitzeinschlages auf dem Monte San Salvatore". Bull. SEV., Bd. 64 (1973) n°3, pp. 120-136.

[8] F. POPOLANSKY – "Distribution de fréquence des amplitudes des courants de foudre". Frequency distribution of amplitudes of lightning currents. Electra n°22 (mai 1972), pp. 139-147.

REF. 12

Mechanism of Breakdown of Laboratory Gaps

C. F. WAGNER
FELLOW AIEE

A. R. HILEMAN
MEMBER AIEE

THE AUTHORS' primary interest in the mechanism of gap breakdown is in its relation to lightning stroke phenomena. In considering the effect of the lightning stroke upon transmission lines, the problem has been resolved into two parts. The first of these is the electrical response of the line to specific assumed stroke characteristics. A method[1-3] to determine this response was recently presented before the AIEE in which it was shown that the time change in the charge in the stroke above the tower may be as important as the current fed into the transmission line. The second part of the problem is the determination of those stroke characteristics that are required to implement this approach. An initial effort[4] along this line was previously presented in which an attempt was made to synthesize the stroke characteristics by correlating the known stroke characteristics with laboratory determined characteristics of long sparks. A further effort[5] was made to utilize the available information concerning the electric field produced at remote points to determine the wavefront of the stroke current. The purpose of this paper is to present a review of available information on laboratory produced sparks, to present new data on this subject, and to co-ordinate the external manifestations of gap breakdown from an engineering point of view. These results have been co-ordinated in a companion paper,[6] in this issue, with similar data from natural lightning.

General Phenomenon

In order to establish the general nature of the phenomenon the experiments of Park and Cones[7] will be described first. Later a more detailed discussion, supported by experimental evidence, of various phases of the discharge will be undertaken. It has been known for a long time that the breakdown of long gaps proceeds in several phases. These are clearly defined by Park and Cones. Their setup, Fig. 1(M), consisted of a metallic sphere of 1.6-cm (centimeters) diameter mounted on a vertical shielded rod connected to ground which permitted measurement of the current from the sphere alone. Above the sphere at a fixed distance above ground a flat insulated plate was mounted to which voltage was applied. Some of their data were obtained with a 0.07×100-μsec (microsecond) wave which may for all practical purposes, be regarded as a rectangular wave. The crest of this applied wave was held constant at 145 kv, and conditions in the gap were varied by changing the gap length by raising or lowering the sphere. The current flowing from the sphere was measured by means of a cathode-ray oscillograph and the setup was housed in a black box to expedite photographing the discharge.

Fig. 1 shows a replot of the current from the sphere as this substantially rectangular wave was applied to gaps of various lengths. Some liberty was taken by the authors to line up the large current pips as this illustrates the phenomenon more clearly. Small distortions of time scales result from this procedure. The time of application of voltage is indicated by the small current ripple just

Fig. 1. Currents resulting when an 0.07×100-μsec 145-kv impulse is applied to the gap setup as shown in M

90004108

Paper 61-489, recommended by the AIEE Transmission and Distribution Committee and approved by the AIEE Technical Operations Department for presentation at the AIEE South East-South Central District Meeting, New Orleans, La., April 5-7, 1961. Manuscript submitted January 9, 1961; made available for printing March 3, 1961.

C. F. WAGNER and A. R. HILEMAN are both with the Westinghouse Electric Corporation, East Pittsburgh, Pa.

The authors wish to acknowledge the valuable assistance of P. H. Long, J. Brado, and L. Kalning for performing the gap breakdown tests and of H. L. Smith for the computer coding of the channel velocity equations for rapid and accurate determination of the gap time lag curves.

preceding the almost vertical current change which represents the charging current to supply the electrostatic field before the gaseous discharge phenomenon occurs. The large abrupt change is termed the "first current pip" by Park and Cones. Generally the current pip does not coincide with the instant of application of voltage but is somewhat delayed. The delay is occasioned by the chance occurrence of a free electron coming within the overstressed region in the vicinity of the sphere and triggering the discharge. This is usually called the "statistical time delay" as it depends upon a chance occurrence. The crest of the first current pip for the sphere positive decreases from 18 amperes for $L=22$ cm as the gap is increased and for the sphere negative from 20 amperes for $L=10$ cm. The magnitudes vary over wide limits. The current rises to crest in about 0.01 μsec and then drops somewhat exponentially to zero in about 0.3 μsec for the sphere either positive or negative.

The current ceases after the disappearance of the first current pip at larger gap settings but with the smaller gaps, such as $L=20$ cm, for the application of the positive potential Fig. 1(L) shows that after the current almost decreases to zero it slowly rises again becoming more rapid and is finally limited by the constants of the circuit. The oscillogram does not record the final current as a protective gap short-circuited the oscillograph element. This rise in current has been termed by Park and Cones the "second discharge rise."

The first current pip is approximately the same for the application of a negative impulse wave, except as to magnitude, as that obtained for an applied positive impulse, but the second discharge rise is not as gradual in its change and has steeper rates of rise. In each case after the second discharge rise has begun, complete breakdown follows unless the voltage wave is chopped.

Positive Discharges

The photographs exhibit different characteristics for positive and negative discharges. Since the discharge is the simpler with the sphere positive it will be described first. For the longer gaps the photographic evidence indicates that streamers that produce light radiate from the sphere but do not complete the passage of the gap. As the gap is reduced to 25 cm some of the streamers do complete passage but the current still drops to zero and breakdown does not occur. For $L=20$ cm complete breakdown occurs. Photographs taken when the waves were chopped by means of a parallel gap show that the appearance of the discharge begins to change after the second discharge rise starts. This change consists of one or more bright discharge channels that start at or near the sphere. These discharges have been termed "channels" by Park and Cones to distinguish them from the first kind of discharge which they termed "streamers." These channels move in zigzag fashion across the gap. The length of the channel as a function of time was measured from the progress of the photographed tip and is shown in Fig. 2.

To form a working thesis on which to base discussion the following explanation similar to Park and Cones' is offered to describe the phenomenon. There is no space charge in the interelectrode space prior to initiation of the discharge. The charge on the sphere is determined by the electrostatic solution for the particular configuration. The field is strong near the sphere and decreases as the plane is approached. If the gap spacing is sufficiently small, a zone in the vicinity of the sphere is stressed beyond the critical value of about 30,000 volts per cm. As a free electron appears in this overstressed zone, streamers form which radiate from the sphere. The streamers are not uniform in length and with a sufficiently large gap none reaches the plate. The net effect of the streamers is to produce a space charge that develops its own field and potential drop. Since the applied voltage across the gap is constant, as the space charge develops, less potential is available to produce the charge on the sphere. Consequently the electric field adjacent to the sphere decreases until it reaches 30,000 volts per cm at which point further supply of current is inhibited. The net result is that when the gap is long, a ball of space charge forms around the sphere. A state of equilibrium is attained for which the formation of the space charge is arrested and ionization processes cease. If the gap is decreased and an impulse is reapplied a new state of equilibrium is attained for which the ball of space charge is larger. Finally, as the gap is further decreased, the space charge expands to occupy the entire interelectrode space and, with additional reduction, conditions become conducive to the development of a channel from the sphere. The discharge is converted from a glow discharge to an arc plasma that begins to grow from the sphere toward the plane at a rate indicated by Fig. 2. The criterion for the critical condition, next to the sphere, appears to be such that a charge distribution will produce an average gradient across the entire gap of about 6,000 volts per cm. Conditions governing the transition from corona to an arc

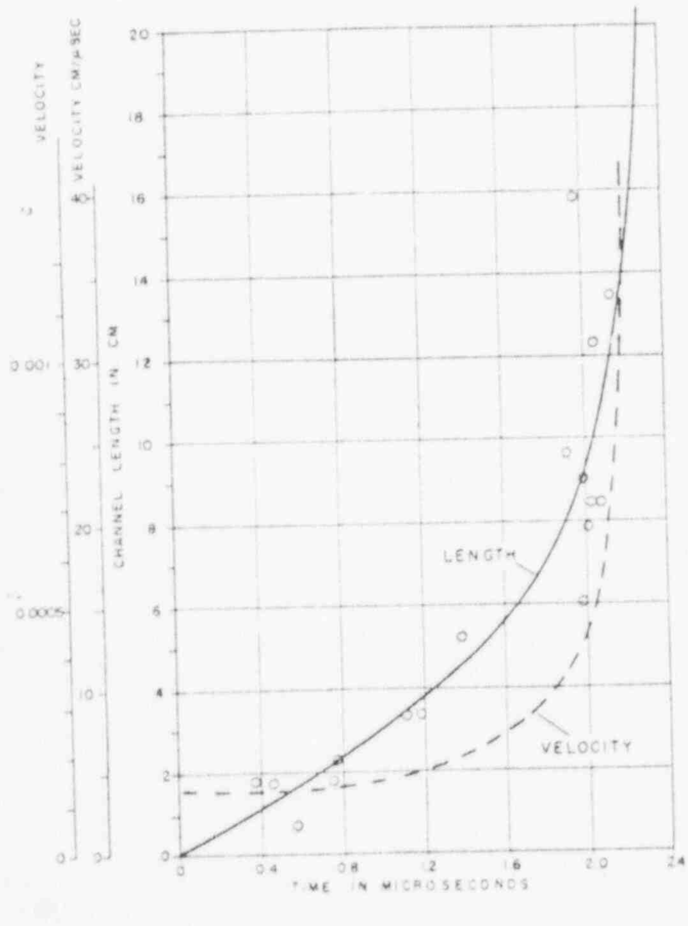

Fig. 2. Progress of channel tip across a 20-cm gap[1] for the conditions of Fig. 1 for the sphere positive. The dotted line is the slope of the distance–time (solid line) curve

90004109

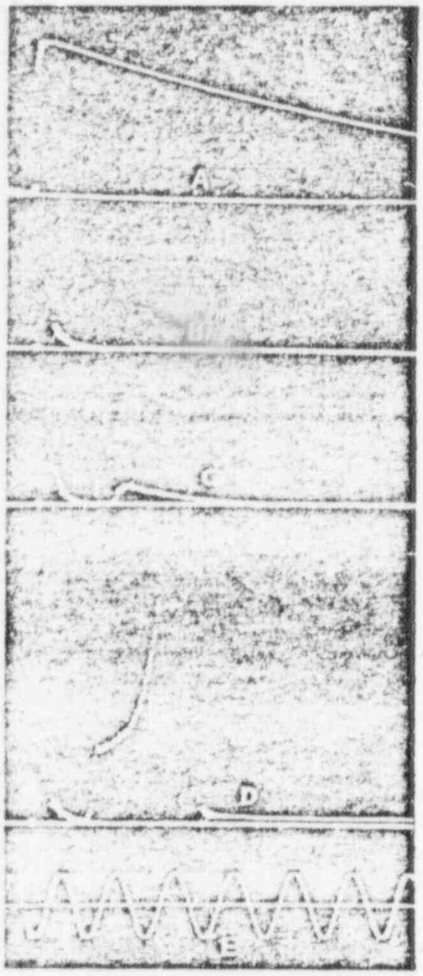

Fig. 3. Current response[13] of a 200-inch rod-rod gap when a 3×50-μsec 3,000,000-volt surge is applied

A—Voltage wave
B, C, and D—Current waves
E—Timing wave of 100,000 cycles per second

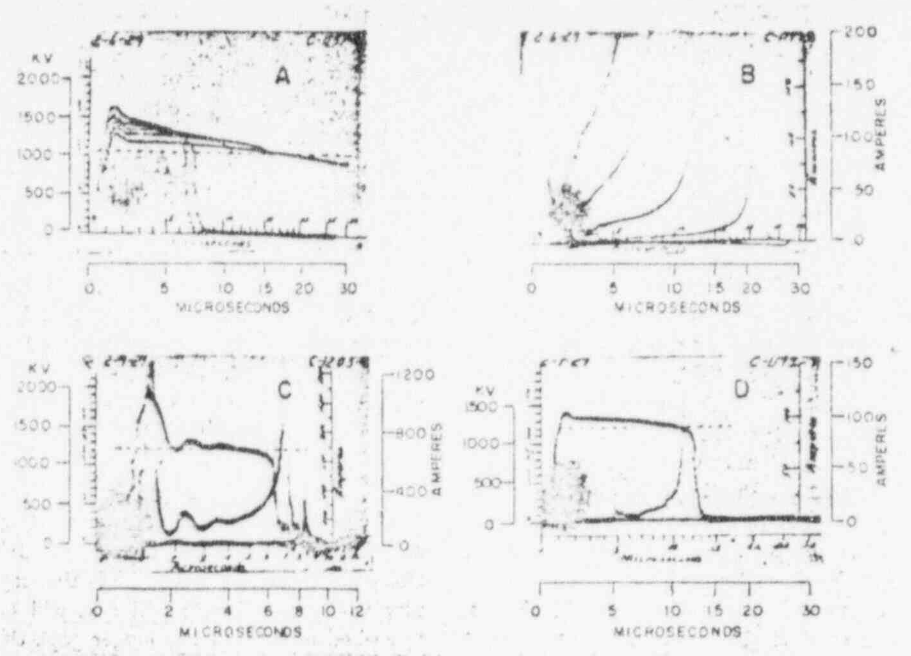

Fig. 4. Sparkover of a 16-unit insulator string equipped with arcing rings of 4-inch-diameter pipe[14]

A—Five successive applications at increasing voltage
B—Currents resulting from A
C—Still higher voltage with corresponding current
D—Application of voltage and resulting current with the insulators only
Note the sudden rise of the current prior to the later increase

are not well understood. It is necessary to wait for further developments by the physicist before a more definite explanation can be given. The drop along the plasma channel is very low and thus when it is initiated the effect is progressive as the channel merely constitutes in effect an elongation of the positive electrode. The continually decreasing gap length encourages all the factors originally responsible for the development of the discharge. When the head finally reaches the plate, the channel constitutes a virtual short circuit of the surge generator and the subsequent current is dependent upon the constants of the generator circuit and the characteristics of the arc. This effect is illustrated by the current oscillogram for the 20-cm gap of Fig. 1.

Negative Discharges

With the sphere negative, the charge develops within the interelectrode space in a similar manner, although the actual mechanism of production may be quite different. The negative discharge is more diffuse than the positive both visually and photographically. It consists of numerous streamers of fine texture while the positive discharge consists of fewer but stronger and more crooked streamers.

In the authors' interpretation of the phenomenon just before sparkover it is assumed that the electric gradient, because of the space charge, is approximately constant across the gap although this assumption is not essential to a general understanding of the phenomenon. For the authors' purposes it is convenient to think in terms of an average gradient across the gap. Returning to the Park and Cones experiments, as the gap is decreased and is sufficiently small, the gradient in the interelectrode space due to the space charge increases and the charge density next to the sphere is higher than at the plane. But the conditions necessary to initiate a channel from the positive plane are reached prior to the conditions necessary to initiate a channel from the negative sphere. So the channel starts from the plane before one starts from the sphere. But as the positive channel progresses from the plate, conditions become more critical at the sphere and a channel is finally initiated from there also. The two channels meet in mid-gap. From this point the current is again determined by the constants of the surge generator and the characteristics of the arc.

Discussion

90004110

The general nature of the breakdown of nonhomogeneous gaps, consisting of a corona discharge followed by the development of a conducting channel, has been known from the earliest days of impulse testing. For example, Slepian and Torok[8] in 1929 by chopping impulse waves showed by means of photographs the stages of progress of the discharge and also some indication of the maximum currents. Utilizing a rotating camera Allibone,[9] in 1938, presented an extensive study of discharges in long gaps and established the chronological sequence of the leader followed by a return stroke in the laboratory. He commented upon the absence of a discharge from the plane when the rod of a rod-plane gap is positive. This distinction between the corona starting voltage and the breakdown was recognized as early as 1931 by Goodlet, Edwards, and Perry.[10]

Komelkov[11] in 1947 working with gaps between 10 and 100 cm concluded that the drop in the channels was very low, about 55 volts per cm, and that the gradient in the corona streamers was in the range of 6,000 to 10,000 volts per cm. Saxe and

Meek[12] also concluded that the drop along the channels is small.

Hagenguth, Rohlfs, and Degnan[13] furnished limited evidence on a vaster geometric scale which might be viewed as supporting the general nature of the discharge discussed here. They measured the current flowing in the ground electrode of a 200-inch rod-rod gap when a 3,000,000-volt negative 3×50-μsec impulse was applied to the free electrode. Fig. 3 is a reproduction of Fig. 12 of their paper. Curve A shows the applied voltage which for this gap was just below critical. With 20 applications of this voltage, nine cases developed a glow that bridged only a portion of the gap and the current in the grounded electrode was as shown by trace B; in nine cases the glow bridged the entire gap and the current was as shown by trace C; and in two cases complete sparkover occurred and the current was as shown by trace D. The magnitudes of the three current pips were remarkably consistent and averaged 7.9 amperes. The duration of the pips was 9 μsec.

As early as 1929 Torok and Fielder[14] measured the predischarge currents of suspension insulators. Fig. 4 is a reproduction of some of their oscillograms. In all of these records the negative pole was grounded. Fig. 4(D) shows the voltage and the current for flashover of a string of 16 insulators. The delay in current occasioned by the necessity of the correct positioning of a free electron is evident and the resultant current is typical of others that have been presented. Figs. 4(A) and 4(B) are mates; the former shows the applied voltages and the latter depicts the resulting cu[illegible]ts as a 16-unit insulator string with an arc[illegible]ng ring of 4-inch pipe was flashed over. Fig. 4(C) shows the same test piece with the application of a still higher voltage. The short-circuit current of the surge generator was most likely about 2,000 amperes. It is not known whether the current trace recorded the true maximum as it may have been limited by the operation of a protective gap placed across the shunt.

Thus with this general background of the phenomenon and limited historical review, a discussion of the component parts of the discharge will be undertaken.

Corona Streamers and Envelope

It is clear from the foregoing that for impulse voltages in excess of the corona threshold voltage but less than the critical breakdown value, a self-limiting space charge is distributed throughout the interelectrode space. This charge must in some manner produce an electric field that inhibits further growth of the discharge.

Average Electric Gradient at Sparkover

For Positive Discharges

As has been mentioned, Allibone commented on the absence of an upward channel from the plane of a rod-plane gap when the rod is positive. Park and Cones also observed that for the sphere positive the channel proceeded from the sphere completely across the gap. Probably the absence of a channel arising from the plate was most dramatically confirmed by Norinder and Salka[15] in their elaborate photographic investigation of spark discharges. The absence of a complication caused by the formation of a channel from the plate insures a somewhat simpler analysis for this type of discharge and for this reason the rod-plane discharge with the rod or small sphere as positive electrode will be considered first.

After a voltage is applied across a gap, the space charge expands and becomes more intense until the gradient next to the electrode drops to 30,000 volts per cm as was mentioned earlier. When the radius of the rod of a rod-plane gap is small, then only a small (in the limit zero, for a pointed electrode) potential is required to produce a charge on the electrode that will result in a gradient at the electrode of 30,000 volts per cm. Then practically all of the applied voltage is available to produce the space charge. For these cases, when the gap is adjusted so that the corona space charge envelops the entire interelectrode space, the applied voltage divided by the gap length is the average gradient along the axis of the corona envelope.

Once the channel has begun to form the discharge develops to ultimate sparkover almost invariably. For the critical sparkover voltage, half of the applications of voltage produce sparkover. Consequently, this voltage constitutes a measure of the average gradient of the space charge to produce sparkover because the cases that do not cause sparkover represent the maximum development of the space charge without the formation of a channel.

In Fig. 5 the average critical sparkover gradients of rod-to-plane and rod-rod gaps from different sources for both polarities are plotted. The positive polarity data are indicated by the full lines. The Bellaschi and Teague[16] data represented the full wave (1.5×40-μsec) critical sparkover values and were made on gaps up to 200 cm. Breakdown occurred at about 8 μsec. The Hagenguth Rohlfs, and Degnan[13] data covered an even greater range up to 640 cm with an impulse wave of 3×50 μsec. They stated further that their unpublished data, with gap spacings up to 50 feet tended to give average gradients of the same value. The Gorev, Zalesky, and Riabov[17] data,

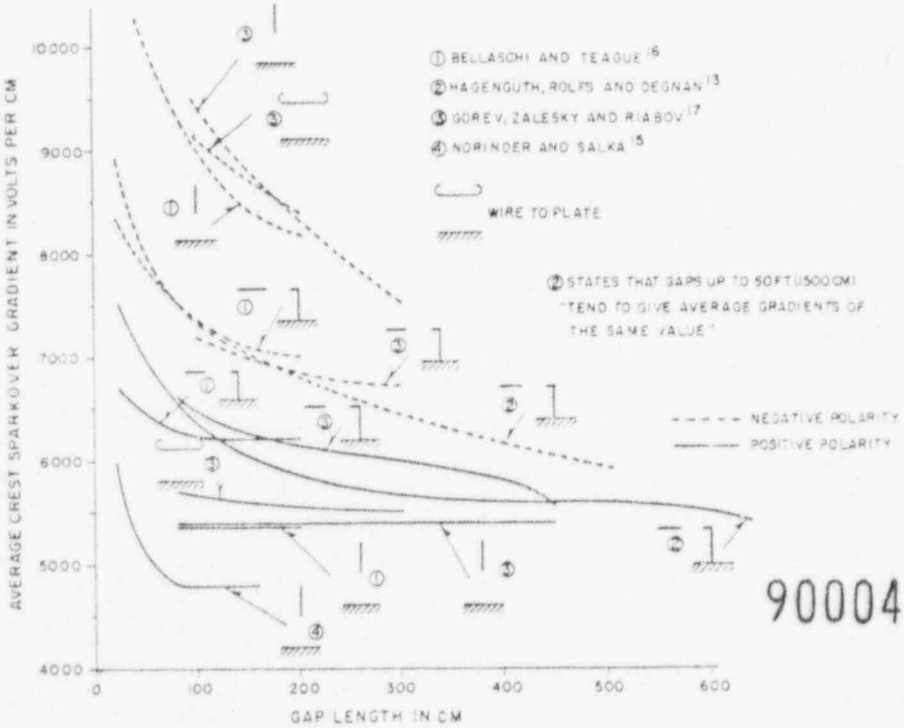

Fig. 5. Average crest impulse sparkover gradient for both positive and negative polarity for gaps of different configuration as a function of gap length

with 1.5×40-μsec impulse waves, agreed quite closely with the other data. The Norinder and Salka[16] curve for the rod-plane sparkover was only 11% below that of the others. The curves marked by a small horizontal line with curled-up end represent horizontal wire-to-plane data. They agree almost exactly with the rod-plane curves. These curves indicate a practical working average of the average crest sparkover gradient for long gaps of about 5,400 volts per cm for rod-plane gaps and about 6,000 volts per cm for rod-rod gaps which can also be interpreted as the average gradient along the axis of the gap produced by the space charge.

Part of the discrepancy between the laboratory data may be ascribed to differences in waveshape of the applied voltages as well as differences in methods of impulse measurements and to laboratory and observational conditions. Berger's CIGRE report,[18] which discussed comparative tests by 14 different laboratories, indicated that the critical sparkover voltage gradient for a 45-cm rod-rod gap for positive polarity gave a range of from 6,000 to 7,600 volts per cm even after air density corrections had been taken into consideration.

For Negative Discharges

In Fig. 1 the waveform of the first discharge pip has approximately the same waveshape for both polarities but the magnitude for positive polarity is somewhat larger than for negative polarity. A corresponding difference in the relative charge for positive and negative applied voltages supplied to the corona envelope of a cylindrical conductor above a plane when impulse has also been noted by Wagner and Lloyd.[19]

As mentioned previously a fundamental difference does exist when a rod-plane gap is impulsed by a negative potential and when impulsed by a positive potential. This difference is the appearance of local discharges at the plate after the negative corona space charge has developed to some extent. One of the plate discharges finally develops into a plasma channel that grows toward the rod before a channel develops from the rod. Because of the presence of the discharges from the plate, the sparkover curves cannot be used directly to determine the average gradient that leads to development of a plasma channel from the rod. One wonders at what value of average gradient would a negative space charge develop into a channel from the cathode if the space charge were permitted to form from the cathode without interference of a corresponding discharge from the anode. During the initial stages of the channel growth the velocity of the channel is small as compared with the later stages. As the head of the channel progresses, the space charge tends to develop ahead of it. The initial channel development from the anode merely serves to shorten the gap length and increases the gradient adjacent to the cathode to a point where a cathode channel will form. The influence of the anode channel on the cathode channel should be proportionately less for the long gaps than for the small gaps and should be less for a plane anode than for a rod anode. So, in order to estimate the average gradient at which channels are developed, one should refer to the sparkover data for rodplate gaps for long spacings, and make some allowance for the development of the channel from the plate. From Fig. 5 the critical average gradient at which the negative channel develops is estimated to be 8,000 to 9,000 volts/cm.

Time to Establish the Charge

Most photographs of the predischarges (used merely to apply to that which occurs before the production of the conducting channels) show very pronounced streamers of high light intensity. The head of some of these streamers travel at very high velocities. For example, Park and Cones stated that the mean streamer velocity was found to be 500 cm per μsec or 1.7% the velocity of light for the sphere negative and 800 cm per μsec or 2.3% the velocity of light for the sphere positive. The average deviation was 90 for the sphere negative and 100 for the sphere positive. However, these numbers cannot be viewed as the actual rate at which charge was developed in the inter-electrode space. Some other mechanism must have been present which the physicist may help to explain. As mentioned by Park and Cones, the streamers "should be thought of as a traveling wave of high charge density which is propagated by a process in which new charges are continually produced at the leading surface of the ball by the high gradient there. In the path behind the ball there is left a high concentration of both positive and negative ions, with an excess of positive ions in case the sphere is positive and an excess of negative ions in case the sphere is negative." The shape of the current wave of the first discharge pip is quite repeatable for the sphere positive and somewhat less repeatable for the sphere negative. The average waveshape rises to crest in about 0.008 μsec and decays approximately exponentially to half value in about 0.08 μsec. As Fig. 1 indicates, the time to reach zero is about 0.3 μsec. The waveshape stays essentially constant for both polarities, for all gap spacings, and for fast and slow applied voltage waves.

Remembering that in Park and Cones' experiments the applied voltage was kept constant and the gap conditions were varied by changing the gap length, the fully developed discharge will be taken as that for which a 0.07×100-μsec positive wave produced 50% sparkovers. From their data this was 24 cm for positive polarity. The effective velocity of charge formation for the positive space charge, v_s^+ will then be defined as the velocity obtained by dividing the half gap length by the time required to produce the fully developed field. Thus

$$v_s^+ = \frac{24}{2\times 0.3\times 10^{-6}} = 4.0\times 10^7 \text{ cm per sec} = 0.0013c \quad (1)$$

For the negative polarity, the effective velocity of charge formation is

$$v_s^- = \frac{11.5}{2\times 0.3\times 10^{-6}} = 1.9\times 10^7 \text{ cm per sec} = 0.0006c \quad (2)$$

The paper by Hagenguth, Rohlfs, and Degnan[13] provided another factor. At the critical sparkover point of a 200-inch rod-gap with a negative impulse applied to the free rod, the time required to develop the space charge was about 9 μsec. This corresponds to a velocity of

$$v_s^- = \frac{200\times 2.54}{2\times 9\times 10^{-6}} = 2.8\times 10^7 \text{ cm per sec} = 0.0009c \quad (3)$$

Considering the wide range in gaps, from 4.3 to 200 inches, to which these values applied it is remarkable that these numbers are so very nearly equal.

Concerning the actual physical process involved in the establishment of the space charge, it will be observed that the electron drift velocity in a field of 30,000 volts per cm and a pressure of 760 mm (millimeters) is, from Loeb,[20] about 1.4 $\times 10^7$ cm per sec or 0.0005 *c*. This field is chosen for comparison purposes because it lies midway between the initial and final fields. This value compares favorably with the values given by equations 1, 2, and 3.

Charge and Electric Field Distribution Within the Gap

So far consideration has been given to characteristics of the space charge that are subject to actual experimental determination such as the average critical breakdown gradient and the external current feeding it. Because of the difficulties of measurement, little is known of the actual structure of the charge distribution or of the field distribution. Doubtless these distributions are a function of time. Photographic evidence points to the early development of streamers which may be quite independent of and unaffected by each other. They probably are responsible for ionization phenomena that produce charge separations. The speed with which the space charge develops suggests strongly that its development is associated with the movement of electrons rather than ions for both polarities. In time the movements of these charges produce a mass or aggregate effect in which all the streamers play a part.

In contemplating the average electric gradient just prior to breakdown, from Fig. 5 for positive polarity, one is immediately struck by the fact that it is constant over a very long range of gap lengths. What sort of charge distribution would give rise to an average gradient that is independent of gap length? Park and Cones suggested a charge concentration that varies inversely as the distance from the spherical electrode in their sphere-plate gap. For either a truly spherical or truly cylindrical charge distribution the resultant electric gradient is a constant. For a rod-plane gap with the rod positive, such distribution can be viewed as being produced by the following mechanism. Suppose that positive ions and electrons are produced uniformly along the numerous very-high-speed streamers that emanate from the positive rod. As the electrons move toward the anode, if the positive ions that are left behind have a uniform radial distribution along each streamer, then the volume distribution would vary inversely with the radius.

The magnitude of the space charge current and the photographs of the discharge both indicate that the mechanism of the negative discharge differs from that of the positive discharge, but the resultant charge distribution may still result in a field that is substantially constant.

Interim Summary

It appears that if a rectangular voltage is applied across a nonuniform gap whose average gradient is just less than the values given in Fig. 5, a self-limiting space charge develops that inhibits further flow of current. The flow of the charge into the gap is at a rate of about 0.001 *c* which corresponds approximately to the electron drift. Park and Cones' data show that for 10- to 20-cm gaps this development requires about 0.3 μsec for its completion and in the Hagenguth, Rohlfs, and Degnan data about 9 μsec with a 200-inch gap. With slower rates of rise and an abundance of electrons to trigger the gap, the current supplying the space charge is reduced in magnitude and spread out over a longer time. A considerable gradient exists within the corona envelope and for the positive discharge, just prior to sparkover, the value is about 5,400 to 6,000 volts per cm and about 8,000 to 9,000 volts per cm for the negative discharge.

Fig. 6. Velocity of the leader development as a function of the terminal voltage, u_t, for three different constant values of the unbridged gap for a rod-plane gap with the rod positive.[21] Gap spacing is 150 cm and series resistance in the circuit is 2,000 ohms

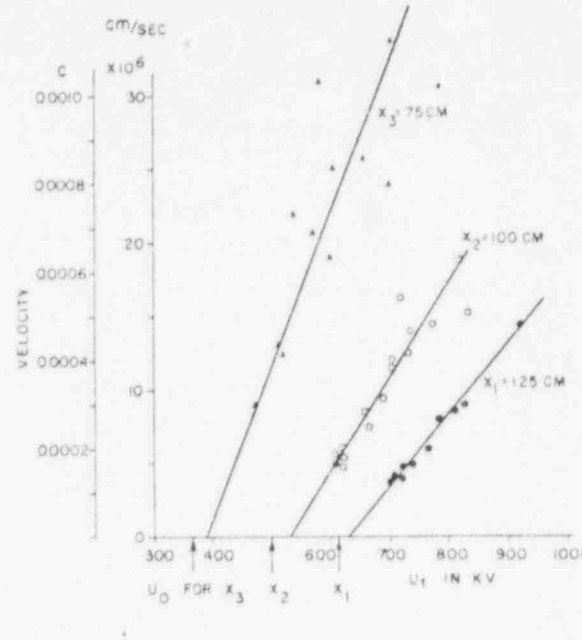

Channels

It has been observed by a number of investigators that the positive discharge from a rod- or sphere-plane gap is much more stable and consistent than the negative discharge. This applies particularly to the development of the channel. Probably this explains why more data are available concerning the positive channel.

Positive Channels

Park and Cones[7] presented the data shown in Fig. 2 concerning the progress of the head of the brightly luminous positive channel as it moved across the gap of the setup mentioned previously. The gap was set for 20 cm and a $0.07 \times t_c$ wave having a crest magnitude of 145,000 volts was applied, which was chopped by a parallel gap. The symbol t_c indicates the time after the first current pip at which the wave was chopped. Corresponding photographs of the discharge showed the distance that the channel had progressed during the chopping time. The slope of this curve is plotted by the dotted line and indicates that the initial velocity is 3×10^6 cm per sec or 0.0001 *c* which rises slowly at first and then more rapidly. According to Park and Cones, at midgap (10 cm) the rate of growth is about 20×10^6 cm per sec or 0.0007 *c*.

Akopian, Larionov, and Torosian[21] undertook elaborately combined oscillographic and rotating drum photographic tests on rod-plane and rod-rod gaps of 100–200 cm with positive impulse potentials applied to the gap. Thus, they were able to co-ordinate the travel of the head of the channel with the instantaneous value of the terminal voltage. Komelkov[11] had previously demonstrated that the drop in the channel was about 50 volts per cm. Therefore, assuming the drop to be negligibly small, the voltage across the unbridged portion of the gap is identical with the terminal voltage. They showed as indicated in Fig. 6 (Fig. 8 of Akopian, et al.) that for a rod-plane gap with positive potential applied to the rod, the velocity of the head of the channel for a constant value of the unbridged gap varied linearly with the applied voltage. In this figure u_t is the applied voltage in kv, *s* is the gap length in cm, and *x* is the unbridged portion of the gap in cm. Curves are drawn for three constant values of the unbridged gap. The velocity rises from zero at a value of terminal voltage u_0 that would produce discharge when applied for some length of time ("prolonged action" according to the language in reference 21). Beyond this voltage the velocity is proportional to the excess of the terminal voltage above this value. The values of u_0 for the three cases are indicated below the abscissa. They also showed that the positions of the straight lines are related and that for rod-plane gaps the following relation for the velocity holds.

90004113

$$v = k\frac{u_i - u_0}{x - 0.23x} \text{ cm per } \mu\text{sec} \qquad (4)$$

For a rod-plane gap up to 200 cm, k is about 9 and for individual discharges the coefficient k may diverge from its mean value within $\pm 20\%$. With u_0 known as a function of x (very nearly linear), the velocity v and consequently x can be solved in terms of the applied voltage u_i. Akopian, Larionov, and Torosian[21] have tested this procedure with applied voltage waves of widely differing shapes with gratifying results.

Negative Channels

The negative channel is much more erratic than the positive channel but, because the experimental results are usually complicated by the presence of positive channels, it is difficult to discriminate between the effects of the two polarities when both are present and in a developmental state. Examination of the channel currents of Fig. 1 reveals that the currents rise more sharply when the sphere is negative. This may possibly indicate a higher velocity for the channel developing from the sphere. It has also been observed photographically that the positive plate channel progressed a considerable portion of the gap before the negative channel started from the sphere. But in spite of this handicap the two channels met in mid-gap. This was possible only if the negative channel traveled with a higher velocity.

Similar evidence has been provided by the experiments of Hagenguth, Rohlfs, and Degnan[13] which were described previously in connection with Fig. 3. In nine out of 20 shots with the same voltage applied, the glow bridged the entire gap without sparkover. In Fig. 11 of their paper a well-defined streamer can be seen "progressing from the grounded positive rod within the glow emanating from the negative electrode." For the particular photograph shown this streamer has progressed about one-fourth or one-third the distance across the gap. "On complete breakdown of the gap (not shown) at the same voltage there is a well-defined split in the spark near the middle of the gap, indicating where the the final streamers [in present terminology, channels] emanating from both electrodes, met." This experiment also strongly indicates higher velocity of the negative channels.

Norinder and Salka[15] related similar experience with rod- and sphere-plate gaps. The plasma channels began at the plate (anode) and proceeded toward the rod or sphere electrode. At a considerably later time similar channels emanated from the rod or sphere and met approximately in the middle of the gap.

Rod-Rod Gaps

For rod-rod gaps, channels form from both electrodes. Akopian, Larionov, and Torosian determined that for an electrode separation of 125 cm the velocity with which the channel tips approach each other can be expressed in the relation

$$v = 11\frac{u_i - u_0}{x} \text{ cm per } \mu\text{sec} \qquad (5)$$

where u_i is again the actual instantaneous voltage in kv across the electrodes and u_0 is the critical voltage in kv of the unbridged gap, x in cm. They generalized no further than this single gap but did show that this relation produced good results when the applied voltage was varied over a wide range of waveshapes.

Rusck,[22] on the other hand, stated that this approach was not a complete solution because tests made in his laboratory "show that the formula given in the above mentioned paper cannot be utilized on other gaps." He cleverly obviated the complexity of taking photographs of the discharge by simply accepting two important assumptions that are also inherent in the work of Akopian, Larionov, and Torosian. First, that the drop in the channel is negligibly small and consequently the channels can be viewed as extensions of the electrodes, and second, that the velocity of approach of the channel tips is a function of the instantaneous electrode voltage and the length of the unbridged gap. As a basis for his work it was necessary to determine experimentally the time to sparkover of gaps to a rectangular applied voltage wave. He found that by applying such a wave to irradiated gaps from 10 to 70 cm the time to sparkover, τ, could be expressed by the following formula:

$$\tau = \left(\frac{20 + 10s}{U}\right)^{4} \text{ in } \mu\text{sec} \qquad (6)$$

where U is the magnitude of the applied rectangular wave in kv and s is the gap length in cm. Rusck also stated that because the critical sparkover voltage, U_0, is approximately a linear function of the distance s, the time lag can be expressed by

$$\tau = 4.7\left(\frac{U_0}{U}\right) \text{ in } \mu\text{sec} \qquad (7)$$

His relations were satisfactorily utilized for different types of applied waveforms. He warned that his work should be applied to time lags less than 4 to 5 μsec, as incorrect results would be obtained for longer times.

Observations by the Authors

If u_0 in equation 5 is explicitly defined as the critical sparkover voltage of a

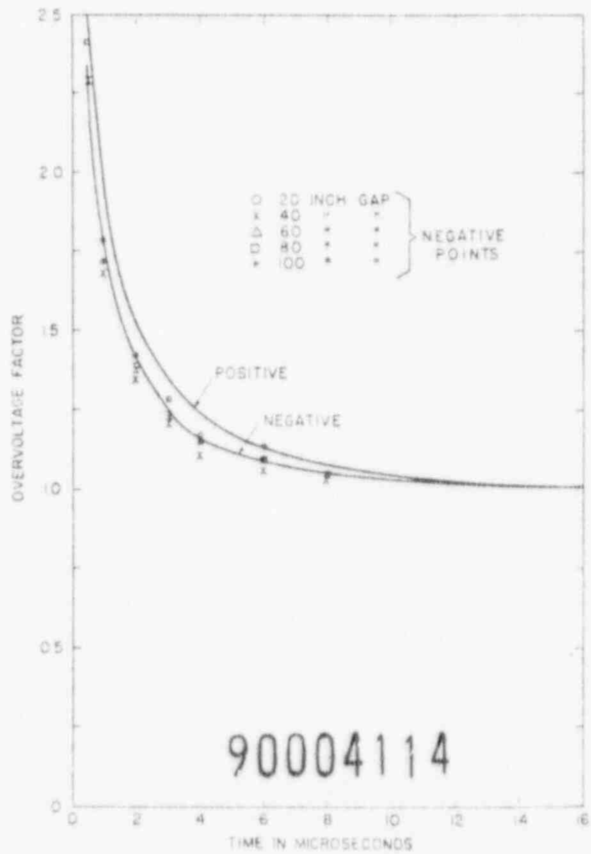

Fig. 7. Time-lag curves for standard rod-rod gaps in response to a 1.5 × 40-μsec voltage wave for spacings from 20 to 100 inches[13]

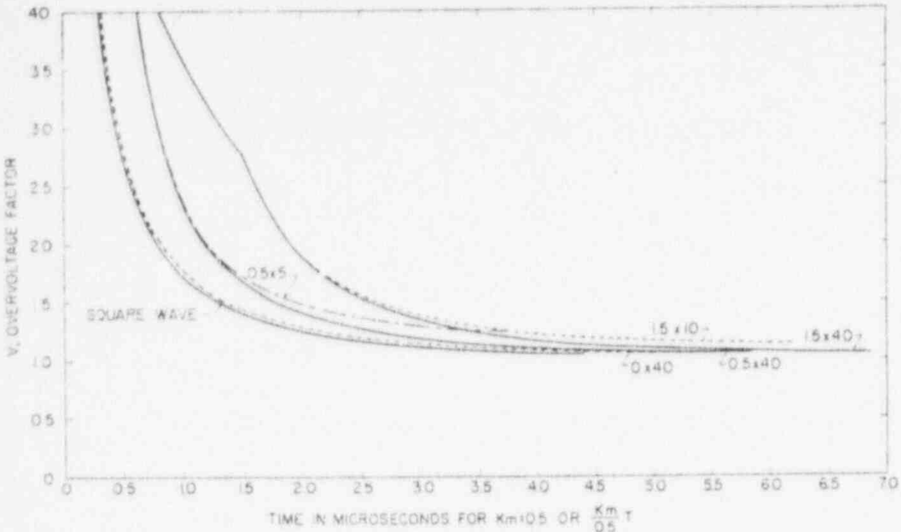

Fig. 8. Calculated time-lag curves for rod-rod gaps for various applied voltage waveshapes

rod-rod gap in response to a rectangular wave and it is assumed that this quantity is proportional to the gap length, then

$$u_0 = mx \text{ in kv} \tag{8}$$

If the difference of the applied waveforms is taken into consideration the factor m corresponds approximately to the average sparkover value in Fig. 5 in kv per cm. Equation 5 can be rewritten as

$$\frac{dx}{dt} = -k\left(\frac{u_t}{x} - m\right) \tag{9}$$

which merely states that the velocity is proportional to the excess of the average gradient across the unbridged portion of the gap over the critical sparkover gradient. Generally the factor k will vary with different gap lengths; the negative sign is inserted for analytical purposes so it may be recognized that the unbridged gap decreases when the quantity with the parenthesis is positive. Further transformation of equation 9 is possible to the following:

$$\frac{km}{s}\,dt = -\frac{\left(\frac{x}{s}\right)}{\frac{1}{m}\left(\frac{u_t}{s}\right) - \left(\frac{x}{s}\right)}\,d\left(\frac{x}{s}\right) \tag{10}$$

The right-hand side is thus reduced to a per-unit gap length basis.

Rusck's equation 7 which is applicable to rectangular voltage waves applied to 10–70-cm gaps shows that the time lag is independent of the gap length. The work of McAuley[23] with 1.5×40 impulse waves on gaps up to 100 inches when replotted in Fig. 7 shows a similar independence of gap length. If, in equation 9,

$$k = Ks \tag{11}$$

then equation 10 is also independent of gap length. This simply means that the velocities of the channel tips, as will be explained in more detail later, are proportional to the electrode spacings. Some such effect can be expected from the physical considerations involved. Suppose as premised earlier, that in their development the corona streamers deposit a charge density in the interelectrode space, such that at the instant of channel initiation the electric gradient between the electrodes is essentially constant and equal to the value m. Furthermore, if it is assumed that this space charge is relatively immobile, then as the arc plasma develops within this space, it forms a good conductor extending as a thin pencil from each electrode. In order to satisfy the condition that the electric gradient along these good conducting pencils is zero, it is necessary that charge be induced along the pencil that will produce an electric field just equal and opposite to that which had existed previously. The induced charge will vary linearly along the pencil and will be proportional to the distance traveled by the tip. The charge density, and consequently the electric field, at the tip will be proportional to the spacing of the electrodes.

Now if a new term, V, is defined as the overvoltage factor

$$V = \frac{1}{m}\left(\frac{u_t}{s}\right) \tag{12}$$

and equations 11 and 12 are inserted into equation 10, then

$$km\,dt = -\frac{x/s}{V - x/s}\,d(x/s) \tag{13}$$

In this same nomenclature, equation 9 expressing the velocity can be changed to the following:

$$\frac{dx}{dt} = -km\left[\frac{1}{m}\left(\frac{u_t}{s}\right)\frac{s}{x} - 1\right] = -sKm\left(\frac{V}{x/s} - 1\right) \tag{14}$$

which confirms the previous statement that the velocity is proportional to gap length.

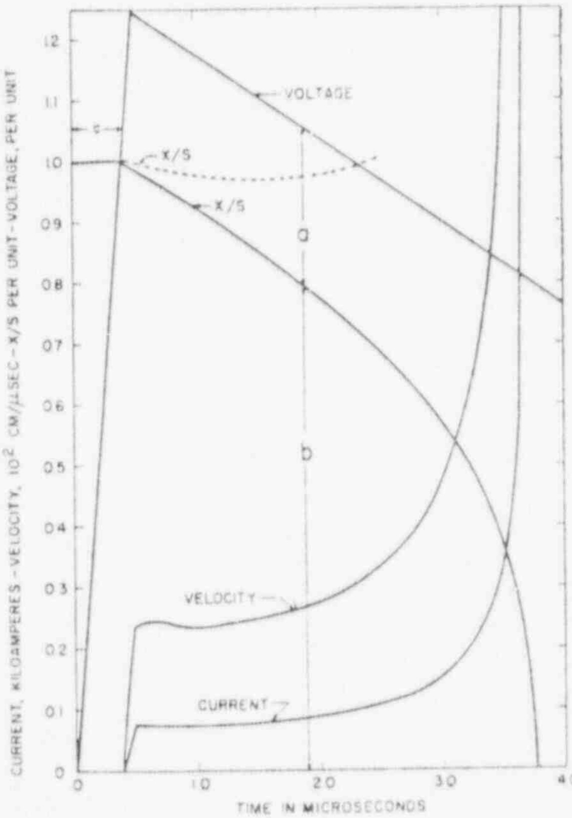

Fig. 9. Determination of the variation of channel velocity, current, and length of unabridged gap with time for an applied 0.5×5-μsec voltage waveshape for a rod-rod gap. Solid line and dotted line x/s curves for an applied surge with crest overvoltage factors of 1.25 and 1.10, respectively

90004115

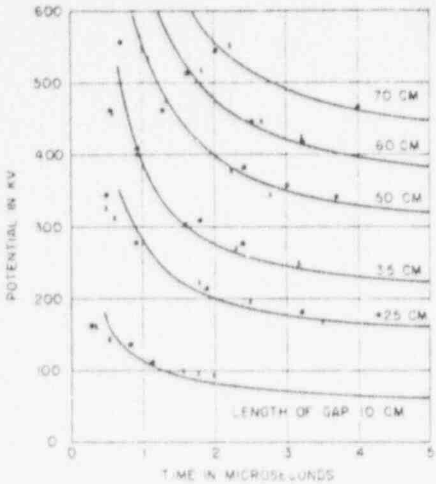

Fig. 10. Calculated time-lag curves for a rod-rod gap with an applied rectangular voltage wave as determined from equation 16 compared with Rusck's[29] test data indicated by the points

X—Positive polarity
O—Negative polarity

Application to Particular Waveshapes

With V known as a function of time, equation 13 permits solution of the determination of the diminution of x with time. Solutions will be obtained for two waveshapes.

Rectangular Wave

With V constant

$$Km\int_0^t dt = -\int_0^{x/s} \frac{x/s}{V-x/s}\, d\left(\frac{x}{s}\right)$$

$$Kmt = -(1-x/s)+V\ln\frac{V-x/s}{V-1} \qquad (15)$$

and for complete sparkover, the time lag T is

$$KmT = -1+V\ln\frac{V}{V-1} \qquad (16)$$

The value of T is plotted in Fig. 8 for Km equal to 0.5 but the curve is applicable to any value of Km. This value of Km was used as it corresponds to a value that, as will be shown shortly, fits the observed test data of Rusck and of Akopian, Larionov, and Torosian.

Linearly Rising and Falling Waves

The time lag, T, for a specific overvoltage factor, V, for other shapes of the applied voltage is most conveniently determined by using a step-by-step solution of equation 14. One such solution for a 0.5×5.0-μsec surge, whose crest overvoltage factor is 1.25, is shown in Fig. 9. The quantity x/s remains at 1.0 per unit until the applied voltage exceeds an overvoltage ratio of 1.0 at which time the channel begins its travel across the gap. Therefore, the time denoted by the distance c is actually a "dead time", that is, during this time the voltage across the gap is not sufficient to initiate a channel. The total time, T, for the channel to complete its passage of the gap is 3.8 μsec.

Also, the velocity of the channel with respect to time is shown in Fig. 9. The significance of this curve is most easily visualized by rewriting equation 14 as

$$\frac{dx}{dt} = sKm\left(\frac{V-x/s}{x/s}\right) \qquad (17)$$

Therefore, from Fig. 9, the velocity for any specific time is the distance a divided by distance b multiplied by the constant sKm. The current curve of Fig. 9 is discussed in a later section.

In Fig. 8 the time lag curves for several waveshapes for $Km=0.5$ are presented. The overvoltage factor is plotted for other than the rectangular wave as defined by equation 12 except that u_i is the crest voltage. At sparkover times when T is less than the front of the wave, the overvoltage factor plotted is the crest voltage actually obtained across the gap. In other words, these curves are constructed and plotted in the same manner as normal time-lag curves. As noted, the time axis can be changed easily for any other value of Km.

It may be seen in Fig. 8 that the critical voltages va[ry] inversely with the wave tail but are independent of the wavefront. For example, the critical voltage for a 1.5×40-μsec wave is about 1.05 and for a 1.5×10-μsec wave is about 1.13. However, the critical voltages for a 1.5×40- and a 0.5×40-μsec waves are equal. As expected, with small values of time the reverse is true; that is, the front is the dominant characteristic. Most of the difference in time lags for short times is due to the differences in dead times.

Consider now the critical voltage for a 0.5×5.0-μsec wave. According to these calculations and theory, at an overvoltage factor of 1.25, $T=3.8$ μsec. It was noted in the calculations that for an overvoltage factor of 1.10 the gap did not spark over but channels were initiated. This is illustrated by the dotted curve of Fig. 9 which shows that x/s starts to decrease when the overvoltage ratio exceeds 1.0. However, because the short wave tail causes a rapid decrease of voltage, the x/s curve reaches a minimum value, and then rises to its original value of unity.

Interpretation of Test Data

Rusck's data are convenient for testing the validity of the relations presented here because he attempted to obtain a rectangular applied voltage wave. It rose to crest in about 0.3 μsec and was flat thereafter with the absence of oscillations. Fig. 10 shows his test points for rod-rod gaps of from 10 to 70 cm. There was no appreciable difference between positive and negative polarity. By choosing $Km=0.46$ and $m=6.15$ kv per cm, the curves represent the computed results for a rectangular wave. For times longer than 1 μsec the agreement is very good, about as good as Rusck obtained with his expression. But below 1 μsec Rusck's relation shows a better agreement with tests.

Fig. 11 is a reproduction from the paper by Akopian, Larionov, and Torosian showing the time-lag curves for several different applied voltage waves for a 120-cm rod-rod gap. The relations are the same as used here for which k or Ks was

90004116

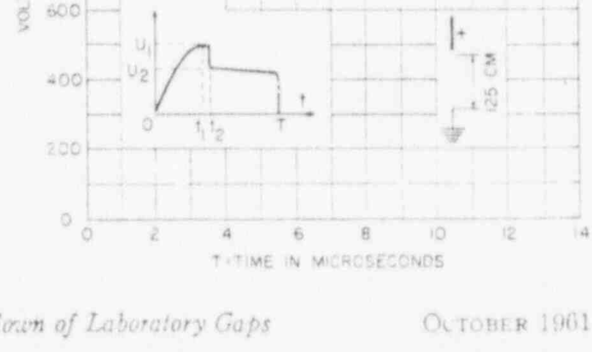

Fig. 11. Time-lag curves for a 125-cm rod-rod gap calculated by equation 5 compared with test data for applied positive polarity voltage waveshapes as illustrated in inset[21]

1—Standard 1.5×40-μsec wave, $t_1=2$ μsec
2—$t_2=2.9$ μsec, voltage ratio $u_2/u_1=0.6$
3—$t_2=1.8$ μsec, $u_2/u_1=0.63$

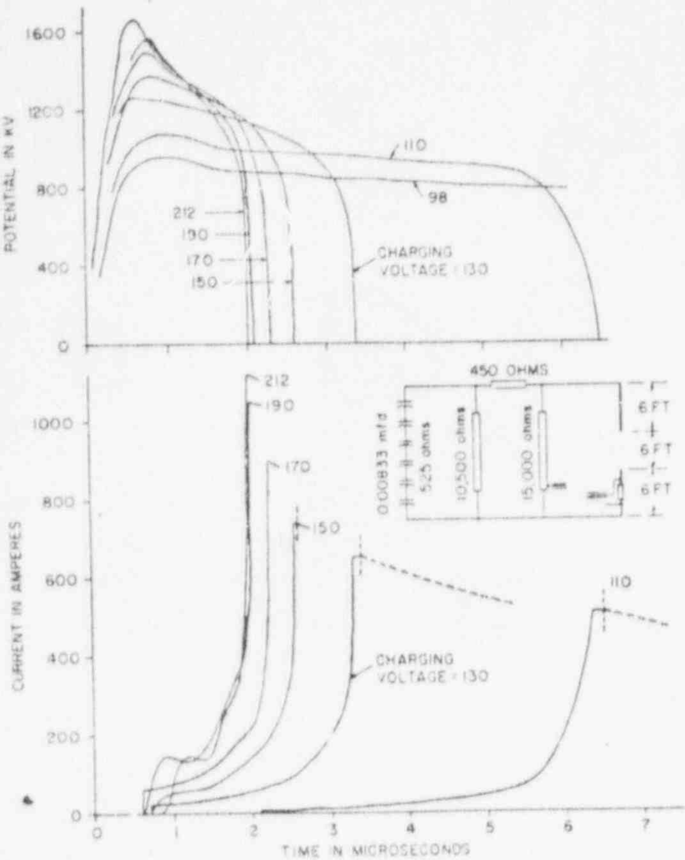

Fig. 12. Voltages across and currents through a 6-foot vertical rod-rod gap for positive polarity applied surges. The surge generator charging voltage for critical sparkover is 98 volts

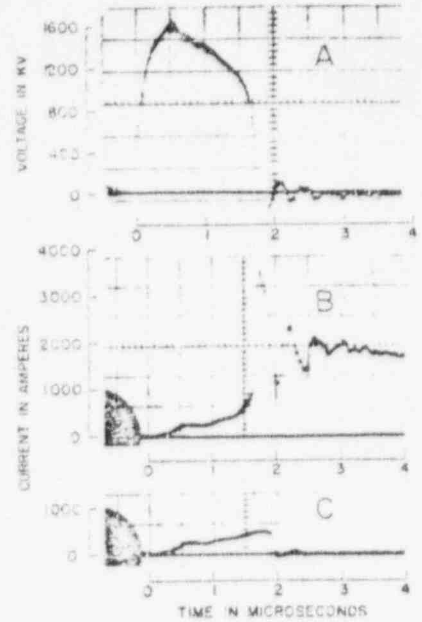

Fig. 13. Typical oscillograms of voltages across and currents through two parallel 6-foot rod-rod gaps separated 18 feet. Charging voltage is 200 volts

A—Voltage across gaps

B—Current through gap which sparked over

C—Current through gap which did not spark over when other gap sparked over

11. The value of K is then 11/125 or 0.088. From the 1.5×40-μsec curve the value of m was estimated as 720/125 or 5.76 kv per cm. The factor Km is then 0.507 which may be compared with 0.46 used in computing the curves in Fig. 13. An average value of 0.5 might very well have been used in both Fig. 10 and Fig. 11. The other two curves of Fig. 11 indicated the degree of agreement obtainable with widely different waveshapes. In their computation it is presumed that Akopian, Larionov, and Torosian used the experimentally observed potentials directly across the electrodes and therefore took into account any internal drop that may have existed in the surge generator.

Experiments by the Authors

The authors undertook measurement of the current in long gaps under sparkover conditions in order to verify some of the discussed concepts and also to study the factors affecting the current variations, because this is the most important variable to the transmission engineers. A surge generator consisting of 30 1/4-microfarad capacitors was used. Other constants of the circuit are shown in the insert of Fig. 12. In one series of tests a vertical 6-foot 1/2- by 1/2-inch rod-rod gap was used. The tip of the lower gap was about 6 feet above the laboratory floor. The voltage across the gap was measured with a 21,000-ohm compensated voltage divider and the gap current was measured simultaneously by means of a shunt located about midway in the lower rod. Successively higher voltages were applied to the gap by increasing the charging voltage of the generator. The charging voltage is an arbitrary number depending upon the a-c voltage applied to the low-voltage winding of the transformer, which supplies the voltage that is subsequently rectified to charge the capacitors of the generator. However, while arbitrary, it is a quantity proportional to the voltage to which the generator is charged, prior to being discharged into the test circuit. For the critical voltage of the 6-foot gap the charging voltage was 98 volts. The resultant waveshape of the critical voltage is shown in Fig. 12. Increasing the charging voltage resulted in drawing more current from the generator during the discharge process and this current drawn through the resistance of the surge generator resulted in considerable distortion of the voltage across the gap. Figs. 13(A) and (B) are typical oscillograms of the voltage and the current. The inductance of the surge generator generally does not play an important role. The oscillation in the current and voltage following completion of the passage of the gap by the arc plasma is caused by the interplay of the inductance and the capacitance. Its effect has been ignored by estimating the current, when necessary, as the average current during this period.

In Fig. 12 a number of curves of voltage and current for different charging voltages are plotted. Contrary to what might be expected from the theory just presented, current does not begin to flow at just the instant that the critical breakdown voltage is exceeded. The time delay at which current is initiated is longer, the smaller the excess voltage over critical. The delay is made up of two components, first, the period of waiting until a free electron enters the overstressed electrical zones at the two electrodes when the corona streamers that form the space charge are released, and second, the time required for the development of the space charge and conditions propitious for the formation of the channels from the electrodes.

It was impossible in the open conditions of the laboratory to obtain a clean-cut oscillogram of current supplying the space charge just under critical voltage as obtained by Park and Cones[1] and Degnan.[13] Apparently the high free electron concentration caused triggering of the gap on the rising portion of the voltage wave and prevented the sharp rise and exponential decay of the current.

90004117

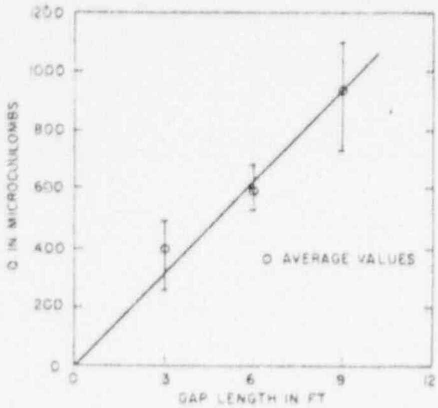

Fig. 14 (left). Relation between the charge fed into the plasma channel and gap length for rod-rod gaps

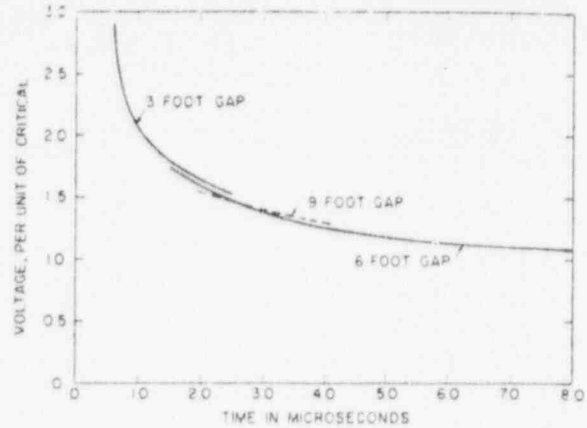

Fig. 15 (right). Experimental time-lag curves for 3-, 6-, and 9-foot rod-rod gaps for applied positive polarity voltages as illustrated

The results obtained did suggest that if the discharge had been delayed a crest of about 25 amperes would have been obtained.

Current-Time Relation

Saxe and Meek[15] concluded that the current "is proportional to the velocity of the leader stroke." For the present this relation will be accepted and it will be assumed that the instantaneous value of the current, i_c, is proportional to the instantaneous velocity. Thus,

$$i_c = -K_c \frac{dx}{dt} \tag{18}$$

The negative sign is introduced because as the unbridged gap becomes smaller the sign of dx/dt must be negative and it is desirable to consider the current as a positive quantity.

If this relation is valid, then upon integrating both sides one arrives at the relation

$$\int_0^T i_c dt = -K_c \int_s^0 dx$$

$$Q = K_c s \tag{19}$$

This states that for any particular value of s, Q should be constant. The area under any one of the curves of current in Fig. 15 to the instant of short circuit is the total charge fed into the channel for a 6-foot rod-rod gap. The range of values thus obtained from Fig. 15 is shown by a bar in Fig. 14. Similar results obtained for a 3-foot and a 9-foot rod-rod gap are also plotted. The slope of this curve gives a value of K_c equal to 3.2 microcoulombs per cm or amperes per cm per μsec. This linearity serves to confirm the proportionality expressed by equation 18.

Saxe and Meek presented a similar curve obtained with a positive rod-to-plate gap for gap lengths of 8 to 55.4 cm which showed a remarkable linear relation for which the slope was 0.88 microcoulomb per cm. It also bears out the general nature of the phenomenon.

In Fig. 9, the velocity was computed for a 0.5×5-μsec wave and an overvoltage factor of 1.25. Applying the factor K_c = 3.2 to this velocity curve gives the current curve indicated. This should be compared with the current curve in Fig. 12 for CV = 130. The comparison, though not perfect, shows a general agreement in nature.

Time Lag Curves

With a given surge generator setting having no adjustments made to maintain a particular waveshape, the time lag curves, according to the theory presented here, should be independent of gap length. This happens because as the gap is doubled, then with the same overvoltage factor, the surge generator voltage, the velocity of the channel, and the current and the voltage drop are doubled and the same time lag should result. Therefore, if these relations are correct, the time lag curves plotted against overvoltage factors for 3-, 6-, and 9-foot gaps should form a continuous curve. This is demonstrated to be the case in Fig. 15.

Progress of Channels

Two vertical 6-foot rod-rod gaps were set up 18 feet apart so as not to influence each other electrostatically. When properly adjusted, on application of the surge potential, one, the other, or sometimes both would spark over. A current shunt was placed in the grounded electrode of gap A only. The upper curve of Fig. 16 shows a replot of the current when gap A sparked over and the lower curve when gap B sparked over as a voltage of 200% of critical was applied to both gaps. Fig. 13 shows the oscillograms applicable to this case. Initially both gaps carried current equally but as the channels developed one traveled slightly faster and hence drew more current. It did so at the expense of the other which then did not have quite enough current to maintain a corresponding velocity. Furthermore, the first one decreased the unbridged gap and tended to travel even more rapidly than the other. The effect was cumulative and the one to spark over robbed more and more of the current. This effect was pronounced only after the differences in velocities and the lengths of the unbridged gaps became great. While the phenomenon is essentially a resistive one, largely dependent on feeding an appropriate amount of energy into the channel to raise the temperature to those of an arc, undoubtedly charges also rush into the channels as they progress and the fields between the approaching tips increase. But upon contract such charges rush toward each other from the opposing channels through the completed paths. Only an inappreciable amount of this

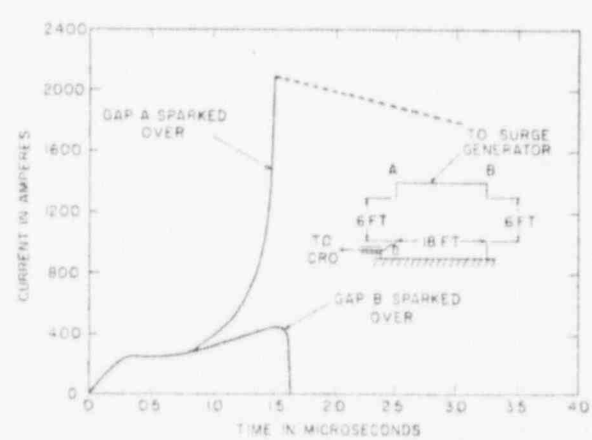

Fig. 16. Current in gap A when gaps A and B are impulsed simultaneously. Charging voltage is 200 volts

90004 13

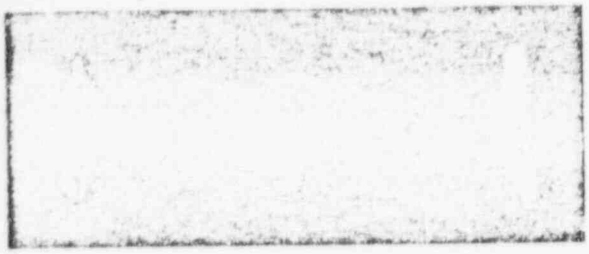

Fig. 17. Channel formation in an unbridged gap when the other gap of two 6-foot paralleled rod-rod gaps sparks over

charge is observed externally as evidenced by the absence of a negative current in the unbridged gap following sparkover of the other gap. Further evidence of this progress of the channels is offered by the still photograph shown in Fig. 17 taken of both gaps simultaneously. Note the extent to which the channels in the gap that did not sparkover have advanced.

Ring-Ring Gaps

A 72-inch-diameter ring made of 2-inch pipe was mounted 94 inches above a 96-inch ring; the latter was located 6 feet above the laboratory floor. Surges of positive polarity were applied with substantially the same surge generator constants as shown in Fig. 12. In Fig. 18 the oscillogram traces of voltages and currents are plotted. The critical sparkover voltage occurred with a charging voltage of 118. The character of the predischarge currents is quite different from and of much greater magnitude than for the 6-foot rod gaps. A very large drop occurs through the resistance of the surge generator. Neither the K nor the K_c constants applicable to rod-rod gaps are applicable to such a gap. The multiplicity of parallel channels apparently affects the fields near the tips of the advancing channels and retards them as compared with the few channels in the simple rod-rod gap. The K constant was determined only approximately and was found to be about 0.05 to 0.06, which is smaller than that for rod-rod gaps. No further work was done on this gap at this time.

Pipe-Pipe Gap

An enlarged form of the ring gap was set up, primarily to simulate a long parallel pipe gap which would have been impossible because of the restricted space of the laboratory. Three 3-inch aluminum pipes each 12 feet long were arranged in triangular configuration about 4 feet from the laboratory floor and a similar set was arranged 6 feet above it. Fig. 19 shows corresponding voltage and current traces. The currents were even larger than for the ring-ring gap. A very pronounced pip occurs at the beginning of the voltage traces. These are formed because of the time required for the formation of the space charge. The channel current forms very rapidly and if there were no inductance in the surge generator circuit would increase almost vertically. Simultaneously a corresponding drop in gap voltage occurs. For example, consider the discharge for a charging voltage of 200. The 900-ampere current through the surge generator produces an internal drop of 900×1,000 or 900,000 volts. The charge drawn from the surge generator capacitor produces an additional but considerably smaller drop which is directly calculable. Because of the distortions

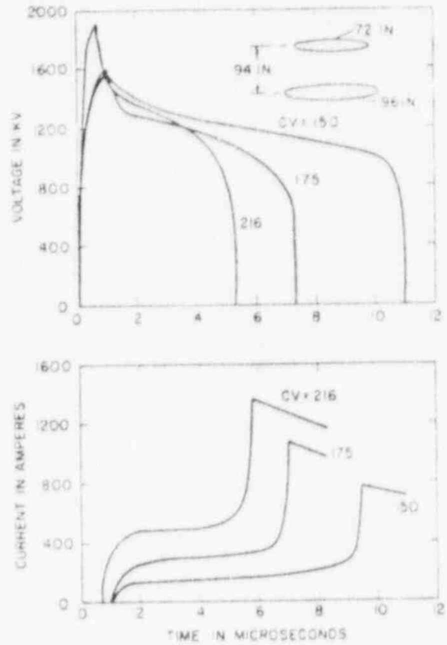

Fig. 18. Voltages across and currents through a 94-inch ring-ring gap

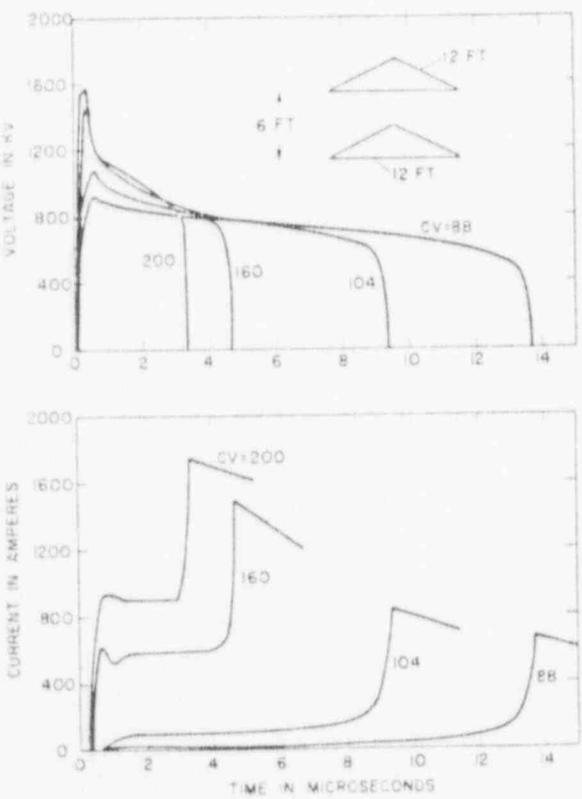

Fig. 19 (left). Voltages across and currents through a 6-foot pipe-pipe gap

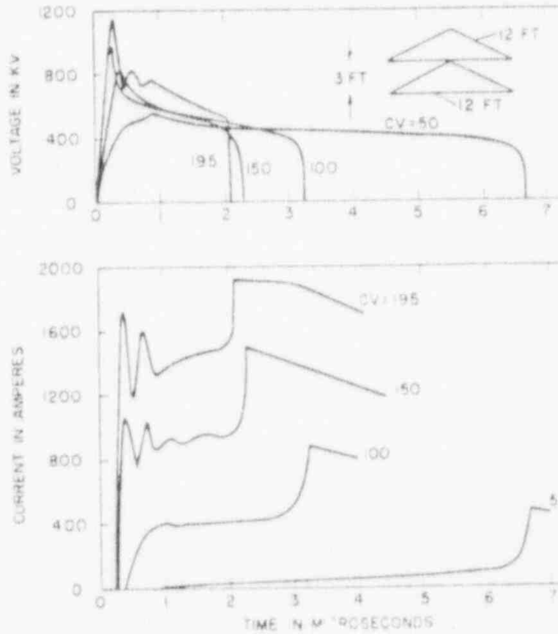

Fig. 20 (right). Voltages across and currents through a 3-foot pipe-pipe gap

90004119

in the waves it was difficult to line up the reference points precisely but it can be assumed that the rapid rise of the current trace should occur simultaneously with the abrupt drop in gap voltage.

Fig. 20 shows a corresponding group of curves for the same gap set for a spacing of 3 feet. Even larger currents result for a particular overvoltage factor. The channel currents were mainly limited by the surge generator's ability to deliver higher currents. The high currents are attained with only modest increases in the electrode voltages. With lower internal resistance even higher currents should result.

No detailed analysis was made of this type of gap at this time, but just as the characteristics of the rod-rod gaps are useful for studying the nature of the stroke proper, and will be considered in this connection in a companion paper, the characteristics of the large parallel pipe gap will be discussed further in a paper concerning the performance of the transmission line tower. The K constant was found to be approximately 0.055 to 0.065.

Energy Fed Into the Discharge

The instantaneous values of current and voltage from Fig. 12 were multiplied and integrated to give the energy fed into the discharge during the breakdown process. The results of this computation are plotted as circles in Fig. 21 against the short-circuit current, I_{sc}, of the surge generator. Four additional points obtained 8 months previously, also on a 6-foot rod-rod gap, are plotted by crosses. While more than one channel is involved some portion of the time, the straight line indicates the value of arc energy required to rise the temperature of a pencil of the gaps to arc temperature as 1.95×10^{-3} joules per ampere per cm.

The energy required to develop the arc should be linearly proportional to the short-circuit current and the length of the gap. It is interesting to contemplate whether this is consistent with the relation that the total charge fed into the production of the arc, such as plotted in Fig. 14, is proportional to gap length only. Assuming that a rectangular voltage wave V is applied to the gap and that W is the total energy supplied to the gap, then

$$W = VQ \qquad (20)$$

If R is the series resistance, then at short circuit

$$W = RI_{sc}Q \qquad (21)$$

and substituting Q from equation 19

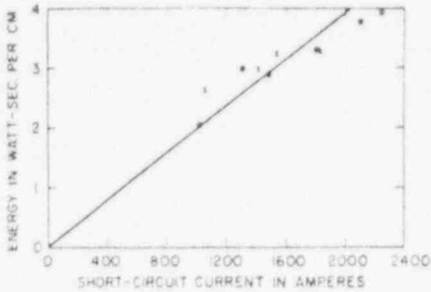

Fig. 21. Energy fed into a 6-foot rod-rod gap

$$W = RK_cI_{sc}s \qquad (22)$$

which demonstrates that W is proportional to I_{sc} and s. Since in equation 19 it was assumed that the current is proportional to the velocity, then the linearity of the energy-current relation lends further support to this assumption for rod-rod gaps.

General Discussion

The authors have kept their conjectures concerning gaseous electronics to a minimum and have confined themselves largely to the external manifestations of the phenomenon. The physical appearance of the corona discharge alone is ample evidence that the gaseous electronics phenomenon is quite different for positive and negative polarity, but externally they differ only in degree. Nevertheless, the authors wish to comment upon some aspects of the discharge.

It was mentioned in the discussion of the space charge that over a considerable range of gaps a rather definite average electric gradient determines the long-time applied voltage at which sparkover occurs and it further appears that the gradient is constant along the center line of the gap. The work of Akopian, Larionov, and Torosian also indicated this as the channel began to develop when u_0 corresponding to the particular gap was exceeded. By "long time" in this connection they implied a time of the order of 100 μsec. With longer times it is quite conceivable that other factors might enter which would alter the nature of the space charge. Thus, for a sustained and continuous potential, as in d-c corona, the charge distribution might be quite different.

It was found by Park and Cones that when a 0.07×100-μsec wave was impressed across their sphere-plate gap, set for a length of between 20 and 50 cm, the current that supplied the space charge rose to crest very rapidly and then decayed to half value in 0.08 μsec. So it may be said that the space charge is substantially established in 0.1 μsec. This period is a function of the phenomenon occurring within the gap, as the regulation of the circuit is sufficiently stiff that the currents required by the space charge do not produce much drop in the external circuit. While Akopian, Larionov, and Torosian used a somewhat larger external resistance it can be assumed that for the length of gaps and for the rates of rise of voltage they used, there was very little lag between the voltage and the establishment of the space charge. This explains why in their analysis of the time to breakdown the phenomenon could be described in terms of the development of the highly conducting channels alone.

For longer gaps, such as the 200-inch rod-rod of Hagenguth, Rohlfs, and Degnan, the time of space charge formation is significant with respect to the total time to breakdown. It remains to be ascertained whether the time lag curves for different waveshapes for such gaps can be computed in a manner similar to that employed by Akopian, Larionov, and Torosian and amplified in this paper.

The foregoing statements may be not completely valid for conditions near the end of travel of the channel. Here the velocity attains very high values and the space charge may not be able to develop sufficiently to keep pace with the values corresponding to the reduced unbridged gap.

As the good conducting channel advances through the relatively immobile space charge, as has been mentioned previously, charges are induced upon this pencil of arc plasma. From the estimates of the current in the channel and from experiments, such as performed by Higham and Meek[24] on the characteristics of rapidly developed arcs, it can be concluded that the diameter of the arc plasma is approximately 2 mm and that the arc is a relatively good conductor. A high charge is induced in the head of the channel that is conducive to the development of a high gradient laterally as well as ahead of it. This charge and gradient, in turn, give rise to copious corona discharges. The head thus expands through the process which might be termed a counter corona discharge that takes place within the original space charge. Conditions conducive to the development of such charges are present even though the field gradient is not uniform as premised by the foregoing simplified assumptions.

More than one channel can form simultaneously, but as they progress in parallel one will advance somewhat farther and tends to shield the others electro-

90004120

statically and thus reduce the field in advance of them. By this process the advance of the others is retarded and this effect becomes progressive. For gap configurations that approach two geometric lines parallel to each other such as formed by two long parallel pipes, this effect should not be as dominant as for a single rod-rod gap. The tests made with two 6-foot rod-rod gaps set 6 feet apart as shown by the insert of Fig. 12, showed that in some cases both gaps sparked over simultaneously which indicates that for separations greater than the gap length the shielding effect is not very great. Tests with smaller separations were not made. Allibone[9] showed that even for two parallel plates two dominant arc paths can form simultaneously.

While more information is available concerning the propagation of channels from the anode than from the cathode, since the process of channel formation is essentially a thermal process, it is expected that the velocity of propagation of the channels from the cathode should be of the same order of magnitude.

Summary

Upon application of an impulse voltage, of such value as not to cause sparkover, a nonuniform field gap, of the proportions frequently encountered in engineering work, the field at first corresponds to that which would be expected from the conventional electrostatic solution. The fields in the vicinity of the electrodes may exceed the critical field momentarily but when this field is exceeded and a free electron appears in the region of the overstressed field, an electron avalance is triggered that develops into a space charge. For rod-rod gaps the space charge develops from both electrodes but for rod-plate gaps from the rod only. The flow of the charge into the intervening gap is at a rate of about 0.001 c which corresponds approximately to the electron drift; so that for a 10-cm gap the charge has diffused through the entire gap in about 0.3 μsec and for a 200-inch gap in 9 μsec. The current feeding the space charge rises very rapidly and decreases somewhat along an exponential curve so that a substantial portion of the space charge is established in slightly less time than these values.

A certain critical average gradient exists for gaps which will produce ultimate sparkover of the gap with prolonged application of the voltage. There is some evidence to indicate that when the space charge is fully developed across the gap the electric gradient in the gap between the electrodes is approximately uniform. The average critical gradients vary between about 5,500 and 10,000 volts per cm depending upon gap configuration and polarity. When the critical average gradient is exceeded a channel is initiated which usually starts from the anode. In the case of a rod-plate gap with the rod positive the channel develops for the entire length of the gap without the development of a plasma channel from the plate. But with the rod negative a plasma channel is first initiated from the plate, and after progressing about halfway across the gap it is met by a more rapidly moving channel, which started at a later time, from the rod. For a rod-rod gap, the plasma channel also starts from the anode and is met in mid-gap by a later initiated channel from the cathode. The drop in the plasma channels is so small that it is considered negligible with respect to the applied voltages concerned in this phenomenon.

For rod-rod gaps, the heads of the two channels approach each other with a velocity that is proportional to the excess of the terminal voltage over the critical sparkover voltage for the instantaneous value of the unbridged gap, and inversely proportional to the length of the unbridged gap. The channels grow with a relatively small initial velocity which is accelerated as the unbridged gap decreases. By using these velocity relations, the time lag of rod-rod gaps can be computed for any applied voltage across the gap. Expressing the applied voltage in terms of the critical sparkover voltage for a rectangular wave, results can be reduced to a per-unit basis that is independent of the length of the gap. These characteristics can be completely described by two parameters.

The channel current is proportional to the velocity of propagation of its head, and therefore can be determined in terms of the instantaneous velocities discussed previously. For small overvoltages, the channel currents are usually concave upward, but for high overvoltages and sufficiently high resistances between the applied voltage and the gap, the current is of a stepped character.

The form of the current wave feeding the initial space charge when a rectangular wave is applied to a gap and the form of the current flowing during the development of the channel is quite opposite; the former decreases somewhat as a negative exponential with time, and the latter increases somewhat as a positive exponential with time. It is shown in the companion paper in this issue that these contrasting characteristics lead to an explanation of the steps in the lightning stroke.

The fact that the magnitude of the currents feeding the initial space charge are quite small, in comparison with the currents that occur during the plasma channel forming phase and with the short circuit currents permitted by the constants of the surge generators, was appreciated quite early. As shown in the companion paper, the currents occurring during the steps of the lightning stroke are also small in comparison with the currents in the return stroke. The phenomenon appears to be essentially a thermal one; sufficient energy must be injected into the gap in order to raise a thin cylinder of air to arc temperatures.

References

1. A New Approach to the Calculation of the Lightning Performance of Transmission Lines. C. F. Wagner. *AIEE Transactions*, pt. III (*Power Apparatus and Systems*), vol. 75, Dec. 1956, pp. 1233-56.

2. A New Approach to the Calculation of the Lightning Performance of Transmission Lines—II. C. F. Wagner, A. R. Hileman. *Ibid.*, vol. 78, Dec. 1959, pp. 996-1021.

3. A New Approach to the Calculation of the Lightning Performance of Transmission Lines—III. A Simplified Method—Stroke to Tower. C. F. Wagner, A. R. Hileman. *Ibid.*, vol. 79, Oct. 1960, pp. 589-603.

4. The Lightning Stroke. C. F. Wagner, A. R. Hileman. *Ibid.*, vol. 77, June 1958, pp. 229-42.

5. Determination of Wave Front of Lightning Stroke Currents from Field Measurements. C. F. Wagner. *Ibid.*, vol. 79, Oct. 1960, pp. 581-89.

6. The Lightning Stroke—II. C. F. Wagner, A. R. Hileman. *Ibid.* (see pp. 622-42 of this issue).

7. Surge Voltage Breakdown of Air in a Non-Union Field. J. H. Park, H. N. Cones. *Journal of Research*, Washington, D. C., vol. 56, 1956, pp. 201-224.

8. Streamer Currents in High Voltage Sparkover. J. Slepian, J. J. Torok. *Electric Journal*, East Pittsburgh, Pa., vol. 26, 1929, pp. 107-10.

9. The Mechanism of the Long Spark. T. E. Allibone. *Journal*, Institution of Electrical Engineers, London, England, vol. 82, 1938, pp. 513-21.

10. Dielectric Phenomena at High Voltages. B. L. Goodlet, F. S. Edwards, F. R. Perry. *Ibid.*, vol. 69, 1931, pp. 695-727.

11. The Structure and Parameters of the Leader Discharge. V. Komelkov. *Bulletin*, Academy of Science, Technical Sciences Section, No. 8, Moscow, U.S.S.R., 1947, pp. 955-66.

12. The Initiation Mechanism of Long Sparks in Point-Plane Gaps. R. F. Saxe, J. M. Meek. *Journal*, Institution of Electrical Engineers, vol. 102, pt. C, 1955.

13. Sixty-Cycle and Impulse Sparkover and Large Gap Spacings. J. H. Hagenguth, A. F. Rohlfs, W. J. Degnan. *AIEE Transactions*, pt. III (*Power Apparatus and Systems*), vol. 71, 1952, pp. 455-60.

14. Ionization Currents and the Breakdown of Insulation. J. J. Torok, F. D. Fielder. *Ibid.*, vol. 49, Jan. 1930, pp. 352-58.

15. Mechanism of Long-Gap Negative Spark Discharges in Air at Atmospheric Pressure. H. Norinder, O. Salka. *Arkiv for Fysik*, Stockholm, Sweden, vol. 5, 1952, pp. 493-529.

16. Impulse and 60 Cycle Strength of Air,

P. L. Bellaschi, W. L. Teague. *AIEE Transactions*, vol. 53, 1934, pp. 1638–45.

17. Impulse Characteristics of Large Gaps, A. A. Gorev, A. M. Zalesky, B. M. Riabov. *Bulletin no. 142*, CIGRE, Paris, France, 1948.

18. Report on the Work of the Study Committee No. 8—Over Voltages and Lightning, K. Berger. *Bulletin no. 326*, CIGRE, 1956.

19. Effects of Corona on Traveling Waves, C. F. Wagner, B. L. Lloyd. *AIEE Transactions*, pt. III (*Power Apparatus and Systems*), vol. 74, Oct. 1955, pp. 858–72.

20. Basic Processes of Gaseous Electronics (book), L. B. Loeb. University of California Press, Berkeley and Los Angeles, Calif., 1955.

21. On Impulse Discharge Voltages Across High-Voltage Insulation as Related to the Shape of the Voltage Wave, A. A. Akopian, V. P. Larionov, A. S. Torosian. *Bulletin no. 411*, CIGRE, 1954.

22. Effect of Non-Standard Surge Voltages on Insulation, Sune Rusck. *Bulletin no. 408*, CIGRE, 1958.

23. Flashover Characteristics of Insulation, P. H. McAuley. *Electric Journal*, July 1938, pp. 273–80.

24. Voltage Gradients in Long Gaseous Spark Channels, J. B. Higham, J. M. Meek. *Proceedings*, Physical Society, London, England, pt. 9, vol. 63, Sept. 1950, pp. 633–648.

Discussion

H. Baatz and A. Fischer (Studiengesellschaft für Hochspannungsanlagen e.V., Nellengen über Esslingen, Germany): The development of a discharge during the breakdown of rod-rod gaps was investigated. Voltage and current were measured simultaneously by a cathode-ray oscillograph at the high-voltage electrode. The high-voltage electrode was chosen as measuring point so that a single rod, without an opposite electrode, could be investigated. Various forms of rods were used; see Fig. 22. The optical view of the discharge figures were taken, as are Lichtenberg figures, by photographic paper which was held axially between the electrodes.

The vertically arranged rod-rod gap with a distance of 350 mm was investigated mainly. The distance was always the same; the peak value of the impulse voltage was varied. For all oscillograms the impulse voltage of 0.3/40 was used. The 100% breakdown voltages for the distance of 350 mm were approximately +305 kv and −315 kv.

Positive Impulse Voltage

Fig. 23 shows a characteristic oscillogram. At t_1 the first part of the impulse generator fires, and at t_2 the impulse voltage is applied to the gap. During the rise of the voltage to its peak value, u_{max}, the capacitive charging current with peak value $i_{c\ max}$ flows. At the moment t_{k1}, a current impulse which may be called current of impulse corona appears. Its peak value is i_{k1}. At t_{k1}, the voltage at the gap is u_k. This value is the inception voltage of impulse corona. The corona current, $i_{k1} = i - i_c$, diminishes as an exponential function. It remains zero for u_{max} voltages at least 20% below the 100% breakdown voltage U_D of the gap.

Negative Impulse Voltage (Fig. 24)

With u_{max} voltages $\leq 0.8\ U_D$ the oscillograms are nearly the same as Fig. 23 with inception of impulse corona at t_{k1} and diminishment of the current $i_{k1}+i_c$ (i_c capacitive current). Sometimes the current impulse of the impulse corona is totally absent. With voltages $0.8\ U_D < u_{max} < U_D$, as shown in Fig. 24, a new event which is not seen in the current oscillogram of positive electrodes appears. After the capacitive charging current belonging to the beginning of the impulse voltage has disappeared, sometimes, during the return of the impulse voltage at t_{k2}, a very steep and high current impulse, i_{k2}, appears. This occasionally is followed by another, smaller impulse. The impulses disappear as an exponential function. In every case when the discharge develops to breakdown, the current impulse, i_{k2}, and sometimes i_{k3}, may be observed. While they are still present the final rise of current up to the breakdown at t_D, follows.

The inception voltage u_k of impulse corona increases slightly with increasing peak value of impulse voltage for all forms of electrodes used. Table I shows the mean values for the different electrodes.

Table I

Electrode	u_k (Kv)	
1	+110	−85
2	+ 96	−78
3	+105	−95
4	+148	−95

All forms of electrodes used clearly show the growth of i_{k1} with increasing u_{max} and therefore with increasing steepness of the impulse voltage. With peak values up to $u_{max}=300$ kv, i_{k1} is directly proportional to u_{max}; see Table II.

Table II

Electrode	i_{k1}/u_{max} (Amps/100 Kv) + Impulse	i_{k1}/u_{max} (Amps/100 Kv) − Impulse
1	2.2	1.35
2	1.7	1.5
3	1.75	1.25
4	3.5	2.0

Figs. 25(A) and 25(B) shows oscillograms of voltage and current without breakdown of the gap, and Figs. 26(A) and (B) with breakdown. The total occurrence including breakdown is shown in Figs. 27(A) and 27(B). In Figs. 28 and 29 the corona streamers bridge the whole gap without breakdown. When the breakdown starts the channels begin again at the electrodes. These pictures cannot be reprinted due to blackened photographic paper. In the original photos the formation of the channels is clearly seen.

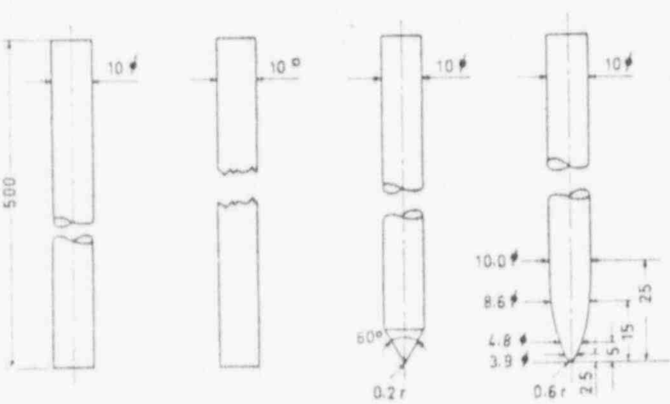

Fig. 22. Various forms of rod electrodes

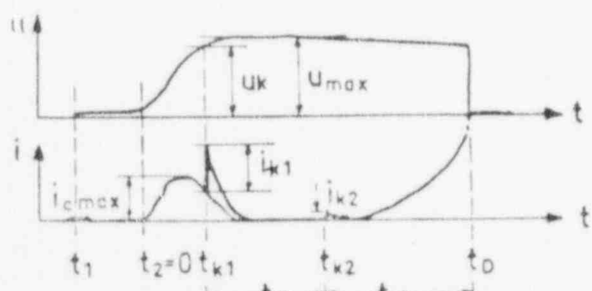

Fig. 23 (left). Characteristic oscillogram with impulse positive

Fig. 24 (right). Characteristic oscillogram with impulse negative

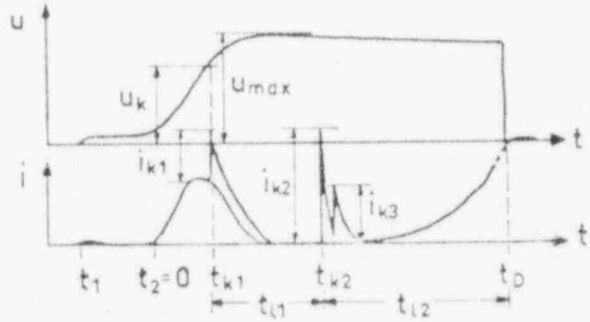

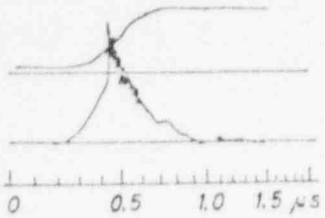

(A)

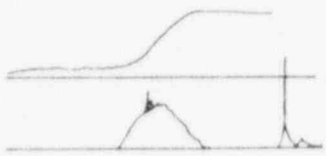

(B)

Fig. 25. Oscillograms without breakdown

A—Impulse positive
B—Impulse negative, time scale as in (A)

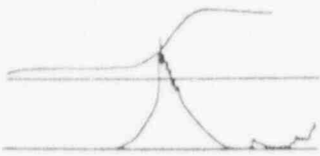

(A)

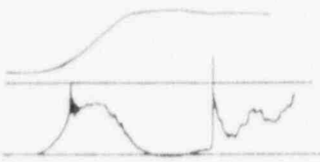

(B)

Fig. 26. Oscillograms with breakdown, time scale as in Fig. 25(A)

A—Impulse positive
B—Impulse negative

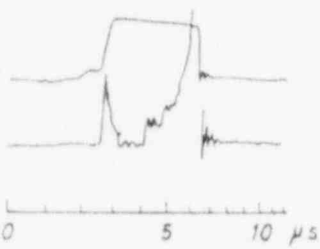

(A)

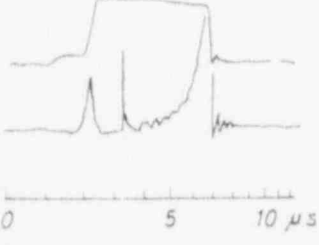

(B)

Fig. 27. Oscillograms with breakdown

A—Impulse positive
B—Impulse negative

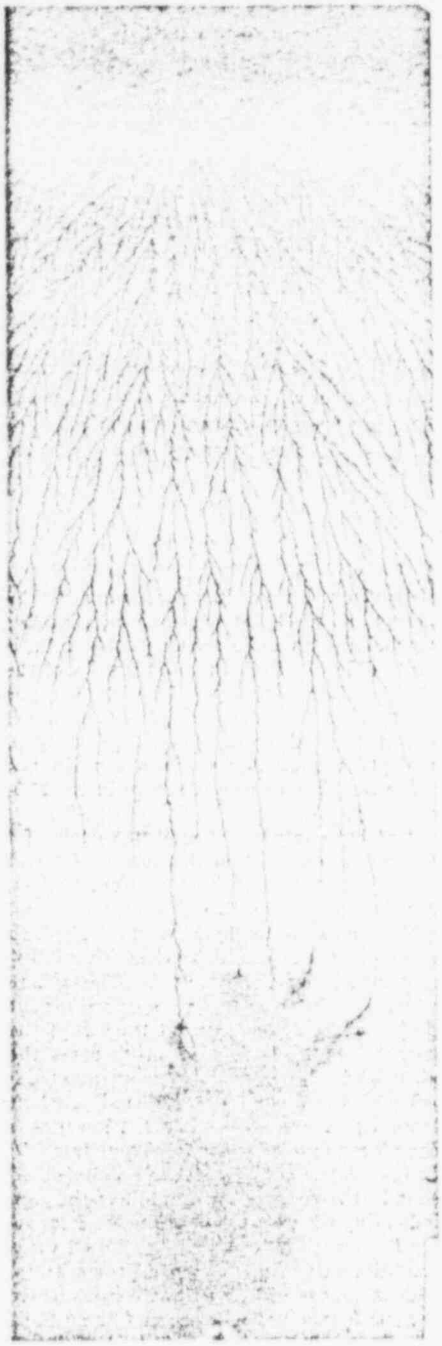

(A)

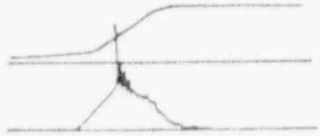

(B)

Fig. 28. (A) Positive and negative streamers, rod-rod gap, 350 mm, impulse positive, $u_{max} = +260$ kv. (B) Oscillogram for Fig. 28(A), time scale as in Fig. 25(A)

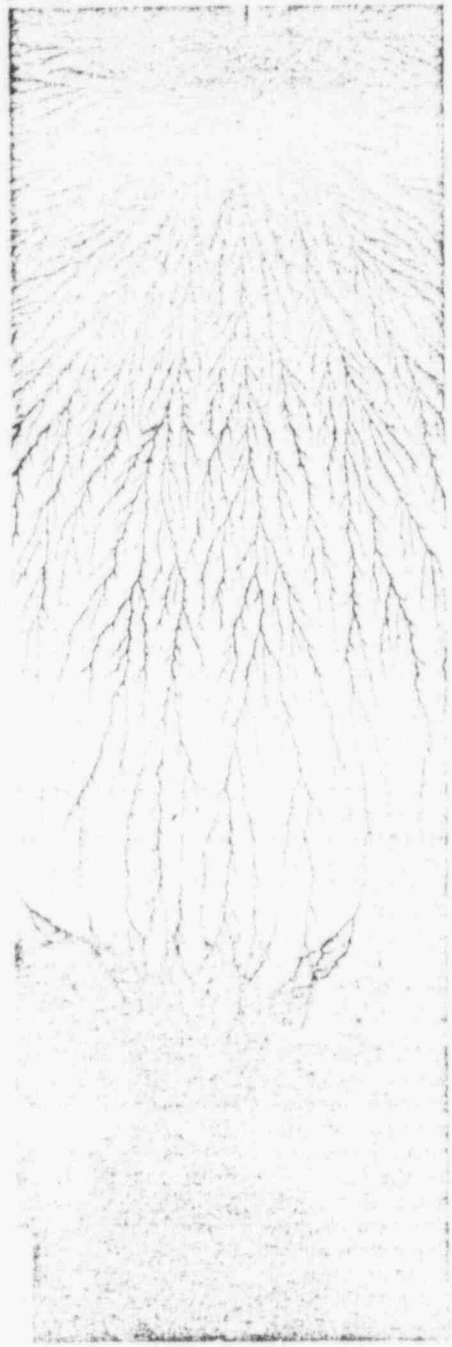

(A)

(B)

Fig. 29. (A) Positive and negative streamers, rod-rod gap, 350 mm, impulse negative, $u_{max} = -255$ kv. (B) Oscillogram for Fig. 29(A), time scale as in Fig. 25(A)

The length of the streamers was measured with one single rod as electrode. Here the length of the corona streamers was proportional to the peak value of impulse voltage (Fig. 30). Some reflections upon the possible field strength at the end of the corona streamers and the distribution of electric charge are given in a publication about this subject.

The same method was used with the rod-rod gap; see Fig. 31. The corona streamers of the positive electrode bridge a great part of the gap before single streamers reach the negative electrode.

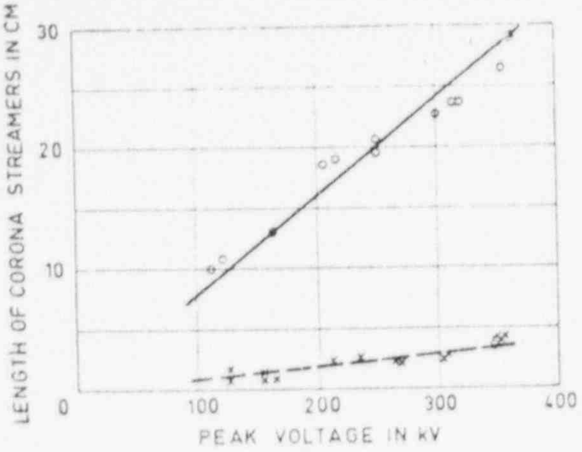

Fig. 30 (left). Length of positive and negative corona streamers measured with one single rod as electrode

Fig. 31 (right). Length of positive and negative corona streamers in the rod-rod gap, distance 35 cm

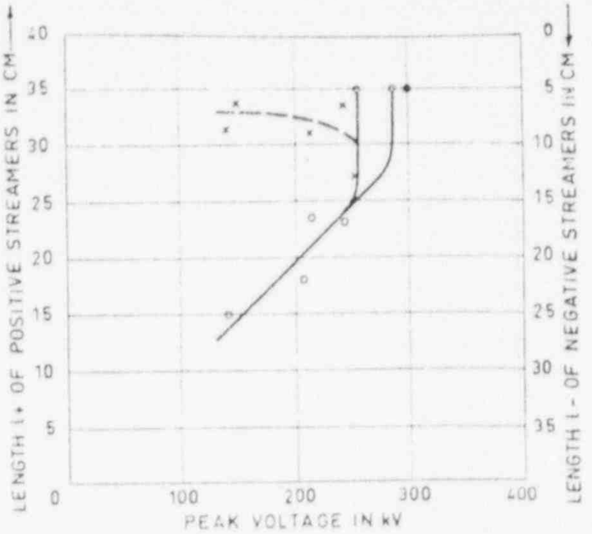

The time, t_{L1} which the corona streamers need to bridge the gap and the time, t_{L2}, of the development of the channel are taken from the oscillograms, depending on the peak value u_{max} of impulse voltage. Figs. 32(A) and 32(B) belong to electrode 1.

The main part of the delay of breakdown is given by the growth of the channels. With increasing impulse voltage the time, t_{L2}, decreases very rapidly. Nevertheless, it is at least twice the time, t_{L1}.

The gap rod-plate as well as the rod-rod gap was investigated. With positive impulses the distance was 500 mm, with negative impulses 200 mm. Both show the same characteristics in principle. The influence of a resistance at the high-voltage electrode was also investigated. Details will be found in a paper soon to be published in the *Elecktrotechnische Zeitschrift*.

J. H. Hagenguth (General Electric Company, Pittsfield, Mass.): This paper is an excellent summary of various laboratory work on the sparkover of nonuniform field gaps. However, I was slightly confused by the interchangeable use of the terms space charge, corona discharge, corona streamers, channels, and discharge channels. One cannot always be certain of interpreting these terms correctly.

The authors discuss the sparkover process of a 200-inch rod-rod gap at 3,000 kv, as shown in reference 13, and current oscillograms of Fig. 3. It seems to me that this mechanism, as indicated by photographs, is quite different from the photographs of the Park and Cones' gaps. The photographs of the latter paper, obtained with chopped waves applied to a sphere-to-plane gap, indicate numerous streamers but do not show the glow discharge shown in the 200-inch gap.

Unfortunately, one cannot be certain of a correct interpretation because only still photographs are available. Nevertheless, my interpretation, based on photos and oscillograms, is as follows: The 200-inch gap voltage was just below the critical (10% sparkover) resulting in nine impulses where a weak, ultraviolet glow spanned about half of the gap, and current trace *B* of the authors' Fig. 3. In nine other cases the glow bridged the gap and a streamer developed from the grounded rod, current trace *C*; and in two cases sparkover was completed and resulted in current trace *D*. In these latter cases there was a well-defined split in the spark in the middle of the gap, indicating where the final streamers emanating from both electrodes met. In all three conditions there was an initial current pip. This is almost equal in the two cases where the spark was incompleted, and about 20% higher for the spark condition. For the spark condition also, the tail was slightly longer and streamer current started directly at the end of the current pip tail, increasing very rapidly at first and then more slowly, in a concave manner, to sparkover current with sparkover being completed in 15 μsec or a total of 27 μsec from current zero. Since it was indicated that the streamers appeared to meet in mid-gap, the ground streamer velocity would be approximately 1.7×10^7 cm/sec which is similar to that given by the authors' equation 2.

In the intermediate condition where the glow bridged the gap and a streamer was seen, a second current pip developed about 8 μsec after the first pip was reduced to zero.

In the case where the glow reached part way, about three-quarters across the gap, there was no second current pip, or if there were, it was less than 1 ampere, the limiting sensitivity of the current measuring circuit. A very short, small glow at the grounded rod appeared.

The very heavy glowing ball from quartz lens photos around the excited negative electrode appeared as very thin streamers of the same lengths when photographed with a glass lens similar to the Park-Cones' photos.

Thus it appears that this glow may be

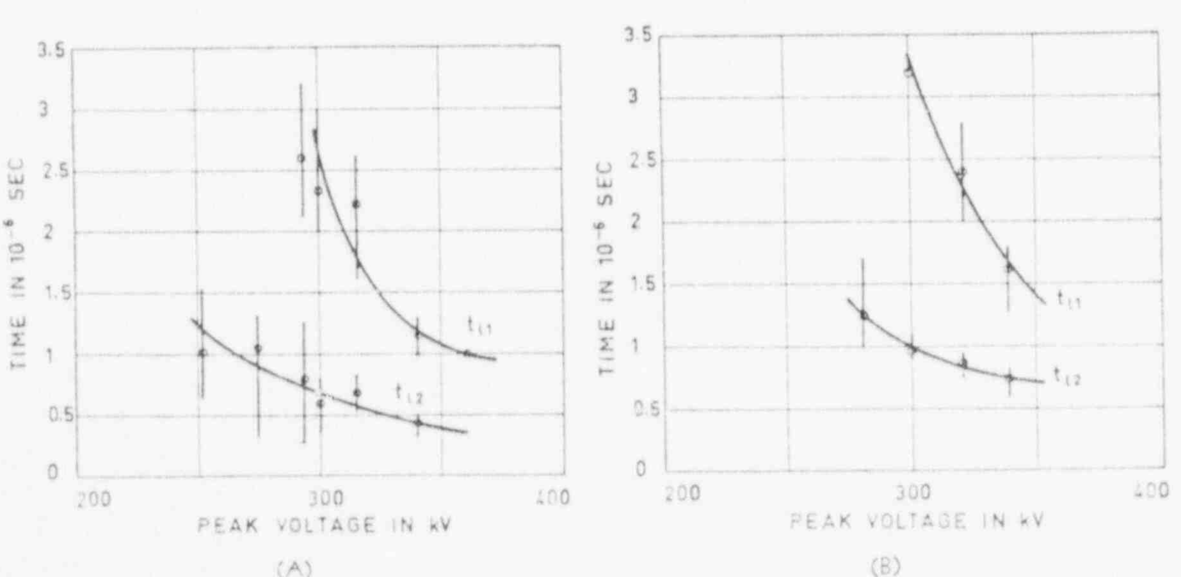

Fig. 32. Time of streamer and channel for 35-cm rod-rod gap

A—Polarity positive

B—Polarity negative

90004124

similar to the pilot leader postulated by Schonland. From the limited data there are at least two possible processes for this under critical voltage conditions:

1. The pilot leader starts at the excited negative rod toward the grounded positive rod, developing a very weak, high-impedance plasma (order of 2.7×10^8 ohms), bridges the gap, and a streamer starts from the grounded rod. This streamer bridges about 17% of the gap and yet no streamer is visible from the negative electrode.

2. The pilot leader starts at the excited negative rod toward the grounded positive rod and is met by a similar leader from the grounded rod. After contact, a streamer starts from the grounded rod, as in 1. However, it is possible that the leader from the grounded rod is a streamer, although oscillograms B and C do not seem to indicate this.

These interesting conclusions state that in this 200-inch rod gap a leader develops across the entire gap without a streamer advancing toward it from the ground electrode, even though the electrode has a nonuniform field around it. The question then is whether a similar process occurs in the lightning stroke.

With regard to average gap gradients, the authors arrive at a figure between 5,500 and 10,000 volts/cm, which is correct for impulse application and the types of gaps studied. In a recent paper,[1] unusual, low, dry flashover strengths are shown in Fig. 21. At 400 inches, the average gradient was 1,800 volts/cm. These flashovers were obtained with slow-front switching-surge-type waves and also with fast-front long-tail waves resembling direct voltage. The lightning stroke pilot leader advanced at about 1.5×10^7 cm/sec and therefore probably resembled a direct voltage excitation rather than an impulse. Consequently, the lower gradients would prevail. This is in conformance with gradient measurements under lightning conditions[2,3] such as 3,400 volts/cm measured on the belly of a *B-25* aircraft just before a lightning stroke.

There is a question regarding the authors' statement that "It was impossible in the open conditions of the laboratory to obtain a clean-cut oscillogram of current applying the space charge just under critical voltage ... Apparently the high free electron concentration caused triggering of the gap on the rising portion of the voltage wave and prevented the sharp rise and exponential decay of the current." Why didn't this occur at voltages above the critical sparkover voltage where time to sparkover was as much as 6 μsec and more?

In their general discussion the authors mention the pencil of arc plasma with a diameter of about 2 mm. It should be noted that in the 200-inch gap there was no pencil until the glow discharge or pilot leader had developed. Thus it might be assumed that there was no pencil in the lightning pilot leader until the return stroke was established. Dr. Flowers has investigated the channel of the spark discharge[4] and found that the current density was about 1,100 amperes/cm.[2]

REFERENCES

1. THE FLASHOVER STRENGTH OF EXTRA-HIGH-VOLTAGE LINE AND STATION INSULATION, A. F. Rohlfs, H. E. Fiegel, J. G. Anderson. *AIEE Transactions, Part III (Power Apparatus and Systems)*, Aug. 1961, pp. 463–71.

2. THE ELECTRICAL CHARGE ON PRECIPITATION AT VARIOUS ALTITUDES AND ITS RELATION TO THUNDERSTORMS, Ross Gunn. *Physical Review*, New York, N. Y., vol. 71, 1947, pp. 181–86.

3. ELECTRIC FIELD INTENSITY INSIDE OF NATURAL CLOUDS, Ross Gunn. *Journal of Applied Physics*, New York, N. Y., vol. 19, May 1948.

4. THE CHANNEL OF THE SPARK DISCHARGE, J. W. Flowers. *Physical Review*, vol. 64, Oct. 1943, pp. 225–235.

C. F. Wagner and A. R. Hileman: The data presented by Professor Baatz and Mr. Fischer are very illuminating and add considerably to the knowledge of the subject. The authors look forward with great interest to the *Elektrotechnische Zeitschrift* paper wherein these tests will be described in more detail. The following comments are directed to their very clear but necessarily limited presentation. Since the primary purpose of the review by the authors of the available laboratory data was to provide a background upon which to base a theory of the lightning discharge, the material presented by Professor Baatz and Mr. Fischer will be discussed as applied to this final end.

One of the pertinent questions in the description and analysis of the steps of the first component of a lightning stroke is the electric gradient within the space charge surrounding the conducting core of the leader. Or expressed in another way, the gradient along the streamers that constitute the corona discharge. Fig. 30 provides information on this point. In the preliminary copy of the discussion it was stated that these data were obtained with the rod placed 2,260 mm above a flat plane. Consider first the case for which the rod is positive. To obtain an approximate estimate of the electric gradients, let it be assumed that the electric fields between the tips of the streamers and the plate correspond to those that would exist between a charged sphere and a plate in which the radius of the sphere is small in comparison with the distance to the plate. Let E_R be the field next to the sphere in volts per cm and R the radius of the sphere in cm. This field is average in character and no attempt is made to consider the higher fields that must surround the tips of individual streamers. The potential in volts between the sphere and plate is then

$$U = R^2 E_R \left[\frac{1}{R} - \frac{1}{446} \right] \qquad (23)$$

If the field is constant at a value of E_R within the sphere then the field becomes a continuous value at the edge of the sphere. The total applied potential is the foregoing expression plus the quantity $E_R R$. Now if the point on the curve of Fig. 32 for which U_{max} is 300 kv and R is 24 cm is arbitrarily chosen then solving for E_R provides a value of 6,050 volts per cm which is quite close to that which we used in our paper.

When this same method is used in cases for which negative potential has been applied to the rod, unreasonably high values of electric fields are obtained. This raises the question of the justification of using the photographic records of the discharge as a criterion of the advance of the space charge. This is acceptable with positive discharges as the electrons produced by the ionization processes at the tip of the streamers are drawn inward toward the rod and the photographic records showed may constitute a true measure of the boundary of the less mobile positive ions that remain. However, with negative potential, the electrons formed in the ionization process having high mobilities can advance outward beyond the boundary indicated by the photographic record. We are somewhat reluctant to express our opinion on the gaseous electronic phenomenon and, therefore, present this point of view more in the nature of conjecture rather than fact.

There is a difference of opinion concerning the magnitude of current involved in the steps of the lightning stroke. The data presented in Table II of the discussion may shed some light on this point. It is stated that for a 350-mm rod-rod gap for negative applied voltage, i_{st} is directly proportional to U_{max} up to 300 kv and less than 2 amperes per 100 kv. Extending this linearity to a stroke potential of 50,000 kv one obtains a current of 1,000 amperes, that confirms the point of view that the current in the steps is small in comparison with the return stroke (usually referred to as the R-change) current.

The authors regret that Mr. Hagenguth was confused by the interchange of terms. The problem is very complicated and we used different terms for the same phenomenon in order to differentiate between two quite different phenomena.

Mr. Hagenguth presents an interesting discussion concerning the occurrence of streamers that appear to bridge the entire gap. We are of the opinion that this phenomenon is similar to that shown by Park and Cones and although the latter used a glass lens their camera was much closer to the discharge. A similar phenomenon is shown in the brilliant photographs of Professor Baatz and Mr. Fischer. As mentioned by Mr. Hagenguth, one must bear in mind that these are still photographs and not instantaneous exposures. We are at a loss to explain this phenomenon but it certainly involves a trail whose impedance is so high that the streamers do not lead to an immediate channel (in this case meaning an arc plasma channel).

Mr. Hagenguth comments on average sparkover gradients and mentions that in a recent paper a value of 1,800 volts per cm was shown. He mentions that these values were obtained with slow-front switching-surge type waves and also with fast-front long-tail waves resembling direct voltage. Examination of the reference reveals that this value was obtained for a rod-plane for which a positive 100×3,200-μsec wave was applied. In reference 13 of the paper, data are given by Mr. Hagenguth that the average gradients of rod gaps up to 250 inches approach a value of 160 kv per foot. They then say that "Other data, not published, with gap spacings up to 50 feet between two generators charged to opposite polarity and with wave tails of the order of 2,300 μsec tend to give average gradients of the same value." According to Mr. Hagenguth's data it appears that this wave might be described as a "fast-front long-tail wave." Perhaps the significant difference in the value to which Mr. Hagenguth referred, namely, 1,800 volts per cm, is that it represented the characteristic of a dry positive rod-to-plane gap upon application of a 60-cycle voltage or an impulse having a slow front and long tail. The higher value of 160 kv per foot or 5,300 volts per cm represents the characteristic of a rod-rod gap to which a negative potential is applied. It would be interesting if data pertaining to a rod-plane gap were obtained in a range of 400 inches for which the applied voltage is a negative slow-front wave. These data could be compared directly with the low gradient of 1,800 volts per cm obtained with a positive wave. Fig. 14 of reference 1 of Mr. Hagenguth's discussion provides some information concerning rod-rod gaps which indicates linearity up to 180 inches and a gradient of about 5,000 volts per cm.

The question raised by Mr. Hagenguth betrays that we were not sufficiently clear in the general exposition of the paper. We tried to convey that sparkover of the gap occurs in two phases, first the development of the space charge (corona discharge), and second, the development of the channel (high conducting arc plasma). Only the first phase develops below critical voltage. Above critical voltage both occur in sequence.

Regarding the development of the space charge, Park and Cones stated that "An analysis of a large number of records obtained with slowly rising surges indicated that the peak current was approximately proportional to the actual value of voltage at the instant the discharge started." Therefore, in an ambient of low free electron concentration and with the application of a steep voltage wave, the crest value of the voltage wave is attained before triggering occurs. But if the concentration of free electrons is high, triggering may occur on the rising portion of the wave with a corresponding reduction in crest value of the current. It is to be presumed that a corresponding lengthening of the current wave would ensue. According to our theory of breakdown, the substantial development of the space charge is a precedent to the development of channel. The current required to develop the space charge is small in comparison with the short-circuit current of the surge generator when ultimate breakdown occurs. Therefore, when the current shunt is adjusted to read the short-circuit current, the space charge current is swamped by the channel formation currents even in the early stages of the channel formation and its presence is not apparent.

In reply to the comment made in the last paragraph of Mr. Hagenguth's discussion, it does not appear that a glow discharge or pilot leader without some sort of conducting core (channel) would possess sufficient conductivity in the form of a cylinder 10,000 or 20,000 feet in length and 100 feet in diameter, to supply the current required to provide the progressing corona discharge (space charge) in front of the leader. Furthermore, if the leader consisted of only such a glow discharge, the gradient per unit length must be approximately 7,000 volts per cm. The drop alone in such leader of 20,000 feet length would be 5×10^8 volts. This would require a deposition of charge along the stroke channel that increases linearly with height. The resultant current at the earth, as the return stroke tapped these charges progressively, would result in a current at the earth that would increase progressively with time up to about 100 μsec and in magnitude would be many times the recorded values. Thus we are of the opinion that a conducting core must exist within the leader.

The Lightning Stroke—II

C. F. WAGNER
FELLOW AIEE

A. R. HILEMAN
MEMBER AIEE

IN A PREVIOUS PAPER,[1] similarly titled, the authors undertook to synthesize certain characteristics of the lightning stroke by applying and extrapolating the results of laboratory experiments. They were supported in this effort by data concerning the transient characteristics of arcs[2] and the properties of corona within cylindrical shells. A companion paper[3] in this issue, discusses the properties of laboratory-produced sparks and the present paper applies this information, together with additional data concerning natural lightning, to a more detailed consideration of the lightning stroke. A new mechanism of the leader steps is presented. Also, a theory of the very important events that occur during the early stages of the return stroke is elucidated.

General Description of the Stroke

Before discussing the various phases of the stroke, a general description of the stroke without detailed substantiation will be presented. The hypothesis pictures the leader as composed of two parts: a very thin good conducting core, which will be called the channel, preceded and surrounded by a negative space charge which will be called the corona sheath. The diameter of the channel is only about 2 mm (millimeters) and its drop about 50 or 60 volts per cm (centimeters). It has characteristics of an arc plasma with very high temperatures and may be highly luminous. The diameter of the corona envelope may be about 100 feet and may extend about 150 feet in front of the channel. The internal gradient of the corona sheath lies between 5,000 and 10,000 volts per cm. It has characteristics of a glow or corona discharge; its temperature is low; it is pierced by streamers; and considerable difficulty is sometimes experienced in photographing it.

As the channel of the leader of the first component of a stroke reaches a particular point it is momentarily arrested and streamers forge ahead into virgin air. These streamers form the corona sheath and as they proceed distribute a space charge that has characteristics similar to a corona discharge and to the space charge associated with the formative stage of the breakdown of long gaps. As the space charge develops, the potential difference across the corona sheath has an increasing effect in restraining the progress of the discharge. But, before the charge can become fully effective in checking the further progress of the streamers, conditions just in advance of the tip of the channel become conducive to the initiation of a channel or arc plasma at this point. This new channel in reality merely constitutes a further extension of the leader channel. Each new channel spurt starts with a relatively low velocity that follows a curve with time that is strongly concave upward. This continues until the channel catches up with the boundary of the corona sheath. The channel cannot progress into virgin air in the form of a highly conducting plasma and, therefore, ceases. In the meantime the corona streamers continue to progress from the new tip of the channel and the whole process is repeated. The photographic studies of Schonland[4] and his associates reveal this rapid extension of the channel as a short step of very high brilliance. And with respect to the development of the channel (which they term streamers) they say, "Definite evidence that the streamers [channels] travel downward is, however, afforded by the broadening of the upper part of their tracks."

According to Schonland, the lengths of the steps vary between 10 and 80 meters with a modal value of about 50 meters or

Paper 61-488, recommended by the AIEE Transmission and Distribution Committee and approved by the AIEE Technical Operations Department for presentation at the AIEE South East-South Central District Meeting, New Orleans, La., April 5-7, 1961. Manuscript submitted January 9, 1961; made available for printing March 3, 1961.

C. F. Wagner and A. R. Hileman are both with Westinghouse Electric Corporation, East Pittsburgh, Pa.

ity, and cost reductions can be made in the core structure. Advances in material development, particularly high strength zirconium alloys suitable for sodium use, have contributed heavily to these new concepts.

Other facets of the advanced program, similarly aimed toward increasing the reliability and decreasing the cost of high-performance sodium graphite reactors in the 300- to 500-mwe range, cover the development and test of high-capacity sodium pumps, control and safety rods designed to operate under high power density conditions, as well as advances in the technology of liquid metal purification.

Aside from these engineering developments, safety is an important aspect of any power reactor design. The low-pressure minimum-stored energy advantages of sodium-cooled reactors have long been known; it has recently become apparent that sodium is exceptional in its ability to retain fission products in the event of accidental failure of cladding, either by a nuclear excursion or by material deterioration. Quantitative studies are in progress to verify the small fission product release from sodium, extending to the release of fission products when contaminated sodium is burned. These studies currently indicate that less than 1/10 of 1% of all fission products generated are released into the containment provided for sodium graphite reactors, and that no accident yet postulated releases sufficient energy to bridge this containment. Thus, it appears that the sodium-graphite system is an extremely safe one from the standpoint of public hazard, as well as in operational performance.

Application of this knowledge to the sodium-graphite concept allows the advanced system design to be kept up to date so that the most modern system may be available to organizations concerned with the economic generation of electric power from nuclear sources.

Conclusions

It appears that the advanced SGR design has initial capital and operating cost competitive with modern fossil fueled stations in many areas of the United States. This system is capable of producing superheated steam with temperatures and pressures comparable with modern steam plant designs. The HNPF is a significant step toward realization of the capabilities of SGR systems.

References

1. 360 Mwe, Uranium-Carbide-Fueled, Sodium-Cooled Nuclear Power Plant. *Report no. AI-6042* (revised), Atomics International Division, North American Aviation, Inc., Canoga Park, Calif., Apr. 1961.

2. Revised Charges for Enriched and Depleted Uranium. *Report no. FR-4761*, Atomic Energy Commission, Washington, D. C., May 1961.

REF. 13

Surge Impedance and Its Application to the Lightning Stroke

C. F. WAGNER
FELLOW AIEE

A. R. HILEMAN
MEMBER AIEE

Summary: Corona effects and a temporary high resistance introduced into the path of the return-stroke current are two factors that contribute to the determination of the velocity of the propagation and surge impedance of the return stroke. Using field theory concepts it is estimated that the surge impedance of the stroke is about 3,000 ohms. This quantity is of value in estimating the length of the last step and wave front of the stroke current.

NORMALLY, the calculation and concept of surge impedance of conductors is approached through circuit theory. Recently, surge impedances of both horizontal and vertical conductors with respect to earth were determined by use of field theory concepts.[1] It is the purpose of this paper to (1) consider further the concept of surge impedance from the viewpoint of electric fields and thus establish a more definite understanding of the nature of surge impedance, and (2) estimate an approximate value of surge impedance that can be applied to the return stroke of natural lightning.

Paper 61-1043, recommended by the AIEE Transmission and Distribution Committee and approved by the AIEE Technical Operations Department for presentation at the AIEE Fall General Meeting, Detroit, Mich., October 15-20, 1961. Manuscript submitted June 15, 1961; made available for printing August 21, 1961.

C. F. Wagner and A. R. Hileman are both with the Westinghouse Electric Corporation, East Pittsburgh, Pa.

Characteristics of Traveling Waves

When it is assumed that the wave of charge and its associated current travel with the velocity of light, certain simplifications result as compared with the assumption that waves of charge and current travel with a velocity less than that of light. In the latter case electric fields that propagate with the speed of light extend in front of the waves of charge and current. As discussed later, reduction in velocity can be attributed to either the effects of corona or to a high ohmic voltage drop that develops as the current in the head of the wave increases rapidly. Both of these effects can occur simultaneously. The development will consider first the case of waves that travel with the velocity of light, and then waves that travel with a velocity less than that of light.

For each case three different combinations of waves will be considered. The first is shown in Fig. 1(A). This is a single rectangular wave of charge (and its associated current) that is initiated at zero time and travels to the right with constant velocity. Such a wave cannot exist by itself but can constitute an elemental building block for more realistic combinations. The electric fields produced by this wave have previously been determined.[2,3] The wave combination of charge shown in Fig. 1(B) is more realistic and does not require a continuous source at the origin to supply the charge fed into

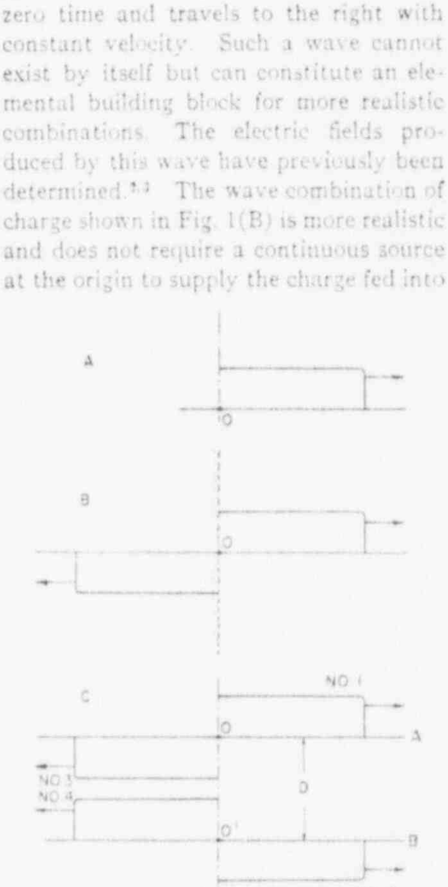

Fig. 1. Combinations of traveling waves used in analysis of surge impedance

90004127

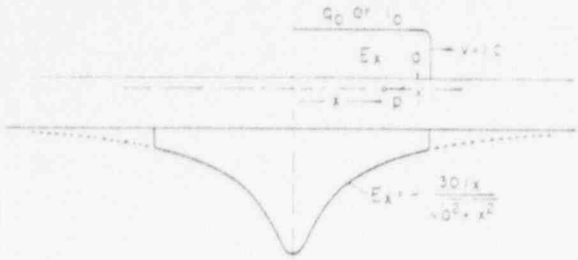

Fig. 2. Tangential component of electric field caused by a single rectangular wave of charge and current traveling with the velocity of light

the waves. The electric field produced by this combination is identical to the field produced when the wave to the left is replaced by a vertical infinitely large plane of zero resistivity, shown by dotted line in Fig. 1(B). Of course, with the infinite plane, a corresponding current flows in the plane that expands radially with the velocity of light. While this case approaches the conditions of the lightning stroke, as will be demonstrated, the integrated effect of the fields increases without limit and for some purposes magnifies the difficulty of drawing precise conclusions. The combination of charge waves shown in Fig. 1(C) results in finite values of potential, and assists in the visualization and evaluation of the nature of surge impedance.

Waves Traveling with the Velocity of Light

1. *Single Wave.* It was shown in reference 2 that when a rectangular wave of charge, q_o in coulombs per cm (centimeter) and its associated rectangular wave of current, i_x, in amperes of the type shown in Fig. 1(A) are suddenly initiated and travel along a straight line with the velocity of light, an electric field is produced that expands also with the speed of light. Fig. 2 shows such a wave. At a point p located a distance x in cm along the path of travel from the point of origin and a distance a normal to the path of travel, the electric field E_x parallel to the x axis is

$$E_x = -9x10^{11}q_o \frac{1}{\sqrt{a^2+x^2}} \text{ in volts per cm} \quad (1)$$

For all points behind the head of the expanding electric field, the field has the shape indicated in Fig. 2. And since

$$i_x = cq_o \quad (2)$$

where c is the velocity of light in cm per second, E_x is also

$$E_x = -30i_x \frac{1}{\sqrt{a^2+x^2}} \quad (3)$$

2. *Oppositely Traveling Waves.* When waves of charge of opposite polarity elongate along the same geometric line as shown in Fig. 3 the electric field parallel to the x axis is just twice as great as for the previous case.

$$E_x = -18\times10^{11}q_o \frac{1}{\sqrt{a^2+x^2}} = -60i_x \frac{1}{\sqrt{a^2+x^2}} \quad (4)$$

Now consider a line parallel to and at a distance a from the x-axis. Within the area bounded by a sphere having a radius given by the expression

$$\sqrt{a^2+x^2} = ct \quad (5)$$

the field is given by equation 4. Outside of this sphere the field is zero. If the cylindrical surface defined by the radius a is replaced by a tube of zero resistivity, the electric field on its surface parallel to the x-axis must be zero. If this tube be broken up into infinitesimal elements and sources of emf (electromotive force) be inserted between the elements whose gradient is just equal and opposite to the field given by equation 4, then both the conditions for zero tangential field and a field necessary for the propagation of the wave are established. The inserted sources of emf will be called the "forcing emf's." These forcing emf's must be inserted progressively just as the head of the field reaches the particular point. The gradient of the forcing emf is shown by the dotted line in Fig. 3.

The total forcing emf introduced up to point x is then

$$V = \int_o^x 60i_x \frac{1}{\sqrt{a^2+x^2}} dx = 60i_x \ln\left[\frac{x}{a} + \sqrt{1+\left(\frac{x}{a}\right)^2}\right] = 60i_x \sinh^{-1}\left(\frac{x}{a}\right) \quad (6)$$

The total voltage that must be inserted to the right and left of zero is shown in Fig. 3.

For $i_x = 1.0$, this voltage properly distributed equals the surge impedance as defined here. Thus, for $x/a = 100$, 1,000, and 10,000, V is 318, 415, and 595 volts, respectively. As x increases, V increases without limit.

Fig. 3 (below left). Tangential component of electric field, forcing emf's, and gradient of forcing emf's caused by waves of opposite polarity elongating along a conductor with the velocity of light

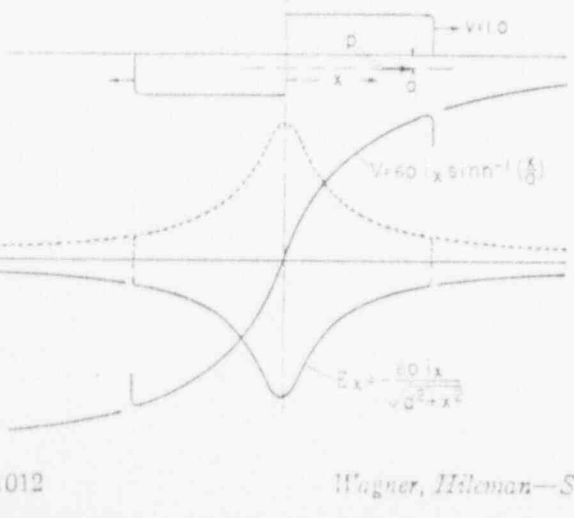

Fig. 4 (right). Forcing emf's necessary in conductor A to produce waves that propagate on conductors A and B with the velocity of light as shown in the inset

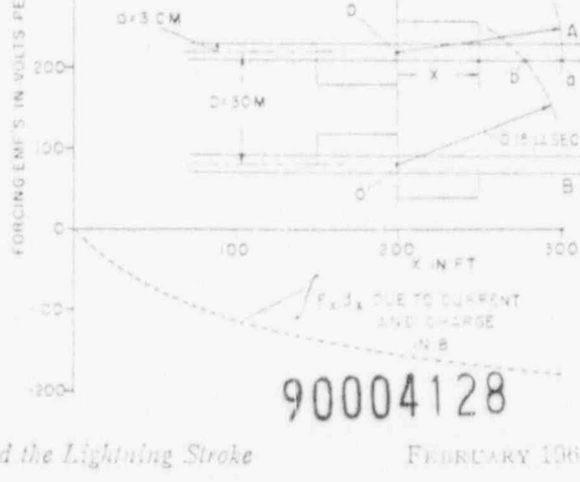

90004128

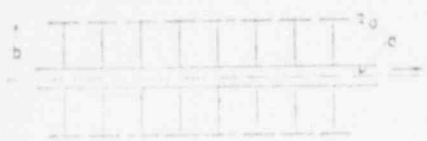

Fig. 5 (left). Simplified assumption used to represent corona effect

Fig. 6 (right). Tangential field caused by a single rectangular wave of charge and current traveling at a velocity less than that of light

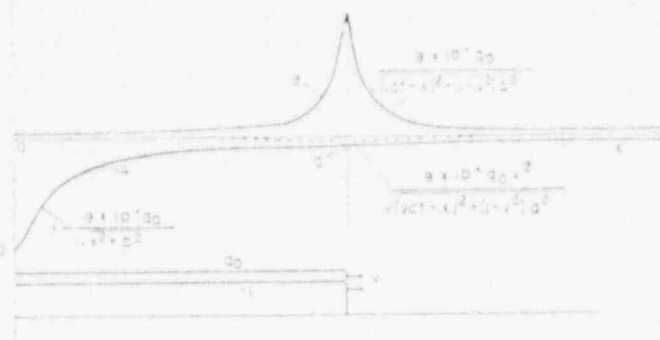

3. *Two Parallel Conductors.* Fig. 4 shows two parallel conductors of radius a, separated a distance D. Assume two pairs of rectangular charge (and current) waves that propagate from O and from O'. The polarities are indicated in the inset. Neglecting for the moment the fact that the fields radiate from two different points and that, therefore, the envelopes of the fields do not coincide, the forcing voltage in each conductor is

$$V=60i_x\left\{\ln\left[\frac{x}{a}+\sqrt{1+\left(\frac{x}{a}\right)^2}\right]-\ln\left[\frac{x}{D}+\sqrt{1+\left(\frac{x}{D}\right)^2}\right]\right\} \quad (7)$$

For x large with respect to a and D

$$V/i_x=60\ \ln\ \frac{D}{a} \quad (8)$$

which is identical with the conventional expression for surge impedance.

The rate at which this limiting value is approached and the noncoincidence of the spheres of influence are best illustrated by an example. Consider two conductors each having a radius of 3 cm (1.18 inches) separated a distance of 30 meters (98.5 feet). The assumed current waves are indicated in the inset of Fig. 4. The upper dotted curve shows the forcing emf in conductor A due to the current and charge in A. Similarly, the lowest dotted curve shows the forcing emf in conductor A due to the current and charge in conductor B. For x large these quantities can be added algebraically and give the conventional value of surge impedance which for this configuration is 414 ohms. For t less than 0.1 microsecond (μsec) the presence of charge and current in conductor B is not felt on conductor A and the emf is simply that for conductor A. For slightly longer times, say for $t=0.15$ μsec, the sum of the two fields is effective up to point b of the inset but between point b and point a only the field due to current and charge in A is effective. The emf for different times are indicated. It can be seen that after 0.1 μsec, which is equal to the travel time between conductors, the conventional value of surge impedance is effective. For instants less than about one-third the travel time between conductors the effective surge impedance is less than the conventional value. It reaches a maximum at an instant equal to the travel time between conductors and then decreases rapidly.

It should be recalled that these forcing emf's represent the voltage whose differential value must be progressively inserted in series on both sides of both conductors to produce the assumed rectangular traveling waves of charge and current. If these forcing emf's were concentrated at $x=o$ (a condition difficult of attainment even with high-voltage surge generators) there results a high current inrush that varies about the final value in inverse proportion of the forcing emf's.

To this point rectangular waves of charge and current only were considered. If the assumed waves possessed sloping fronts, the effect can be determined by resolving the wave into a group of infinitesimal rectangular waves displaced appropriate distances. For such waves the surge impedance approaches the conventional value even more rapidly and smoothly than the rectangular waves, as a portion of the wave has progressed along the line, and has already reached the conventional value before the later increments are applied to the line. Another characteristic should be noted. Even though the front of the waves of current and charge remain sloped as they continue to travel along the line, the tangential component of electric field is equal to zero. This may seem anomalous but it should not be confused with the radial field which changes as the front of the charge wave passes a particular point in the line.

Waves Traveling with Velocity Less Than Light

Two practical cases occur to the authors in which traveling waves propagate with a velocity less than that of light. One is that of corona in which the charge associated with the corona discharge takes a position more removed from the axis of propagation than the associated current. The other case is that of lightning. For the return stroke the charge again is farther removed from the axis than the current, but, in addition, as the current rises rapidly, a temporary high resistance drop that travels with the head of the wave is inserted progressively in the path of the wave.

In this development corona effects will be represented by a simplified assumption. In Fig. 5, the current will be assumed to flow through the central continuous perfectly conducting cylinder of radius a. The charge, however, will be assumed to reside on the surface of short sections of a discontinuous cylinder of radius b connected electrically to the inner cylinder. This is oversimplified for representing actual corona conditions on transmission lines, as the radius in this assumption is independent of the charge, whereas, on transmission lines it varies with the charge and the voltage to ground. It does serve to illustrate the fundamental principles of wave propagation.

1. *Single Wave.* As previously derived in reference 2, Fig. 6 shows the relations governing the tangential component of the electric field surrounding a rectangular wave of charge, q_0, in coulombs per cm, and a rectangular wave of current i_0, in amperes, that propagate with a constant velocity vc, where c is the velocity of light and v is a fraction. The current and charge are related by the expression

$$i=vcq_o \quad (9)$$

Curve A is a stationary wave of electric field symmetrical about the origin produced by the charge whose head travels with the velocity of light. Curve B is likewise associated with the charge, but is symmetrical with respect to the head of the wave. Curve C is associated with the current and is of opposite polarity to B. Cognizance has been taken in the expressions that b might differ from a. When they are equal, curves B and C have the same shape.

2. *Oppositely Traveling Waves.* Schonland, among others, has shown that the head of the return stroke of lightning travels at a velocity less than that of light. Since Fig. 1(B) approaches the condition

90004129

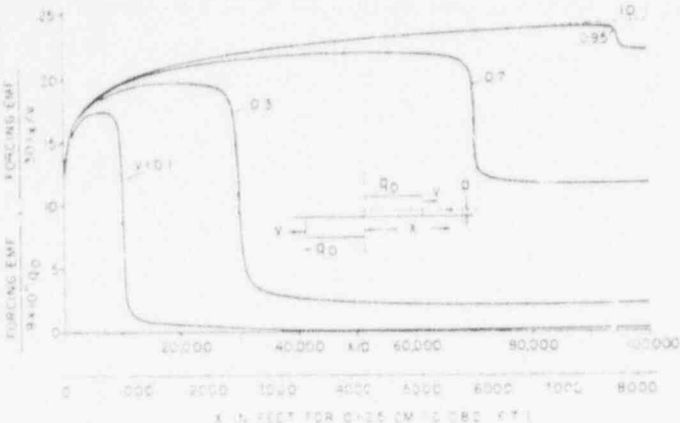

Fig. 7. Forcing emf's necessary to produce rectangular waves of charge and current traveling at a velocity less than that of light with no corona. Wave combination is given in the inset. Charge radius b-current radius a, ct/a = 100,000

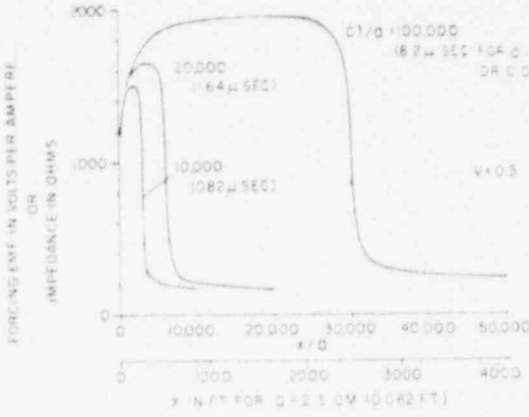

Fig. 8. Variation with time as parameter of forcing emf's for same conditions as Fig. 7 except the velocity is constant at v = 0.3

of the return stroke the equivalent surge impedance in this case will be analyzed. Fig. 7 has been computed with the assumption that the charge radius b is equal to the current radius, a. It shows the forcing emf's necessary to produce a rectangular wave of charge and current that travels with a constant velocity equal to 0.1, 0.3, 0.7, and 0.95 that of light. The particular instant chosen for this figure is $ct/a = 100{,}000$. A second scale for a and b equal to 2.5 cm (0.082 foot) has been added to the abscissa. For this particular value, the instant corresponds to 8.2 μsec.

Consider the curve for $v = 0.3$, that shows how a positive forcing emf of $19.8 \times 30 i_z/0.3$ must be distributed between zero and about $x/a = 15{,}000$, and how a negative forcing emf of about $17.5 \times 30 i_z/0.3$ must be distributed between $x/a = 15{,}000$ and $x/a = 50{,}000$ so that a rectangular wave of charge and current would reach a point $x/a = 30{,}000$ at this instant. In general there exists a roughly rectangular wave of potential equal in length to the elongating charge and current wave, and whose crest increases gradually as a logarithmic function of time. The manner in which the wave varies with time is illustrated in Fig. 8. Of course, if a be larger than this number, for the same instants of time, the forcing potentials would be correspondingly smaller.

The curves of Fig. 7 are plotted to show the relative values of the forcing emf's with the charge q_0 kept constant. As applied to the lightning stroke the comparison is more revealing when based upon a unit of current as this reveals the surge impedance. This has been done in Fig. 9, from which it can be seen that the effective impedance increases almost inversely as the velocity of propagation of the head of the wave.

The foregoing curves assumed that the radius of *charge* concentration, b, is the same as the *current* radius, a. The solid curves of Fig. 10 present the impedance characteristic for $v = 0.1$ and 0.3 for the condition that $b = 10$ feet and $a = 0.082$ foot for an instant equal to 8.2 μsec. It should be noted that the forcing emf's in this case are smaller than for Fig. 9 in which $a = b = 0.082$ foot for the same instant. The dotted curves of Fig. 10 are for the case of $a = b = 10$ feet. It can be seen that the impedance characteristic is more responsive to b than to a.

Without going into detail at this point, it will be observed that the return channel of the lightning stroke possesses a characteristic of the general nature described in Figs. 7–10. The return channel tends to propagate with the velocity of light but the current, in rising rapidly at the head of the return channel, introduces into the path of the channel a high-voltage drop that corresponds to a high negative forcing emf. The higher the transitory drop introduced by the increasing current, the more head of the current is retarded and its magnitude decreased.

If the wave front of the current wave is sloped, then the wave can be resolved into small incremental rectangular waves and the voltages of the component elements can be added. In this case, the voltage would be approximately proportional to the product of the instantaneous current and surge impedance, and the voltage drop along the path would be

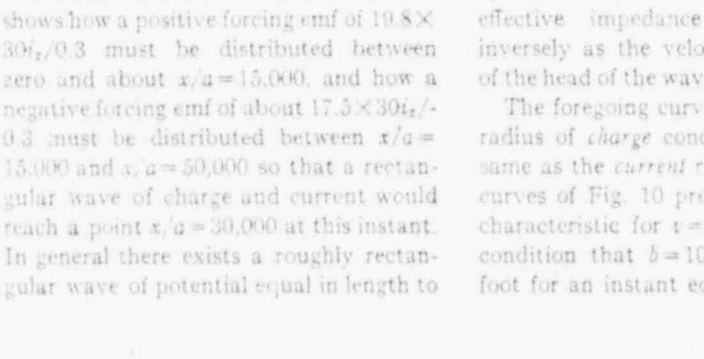

Fig. 9. Curves of Fig. 7 replotted to show relative values of impedance or forcing emf's based upon a unit current wave

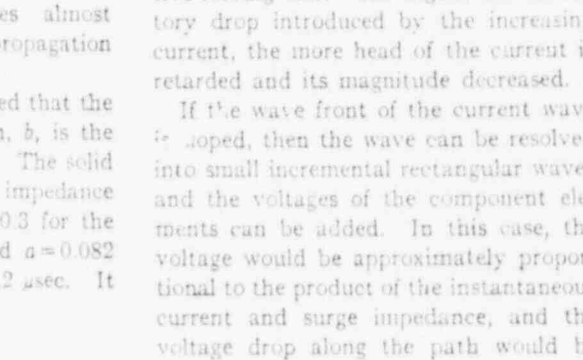

90004130

Fig. 10. Impedance characteristics showing the effect of corona for two different velocities

independent of the slope of the wave front, but in proportion to the magnitude of the current. Thus the total negative voltage that would have to be inserted in the front of the moving wave would be the same whether the current attained its maximum value in 1 μsec or in 2 μsec, that is, so far as the computation of the velocity of the current in terms of the drop is concerned. The actual total drop is determined by the arc characteristics.

3. *Two Parallel Conductors.* Four waves will be assumed to propagate from O to O' as in Fig. 1(C) and will be numbered as indicated. Just as in Fig. 4, so in this case also for x large in comparison with D, the forcing emf's reach limiting values. Fig. 11 has been prepared to illustrate the difference between corona effects and high arc drops occasioned by rapid changes in current magnitude. In the three cases depicted here, it is assumed that the distance between the conductors in all cases is 200 feet and that the head of the waves of charge and current have traveled 1,000 feet. In all three cases the electric fields tangent to the axis of propagation are plotted by the dotted curves. In computing the field in conductor A due to the charge in conductor A the radius a is used and due to the charge in B the radius D is used. For current, radius b is replaced by radius a. The negative of these fields are then integrated and the results plotted by the solid-line curves. In all cases the forcing emf's are computed for unit current.

In Fig. 11(A) the effect of corona is illustrated. The particular value of $v=0.62$ was chosen for a reason to be developed later, and results in a negative forcing or retardation voltage at the head of the wave that equals zero. The integrated effects of the traveling field due to charge, E_{xe}, and the traveling field due to current, E_{xm}, just cancel each other at this particular velocity and for these particular values of a and b for times greater than about the travel time between conductors. Figs. 11(B) and 11(C) were computed for a lower velocity of $v=0.3$. To attain the velocity, if $a=b=0.082$ foot would require a retardation voltage of 1,420 volts per ampere, but if $a=0.082$ foot and $b=10$ feet only 460 volts per ampere would be required. In Figs. 11(A), (B), and (C), the curve V represents the integrated effect of the stationary field; V_e, the integrated effect of the traveling field due to the charge; V_i, the integrated effect of the traveling field due to the current and the dot-dash curve the total of these three values.

It should be noted that, for the configuration used in the calculations of Fig. 11,

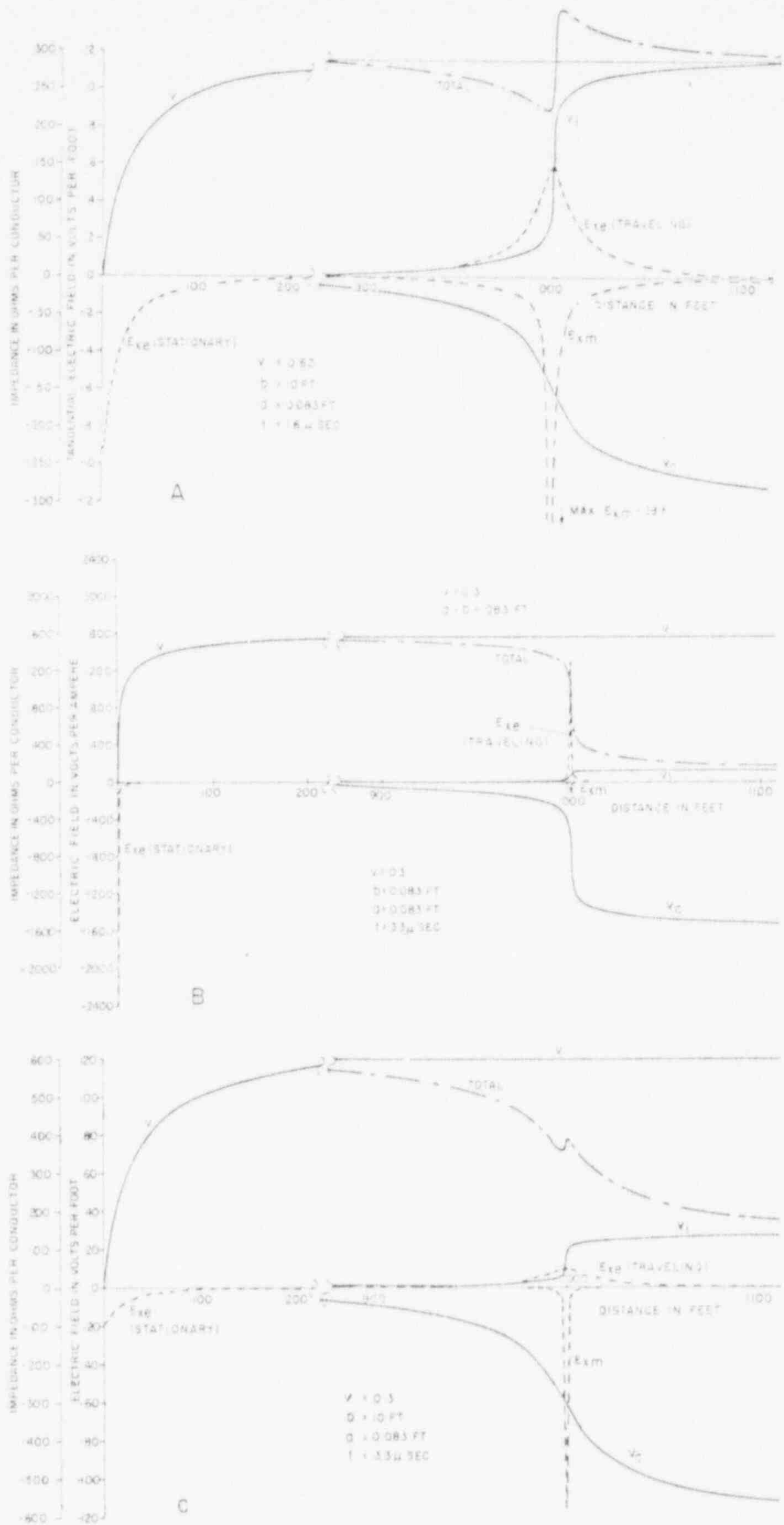

Fig. 11. Impedance and tangential electric fields on one conductor for wave combination of Fig. 1(C)

A—With corona and zero retardation voltage at head of wave, v = 0.62
B—No corona but with retardation voltage, v = 0.30
C—With corona and with retardation voltage, v = 0.30

90004131

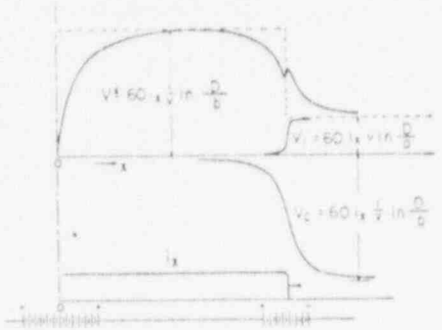

Fig. 12. Limiting values of forcing and retarding emf's on one conductor for wave combination of Fig. 1(C)

if the waves traveled at the velocity of light the limiting value of surge impedance would be 468 ohms. From Fig. 11(A) it is shown that corona tends to decrease this value to about 290 ohms, but Fig. 11(B) shows that high arc drops for retardation voltages tends to increase the surge impedance to about 1,560 ohms. Fig. 11(C) shows that for the particular values considered, when both corona and a retardation voltage are present, the net result is to increase the surge impedance to about 600 ohms.

The limiting values of the forcing and retardation emf's can be determined as follows. The forcing emf for the stationary component, V, in conductor a of Fig. 1(C) due to waves 1–4 is the same as equation 7 but expressed in terms of q_o is

$$V=18\times10^{11}q_o\left\{\ln\left[\frac{x}{b}+\sqrt{1+\left(\frac{x}{b}\right)^2}\right]-\ln\left[\frac{x}{d}+\sqrt{1+\left(\frac{x}{d}\right)^2}\right]\right\} \quad (10)$$

and for x/b large

$$V=18\times10^{11}q_o\ln\frac{D}{b} \quad (11)$$

From Fig. 6 it can be seen that the tangential component of electric field caused by charge in front of the head of the wave at a radius b due to wave 1 is

$$9\times10^{11}q_o/\sqrt{(vct-x)^2+(1-v^2)b^2} \quad (12)$$

and for wave 2 where b is small in comparison with D

$$-9\times10^{11}q_o/\sqrt{(vct-x)^2+(1-v^2)D^2} \quad (13)$$

Let $vct-x=y$ and the total field is

$$E_x=9\times10^{11}q_o\left\{\frac{1}{\sqrt{y^2+(1-v^2)b^2}}-\frac{1}{\sqrt{y^2+(1-v^2)D^2}}\right\} \quad (14)$$

Then V for this component of field upon integrating with respect to y from $y=0$ to y is

$$V=-9\times10^{11}q_o\left\{\ln\left[\frac{y}{b\sqrt{(1-v^2)}}+\sqrt{\frac{y^2}{b^2(1-v^2)}+1}\right]-\ln\left[\frac{y}{D\sqrt{(1-v^2)}}+\sqrt{\frac{y^2}{D^2(1-v^2)}+1}\right]\right\} \quad (15)$$

and for y very large

$$V=-9\times10^{11}q_o\ln(D/b) \quad (16)$$

The integral of the component of field behind $x=vct$ has a like forcing emf. Therefore, the total retarding emf due to the charge, V_c, is

$$V_c=-18\times10^{11}q_o\ln(D/b) \quad (17)$$

The expression for the retarding emf due to the current, V_i, has a similar form with b replaced by a, is of opposite polarity, and has a factor v^2.

$$V_i=18\times10^{11}q_ov^2\ln(D/a) \quad (18)$$

Since i_x is related to q_o by equation 9, equations 11, 17, and 18 become, respectively,

$$V=60i_x\frac{1}{v}\ln\frac{D}{b} \quad (19)$$

$$V_c=60i_x\frac{1}{v}\ln\frac{D}{b} \quad (20)$$

$$V_i=60i_xv\ln\frac{D}{a} \quad (21)$$

Fig. 12 shows graphically the relations involved and how the forcing emf is inserted in series between the origin and elements of the conductor and the equivalent retarding emf's. In the limit the relations are given by the dotted lines.

In connection with Fig. 11(A) it was mentioned that when corona effects only are present, the retardation voltage is zero. This means that V_c from equation 20 must equal V_i from equation 21. Then

$$60i_x\frac{1}{v}\ln\frac{D}{b}=60i_xv\ln\frac{D}{a} \quad (22)$$

and consequently

$$v=\sqrt{\ln\frac{D}{b}\Big/\ln\frac{D}{a}} \quad (23)$$

The conventional expression for the velocity of traveling waves is

$$v_c=1/\sqrt{LC} \quad (24)$$

where L is the inductance in henrys per cm length and C is the capacitance per cm length. This can be seen to be equal to

$$v_c=c\sqrt{\ln\frac{D}{b}\Big/\ln\frac{D}{a}} \quad (25)$$

which verifies equation 24.

An expression for surge impedance can be obtained in a similar manner. By definition

$$Z_c=\frac{V}{i_x} \quad (26)$$

And substituting V from equation 19 and then v from equation 23

$$Z_c=60\sqrt{\left(\ln\frac{D}{a}\right)\left(\ln\frac{D}{b}\right)}=60\ln\frac{D}{a}\sqrt{\frac{\ln D/b}{\ln D/a}}$$

$$=Z\sqrt{\frac{\ln D/b}{\ln D/a}} \quad (27)$$

where Z is the normal value of surge impedance for which no corona exists. This value of Z_c is also equal to $\sqrt{L/C}$.

Predischarge Currents of Rod-Rod Gaps

In the lightning stroke the leader of the first component moves earthward in halting steps, distributing as it does so a charge along its entire length. As it approaches the earth the steps become smaller, and as an approximation the leader may be regarded as moving slowly and continuously. As the tip reaches a point such that the distance to the earth equals the breakdown value for the potential at which the stroke channel is charged, breakdown occurs much as in a very long gap. The current for the discharge is drawn from the distributed charge along the channel in the form of a traveling wave that propagates with a velocity having a modal value 0.12 that of light. It is the surge impedance of this channel from the tip of the upward-moving leader that is the point of this investigation. It can be seen that the discharge resembles in considerable detail the discharge of a long rod-rod gap through a series of resistance, i.e., the surge impedance of the stroke, from a source of constant voltage, the potential of the charged leader. It is the purpose of this section to discuss the characteristics of just such a circuit.

For this development, let

U = constant voltage of the source in kv
R = series resistance in kilohms
u_i = instantaneous voltage across the gap in kv
i = current in amperes through the gap and the series resistance

In reference 4 the process of breakdown was discussed in considerable detail, and it was shown that it normally consists of the development of channels from each electrode that approach each other with ever-increasing velocity. The voltage drops along the channels are small in comparison with the potential across the gap, and, therefore, the channels can be regarded as extensions of the electrodes.

90004132

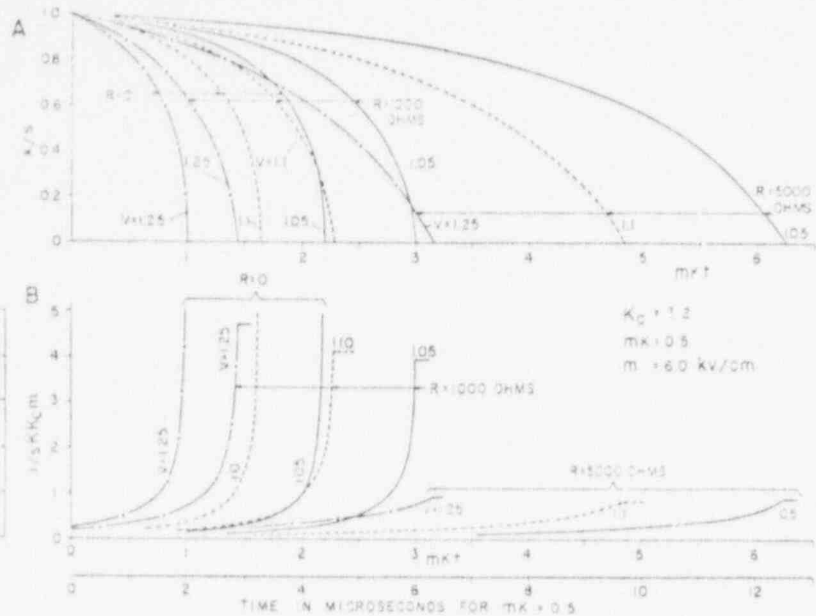

Fig. 13. Calculated predischarge channel development in rod-rod gaps for different values of series resistance and overvoltage factor

A—Channel growth
B—Predischarge current

If x be the distance between the ends of the channels in cm, that is, the length of the unbridged gap and t be the time in µsec, the velocity with which the ends of the channels approach each other is given by

$$\frac{dx}{dt} = -sK\,\frac{u_t - mx}{x} \qquad (28)$$

where

s = original gap spacing in cm
m = average critical breakdown gradient in kv per cm (about 6)
K = constant determined from experiment
t = time in µsec

In reference 4 it was also shown that the current is approximately proportional to the velocity with which the channel ends approach other. Thus

$$i = -K_c\,\frac{dx}{dt} \qquad (29)$$

in which K_c is a constant, which for rod-rod gaps is about 3.2. The voltage across the gap is simply the source voltage minus the iR drop, or

$$u_t = U - Ri \qquad (30)$$

Inserting i from equation 29 into equation 30, and using this result in equation 28, there results that

$$dt = \frac{(x/s) + KRK_c}{mK[V-(x/s)]}\,d(x/s) \qquad (31)$$

where V is the overvoltage ratio defined by

$$V = U/sm \qquad (32)$$

To obtain the progress of the channels as a function of time

$$mK\int_0^t dt = -\int_1^{x/s} \frac{(x/s)+KRK_c}{V-(x/s)}\,d(x/s)$$

or

$$mKt = -1 + (x/s) + (V + KRK_c)\ln\frac{V-(x/s)}{V-1} \qquad (33)$$

And for complete passage of the gap in time T

$$mKt = -1 + (V + KRK_c)\ln\frac{V}{V-1} \qquad (34)$$

This equation is of greatest interest in laboratory testing when the circuit is such that the inductance can be neglected. Of course, the drop in the voltage of the capacitors as they discharge must also be taken into consideration if the overvoltage is large and considerable charge is drained from the capacitors of the surge generator. This expression is of value in studying the process of breakdown. It is interesting to observe in passing that T is a function of the product RK_c which means that the effect of a given applied voltage on two similar gaps can be simulated by using one gap and doubling the resistance of the surge generator. Similarly, the breakdown characteristics of two very long parallel pipe gaps can be simulated by a gap of smaller length pipe if the same time the series resistance is increased inversely proportional to the length of the pipes.

For the lightning stroke it is important to know the current-time as well as the distance-time relation.

Combining equations 28, 29, and 30 to eliminate dx/dt and u_t and then inserting equation 32, the result is

$$\frac{i}{sKK_cm} = \frac{V-(x/s)}{(x/s)+KRK_c} \qquad (35)$$

And so after (x/s) is determined as a function of time from equation 33, i can be computed likewise as a function of time from equation 35.

The parameters in these expressions occur in such fashion that with the selection of three of them the nature of the phenomenon can be shown graphically. In Fig. 13 the three parameters m, K, and K_c are given specific values that have been found to lie within the practical range. For a discussion of the determination of these values see reference 4. The variation of (x/s) and i as the overvoltage factor and the series resistance are varied is shown in the upper and lower set of curves, respectively. To further elucidate these effects the total breakdown time of the gap, T, is plotted from Fig. 13 in Fig. 14 in the form of the conventional time-lag curve for a rectangular applied impulse wave.

Two scales are provided for both the ordinate and the abscissa of the lower set of curves of Fig 13. For a given R, the final steady-state value of the current varies directly with the gap length s. This may seem strange at first, but it should be remembered that the applied voltage is a rectangular wave of magnitude $U = ms$. Therefore, the final current is

$$I_f = U/R = Vms/R \qquad (36)$$

Thus, I_f in Fig. 13 is proportional to the overvoltage factor V and inversely proportional to R.

The extension of the magnitude of these currents into the realm of lightning strokes may be clarified by letting s equal 100 feet (or 3,045 cm). The length of the last step can be visualized as of this order of magnitude. Assuming an over-

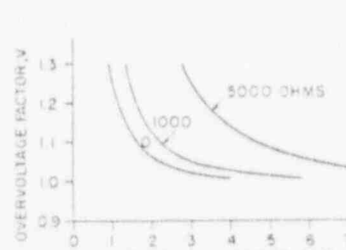

Fig. 14. Total breakdown time of rod-rod gap obtained from Fig. 13 and plotted in form of conventional time-lag curve

90004133

voltage factor of unity for this length, I_f = , $1\times6\times100\times30.48/1$ or 18,300 amperes for a stroke surge impedance of 1,000 ohms and 6,100 amperes for a stroke surge impedance of 3,000 ohms. The corresponding stroke potential per 100 feet would be 18,300,000 volts. Thus also for a given stroke impedance, the length of the last step, the potential and the current are all proportional.

One element in the development of relations in Fig. 13 was the assumption that the instantaneous velocity with which the channels approach each other is proportional to the instantaneous value of the current. This relation is expressed in equation 29. Designating this velocity by v_s

$$v_s = -i/K_e \tag{37}$$

in which i is expressed in amperes and v_s is expressed in cm per μsec. The lower curves in Fig. 13 express the current as a function of $i/s\ K_eKm$. The instantaneous velocity is then given in terms of these curves as

$$v_s = (i/sKK_em)sKm \text{ cm per } \mu\text{sec} \tag{38}$$

or

$$v_s/c = (i/sKK_em)sKm/3\times10^4 \text{ as a fraction} \tag{39}$$

The final value of this expression as contact is made, according to the theory advocated by the authors, should be equal to the velocity of propagation of the return stroke. Observation places this value between about 0.1 and 0.5 c.

In the computation of Fig. 13, mK was taken as 0.5 and (i/sKK_em) for R between 1,000 and 5,000 ohms had a value between 1 and 5. Now if for the moment the striking distance, which will be designated as X_1, and which is equivalent to s be taken as 200 feet then v_s/c also lies between 0.1 and 0.5 c. But, of course, if different values of X_1 had been chosen, the check would vary with the assumed value of X_1. This comparison does indicate that the relation between velocity and current appears to apply to the lengths of gaps involved in lightning.

While at the present time no particular grouping of the parameters determining the stroke characteristics are known with great precision, it is possible through a comparison of the different sets of data to arrive, through judgment, at a set of parameters that appear reasonable. Much can be determined when once the surge impedance of the stroke is known.

Application to the Lightning Stroke

The authors' conception of the stroke mechanism is presented in detail in reference 5. One characteristic of the stroke that has not been given much consideration is its surge impedance. One application of this quantity is to co-ordinate the potential of the stroke with the resultant final current at the ground. With this factor known one can estimate the extent to which reflections within the impedance of the stricken object might affect the stroke characteristics, or with the stroke current known one can determine the stroke potential and thereby estimate the length of the last step. These latter characteristics are also of value in estimating the number of shielding failures that may occur for a particular configuration of ground wires and conductors of transmission line. This section is devoted to the determination of the stroke surge impedance from three different aspects.

1. *A comparison of the statically determined potential of the stroke channel with the subsequent current that flows in the stroke channel next to the earth.* In Fig. 1 of reference 5 and the discussion accompanying it, a channel tip was assumed to be momentarily halted as it approached the earth at a point 1,000 feet above the earth at an instant at which the space charge in advance of the channel tip is fully developed for that particular step. It was assumed that the density of the space charge surrounding the channel varied inversely as the distance of the point from the channel. It was shown that for a charge distribution of 5×10^{-6} coulombs per cm some distance back from the tip where the charge per cm length became substantially uniform, the potential of the channel with respect to the earth was about 50,000,000 volts. This computation served to establish the potential of the channel for such a charge per unit length. While the actual path of the stroke is tortuous and branched, this same potential and charge distribution will be assumed to apply as the tip approaches the earth. As the return channel from the earth taps the charge in a cross section of the downward leader, the current released to the earth is given by equation 9. If v be let equal to 0.12, the modal velocity, then $i = 0.12\times3\times10^{10}\times5\times10^{-6} = 18{,}000$ amperes, and if $v = 0.3$, the stroke current is 45,000 amperes. Using these values to determine a surge impedance of the stroke, one obtains 50,000,000/18,000 or 2,780 ohms for $v = 0.12$ and 1,100 ohms for $v = 0.3$.

2. *Velocity of the return channel.* The diameter of the cylindrical volume of charge deposited by the downward leader and the volume distribution of charge are still somewhat controversial. They doubtless vary with the stroke potential and also with height. If it is desired to replace a charge distribution that varies inversely as the radius from the channel core to the boundary of the corona sheath with a charge all of which is concentrated at a given radius, this radius is theoretically equal to 37% of the radius of the boundary of the corona sheath. For the present purpose a radius of 10 feet is arbitrarily chosen as an approximate value, bearing in mind that the radius doubtless varies with potential, and also that use is being made of the still unproven premise that the charge does in fact vary inversely as the radius. After the current in the upward channel from the earth has risen to crest, the highly conducting channel in its upward progress successively taps different lateral sections of this charge. The diameter of the upward channel varies with the current in the upward channel. An arc plasma for currents of the order of magnitude of those met in lightning will have a radius of about 2.5 cm (0.082 foot). The resistance of such an arc channel attains a low drop in a fraction of a μsec, but during the interval in which the current is rising, which at a particular point may also be a very short time, the voltage drop attains very high values. These high values of resistance of the arc constitute the retardation emf's discussed in connection with waves that travel with a velocity less than that of light. And so the upward channel as it taps the charge from the downward leader can be conceived as a good conductor of radius 0.082 foot extending upward from the earth at a velocity of about 10 to 30% of that of light and fanning out laterally at the tip to deposit a neutralizing charge at a radius of 10 feet. At the same time a very considerable impedance is offered to the formation of the good conducting quality at the head of the wave.

Fig. 10 shows the impedance characteristics of such wave for $v = 0.1$ and for $v = 0.3$ at 8.2 μsec. In the former case the impedance is shown to be of the order of 2,400 ohms and in the latter about 1,000 ohms.

3. *Waveshape of current in return channel.* The shape of the predischarge current in rod-rod gaps is affected strongly by the external resistance. By comparing these currents with the currents of those observed for natural lightning the impedance of the stroke can be estimated, provided that extrapolation from gap separations attainable in the laboratory to gap distances of lightning proportions is justifiable.

Fig. 15. Evaluation of return stroke surge impedance from the shape of the return stroke current wave front

A—Calculated predischarge currents in rod-rod gaps

B—Lightning stroke currents measured by Berger[6]

C—Measured predischarge currents in rod-rod gap

D—Measured predischarge currents in rod-plane gap, negative polarity

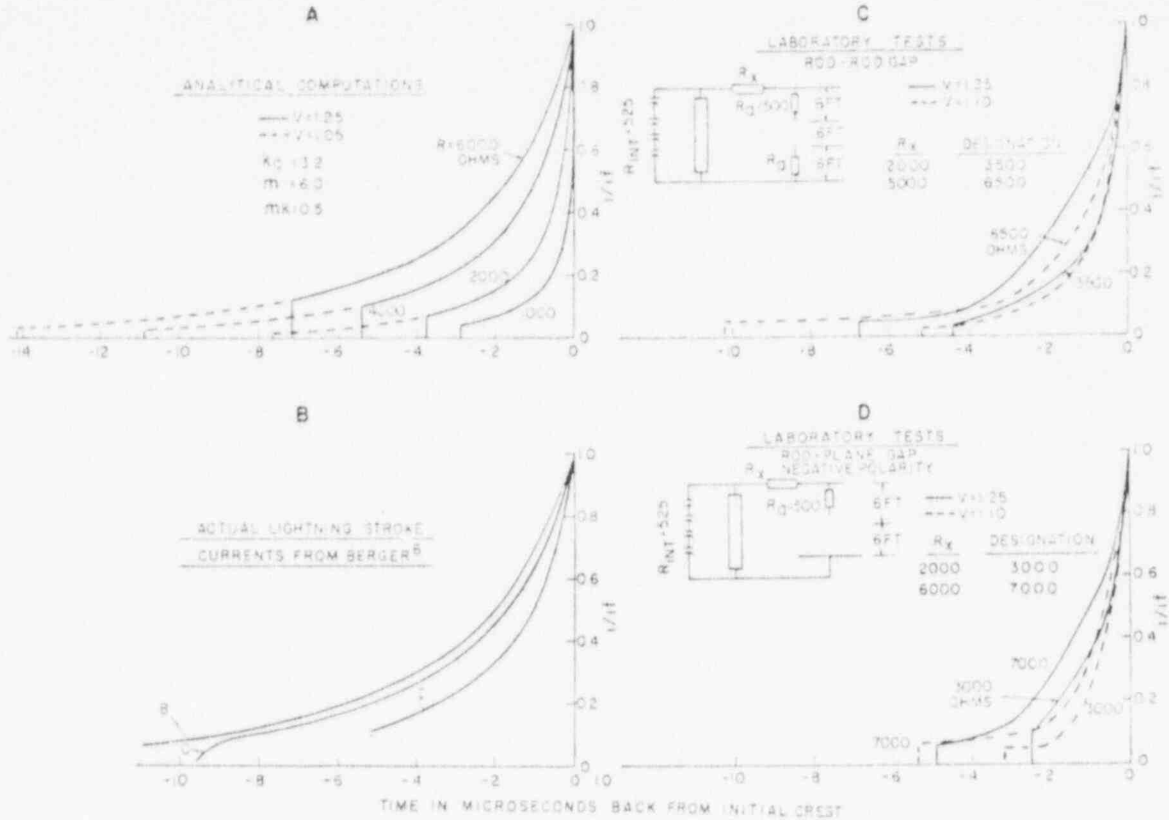

The computed curves of Fig. 13 have been replotted in Fig. 15(A) together with similar curves for $V=1.05$ by using as ordinate the ratio of the instantaneous of the final current and as abscissa the time measured backward from the instant that the current reached its maximum or final value. It is interesting to observe that for this range of parameters there is little difference in the curves for $V=1.05$ and those for $V=1.25$, except for the extension for low values of current. In Fig. 15(B) is plotted on a similar basis the three most complete curves of natural lightning currents obtained by Berger in Switzerland,[6] whose data had been reproduced in reference 5. The curve designations are the same as those used in Fig. 8 of reference 5. The curves of Fig. 15 (A) in their computation involve intermediate assumptions and evaluation of constants. These intermediate steps can be circumvented by the use of only one of the assumptions used, namely, that the time lag of rod-rod gaps in independent of the gap length,[4] and by then obtaining experimentally the wave shape of the predischarge currents for different series resistances. The results of such tests are plotted in Fig. 15(C). The applied voltage in these tests rose to an effective crest in about 1/4 μsec and the overvoltage factor was 1.10 and 1.25. In these curves the designation numbers are simply the sum of $R_{int}+R_x+2R_g$. It should approximate the effective resistance as R_x is large in comparison with the other values.

It was found in previous tests on rod-rod gaps that a considerable oscillation in current resulted as the average peak of current was approached. The oscillation was decreased very greatly by placing the resistors R_g close to the gaps. These were arranged in a vertical position and the 1/2×1/2-inch rod gaps were only about 8 inches long. Fig. 16(A) shows the nature of the resulting current.

It is recognized that natural lightning to open ground would be more closely simulated in the laboratory by discharges between a rod of negative potential and a flat plate. The results of such tests with the same type of applied voltage wave are shown in Fig. 15(D). The results show a somewhat faster travel time, but the general shape of the curves are the same as for rod-rod gaps. A typical oscillogram from these tests is shown in Fig. 16(B).

The inductance of the circuit doubtless has some effect upon retarding the rate at which the current rises. This effect is particularly important near the later stages of the current rise. And so in comparing the curves of Figs. 15(A), (C), and (D) with the curves of Fig. 15(B), some consideration should be given to the effect. Greater refinements in the investigations to determine these effects would be warranted.

Estimate of Surge Impedance of Stroke. The great variation in stroke parameters enhances the difficulty of estimating the stroke surge impedance, for not only do such quantities as currents, potentials and velocities of the return channel vary over wide limits, but the equivalent surge im-

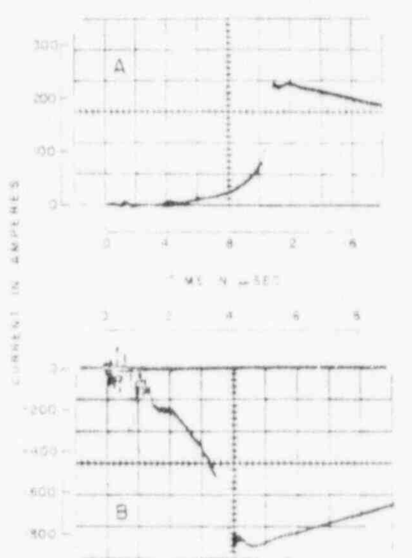

Fig. 16. Oscillograms showing predischarge currents in gaps; see insets of Fig. 15

A—Six-foot rod-rod gap, $v=1.10$, $R_x=3{,}000$ ohms

B—Six-foot rod-plane gap, negative polarity, $v=1.25$, $R_x=1{,}000$ ohms

90004135

pedance is interdependent with them. The velocity method of Fig. 10 is probably the most accurate method of estimating the surge impedance, but it also requires a knowledge of the equivalent corona radius, and it varies with time. But since the corona radius enters the expression for the surge impedance as a logarithmic relation, it may not be essential to know its value precisely. From Fig. 10 it can be estimated that for $v = 0.1$ and 0.3 the surge impedance values are 2,400 and 1,000 ohms, respectively. Since 0.12 is the modal value of v, one would lean to a value of about 2,400 ohms.

From the electrostatically determined potential of the stroke and the resulting current that flowed to earth upon contact of the leader with the earth, it was determined that the surge impedance of the stroke was about 2,780 ohms when v was assumed equal to 0.12 and 1,100 ohms when v was assumed equal to 0.3. These values are not much different from those just given and they involve much the same kind of assumptions.

In comparing the analytically determined predischarge currents of Fig. 15(A) with Berger's first component stroke currents of Fig. 15(B), the computation of necessity was based upon a stationary upper electrode. It was necessary to extrapolate the time-lag curves from laboratory distances to last-step stroke distances. Within these limitations the stroke impedance appears to be of the order of 4,000 to 6,000 ohms. In comparing the more direct laboratory predischarge curves of Figs. 15(C) and (D) with Berger's results of Fig. 15(B) which were obtained with a 230-foot mast would indicate an even larger surge impedance in excess of 6,000 ohms.

Thus, these methods give a wide range of surge impedances, but in judging the various methods the authors give greatest weight to the velocity method. The values estimated from the statically determined potentials would then be next in accuracy. The curves of Figs. 15(C) and (D) are of greatest value in confirming the general shape of the current curves. If only one value must be chosen the authors suggest a value of about 3,000 ohms.

Conclusions

In the different approaches so diverse in character to the consideration of the surge impedance of a lightning stroke, a number of conclusions can be drawn.

1. The surge impedance of two parallel conductors is equal to its conventional value after a time equal to the travel time of light between them, and the surge impedance of a conductor parallel to a perfectly conducting earth plane is equal to its conventional value after a time equal to twice the travel time of light between the conductor and earth.

2. The surge impedance of a vertical conductor, one end of which is connected to a perfectly-conducting earth plane and upon which waves of current and charge travel upward, increases with time without limit. The surge impedance also increases almost inversely as the velocity of propagation of the head of the wave.

3. In the lightning stroke two factors contribute to the determination of the velocity of propagation of the return stroke and its surge impedance. These are (1) the fact that the charge distribution in the downward leader has a much greater radius than the column of the arc by which the charge is subsequently drained to the earth (corona effect), and (2) the temporary high resistance introduced into the path of the current as the current at the head tends to increase rapidly. The effects of these quantities have been analyzed in terms of observed lightning characteristics.

4. Corona decreases both the velocity of propagation and surge impedance, while the temporary increase in voltage drop over the normal arc drop at the head of the wave decreases the velocity of propagation, but increases the surge impedance. In a lightning stroke these effects combine to produce a large decrease in velocity and an increase in surge impedance.

5. An expression has been derived for the growth of the channel current in a gap to which a rectangular voltage wave is applied through a constant resistance.

6. For general purposes it is estimated that the surge impedance of the stroke is of the order of 3,000 ohms.

References

1. A New Approach to the Calculation of the Lightning Performance of Transmission Lines III—A Simplified Method: Stroke to Tower, C. F. Wagner, A. R. Hileman. *AIEE Transactions*, pt. III (*Power Apparatus and Systems*), vol. 79, Oct. 1960, pp. 589–603.

2. A New Approach to the Calculation of the Lightning Performance of Transmission Lines, C. F. Wagner. *Ibid.*, vol. 75, Dec. 1956, pp. 1233–56.

3. A New Approach to the Calculation of the Lightning Performance of Transmission Lines, C. F. Wagner, A. R. Hileman. *Ibid.*, pt. III-B, vol. 78, Dec. 1959, pp. 996–1021.

4. Mechanism of Breakdown of Laboratory Gaps, C. F. Wagner, A. R. Hileman. *Ibid.*, pt. III, vol. 80, Oct. 1961, pp. 604–22.

5. The Lightning Stroke—II, C. F. Wagner, A. R. Hileman. *Ibid.*, pp. 622–42.

6. Measuring Equipment and Results of Lightning Research During 1947–1954 on Mount San Salvatore, K. Berger. *Bulletin*, Schweizerischen Elektrotechnischen Vereins, Zurich, Switzerland, vol. 46, nos. 5 and 9, 1955.

Discussion

Charles J. Miller, Jr. (The Ohio Brass Company, Barberton, Ohio): The phenomenon of electrical breakdown of air is one which has attracted the attention of many investigators, starting with Benjamin Franklin in 1752. This present paper by Wagner and Hileman is another milestone in their series of important contributions to the over-all effort being made by contemporary scientists around the world to relate the theoretical aspects of electricity with observed phenomena.

One result of practical importance for laboratory impulse testing is equation 34 which, as the authors indicate, may be used to calculate the time to flashover of air gaps for various overvoltage ratios V. This equation has been checked against some volt-time data obtained on rod-rod gaps in 1938, and the results of this comparison are given in Fig. 17.

For these calculations the following values were used in equation 34:

$K_c = 3.2$, the value recommended by the authors for rod gaps.

$R = 0.8$ kilohm, the impulse-generator series resistance.

$m = 6$ kv per cm, the value indicated by the authors.

$m = 0.20$ determined by fitting the calculated curve to the data.

Note that a value of 0.50 is suggested by the authors for rod-rod gaps, and is the value which they used in their calculations for Fig. 13.

It is recognized that an impulse generator having a $1\frac{1}{2}\times 40$-μsec output wave, as was used in the 1938 rod-rod gap tests, may not conform exactly to the simple constant-voltage series-resistance circuit visualized by the authors for the derivation of equation 34, but a little reflection indicates that for practical purposes, the impulse generator circuit approximates this condition. In any event, the comparison between the laboratory data and the calculated values gives a remarkably close correlation, and this by itself would seem to indicate that this theoretical approach to the breakdown of air gaps in the laboratory warrants further study.

90004136

H. Linck and L. Lishchyna (Ontario Hydro, Toronto, Ont., Canada): Sparked by the high lightning-outage rates of certain high-voltage transmission lines, the authors in a very commendable way decided several years ago to undertake a thorough theoretical investigation of the characteristics of the lightning discharge and its effects. Their present paper indicates that they have advanced in their studies to the stage where the correlation of field theory and physical processes in the stroke formation can be attempted in order to arrive at a practical method of line-outage calculations. Due to the complexity of the subject, a detailed discussion of the authors' work must be left to those experts who have an intimate knowledge of both electromagnetic field theory and the physics of the spark phenomenon, but some questions of a more general nature may be permitted here.

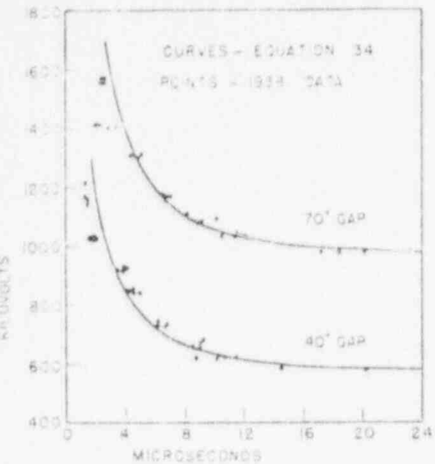

Fig. 17. Comparison of rod-rod gap data obtained in 1936 with calculated curves obtained by using equation 34 for the time to flashover

In Fig. 7, the forcing emf's for rectangular waves of charge and current at a velocity less than that of light and without corona are shown. If the head of the return stroke has progressed to a point $v.c.t$ above the ground, is it correct to assume that the forcing function for the return stroke current is composed of the integral of the electric field from ground to point $v.c.t$ as it existed along the stroke channel just before the return stroke commenced, plus the temporary high-voltage drop at the return stroke head?

A simplified formula for the forcing voltage in each conductor of a traveling wave system of two parallel conductors is given in the paper. It is also shown that the surge impedance of such a system is not a constant for travel distances from the source up to the equivalent of the conductor spacing. The question arises how the impedance of a short-line section should be represented for the case where lightning strikes a line 100 or 200 feet from the station entrance.

The authors state that they are aware of two practical cases for which traveling waves propagate with a velocity less than that of light, firstly, the propagation of charge under corona, and secondly, lightning. A third important case can be added, namely traveling waves in cables. It is known that the velocity of wave propagation in a medium of permittivity k varies inversely as the square root of the permittivity, and it follows that reduced velocity is not limited to wave phenomena in an electrically excited gas. But it would appear that basic differences exist in velocity reduction due to increased permittivity and due to ionization. One difference, for instance, would be that in the case of a cable the electromagnetic field is guided by the inner and outer conductor with losses normally neglected, whereas in lightning the return stroke in expanding its own conducting path has to force its way ahead, consuming energy in doing so. Remembering that at the beginning of their investigations the authors did not recognize as valid the concept of stroke-surge impedance, it is gratifying to note that now, based on a different principle, it may be possible to describe certain stroke characteristics in terms of an impedance, a parameter that can easily be fitted into conventional calculations.

There are still some areas of doubt concerning simplified assumptions in lightning calculations. It has been proposed by one of the authors that the stroke potential can be expressed as the product of stroke-surge impedance and current crest; considering that stroke currents in the range of about 1,000 to 250,000 amperes have been measured, and assuming an average stroke impedance of 3,000 ohms as suggested in the paper, then stroke potentials would fall between 3 to 750 million volts. If, on the other hand, one argues that the development of the leader depends on a critical voltage condition, and therefore the stroke potential does not vary greatly, being of the order of 50 million volts, then for the currents mentioned above the surge impedance would be between 50,000 and 200 ohms; the authors quote figures from 1,000 to over 6,000 ohms. It appears that it is too early to accept any average data on stroke parameters, and I agree with Mr Wagner that still further field measurements of the properties of lightning are required before we can claim to understand it fully.

C. F. Wagner and A. R. Hileman: We wish to thank Dr. Miller for his gracious comments. We are particularly pleased because he has been an outstanding contributor to the art in this particular field. It is most interesting that by using the formula given in the paper he has been able to determine a curve that fits the data for a 40-inch and a 70-inch gap that was obtained in an entirely different laboratory. We realize that Dr. Miller appreciates the implications of using equation 34, that had been developed for the application of a constant voltage to a gap through a series resistance, to a surge generator circuit whose constants had been set for a 1.5×40 wave. We merely wish to comment that some danger might be implicit in such procedure because of the change in the constants of the surge generator necessary to produce such a wave.

We appreciate also the penetrating comments of Messrs. Linck and Lishchyna. They comment first upon the use of Fig. 7. In determining the forcing emf we did not use the radius of the leader as it existed along the stroke channel just before the return stroke commenced. Had we done so, we would have used a radius of about 1 mm (millimeter) instead of the value of 2.5 cm that is indicated in the caption for the abscissa. Perhaps a more detailed discussion of our philosophy might be in order. To determine the stroke potential as the leader of the first component approaches the earth, we could have made some assumption regarding the distribution of charge across the lateral sections of the leader which in the previous paper we assumed to vary inversely as the radius from the core. Then from such an assumption the leader potential could have been determined. Any such calculation would be affected both by the tortuosity of the downward leader and also by the effect of the charge on branches from the main channel of the downward leader. By operating upon the return stroke we start with an assumption of current, of the velocity of the return stroke, of the diameter of the plasma core of the return stroke, and of the location of the charge that had to be fed into the upward leader as it taps any lateral section of the channel. In this case, the assumption concerning the location of the charge is not an important factor. We feel that this approach to the determination of the potential of the core is likely to be more accurate than the first approach.

The discussers ask the very practical question concerning the representation of a short line section where a lightning stroke impinges on a line a short distance from the station entrance. Equation 7, which is plotted in Fig. 4, shows that the surge impedance for the system of waves shown in the inset does not reach the conventional value of surge impedance as given by equation 8 until a time equal to the travel time of the field between the conductors. However, as shown in Fig. 4, the surge impedance is equal to about 85% of its final value within about 1/4 of the travel time. Also, the curves of Fig. 4 are applicable only for a rectangular wave. As discussed in the last paragraph under section 3, if the assumed waves possessed sloping fronts, the error in using the conventional surge impedance when expressed in terms of the final values becomes smaller. Therefore, in direct answer to the discussers' question, it appears that the conventional value of surge impedance should be used to represent the short line section.

The authors wholeheartedly endorse the discussers' observations that there are still some areas of doubt concerning simplified assumptions in lightning calculations and in the opinion of the authors this statement applies not only to the characteristics of the stroke, but to the characteristics of the transmission line. The danger of accepting average stroke parameters was brought out very clearly by Messrs. Linck and Lishchyna, and the authors wish to develop this thought further. The stroke potential certainly varies from stroke to stroke depending upon the charge distributed along the path of the downward leader, and since the return stroke current varies over wide limits and is proportional to the charge laid down by the downward leader, then for a given return stroke velocity, the stroke potential should vary over about the same range as the return-stroke current. The evidence indicates that the velocity is not constant but is higher for the higher currents

90004137

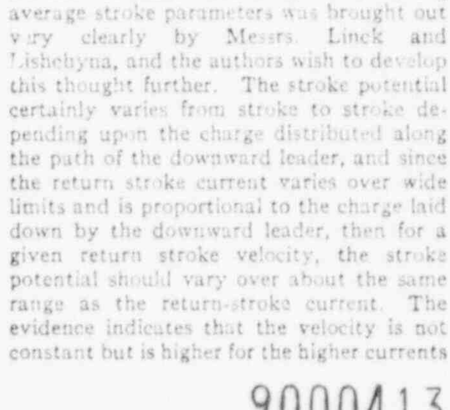

Fig. 18. The velocity of the return stroke as a function of the lightning current. The unbroken curve is calculated by equation 40. The dotted curve is obtained from analysis of field measurements (Fig. 7 of reference 4)

than for the lower currents. This variation of return-stroke velocity with current affects the computation of the stroke potential when computed through the medium of the surge impedance because the surge impedance decreases with increasing velocity. In this connection it would be well to review the present knowledge concerning the relation between velocity and current.

In 1942 Wagner and McCann[1] in reviewing the data of Schonland[2] and his associates state that "the evidence is quite strong that higher return-streamer velocities are associated with higher stroke currents." From their data[2] Wagner and McCann also derived percentage distribution curves of the effective upward velocity of the return streamer (Fig. 20 of reference 1). Assuming that the higher return-streamer velocities are associated with the higher stroke currents then from the distribution curves of return streamer velocity and distribution curves of current, it is possible to obtain a curve relating to these two quantities. Lundholm[3] compared these quantities for three ranges of stroke currents and Rusck[4] plotted the curve shown by a dotted line in Fig. 18 (Fig. 7 of reference 4). The full line in Fig. 18 is an analytical relation developed by Rusck[4] which is given by

$$v = 1 \Big/ \sqrt{1 + \frac{500}{I}} \qquad (40)$$

where v is the velocity of the return streamer expressed as a fraction of that of light and I is the return stroke current. According to Rusck this relation is based upon the previous work of Lundholm[3] and Toepler[5] and includes some degree of empiricism. Nevertheless, the equation fits the observed results very nicely and can be used for the present for extrapolating into the unknown region of Fig. 18.

REFERENCES

1. INDUCED VOLTAGES ON TRANSMISSION LINES. C. F. Wagner, G. D. McCann. *AIEE Transactions*, vol. 61, 1942, pp. 916-29.

2. PROGRESSIVE LIGHTNING—II. B. F. J. Schonland, D. J. Malan, H. Collens. *Proceedings*, Royal Society, London, England, Series A, vol. 152, 1935, p. 595.

3. INDUCED OVERVOLTAGES ON TRANSMISSION LINES AND THEIR BEARING ON THE LIGHTNING PERFORMANCE AT MEDIUM VOLTAGE NETWORKS. R. Lundholm. *Transactions*, Chalmers University of Technology, Gothenburg, Sweden, no. 188, 1957.

4. INDUCED LIGHTNING OVER-VOLTAGES ON POWER-TRANSMISSION LINES WITH SPECIAL REFERENCE TO THE OVER-VOLTAGE PROTECTION OF LOW-VOLTAGE NETWORKS. Sune Rusck. *Transactions*, Royal Institute of Technology, Stockholm, Sweden, no. 120, 1958.

5. FUNKENKONSTANTE, ZUNDFUNKEN UND WANDERWELLE. M. Toepler. *Archiv fur Elektrotechnik*, Berlin-Charlottenburg, Germany, vol. 14, 1924, pp. 305-18; also vol. 18, 1927, p. 549.

Radio-Influence Testing on 70 Miles of 345-Kv Horizontal Bundle Conductor

R. E. GRAHAM
ASSOCIATE MEMBER AIEE

C. R. BOND
ASSOCIATE MEMBER AIEE

Summary: Radio-influence (RI) test results on 70 miles of 345-kv transmission line are presented. The design of the 345-kv transmission line using 954-MCM (thousand circular mils) ACSR (aluminum cable, steel reinforced) conductor bundled at 18-inch spacing, the use of standard suspension clamps, triangular space plates, and a horizontal phase spacing of 27 feet resulted in satisfactory RI level without control rings at the conductor hardware assemblies. Attenuation tests show that RI readings at one site are not materially affected by precipitation on the line a few miles away.

LABORATORY TESTS were conducted by the Ohio Edison Company, previous to the construction of 70 miles of the 345-kv line, to determine the corona and radio-influence levels of the line hardware to be used on its 345-kv transmission lines, and field tests were conducted on the completed transmission line to evaluate the selection of hardware.

On January 31, 1961, the Sammis–Star North 345-kv transmission line was energized for RI testing; Figs. 1 and 2. These tests ran for approximately 8 weeks.

Laboratory Tests

In 1958, the Ohio Edison Company conducted laboratory tests on various types of hardware and conductors for corona and RI, and the results are shown in Table I (all voltages are line to ground). These test data provided the basis for the selection of the hardware assembly for the 345-kv transmission lines.

Tension stringing was adopted after a comparison of laboratory data of "cleaned" and "as received" conductor corona and RI tests indicated that a significant reduction in the RI could be expected if tension stringing was used. The "as received" condition would be similar to conductors strung in a normal manner.

Realizing that differences exist when moving from laboratory to the field, it was decided that RI field tests would be conducted on the Sammis–Star North 345-kv transmission line to evaluate the laboratory tests further.

Laboratory tests had indicated that control rings might not be necessary on conductor hardware assemblies and, since RI field tests were necessary to substantiate the laboratory results, it was decided to construct the Sammis–Star North 345-kv transmission line without control rings on the 26-mile section at the plant end, and with control rings on the remaining 44 miles of line.

Ambient Level Tests

Prior to and during the construction of the 345-kv transmission line, ambient-noise-level readings were taken along the right of way to establish an ambient level for the area and for some of the existing lines crossed by the 345-kv line. The normal ambient level ran from about 5 to 10 μv (microvolts) per meter as read on the Quasi-Peak scale of a Stoddart *NM 20B* meter with a 1/2-meter rod antenna.

Tests were conducted on other lines throughout the system to gain a better knowledge of acceptable levels of RI and the methods of measurement.

345-Kv Long-Line Tests

PRELIMINARY WORK

90004138

Two sites were selected as the primary test locations. One test site was in the center of the 26-mile section of line without control rings, while the other was in the 44-mile section with control rings, 13 miles from where the rings start. These test sites were selected since they were nearly identical in all respects and thus eliminated some of the possible variables.

These two particular sites were then staked so that all lateral and longitudinal readings would be taken at exactly the same location regardless of the number of readings. Lateral stakes were placed 25 feet apart for 300 feet either side of the centerline while the longitudinal stakes were 20 feet apart 75 feet either side of the centerline for about 600 feet.

Paper 61-1027, recommended by the AIEE Transmission and Distribution Committee and approved by the AIEE Technical Operations Department for presentation at the AIEE Fall General Meeting, Detroit, Mich., October 15-20, 1961. Manuscript submitted June 15, 1961; made available for printing August 8, 1961.

R. E. GRAHAM and C. R. BOND are both with the Ohio Edison Company, Akron, Ohio.

The authors wish to express their thanks to the many members of the Ohio Edison Company who aided in all phases of the testing, and to Commonwealth Associates Inc., of Jackson, Mich., the Ohio Brass Company, and the Westinghouse Electric Corporation for their advice and assistance.

on the other hand emphasize that on the basis of only 2 years of experience, about 4% of the strokes produce flashovers. They further point out the difference between this value and the value of 7% used by the authors. The authors wish to call attention to these contradictory criticisms and emphasize their own recognition of the need to handle averages carefully. But even if one would use the 4% value mentioned by Mr. Johnson and Mr. Schultz, it does not constitute a contradiction of the authors' thesis but rather indicates in viewing Fig. 2 that a relatively large value of time to crest is indicated. This follows because, in general, the average rate of rise increases with increasing current, regardless of the lower limit of current chosen. But in spite of these comments, the authors will also agree that the available data are still meager. Had they been completely satisfied with the published data, there would have been no urge to undertake the investigation described in the paper. But even in this investigation, the results were not too conclusive. As mentioned in conclusion 6, to achieve times to crest of the order of 1 or 2 μsec the neutralizing processes in a section of the lightning channel proceed by lateral discharges and develop at about the same speed as spark discharges.

The authors wish to concur with Mr. Linck that a sufficiently large amount of information can best be obtained through a combined effort of the industry.

Returning to the comments of Mr. Johnson and Mr. Schultz, the authors note that they emphasize and quote our statement "There must be a limit of crest current below which the data need not be given consideration." We wish to reassert this statement. For example, even if the current has a rectangular front with an infinite rate of rise, it does not follow that the voltage across the insulator string will be infinitely large or that the insulator string will flash over. There certainly exists a lower limit of current, even of rectangular shape that would not cause flashover. The most desirable information regarding current is the instantaneous values as a function of time. Lacking this, the average values of slopes to several definite instants would be next most desirable. At this point in the art of calculating the performance of a line, one cannot say with assurance which is the most important average. It is conceivable that the most desirable average must be coordinated with the breakdown characteristics of the insulator string. But given only one average, the average to crest would appear to be the most informative.

Of course, the current and its time variation are not the only factors that must be considered in determining the performance of a line. The time variation of the charge and current in the stroke channel above the towers can also be of importance. The authors' discussion of Fig. 2 does not imply in any way that the actual currents in the tower and ground wires and their time variations are the only factors that must be computed.

Mr. Johnson and Mr. Schultz indicate that high rates of rise or short fronts of stroke currents are the cause of the high lightning outage rates on existing high voltage lines. They base this observation on the field data shown in Fig. 2 and on use of the tower surge impedance or inductance concept as given in their paper.[1] A discussion of this paper[2] shows that using the existing data on wavefronts and the concept of tower surge impedance or inductance does not result in line flashovers, and therefore does not explain the high outage rates on existing high-voltage lines.

The authors have not attempted in their paper to analyze all aspects of the lightning stroke. They are concerned primarily with those characteristics that might have a bearing upon the lightning protection of transmission lines. Mr. Rorden has raised the question of a theory to explain branching. The authors feel that the logical starting point in the analysis of stroke for its effect upon the line is the current fed into the tower top and ground wires. Considerable statistical information is available concerning the crest magnitude and the frequency of occurrence of different crest values. Less information concerning the rate of rise of the current is available. This current and the variation of charge and current above the tower within a height of say 300 or 500 feet, as influenced by the velocities of the stroke or the presence of upward streamers, are probably all that is significant. Branching in parallel or above this zone may influence the value of these quantities within this zone, but if the quantities within this zone are postulated in terms of the tower-top currents and their rates of rise, the effects of branching would automatically be included in the computations. The time variation of the charge and current above the tower should take into account the probability of occurrence of upward streamers.

References

1. See reference 3 of the paper.
2. Discussion by C. F. Wagner and A. R. Hileman of reference 3 of the paper, p. 1478.

90004139
REF. 14

Arc Drop During Transition from Spark Discharge to Arc

C. F. WAGNER, FELLOW AIEE
C. M. LANE, ASSOCIATE MEMBER AIEE
C. M. LEAR, ASSOCIATE MEMBER AIEE

OF RECENT YEARS, renewed interest has developed in the rate of rise of the current on the wavefront of a lightning stroke as it strikes the earth. In a companion paper it is shown that an essential element in determining the stroke-current characteristics is the transient arc drop of the stroke current. The purpose of this paper is to present experimental results of tests on laboratory-produced oscillatory arcs having crest values up to 50,000 amperes and times to crest as short as 1.2 μsec (microseconds).

Review of Present Knowledge

The earliest work of this nature is that of Norinder and Karsten,[1] who reported the voltage drop for impulse currents having a crest amplitude up to 102 ka (kiloamperes). Most of these data are for times much longer than 1 μsec. Fig. 1, however, replotted from their work, shows the arc drop taken across an 18-cm (centimeter) gap that was broken down and through which an oscillatory current passed whose first crest of 26,000 amperes occurred at 1.3 μsec. The plotted points represent the voltage drops at successive positive and negative current crests. By 14.3 μsec, the current crest had reduced to 15,600 amperes.

In 1930 Higham and Meek[2] investigated impulse currents in the range 60 to 500 amperes, that attained their peak values in about 1/4 μsec and decayed to half value in 10 or 28 μsec. Their work was carried out on spark gaps up to 40 cm in length. Fig. 2 taken from their paper is an oscillogram that shows the general nature of the voltage drop across the arc immediately after the spark has occurred and current begins to flow. From other data given in the paper it is deduced that this oscillogram probably applies to a 20-cm gap. In the range of currents covered by their investigations they found that the drop was independent of the current. For the higher currents the diameter of the arc channel increased to maintain the same current density. From the data for different decay times they estimated the drops that would result if the current increased to crest in 1/4 μsec and continued at crest value without decaying.

Paper 58-176, recommended by the AIEE Transmission and Distribution Committee and approved by the AIEE Technical Operations Department for presentation at the AIEE Winter General Meeting, New York, N. Y., February 2–7, 1958. Manuscript submitted October 10, 1957; made available for printing November 13, 1957.

C. F. Wagner, C. M. Lane, and C. M. Lear are with Westinghouse Electric Corporation, East Pittsburgh, Pa.

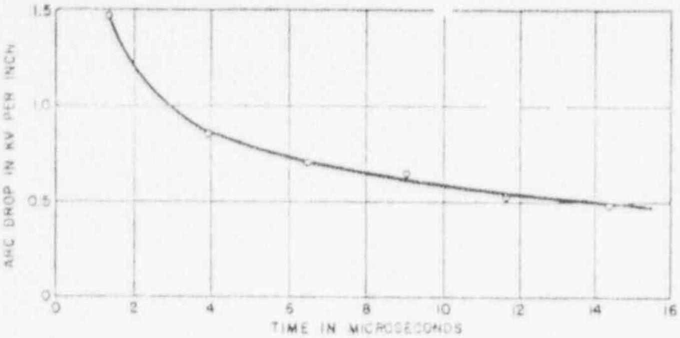

Fig. 1. Arc drop[1] at current crests of an oscillating current whose first crest is 26,000 amperes and whose period of oscillation is 5.2 μsec

These values, for air, are plotted in Fig. 3. Higham and Meek state that, "this curve may be expected to apply with reasonable accuracy to spark channels in air at atmospheric pressure when conducting unit function currents of magnitudes ranging from 50 to 1,000 amperes."

It is this curve that encouraged the authors to investigate the transient-voltage-drop characteristics of the impulse currents as a likely factor in determining the front and other characteristics of the stroke current. Higham and Meek also took into consideration the tortuous character of the arc path and showed that the total drop was proportional to the total arc path for gaps up to 40 cm in length. Tungsten electrodes were used and the electrode drop was about 100 volts.

More recently, Allen and Craggs[3] continued this work with currents up to 265 ka. Their currents were oscillatory reaching a crest in 7.7 μsec. The maximum length of their gap was 7 millimeters. Because of the inductive drop in the measuring circuit they report voltage gradients only at the instant at which the rate of change of current is zero. For air the voltage gradient at 188 ka is 180 volts per cm and for 265 ka, 360 volts per cm.

There thus remains an area of currents in the order of tens of thousands of crest amperes rising to crest in the order of several μsec that remains to be investigated.

Considerable data are available regarding the diameter of the arc channel under transient conditions. Higham and Meek[4] have measured the diameter during the first 12 μsec following the development of impulse currents that rise to crest in 1/4 μsec. Fig. 4 is typical of their data and applies to currents from 150 to 500 amperes that decay to half value in 9 μsec. The values were obtained photographically by means of a rotating-mirror technique.

Allen and Craggs[3] by a similar method determined that for a current that rose from zero to a crest of 188,000 amperes in 7.7 μsec as a sinusoid, the channel radius increased almost uniformly during this time, and at 7.7 μsec attained a radius of 1.25 cm. The radius of the core at the same instant was 0.95 cm. These arcs were in air at atmospheric pressure.

Apparatus

The test setup used in this investigation is shown schematically in Fig. 5. From one to five 100-kv 0.25-microfarad capacitors were connected in parallel and charged through high resistances from a source of d-c potential. Two gaps, a "tripping" or "external" gap, and a "test" gap, were connected in series with a current-measuring shunt and placed directly across the terminals of the capacitor. The electrodes B and C forming the test gap were made of 0.125-inch tungsten rods and electrode A of copper rod. Current was measured by taking the drop across the shunt to the oscillograph through coaxial cable.

Anticipating voltages as high as 30 or 40 kv across the test gap before breakdown, then to measure arc drops as low as 1 kv with a satisfactory accuracy, required a special technique for the measurement of the voltage. A scheme similar to that used by Higham and Meek[2] was used. As shown in Fig. 5, a nonlinear shunt parallels a 100-ohm resistor and the 52-ohm coaxial cable to the oscillograph. A 1,600-ohn resistor is in series with the parallel combination. For low voltages the nonlinear resistor has a high resistance, but for high voltages its resistance is low. The resultant calibration is shown in Fig. 6.

It was found that a considerable voltage was induced in unavoidable loops of the voltage-measuring circuit by the heavy currents in its vicinity. This voltage was almost completely neutralized by placing a compensating coil in each of the loops of the voltage-measuring circuit. These consisted of coils mounted on rods that could be turned until a minimum deflection of the voltage element was obtained with electrode C moved inward to short circuit the test gap. To ensure that good contact was made, a small brass sleeve with two clamping screws was fastened across the gap.

To a large extent the external gap determined the current obtained since this controlled the voltage to which the capacitors would rise before discharging. The proportions of the external gap to test gap could be varied only within relatively small limits. To increase the current that

90004140

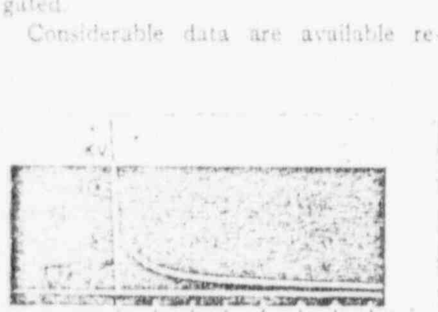

Fig. 2. Oscillogram[2] of voltage drop across spark channel. Authors state that the original oscillogram shows a clearly defined trace above 10 kv

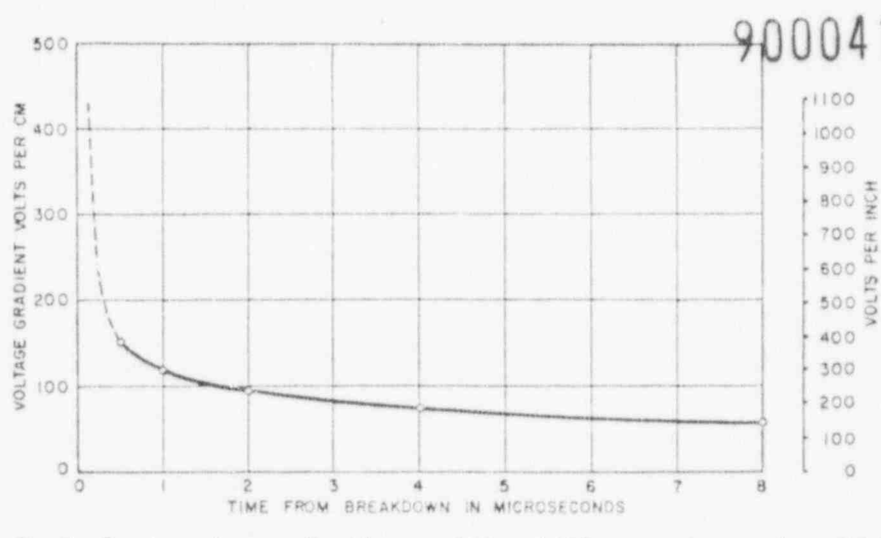

Fig. 3. Transient voltage gradient[1] for arcs of 50 to 1,000 amperes having a front of 1/4 μsec and a flat top

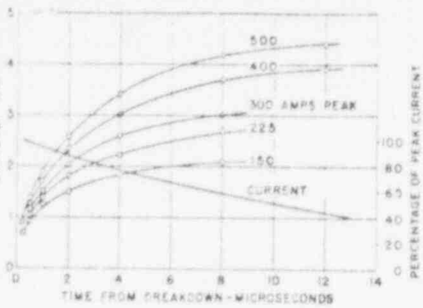

Fig. 4. Diameter of arcs[4]

could be obtained for small values of the test gap (1/2 inch), an auxiliary electrode shown by the dashed line in Fig. 5 was inserted in the circuit. The resistance across this gap approximated that across the test gap. This permitted an artificial increase of the test gap without disturbing the voltage measurements across the small gap.

The shortest time for the current to reach crest, 1.2 μsec, was attained when the capacitors were discharged with no external inductance. The time to crest was increased, but at the cost of decreasing the crest current, by inserting an inductance (3.3 or 9.4 millihenrys) as shown by the dashed lines.

Measuring Technique

For preliminary observations, the oscillograph was tripped by means of a probe located near the high-voltage electrode. In this way tripping occurred in the early stages of breakdown of the external gap. Only a very small element of the voltage record was lost and the entire sequence of events of breakdown became evident. Fig. 7(A) is an oscillogram of the voltage across the test gap, obtained by tripping in this manner. As the capacitors became charged, the voltage across their terminals increased slowly until the external gap broke down and the oscillograph tripped. Prior to breakdown of the test gap the current through the external gap is limited by the resistance in the voltage-metering circuit. These predischarge currents are of the order of 50 amperes, depending upon the setting of the external gap. As illustrated by Fig. 2, the voltage across the gap does not decrease to zero instantly. The time required for the decrease in voltage of the external gap is reflected in the time required for the voltage across the test gap to build up, which requires a fraction of a μsec. After this interval, substantially all of the capacitor voltage is applied across the test gap which also requires a small time to break down. With the breakdown of the test gap, a similar phenomenon occurs in both gaps, the current in the test gap increases from substantially zero (neglecting the preionization currents) and the current in the external gap increases from about 50 amperes, both currents increasing to the current determined by the rate at which charge on the capacitors can discharge into the inductance of the circuit, which is controlled largely by the internal inductance of the capacitors. From this instant the voltage across the test gap describes the characteristics of the test-gap arc as the current through it increases in response to the circuit parameters. The deflection of the oscillogram is not, of course, proportional to the voltage but includes the effect of the nonlinear calibration of Fig. 6.

The voltage across the current shunt is shown in Fig. 7(B) with the sudden, almost vertical, trace lined up to correspond to the instant of breakdown of the test gap. Prior to this instant the indication is zero, which corresponds to the 50 amperes to which the resistance of the voltage circuit limits the current. The vertical trace represents the inductive drop of the shunt, an observation that was subsequently checked by other measurements. Limitations in available laboratory time did not permit of the construction of a more accurate shunt.

Except for about the first 0.1 μsec the arc voltages of the test and trip gaps should not influence the waveshape of the current appreciably. To eliminate the inductive error of the current shunt it was assumed that the current was sinusoidal. From the actual record the crest value and the time to crest of the assumed sinusoidal current were calculated. The crest value and time to crest (quarter period) in μsec was indicated by the designation such as 32,300 amperes per 3.0 μsec.

Tripping by the method just described was found to be erratic. The trip circuit was transferred to the terminals of the current shunt so that the vertical rise which was always associated with the initial rise of current would provide positive tripping. At the same time about

Fig. 6 (right). Calibration curve for voltage element

Fig. 5 (below). Schematic diagram of apparatus

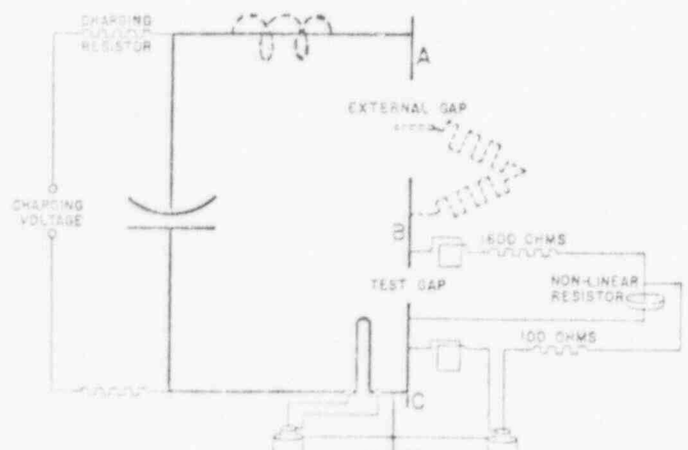

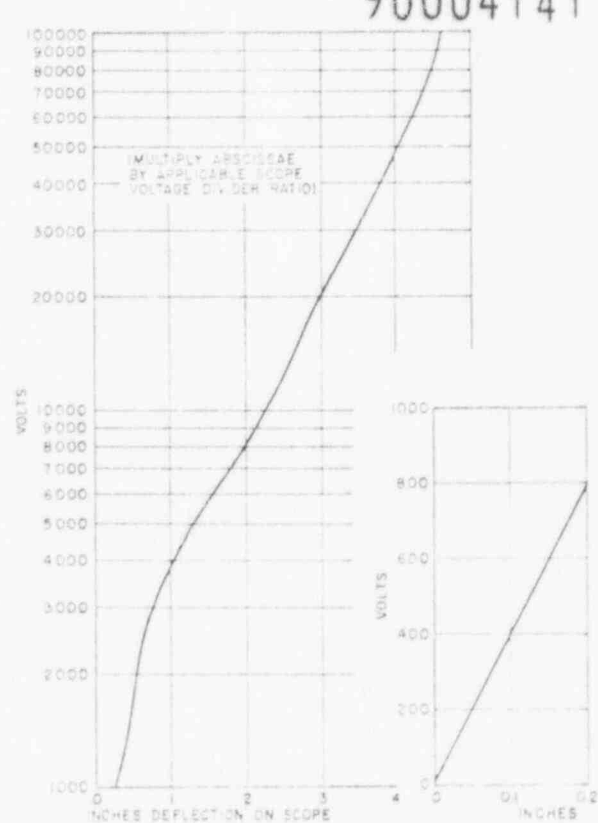

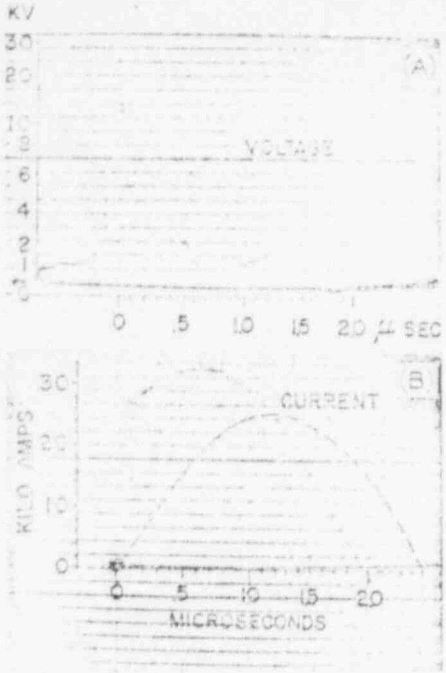

Fig. 7 (left). Oscillograms

A—Voltage drop across the arc

B—Current through the arc

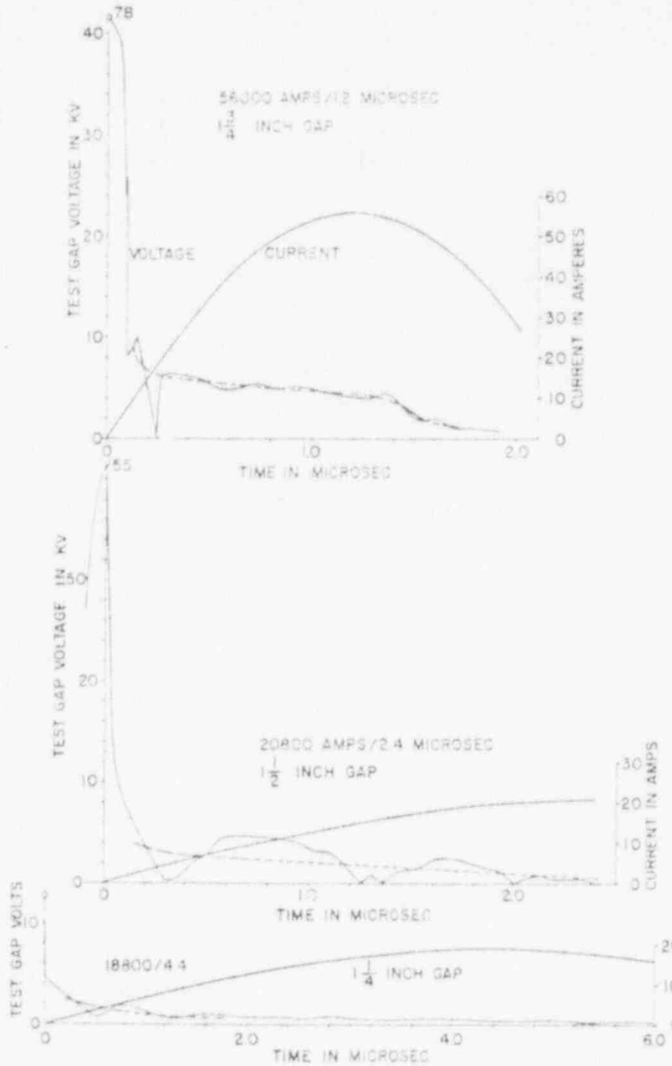

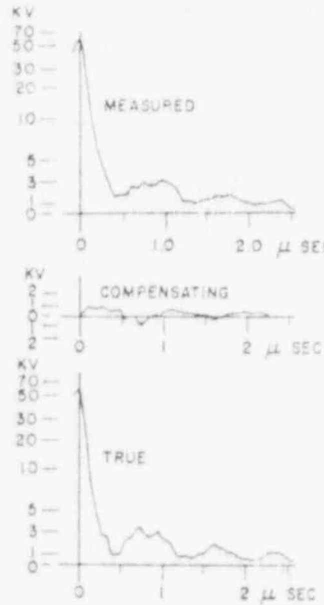

Fig. 8 (left). Replots of typical oscillograms showing measured drop, compensating voltage, and difference

Fig. 9 (right). Variation of arc with time for three typical conditions

90004142

100 feet of delay cable was inserted in the coaxial cable to the voltage plates which introduced sufficient delay so that a small element of the voltage just prior to the gap breakdown was included in the oscillogram.

For each setting of the gaps, several records of the compensated voltage (voltage across the short-circuited test gap), the voltage across the test gap, and the current were made. The records were found to be sufficiently repetitive. Fig. 8 is illustrative of the results obtained. These are replots of the oscillograms for a 32,300-ampere-per-3.0-current wave. The upper oscillogram is the record of the measured voltage across the 1.5-inch test gap. The middle oscillogram is the record of the compensating voltage, the voltage obtained with the test gap short-circuited to measure the remanent induced voltage in the measuring circuit. Subtracting the compensation values from the upper curve provides the true arc voltage plotted by the bottom curve. As will be seen from subsequent records, the oscillation in the voltage record is affected to some degree by the amount of inductance in the discharge circuit. The actual voltage was taken as the smooth curve through the bottom curve. Doubtless also some error exists in the record for times less than 0.2 μsec.

Results

Typical arc-drop and current curves are shown in Fig. 9 for the three external inductances used in the tests. The top illustration in Fig. 9 is for the maximum current and shortest time, the current in this case attaining maximum is 1.2 μsec. The current the middle illustration attains its crest in 2.4 μsec, and for the bottom one in 4.4 μsec. Summaries of the results are shown in Fig. 10(A) and (B): (A) being for an external inductance of zero, and (B) for 3.3 microhenrys. The voltage across the arc decreases very rapidly for the first few tenths of a μsec. In Fig. 10(A) it can be observed that this effect is quite erratic. Doubtless part of the lag in approaching a low voltage can be attributed to a lag in the measurement circuit, but a portion must represent an actual time required for the channel to become conducting. If the lag were simply a measurement error one would expect a greater consistency. Perhaps a portion of the inconsistency can be attributed to the sharp rise in voltage prior to actual breakdown. It was found in selecting the relative lengths of test and external gaps that no great variation was permissible. The desired current is set by the external gap. Then if the test gap is too small breakdown occurs in the rising front of the wave, and if too small breakdown does not take place at all. In general, a ratio of about one to two was

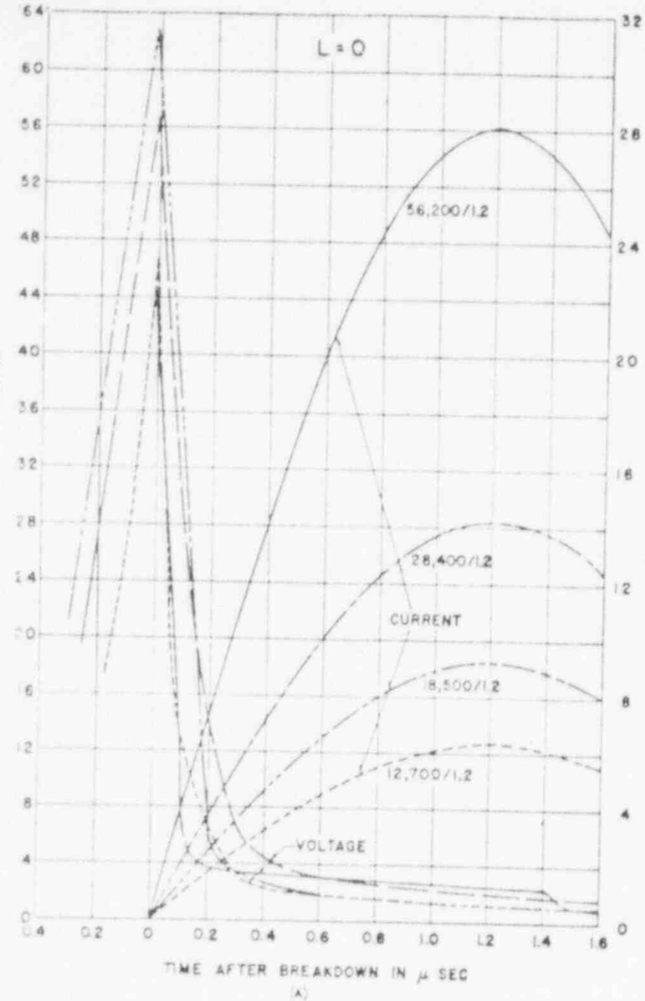

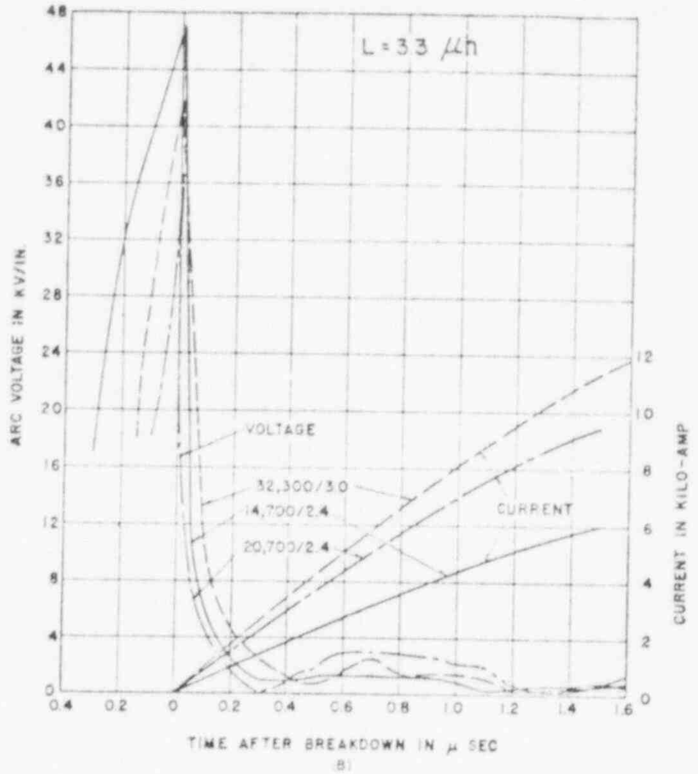

Fig. 10. Summary of arc drop as a function of time and crest current

A—Zero external inductance

B—3.3-microhenry external inductance

maintained between the test and external gap. Perhaps a somewhat smaller ratio would have developed more consistent results.

Averaging the observed results in a manner indicated by the dashed lines of Fig. 9, the curves of Fig. 11 were prepared which show the voltage gradient along the arc at different instants as a function of current. In plotting the abscissa it was assumed for any given instant that the current increases linearly with time up to that instant, and that the average value of the actual current and the average value of the assumed linear relation were the same. The crest value of the linear relation was then plotted as the current. The effect of high rates of rise of current is shown clearly. At 20,000 amperes, the gradient is eight times as great if the full value is attained in 0.25 μsec than if attained in 4.0 μsec.

For comparison purposes a point from previous work by Norinder and Karsten[1] is included. For this case the voltage is given at the first peak of an oscillatory current, the crest of which was 26,000 amperes and the time to crest was 1.3 μsec. The same kind of averaging was applied to this point. The values obtained by the authors are somewhat higher than those reported by Norinder and Karsten.

Using the curves of Fig. 11 as a basis, the gradient curves of Fig. 12 were plotted to illustrate more clearly than Fig. 9 the effect of changing the wavefront, maintaining at the same time the same crest value of 30,000 amperes. The curves are plotted for the period during which the currents continue to increase.

The limits of the available facilities prevented collection of data for currents of high magnitude with flat tops. The data by Higham and Meek for which Fig. 2 is typical shows a rather rapid decrement in voltage drop to 72 volts per cm at 4 μsec. After this there is a further gradual drop to 35 volts per cm at 24 μsec. A similar phenomenon probably occurs at the higher currents studied in this investigation. At the instant of flattening of the current the voltage drop probably decreases slowly and by 30 to 100 μsec reaches a steady

90004143

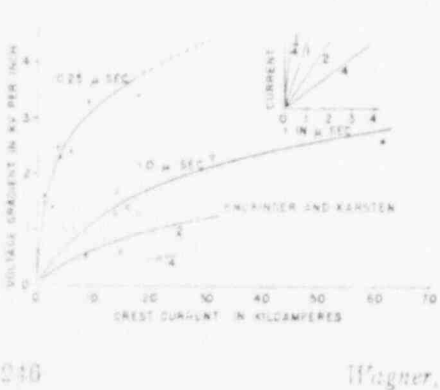

Fig. 11 (left). Voltage gradient of arcs. For each curve it is assumed that the current increased linearly with time up to the time indicated on each curve

Fig. 12 (right). Gradient-time curves for current increasing linearly to crest of 30,000 amperes at times indicated on the curves

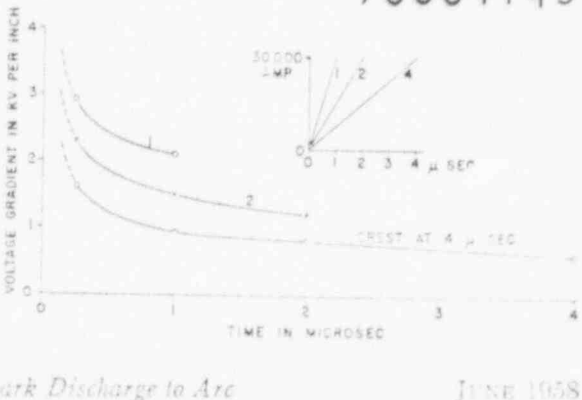

value of about 50 volts per inch. Strom[5] obtained for 60-cycle arcs in air a drop of 40 volts per inch for a current of 14,000 crest amperes.

Conclusions

1. Oscillatory current discharges have been obtained from capacitors that have a crest up to 56,000 amperes. The maximum current of 56,000 amperes reached crest in 1.2 μsec. Lower currents were obtained with longer times to crest.

2. The initial discharge was accompanied by a very high voltage drop having a duration of about 0.2 μsec that might be of the order of 20 to 40 kv per inch.

3. The initial high drop is followed by a longer duration but still high drop of the order of 1 to 4 kv per inch. This drop increases with the steepness and with the magnitude of the current crest.

4. The primary purpose of these tests was to determine whether the transient voltage drop of high-current arcs might be of significance in determining the characteristics of the lightning-stroke currents. If one were to consider an arc gradient of, e.g., 3.0 kv per inch, then an arc length of 100 feet would possess a drop of 3,600,000 volts. Since the stroke potential has been estimated at from 1 to 5×10^7 volts, it would not require many 100-foot lengths to have a very significant effect upon the characteristics.

This much has been demonstrated. It would be desirable if this work were continued under more carefully controlled conditions and over a greater range of the parameters.

References

1. Experimental Investigations of Resistance and Power Within Artificial Lightning Current Paths, H. Norinder, O. Karsten. *Arkiv för Matematik, Astronomi och Fysik*, Stockholm, Sweden, band 36A, no. 16, 1949, pp. 1–48.

2. Voltage Gradients in Long Gaseous Spark Channels, J. B. Higham, J. M. Meek. *Proceedings*, Physical Society, London, England, vol. 63, pt. 9, no. 369B, Sept. 1950.

3. High Current Spark Channels, J. E. Allen, J. D. Craggs. *British Journal of Applied Physics*, London, England, vol. 5, Dec. 1954, pp. 446–53.

4. The Expansion of Gaseous Spark Channels, J. B. Higham, J. M. Meek. *Proceedings*, Physical Society, vol. 63, pt. 9-B, Sept. 1950, pp. 649–61.

5. Long 60-Cycle Arcs in Air, A. P. Strom. *AIEE Transactions*, vol. 65, Mar. 1946, pp. 113–18.

90004144

Electromagnetic Field Phenomena in Shielded Aerial Cables Under Surge Conditions

J. K. DELSON
ASSOCIATE MEMBER AIEE

WHEN shielded aerial cable is surrounded by a coaxial shield, the shield may be of metal ribbon and be applied in the form of a helix. See Fig. 1. If the shield ribbon is wound with an intercalated insulation so that the turns do not touch each other, the current path in the shield would necessarily be along the helix formed by the conductor. On the other hand, if the individual turns of the insulation were not intercalated, but rather allowed to overlap in the manner shown in Fig. 1, the current path having least resistance would be neither strictly along the ribbon nor along the straight path of the cable shield in the axial or z-direction, both would be somewhere between these two extremes. Thus the current path in the shield would be in the form of a helix the pitch angle of which would be greater than that of the helix formed by the construction of the shield, but less than 90 degrees, angular measure, which corresponds to flow in the axial or z-direction.

If it is assumed that the currents in the shield follow the path of least resistance, as discussed above, namely a helical path of pitch angle ψ, the spiraling flow of the shield currents should affect the performance of the cable by increasing the inductance of the cable over the value of inductance expected for a cable in which the shield currents did not spiral, such as in an extruded-lead sheath. This effect has been postulated in a study by Van Wormer, Schultz, and Lee.[1] These authors allowed for an increase in inductance which would correspond to the spiraling of the shield current, and thereby increase the value of surge impedance of the cable while decreasing the velocity of wave propagation. The authors also carried out measurements, which they compared with their theory. The cable measured was of the type illustrated in Fig. 1, and was made up of an inner conductor, the adjacent insulating material, the shield and a jacket, and the messenger and binder. In addition to waves propagating between the inner conductor and shield of the cable, waves attributed to the presence of the messenger and binder were also observed. The waves each traveled at individual velocities and were coupled to each other, and at points of reflection complex waveforms of current and voltage resulted. In a discussion of this study, observations on the cable were compared with an analysis based on electromagnetic field concepts.[2] This analysis omitted the influence of the messenger and binder, and the resulting multivelocity waves, it concentrated instead on the influence which the helical shield construction has on the principal waves propagated. The analysis corresponded, therefore, to the case in which the messenger and binder were grounded continuously to the shield. In the observations made on the case where the messenger and binder were grounded at periodic intervals to the shield, the surge impedance and velocity of wave propagation agreed with the values from the analysis of electromagnetic fields for a pitch angle in the range of 45 degrees to 50 degrees.[1,2] This value of pitch angle appears quite reasonable, serving as a check between theory and observation. The purpose of this paper is to present the details of the analysis referred to, paying particular attention to those components of electric field intensity which arise in the cable in the presence of shield current flowing in a helical path.

The mathematical analysis is presented in the Appendix. Here, the cable is understood to be made of an inner, cylindrical conductor (assumed to be smooth-surfaced), covered with an insulating dielectric, which in turn is wrapped helically with a metallic ribbon to form the outer conductor or shield. The boundary conditions, used in the analysis to describe the flow of currents in the shield, are the same as those

Paper 58-76, recommended by the AIEE Insulated Conductors Committee and approved by the AIEE Technical Operations Department for presentation at the AIEE Winter General Meeting, New York, N. Y., February 2–7, 1958. Manuscript submitted October 14, 1957; made available for printing December 18, 1957.

J. K. Delson is with the General Electric Company, Schenectady, N. Y.

REF. 15

Lightning and Transmission Lines

by C. F. WAGNER

Westinghouse Electric Corporation
East Pittsburgh, Pennsylvania

Introduction

The phenomenon of natural lightning is of interest to a wide range of workers in varied disciplines, among them are the meteorologist, the physicist, the radio engineer and the power transmission engineer. It has become increasingly difficult to follow the research that is currently in progress in all of these fields. The power transmission engineer limits his attention largely to aggregate or terminal effects and, in consonance with his knowledge of the equipment which he must protect, attempts to understand and explain the lightning stroke by analogy with the corona characteristics and breakdown characteristics of rod gaps and parallel conductors.

The engineer often does not possess the luxury to await complete information on a particular problem before attempting its solution. Lightning protection of transmission and distribution lines is one such case where he must speculate upon the problem of the nature of stroke characteristics. To this background, the present structure of the stroke and its application are submitted.

First Component

During the process of charge separation, charge of one polarity may form in a volume distribution within the cloud while charge of the opposite polarity is carried to earth. Or with charge cells of opposite polarities within a cloud separated great distances, the earth can form a neutral plane upon which charges are separated by induction. In either event, for the purpose of this discussion it will be assumed that a negative volume distribution of charge exists in the cloud and a corresponding charge of positive polarity exists on the earth. By a process not within the scope of this article an incipient spark develops within the cloud and initiates a leader that travels earthward. We omit a detailed discussion of the characteristics of these leaders, which propagate in a stepped fashion to earth, since this information may be found elsewhere (**1**–**6**).

According to Schonland (**1**, **2**) the lengths of the steps vary between 10 and 80 meters with a modal value of 50 meters or 150 feet. The time between steps is about 50 microseconds (**1**, **2**), but as the leader approaches the earth the interval decreases to about 13 microseconds (**7**). As a result of field measurements Schonland concluded very early that the current in the steps is less than

10 per cent of that
in structure and h
like an inverted t
For this analysis,
charge vertical to
core of relatively
carried from point
tivity to accommo
of arc-like charac
axis. This central

The potential
illustration, we wi
stroke impinges u

Udo (**8**) has s
sparkover voltage
about 500,000 vol
leader comes with
discharge changes

In the particul
the downward le
this is the point
will eventually
crimination."
virgin
leader
the leade
before this po
ward leader m
tower, and the s
streamers are on
external to the di
The ensuing disc
broken down by
tributed along th
the nature of the
mediately availab

If the downwa
distributed, the c
with which a wav
the impedance off
be about 300 ohm
can be more prop
tens or hundreds
suddenly increase
This may be view

90004145

10 per cent of that in the main return stroke. Actually, the leader is complicated in structure and has many branches emanating from the central member, much like an inverted tree. Each branch has charges deposited along its members. For this analysis, the leader is assumed to be a straight cylinder of negative charge vertical to the earth. The cylinder of charge presumably has a central core of relatively high conductivity as the charge for each advance must be carried from points higher up to the head of the leader. The necessary conductivity to accommodate the current involved can only be achieved by a discharge of arc-like character. Such discharge possesses a low voltage gradient along the axis. This central core will be called the "channel of the downward leader."

The potential of the downward leader varies from stroke to stroke, but for illustration, we will assume it to be 50,000,000 volts. It is also assumed that the stroke impinges upon a transmission tower so that rod-rod conditions apply.

Udo (8) has shown that for spacings between 3 and 8 meters the critical sparkover voltage is substantially linear with the length of gap and is equal to about 500,000 volts per meter (150 Kv per ft.). Therefore, when the tip of the leader comes within a distance of 50000/150 or 330 feet, the character of the discharge changes radically.

In the particular theory of the stroke we propose, this point in the path of the downward leader is important because with earth surface protuberances, this is the point from which discrimination is determined as to where the earth will eventually be struck. Thus, this point will be called the "point of discrimination." Prior to this instant the advance of the leader was projected into virgin air and the impedance of the discharge circuit for the advance of the leader tip involved both the surge impedance of the leader and the capacity of the leader head to earth. But from the point of discrimination, or perhaps just before this point is reached, some of the high resistance streamers of the downward leader meet similar streamers that extend upward from the stricken tower, and the series capacity no longer exists. At most, the currents in these streamers are only a few hundred amperes. From this instant, the impedance external to the discharge is simply the surge impedance of the downward leader. The ensuing discharge should be similar to that in any other long gap being broken down by a surge generator, except that the generator charge is distributed along the vertical leader. However, a further limitation is imposed by the nature of the stroke. The charge along the length of the leader is not immediately available to the discharge for the following reasons:

If the downward leader were a metallic conductor along which the charge is distributed, the charge would be available for discharge to earth at the velocity with which a wave could travel upward with the velocity of light. In this case the impedance offered to the flow of current from the vertical conductor would be about 300 ohms. For the present case, the channel of the downward leader can be more properly approximated by an arc that had been carrying a few tens or hundreds of amperes. It is the property of an arc that as its current is suddenly increased the voltage gradient along its axis increases for a short time. This may be viewed as a means of supplying the greater internal energy required to produce the greater conductivity of the arc for higher currents. As a consequence of the high temporary gradient along the channel, the charge in the downward leader becomes available at a slower rate; this effect is reflected by the slower velocity of the head of the return streamer which travels at a velocity of between 0.1 and 0.3 that of light. This effect discussed by the author in 1962 (**9**) showed that the observed relation between stroke current and velocity of the return stroke was matched closely by an analytical relation based upon the energy required to establish an arc. The degree of conformance is shown in Fig. 1 and is better than expected for the data available. It should not be

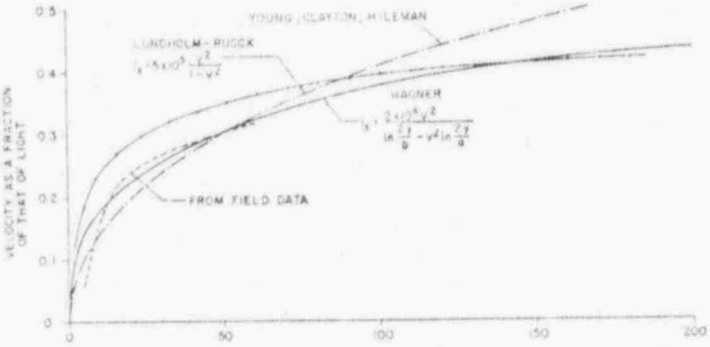

Fig. 1. Relations between stroke current and velocity of return stroke.

accepted as the degree of precision in either the analytical expression or the field data.

Prior to the Wagner development, a similar relation was presented by Lundholm (**10, 11**) in 1957 in which he related the resistance obtained from traveling wave theory to the resistance of an electric discharge, obtained empirically by Toepler (**12**), which stated that the resistance is inversely proportional to the charge passing a particular point. The Lundholm relation is also shown in Fig. 1.

The period of the temporary high gradient is very short. Tests made by the author (**13**) indicate a time less than a microsecond. Thus, except for this short interval, the return stroke constitutes a relatively good conductor whose head extends upward along the axis of the cylindrical charge constituting the downward leader. As it advances streamers must extend outward and upward, a sort of counter-corona that collects the charge originally deposited on and around the channel of the downward leader. If this collection process were neglected a heavy neutralizing charge, opposite in polarity to the downward leader, would be drawn from the earth by mutual capacitance coupling. Because of the low arc drop, the return channel being blazed up the channel of the downward leader is at substantially earth potential over its entire length. This condition requires that the leader charge be substantially neutralized by this coupling effect, estimates of which by Wagner and McCann (**14**) in 1942 indicated a 70 per cent neutralization.

It follows also
streamer the im
more likely aro
progress of the le
3,000 ohms from

We might loo
to anticipate the
of the downwar
only slightly gre
larger series resi
are available as
means for slowin

Fig. 2. Voltages acr
applied surges.

Figure 2 is a
rod–rod gap with
around the maxi
tions in the circu
termed the "non

90004147

It follows also that because of the slow velocity of propagation of the return streamer the impedance of the vertical leader, instead of being about 300, is more likely around 3,000 ohms. Therefore, the last 330 feet of the downward progress of the leader can be represented as being fed through a resistor of about 3,000 ohms from a capacitor charged to 50,000,000 volts.

We might look to the current that flows in a laboratory gap when impulsed to anticipate the nature of the lightning discharge. Because of the slow approach of the downward leader, the voltage applied to the laboratory gap should be only slightly greater than the minimum breakdown value and should have a larger series resistance than is normally used in commercial testing. Such data are available as the insertion of a high resistance in the circuit is a favorite means for slowing the process of breakdown to facilitate its study.

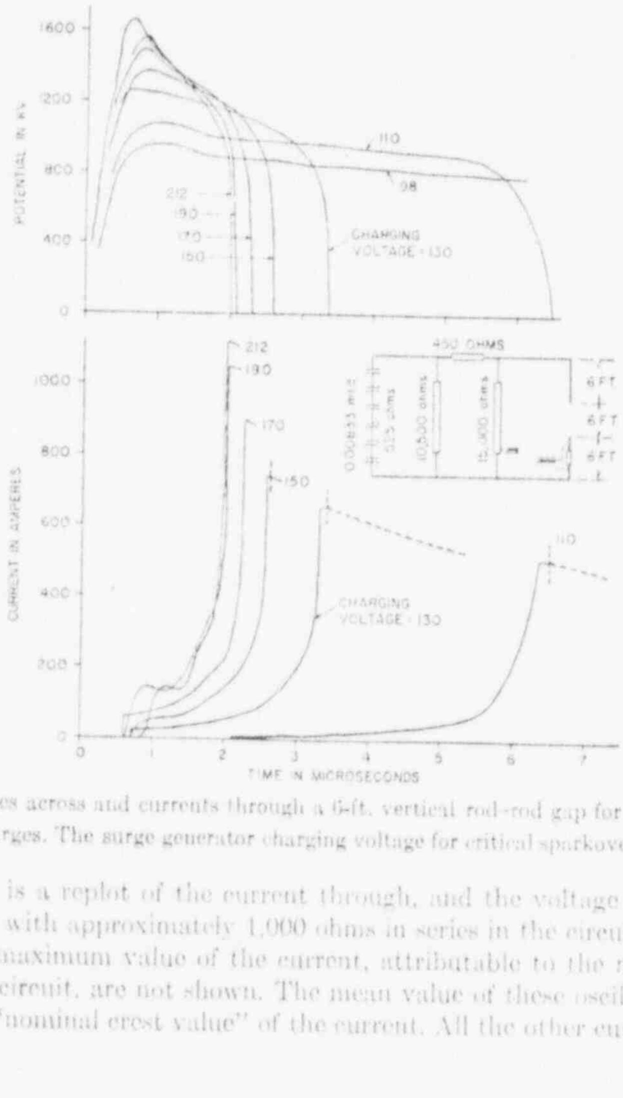

FIG. 2. Voltages across and currents through a 6-ft. vertical rod-rod gap for positive polarity applied surges. The surge generator charging voltage for critical sparkover is 98 volts.

Figure 2 is a replot of the current through, and the voltage across, a 6-ft. rod-rod gap with approximately 1,000 ohms in series in the circuit. Oscillations around the maximum value of the current, attributable to the natural oscillations in the circuit, are not shown. The mean value of these oscillations will be termed the "nominal crest value" of the current. All the other curves that have

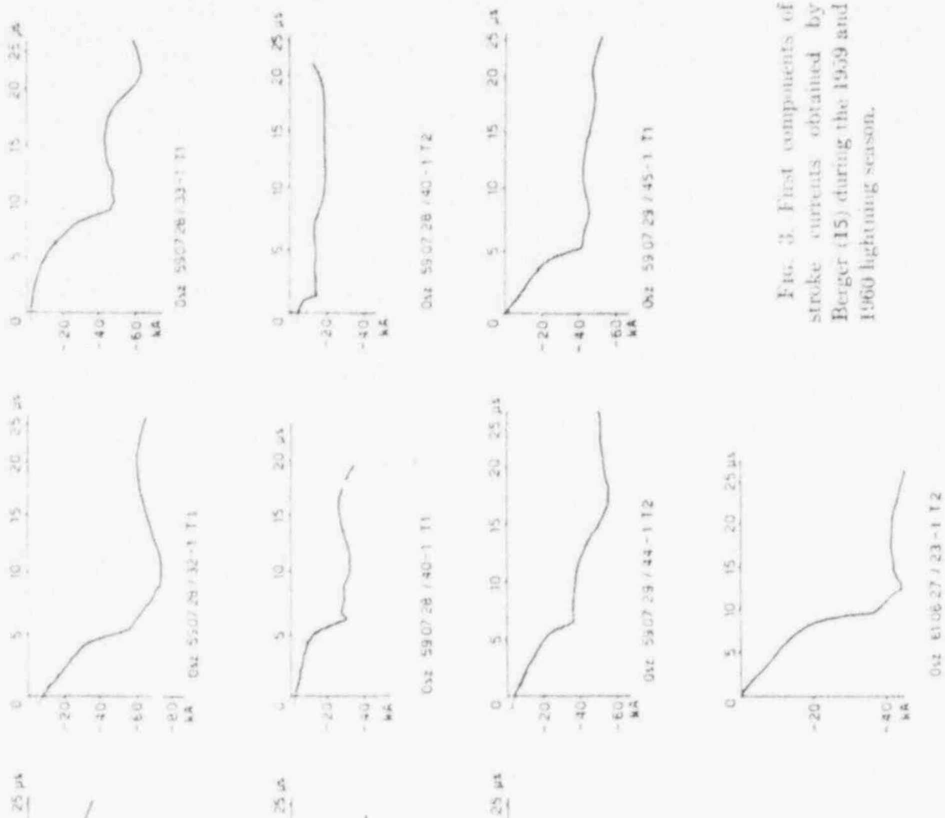

FIG. 3. First components of stroke currents obtained by Berger (15) during the 1959 and 1960 lightning season.

come to the au
characteristic. T
sistance and th

With this b
tained for act
component of
Note that all of
and that this c
cases a flattenin
crest current.

This discuss
depicted in Fig.
the channel of t

shows the posi
channel tip and
sheath has alre
later instant at
point of discrim
channel) tip an
active discharg
channels appro
number and int
impression of th
met; perhaps so
curred and the
Berger's curves
flatten out. Sub
due to the trigg
different branch

come to the author's attention possess this identical concave upward current characteristic. The time to crest may be extended by increasing both the resistance and the gap length.

With this background, comparison can be made with current records obtained for actual strokes. Figure 3 shows a number of such records of the first component of strokes obtained by Berger (**15**) atop Mount San Salvatore. Note that all of these records contain the same concave upward characteristic and that this concavity terminates with a sudden change of slope—in most cases a flattening out. This point in the laboratory corresponds to the nominal crest current.

This discussion thus leads to the model (**6**) of the first component of a stroke depicted in Fig. 4. The dotted lines indicate the corona sheaths that surround the channel of the downward leader and the mast next to the earth. Figure 4(a)

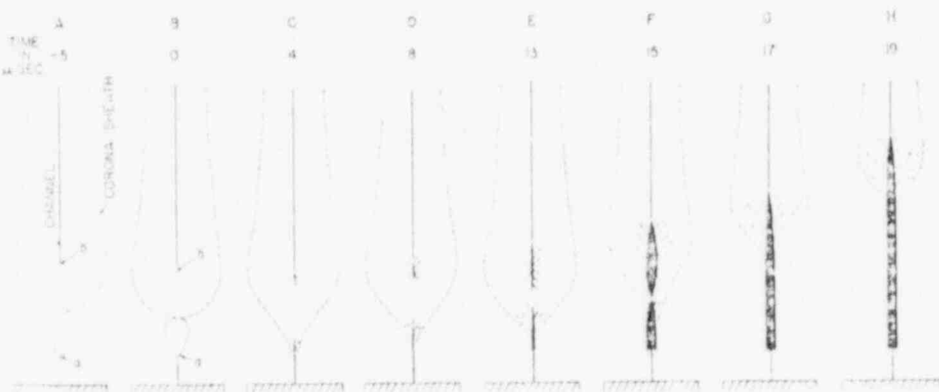

FIG. 4. Stages in the development of an upward channel.

shows the position of the downward leader channel when separation of the channel tip and mast still exceeds the minimum breakdown value. A corona sheath has already formed around the mast. Figure 4(b) shows a somewhat later instant at which the minimum breakdown position is attained. This is the point of discrimination. Channels begin to develop from both the leader (or channel) tip and the mast. By "channels" in this case we mean a thermally active discharge of high temperature and relatively good conductivity. The channels approach each other progressively and at the same time increase in number and intensity. The width of the heavy lines is intended to convey an impression of the current flowing at the instant. Finally at *G* the channels have met; perhaps some final stabilization of the channel voltage gradients has occurred and the breakdown process in the final gap is completed. This point in Berger's curves is where the upward concavity ceases and the current tends to flatten out. Subsequent fluctuations in current in Berger's records are probably due to the triggering of additional charge pockets as the return stroke reaches different branch points. Figure 5 shows more graphically the probable distribu-

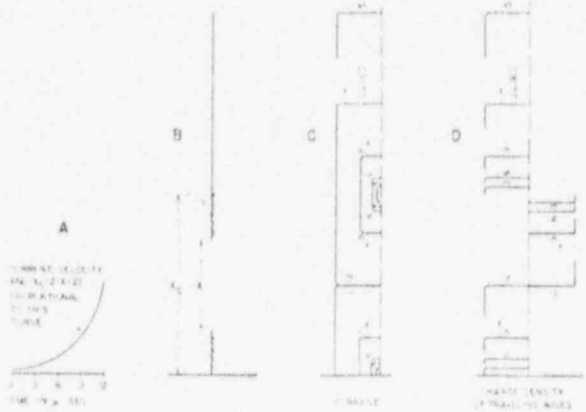

FIG. 5. Illustrating approximate length of unbridged gap of leader (B), current (C), and charge (D) resulting from assumption (A) regarding length of unbridged gap and current. Time is measured from instant of initiation of leaders of last step.

tion of current and charge resulting from the stroke (16). This model assumes that the transition of the current in the upward streamer occurs instantly, which is not the case. The high transitory voltage gradient in the arc as it accommodates itself to a condition of higher conductivity prevents an instantaneous rise in the current. The current in the return stroke should therefore be sloped to some extent.

The sketch reproduced in Fig. 6 shows the earth terminal of a stroke which occurred on flat, bare country. It is a Boys' camera record taken by Malan and reproduced by Golde (17) in a discussion of upward leaders. Point x, about 50

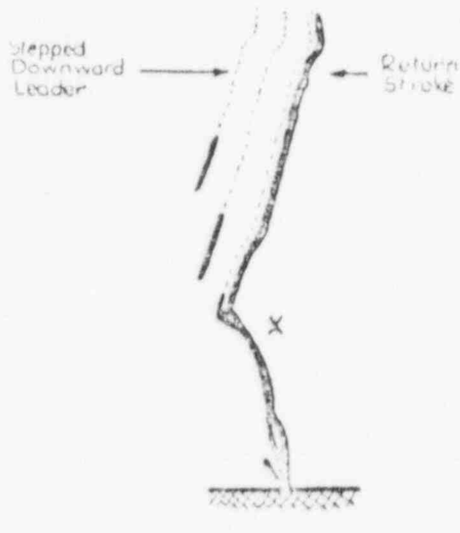

FIG. 6. Boys' camera photograph of stroke to ground (17).

meters above
terminated. It
character and
are clearly show

It should
records obtain
strokes to leve
Fig. 6, there s
data as typical
conditions at t
argument is ce
line.

In Fig. 7 is

FIG. 7. Oscillo

from a direct s
ing equipment
torted by prop
on a section of
vania Power a

meters above the earth, indicates where the downward leader (or channel) terminated. It is from this point that the downward and upward leaders change character and develop into the last big step. The lengths of the last few steps are clearly shown.

It should also be noted that some transmission engineers (18) discount records obtained on a tall mast atop a high hill as not typical of downward strokes to level ground or to low earthed objects. According to the stroke in Fig. 6, there should be no appreciable difference, and the author accepts the data as typical of strokes to transmission lines. It is frequently advanced that conditions at the earth end of a stroke correspond to those of a plane gap. This argument is certainly not applicable to strokes that terminate on a transmission line.

In Fig. 7 is shown the only oscillogram (to the author's knowledge) obtained

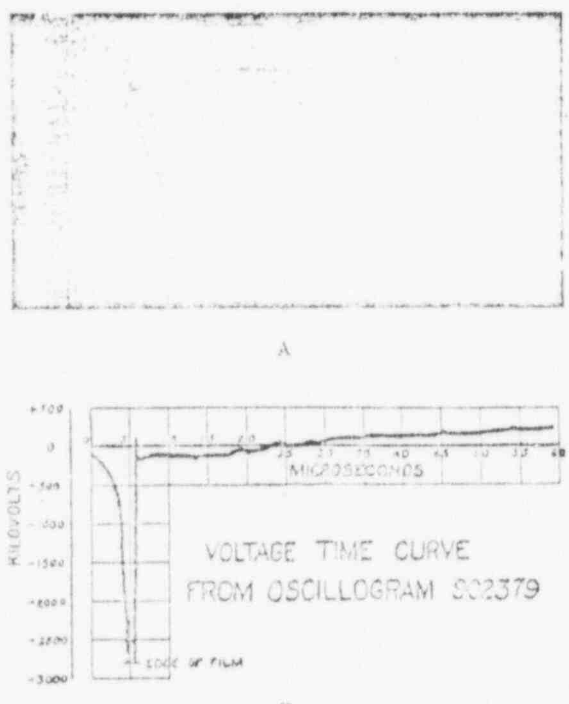

FIG. 7. Oscillogram of lightning surge voltage measured 125 feet from point struck (19).

from a direct stroke to a transmission line that was close enough to the recording equipment so that the wave shape of the voltage to ground was not distorted by propagation. This oscillogram was obtained by Bell and Price (19) on a section of 220-kv steel-tower line, without ground wires, of the Pennsylvania Power and Light Company. Flashover occurred 125 feet from the oscillo-

90004152

graph on the phase to which it was connected—an outer conductor of a horizontal single-circuit configuration. The insulation level of the line was about 1300 kv and the voltage reached 2800 kv before flashover took place. The interval between the time the voltage was high enough to operate the oscillograph and flashover occurred was about 6 microseconds. This record helps to support the contention that strokes to towers have the same upward concave character as do Berger's.

As observed by many investigators (**20**, **21**), most notably Berger (**22**, **23**, **15**), many strokes of negative polarity are of relatively small magnitude and long duration. These strokes are initiated from the earth and propagate upward. Berger, in his companion article (page 451), discusses this type of discharge in detail. But in the problem of lightning protection of transmission lines this type of stroke is of little significance. Berger (**23**) has also demonstrated more clearly than others that occasional positive strokes occur which are characterized by much higher values than conventional strokes but have slower rates of rise.

Subsequent Components

A lightning stroke (or flash) may consist of one or more components. As many as 42 have been recorded. All of the components take the same path as the return stroke of the first component. Compared to the average velocity of the leader of the first component, the leaders for subsequent components have very high velocities (about 0.03c) and are almost entirely free of steps, although

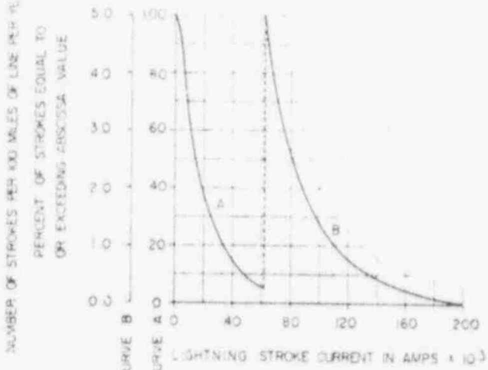

Fig. 8. Lightning stroke probability curve.

Kitagawa and Kobayashi (**7**) report very high frequency steps. These leaders are called "dart leaders" by Schonland (**1**, **2**). It is still regarded as controversial whether a significant current continues to flow down the path of the return stroke in the interval between components. McCann (**21**) states that for some strokes the current between components is less than 0.1 ampere, and Berger (**22**) also refers to the absence of current between components. McCann and Clarke (**24**) have suggested that time is required for the hot gases comprising the arc plasma to diffuse into the surrounding cooler air. This process involves the expansion of the small arc core into a progressively larger cylinder that gradually drops in temperature and density. Since a rarefied gas requires a lower voltage for breakdown it may be argued that a similar discrimination is active in the formation of dart leaders. If it is true, as with laboratory gaps, that the current increases with the approach velocity of the leaders as reported by Akopian, Larionov and Torosian (**25**), then the return current associated with subsequent components should rise more rapidly than the first component. While much of this argument is speculative, it is a fact, as recorded by Berger (**15**), that the front time of the return stroke currents is about 1.0 microsecond. The crest value of these currents is stated by Schonland to be less than those of the first component. Direct measurements by Berger have verified this statement.

Stroke Current Probability and Stroke Density

One of the most important criteria as to whether flashover of a transmission line insulator occurs, is the crest value of the stroke current. An enormous amount of data has been collected in this country and elsewhere, principally through the use of magnetic links. In 1950, after a study of the available information, the Lightning and Insulator Subcommittee of the *AIEE* (**26**) agreed that the curve shown in Fig. 8 is sufficiently representative to be used in determining the lightning performance of transmission lines. It shows the percentage of strokes that equal or exceed the values of current indicated by the abscissa. The minimum current considered in the preparation of this curve is 2400 amperes.

Stroke density is usually measured by the isokeraunic level, which is simply the number of days in the year that U.S. Weather Bureau attendants hear thunder at a particular location. In the U.S. the levels vary from substantially none to a high of 90 in western Florida. Based upon the actual number of strokes to a line, the *AIEE* Lightning and Insulator Subcommittee agreed that in a region where the isokeraunic level is 30, about 100 strokes occur for 100 miles per year. On this basis the curve of Fig. 8 also gives the number of strokes per 100 miles per year that exceed the abscissa. This corresponds roughly to between 10 and 15 strokes per square mile per year. Isokeraunic levels are a crude measure but they are the best indicators available to date. During the past few years a considerable amount of work has been done, notably in Europe and South Africa, in the development and installation of a "lightning counter" to measure the number of strokes that occurs in a given area. The more general use of this instrument should be of considerable value.

Surge Impedance and Potential of Stroke

To obtain a more precise method of computing the voltage across a string of insulators on a transmission line when the tower is struck by lightning, the author (**27**) derived expressions for the field around a rectangular wave of charge and current that elongates from a zero position with a constant velocity

90004154

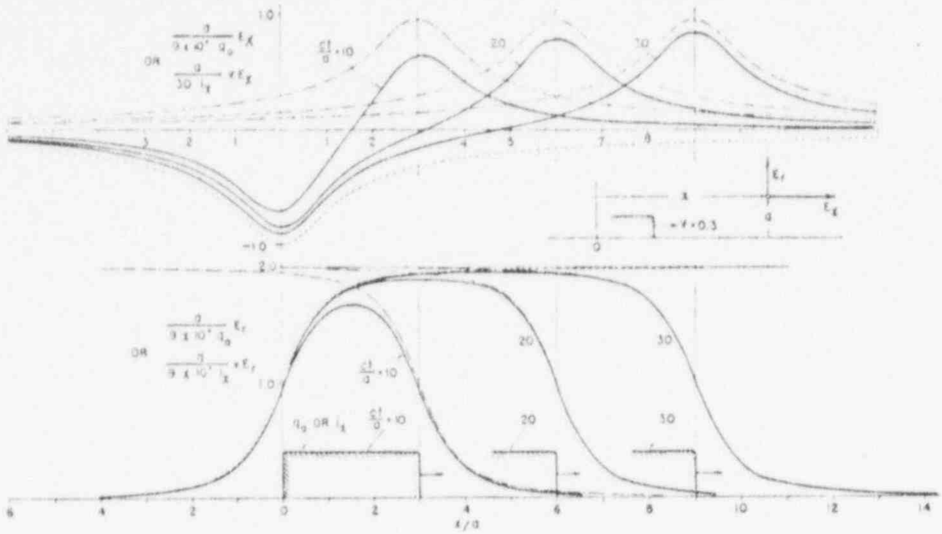

FIG. 9. Space distribution of fields, E_x and E_r, at different instants illustrating wave nature of electric fields produced by a square-front wave of charge and current originating at $x = 0$ and traveling with velocity v, expressed in terms of light, along x-axis.

v, expressed as a fraction of the velocity of light c. Figure 9 gives the values of such fields at a constant radius a from the geometric axis of propagation, where E_x is the component parallel to the axis and E_r the component perpendicular to the axis. The fundamental relations for this development are given in (**14**). As Fig. 9 shows, the values of fields for different instants are plotted as a function of x, the distance from the origin.

Through the device of a mirror image these relations can be used almost directly to determine the fields associated with a wave of constant magnitude and velocity that travels upward from a perfectly conducting earth. Integrating the vertical field at radius b gives the following approximate expression (**28, 29**)

$$V = 60i\,\frac{1}{v}\ln\frac{2D}{b} \qquad (1)$$

where V is the potential to point D. The symbol b in this case represents the radius at which the charge can be assumed to be concentrated, being different than the current radius because of corona. This expression can likewise be used to determine the current when a constant voltage is applied between a vertical conductor and the earth. For a more detailed discussion of this point see (**25**). With this as a basis, the values of V (the potential of the stroke) and the surge impedance to any point can be determined. For protection purposes we are interested in the length of stroke when the current has reached nominal crest value, as this determines the approximate surge impedance to use in connection with the current for fixing V. Taking D for this case as 300 feet the values indi-

i, an
D, f
b, f
v,
V,
Z,
Stri

cated in Table I w
to the values of th
From Eq. 1, th
stroke rises, which
the nominal crest is
also decreases with

Shielding of Tra

It has long been
lines is the installa
strokes. These are
is important beca
ing failure) nea
location has be
was done on

FIG. 10. Shielding
Young, Clayton an
fifteen 5¾ inch insula

90004155

TABLE I

i, amperes	50,000	10,000
D, feet	300	300
b, feet	6	2
v, a numeric	0.3	0.17
V, kv	46,000	20,000
Z, ohms	920	2,000
Striking distance, feet	310	135

cated in Table I were computed. These values serve to orient one with respect to the values of the stroke potential, V, and the surge impedance, Z.

From Eq. 1, the surge impedance is seen to increase as the head of the return stroke rises, which partially accounts for the decrease in stroke current after the nominal crest is reached. The charge density per unit length of leader channel also decreases with the leader height.

Shielding of Transmission Lines

It has long been accepted that the principal means for protecting transmission lines is the installation of wires above the conductors to shield them from direct strokes. These are usually called ground wires. The location of such conductors is important because failure of the ground wire to intercept the stroke (a shielding failure) nearly always results in flashover of the insulator string. Proper location has been the subject of much investigation. Some of the earliest work was done on simulated models (**30**). Another approach is purely geometric in

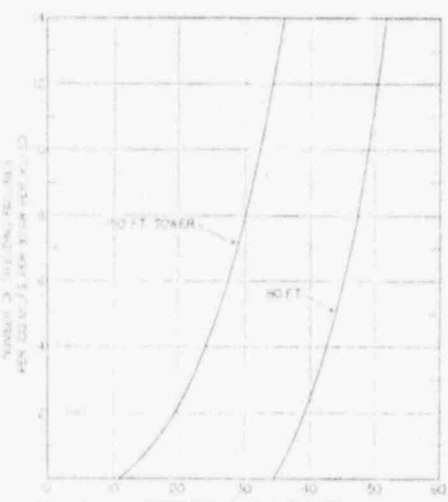

FIG. 10. Shielding failures according to Young, Clayton and Hileman (**31**), with fifteen $5\frac{3}{4}$ inch insulators.

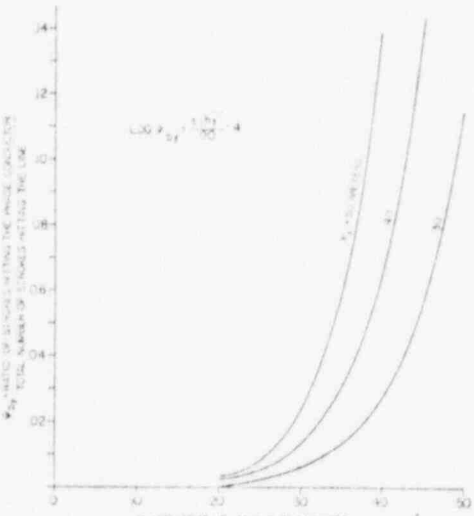

FIG. 11. Probability of shielding failures according to Kostenko, Polovoy, and Rosenfeld (**32**).

nature, but its application is dependent upon setting up a criterion to determine the location of what is called here the point of discrimination. A third approach involves an analysis of the actual outage performance of transmission lines and a discrimination as to what proportion is due to shielding failures. A detailed discussion of different methods is found in (**16**).

According to the stroke theory as enunciated here, the striking distance is equal to the stroke potential divided by the breakdown gradient per ft. of rod-rod gaps. The direction of leader propagation is influenced by the random field at its head, which produces the sudden changes in direction at each step, and by the directive field that controls its general direction. The latter sometimes produces rather bizarre effects. But according to this theory the path of the stroke above the point of discrimination is irrelevant. The assumption implies a uniform area distribution to a point just above this point. Young, Clayton and Hileman (**31**) have adopted this general approach but have made some modest changes in other assumptions: The principal one being in the relation between current and velocity, shown in Fig. 1, so that the results of their analysis match the presently available experience data on actual lines. The assumption was also made that the number of strokes per 100 miles per year for a ground wire height

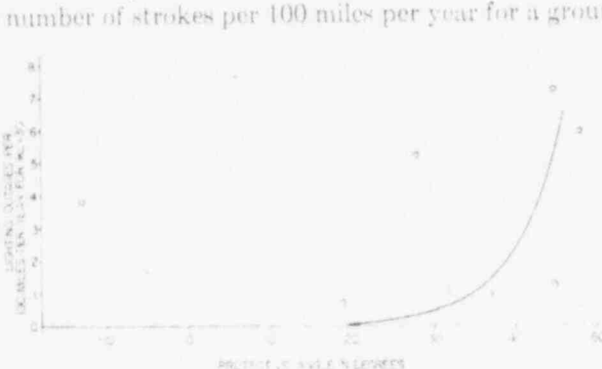

Fig. 12. Lightning outages as a function of protective angle (**30**) for 110 to 165 kv, with average tower-footing resistances less than 10 ohms.

of 100 feet in a region of isokeraunic level of 30 was 100. Figure 10, taken from their paper (**31**), illustrates the effect of protective angle (the angle made by a line drawn through either the outside or the upper conductor and the ground wire) and the height of the ground wire upon the number of shielding failures. Figure 11 shows similar curves from Kostenko, Polovoy and Rosenfeld (**32**) based upon subtracting computed back flashovers from actual performance to obtain the shielding failures. We have taken here the liberty of basing the performance on 100 strokes per 100 miles. It is also of interest to compare these curves with the curves in Fig. 12 presented by Wagner, McCann and MacLane (**30**) in 1941 based upon operating experience as reported by *AIEE* in 1938 for 110 to 165 kv lines for which the tower footing resistances were less than 10 ohms. It may be tacitly assumed that for this case all are shielding failures.

More recently, Armstrong and Whitehead (**33**) developed a device called the "Pathfinder" that is intended to distinguish, after flashover of a string of

insulators has oc
to a tower and g
provided a meth
used substantiall
the striking di
teristics inste
leader of the
approach of the
front voltage tha
breakdown occu
question arises a
steps, so the imp

Figures 10, 1
Fig. 10 is partly
better concept
shielding, protect
heights of 50, 10

Direct Strokes

An early exp
Fortescue (**35**),
Not Induced S
that time de
directly and
Maxim
indir

Fig. 13. S

this time, activi
was just being p
conducted; and t
Methods of comp
so that in 1950
committee prepa
Performance of
paper that had b
the general accep
principal element

90004157

insulators has occurred, between whether the stroke occurred to a conductor or to a tower and ground wire combination. Improvements in the device (**34**) also provided a method for computing the number of shielding failures. The method used substantially the same model for the stroke as given here but in computing the striking distance of the stroke it used switching surge breakdown characteristics instead of the impulse breakdown characteristics of a rod gap. If the leader of the initial component of a stroke is truly devoid of steps then the slow approach of the head would justify the breakdown characteristics of a slower front voltage than a 2 × 40 microsecond wave. At the front for which minimum breakdown occurs the breakdown value is less than the impulse value, but the question arises as to what front would apply. Actually, the leader advances in steps, so the impulse value might be as good as a switching surge value.

Figures 10, 11 and 12 are based upon actual operating experience, but since Fig. 10 is partly based upon the stroke model presented here, it provides a better concept of the principles involved. In resume, for essentially perfect shielding, protective angles of 45, 30 and 12 degrees are required for ground wire heights of 50, 100 and 150 feet, respectively.

Direct Strokes

An early exponent of the direct stroke theory of line protection was C. L. Fortescue (**35**), who, in 1930, introduced the idea in his article "Direct Strokes, Not Induced Surges, Chief Cause of High-Voltage Line Flashover." Prior to that time designers thought it highly improbable that lines would be struck directly and many believed it practically impossible to cope with direct strokes. Maximum coupling of the ground wire with phase conductors to protect against indirect strokes was the controlling criterion in locating the ground wire. About

FIG. 13. Schematic diagram of a single phase conductor and ground wire.

this time, activities in related fields took place: The cathode ray oscillograph was just being perfected; laboratory tests on insulators and gaps were being conducted; and the theory of transmission line performance was being refined. Methods of computation and confidence in the results had sufficiently advanced so that in 1950 a working group of the *AIEE* Lightning and Insulator Subcommittee prepared a report (**26**) on "A Method of Estimating Lightning Performance of Transmission Lines." This method was based largely upon a paper that had been presented earlier by Harder and Clayton (**36**). Because of the general acceptance of the *AIEE* method, a brief review will be given of its principal elements.

Figure 13 is a schematic diagram of a transmission line showing only one phase conductor. Assume that a stroke strikes a tower top. When this occurs the tower top rises in potential above the earth, carrying with it the arm supporting the insulator string. The first step is to compute this potential, and to this end the following assumptions are made:

1) *The crest value of the stroke current.*

2) *The wave shape of the stroke current.* A 2 × 40 microsecond wave shape was originally selected and for currents in excess of 30,000 to 40,000 amperes a 4 × 40 microsecond wave was chosen.

3) *The inductance and ground resistance of the towers.* The inductance was held constant at 20 microhenries for all cases and the tower footing was taken as a constant for any case, *i.e.*, it was not permitted to vary with time but held as one of the variables

4) *The span length.*

5) *Tower footing resistance.*

It was further assumed that the impedance of the tower and ground wires, and the tower footing resistance, would not affect the current forced into the tower

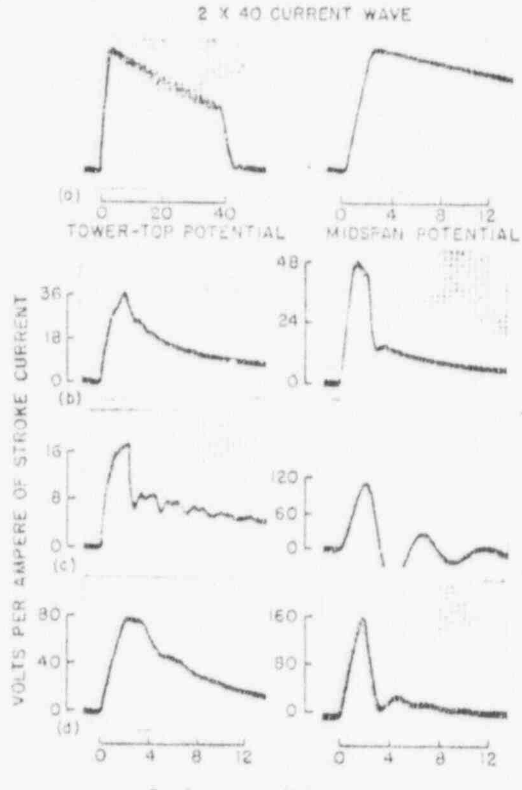

FIG. 14. Typical tower-top and midspan potentials (37) from Anacom study resulting from the introduction of a 2 × 40 current wave shown in (a) into the tower top. (b) 400-ft. span, 50 ohm tower-footing resistance; (c) 1000-ft. span, 10 ohm tower footing resistance; (d) 1000-ft. span, 100 ohm tower-footing resistance.

top. With these a
tower top potentia
determined with th
potential per unit
is the coupling fac
root of the electro
follows that the p
V_{ts} be designated
from standard time
ence time lags, and
then

where I is the crest
to the distribution
per 100 miles per y

Following such
in Fig. 15 for differe

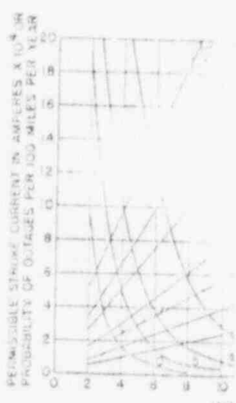

FIG. 15. Curve for
formance and insulatio
(26).

shows a comparison
published data with
Upon examining this
reflection it will be o
ance, probably resul
with high performan
was used as the towe

90004159

top. With these assumptions, applying the evolved methods of computations, tower top potentials and midspan potentials (37) such as shown in Fig. 14 were determined with the aid of an analog computer. Assigning the symbol P to this potential per unit stroke current, the potential of the conductor is CP, where C is the coupling factor between the ground wire and the conductor. The square root of the electrostatic and magnetic couplings was used for computing C. It follows that the potential across the insulator string is simply $(1 - C)P$. If V_{in} be designated the flashover voltage of the insulator string as determined from standard time lag curves for 1.5×40 microsecond waves at specified reference time lags, and k the time lag of an equivalent 1.5×40 microsecond wave, then

$$I = \frac{V_{in}k}{(1 - C)P} \tag{2}$$

where I is the crest current of the stroke that will cause flashover. Next, referring to the distribution curve of Fig. 8, it is possible to obtain the number of strokes per 100 miles per year that will cause flashover for an isokeraunic level of 30.

Following such procedure we can compute curves (26) such as those shown in Fig. 15 for different span lengths. Figure 16, taken from the Committee report,

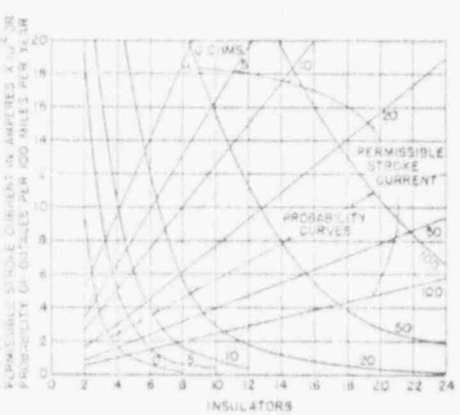

FIG. 15. Curve for estimating line performance and insulation for a 1200-ft. span (26).

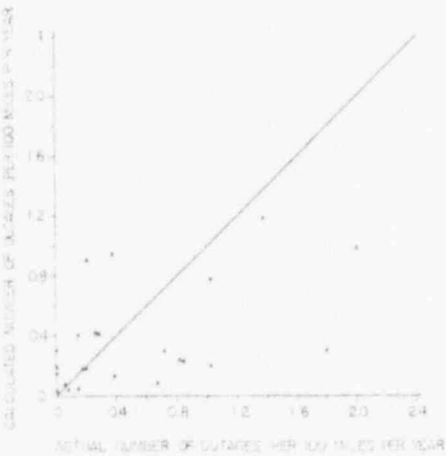

FIG. 16. Comparison of estimated performance with experience.

shows a comparison of performance of the transmission lines as taken from published data with calculated performance as determined by the *AIEE* method. Upon examining this comparison, the first impression is not favorable but upon reflection it will be observed that low estimates agree generally in low performance, probably resulting from low tower footing resistances and high estimates with high performance. The average resistance of all towers on a particular line was used as the tower resistance for computing the estimated performance. Had

90004160

actual resistances been used the comparison would presumably have been better.

The *AIEE* method applies only to systems of 230 kv and below. With the introduction of higher voltages some of the assumptions are no longer adequate. Clayton and Young (**38**) extended the method to apply to voltages ranging from 115 to 700 kv, and included the effect of 60 cycle voltage and the variation of ground wire height with voltage.

This review of the generally accepted methods of calculation has been sketchy but it is hoped that it has served to delineate the important elements in the analysis.

It is difficult to quarrel with success but in the light of more recent information some factors are questionable. Doubtless there are some counter-balancing effects in the simplified assumptions of the *AIEE* method. From the results of Berger (**15**), particularly, it is evident that the front of the wave is concave upward rather than that corresponding to a 4 × 40 microsecond wave. Just what the equivalent straight front wave would be is difficult to judge without calculations. It would seem also that the nominal crest value, *i.e.*, the value at which concavity ceases, would be more logical to use than the actual crests shown in Fig. 3. Furthermore, as will be discussed in greater detail later, the predischarge currents—the currents associated with the development of leaders—become very great between parallel conductors such as the ground wire and the conductors. This effect may explain the infrequency of midspan sparkovers mentioned in the Committee report and which prompted the Committee to favor a 4 microsecond front.

Indirect Strokes

In addition to shielding failures and back-flashes resulting from strokes to a ground wire, a third possibility of insulator flashover exists in the form of a sufficiently high voltage being induced by a stroke near the line that strikes neither a conductor nor a ground wire. The induced voltage is greater, the nearer the stroke is to the line, but for high-voltage lines—even for the stroke that just misses the line—the induced voltage is innocuous. For low-voltage lines, especially in the absence of ground wires, the insulation level may be so low that the induced voltages become important even for strokes a considerable distance from the line. Using substantially the same stroke mechanism as presented here, Wagner and McCann (**14**) studied this problem in 1942.

The basic mechanism of the stroke is divided into three distinct stages:

a) *Condition before the start of the discharge to earth.* A charge of $-Q_0 = -6.66$ coulombs was assumed concentrated at a point 2,000 meters or 6,560 feet above ground.

b) *First stage of lowering charge.* At the initiation of the discharge the charge, $-Q_0$, was lowered at a constant velocity of 1/20 or 1 percent of the velocity of light (or approximately 0.5 ft. per microsecond) so that a uniform charge of $q = -1.02 \times 10^{-3}$ coulombs per ft. was deposited along the downward leader

and the leader curr
this stage ended an
the ground was con

c) *Second st*
to rise from th
ously discharged
The current behind
length. For the co
I_s = 100,000 ampere

The electric gra
then calculated for
The gradient will h
instantaneous distri
tions change rapidly
recognize the finite
in space under con

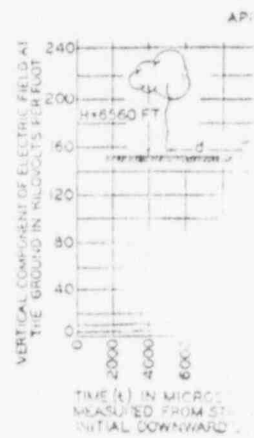

FIG. 17. Ground gradie
and distance from

retarded vector pot
ground gradient for
distances from the s
extended at the inst
18. Changing the ti
streamer, the right-
stage due to the ch
including the props

and the leader current was 500 amperes. When this leader reached the ground this stage ended and the return streamer was initiated. No upward leader from the ground was considered for the fundamental case.

c) *Second stage of lowering charge.* The return streamer was then assumed to rise from the ground at a uniform velocity of 1/10 that of light. It instantaneously discharged each section of the downward leader as that section was reached. The current behind the head of the return streamer was constant along its entire length. For the conditions assumed, this results in a return stroke current I_s = 100,000 amperes.

The electric gradient at any point P at a distance d from the stroke was then calculated for these three stages for the assumption of a perfect ground. The gradient will have only a vertical component; it can be computed from the instantaneous distribution of the charges and currents. When these distributions change rapidly, using the velocity of light as a criterion, it is necessary to recognize the finite time required for the disturbance to propagate to the point in space under consideration by using the retarded charge potential and the

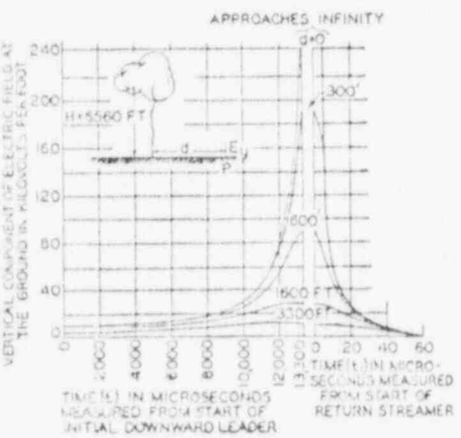

Fig. 17. Ground gradient as function of time and distance from stroke channel.

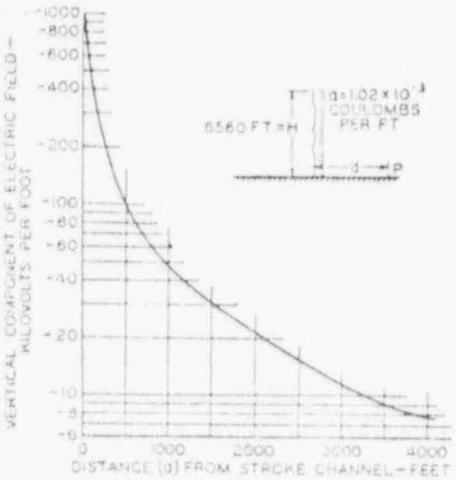

Fig. 18. Maximum value of ground gradient that occurs the instant initial streamer reaches earth.

retarded vector potential of current. The left-hand side of Fig. 17 shows the ground gradient for the (b) stage as a function of time for different horizontal distances from the stroke. Maximum gradients occur when the leader is fully extended at the instant the head reaches the ground. These are plotted in Fig. 18. Changing the time-scale so that zero represents the beginning of the return streamer, the right-hand side of Fig. 17 gives the ground gradient for the (c) stage due to the charge alone, and Fig. 19 due to the current. The effect of including the propagation time—the retarded magnetic vector potential—is

90004162

shown clearly in Fig. 19 by the time-delay of the sudden increase in current. For distances less than 10,000 feet, the gradient due to the current is negligible compared to that produced by the charges. For fixed velocities of the downward leader and return streamer the relative contribution of the charges and current is independent of I_s, both being proportional to I_s.

Consider a single conductor parallel to and 50 feet above ground and insulated from it. Let a vertical stroke occur 300 feet from this conductor. Further assume that the conductor is divided into 50-ft. sections insulated from each other. By computing the square root of the sum of the squares of 300 and the distance x along the line, the distance from the mid-point of each section to the stroke can be determined and thus the gradient beneath each element is

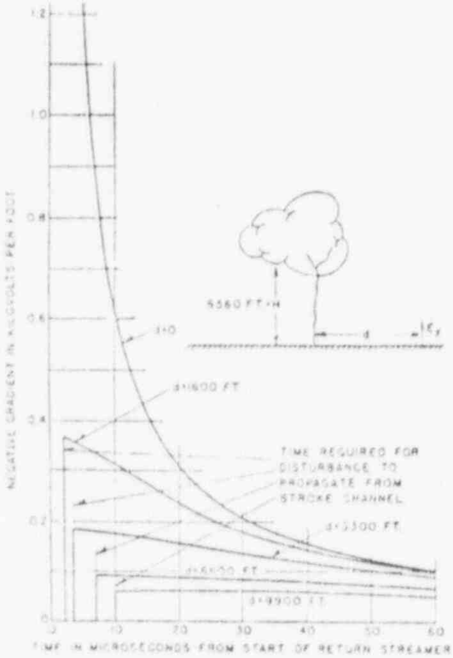

Fig. 19. Ground gradient due to current in return streamer.

found. The potential induced in each section is proportional to the height of the conductor. The maximum potential, the point nearest to the stroke at the instant the downward leader reaches the earth, is from Fig. 18 about −150,000,000 volts. However, the actual conductors do not consist of isolated sections but one continuous conductor, so as the inducing voltages increase they are simultaneously being drained off along the line. The actual voltage that does occur is a function of the velocities of the downward leader and the return stroke current. The velocity of the downward leader is so low that the conductor rises only a very small amount during this stage. But the velocity of the return stroke is sufficiently high so that a very significant voltage can appear.

Figure 20 shows th
the line to 500,000
stroke current, by
probability of occu

Following this
induced voltages,
for low-voltage dis
duced voltages even

Golde (39), usi
concerning charge
tion of the return
studies were directe
information availab
surges exceeding 20

In 1958, Rusck
this problem in m
charge along the st

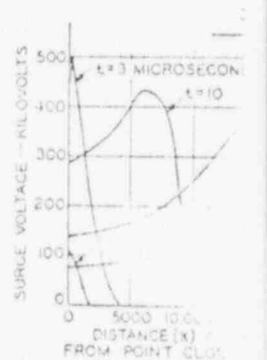

concluded that the
point in the line whi
has no great influen
lightning strokes vo
time constants. He
portance in the case
On the other hand,
lower are caused by
the effect of lightnin

More recently O
the effect of lightni
interesting element
individual steps in t
vances produce dang

90004163

Figure 20 shows the computed voltage waves as a function of the distance along the line to 500,000 volts. Since the voltage is proportional to the inducing or stroke current, by combining the results with the stroke probability curve the probability of occurrence of voltages of different magnitudes can be deduced.

Following this type of reasoning, Wagner and McCann concluded that induced voltages, even for strokes that just miss the line, are important only for low-voltage distribution lines. Ground wires reduce the importance of induced voltages even more.

Golde (39), using somewhat more sophisticated and realistic assumptions concerning charge distribution along the downward leader and velocity variation of the return stroke, arrived at substantially the same conclusions. His studies were directed primarily to distribution circuits, and he states: "statistical information available indicates that indirect surges rarely reach 100 kv and that surges exceeding 200 kv are almost exclusively due to direct strokes."

In 1958, Rusck (11) presented a comprehensive and rigorous analysis of this problem in mathematical form. He assumed a uniform distribution of charge along the stroke channel and a uniform velocity of the return stroke. He

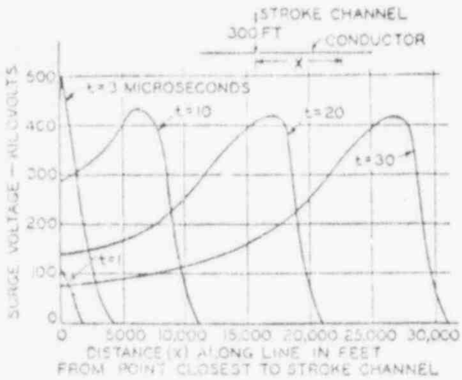

FIG. 20. Distribution of induced voltage along an infinitely long conductor 50 feet above ground at successive times after start of return streamer.

concluded that the resultant voltage on the line obtains its maximum at that point in the line which is nearest to the lightning stroke and that the front-time has no great influence on the magnitude of the voltage, except in the case of lightning strokes very close to the line, which will be decreased with longer time constants. He further concludes that the induced voltages are of no importance in the case of lines insulated for a system voltage higher than 70 kv. On the other hand, the majority of the lightning faults on lines for 20 kv and lower are caused by the induced voltages. His studies included an evaluation of the effect of lightning arresters on low-voltage distribution circuits.

More recently Ohwa (40) repeated the analysis with greater emphasis upon the effect of lightning arresters distributed along the line at transformers. An interesting element was added in these investigations as he concluded that the individual steps in the stepped leader during the momentary high velocity advances produce dangerously high voltages of very short duration in low-voltage distribution circuits. A study of the ground gradients produced at a distance by the return stroke was presented by Wagner (**41**) in 1960. This study excluded the interesting effects described by Ohwa that are produced by the stepped leader.

Prestrike Theory

Of the various theories advanced to explain the nature of the lightning stroke, the only other author who discusses those aspects of the stroke which affect transmission line performance is Griscom (**18, 42, 43, 44**). He designates his theory the "Prestrike Theory" because the main stroke current at the ground was expected to be preceded by a spike of current of very high magnitude but short duration. According to Griscom the head of the downward leader forms a large bulbous volume of charge which is responsible for a disproportionate amount of charge in the head. Upon approaching earth this charge is dumped out quickly and accounts for the large pip of current before the main return stroke current forms. The Griscom theory predicts [see Fig. 6, (**43**)] that for a crest return stroke current of 75,000 amperes, the prestrike

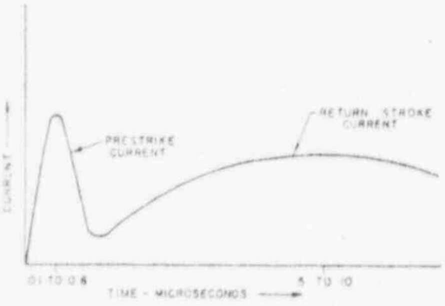

FIG. 21. Early estimate of relative magnitude of the prestrike pulse and the crest magnitude of the main portion of the stroke current and also the general shape of the stroke current.

current consists of a pip of current that rises to a crest of about 200,000 amperse in a sort of sinusoidal fashion and then falls to zero in about 1.2 microseconds. Such a pulse, if it actually existed, could produce previously unsuspected flashovers and outages of transmission lines. Before any field data had been obtained, publicity in connection with this theory portrayed the stroke current as indicated in Fig. 21. On 1965, based upon a considerable amount of data collected with the newly devised Kine-klydonograph, Griscom and his associates (**18, 44**) published Fig. 22 as their conception of the stroke current at the earth. Referring to the lower figure, the crest of the prestrike pulse is now only about 0.4 of the return stroke current and is to some extent absorbed into the front of the first component. Instead of being more than 2.5 times the main stroke current as previously predicted, the magnitude of the pulse, according to their interpretation of the records, is now only 0.4 times the main stroke current. We would not expect a prestrike current of the character depicted in Fig. 21 to exert much influence upon line performance.

Referring to Berger's oscillograms of stroke currents in Fig. 3, we observe that the shape is entirely different from that deduced by Griscom and his associates.

The prestrike pulse is absent in the Berger oscillograms, and the Griscom curve does not evidence the strong upward concavity that ends abruptly at what is here termed the nominal crest value. Subject to a ±25 per cent error characteristic of Lichtenberg figure techniques, the Kine-klydonograph measures the change in voltage that occurs within certain fixed intervals of time. It can be viewed as measuring roughly the slope of the current. In a closure discussion (**18**), Griscom states that from the character of the Lichtenberg figures it is possible to distinguish the time sequence of occurrence of successive voltage pulses. It appears that since oscillogram 61 06 27/23–1 T2 of Fig. 3 and the lower curve of Fig. 22 consist of a high rate of rise followed by a slower rate of

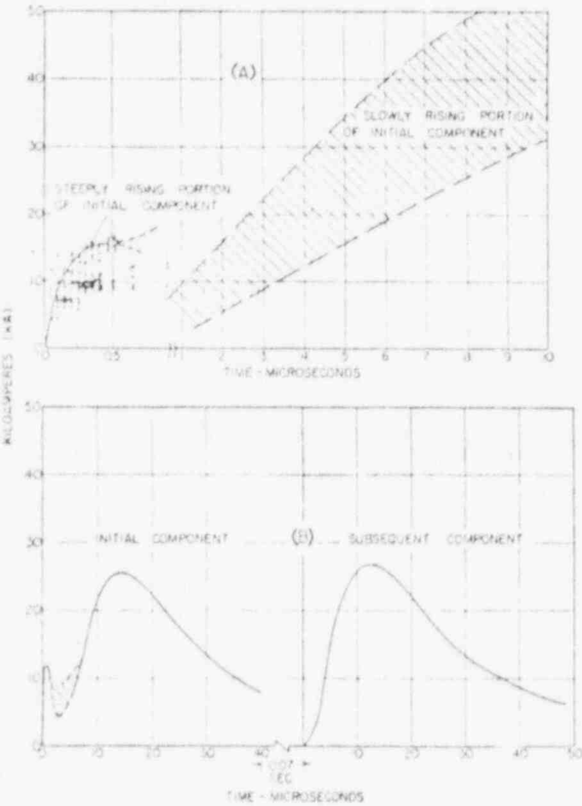

FIG. 22. Concept of wave form of lightning stroke as constructed from kine-klydonograph records (**18**).

rise, they would produce the same kind of Kine-klydonograph record. Griscom's deductions are rather strained in comparison with the more reliable oscillographic evidence of Berger, supported by the nature of the discharge current obtained in the laboratory and the actual line voltage oscillogram of Fig. 22. In Fig. 22(b) the wave shape of the subsequent components is identical with

90004166

that of the first component minus the prestrike current. These curves likewise contradict the actual oscillographic records of Berger's subsequent strokes. In the author's judgment, theoretical explanations support Berger's results.

In connection with his studies Griscom and his associates also used an instrument they term a "klydonograph gradient recorder." It consists of a screen raised up from and parallel to the earth across which a modified klydonograph and drainage resistors are connected. The time constant of the combination is 75 microseconds. They state (44) that field gradients of about 100 kv/m have been measured by this instrument, and they conclude that "while there is still insufficient data to claim absolute proof, the existence of very high field gradients close to downward strokes does substantiate the *prestrike* concept of stroke development." Note that Figs. 17 and 18 show calculated values of gradients, based upon a more conventional stroke mechanism, that are of the same order of magnitude as those reported by Griscom. Golde (39) and Rusck (11) also refer to similar ground gradients. The prestrike th[illegible] is not essential to explain gradients of this magnitude.

Difficulties of Computations

Frequently, the competence of an investigator resides in his ability to choose adequate simplifying assumptions. One of these assumptions refers to the tower. Great simplification results if a specific surge impedance, Z_t, is assigned to the tower and the tower is treated as though it were a short line of this surge impedance grounded at the end. This assumption also gives a particular meaning to the term "tower top potential." This is a generally accepted practice, but considerable theoretical doubt exists as to its validity. Some of these doubts will now be explored.

Consider a transmission line whose inductance is L henries per cm and whose capacitance is C farads per cm. The surge impedance, Z, in ohms is

$$Z = \sqrt{L/C}. \tag{3}$$

A disturbance propagates along the line with the velocity of light, c, equal to 3.0×10^{10} cm per sec. This velocity can also be stated as equal to

$$c = 1/\sqrt{LC}. \tag{4}$$

Eliminating C between Eqs. 3 and 4

$$Z = 3 \times 10^{10}\, L. \tag{5}$$

Suppose now that a 100-ft. (30.5 m) tower, which is actually a vertical conductor, is represented as a horizontal conductor 100 feet long grounded at the

end. Suppose furth
constant rate to cr
AIEE committee
height of 100 fe
inductance per
responding value
wave theory that t
such a current, is
of current, or if I
$10^6 = 5.0I$ in volts
the tower it may b
duces a drop of 20
tower would corres
fore, only for towe
in the tower becom

One of the prin
erroneous practice
in space. Such a va

where L_t is the in
cylinder in cm. T
duced by a unit
to infinity
in conj
other ele
by itself has no
clear that the ind
length when each
inductance of the o
flux around an infi
grated over the len
unit length so com
ductance has been
mission lines, the ef
included.

Various attempt
actual tower in the
proper placement o
illustrate the point
top of a right cylin

end. Suppose further that a current is forced into the free end that rises at a constant rate to crest at 4 microseconds. This is the assumption made by the *AIEE* committee regarding wave front. The committee also assumed a tower height of 100 feet and a tower inductance of 20 microhenries. Computing the inductance per unit length and inserting into Eq. 5 it can be seen that the corresponding value of Z is 200 ohms. It can be shown by conventional traveling wave theory that the voltage at the free end of such a line, when subjected to such a current, is equal to the total inductance times the time rate of change of current, or if I be the crest current the voltage is $(20 \times 10^{-6})(0.25)\ I \times 10^{6} = 5.0I$ in volts. To form an idea of the relative importance of the drop in the tower it may be observed that a tower footing resistance of 20 ohms produces a drop of $20I$. For this value of tower footing resistance the drop in the tower would correspond to about 20 per cent of the whole voltage drop. Therefore, only for tower footing resistances below 20 ohms does the inductive drop in the tower become important from the conventional point of view.

One of the principal difficulties encountered in the past is similar to the erroneous practice of assigning a self inductance value to an isolated cylinder in space. Such a value is given by Rosa (**45**), i.e.,

$$L_t = 2l\left(\ln \frac{2l}{\rho} - 1\right) \times 10^{-9} \qquad (6)$$

where L_t is the inductance in henries, l is the length, and ρ the radius of the cylinder in cm. This value was obtained by integrating the flux linkages produced by a unit current in the cylinder over the length of the cylinder and out to infinity. Rosa cautions that this quantity cannot be used by itself but only in conjunction with similar self and mutual inductances that apply between other elements comprising a complete current circuit. That this quantity taken by itself has no significance can be illustrated by two simple examples. It is clear that the inductance of two cylinders of the same diameter but half the length when each is computed separately by this formula is not equal to the inductance of the original cylinder when calculated by this formula. Also, if the flux around an infinitely long cylinder be computed and the linkages be integrated over the length of the cylinder and out to infinity, the inductance per unit length so computed is infinitely large. In the manner in which this inductance has been used in connection with the lightning performance of transmission lines, the effects of other parts of the circuit upon this element are not included.

Various attempts have been made to measure the surge impedance of an actual tower in the field (**46**). In this case the question arises concerning the proper placement of the voltage lead in measuring the tower top potential. To illustrate the point consider Fig. 23 that shows a ground wire connected to the top of a right cylinder representing a tower (**47**). The cylinder material will be assumed to have perfect conductivity. Suppose a traveling wave of charge and current, that moves from left to right, is impressed upon the ground wire. It is desired to measure the tower top potential at B. Of the three positions of the voltage divider, FB, EB, or DB, which is the correct one for measuring the potential of B above ground? Position FB, making about a 45° angle with the ground, has been used in some field testing. For position DB, lying along

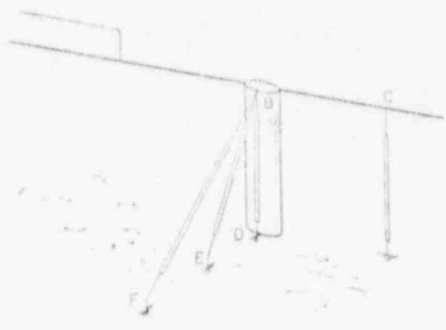

Fig. 23. Different lead positions for measuring tower-top potentials.

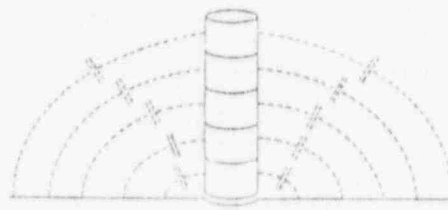

Fig. 24. Incremental-capacitance elements of right cylinder insulated from the earth.

the surface of the cylinder, the measured voltage is simply the resistance drop along the surface of the cylinder, but since the material has a zero resistivity the measured value is zero. Since there is no basis for discrimination between the three different positions, doubts arise as to whether any of them is correct.

As early as 1941, efforts (**48**) were made to measure the surge impedance of a tower by pulsing the top directly from a surge generator through a lead making a small angle with the ground and by measuring the tower top potential by another lead making a sharper angle with the ground. Such a method, interpreted in terms of the previous discussion, has definite apparent errors.

Another way of illustrating the questionable nature of tower surge impedance is shown in Fig. 24. A right cylinder is raised slightly above the earth and a voltage is applied between the cylinder and the earth. By graphical construction or otherwise, the electrostatic field pattern is obtained. The tower is then divided into sections as shown and a capacitance number assigned in proportion to the lines of force that emanate from each section. The argument then continues that a wave moving down the tower must travel at the velocity of light and from the relation for velocity, $1/\sqrt{LC}$, the inductance for the element is determined. Thus the surge impedance of any particular element is obtained from the expression $\sqrt{L/C}$. With this argument the surge impedance decreases from a maximum value at the top to zero at the bottom. Actually, if a wave starts from the top and travels to the bottom (an untenable assumption without considering the source of the wave), the lines of force must move out from the section with the velocity of light and cannot develop instantly to the earth.

In an effort to c
new approach based
by Wagner and H
along similar lines,
and Price (**52**) in 1
besetting the loop
based upon functio
and current as it w
proach, the primary
rectangular wave of
a velocity less than
with (a) which fed
calculate the voltag
wires, conventional
the proper values of
compute the voltag
stroke above the t
mechanism the volt
tower were signific
first component of
components. Until
above the tower t

In the work
that the
checked

This value is suppo
value of surge imped

a value supported b
et al. A value of to
also be obtained by
resulting in

Concerning the num
cases used without a
100; Jordan (**53**), 7

In an effort to clarify these calculations Wagner (**27**) undertook in 1956 a new approach based upon field theory. Later these concepts were carried further by Wagner and Hileman (**49, 50**). Lundholm (**51**), who had been working along similar lines, presented a paper before *CIGRE* and another with Finn and Price (**52**) in 1958 that introduced his "loop voltage" method. Difficulties besetting the loop voltage are discussed in (**52**). These new approaches were based upon functions that defined the electric field around a wave of charge and current as it was initiated from a zero position. Citing the Wagner approach, the primary forcing function of the lightning stroke was (a) a positive rectangular wave of charge that moved vertically above the stricken tower with a velocity less than that of light and (b) a positive wave of current associated with (a) which fed a negative current into the tower top. It was shown that to calculate the voltage produced by the current fed into the tower and ground wires, conventional traveling wave theory and methods can be used provided the proper values of surge impedance are used. Methods were also developed to compute the voltages across the insulator string due to (a), the charge in the stroke above the tower. For the particular assumption regarding the stroke mechanism the voltages across the insulator string due to the charge above the tower were significant. This stroke mechanism is probably not typical of the first component of the stroke but may approach somewhat that of subsequent components. Until more specific information regarding the movement of charge above the tower becomes available, no definitive judgment can be assessed.

In the work of Wagner and Hileman (**50**) the surge impedance of the tower that they developed (when used in the conventional methods of calculation checked their results) is

$$Z_t = 60 \ln \sqrt{2}\,\frac{2h}{r_t}. \tag{7}$$

This value is supported by Clayton and Young (**38**). On the other hand, the value of surge impedance given by Jordan (**53**) without proof is

$$Z_t = 60 \ln \frac{h}{r_t} + 45 \frac{d}{h} - 60 \tag{8}$$

a value supported by Anderson and Hagenguth (**54**) and also by Griscom (**18**), *et al.* A value of tower surge impedance (**54**) based upon Rosa's formula can also be obtained by dividing Eq. 6 by the tower height and inserting in Eq. 5, resulting in

$$Z_t = 60\left(\ln \frac{2h}{r_t} - 1\right). \tag{9}$$

Concerning the numerical values of tower surge impedance which were in many cases used without any effort to substantiate them are: Torok and Ellis (**55**), 100; Jordan (**53**), 78; Clayton and Young (**38**), 200, for the higher towers used at 345 kv and above. Harder and Clayton (36) and also the *AIEE* committee (26) used a tower inductance of 20 microhenries which they stated applied to a 100-ft. tower. Applying Eq. 5, this corresponds to a Z_t of 200 ohms.

Returning to the question of measuring the tower surge impedance in the field, another method used is to place a lead, as shown by *FB* in Fig. 23, making a 45° angle with the earth and apply a surge to the bottom end. The surge impedance is then computed from the reflections produced by the tower (56). Kawai (57) in using this method reported that no reliable result could be obtained. There are certain theoretical objections to this approach, such as the coupling between the tower and the lead. He devised alternate methods but the results are at variance with all other methods of evaluation.

In an entirely different approach to the clarification of transmission line performance, Hagenguth, Anderson and Fischer (58) resorted to the construction and testing of models. The model described by them was built to a 25-to-1 scale which requires that all measurements must likewise be reduced correspondingly in time. They reported an agreement with the Lundholm "loop voltage" method, but in a discussion Lundholm indicated that the discrepancy was too great and attributed it either to inaccuracy in the loop voltage theory or to some error in the measurements, or to both. Later, Braunstein (59) continued his work on models in Sweden with improved measuring techniques. The model approach is unique because it eliminates the need for computing a tower surge impedance or coupling between the ground wire. But measurements are a problem with this arrangement. For example, if it is desired to measure the tower top potential, the same questions arise as with actual towers in the field. Similar questions apply regarding placement of leads in measuring the potential across the insulator string. Should leads be brought out horizontally from the top and bottom of the insulator string, or should one lead be tapped from the bottom of the insulator string, brought up to the top and then taken off along a similar lead tapped from the top of the insulator string? Another disadvantage of model testing is the inability to introduce the change in coupling arising from corona effects, although this might be a secondary consideration. It is also difficult to properly simulate actual stroke characteristics.

In resumé, then, a true equivalent tower surge impedance can only be evaluated through an analysis, such as undertaken by Wagner and Lundholm or similar development. The value given by Eq. 7 is therefore recommended. This quantity applies only for the current injected into the tower top. While not proved definitely, it appears that to determine the effect of charge variation above the tower associated with the stroke mechanism, the tower surge impedance can be neglected.

The equivalent tower surge impedance may differ with the circuit conditions and the element along which the forcing function is applied, being different for the case of a wave approaching the tower along the transmission conductor as compared to a stroke to the tower.

To date, in line c
to rise linearly with
is not true. The eff
fronts of compon
component, and
smaller it is questi
more severe. The eff
evaluated.

Pipe-Pipe Gaps

The left-hand o
injected into a powe
duration (several h
quently the voltage
(2 or 3 microsecond
towers on both sides
paths to earth.

So long as the vo
flashover value only
is exceeded leaders
them. From Fig.
flowing thro
an imped

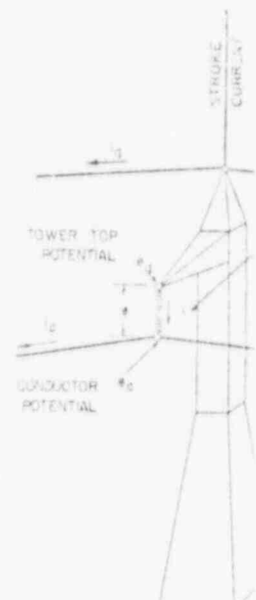

To date, in line calculations the wave fronts of lightning strokes are assumed to rise linearly with time to the crest value. Berger's data show conclusively this is not true. The effect of the concave front is still to be determined. The wave fronts of components subsequent to the first rise much faster than the first component, and thus should be more severe, but since the crest values are smaller it is questionable whether the first or subsequent components are the more severe. The effect of the charge in the stroke above the tower is still to be evaluated.

Pipe-Pipe Gaps

The left-hand oscillograms in Fig. 14 demonstrate that while the current injected into a power system when lightning strikes a line is of relatively long duration (several hundred microseconds), the tower top potential, and consequently the voltage across the insulator string, is of relatively short duration (2 or 3 microseconds). Such short durations are the result of reflections from towers on both sides of the stricken tower as the stroke current seeks additional paths to earth.

So long as the voltage across the insulator string is smaller than the critical flashover value only a relatively small current flows. But when the critical value is exceeded leaders begin to flow that require much larger currents to support them. From Fig. 25 it is clear that the leader current, i, must be supplied by flowing through the conductor on both sides. In seeking a path of current flow, an impedance, Z, is offered. Because the predischarge currents of insulator

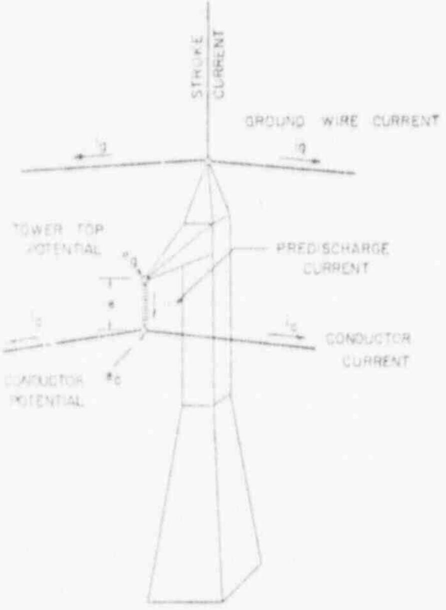

FIG. 25. Diagrammatic sketch of tower with ground wire and conductor showing nomenclature used.

90004172

strings and other types of equipment are so small, the Zi drop encountered is also small and is usually neglected. However, by suitably modifying the line construction, the predischarge currents can be magnified many times (60 64) and to such an extent that the Zi drop becomes sufficiently large in comparison with the critical flashover value of the insulator as to radically modify the line performance. Several means will be shown whereby the predischarge current can be increased. They are all based upon the breakdown characteristics of long parallel electrodes. Since in the literature such terms as rod–rod, rod–plane and sphere–sphere are used to designate particular types of electrode configurations, we apply the term *pipe–pipe* to specify this type of gap because pipes were used in making the tests.

Figure 26 shows typical oscillograms of the voltage across such a gap and the

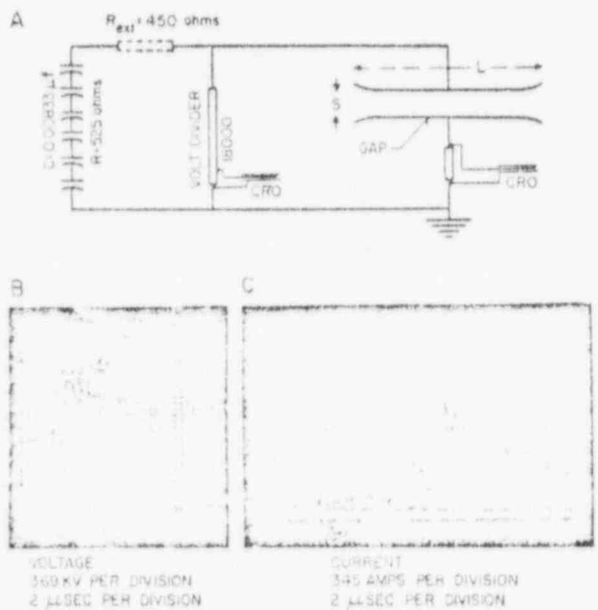

FIG. 26. Surge generator circuit and typical oscillograms of current and voltage in a parallel electrode gap consisting of two pipes, 50 feet in length, spaced 6 feet apart, and with 975 ohms in the circuit.

current through it. The gap consists of two pipes L ft. in length, spaced S ft. apart. To the point a only a small current flows which represents the current necessary to supply the charging current of the gap and the corona discharge. At point a the current rises abruptly and continues at a high value until breakdown occurs. This current is associated with the growth of arc-like streamers that extend from both electrodes. To obtain a sort of working relationship, it has been found, as the result of a large number of tests, that the total average current, i_p, in amperes is proportional to L and S and inversely proportional

90004173

to the square of T in microseconds, the time of leader growth from each of the electrodes or until the gap voltage drops to zero. Thus,

$$i_p = \frac{10LS}{T^2}. \tag{10}$$

If the voltage is removed before the time T, that is, before the approaching leaders make contact or attain sufficient conductivity, flashover will not occur.

Figure 27 is a still camera photograph of the discharge of such a gap. It

FIG. 27. Photograph of the discharge across a gap of 50-ft. length and 6-ft. spacing. Surge generator set for 1.85 times critical breakdown value.

shows clearly the simultaneous development of numerous leaders until one finally dominates and flashover occurs at that point, although the author has photographs that show simultaneous flashovers at several points—evidence that a finite time is required for good conductivity to be achieved at any point. We might view a gap of this nature as a large number of rod–rod gaps in parallel electrically, each of which has a very high resistance connected in series. It is known from the previous discussion of rod–rod gaps that the time of breakdown increases as the series resistance increases.

Suppose a gap of this nature is connected across a string of insulators and the spacing S is adjusted so that the critical breakdown voltage is just less than the critical flashover of the insulator. This spacing is a very important consideration. The critical breakdown value (63), e_p, is approximately

$$e_p = 186000S. \tag{11}$$

It was stated previously that the current, i_p, must be drawn through the impedance of the transmission line Z. To assess the value of the gap, the Zi_p drop will be compared with the critical breakdown voltage. Let this ratio be designated N. Then from Eqs. 10 and 11

$$N = \frac{40LZ}{T^2} 186000. \tag{12}$$

Note that N is independent of S. Assuming the effective surge impedance of the line to be 500 ohms, and since the current is supplied from both sides, this value must be divided by 2. Therefore, inserting 250 for Z Eq. 12 becomes

$$N = \frac{(0.054)L}{T^2}. \tag{13}$$

Suppose, further, that two rods that extend 15 feet on each side of the tower are mounted on each phase. The effective length of the combination is then 60 feet. Assume also that the duration of the tower top voltage is 2 microseconds. Then

$$N = \frac{0.054 \times 60}{4} = 0.8 \tag{14}$$

or, if T is 3, $N = 0.36$.

While these numbers are only crude approximations, they do provide an estimate of the order of the effect. Thus, to maintain the same voltage across the insulator string with the gap as without the gap requires a forcing voltage (or stroke current), $(1 + N)$ times as great.

While the ground wire and phase conductors constitute a very long pipe–pipe gap, they are of no value in developing predischarge currents until the spacing between them is reduced to the point where its critical flashover value is slightly less than that of the insulator string. This requirement involves a quite different location of the ground wire or wires than usual. While galloping might be a deterrent in reducing the distance between the ground wire and the conductor, this is not the case in some localities even for transmission lines with their large spacings. Galloping is an even lesser danger for distribution lines. Perhaps the very simple energy-absorbing non-galloper of A. H. Kidder (65) could find application. Two schemes, indicated merely to illustrate the principle, are shown in Figs. 28 and 29.

In Fig. 28 two pipes for each phase conductor are mounted on the tower and the gap spacing is adjusted so that the sparkover value of the gap is equal to or a little less than that of the insulator string. Predischarge currents begin to flow just as soon as the voltage across the gap and insulator string combination

90004175

exceeds the critical breakdown value. For surges of short duration quite high impulse voltages are required to cause breakdown of the combination. With the application of such voltages high predischarge currents flow that must be drawn through the conductor which offers an impedance to their flow. The benefits of drawing the high predischarge currents through the surge impedance of the line can be expressed by stating that a higher stroke current is required to produce a specified voltage across the insulator string or by stating that for a given stroke current a smaller voltage, that can be applied for a longer time before flashover occurs, appears across the insulator string. In Fig. 29 the pipe–pipe gap is formed by the ground wire as one electrode and phases A and B as the other. In order that this gap be effective the clearances of both conductors A

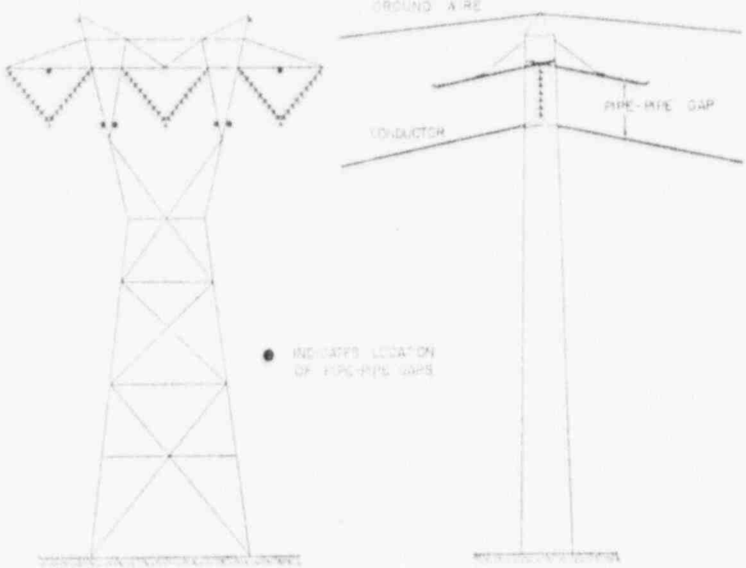

FIG. 28. Pipe–pipe gaps installed on a steel transmission tower, with pipes mounted geometrically parallel to the conductor, which forms one electrode of the gap.

and B to the downlead, R_2, must be greater than the spacing of the pipe–pipe gap, R_1; otherwise clearance distance R_2 would break down before the pipe–pipe gap, R_1, becomes effective. Lowering the ground wire also increases the coupling with the phase conductors which in turn reduces the tower top potential, but this is very secondary in comparison with the pipe–pipe effect *provided* that it is lowered sufficiently. Even with present spacings of the ground wire the pipe–pipe effect influences the flashover for strokes to midspan. It has long been known that flashovers at midspan are less frequent than would be expected by conventional theory; in fact, this is what prompted the *AIEE* committee to choose a 4 microsecond front for the stroke current. However, it must be pointed out that with present configurations strokes that might otherwise cause flashover at midspan are now merely transferred to the insulator string.

90004176

Around 1958, Griscom (18, 66) suggested the use of cantilever rods mounted at the top of the insulators parallel to the conductor. This would appear to be identical to the pipe–pipe scheme, but such is not the case. The pipe–pipe arrangement depends for its operation upon the high energy leaders that emanate from both pipes before the discharge (the final short circuit of the gap), whereas the Griscom "cantilever co-planar" rods depend upon increasing the coupling between the tower top and the conductor to absorb the high frequency prestrike pulse. The spacing between the pipe–pipe gap of Wagner is very critical and must be adjusted so that the critical breakdown value is just smaller than that of the insulator string, whereas Griscom indicates that the rods should be placed as close as mechanically convenient. Griscom and his associates (18) state that

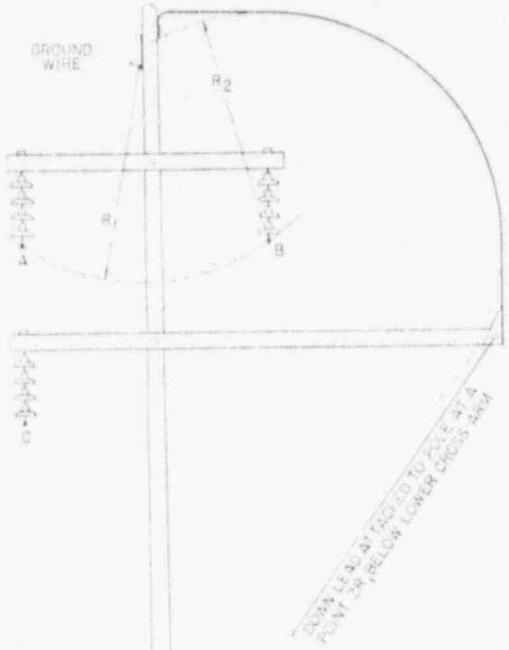

FIG. 29. Illustrative example of distribution circuit designed so that the flashover voltage of distance R_2 from the conductor B to the downlead is greater than the flashover voltage of the distance R_1 from the conductors A and B to the ground wire.

with their co-planar rods couplings as high as 70 to 80 per cent can be attained. This could be the case if the duration of the prestrike pulse were only about 0.05 or 0.10 microseconds rather than the indicated one microsecond duration, for then the wave need not travel any great distance before the crest voltage is attained. But for a pulse duration of one microsecond to increase the coupling sufficiently would involve lengths of cantilever co-planar rods of about 500 feet.

Discussion and Conclusions

The phenomenon of natural lightning is so complicated that perforce simplifying assumptions must be made to describe even its fundamental nature. The

model of the strok
garding shielding,

Much detailed
continually bein
strokes. Labor
the new high-vo
however, the actu
tations for the desi

Regarding shiel
shielding, protecti
wire heights of 50,
the working curve
and Young to the
siderations presum
Distribution lines
insulation levels, a
strokes to constitut
ground wires. Thi
should be disconti
undertaken to dete
the current wave
movement, the i
the stroke above
sparks should

Sin
number
duction of the
uneconomical. Li
since these consi
promising lead for
nomenon of predis
those systems in w
and 60-cycle volta
principles should
means for eliminati
are developed at a
insulation along t
tamination, space f
similar to strain
insulators can be
infer that tangent
resist tangential str

90004177

model of the stroke presented here provides a vehicle for basing judgment regarding shielding, direct strokes and indirect strokes.

Much detailed information has already been obtained and new data are continually being accumulated concerning the characteristics of individual strokes. Laboratory data on the longest gaps that can be broken down with the new high-voltage surge generators should be of value. We do not foresee, however, the actual incorporation of much of the detailed knowledge in computations for the design of lines. Such calculations must be simple and practical.

Regarding shielding, it is sufficient to know that for substantially perfect shielding, protective angles of 45, 30 and 12 degrees are required for ground wire heights of 50, 100 and 150 feet. And for direct strokes to the ground wire the working curves of the *AIEE* committee and their extensions by Clayton and Young to the higher voltages seem to be adequate. Of course, these considerations presume the use of ground wires in regions of high isokeraunic level. Distribution lines in the range of 33 kv and below, because of their very low insulation levels, are subject to sufficiently high induced voltages from nearby strokes to constitute a problem. Such outages are reduced greatly by the use of ground wires. This does not imply that general investigations and analyses should be discontinued. Quite the contrary, it is suggested that studies be undertaken to determine by conventional means the effect of the concavity of the current wave fronts. With the somewhat arbitrary assumptions of charge movement, the investigations begun by the author on the effect of charge in the stroke above the stricken point should be continued. Studies of very long sparks should reveal more information.

Since the introduction of the ground wire, except for a slight choice in the number of insulators, the conventional means for reducing outages is the reduction of the tower footing resistance. In certain types of soil this becomes uneconomical. Little of a fundamental nature has been added to the technique since these considerations were established. Therefore, it appears the only promising lead for reducing line insulation lies in the application of the phenomenon of predischarge currents as exemplified by the pipe-pipe gaps. For those systems in which switching surges and the combination of contamination and 60-cycle voltages do not constitute the limits of insulation, the pipe-pipe principles should have direct application. Where these other limitations exist, means for eliminating them should be sought. Certainly switching surges which are developed at a few specific points should not be permitted to control the insulation along the entire line. With respect to 60-cycle voltages and contamination, space for additional units could be found by utilizing a construction similar to strain towers—a construction in which an unlimited number of insulators can be added without increasing the tower height. This is not to infer that tangent towers have the strength of strain towers built into them to resist tangential strains; they merely continue to function like clothesline props.

The flexibility of the vertical string can be introduced by making the tower flexible, if this is essential. These ideas are merely injected in order to vitalize the plea that some consideration be given to the pipe pipe gap phenomenon.

References

(1) B. F. J. Schonland and H. Collens, "Progressive Lightning," *Proc., Royal Soc. London*, Vol. 143, pp. 654–71, 1934.

(2) B. F. J. Schonland, D. J. Malan and H. Collens, "Progressive Lightning II," *Proc., Royal Soc. London*, Series A, Vol. 152, pp. 595–625, 1935.

(3) D. J. Malan and H. Collens, "Progressive Lightning III, The Fine Structure of the Return Stroke," *Proc., Royal Soc. London*, Vol. 162, pp. 175–203, 1937.

(4) B. F. J. Schonland, D. B. Hodges and H. Collens, "Progressive Lightning V, A Comparison of Photographic and Electrical Studies of the Discharge Process," *Proc., Royal Soc. London*, Vol. 166, p. 56, 1938.

(5) I. S. Stekolnikov, "The Nature of the Long Spark," *Izdatel'stvo Akademii Nauk SSSR*, pp. 1–272, 1960. English trans. available from Foreign Tech. Div., Air Force Systems Command, Wright-Patterson AFB, Ohio.

(6) C. F. Wagner and A. R. Hileman, "The Lightning Stroke II," *AIEE Trans.*, Pt. III (Power Apparatus and Systems), Vol. 80, pp. 622–42, Oct. 1961.

(7) N. Kitagawa, M. Kobayashi, "Field Changes and Variations of Luminosity Due to Lightning Flashes," pp. 485–501, "Recent Advances in Atmospheric Electricity," New York, Pergamon Press, Inc., 1958.

(8) T. Udo, "Sparkover Characteristics of Large Gap Spaces and Long Insulation Strings," *IEEE Trans. on Power Apparatus and Systems*, pp. 471–83, 1964.

(9) C. F. Wagner, "Relation Between Stroke Current and Velocity of the Return Stroke," *IEEE Trans. on Power Apparatus and Systems*, pp. 609–17, 1963.

(10) R. Lundholm, "Induced Over-Voltage Surges on Transmission Lines, and Their Bearing on the Lightning Performance at Medium-Voltage Networks," *Trans. Chalmers Univ Tech.*, Gothenburg, Sweden, No. 188, 1957.

(11) S. Rusck, "Induced Lightning Over-Voltages on Power Transmission Lines with Special Reference to the Over-Voltage Protection of Low-Voltage Networks," *Trans. Royal Inst. Tech.*, Stockholm, Sweden, No. 120, 1958.

(12) M. Toepler, "Funkenkonstante, Zündfunken und Wanderwelle," *Arch für Elektrotechn*," Vol. 14, pp. 305–318 and Vol. 18, p. 549.

(13) C. F. Wagner, C. M. Lane and C. M. Lear, "Arc Drop from Spark Discharge to Arc," *AIEE Trans.*, Pt. III (Power Apparatus and Systems), pp. 242–47.

(14) C. F. Wagner and G. D. McCann, "Induced Voltage on Transmission Lines," *AIEE. Trans.*, Vol. 61, pp. 916–30, 1942.

(15) K. Berger, "Front Duration and Current Steepness of Lightning Strokes to the Earth," *Proc. Internat. Conf. Central Electricity Res. Labs.*, Leatherhead, Surrey, England, May 7–11, 1962, London, Butterworths, 1962.

(16) C. F. Wagner, "The Lightning Stroke as Related to Transmission Line Performance," Parts I and II, *Elec. Eng.*, May and June, 1963.

(17) R. H. Golde, "Occurrence of Upward Streamers in Lightning Discharges," *Nature*, London, England, Vol. 160, p. 395, Sept. 20, 1947.

(18) S. B. Griscom, et al., "Five-Year Field Investigation of Lightning Effects on Transmission Lines, I—Data Summary and Suggestions for Improved Line Performance;" II—"Instrumentation and Installations;" III—"Lightning Stroke Characteristics and Their Effects in Transmission Systems," *IEEE Trans. Power Apparatus and Systems*, pp. 257–80, April 1965.

(19) E. Bell and A. L. Price, "Lightning Investigation on the 220-kv System of the Pennsylvania Power and Light Company," *AIEE Trans.*, pp. 1101–10, Sept. 1931.

(20) J. [illegible] Hagenguth and J. G. Anderson, "Lightning to the Empire State Building," Part III, *[illegible]E Trans.*, Pt. III (*Power Apparatus and Systems*), Vol. 71, pp. 641–49, Aug. 1952.

(21) G. D. McCann,
Trans., Vol. 63,
(22) K. Berger, "M
1954 on Mount
Switzerland, Vol
(23) K. Berger and
Salvatore for t
Bd. 57, 1966.
(24) G. D. McCann
AIEE Trans., V
(25) A. A. Akopian,
Across High-Vo
No. 411, *CIGRE*
(26) "A Method of
mission and Dis
(27) C. F. Wagner, "
AIEE Trans., P
(28) C. F. Wagner an
Stroke," *AIEE*
1961 (Feb. 1962
(29) C. F. Wagner, "
IEEE at New C
(30) C. F. Wagner,
AIEE Trans., V
(31) F. S. Young, J.
IEEE Trans. P
(32) M. V. Kostenk
Ground Wi
USSR, No
(33) H.
(34) H.
Line Shiel
1967.
(35) C. L. Fortescu
Line Flashover,
(36) E. L. Harder an
Direct Lightnin
(37) A. C. Monteith,
and Distributio
(38) J. M. Clayton
Lines," *Trans.*
(39) R. H. Golde, "
III-A, (*Power*
(40) Genichi Ohwa, "
Electrical Engin
(41) C. F. Wagner, "
Field Measurem
pp. 581–89, 1960
(42) S. B. Griscom, "
Trans., Pt. III,
(43) S. B. Griscom,
Performance,"
Dec. 1958.
(44) E. Beck, et al
Records," *Westi*

(21) G. D. McCann, "The Measurement of Lightning Currents in Direct Strokes," *AIEE Trans.*, Vol. 63, pp. 1157–64, 1944.
(22) K. Berger, "Measuring Equipment and Results of Lightning Research During 1947–1954 on Mount San Salvatore," *Bull. Schweizerischen Elektrotechnischen Vereins*, Zurich, Switzerland, Vol. 46, Nos. 5, 9, 1955.
(23) K. Berger and E. Vogelsanger, "Photographic Lightning Investigations on Mount San Salvatore for the Years 1955–1965," *Bull. Schweizerischen Elektrotechnischen Vereins*, Bd. 57, 1966.
(24) G. D. McCann and J. J. Clark, "Dielectric-Recovery Characteristics of Large Air Gaps," *AIEE Trans.*, Vol. 62, pp. 45–52, Jan. 1943.
(25) A. A. Akopian, V. P. Larionov and A. S. Torosian, "On Impulse Discharge Voltages Across High-Voltage Insulation as Related to the Shape of the Voltage Wave," Rep. No. 411, *CIGRE*, Paris, France, 1954.
(26) "A Method of Estimating Lightning Performance of Transmission Lines," Rep. Transmission and Distribution Cte. AIEE, *Trans. AIEE*, Vol. 69, pp. 1187–1196, 1950.
(27) C. F. Wagner, "A New Approach to the Lightning Performance of Transmission Lines," *AIEE Trans.*, Pt. III (*Power Apparatus and Systems*), Vol. 75, pp. 1233–56, Dec. 1956.
(28) C. F. Wagner and A. R. Hileman, "Surge Impedance and Its Application to the Lightning Stroke," *AIEE Trans.*, Pt. III (*Power Apparatus and Systems*), Vol. 80, pp. 1022–22, 1961 (Feb. 1962 section).
(29) C. F. Wagner, "Surge Impedance," Paper No. 31, pp. 66–419, Summer Power Meeting *IEEE* at New Orleans, La., July 15, 1966.
(30) C. F. Wagner, G. L. MacLane and G. D. McCann, "Shielding of Transmission Lines," *AIEE Trans.*, Vol. 60, pp. 313–28, 1941.
(31) F. S. Young, J. M. Clayton and A. R. Hileman, "Shielding of Transmission Lines," *IEEE Trans. Power Apparatus and Systems*, Spec. Sup., Vol. S82, pp. 132–154, 1963.
(32) M. V. Kostenko, et al., "The Role of Lightning Strikes to the Conductors Bypassing the Ground Wires in the Protection of High-Voltage Class Lines," *Elektrichestvo*, Moscow, USSR, No. 4, pp. 20–26, 1961.
(33) H. R. Armstrong and E. R. Whitehead, "A Lightning Stroke Pathfinder," *Trans. IEEE, Power Apparatus and Systems*, Vol. 83, pp. 1223–27, 1964.
(34) H. R. Armstrong and E. R. Whitehead, "Field and Analytical Studies of Transmission Line Shielding," Paper No. 31, pp. 67–103, Winter Power Meeting of the *IEEE*, Feb. 1, 1967.
(35) C. L. Fortescue, "Direct Strokes—Not Induced Surges—Chief Cause of High-Voltage Line Flashover," *The Electric Journal*, Vol. 27, pp. 459–62, Aug. 1930.
(36) E. L. Harder and J. M. Clayton, "Transmission Line Design and Performance Based on Direct Lightning Strokes," *AIEE Trans.*, Vol. 68, Part I, pp. 439–49, 1949.
(37) A. C. Monteith, et al., "Line Design Based Upon Direct Strokes," Chap. 17, Transmission and Distribution Ref. Book Westinghouse Elec. Corp., 1950.
(38) J. M. Clayton and F. S. Young, "Estimating Lightning Performance of Transmission Lines," *Trans. IEEE on Power Apparatus and Systems*, pp. 1102–1110, 1964.
(39) R. H. Golde, "Lightning Surges on Overhead Distribution Lines," *AIEE Trans.*, Part III–A, (*Power Apparatus and Systems*), Vol. 73, pp. 437–47, 1954.
(40) Genichi Ohwa, "Study of Induced Lightning Surges and Their Frequency of Occurrence," *Electrical Engineering in Japan*, Vol. 84, No. 12, Dec. 1964.
(41) C. F. Wagner, "Determination of the Wave Front of Lightning Stroke Currents from Field Measurements," *AIEE Trans.*, Pt. III (*Power Apparatus and Systems*), Vol. 79, pp. 581–89, 1960.
(42) S. B. Griscom, "The Prestrike Theory and Other Effects in the Lightning Stroke," *AIEE Trans.*, Pt. III, (*Power Apparatus and Systems*), Vol. 77, pp. 919–33, Dec. 1958.
(43) S. B. Griscom, et al., "The Influence of the Prestrike on Transmission Line Lightning Performance," *AIEE Trans.*, Pt. III (*Power Apparatus and Systems*), Vol. 77, pp. 933–40, Dec. 1958.
(44) E. Beck, et al., "Results from Five Years of Lightning Study with Klydonograph Records," *Westinghouse Engineer*, pp. 148–53, Sept. 1966.

(45) E. B. Rosa, "The Self and Mutual Inductance of Linear Conductors," Reprint No. 80, *Bull., Bureau of Standards*, Wash., D. C., Vol. 4, No. 2, 1908.

(46) G. D. Brener, et al., "Field Studies of the Surge Response of a 345-kv Transmission Tower and Ground Wire," *AIEE Trans.*, Pt. III (*Power Apparatus and Systems*), Feb. 1958 Section, Vol. 76, pp. 1392–96, 1957.

(47) Discussion by C. F. Wagner of Ref. (**46**).

(48) "Surge Phenomena" (book), British Elec. and Allied Ind. Res. Assoc., p. 216, 1941.

(49) C. F. Wagner and A. R. Hileman, "A New Approach to Calculation of Lightning Performance of Transmission Lines, II," *AIEE Trans.*, Pt. III (*Power Apparatus and Systems*), Vol. 78, pp. 996–1021, Dec. 1959.

(50) C. F. Wagner and A. R. Hileman, "A New Approach to the Calculation of the Lightning Performance of Transmission Lines, III, A Simplified Method: Stroke to Tower," *AIEE Trans.*, Pt. III (*Power Apparatus and Systems*), Vol. 79, pp. 589–603, Oct. 1960.

(51) R. Lundholm, "Over-Voltages in a Direct Lightning Stroke to a Transmission Line Tower," *CIGRE* Rep. No. 333, Paris, 1958.

(52) R. Lundholm, et al., "Calculation of Transmission Line Lightning Voltages by Field Concepts, *AIEE Trans.*, Pt. III, (*Power Apparatus and Systems*), Vol. 76, pp. 1271–83, 1957.

(53) C. A. Jordan, "Lightning Computations for Transmission Lines with Overhead Ground Wires," *General Electric Review*, Schenectady, N. Y., Vol. 37, No. 3, pp. 130–37, March 30, 1934.

(54) J. G. Anderson and J. H. Hagenguth, "Magnetic Fields Around a Transmission Line Tower," *AIEE Trans.*, Pt. III (*Power Apparatus and Systems*), Vol. 77 (Feb. 1959 Section), pp. 1644–50, 1958.

(55) J. J. Torok and W. R. Ellis, "Design of Transmission Lines," *The Electric Journal*, pp. 467–71, Nov. 1933.

(56) R. W. Caswell, et al., "Lightning Performance of 138-kv Twin-Circuit Transmission Lines of Commonwealth Edison Company—Operating Experience and Field Studies," *AIEE Trans.*, Pt. III, (*Power Apparatus and Systems*), Vol. 76 (Feb. 1958 Section), pp. 1480–91, 1957.

(57) M. Kawai, "Studies of the Surge Response on a Transmission Line Tower," *IEEE Trans. Power Apparatus and Systems*, Vol. 83, pp. 30–34, Jan. 1964.

(58) F. A. Fischer, et al., "Determination of Lightning Response of Transmission Lines by Means of Geometrical Models," *AIEE Trans. Power Apparatus and Systems*, Feb. 1960; Vol. 78, pp. 1725–34, 1959.

(59) A. Braunstein, "Lightning Response of Power Transmission Lines," Doctorate Thesis, Chalmers Tekniska Hogskola, Göteborg, Sweden, 1963.

(60) C. F. Wagner and A. R. Hileman, "Effect of Predischarge Currents upon Line Performance," *AIEE Trans.*, Pt. III (*Power Apparatus and Systems*), Vol. 82, pp. 117–31, April 1963.

(61) C. F. Wagner and A. R. Hileman, "Predischarge Currents of Parallel Electrode Gaps," *CIGRE*, Paper No. 320, 1964.

(62) C. F. Wagner and A. R. Hileman, "Predischarge Current Characteristics of Parallel Electrode Gaps," *IEEE Trans. Power Apparatus and Systems*, pp. 934–44, 1964.

(63) C. F. Wagner, "Application of Predischarge Currents of Parallel Electrode Gaps," Western Electronic Show and Convention, Los Angeles, Cal., August 25–28, 1964.

(64) C. F. Wagner, "New Line-Protection Concepts Lack Field Trials," *Electric Light and Power*, pp. 70–73, March 1965; pp. 88–92, April 1965.

(65) A. H. Kidder, "A Proposed Friction Damper for Galloping Conductor Waves," Paper No. 31, pp. 66-307, Summer Power Meeting of *IEEE*, New Orleans, La., July 13, 1966.

(66) Discussion of Ref. (**60**).

rainer, we anticipate that great advantages will be found from this circuit, namely, the flexibility of adjustment of the different circuit parameters and the possibility of making many more tests in the failure area since the failure, though it can be readily detected from the oscillograms, will not be damaging to the breaker beyond the normal erosion associated with successful operations.

We appreciate the good wishes of Dr. Hochrainer who has had a number of years experience with a circuit rather similar to the one we have proposed and has made "many comparison tests . . . to show the equivalence of synthetic testing to direct testing."

A Lightning Stroke Pathfinder

REF. 16

H. R. Armstrong, Fellow IEEE *E. R. Whitehead*, Fellow IEEE

Summary: Extra-high-voltage transmission lines, designed in accordance with the AIEE lightning outage estimation method published in 1950, have actually experienced several times the outages predicted. Recent studies, based on new concepts of the lightning stroke mechanism, strongly indicate that lightning strokes to the phase conductors, or shielding failures, account for this sharp discrepancy.

A low-cost instrument, rugged in design and readily installed, has been developed to discriminate between strokes to the shielding system or a phase conductor. Signals are easily read either from the ground or from a helicopter. Power follow current is similarly indicated. A minimum of 100 records are deemed essential to firmly allocate lightning outages to phase conductor or shield wire stroke terminations. To secure these records, it is recommended that a field study be conducted on a suitable mile-year sample of transmission lines.

With this information available, the engineering prediction of the lightning performance of transmission lines can be placed on a much sounder basis and lines can be designed to a preselected level of tripout probability.

In 1950, the AIEE published a report on a method of estimating lightning performance of transmission lines.[1] This method assumed that virtually perfect shielding was obtainable on all lines with a shielding angle of 30 degrees and considered that flashovers that did occur were the result of voltages developed across the insulator string resulting from the flow of current to earth through the tower.

Extra-high-voltage (EHV) lines, designed on the recommendations of the AIEE report, actually experienced many times the predicted number of lightning tripouts per 100 miles per year. This situation has led to an extensive reappraisal of the theoretical basis for the conclusions reached in this report along one or more of the following lines:

1. The rates of rise of lightning stroke currents may be much higher than commonly supposed, in which case the electrodynamic response of the transmission line must be calculated from the concepts of fundamental electromagnetic field theory rather than from those of distributed-constant circuit theory.

2. The charge in the lower portion of the leader channel may be highly concentrated and immediately available, resulting in high tower currents as well as high induced voltage components.

3. The shielding of EHV lines is much poorer than that of lower voltage lines and is critically dependent on the height of the EHV lines.

4. The lightning stroke mechanism is essentially involved in a little understood and complex manner with all of the foregoing items.

In recent years important progress has been made in the theory of the lightning stroke[2,3] and in the careful analysis of field data over a significant period of time.[4] It is clear, however, that any final adjustment of theoretical models to field data must include additional data which definitely assign every flashover to one of two classes:

1. Those arising from direct strokes to the phase conductor.
2. Those arising from direct strokes to the shielding system.

The purpose of this paper is two-fold: first, to outline briefly the most promising developments with respect to the shielding problem and to describe a low-cost instrument designed to indicate the ground wire or phase conductor as the terminus of the lightning stroke; and second, to suggest its use in a large-scale field test to provide the information essential for a meaningful advance in the application of the theory of lightning protection of high-voltage transmission lines.

Theoretical Background

The authors have followed with great interest the fundamental work of C. F. Wagner, A. R. Hileman, and their associates in developing the theoretical mechanism of the lightning stroke. This mechanism was under active investigation in relation to the shielding problem when the excellent paper by Young, Hileman, and Clayton appeared.* This paper confirmed the basic ideas upon which the present studies were premised but indicated that future effort should be concentrated on the problem of providing economical instrumentation which could be installed in the field in sufficient numbers to provide experimental confirmation of the shielding theories.

The new approach to the shielding problem assumes that

Paper 64-40, recommended by the IEEE Transmission and Distribution Committee and approved by the IEEE Technical Operations Committee for presentation at the IEEE Winter Power Meeting, New York, N. Y., February 2–7, 1964. Manuscript submitted November 4, 1963; made available for printing December 12, 1963.

H. R. Armstrong is with the Detroit Edison Company, Detroit, Mich., and E. R. Whitehead is with the Illinois Institute of Technology, Chicago, Ill.

The authors take pleasure in acknowledging the contributions of both organizations and individuals to the development of the device described in this paper. Sponsorship of the project by the Edison Electric Institute made it possible to carry out the necessary development and testing in parallel with a review of the theoretical background applicable to the problem. D. W. Gilman and W. S. Price of the Edison Electric Institute gave valuable advice and enthusiastic support. Special acknowledgment is due the Josiyn Manufacturing and Supply Company for the development of the hot-line tool for the collector ring and for furnishing laboratory testing time at cost as a contribution to the feasibility project. R. J. Arndt of the IIT Research Institute furnished valuable preliminary information on suitable electroexplosive and rectifier elements. L. S. Van Slyck, graduate student at Illinois Institute of Technology, made substantial contributions to the theoretical phases of the investigation.

* Shielding of Transmission Lines, F. S. Young, J. W. Clayton, A. R. Hileman (Paper 62-1313).

90004182

the point to be struck is determined by long-spark theory[4] involving distances of the order of 100 feet or less and average voltage gradients of the order of 0.6 megavolt per meter. In applying this approach, Young, Hileman, and Clayton found initially that more shielding failures were estimated than experienced when Wagner's velocity–current relation[3] was used as the key transition relation between the stroke current frequency distribution and the stroke voltage frequency distribution. Accordingly, they made an appropriate adjustment of this curve to bring the estimated shielding failures down to the level of lightning tripouts experienced on important EHV lines. Recent studies[6] suggest that the actual stroke model may require modification, probably on a statistical basis, to include effects of branching on both the velocity current curve and the effective striking distance. When this is done, little or no important modification in Wagner's velocity–current relation may be needed.

It is becoming apparent that even a modest increase in the precision of knowledge in one area of this problem only highlights the uncertainties in others. Painstaking fitting of the theoretical calculations of shielding failures to field experience seems at least highly questionable when we really do not know the division between outages so caused and those resulting from strokes to the ground wire or tower.

The Pathfinder

Recognizing that the problem posed in the foregoing is of key importance, the Edison Electric Institute supported a research project designed (1) to evaluate existing theories relating to shielding failures, (2) to develop a low-cost instrument suitable for large-scale field studies, and (3) to outline preliminary plans for such a field investigation.[6] This paper is primarily concerned with the second of these tasks. Professor L. S. Van Slyck has in preparation a thesis for an advanced degree which will deal more fully with the other phases of this investigation at a later date.

It is estimated from available, but scattered, data sources that 90 to 95% of the lightning strokes to earth lower negative charge. This fact serves with acceptable accuracy as the physical basis for discrimination as to the probable location of the stroke terminus on the transmission line.

In the original concept, the device named the "Pathfinder" was to consist of (1) a flashover current interceptor ring affixed to the cap of the second insulator from the tower arm directing this current to (2) a polarity-sensitive but power-follow-rejective circuit which would activate signals furnishing the corresponding information to an observer on the ground or in a helicopter. Accordingly, a simple device using a high-current inductor for time discrimination and silicon diodes for polarity discrimination was initially proposed as a point of departure for further development.

If the lightning stroke terminates on the phase conductor, and its current exceeds a very low threshold level depending upon the number of insulators, negative current is supplied to the collector electrode, probably by cascade flashover, and directed through the device. The silicon diodes sense the polarity and direct a small fraction of the current through an electroexplosive device of a highly reliable type. This device, known as a squib, is installed in a gun designed to eject a large disk covering a distinctive signal employing both shape and color as a means of visual discrimination.

Should the stroke contact the shield wire or tower, and sufficient voltage develop across the insulator string to result in flashover, a current of opposite polarity flows from the phase wire through the instrument and an alternate characteristic signal is exposed in a similar fashion. In either case, care must be taken to prevent any ensuing power follow current from activating the remaining surge current signal and destroying the information.

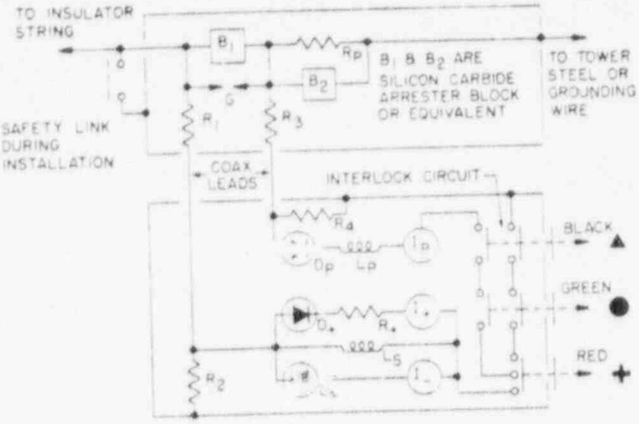

Fig. 1. Pathfinder circuit employing electroexplosive power-follow-current signal

Table I. Indicator Coding

Signal			Stroke Terminated on		Stroke Polarity		Power Follow Current	
Red Cross	Green Disk	Black Triangle	Conductor	Ground Wire	Positive	Negative	Yes	No
x			x			x		x
x		x	x			x	x	
x	x		x		x (1)			x
x	x	x	x		x		x	
	x			x		x		x
	x	x		x		x	x	
		x		x	x (2) or	x	x	

1. Instrument biased for high positive current to conductor.
2. Low-magnitude short-duration current caused by "backflash" below threshold current of instrument.

Many circuits employing resistors, inductors, and capacitors in various combinations were investigated as time-discrimination networks, and in the interest of low cost it was decided that time discrimination should be assigned to the low-current circuit. Moreover, the wide range of lightning current expected dictated the use of a nonlinear shunt resistor of the type used in lightning arresters to provide both low-current sensitivity and high-current withstand ability.

As the development progressed, it became evident that a signal showing power follow current would be useful inherently and also serve as a flashover indicator if the surge current from a stroke to the ground wire were below the threshold of the instrument; see note 2 of Table I. It was also felt desirable to indicate the presence of a very high positive current, as this would be most unlikely except for a positive stroke to the phase conductor. A bias resistor in the positive diode circuit results in rupture of the negative diode to provide the indication in such a case; see note 1 of Table I.

From the foregoing considerations it was deter[illegible] three signals would be used with the associat[illegible] yield information in accordance with the signa[illegible]own in Table I. A red cross is used for a negative current from the insulator string, a green disk for a positive current, and a black triangle is used to indicate power follow current. In the production model the signals will be about 5 inches in diameter and will be readily visible for a distance of 150 to 200 feet.

Fig. 1 shows one of the circuits which employs electro-

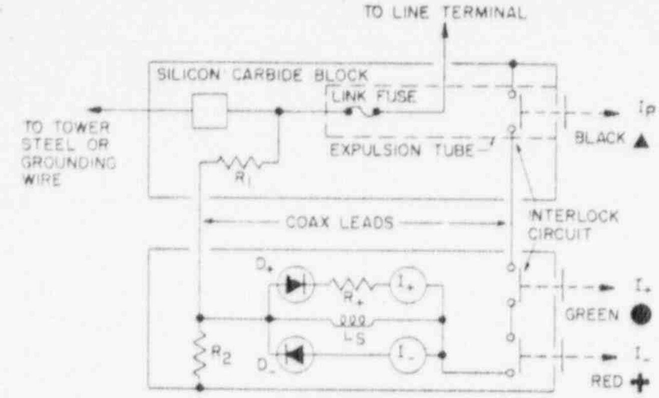

Fig. 2. Pathfinder circuit employing expulsion fuse for power-follow-current signal

explosive actuation of all three signals, while Fig. 2 shows a simpler circuit which employs expulsion fuse operation to uncover the power follow signal.

It has been suggested that when performance records of transmission lines are analyzed the ratio of double-circuit to single-circuit can be used to estimate the division between backflash and shielding failure tripouts. Application of the Pathfinder to both circuits of a double-circuit line should yield data relating to such a possibility. In such applications the existence of shielding failure on one circuit with backflash on the other could be detected if the signals were definitely known to be coincident.

Fig. 3 shows a developmental model of the Pathfinder with Fig. 3(A) all signals covered, Fig. 3(B) a stroke to the phase conductor without power follow current, and Fig. 3(C) the power follow current indication added.

Field Tests

Extremely valuable data could be obtained if the instrument described were applied to a sufficiently large sample of electric power transmission lines, 100 kv and above. The choice of such a sample is of critical importance, however, because of the small number of flashovers per 100 miles per year. Moreover, the sample must be selected so that some lines may be expected to furnish flashovers arising from strokes to the ground wire, while others may be expected to furnish flashovers arising largely from shielding failures. Obviously, the sample should not include lines exceptionally free from flashovers caused by lightning. Viewed in this perspective, the vagaries of thunderstorm-days per year and storm paths are, fortunately, already included in the record of the performance of lines, and it is on this basis that a proper statistical sample should be based.

A preliminary study of statistical considerations suggests that about 100 records are desirable to give a reasonably reliable allocation of lightning tripouts to backflash or to shielding failure causes. This study also indicates clearly that experimental evaluation of various shielding angles, ground resistances, and other design parameters is completely unrealistic. It is believed, however, that extremely valuable data could be obtained from a sample of perhaps 1,500 to 2,500 mile-years distributed equally in three categories as indicated in Table II.

An important factor in any widespread application of the Pathfinder is a means of rapid and safe installation of both the current collector ring and the indicator housing. A spring-loaded clamp secures the ring to the insulator hardware below the unit which is first from the grounded end of the insulator string. The clamp is held open by a toggle action hot-line tool, as shown in Fig. 4, in order to provide easy access to the installation location. Fig. 5 shows the collector ring in place and the unlatched tool in the withdrawal stage. The collector ring causes a negligible reduction in impulse flashover for insulator strings of seven or more units.

Conclusions

1. Recent advances in theoretical models of the lightning stroke mechanisms have led to corresponding applications to

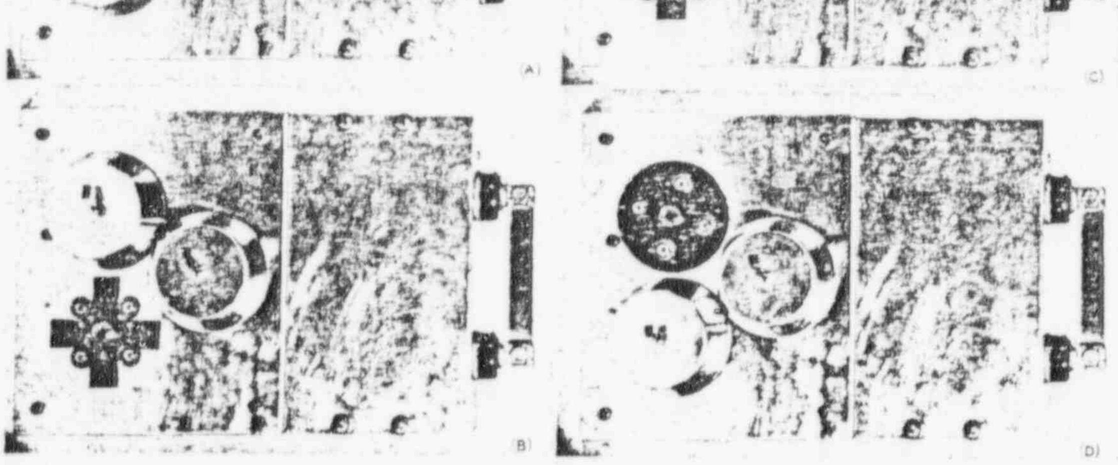

Fig. 3 Developmental model of pathfinder
A—All signals covered
B—Stroke to phase conductor without power follow
C—Power-follow-current signal added
D—Stroke to shield wire without power follow

90004184

Table II. Suggested Transmission Line Sample

Sample	Description of Sample	Mile-Years	Number of Records Expected: 90% Certain	Number of Records Expected: 50% Certain
A(15)*	High flashover rate Shielding and backflash Shielding angle 45 degrees or more High footing resistance	500	64	75
B(5)*	Few backflashes expected Shielding suspected Shielding angle 30 degrees or less Low footing resistances High towers	500	19	25
C(2)*	Few shielding failures expected Backflash suspected Shielding angle 0–12 degrees High footing resistances Low towers	500	6	10
	Totals	1,500	89	110

* Average tripout rate per 100 miles per year.

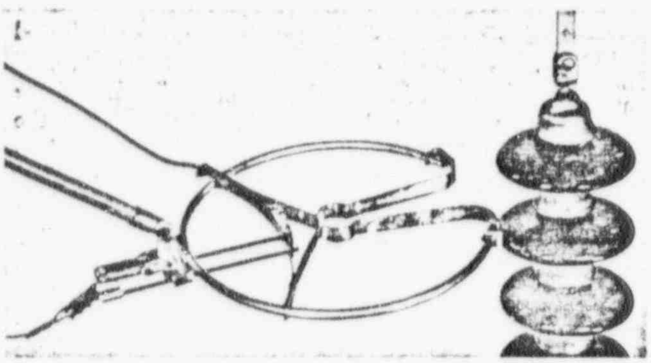

Fig. 4. Collector ring and hot-line tool

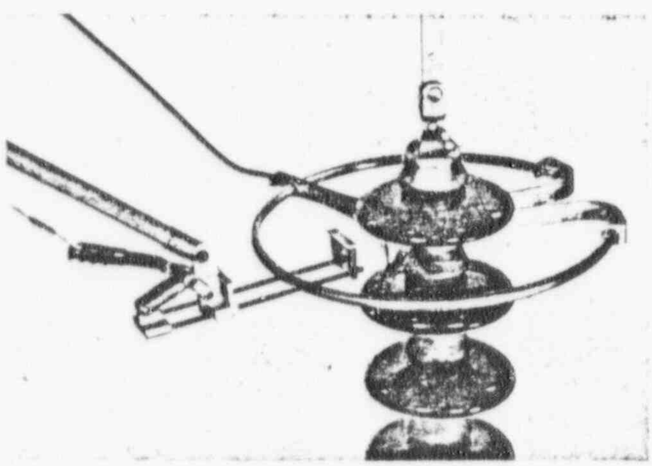

Fig. 5. Collector ring in position

the calculation of shielding failures which may account for the poor performance of certain EHV lines. It seems clear that a much more complete knowledge of the total mechanism of the lightning stroke is necessary for any meaningful advance in the engineering design of high-voltage lines for protection against lightning tripouts.

2. The AIEE method erred in assuming shielding failures as negligible with angles of 30 degrees or less. With our knowledge of shielding performance it may be wise to be cautious before dismissing backflash flashovers as being negligible.

3. Any feasible method of reliably assigning every flashover to a backflash category or a shielding failure category would not only yield results of immediate value in terms of design evaluation but would also provide a basis for adjustment of the lightning stroke model to account for the experimental facts. The authors urge the industry to support a cooperative field investigation of sufficient scope to yield adequate data.

4. The present paper describes a low-cost device which can readily and safely be installed on transmission lines and which is capable of yielding seven responses from three visual signals. Athough this device operates on a "one-shot" basis, spent units can easily be replaced on lines with high data potential.

References

1. A Method of Estimating Lightning Performance of Transmission Lines, AIEE Committee Report. *AIEE Transactions*, vol. 69, pt. II, 1950, pp. 1187–96.

2. The Relation Between Stroke Current and Velocity of the Return Stroke, C. F. Wagner. *AIEE Transactions*, pt. III (*Power Apparatus and Systems*), vol. 82, Oct. 1963, pp. 601–08.

3. The Lightning Stroke as Related to Transmission Line Performance, C. F. Wagner. *Electrical Engineering*, vol. 82, May 1963, pp. 339–47; pp. 388–403.

4. Performance of 161-Kv and 115-Kv Transmission Lines, Fred Chamber, C. P. Almon, Jr. *AIEE Transactions*, pt. III, vol. 81, Oct. 1962, pp. 431–59.

5. Mechanism of Breakdown of Laboratory Gaps, C. F. Wagner, A. R. Hileman. *Ibid.*, vol. 80, Oct. 1961, pp. 604–18.

6. Mechanism of Lightning Flashover Research, E. R. Whitehead, L. S. Van Slyck. *Report of Project No. E8004*, I.I.T. Research Institute, Sept. 1963.

Discussion

C. F. Wagner (Westinghouse Electric Corporation, East Pittsburgh, Pa.): It is very encouraging to note the recognition of the need for field work to determine directly the degree of shielding afforded by overhead ground wires. It is also gratifying that some steps have been taken to implement such field work. The results of such investigations, in order to be really meaningful, must be carried out by instrumentation and deductions which are unquestionable. This is particularly important because of the great expense of instrument manufacture and field installation and supervision.

One factor in the assumption of the authors should be given further consideration. The authors state quite correctly that 90 to 95% of all lightning strokes to earth lower negative charge and imply thereby that the number of shielding failures should also be accurate within these limits. This conclusion might be correct if the same percentage applied over the entire range of lightning stroke currents, but since in high-voltage lines it is usually the very high stroke currents that produce backflashes, the analysis of the percentage of negative strokes should be directed to the high values for which the value of 90 to 95% may not apply.

Of greater importance is the assumption that if the polarity of the stroke itself is known, then from the polarity of the impulse current flowing through the insulator flashover it is possible to discriminate between a shielding failure and a backflash. This would be true according to generally accepted theories in which the effects of predischarges are neglected, but predischarges can have a very important effect. Consider the case of a negative stroke of high current value to midspan. The potential from the ground wire to the conductor rises above the value at which channels form in the discharge between them. Because of the great length of the distance for which the ground wire and conductor are parallel, the currents that flow through this discharge attain large values. By the time the head of the wave reaches the tower, large currents are flowing in the conductor. But if the tower footing is low the tower top is held at substantially ground potential and the conductor rises to a high negative value relative to the tower top. In the usual constructions the insulation level of the insulator string may be only a quarter of that of the distance between the ground wire and conductor at midspan, and flashover of the insulator string may occur. The resultant polarity of the current that flows across the insulator string is of the same polarity as that which would result for a stroke to the conductor. For a stroke to midspan the measured polarity does not provide a proper discrimination between a shielding failure and a backflash.

H. R. Armstrong and E. R. Whitehead: We appreciate the discussion of our paper very much. Mr. Kalb has asked about the tests made on the device. The Pathfinder model described in the paper was a developmental model intended primarily to demonstrate the feasibility of such an instrument. The lowest current was about 2.3 crest kiloamperes, the signal duration approximately 7 microseconds, and the upper limit of current used about 90 kiloamperes. Within these limits no polarity discrimination failures were experienced. The parameters of the circuit have not yet been optimized, and this remains a task in connection with the production prototype now being designed.

Dr. Wagner cautions that predischarge current to the phase conductor caused by a stroke to midspan may cause insulator flashover and incorrectly signal a shielding failure. While we have given some thought to such streamer currents, it may well be that more careful consideration is required to guard against them. We believe there are three reasons why the probability of misinformation from this source can be made sufficiently small:

1. For normal spans, the duration of insulator voltage should be of the order of 1 microsecond and the insulator sparkover voltage would be quite high.

2. Perhaps fewer than one-half the strokes to the ground wire can be considered as terminating in the critical region.

3. Time discrimination for the negative current indicator can provide a delay in the order of 10 microseconds at an acceptable incremental cost.

If suitable time discrimination is employed, the false signal can be avoided and reliance is then placed on the power follow signal in the same manner as indicated in the signal chart of the paper.

During the program of the investigation leading to the paper, many circuits were devised to provide varying degrees of discrimination. One such circuit included a linear resistor and a parallel indicator branch designed to operate only at a predetermined magnitude of current irrespective of polarity. In the interest of reduced cost and complexity this additional indicator was discarded.

We would very much appreciate Dr. Wagner's estimate of the order of magnitude of the predischarge currents which were discussed.

Calculating Loss Reduction Afforded by Shunt Capacitor Application

R. F. Cook, Member IEEE

Many papers have been written and much controversy exists concerning the correct technique for evaluating losses in power distribution systems. One of the greatest bones of contention concerns the loss reduction afforded by application of shunt capacitors. Some points of dispute arise from different economic and operating principles governing the operation of various electric systems. Other points represent differences of opinion between engineer-economists.

No matter how the loss reduction afforded by shunt capacitors is evaluated, assuming the losses are worth something, one common step must be taken; the amount of loss reduction, peak losses and energy losses, must be calculated. This calculation is the subject of this paper.

Most but not all previous papers, including those for *AIEE Transactions*, which studied the application of shunt capacitors to distribution systems, have used an incorrect method of calculating the energy loss reduction, some authors calling it an approximation, which it is not. Approximate data—which is all that is usually available—may be used in an incorrect calculation and may result in a correct or approximate answer, but this is sheer luck. Moreover, use of the particular incorrect calculation shown in the next section cannot be justified on the basis of less effort because the correct calculation is almost as simple as the incorrect. This will be shown.

Paper 64-60, recommended by the IEEE Transmission and Distribution Committee and approved by the IEEE Technical Operations Committee for presentation at the IEEE Winter Power Meeting, New York, N. Y., February 2-7, 1963. Manuscript submitted November 4, 1963; made available for printing December 6, 1963.

R. F. Cook is with the Westinghouse Electric Corporation, East Pittsburgh, Pa.

Example of Incorrect Loss Reduction Calculation

A simple hypothetical primary feeder circuit is shown in Fig. 1(A). Accepting the assumption that shunt capacitors affect

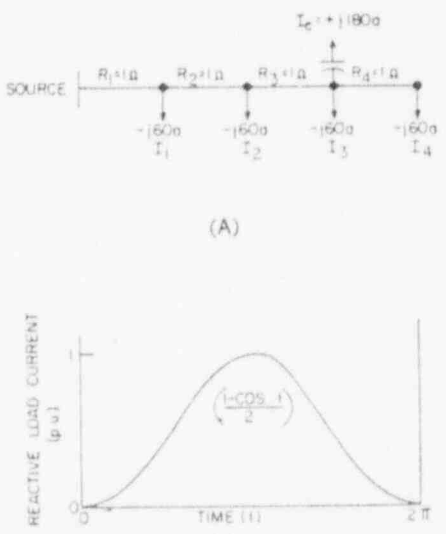

Fig. 1

A—Simple circuit with reactive load currents, capacitor current, and line section resistances

B—Reactive load cycle for loads of A

90004186

2) In some tests, we measured a current through a sample at the ground side. We found that the leakage current is very small, on the order of less than a few mA, except in the case of the snow test. Just before the occurrence of flashover, somewhat larger amounts of predischarge current may appear, but the large capacitance in the loading capacitor prevented this from being a problem. We encountered no difficulty with voltage regulation, except in the case of the snow tests. H. L. Hill in his report[4] stated that "the current surging seldom exceeds 3 mA until immediately prior to flashover on standard and semifog insulators." In the case of the snow test, the larger current capacity of the power source would give a lower flashover voltage.

3) In the case of dry or wet flashover tests, the applied voltage was kept about 85 percent of the sparkover voltage, and the remaining 15 percent was raised and dropped for each occurrence of flashover without interrupting the applied voltage. The voltage was controlled at the 50-cycle power source using a tap-changing transformer. One step of tap-changing resulted in a 5-kV change of the dc output.

It appears that the mean rate of voltage rise has little effect on flashover voltage when the maximum rate of voltage rise is in a range smaller than 5 kV/s.

4) No tests were performed using an instantaneously applied voltage.

5) Sparkovers sometimes take place across a pair of sphere gaps at an abnormally lower voltage, such as 80 percent of the standard value; however, it is not difficult to eliminate these abnormalities by the same method used for 50–60 cycle voltage calibration.

Although a pair of sphere gaps is not always an accurate measuring device for direct current, it is good for confirmation of the operation of modern measuring equipment. In the case of dc voltage measurement, any corona from the voltage divider would introduce a large error, because of the extremely high value of resistance. The use of sphere gaps is a good method to avoid an accidental error of voltage measurement.

References

[4] ASEA, Ludvika, Switzerland, Tech. Memo. 9535, September 13, 1966.

REF. 18

Field and Analytical Studies of Transmission Line Shielding

H. R. ARMSTRONG, FELLOW, IEEE, AND EDWIN R. WHITEHEAD, FELLOW, IEEE

Abstract—During the past two years, 4615 Pathfinder devices were installed on approximately 433 miles of EHV and EHV transmission lines suitably divided into sample classes for significant data yield.

Over approximately 70 percent of a full lightning season, 14 Pathfinder operations were recorded of which 12 were caused by lightning strokes to the top phase conductors and two resulted from a double-circuit fault caused by a stroke to the ground wire or tower.

Fifty transmission lines showing an average lightning trip-out rate of only 0.175 per 100 miles per year were considered effectively shielded over the sample period of 52 000 mile-years, and were accordingly analyzed for their average ground wire heights and average shield angles. The data were plotted by insulation levels and the results compared with the predictions of an analytical model developed to serve as an extrapolating device to relate field experience to the design of new lines. Important parameters of the model were determined by calibration against the field data.

It is concluded that terrain factors, as determined by the actual line profile, are of major significance and must be carefully considered in establishing effective conductor and ground wire heights.

While the analytical model is theoretically capable of extension to the prediction of trip-out rates for partially effective shielding, it is concluded that more data are needed before this can be done with satisfactory confidence.

Paper 31 TP 67-103, recommended and approved by the Transmission and Distribution Committee of the IEEE Power Group for presentation at the IEEE Winter Power Meeting, New York, N. Y., January 29–February 3, 1967. Manuscript submitted October 31, 1966; made available for printing November 21, 1966.

H. R. Armstrong is with the Detroit Edison Company, Detroit, Mich.

E. R. Whitehead is with the Illinois Institute of Technology, Chicago, Ill.

A REPORT has been previously made[1] on the Pathfinder research program which was designed to study the mechanism of lightning strokes to transmission lines. The investigation is still in progress in the third, or data-gathering phase, and will not be completed for several years. It seems timely, however, to report on the progress of the field investigation and the parallel analytical studies. This paper will discuss

1) the final form of the Pathfinder shielding failure indicator
2) the interpretation of the Pathfinder signals
3) a description of the transmission line samples studied
4) a summary of the Pathfinder operations to date
5) the development of an analytical system model consisting of the lightning stroke, the transmission line tower and conductors, and the surrounding terrain. The model is then used as a correlating and extrapolating mechanism to relate line performance to the characteristics of the lightning stroke. The model is also useful in interpreting Pathfinder data.

The final form of the Pathfinder instrument installed in the field differs in detail, though not in function, from that described before.[1] Fig. 1 shows the circuit diagram of the production device, while Fig. 2 shows an installation on a 345-kV transmission tower.

The device operates only upon complete flashover across the insulator string when the flashover current path to ground is intercepted by the current collector ring normally mounted on the ground-end insulator unit. It is simplest to explain the operation using electron flow as negative current. If the collector ring receives electrons or negative current from the phase conductor as a result of a shielding failure, the silicon carbide voltage-limiting element transmits a voltage signal by way of the dropping

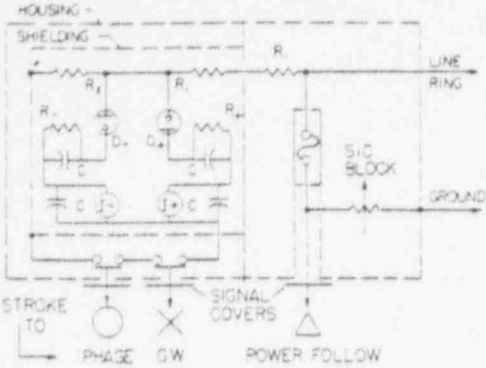

Fig. 1. Circuit diagram of Pathfinder.

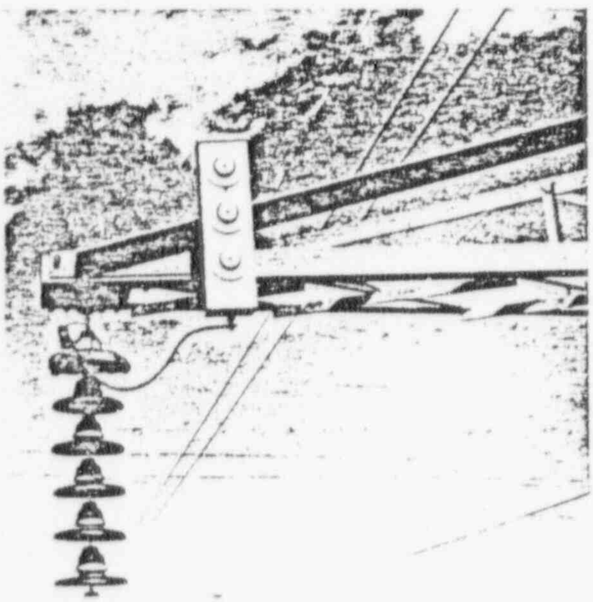

Fig. 2. Pathfinder installation on a 345-kV tower.

resistor R_1 to the sensing system tapped at R_2. The negative current enters dioide D(−) and is rejected by diode D(+). If the time duration of the signal is under 3 μs the indicator current drops very rapidly as this time approaches zero. Corona and small streamer currents will not operate the indicator. On the other hand, the response drops somewhat more slowly as the duration increases above 20 μs so that power frequency current will not operate the surge current indicator. Thus, with current in the operating range, the electro-explosive "squib" I(−) absorbs sufficient energy to activate the detonating charge and expel the aluminum disc covering the red disc signal on the exterior of the instrument housing. In doing so, the interlock circuit is opened, preventing any subsequent surge operation. Should system fault current follow the initial impulse flashover across the insulator string, the expulsion fuse in series with the voltage-limiting element is activated, and the disc covering the black triangular power-follow signal is expelled to reveal this signal in addition.

If lightning strikes the tower or ground wire and an insulator flashover ensues, electron current enters the grounded housing and passes through the voltage-limiting element to the collector ring and then to the phase conductor. This current is much less than that for a stroke to the conductor because a surge impedance of the order of 200 ohms is in parallel with the tower impedance. Here the nonlinear character of the current shunt permits sufficient voltage to activate the I(+) squib by way of the diode D(+) provided the current duration exceeds the intentional time delay. Tests indicate a current threshold of approximately 3–4 kA, providing further insurance against spurious operation.

The functions of the Pathfinder device are to signal the probable point of stroke termination, either phase conductor or shielding system, for each instrumented insulator string flashover and to signal the presence or absence of power follow.

Most of the Pathfinders are installed on the two top phases of double-circuit vertical-configuration towers. In Table I several single and multiple signals are interpreted. For a complete and more accurate analysis of the signals it is necessary to know the tower footing resistance, the phase sequence of the circuits, and the relay and circuit breaker operating records.

The selection of the lines for a shielding efficiency study is of great importance because line performance governs the quality and quantity of the expected data. Accordingly, the structural and electrical features of 45 selected steel-tower lines were examined, and three classes of line samples were established together with an approximate mileage needed for each class. These sample classes are defined in broad terms in Table II.

TABLE I

SIGNAL CODE WITH PROBABLE INTERPRETATIONS

Red Disc Circuit 1	Red Disc Circuit 2	Green Cross Circuit 1	Green Cross Circuit 2	Black Triangle Circuit 1	Black Triangle Circuit 2	Signal Interpretation
X						Stroke to conductor without power follow
X				X		Stroke to conductor with power follow
		X				Stroke to ground wire without power follow
		X		X		Stroke to ground wire with power follow
		X	X	X		Stroke to ground wire, double-circuit fault, no power follow
		X	X	X	X	Stroke to ground wire, double-circuit fault with power follow
				X		Stroke to ground wire; conductor current below surge threshold
X		X				Stroke to no. 1 backflash on no. 2 without power follow
X			X	X	X	Stroke to no. 1 backflash to no. 2 with power follow
X	X			X	X	Stroke (+) of high current to ground wire with power follow
						Single-conductor or circuit events may similarly initiate on no. 2

TABLE II

CLASSES OF TRANSMISSION LINE SAMPLES

Sample Class	Line Voltage, kV	Shield Angle, degrees	Trip-out Rate	Mileage Needed	Number of Towers
A	110–138	45 (or more)	6–18	150	980
B	330–345	25–35	4–10	150	720
C	110–138	10 (or less)	2–6	150	1000
			Totals	450	2700

90004188

TABLE III

ANTICIPATED DATA YIELDS

Sample Class	Miles	Years	Rate	Lines With Favorable* Trip-out Rates 50 Percent certainty	Lines With Favorable* Trip-out Rates 90 Percent certainty	Rate	Lines With Unfavorable Trip-out Rates 50 Percent certainty	Lines With Unfavorable Trip-out Rates 90 Percent certainty
A	150	5	0.10	75	64	0.06	45	37
	150	6	0.10	90	79	0.06	54	46
B	150	5	0.07	52	43	0.04	30	23
		6	0.07	63	55	0.04	36	28
C	150	5	0.04	30	23	0.02	15	10
		6	0.04	36	28	0.02	18	13
Total Records				157–189	136–162		90–108	70–87
Years				5–6	5–6		5–6	5–6

* For study purposes a favorable rate is a high number of lightning trip-outs per 100 tower line miles per year.

TABLE IV

SUMMARY OF PATHFINDER OPERATIONS TO OCTOBER 15, 1966

Company	Line, kV	BIL, kV	$\hat{H}$, feet	$\hat{Y}$, feet	$\hat{\theta}$, degrees	Tower Number	Signals Red	Signals Green	Signals Black	Trip-outs Yes	Trip-outs No	Fault Type
A	120	790	67	58	44	200	X		X	X		L-G
A	120	790	67	58	44	201	X		X	X		L-G
A	120	790	67	58	44	202	X		X	X		L-G
A	120	790	67	58	44	271	X		X	X		L-G
A	120	790	67	58	44	272	X		—	X		L-G
A	120	790	67	58	44	312	X		—		X	L-G
B	115	690	83	71	43	99	X		X	X		L-G
B	115	690	70	58	45	100	X		—	X		L-G
B	115	690	70	58	45	101	X		X	X		L-G
C	115	790	65	56	63	85	—	X	Double	X		L-G
C	115	790	65	56	63	85	—	X	Circuit	X		L-G
D	345	1600	129	102	33	53	X		X	X		L-G
D	345	1600	129	102	33	79	X		X	X		L-G
D	345	1600	120	102	33	106	X		X	X		L-G

Note: These data reflect approximately a 70-percent installation for one lightning season.

Anticipated data yields, computed from standard Poisson tables, are given in Table III.

To determine whether actual outage experience over 5-year periods conforms approximately to mathematical expectations, an analysis was made of about 2600 mile-years of transmission line operation reported in the literature. It was found that the actual performance experienced either agreed reasonably well with the theoretical variability of 5-year samples or was more consistent than expected. This comparison lent credence to the basis on which Table III was prepared. The conclusion drawn from the statistical review was that, if lines with favorable trip-out rates could be obtained as samples, the desired number of approximately 100 records would be virtually certain in five years. On the other hand, if only samples with unfavorable rates were available, there would still be about an even chance of securing the desired data in five or six years. When all factors were considered, including the cost of the production Pathfinder, the final field installation included 4615 instruments distributed over 433 miles of transmission line in three categories as outlined before. The instruments were distributed among 12 participating companies located in a rectangle bounded by Florida, New England, Texas, and Colorado. Table IV summarizes the Pathfinder operations to October 15, 1966.

The first 285 Pathfinder units in service in 1965 were installed on 25 miles of Detroit Edison Company 120-kV lines with a shielding angle of 45 degrees. The installation was less than a month old when a reasonably severe thunderstorm over the line yielded four indications of insulator flashover due to strokes to a phase conductor. It was possible to relate power follow indications to circuit breaker operations—a good omen for a successful project.

ANALYTICAL MODEL

While attempts to quantify transmission line shielding theory are not new,[8]–[4] none of the preceding models has seemed fully satisfactory as a means of coordinating the performance of existing transmission lines with those characteristics of the lightning stroke which appear applicable. The model presented here has been useful in several directions, but it, too, must be considered a tentative step which may well be modified substantially as new data are evaluated. One important advantage of even a tentative model is that it classifies and separates the variables so that attention can be focused on its defects. It is with the foregoing firmly in mind that the following model is presented.

In the use of geometrical quantities, the term *effective* means that quantity which, when employed in the model, characterizes

90004189

the variable in the field. Usually this really means an average value. In the use of electrical or electrogeometrical quantities such as voltage, current, or strike distance, the term employed for the same purpose will be the *expected* value. In the latter case it is usually meant that the deviations from the expected value are really not known. In both cases, however, the superscript bar will be employed to designate such quantities.

Geometry of Shielding

Fig. 3 illustrates the geometry of shielding for a single-circuit horizontal configuration of phase conductors w and x, shielding conductors s at an average angle $\bar{\theta}_s$ with respect to the phase conductor, and their respective average heights above earth. Although transverse slope of the earth is easily incorporated into the model, it is omitted here in the interest of simplicity. The arcs centered on the ground wires with strike radius $\bar{r}_{ss}$ and the horizontal line through y_1 represent the intersection of the shielding surfaces with the plane of the paper, while the arc $y_1x_2y_2$ represents the intersection of the exposed surface. The phase conductor w is the origin of polar coordinates and counter-clockwise angles are positive. For convenience in subsequent reference, the leader terminating on the exposure arc above the horizontal is designated type 1 exposure, while that terminating on the portion of the exposure below the horizontal is designated type 2 exposure.

Effective Shielding

The expected exposure is clearly reduced to zero when the triangle wy_1s of Fig. 3 is rotated clockwise about the origin to make $\bar{\theta}_1 = \bar{\theta}_2$, as is depicted in Fig. 4. Analysis of these figures will show that zero exposure for one outside phase conductor results when:

$$\bar{\theta}_s \leq \bar{\theta}_1 - \bar{\beta} \tag{1}$$

$$\bar{\theta}_1 = \sin^{-1}\left[K_{sg} - \bar{y}/\bar{r}_{ss}\right] = \bar{\theta}_2 \tag{2}$$

$$\bar{\beta} = \sin^{-1} \bar{c}/2\bar{r}_{ss} \tag{3}$$

which hold for the assigned expected strike distances

$\bar{r}_{ss}$—expected strike distance from the leader core to the shield wires.

$\bar{r}_{sg} = K_{sg}\bar{r}_{ss}$—expected strike distance to earth.

(A complete list of symbols will be found in Appendix I.)

The strike distance is here taken as

$$\bar{r}_{ss} = K_{rs}I_0^{s} \tag{4}$$

where I_0 is the lightning stroke current to a zero-resistance ground and K_{rs} and s are constants to be developed. The strike distance $\bar{r}_{ss}$ cannot really be considered an invariable value for an assigned value of current, but there is presently little to assist in determining its deviation.

In the derivation of (4), first associate a leader voltage V_s with the stroke current I_0 and next associate a strike distance with V_s. In recent years there have been various approaches to the first step,[5]-[6] and the latest data on switching surge strike distances[7]-[8] aid in the second step. Regardless of the approach adopted, the stroke voltage–current relation requires very great simplification of the electrogeometry to afford tractable solution, and the voltage–distance relation requires very great extrapolation of available test data. For these reasons, the justification for any analytical approach can only lie in a demonstrated usefulness in describing actual line performance and in indicating directions in which to proceed to improve the model.

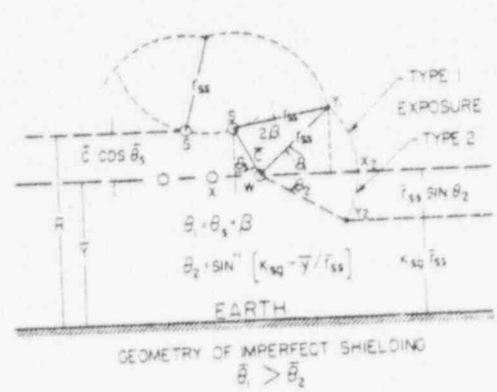

Fig. 3. The geometry of shielding.

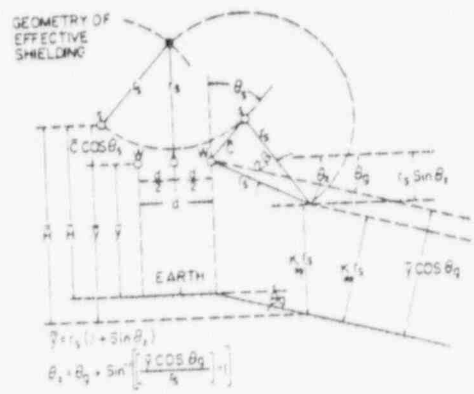

Fig. 4. The geometry of effective shielding.

With the foregoing in mind, the Wagner[6] stroke model is then employed in the following form:

$$V_s = 60\,(I_0/v_1)\ln(2\bar{r}_{sg}/d) \tag{5}$$

where

- V_s leader voltage, kV
- I_0 stroke current to zero resistance earth
- v_1 velocity of return channel in per unit velocity of light
- $\bar{r}_{sg}$ strike distance to ground
- d expected corona radius of the leader at heights well above $\bar{r}_{sg}$.

Since V_s depends on $\bar{r}_{sg}$ and $\bar{r}_{sg}$ depends on V_s, trial solutions are necessary to proceed. Because both $\bar{r}_{sg}$ and d increase with V_s, the logarithmic factor varies very slowly, and a value of 4.6 has tentatively been selected for it.

Within the appropriate accuracy requirements, the various relations which have been proposed for the relation between the current I_0 and the return channel velocity v_1 may be represented by

$$I_0 = K_i v_1^{q}. \tag{6}$$

Among the several relations investigated, the relation

$$I_0 = 2400\,v_1^{3} \text{ or } v_1 = I_0^{1/3}/13.4 \tag{7}$$

has been tentatively adopted as a useful compromise. Substitution of (7) in (5) gives

$$V_s = 3.7\,I_0^{2/3} \text{ MV for } I_0 \text{ in kA.} \tag{8}$$

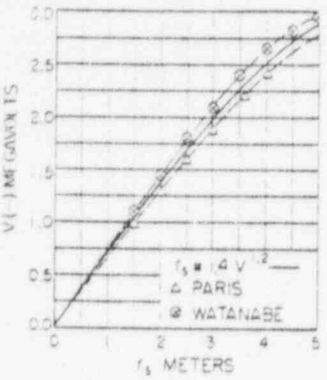

Fig. 5. Point-point sparkover distance for negative polarity switching surges.

To determine the strike distance, there is no recourse but to extrapolate the laboratory strike distances for the highest voltages available. Fig. 5 shows the relatively close agreement between the data of Paris[6] and Watanabe.[7] The mean of these data is given by the solid line, empirically given by

$$r_s = 1.4 V_s^{1.2} \tag{9}$$

for V_s in megavolts and r_s in meters.

Substituting (8) into (9), the desired distance–current relation becomes

$$r_{ss} = 1.4 \times 3.7^{1.2} I_0^{(2\times1.2)/3} \tag{10}$$

$$r_{ss} = 6.72\, I_0^{0.8} \text{ meters}$$

$$r_{ss} = 22\, I_0^{0.8} \text{ feet.}$$

The critical lightning current which can be accepted by the phase conductor without insulator flashover is given by

$$I_c = 2E/Z = \frac{\text{basic insulation level in kV}}{\text{one half the conductor surge impedance}} \tag{11}$$

where the surge impedance Z is determined by the usual methods taking into account the presence of the ground wires.[8] For estimating purposes, the following tabulated values are useful as applying to HV and EHV lines.

Conductor	One Half Z, ohms
Four-bundle	160
Two-bundle	180
Single (EHV)	200
Single (HV)	220

I_0 is slightly greater than I_c and a correlation curve may be used if desired (see Fig. 11).

Terrain Parameters

The geometry of shielding requires the use of certain effective parameters which can be determined from existing or proposed tower design and line profile. The effective conductor and shield wire heights must not only take into account their respective sags, but also the "earth sag" as determined from the profile of the line. These considerations are shown in Fig. 6 where, for estimating purposes, flat, rolling, and mountainous terrains are defined. In the field research program, each individual shielding failure event is analyzed in terms of the profile on both sides of the tower involved. The conductor and shieldwire heights averaged for these adjacent spans are then used, together with the tower configuration, to determine the effective separations and angles. Theoretically, the analytical model provides for a sloping earth plane. Examination of numerous lines, however, shows that the longitudinal profile is by far the controlling factor in transmission line shielding.

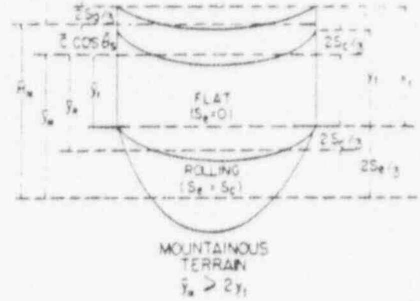

Fig. 6. Terrain and structural parameters.

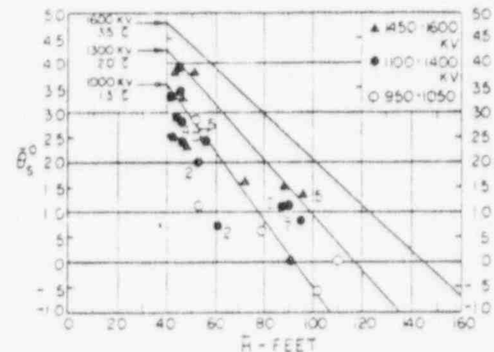

Fig. 7. Effective shield wire height vs. effective shielding angle for 50 lines showing superior performance.

TABLE V
DATA FOR FIFTY TRANSMISSION LINES SHOWING SUPERIOR PERFORMANCE*

Characteristic	Minimum	Average	Maximum
Lightning trip-outs for 100 miles per year at 40 T.D.†	0.00	0.175	0.50
Experience per line in mile-years	210	1040	6500
BIL, kV	950	1300	1625
Average ground resistance in ohms (35 lines)	2	23	94
Total mile-years: 52 000			

* From Chambers and Almon[10] and Ohio Brass Company.[11]
† Thunderstorm days.

Calibration of Analytical Model

It has been pointed out earlier that any model must satisfactorily account for the good or poor performance of existing lines. On one hand, the model may be "calibrated" by examining the geometry of high-performance lines and comparing it with analytical results. On the other hand, it is necessary to compare the analytical results with conditions known to produce shielding failure. Such conditions are evidenced by the corresponding type of Pathfinder operation. In the final analysis, therefore, the param-

90004191

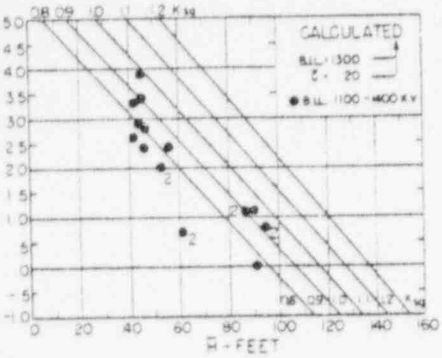

Fig. 8. Tentative calibration of K_{sg} using a subgroup of lines from Fig. 7.

eters of the model must be adjusted so as to provide the fullest possible agreement with field experience. Adjustments must be made with maximum objectivity and within the context of known theoretical considerations, so that they do not obscure basic defects in the model.

Fig. 7 shows the height-angle characteristics of 50 transmission lines showing superior lightning performance as indicated in Table V. The total experience sampled in this table is 52 000 mile-years. While common practice in the United States has been to refer performance to a level of 30 thunderstorm days (T.D.) per year, these data have been adjusted to 40 T.D. to minimize the possibility that linear correction over the wider range might be invalid.

The solid lines of Fig. 7 have been calculated from the analytical model for the three groups of lines as indicated by the symbol code. It is important to note that a given line may, of course, have an effective shield angle well below its critical value, so the upper envelope of the points in each group carries the essential information with which to compare the lines. K_{sg} has been taken as 0.9 in these calibrations.

At the suggestion of Dr. R. H. Golde, the model has been modified to permit a difference in the sparkover-distance relation for leader to ground wire or tower (nominally point-point) and for leader to ground (nominally point-plane). It is by no means clear that laboratory differences in point-point and point-plane extend to the actual situation in the field. For example, in heavily wooded country, k_{sg} might actually be equal to or greater than unity.

Fig. 8 shows height-angle data for a reasonably homogeneous subgroup of Fig. 7. The solid lines have been calculated for several values of K_{sg}, and from this figure a value of $K_{sg} = 0.9$ has been tentatively adopted.

The line samples shown for Pathfinder installations have been selected primarily to detect both shielding and "backflash" events. Some attention has been given, however, to selecting sample lines whose configurations lie close to the critical one. By this means it is hoped to sharpen the determination of the model parameters when sufficient data become available. For the same reason, a limited number of instruments have been installed on the top and middle phases on one side of a double-circuit tower, and, in one case, top and middle phases on both sides of the double-circuit tower have been instrumented for a limited distance in mountainous terrain. The lines contributing the data in Table IV all have effective shielding angles much greater than calculated by the present model, so that these data do not yet aid substantially in the calibration of model parameters.

Shielding Design

The authors feel that the data of Table V and Fig. 7 demonstrate that effective shielding can be and has been achieved in practical designs. For this reason it is recommended that design of the shielding system, that is, placement and spacing of the ground wires, be predicated on zero expectation of shielding failures. To design a tower line for a predetermined number of shielding failures is vastly more complicated and cannot be done to a satisfactory degree of confidence at this stage of the art. The reasons for this conclusion stem from the fact that, since the parameters have been selected for expected perfect shielding, no measure is yet available for deviations from their mean values. On the other hand, deviations in thunderstorm days, stroke density per storm, and leader angles are eliminated from consideration. Some of the problems associated with partially effective or imperfect shielding are discussed in the following.

Partially Effective Shielding

Extension of the analytical model to partially effective shielding, while theoretically straightforward, involves numerous uncertainties, statistical variations, and necessary assumptions. Nevertheless, the extension is essential to use fully the data anticipated from the field study, since most of the sample lines are obviously only partially shielded.

Fig. 3 shows that conductor w has an exposure arc $Y_1X_2Y_2$. Leader angles other than zero referred to the y axis can result in type 1 or type 2 intersections. Since the shielding geometry is expressed in trigonometric form, it is advantageous to postulate a probability density function

$$f(\alpha) = K_m \cos^m \alpha \tag{12}$$

so that the probability of finding a leader in the angle range α_1 to α_2 is

$$P_{\alpha_1}^{\alpha_2} = \int_{\alpha_1}^{\alpha_2} K_m \cos^m \alpha \, d\alpha$$

with

$$\int_{-\pi/2}^{+\pi/2} K_m \cos^m \alpha \, d\alpha = 1 \tag{13}$$

so that the normalizing constant K_m becomes

$$K_m = 1 / \int_{-\pi/2}^{+\pi/2} \cos^m \alpha \, d\alpha.$$

The meaning of the constants K_m and m is illustrated by the probability curves of Fig. 9. As m and K_m approach infinity

$$P_{\alpha_1}^{\alpha_2} \rightarrow \int_{\alpha_1}^{\alpha_2} \delta(\alpha) \, d\alpha = 1 \text{ for } \alpha_1 < 0 < \alpha_2 \tag{14}$$

where $\delta(\alpha)$ is the unit impulse of α.

Preliminary evaluation of the performance of partially shielded lines suggests that m may lie between 1 and 2 with values near 2 more probable. Further detailed study of the calculations for partially shielded lines is beyond the scope of the present paper, but the process involves evaluation, using suitable trigonometric substitutions for x, of integrals of the form

$$\int_{r_{st}}^{R_c} P(r) \int_{-\infty}^{+\infty} K_m \int_{\alpha_1(x,r)}^{\alpha_2(x,r)} \cos^m \alpha \, d\alpha \, dx \, dr. \tag{15}$$

In practice, the outer integral will be evaluated from the lower critical value r_{st} to the upper critical value R_c (at which the ex-

90004192

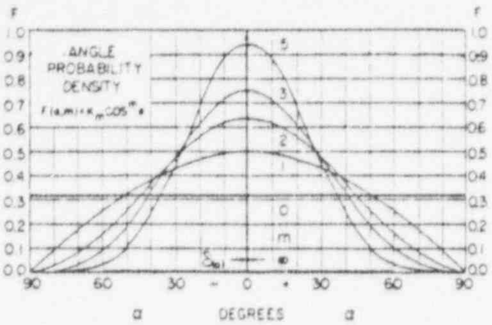

Fig. 9. Leader angle probability density curves.

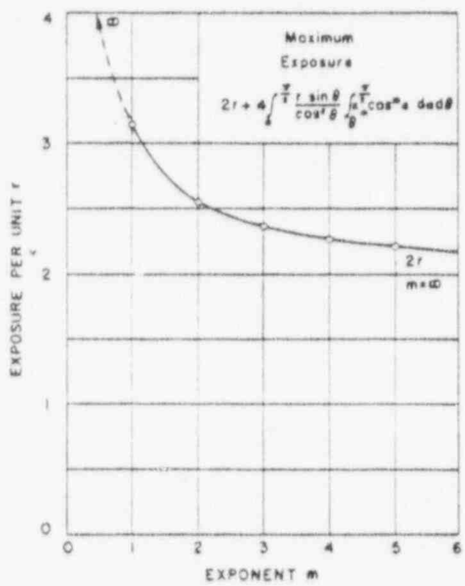

Fig. 10. Maximum exposure for a single strike radius r and $y = 2r$.

posure becomes zero) by summation using

$$P(r)\Delta r = P(i)\Delta i \tag{16}$$

where

$$r = 22i^{0.8}$$

and the probability density function $P(i)$ is adopted from the AIEE or more suitable current-probability curves.[12] For present purposes it has been found useful to take the probability density function as

$$P(i) = 4.75\epsilon^{-i/20} + 0.10\epsilon^{-i/80} \text{ percent} \tag{17}$$

where i is in kiloamperes and the increment Δi has been chosen as

$$\Delta i = 2 \text{ kA for } i < 10 \text{ kA.}$$
$$\Delta i = 5 \text{ kA for } i > 10 \text{ kA.}$$

For distributions other than those of the AIEE report,[12]

$$P(i) = K_1\epsilon^{-i/I_1} + K_2\epsilon^{-i/I_2} \tag{18}$$

will also be found useful.

As a clue to the possible values of the angle distribution exponent m, Fig. 10 shows the result of evaluating the α and x integrals for one value of the radius r and an unshielded conductor at a height $y = 2r$. The figure shows that these integrals are not convergent for $m = 0$ so this is not a valid exponent. As m approaches infinity the curve approaches the value $2r$ as the necessary exposure for all-vertical strokes.

When sufficient data become available from the various field installations of the Pathfinder instrument, it is hoped that more accurate analysis of the leader angle effect will be possible along the lines illustrated in Appendix III.

Conclusions

1) During approximately a 70-percent lightning season, 14 Pathfinder operations have been obtained on an indicated nine separate strokes. Eight of these strokes were indicated as strokes to the phase conductor, and one was indicated as a stroke to the ground wire which resulted in a double-circuit fault.

2) An analytical model has been developed which appears capable of correlating the more important factors affecting the shielding of transmission lines from strokes to the phase conductors.

3) Terrain factors are of major significance and must be carefully considered to determine the effective heights of the conductors and ground wires.

4) Fifty transmission lines having superior performance over an aggregate of 52 000 mile-years experience have been analyzed for effective shield angle and effective heights of conductor and ground wire as a means of calibrating some of the parameters of the analytical model. There is great need for extending this type of statistical study into more recent experience on EHV lines.

5) Design of EHV lines should be based on an outage expectation of zero, as determined by the correlating model of this paper or similar equivalent models.

6) The analytical model is capable of extension to the estimation of shielding failure trip-out rates resulting from partially effective shielding, and there are reasons to expect that progess can be made in this phase of the problem as data accumulate from the Pathfinder installations. The problem is complex, challenging, and interesting, but the relevant parameters require further study and evaluation.

7) Basic research on the plasma thermodynamics of the lightning stroke should be encouraged and supported, for new knowledge in this area will undoubtedly find early application to improved engineering models of the lightning mechanism.

Appendix I
Nomenclature and Terminology

General

- T.D. Thunderstorm days per year
- N Strokes to ground per square mile per year
- BIL Basic insulation level
- $P(r)$ Probability of strike radius r
- $P(i)$ Probability of stroke current i.

Electrogeometric and Electric

- V_s Leader voltage to ground, kV or MV
- I_0 Stroke current to zero resistance ground, kA
- I_c Critical current to conductor, kA
- ln Natural or Naperian logarithm
- v_1 Velocity of return channel in per unit v_0
- v_0 Velocity of light, m/s
- d Expected corona radius of leader
- E Line BIL, kV
- Z Surge impedance of line conductor struck
- $\bar{r}_{ss}$ Expected strike radius—leader to shield wire
- $\bar{r}_{sg}$ Expected strike radius to earth
- $\bar{r}_{sc}$ Expected strike radius to conductor ($\bar{r}_{sc} \cong \bar{r}_{sg}$)
- K_{sg} $\bar{r}_{sg}/\bar{r}_{ss}$
- K_m Angle probability density normalizing coefficient
- m Angle probability density exponent
- α Angle of leader from the vertical.

90004193

Terrain

- h_t Ground or shield wire height at tower
- y_t Conductor height at tower
- s_g Ground or shield wire sag
- s_c Conductor sag
- $\bar{H}$ Mean around wire height
- $\bar{y}$ Mean conductor height
- s_e Earth sag
- $\bar{\theta}_g$ Mean transverse ground plane angle from horizontal.

Flat terrain	Plane earth between tower footings
Rolling terrain	Earth sag equal to conductor sag
Mountainous terrain	Mean conductor height equal to or greater than twice that for flat terrain.

Geometrical

- $\bar{\theta}_s$ Mean value of shielding angle
- $\bar{\theta}_1$ Upper exposure angle (mean)
- $\bar{\theta}_2$ Lower exposure angle (mean)
- $\bar{c}$ Mean separation between shield wire and conductor
- $\bar{\beta}$ Angle whose sine is $\bar{C}/2\bar{r}_{ss}$
- b $\bar{C}\cos\bar{\theta}_s$ (mean shield wire superelevation)
- a $\bar{C}\sin\bar{\theta}_s$ (mean shield wire offset from conductor)
- x Distance from conductor at right angle to line.

Appendix II
Sample Calculations for Effective Shielding

A review of Olmstead[18] suggests the following typical values useful for preliminary design of structures for zero expectation of shielding failures:

Voltage Class, kV	BIL, kV	Z/2, ohms	$\bar{C}$, feet	I_c, kA	Notes
500	1800	160	35	11	4-bundle conductor
		180	35	10	2-bundle conductor
300–400	1600	180	30	9	2-bundle conductor
		200	30	8	single conductor
220–230	1400	200	25	7	
115–161	1000	200	20	5	

The following data refer to a proposed double-circuit 345-kV line, which will traverse virtually flat terrain, which has the following tentative electrical and structural characteristics:

Conductor sag S_c = 54 feet
Ground wire sag S_g = 36 feet
y_t = top conductor height at tower = 136 feet
$\bar{c}$ = mean separation—ground wire to conductor
$Z/2$ = one half conductor surge impedance = 180 ohms
BIL = 1600 kV and I_c = 1600/180 = 8.9 kA.

Estimate the location of the ground wire for zero expected shielding failures.

Step	Quantity	Source of Data or Calculation
1	I_0 = 10 kA	Fig. 11
2	r_{ss} = 139 feet	Fig. 12
3	y	$y = y_t - (2/3)S_c$ = 136–36 = 100
4	y/r_{ss}	100/139 = 0.720
5	$\bar{\theta}_1$ = 11.0°	To enter Fig. 13 if K_{sg} = 0.9
5	$\bar{\theta}_1$	Add 0.1 to 0.720 to get 0.82
6	$\bar{\beta}$	Enter Fig. 14 with
6	$\bar{\beta}$ = 7.2°	$\bar{c}/2r_{ss}$ = 35/278 = 0.126

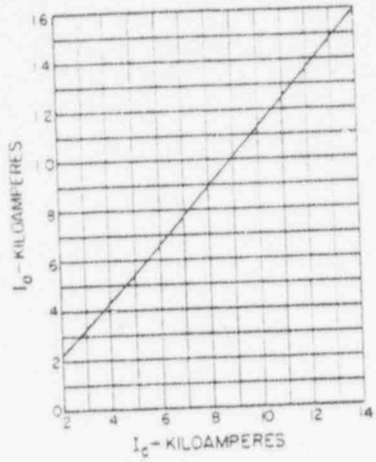

Fig. 11. Adjustment curve for determining I_0 from I_c.

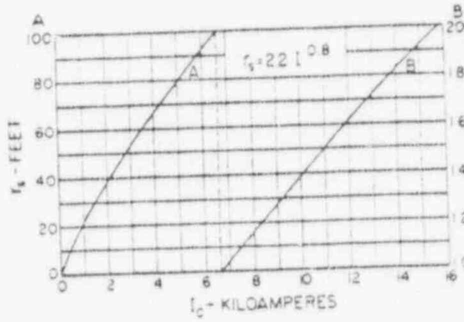

Fig. 12. Strike radius r_s as a function of I_0.

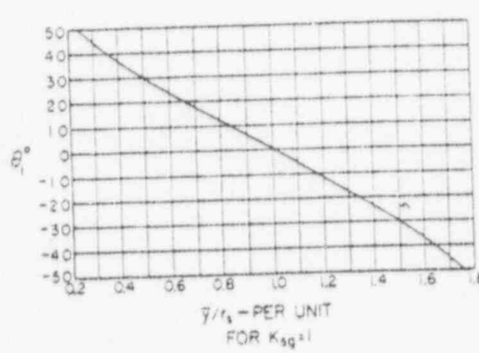

Fig. 13. The angle θ_1 as a function of y/r_s for K_{sg} = 1.0.

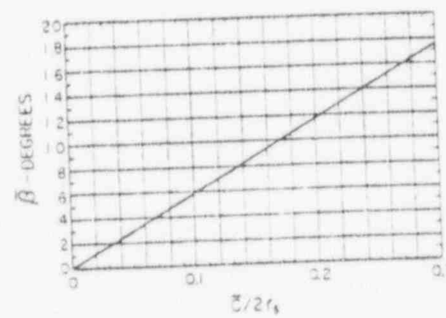

Fig. 14. The angle β as a function of $c/2r_s$.

7	$\hat{\theta}_s$	$\theta_s = 11.0° - 7.2° = 3.8°$
7	$\hat{\theta}_s = 3.8°$	
8	$\bar{b}$	$\bar{b} = \bar{c}\cos\hat{\theta}_s = 35$ feet
9	$\bar{H} = 135$ feet	$\bar{y} + \bar{b} = 100 + 35$
10	$\bar{H} = 135$ feet	Check from curve of Fig. 7
11	$h_t = 159$ feet	$h_t = H + 2/3\, S_g = 135 + 24 = 159$
12	$a_t = 2.45$ feet	$a_t = \bar{c}\sin\theta_s$
13	$b_t = 23$ feet	$b_t = h_t - y_t = 159–136$
14	$\theta_{st} = 6.1°$	$\theta_{st} = \arctan 2.45/23.$

Summary

$y_t = 136$ feet $h_t = 159$ feet
$\theta_s = 6.1°$ at the tower
$b_t = 23$ feet $a_t = 2.45$ feet (inboard)
$\hat{\theta}_s = 4°$ $\bar{H} = 135$ feet.

Appendix III
Application of Analytical Model to Imperfect Shielding

In the body and conclusions of this report it has been emphasized that additional and rather indefinitely-known parameters are necessary to permit estimation of trip-out rates from shielding failures to a satisfactory degree of confidence. Some of these are

1) N = number of strokes to ground per square mile per year. This number has been variously estimated from 10 to 15 for 30 thunderstorm days per year.

2) the leader angle probability density function $F(\alpha)$ which is here taken as

3) $K_m \cos^m\alpha = F(\alpha)$

4) the exponent m if this form of $F(\alpha)$ is satisfactory.

5) K_1, K_2, I_1, and I_2 if the probability density function for current has the assumed form

$$P(i) = K_1\epsilon^{-i/I_1} + K_2\epsilon^{-i/I_2}$$

6) the ratio (or relation) between N and the number of thunderstorm days (isokeraunic level)

7) unknown effects of stroke branching.

Despite the lack of precision in our knowledge of these parameters, it is useful to make reasonable estimates of their average values and to apply the analytical model to estimate the number of trip-outs caused by shielding failures for an assigned geometrical situation. These estimates can then be compared with the actual performance of the line over an extended period in the past and over the period of the Pathfinder field study.

The sample lines have been selected with a view to providing a range of height, angle, and terrain conditions so that, with sufficient data, one may hope to narrow the range of uncertainty to some degree. If parameters can be determined which enable the analytical model to meet the requirements of effectively shielded lines while accounting satisfactorily for the performance of partially shielded lines, a most useful result will have been obtained.

Table VI shows the steps by which the analytical model is applied for one of the 345-kV lines of the field study, but it is not presented as a "calculation" of the trip-out rate. For the purpose of this illustration the angle-exposure integrals have been evaluated for

$$F(\alpha,m) = 1/2\cos\alpha$$

$$K_m = 1/2$$

$$m = 1$$

TABLE VI
Illustrative Application of Analytical Model to Imperfect Shielding

Line	Item	Computations for $\bar{y} = 130$ $\bar{c} = 32$							Notes
1	Stroke current I_0	*9.0*	*12.5*	*17.5*	*22.5*	*27.5*	*32.5*	*37.5*	Kiloamperes
2	Probability $P(r)\,\Delta r$	6	13	10	9	6	5	4	Percent
3	Strike Distance r_{st}	127	166	217	264	312	356	400	Feet
4	Angle $\hat{\theta}_s$	33	33	33	33	33	33	33	Degrees
5	Angle $\hat{\beta}$	7.0	5.5	4.2	3.5	2.9	2.6	2.3	Degrees
6	Angle $\hat{\theta}_1$	40.0	38.5	37.2	36.5	35.9	35.6	35.3	Degrees
7	Angle $\hat{\theta}_1$	0.70	0.67	0.65	0.64	0.63	0.62	0.62	Radians
8	Angle $\hat{\theta}_2$	−7.2	6.6	17.2	24.0	29.2	32.1	35	Degrees
9	Angle $\hat{\theta}_2$	−0.125	0.115	0.30	0.42	0.51	0.56	0.61	Radians
10	Cosine $\hat{\theta}_2$	0.99	0.99	0.96	0.92	0.87	0.85	0.82	Units
11	Cosine $\hat{\theta}_1$	0.76	0.78	0.80	0.80	0.81	0.81	0.82	Units
12	Line 10 − Line 11	0.23	0.21	0.16	0.12	0.06	0.04	0.00	Units
13	Line 7 − Line 9	0.82	0.55	0.35	0.22	0.12	0.06	0.01	Radians
14	Line 12 + Line 13	1.05	0.76	0.51	0.34	0.18	0.10	0.01	Numeric
15	Line 3 Line 14/2	67	63	55	45	28	18	2	
16	$19N \times 10^{-3}$	0.190	0.190	0.190	0.190	0.190	0.190	0.190	
17	Line 15 × Line 16	12.7	12.0	10.4	8.6	5.3	3.4	0.38	
18	Line 17 × Line 2	76	156	104	77	32	17	1.6	
19	Summation Line 18								464
20	Trip-out rate for one side of line 464/100 = 4.64								
21	Trip-out rate for both sides of the line 2 × 4.64 = 9.28 for $N(30)(= 10)$								
22	Trip-out rate for both sides of the line at $N(30)(= 12.5) = 11.6$								
23	Trip-out rate for both sides of the lines at $N(30)(= 15) = 13.9$								
24	Actual trip-out rate = *9.17*, showing need for further investigation of model parameters.								

Note: Illustrated computation is for $N(30) = 10$ strokes per square mile per year and 100 percent rolling terrain. Line profile is estimated to be 75 percent flat, 16 percent rolling, and 9 percent mountainous. When adjusted for profile distribution and 35 thunderstorm days the results are as follows, for the indicated $N(30)$ values, $m = 1$, $K_m = 1/2$:

	$N(30) = 10$	$N(30) = 12.5$	$N(30) = 15$
Trip-out rate	7.8	9.8	11.7

yielding the result, for $2\bar{r}_{11}$ much larger than $\bar{c}$,

$$\text{Transverse exposure distance} = \frac{\bar{r}}{2}\left[\cos\hat{\theta}_2 - \cos\hat{\theta}_1 + \hat{\theta}_1 - \hat{\theta}_2\right]$$

which is evaluated in lines 12, 13, 14, and 15.

Acknowledgment

The authors wish to express their thanks to the Edison Electric Institute for the extensive support which has made this research possible and to the cooperating companies for their enthusiastic participation. Thanks are also extended to Dr. K. Berger, Dr. D. H. Baatz, and Dr. R. H. Golde for most helpful conferences and to G. Brown for verifying many of the analytical developments.

References

[1] H. R. Armstrong and E. R. Whitehead, "A lightning stroke pathfinder," *IEEE Trans. Power Apparatus and Systems*, vol. 83, pp. 1223–1227, December 1964.

[2] R. H. Golde, "The frequency of occurrence and the distribution of lightning flashes to transmission lines," *Trans. AIEE*, vol. 64, pp. 902–910, 1945.

[3] F. Schwab, "Lightning proof overhead lines," *Bull. S.E.V. (Switzerland)*, vol. 55, pp. 87–90, 1964.

[4] F. S. Young, J. M. Clayton, and A. R. Hileman, "Shielding of transmission lines," *IEEE Trans. Power Apparatus and Systems (Supplement)*, vol. 83, pp. 132–154, 1963.

[5] R. H. Golde, "Theoretical considerations on the protection of lightning rods," *ETZ-A*, vol. 82, pp. 273–277, 1961.

[6] C. F. Wagner, "Relation between stroke current and the velocity of the return stroke," *IEEE Trans. Power Apparatus and Systems*, vol. 82, pp. 609–617, 1963.

[7] Y. Watanabe, "Switching surge flashover characteristics of extremely long air gaps," presented at the IEEE Summer Power Meeting, New Orleans, La., July 10–15, 1966.

[8] L. Paris, "Influence of air gap characteristics on line to ground switching surge strength," presented at the IEEE Summer Power Meeting, New Orleans, La., July 10–15, 1966.

[9] L. V. Bewley, *Travelling Waves on Transmission Systems*. New York: Wiley, 1951.

[10] F. Chambers and C. P. Almon, Jr., "Performance of 161-kV and 115-kV transmission lines," *Trans. AIEE (Power Apparatus and Systems)*, vol. 81, pp. 431–360, October 1962.

[11] *Lightning Performance of Typical Transmission Lines*. Mansfield, Ohio: Ohio Brass Company, 1955.

[12] AIEE Committee Report, "A method of estimating lightning performance of transmission lines," *Trans. AIEE*, vol. 69, pt. II, pp. 1187–1196, 1950.

[13] B. F. J. Schonland, *Flight of Thunderbolts*. Oxford: Clarendon, 1950.

[14] D. Muller-Hillebrand, "On the frequency of lightning flashes to high objects—a study on the gulf of Bothnia," *Tellus*, vol. 12, no. 4, pp. 444–449.

[15] K. Berger, "Electric requirements of overhead lines for very high voltages," *Bull. S.E.V. (Switzerland)*, vol. 54, pp. 749–754, 1963.

[16] L. M. Olmsted, "Design survey reveals patterns of EHV expansion," *Elec. World*, pp. 104–116, November 15, 1965.

Discussion

J. G. Anderson (General Electric Company, Pittsfield, Mass.): It would appear that, at long last, we are obtaining some good data on the shielding failure characteristics of actual transmission lines. The authors are making a very important contribution with this Pathfinder study.

One possible application of the Pathfinder measuring device is in study of the lightning response of distribution lines. Have the authors any plans to do such work? Another possible application is the study of suppression of power-follow current by wood crossarm when [illegible] Pathfinder data would be of interest in such situations.

As discussed to some extent in the paper, the data obtained on shielding failures will normally deal with shielding failure probabilities of only a few percent of the strokes contacting the line, hence data from many strokes are necessary. To obtain a good workable number to calculate outage frequency, one needs to know:

1) How many strokes contact the line?

2) Of these strokes, how many contact the ground wire and how many the phase conductor?

3) Of the strokes contacting either location, how many of each caused flashover?

If, on the lines where Pathfinders are installed, the footing resistances are low, then most failures would naturally be shielding failures and the Pathfinder indication that this is the case would only be what was expected anyway. Hence, shouldn't the footing resistances of each of the test lines be carefully examined in their statistical aspects, and not just at the towers where a target indication is obtained? Also, unless one measures the total number of strokes contacting the line, can shielding failure probability be obtained with any confidence? Some of the rules of thumb for estimating the total strokes are of dubious accuracy for this kind of work.

The authors are making a notable contribution, and their measurements appear likely to create some new concepts in transmission line design.

90004196

F. S. Young (Westinghouse Electric Corporation, East Pittsburgh, Pa.): In the study of subjects such as shielding of transmission lines, several important phases of investigation are found to exist. There must be an understanding of the phenomena that interact to produce the problem; in this case the mechanics of the lightning stroke. A suitably accurate model must be developed for use in study of this interaction of components and data finally supplied to support and verify the hypothesis. All these phases are found in various stages of development in this paper.

The authors have isolated the important parameters that affect the shielding of transmission lines and have developed an instrument to record data for each outage experienced on a line. They have perfected a model that can be used for extensive analysis of the problem. All that remains now is completion of their field investigations. Although the data presented here represent only a small sample of the total expected to be obtained in this project, it is interesting to see how it compares with theoretical work.

Referring particularly to the analytical model developed in the paper, the authors discuss their calculation procedure. This has proven to be a useful technique in the analytical study of shielding of transmission. In work[4] presented in 1963, we chose to use two points of calibration. First we selected a line of known performance where shielding failures were thought to produce the majority of the outages. When properly calibrated our model successfully produced this outage rate and also showed that lines of good performance, i.e., those with zero outage rates, were represented properly. The authors have wisely chosen to calibrate their model only with lines showing superior performance. Fig. 7 however shows a considerable margin of safety for the lines used. It would be most instructive if the authors would comment on how accurate the model appears to be when the effective shielding angle of a line may in fact exceed the critical. It is realized that more data will be required before definite conclusions can be reached, but some indication of the degree of conservatism included would be helpful in evaluating this method.

In developing this model the authors have included several interesting and useful features that have not been included in previous work. The discussion of the terrain factors is important. They will also be useful to the authors in evaluating data from particular towers when more field experience has been gained.

The line designer should always strive to achieve perfect or, in the authors' terms, effective shielding, then concentrate his efforts on limiting the number of backflashes or outages due to strokes to the ground wire. Analytical work, however, should not be limited to perfectly shielded lines but should permit analysis of all conditions.

Finally, in comparing the effective shielding angle data presented in Fig. 7 with data presented previously, one immediately notices a large preponderance of negative angles for lines over 100 feet of effective height. Care should be exercised in comparison of data presented in such fashion. Work we did has been presented in terms of height of the tower; therefore, if some sag is assumed it is found that the two sets of analytically derived data agree fairly well. We hope this provides as much comfort and encouragement to the authors as it did to us in reviewing their paper.

C. F. Wagner (Pittsburgh, Pa.): Shielding still remains one of the important factors in the protection of transmission lines against lightning that is not quite completely resolved, although presently available operating experience directs one to conclusions that should be acceptable. I agree completely with the authors that it is difficult to specify lightning characteristics and particularly those that apply to definition of an adequate or acceptable model of the stroke. I am gratified that the authors have adopted the same stroke model as I have advocated, but I would like to comment on some of the difficulties that attend the adoption of any stroke model.

First, I would like to call attention to the quantity r_{sg} that appears in (5). In the model that I prefer, this quantity should refer to the distance that the head of the return stroke has traveled by the time crest return stroke current has been attained. The argument behind this statement is somewhat as follows: If the downward leader be regarded as a vertical cylinder charged to a uniform potential of V_x and if such a cylinder be discharged to ground at a uniform velocity v_1, then neglecting other phenomena in the last step, the current flowing to ground from such a circuit can be determined approximately by

$$V_x = 60\ (I_0/v_1) \sinh^{-1} (x/a)$$

or approximately

$$V_x = 60\ (I_0/v_1) \ln (2x/a).$$

In this expression x is the vertical distance above the earth at any instant and a is the radius, neglecting corona to simplify the discussion. The principal point I wish to make is this: As the head of the return streamer advances upward the impedance increases logarithmically. The current consequently decreases inversely as this quantity increases. Actually, of course, all the phenomena associated with the breakdown of long gaps are present to limit the initial current and to produce an upward concave current flow until crest is reached. After this, in the simple model, the current should decrease as the impedance increases. In my model I have thus chosen r_{sg} to be that value of x at which crest current is attained.

I have also observed that in determining the striking distance in (9), the switching surge values of the breakdown voltage of the gap have been used, whereas I used the impulse breakdown values. If the leader of the initial component of the stroke in its downward progress is truely devoid of steps, then it would appear that some value of switching surge breakdown should be used. But what wave front? The authors do not specify the front that they used. There is nothing distinctive about the velocity of the head of the leader to indicate the use of any particular switching wave front. On the other hand, if the influence of the steps is considered, then the potential applied to the striking distance might be applied suddenly so as to justify the use of an impulse value of sparkover voltage.

The authors have also introduced the concept of the "probability density function," in which the density of the strokes, instead of being uniform above the loci of the striking distance radii, is a function of the angle of incidence of the strokes. Unquestionably, before the leader actually comes within the range of the striking distances, they are attracted to some degree by the transmission line as it projects above a level plane. Young *et al.*[9] provided for this condition by means of an attractive factor that is a function of the height of the transmission line. The probability density factor might conceivably go further than this assumption by discriminating between exposures that the authors have designated as type 1 and type 2 in Fig. 3.

The nature of individual lightning strokes is very complex, combining as it does phenomena involved in spark breakdown, corona discharges, and the transient and steady-state characteristics of arcs. Over and above these variables are such factors that affect individual area stroke incidences, seasonal effects, and year to year effects. Any practical representation of the stroke must, of necessity, represent a greatly oversimplified model of the actual phenomenon. It behooves the lightning specialist, therefore, to exercise extreme caution in attributing too great a rigidity or too great a refinement in the representation of the stroke. The lightning specialist must have his head in the clouds and his feet on the ground. While he aspires to learn more concerning the theoretical aspects of the phenomenon, he should provide the designing engineer with a simple relation between shielding angle and height to insure satisfactory shielding and a method of computing lightning outages as simple as the old AIEE method of computation.

Manuscript received March 6, 1967.

Edward Beck and **D. F. Shankle** (Westinghouse Electric Corporation, East Pittsburgh, Pa.): In this interesting paper, our attention was attracted immediately to Table IV which indicates that of a total of 14 flashovers recorded by the Pathfinder, 12 were caused by direct hits on conductors and only two by back flashes from struck towers or shield wires to a conductor.

Accepting these records as factual, it is a startling finding which is contrary to the general view held so far that most flashovers on shielded lines are caused by backflashes and only a few by direct hits on a conductor. But that has been the history of lightning research. What we once thought was so is found to be not so. Furthermore, the two cases of backflash were recorded on a line with a shielding angle of 66 degrees, the largest listed in the table. According to our traditional way of thinking, if the records were reversed, 12 caused by backflashes and two by direct hits, we would not be startled.

We think that significant comment and conclusions must be reserved until more data are available, which should not be long forthcoming in view of the great scope of this promising investigation.

Manuscript received February 21, 1967.

J. C. Engimann and **R. W. Caswell** (Commonwealth Edison Company, Chicago, Ill.): The authors indicate that, to keep the trip-out rate down to an acceptable value, it is necessary to have a smaller shielding angle than has been considered necessary in the past.

It is of interest to consider the performance of one of our 345-kV double-circuit tower lines which has two ground wires installed at a shielding angle that in the past was considered very good. The overall length of the ground wire arm is 20 feet; the top and bottom conductor arms are each 38 feet long and the middle conductor arm is 68 feet long. The shielding angle for top conductor is approximately 20° and approximately 26° for the middle conductor. The insulation consists of twenty 5 by 10-inch insulator units. The footing resistance of each tower is 10 ohms or less. The isokeraunic level is between 40 and 45. The tower line is 89 miles long.

The two circuits, numbers 11601 and 11602, have been in service for nine years. For this period, line 11601 has an annual trip-out rate (due to lightning) of 2.36 per 100 circuit miles, and for line 11602 it is 2.49. This high trip-out rate is not considered satisfactory performance.

The following information about which phase position was involved in the flashover is based on oscillograms and aerial patrols.

For line 11601, 64 percent of the flashovers involved the middle phase, 26 percent the top phase, 5 percent the bottom phase, and 5 percent not known.

For line 11602, 75 percent of the flashovers involved the middle phase and 25 percent the top phase.

There have not been any instances where these two circuits have had a simultaneous flashover due to lightning.

The height of the ground wire arm on the majority of the towers on which flashovers have been located is in the range of 140 to 160 feet, with one having the maximum height of 225 feet.

Manuscript received March 6, 1967.

We believe this tower line is a good example of why additional information, as we hope will be obtained by the Pathfinder instrument, is essential for the economical design of transmission lines that will give satisfactory performance. In an attempt to secure more information, we are installing the Pathfinder in a portion of one circuit on the top and middle phase.

A comparison of the unsatisfactory performance of the 345-kV lines just discussed with those of more recent design is interesting. We have had in service for two years approximately 102 circuit-miles of double-circuit 345-kV tower lines with two ground wires installed. The shielding angle for the top phase is negative 17°. The insulation consists of eighteen $5^3/_4$ by 10-inch insulator units. During this 2-year period we have not had any tripouts of these circuits due to lightning. While this record is for only a short period of time, we do know that they have been exposed to lightning, as a 138-kV circuit adjacent to one of these lines has had two trip-outs in each of these two years due to lightning. Also, lines 11601 and 11602, which are in the same area, had higher than usual trip-out rates for these two years.

This limited experience indicates that better shielding will materially improve the performance. To design the most economical line, consistent with desired performance, it is necessary to know more about shielding requirements.

We believe that the data to be secured by the Pathfinder with its analysis and development of design parameters by Dr. Whitehead will assist in the economical design of better performing transmission lines.

R. J. Bronikowski (McGraw-Edison, Power Systems Division, Milwaukee, Wisc.): Our compliments are extended to the authors of this interesting study of shielding characteristics. As one of the McGraw Edison engineers who worked with Dr. Whitehead on the development and production design of Pathfinder instruments, I have a keen interest both in the significance of the findings and the performance of the device. One of the design criteria was that the Pathfinder safely withstand a 60-cycle fault current of 30 000 amperes for 12 cycles without blowing up or dropping the line lead to the phase conductor. This level provides a substantial safety margin between expected fault currents and breaker operating times so that the devices could be installed at most locations on transmission systems. To meet this requirement, vent panels were built into two sides of the instrument. In our testing we learned that the vents would not operate at 3000 ampers fault current, that at about 6000 amperes one vent operated, and that at 10 000 amperes or higher, both vent panels would be released. It would be interesting to learn if the reports of Pathfinder operations mention vent panels blowing at any of the installations.

Manuscript received February 23, 1967.

H. R. Armstrong and E. R. Whitehead: We are most gratified by the interest in our paper as indicated by the several pertinent discussions. We shall endeavor to respond to particular questions as possible or concur in the remaining uncertainty.

Mr. Anderson inquires about possible plans to extend the study to distribution lines. There are no plans for a field study utilizing the Pathfinder device, but it is possible that the general conclusions of the overall study can be extrapolated to distribution systems at the higher voltages. We agree that studies using the Pathfinder device on wood crossarm lines could be of value in the study of follow-current suppression by the deionizing action of wood. Such lines were eliminated from the present study because, in general, their excellent performance promised too little data toward the principal objective of the study. We further concur in the desirability of the data Mr. Anderson quite correctly enumerates as 1) total strokes to any part of the line, 2) division of strokes between phase conductors and shield wires, 3) how many to either phase conductor or ground wire cause flashover? In the early phases of research on the Pathfinder device, these were precisely the questions we asked ourselves. It was immediately realized, however, that an economically-feasible experimental study would have to concentrate on the division of actual flashovers between those arising from shielding failure and those from the response of the line to strokes to the tower or ground wire. As Mr. Anderson points out, the footing resistances of the sample lines should be studies as carefully as possible and present plans are to obtain the maximum information available.

Mr. Young requests the authors' estimate of the degree of conservatism represented by the calculated lines of Fig. 7. In doing so he points up the most important objective of the field study which will require a great deal more data. What makes the question even more pertinent is that lines showing superior performance may indeed be conservatively shielded; that is, have shielding angles well below the "critical line" referred to a particular electrogeometrical model. We cannot yet answer his question in an objective manner, but we have chosen some lines whose shielding angles are *believed to be* very close to the critical lines of Fig. 7 and perhaps in another few months we can be somewhat more helpful in this respect. We appreciate his comment in connection with the use of terrain factors and effective height, and can assure him we share his comfort and encouragement at the reasonable agreement between the results obtained from his data[4] and those of our paper when adjusted for such factors.

Dr. Wagner comments on his preference for somewhat different values in connection with the estimate of the stroke voltage and strike distance. The result of the use of these different values would yield slightly higher voltage for an assigned current together with larger strike distances for the larger voltage on an impulse basis. Unfortunately, the laboratory data must be extrapolated inordinately in any event so that, as pointed out in the paper, calibration with field results must be employed in any reliable engineering design. One of the secondary objectives of the present study is, however, to throw light on such questions as Dr. Wagner has raised. We agree that the lightning specialist should "have his head in the clouds and his feet on the ground" though someone remarked that this could easily result in his conversion to "the late lightning specialist!" Moreover, we agree that the line designer should be provided with simple relations between shielding angle and height. Such relations between shielding angle and height have indeed been provided the designer, on a tentative basis, in a recent IIT status report.[4] We appreciate Dr. Wagner's comments and have used his stroke model as the simplest and best for our purposes. We accept full responsibility for such results as accrue from the simplifications made to adapt it to our overall electrogeometrical shielding model.

We thank Mr. Shankel and Mr. Beck for their comments and could not agree more that further comment and conclusions must await further data. As in many studies, however, EHV lines are being designed now and we felt it important that even these early results should be made available, particularly since they are in agreement with less extensive studies in this country and abroad.

Mr. Engimann and Mr. Caswell cite some exceedingly interesting data on the performance of the line to which the Pathfinder devices are applied on their system. It will be most interesting if and when the first Pathfinder records are received showing impulse flashover on a middle phase. There are two other lines, one 138 kV and one 345 kV, where a limited application of the Pathfinder device is made to a middle phase, but neither is as extensive as that reported by Mr. Engimann and Mr. Caswell.

Mr. Bronikowski asks about the performance of the pressure relief vent panels of the Pathfinder device. We have estimated fault current values for only one operation on which both vent plates operated. This current was 6800 amperes. On several other operations, one plate was blown off. It appears, therefore, that these plates are functioning properly. The McGraw Edison Company and the Joslyn Manufacturing and Supply Company furnished the instrument and current collector rings, respectively. Much favorable comment has been received from the field concerning the speed and ease of installation of, and the evident attention to reliability given to, the manufacture of these devices.

References

[17] "Current status report on the E.E.I. research project—Mechanism of lightning strokes to transmission lines—1967," Rept. of the Steering Committee, H. R. Armstrong, Chairman, IIT Research Institute, Chicago, Ill., January 16, 1967.

Manuscript received May 11, 1967.

90004198

TABLE IX
Comparison of Elimination and Impedance Methods

Nodes	Branches	Links	Sources	Complex Multiplications: Elimination Method	Complex Multiplications: Impedance Method
50	100	25	25	40 200	41 800
50	125	25	50	40 200	62 575
50	125	50	25	59 300	62 825
50	150	50	50	59 300	83 600
50	175	100	25	99 350	104 875
50	200	100	50	99 350	125 650
100	175	50	25	159 200	238 150
100	200	50	50	159 200	317 200
100	225	100	25	243 600	397 250
100	250	100	50	243 600	476 300
100	325	200	25	410 700	715 450
100	350	200	50	410 700	794 500

izes the elimination method since no advantages can be taken of the ordering feature.

For the impedance method, no computations are included for matrix terms below the diagonal. If the off-diagonal terms were not symmetrical, the number of calculations for the impedance method would approximately double. Conversely, no credit is given to the impedance method for gradually increasing the size of the matrix. It is assumed that the original network is actually larger than the final that is retained, and the tabulated computations include only those that occur after the network has been built up to full size. Comparable techniques are applicable for both the impedance and elimination methods for erasing nodes that are not required in the final analysis.

To take advantage of network sparsity, the elimination method requires more logical operations than the impedance method. No reliable assessment can be made of the penalty attributable to this difference other than to note that numerous logical steps can be made during the time that it takes to make one complex multiplication.

To open a line, fewer computations are required by the impedance method than by elimination if the opening is temporary, and if there is no mutual coupling to the line, such that only one column of the matrix need be modified. For simultaneous faults and/or line-open conditions, it is generally necessary to modify the entire impedance matrix, and the elimination method would be faster.

For transient stability studies, only one solution by elimination would be required for each time interval, even though several generators may be swinging. The number of computations for the impedance matrix solution would be proportional to the number of generators. The impedance method would generally be faster except during switching operations which would require 1) modification of the entire matrix or 2) input of a precalculated matrix from bulk storage. Overall, one would expect the time requirements of the two methods to be comparable for transient stability studies.

One could go on comparing the efficiencies of the impedance and elimination methods for different problems and show that either may have advantages in certain respects but are comparable overall. We prefer the elimination method primarily because it requires less storage than the impedance method. True, computers are getting larger, faster, and cheaper. At the same time our problems are getting more complex such that one never seems to have a computer that is large or fast enough. Thus there is always an incentive to strive for better programs. Off-line problems can generally be taken to large computer centers where storage may not be a problem. For on-line systems, storage and time requirements may be all important.

Our company selected a 16 K IBM 1130 computer instead of a 32 kbyte IBM 360. As Mr. Lipson noted, we were indeed somewhat optimistic in estimating 300 nodes internal storage. Our present program is dimensioned for 200 nodes, with provision to transfer a block of terms to temporary bulk storage any time that the principal matrix area cannot hold all the terms that are developed. It is, however, expected that this feature will not be required except possibly for very dense networks of 200 nodes. Normally, the data for large networks will be transmitted to a large computer center, except for cases where only a few solutions are required.

REF. 19

Field and Analytical Studies of Transmission Line Shielding: Part II

GORDON W. BROWN, MEMBER, IEEE, AND EDWIN R. WHITEHEAD, FELLOW, IEEE

Abstract—An analytical model for the shielding of transmission lines against lightning is extended to the case of partially effective shielding, including the effect of possible leader approach angle distributions. Results of the Pathfinder projects are brought up to date, and the data are shown to be consistent with the model. An index number is developed to aid in classifying line performance, and suggestions are made regarding the study of the backflash problem.

Paper 68 TP 616-PWR, recommended and approved by the Transmission and Distribution Committee of the IEEE Power Group for presentation at the IEEE Summer Power Meeting, Chicago, Ill., June 23-28, 1968. Manuscript submitted February 7, 1968; made available for printing April 2, 1968.

G. W. Brown is with the University of Pittsburgh, Pittsburgh, Pa.
E. R. Whitehead is with Illinois Institute of Technology, Chicago, Ill.

Introduction

OVER the past ten years the theory of shielding HV and EHV electric power transmission lines has been significantly advanced both in Europe and in the United States, although some of the underlying ideas were advanced much earlier. The work of Golde, and more recently that of Wagner on the relation between prospective stroke current and the strike distance from the leader tip provided the missing link between the electrical parameters of the lightning stroke and the geometrical parameter of the transmission line leading to the development of what may be termed the electrogeometric theory of transmission line shielding [1]–[3].

In January, 1967, Armstrong and Whitehead reported on the development of an analytical model based on the Wagner lightning stroke mechanism and its application to the design of effectively shielded lines. This model was tentatively calibrated against the parameters of 50 effectively shielded lines for a total experience of 52 000 mile years. The paper also reported on the design and operating characteristics of the Pathfinder device and the initial results of its installation on 433 tower line miles to determine the effects of partially effective shielding and other causes of insulator flashover from lightning. The extension of the electrogeometric model to partially effective shielding was, however, indicated only briefly [4].

The present paper will extend the application of the analytical model to the case of partially effective shielding, including the effects of an assumed leader angle probability density function, give typical samples from the 240 curves obtained in a computer study, and bring the Pathfinder field data up to date [5].

Electrogeometry of Transmission Line Shielding

The geometry of the transmission line model is given in Figs. 1 and 2. In Fig. 1, for the illustrated strike distance r_s to the conductors and r_{sg} to earth, there will be an effective horizontal swath X which will depend upon the leader angle probability density function. The exposed cylindrical surface is indicated by the arc abc. If all leaders are vertical, the swath for one side of the line is the projection of the arc ab on the horizontal axis. If a frequency distribution $f(r_s)$ of strike distances can be found, the number of shielding failure outages per unit length and time in a region of known stroke density N_0 is given as

$$n = kN_0 \int_{r_{s\,\min}}^{r_{s\,\max}} Xf(r_s)\, dr_s. \tag{1}$$

Here, $r_{s\,\min}$ is the minimum strike distance for which an outage could possibly occur and $r_{s\,\max}$ the maximum strike distance for which a stroke can hit the phase conductor. The coefficient k is the proportion of shielding failure flashovers which cause outages (i.e., which allow power follow current), and X the effective swath at r_s for both sides of the line.

Effect of Leader Angular Distribution

Since not all stroke leaders approach earth (or line) from a vertical direction, some angular distribution must be found for the approach angle of the leader. If ψ is defined as in Fig. 1, and a frequency function $g(\psi)$ is determined, it can be shown that (1) applies if the swath X is reinterpreted as an effective swath

$$X = r_s \int_{\theta_2}^{\theta_1} \int_{\psi_2(\theta)}^{\psi_1(\theta)} \frac{\sin(\theta - \psi)}{\cos\psi}\, g(\psi)\, d\psi d\theta. \tag{2}$$

The trigonometric coefficient results from the fact that the number of strokes to an elementary arc $r_s d\theta$ from strokes at angle ψ with total variation $d\psi$ is as follows:

$$r_s d\theta \sin(\theta - \psi) = dA$$

is the elemental area presented perpendicular to the oncoming strokes at angle ψ.

$$N_0 g(\psi) d\psi = N_h \tag{3}$$

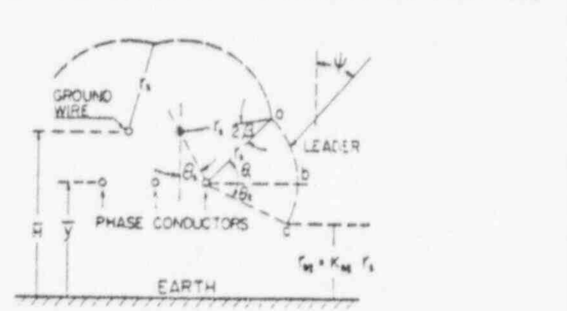

Fig. 1. Geometry of transmission line shielding.

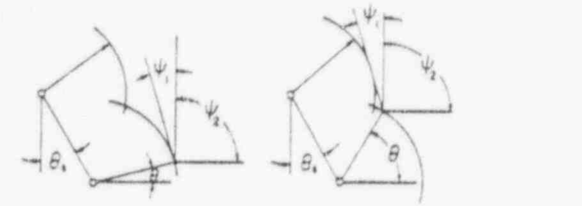

(a) (b)

Fig. 2. Common limitations on approach angle. (a) Region I—$\theta < \theta_s$. (b) Region II—$\theta > \theta_s$.

is the stroke density measured at the horizontal, while

$$\frac{N_0 g(\psi) d\psi}{\cos\psi} = N_\psi \tag{4}$$

is the stroke density as would be measured in the plane of the above elemental area. Hence, the number of strokes striking this element is

$$dn = \frac{N_0 g(\psi) d\psi}{\cos\psi} r_s \sin(\theta - \psi) d\theta f(r_s) dr_s. \tag{5}$$

The limits of integration ψ_2 and ψ_1 depend on several factors, as indicated in Fig. 2. It is assumed that no leaders approach from below the horizontal.

Effective Shielding

If in (1), $r_{s\,\min}$ is equal to $r_{s\,\max}$, no shielding failures can occur. However, since most quantities used are averaged quantities, use of the term perfect should be avoided. The term effective shielding is preferred.

Determination of Variables

Distribution of Strike Distance

The frequency distribution $f(r_s)$ rests upon the relation between strike distance and current, and the frequency distribution of current. The connection between the distribution of monotonically related functions is

$$f(r_s) = h(I) \frac{dI}{dr_s}. \tag{6}$$

The function $h(I)$ is the frequency distribution of currents, which can be determined from the cumulative or probability distribution, such as found in [6]. The connection between r_s and I is found by the series of functional dependencies

$$v = v(I)$$
$$V_s = V_s(I, v) \tag{7}$$
$$r_s = r_s(V_s).$$

Thus

$$r_s = r_s(I).$$

Here, v is the return stroke velocity and V_s the leader voltage [4], [5].

Distribution of Approach Angle

The distribution of leader approach angle can at present only be estimated. However, a reasonably wide class of solutions is represented by

$$g(\psi) = \begin{cases} 0, & \psi < -\pi/2 \\ K_m \cos^m \psi, & -\pi/2 \le \psi \le \pi/2 \\ 0, & \pi/2 < \psi. \end{cases} \tag{8}$$

Three of this class are of greatest interest; namely, $m = 1$ ($K_1 = 1/2$), $m = 2$ ($K_2 = 2/\pi$), and $m = \infty$ which is the case for all strokes vertical, and for which $g(\psi)$ degenerates to the Dirac function. Calibration of the end result and limited visual observation by one of the authors suggest that m is about 2 [4], [5].

Real-Line Geometry

For a real line, factors such as terrain and conductor sag determine the angular parameters and heights of Fig. 1. Under these circumstances, (1) can be interpreted as outages per unit length at a given point on the line, and the total outages for the line will be

$$N = \int_0^L n(x)\, dx \tag{9}$$

where x is the dimension along the line and L the total line length. It is felt, however, that there is insufficient justification in going to this extreme, as long as the caution in the previous section on effective shielding is observed. Calibration of the above formulas, based on averaged heights, sags, and shielding angles indicates that lines designed for effective shielding and ground resistances of less than 25 ohms can be expected to have fewer than 0.5 outage per hundred miles and year.

Tentative Calibration of Analytical Model

Numerical representation has been left to one section, since in large measure numerical values are interdependent. For example, the frequency distribution of strike distance depends on both the velocity–current relation and the probability distribution of current. In addition, many of the factors are relatively poorly known, resulting in the necessity of calibrating the final analytical model against actual field results. With this in mind, the following formulas are given as a unit, based on the work indicated in [4] and [5]:

$$r_s = 7.1\, I^{3/4} \text{ meters } (I \text{ in kA}) \tag{10a}$$

$$f(r_s) = \begin{cases} 0, & I < 5\,\text{kA} \\ 7.4 r_s^{-4/3}, & I \ge 5\,\text{kA} \end{cases} \tag{10b}$$

$$g(\psi) = \frac{2}{\pi}\cos^2\psi \tag{10c}$$

$$N_0 = 0.4\,\text{TD} \tag{10d}$$

$$K_{sg} = 0.9 \tag{10e}$$

$$k = 0.9 \tag{10f}$$

$$r_{s\,\min} = r_s \text{ for } I_{\min} \tag{10g}$$

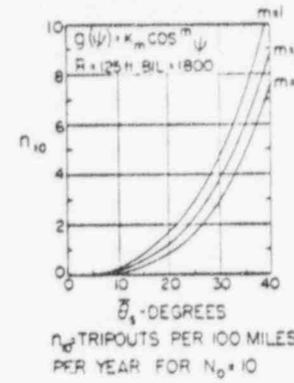

Fig. 3. Influence of exponent m on shielding failures.

where

$$I_{\min} = \frac{2\,\text{BIL}}{Z} \tag{10h}$$

and TD is thunderstorm days per year.

It is noted that (10b) is an approximation which may be valid only for transmission lines. For applications where precision is necessary in calculating strike distances having currents outside the range of about 5–80 kA, such as backflash and area protection, the current probability distribution and (6) must be utilized [4].

It has been pointed out that $g(\psi)$ cannot presently be accurately estimated. Perhaps it will never be isolated. Nevertheless, it is believed prudent to provide for a reasonable possibility of leader angle deviation from the vertical. Fig. 3 shows the influence of the exponent m on shielding failures under one set of line parameters. The exponent $m = 2$ has been selected tentatively as preferable to either $m = \infty$ or $m = 1$ (as are used in [3] and [4], respectively).

The estimate for N_0 is quite close to that of other investigators, yielding a value of 12 strokes per square mile per year for 30 thunderstorm days per year. It is clear that a significant improvement would be made if storm frequency could be expressed in thunderstorm hours per year as is reported abroad [12].

K_{sg} was originally intended to reflect a possible difference in strike distance for a leader-to-earth and a leader-to-ground wire for the same leader voltage. The use of this constant is such that it actually subsumes uncertainties in r_s, in the angle distribution function, and in the smoothness of terrain such as the averaged effect of trees, brush, or buildings along the right of way. It serves as a calibration constant having values variously estimated from 0.85 to 1.00 with the value 0.9 selected for the estimates reported.

It is important to note that all calculations for partially effective shielding have been made using the so-called AIEE current magnitude distribution curve as numerically adapted for computation. It follows that $f(r_s)$ is affected by any uncertainty in this curve. While the AIEE curve has the merit of quantity, its quality is open to considerable question. Recent oscillographic measurements by Berger tend to support the higher current levels reported by Baatz and others. Since larger values of current could increase r_s and affect $f(r_s)$, it is possible that compensating adjustments in the exponent m of $g(\psi)$ and perhaps in the value of K_{sg} might be required [7], [8].

Estimates of the height–angle relation for effective shielding depend upon the more accurately known values of BIL and conductor surge impedance, and any uncertainty in this relation

90004201

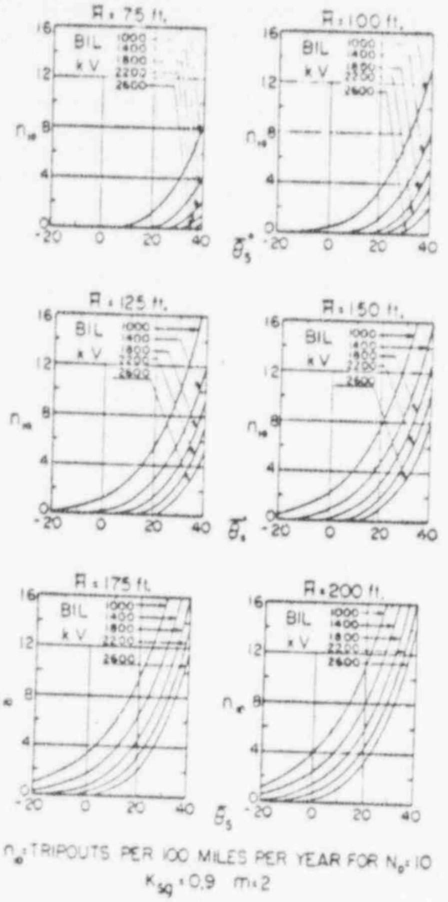

Fig. 4. Estimated shielding failures for partially effective shielding.

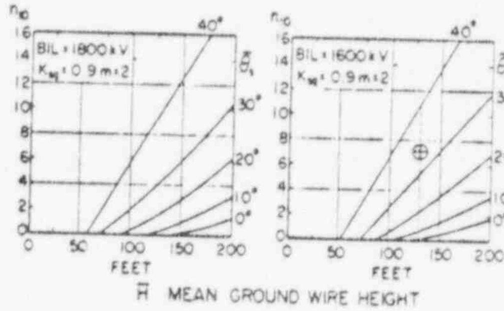

Fig. 5. Estimated shielding failures as function of height for constant shielding angle.

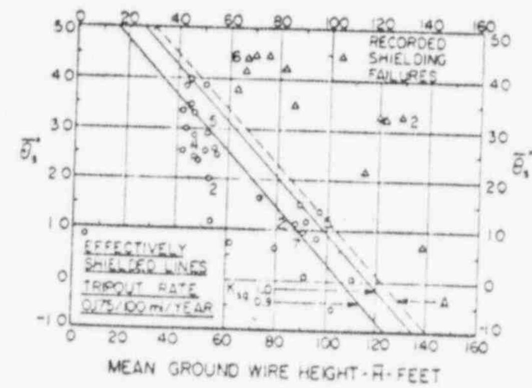

Fig. 6. Height–angle relations for effectively shielded and partially shielded lines.

would derive from the mean strike distance-current formula. Moreover, the final calibration of the analytical model for effective shielding depends on a very satisfactory volume of statistical data as discussed later in connection with Fig. 6 [4].

Computer Study

Utilizing the above equations, shielding failure outages for over 200 combinations of possible line heights, values of BIL, and various assumptions regarding $g(\psi)$ and K_{sg} were calculated. For these, it was assumed that $N_0 = 10$ strokes per square mile and year and $Z = 400$ ohms.

Several typical sets of curves are shown in Fig. 4. In order to stress the effect of height, data derived from these curves is shown in another form in Fig. 5. In connection with these figures, it cannot be overemphasized that $\bar{H}$ is the mean height of the ground wire above the earth surface which must take into account the actual or estimated earth profile [5]. If higher accuracy is justified, (9) can be employed.

Current Pathfinder Data from Edison Electric Institute Field Study

Table I shows the accumulated Pathfinder operation as reported by the Edison Electric Institute. This table may be summarized as reflecting a total of 40 Pathfinder operations on 29 individual strokes. Nineteen of these strokes caused shielding failures, eight caused backflash events, and two caused implied backflash events. In the last two cases the instruments were returned from the field for checking. Laboratory tests verified the integrity of the impulse circuitry, and the electro-explosive devices functioned properly. It is therefore assumed that the failure to indicate resulted from volt-time signals below the activation level of the electroexplosive elements. Such cases are expected to be rare [9].

The Pathfinder devices have been in the field for only 1.7 lightning seasons and the 1967 season was noteworthy for a low level of thunderstorm activity over most of the sample lines. Only one company reported above average activity. It is expected that a resumption of normal thunderstorm incidents will accelerate the accumulation of operations. The data yield is only slightly below projections for the actual instrumented time, but it is expected that the full five-year period will be required to yield the variety and number of data needed.

Interpretation of Pathfinder Data

The estimation of shielding failure tripouts is subject to much more variability than the estimation of a critical height–shielding angle relation and it has long been recognized that the Pathfinder data taken alone could never yield sufficient data to permit statistical curves of tripout rates versus height and shielding angle. The approach to the problem is threefold: 1) a large-scale statistical study of the height-angle relations for lines showing excellent performance, 2) verification of shielding failure or backflash events for a variety of line geometry, insulation, and grounding conditions, and 3) the use of an analytical model as an extrapolation mechanism consistent with the findings of 1) and 2). While it is yet too early to form firm

TABLE I

Operation Number	Operation Company	Line (kV)	BIL (kV)	$\bar{H}$ (feet)	$\bar{Y}$ (feet)	$\bar{\theta}_s$ (degrees)	Tower Number	Tower Ohms	Signals* Red	Signals* Green	Signals* Black	Tripout Yes	Tripout Number	Fault Type	Notes
1	A	120	790	67	58	44	200		×		×	×		L_1G	
2	A	120	790	67	58	44	201		×		×	×		L_1G	
3	A	120	790	67	58	44	262		×		×	×		L_1G	
4	A	120	790	67	58	44	271		×		×	×		L_1G	
5	A	120	790	67	58	44	272		×			×		L_1G	
6	A	120	790	67	58	44	312		×				×		
7	B	115	690	83	71	43	99		×		×	×		L_1G	
8	B	115	690	70	58	45	100		×			×		L_1G	
9	B	115	690	70	58	45	101		×		×	×		L_1G	
10	C	115	790	65	56	63	85	CP		×		×		DC	1
11	C	115	790	65	56	63	85	CP		×		×		DC	1
12	D	345	1600	129	102	33	53	1.0	×		×	×		L_1G	
13	D	345	1600	129	102	33	79	2.5	×		×	×		L_1G	
14	D	345	1600	120	102	33	106	1.5	×		×	×		L_1G	
15	D	345	1600	136	110	34	184	2.0			×	×		L_1G	2
16	B	115	690	78	68	45	136				×	×		L_1G	2
17	E	69/138	945	82	68	42	81		×		×	×		L_1G	
18	E	69/138	945	86	68	35	59	4.2	×			×		L_1L_4G	3
19	E	69/138	945	86	68	35	61	6.2	×		×	×		L_1L_4G	
20	E	69/138	945	91	68	28	318	250		×	×	×		$L_1L_2L_4G$	
21	E	69/138	945	86	68	35	255	140		×	×	×		$L_1L_2L_4G$	4
22	B	115	690	76	66	45	114		×			×		L_1G	
23	B	115	690	76	66	45	115		×		×	×		L_1G	
24	F	138	945	138	107	7	93		×		×	×		L_1G	
25	F	138	945	138	107	7	94		×		×	×		L_1G	
26	A	120	790	67	58	44	239		×		×		?	L_1G	5
27	A	120	790	67	58	44	240		×		×		?	L_1G	5
28	A	120	790	67	58	44	260		×		×	×		L_1G	
29	E	69/138	945	92	68	27	215	37		×	×	×		DC	6
30	G	110	744	66	55	42	139		×		×	×		L_1L_2G	
31	G	110	744	66	55	42	140		×		×	×		L_1L_2G	
32	H	115	690	63	53	38	138	CP	×				×	L_1G	
33	H	115	690	63	53	38	217	CP		×	×	×		DC	7
34	H	115	690	63	53	38	217	CP		×	×	×		DC	
35	H	115	690	63	53	38	171	CP		×	×	×		L_1G	
36	H	115	690	63	53	38	168	CP		×	×	×		L_1G	
37	D	345	1600	122	95	32	88	3.5	×		×	×		L_1G	
38	C	115	790	65	56	63	227	CP		×	×	×		L_1G	
39	A	120	790	67	58	44	308		×				×		
40	I	345	1600	113	50	21	31/4	1.5	×			×		L_4G	8

* red — stroke-to-phase conductor (shielding failure)
green — stroke-to-ground wire followed by backflash to the phase conductor
black — power follow.

Notes:

1 no black signal, but pressure plates ejected, double circuit fault
2 see special discussion in text
3 no instrument on tower 60 (strain tower)
4 black target cover failed to eject completely
5 records not clear on breaker operation, perhaps no power follow
6 double-circuit fault, Pathfinder operation top phase 138-kV side only
7 lines operated as single circuit
8 black signal covers did not eject properly.

conclusions, some interesting patterns are beginning to emerge which suggest that sound conclusions can be reached with sufficient data. Fig. 6 shows height–angle relations for 50 effectively shielded lines as indicated by their mean tripout rate of only 0.175 per 100 miles per year. Plotted on the same figure are the estimated critical height–angle lines for $K_{sg} = 1.0$ and $K_{sg} = 0.9$. The mean BIL value for the circled points is 1300 kV. Numbers adjacent to points indicate the number of lines having the same geometry. Also plotted on this figure are the height–angle points for the confirmed shielding failures of Table I. The group of triangles near $\bar{H} = 70$ feet and $\bar{\theta}_s = 40$ degrees has an averaged BIL of 760 kV, the group near $\bar{H} = 125$ feet and $\bar{\theta}_s = 33$ degrees has a BIL of 1600 kV, and the triangle at $\bar{H} = 138$ feet and $\bar{\theta}_s = 7$ degrees has a BIL of 945 kV. It is interesting to note that the upper envelope line A corresponds to the maximum BIL of 1600 kV for the circle points and that effective shielding for 125 feet and 1600 kV would be indicated for a shielding angle slightly less than zero degrees. The data of Fig. 4 confirms this estimate. The circled cross of Fig. 5 represents the performance of this same line plotted for the mean height and angle where shielding failures occurred. These parameters may not conform exactly to the average for the entire line, but marked departure is not anticipated.

Application of Shielding Theory to the Backflash Problem

Shielding theory affects the backflash problem through its application to the estimation of the number of strokes to the ground wire system. Although an extended study of this application is beyond the scope of the present paper, it is appropriate to suggest the directions to be taken in such a study.

90004203

Assuming the transmission line to be effectively shielded, the effective transverse exposure or swath depends upon the location and mean height above earth of the ground wires. Any attractive effect of grounded objects on the leader and its corona envelope is considered to be absorbed in the angle distribution function $g(\psi)$.

The backflash problem is acute for large values of current. A reasonable value of time invariant tower footing resistance is 20 ohms, and a representative BIL value might be 1000 kV for an HV line. If the coupling factor is assumed to be offset by the electric induction from the stroke, there results an estimate of 50 kA as a significant threshhold current. The corresponding strike distance is $r_s = 435$ feet. For an EHV line, a significant current might be 100 kA for which the estimated strike distance is 735 feet. Table II illustrates the effect of mean ground wire height and angle distribution parameter on the total swath for these two currents.

Table II brings out two useful points: 1) the effect of increased height on backflash events is less than proportional to height, and 2) the influence of the angle parameter on this effect is trivial at high currents. It should be noted that the swaths of Table II are specific for the current involved and are not integrated effective swaths.

Stroke Density and Power Follow Ratio

Based on the analytical model presented here and the performance of typical lines, a tentative stroke density is given by

$$N_0 = 0.4\,\mathrm{TD}$$

where

N_0 number of strokes per square mile per year
TD number of thunderstorm days per year.

The tentative tripout-to-flashover ratio from the Pathfinder study is approximately 0.9.

Line Performance Index

A useful concept, developed in [10], is that of a broad index number describing the lightning performance of transmission lines for discussion purposes which avoids the minutiae of the problem. The performance index M defines the specific performance in tripouts per 100 miles or kilometers per year, for a range of 30–50 thunderstorm days per year, by the relation specific performance = 10^M.

Table III is expressly applicable to shielded HV and EHV lines, and the qualitative classification is that of the authors, not necessarily that of CIGRE Committee 33. This table is useful in evaluating the performance of existing lines, and in formulating realistic predictions of the performance of new lines [10].

Variation of Tripout Rates

The application of analytical models to the multivariate problem of the lightning performance of transmission lines leads to numerical results which must necessarily be viewed in relation to the variability of line performance. Fig. 7 has been derived from data given in [11], the particular example being selected because of a continuous record kept for 27 years. This figure exhibits the relative stability of five-year averages about the mean tripout rate of 8.8 per 100 miles per year as compared to the spread of the yearly tripout rates. It is for this reason that the Pathfinder study was planned for a five-year period and it is recommended that averages for five or more years be used in comparing analytical estimates with line performance.

TABLE II
TOTAL SWATH X IN FEET

$\bar{H}$ (feet)	I (kA)	r_s (feet)	$m = \infty$	ratio	$m = 2$	ratio	$m = 1$	ratio
75	50	435	487	1.00	490	1.00	500	1.00
150	50	435	720	1.48	757	1.53	800	1.58
75	100	735	646	1.00	646	1.00	646	1.00
150	100	735	880	1.36	896	1.39	910	1.41

TABLE III

Exponent m	Specific Lightning Performance	Qualitative Classification
−2	0.00–0.05	exceptional
−1	0.06–0.59	excellent
0	0.60–5.99	common
+1	6.00 or more	poor

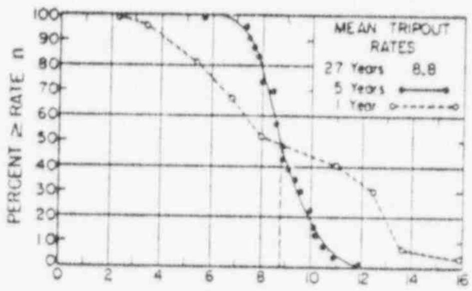

Fig. 7. Variability of tripout rates.

Conclusions

1) The extension of the analytical model developed by Armstrong and Whitehead [4] to the estimation of lightning tripouts resulting from partially effective shielding leads to results consistent with limited data on the known performance of existing transmission lines.

2) Two specific degrees of freedom for the calibration of the analytical model, the parameter K_{sg} and the angle distribution parameters m, have been studied for K_{sg} values of 1.0, 0.9, and 0.85 and for m values of 1.0 and 2.0. Typical results for $K_{sg} = 0.9$ and $m = 2.0$ have been presented as illustrative of the numerous studies made. It is believed that these parameters, along with small adjustments of N_0, allow sufficient flexibility to accommodate any moderate adjustments which may later be made in the current magnitude frequency distribution curve, or in the strike distance–current relation.

3) Over a cumulative period of 1.7 lightning seasons marked by subnormal lightning incidents, 40 Pathfinder operations have been reported. These records resulted from 29 separate strokes, 19 of which caused shielding failures, 8 caused known backflash events, and 2 are thought to reflect backflash events. Of the 8 known backflash events, 4 were on towers having counterpoise grounding in high-resistivity soil and 3 were on towers having localized ground resistances of 250, 140, and 37 ohms, respectively. Five of the 8 known backflash events caused double-circuit or multiple conductor faults.

4) All of the 17 known shielding failures resulted from height-angle parameters well above the critical lines tentatively established for effective shielding. The most significant single shielding failure resulted from a mean shielding angle of only 7 degrees and a mean ground wire height of 138 feet in mountainous terrain.

90004204

TABLE IV

	Pathfinder's Records	Commonwealth Edison 345-kV Line		OVEC	Ontario Hydro
		Line 11601	Line 11602	345-kV Line	230-kV Line
Shielding failures	66%	58%	62%	82%	61.1%
Backflashovers	34%	37%	38%	13%	30.5%
Flashes to unknown destination	0	5%	0	5%	8.3%
References	Brown and Whitehead	Engimann and Caswell [13]	Engimann and Caswell [13]	Schlomann *et al.* [14]	Lishchyna [15]

5) A broad index number M has been developed to classify lightning performance of HV and EHV lines, according to the relation

$$\text{specific performance} = 10^{M}$$

with numerical and qualitative classification as given in Table III. This index is useful in characterizing existing or estimated line performance.

6) Excellent lightning performance, $M = -1$, has been achieved for HV and EHV lines having conventional basic insulation levels, effective shielding, and localized ground resistances of 25 ohms or less.

7) Electrogeometric shielding theory is applicable to the estimation of the backflash performance of lines having effective shielding through its connection with the attractive swath of the ground wire system. While the effect of mean ground wire height is a controlling factor in shielding failures, it is a relatively minor factor in increasing the number of strokes to the ground wire.

8) As improvements in shielding theory lead to better allocation of the cause of lightning tripouts, it should be possible to renew the attack on backflash performance with greater effectiveness.

References

[1] R. H. Golde, "Theoretische Betrachtungen über den Schutz von Blitzableitern," *ETZ-A*, vol. 82, pp. 273–277, 1961.
[2] C. R. Wagner, "The lightning stroke as related to transmission-line performance," *Elec. Engrg.*, vol. 82, pp. 388–394, June 1963.
[3] F. S. Young, J. M. Clayton, and A. R. Hileman, "Shielding of transmission lines," *IEEE Trans. Power Apparatus and Systems* (Supplement), vol. S82, pp. 132–154, 1963.
[4] H. R. Armstrong and E. R. Whitehead, "Field and analytical studies of transmission line shielding," *IEEE Trans. Power Apparatus and Systems*, vol. PAS-87, pp. 270–281, January 1968.
[5] G. W. Brown, "The electrogeometry of shielding against lightning," Ph.D. dissertation, Illinois Institute of Technology, Chicago, Ill., 1967.
[6] AIEE Committee Report, "A method of estimating lightning performance of transmission lines," *AIEE Trans.*, vol. 69, pp. 1187–1196, 1950.
[7] K. Berger, "Novel observations on lightning discharges: results of research on Mount San Salvatore," *J. Franklin Inst.*, vol. 283, pp. 478–525, June 1967.
[8] H. Baatz, "Lightning stroke measurements on transmission lines," *ETZ*, vol. 72, pp. 191–198, April 1951.
[9] E. R. Whitehead, "Current status report on the E.E.I. Research Project 50—mechanics of lightning strokes to transmission lines," IIT Research Institute, Chicago, Ill., January 1968.
[10] E. R. Whitehead, "The lightning performance of EHV lines," CIGRE Rept. of Study Committee 33 on Lightning and Surges, 1968.
[11] F. Chambers and C. P. Almon, Jr., "Performance of 161-kV and 115-kV transmission lines," *AIEE Trans. (Power Apparatus and Systems)*, vol. 81, pp. 431–400, October 1962.
[12] V. V. Burgsdorf, "Lightning protection of overhead transmission lines and operating experience in the U.S.S.R.," CIGRE, Paper 326, 1958.

TABLE V

I (kA)	r_s (m)		
50	134	70	73
100	224	120	112
	Brown and Whitehead	Golde [16]	Wagner [17]

Discussion

Y. H. Chan (The Hydro-Electric Power Commission of Ontario, Toronto, Canada): This paper makes an excellent combination of theoretical analysis and engineering application. In the analysis, many factors, including leader angle and terrain effect, were carefully weighted and the final estimation of shielding failures is precisely represented as a function of shielding angle, earth wire height, and BIL of the line.

The number of flashes to unit length of a transmission line was extensively studied by Lewis and others in the 1930's. It took us over 30 years to realize the need of separating the number of flashes to phase wires and that to the earthed parts of a line, i.e., towers and earth wires. Surely the Pathfinder is the device to fulfill this function. Probably in the very near future its records will provide a fair judgment on the merits of the lightning performance theories which came from various schools. The records obtained so far are very encouraging. They compare well with the observation of Engimann and Caswell [13] as shown in Table IV which is constructed under the assumption that flashes to the top phase are due to shielding failure, those to the bottom phase are due to backflashovers, and those to the middle phase are equally contributed by shielding failures and backflashovers.

I would like to know the authors' opinion on the following questions:

1) The authors relate the stroke current I with the strike distance r_s, by

$$r_s = 7.1\, I^{3/4} \; (I \text{ in kA}, r_s \text{ in meters}).$$

This equation seems to give too high a flashover distance for the corresponding lightning current as compared with Golde's recent estimation [16] and Wagner's result [17] as seen in Table V.

2) For leader angle other than vertical, the transmission line cannot be considered as symmetrical, did the authors include this effect in their calculation?

References

[13] J. C. Engimann and R. W. Caswell, discussion of [4], p. 280.
[14] R. H. Schlomann, I. B. Johnson, W. S. Price, and J. G. Anderson, "1956 lightning field investigation on the OVEC 345-kV system," *AIEE Trans. (Power Apparatus and Systems)*, vol. 76, pp. 1447–1459, 1957 (February 1958 sec.).
[15] L. Lishchyna, Ontario Hydro Technical Report.
[16] R. H. Golde, "The lightning conductor," *J. Franklin Inst.*, vol. 283, p. 1, June 1967.
[17] C. F. Wagner, Contribution to *Gas Discharge and the Electricity Supply Industry*. London: Butterworth, 1962.

Manuscript received June 2, 1968.

90004205

R. H. Golde (The Electrical Research Association, Cleeve Road, Leatherhead, Surrey, England): The authors are to be congratulated on having presented an outstanding contribution to the solution of the question of the lightning performance of EHV transmission lines. In fact, as one of the early contributors to what the authors call the electrogeometrical approach, I would suggest that the authors have perfected this method to such an extent that attention should now be concentrated on the main parameters on which this investigation is based. With this in view, the following comments are offered as a constructive contribution to the discussion.

Equation (6) expresses the striking distance[1] as a function of the intensity of the lightning current. From this concept it follows that the frequency distribution of the amplitudes of lightning currents to open ground differs from that determined from magnetic link measurements on transmission lines to which the authors refer as AIEE current magnitude distribution curve. The resulting differences are clearly shown in Fig. 6 of [19]. To what extent the current distribution determined in a tall tower on top of a Swiss mountain [7] can be related to strokes to open ground is a matter which is open to argument.

The question as to whether the striking distance should be estimated from laboratory tests with standard 1.2/50 impulses or with long-fronted impulses depends on the nature of the pilot streamer preceding a step in a leader stroke. In my view, the potential drop in the pilot streamer is sufficiently low for the second alternative to be preferable. Values derived from (10a) are somewhat greater than those obtained from this interpretation (see [18], Fig. 3.) On the same argument there are indications that the authors' factor K_s, may not be far from unity.

Equation (10h) appears to be over-simplified since the potential at the point struck is materially affected by reflections from adjacent towers [20].

The authors' estimate for N_s is acceptable but their attention may be drawn to the intensive work carried out by CIGRE Study Committee 8 on determining this all-important factor from lightning flash counter measurements.

Prof. Whitehead's pioneering work in the Pathfinder investigation deserves highest commendation and further results are awaited with greatest interest. As he is aware, CIGRE Study Committee 33 is currently engaged in an attempt at elucidating the relative frequencies of shielding failures and backflashovers on EHV lines by statistical evidence to be provided from existing transmission systems all over the world.

It would be appreciated if the authors could explain the significance of the points indicated in Fig. 7. From the data in Table I, one would have expected to find 27 points on the curve relating to one year but considerably fewer points on the curve relating to five years.

References

[18] R. H. Golde, "The lightning conductor," *J. Franklin Inst.*, vol. 283, pp. 451–477, June 1967.
[19] —— "Lightning surges on overhead distribution lines caused by indirect and direct lightning strokes," *AIEE Trans. (Power Apparatus and Systems)*, vol. 73, pp. 437–447, June 1954.
[20] —— "Lightning currents and potentials on overhead transmission lines," *J. IEE* (London), vol. 93, pp. 559–569, 1946.

Manuscript received June 24, 1968.

[1] In honor of Benjamin Franklin, who introduced the term "striking distance," I prefer this term to the authors' "strike distance" and hope that it will find wider application.

L. Lishchyna (The Hydro-Electric Power Commission of Ontario, Toronto, Canada): Over the past eight years we at Ontario Hydro have retained records of the lightning performance of a 230-kV double-circuit line as shown in Fig. 8. The relay operation records show that during the years of 1960–1967 this line had a total of 27 lightning tripouts of which 18 involved only one of its two circuits.

Manuscript received July 24, 1968.

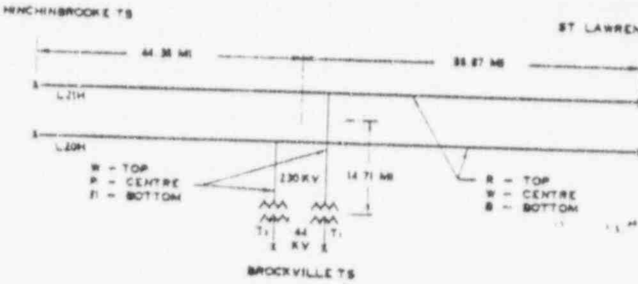

Fig. 8. 230-kV double-circuit line from St. Lawrence TS to Hinchinbrooke TS with tap to Brockville TS.

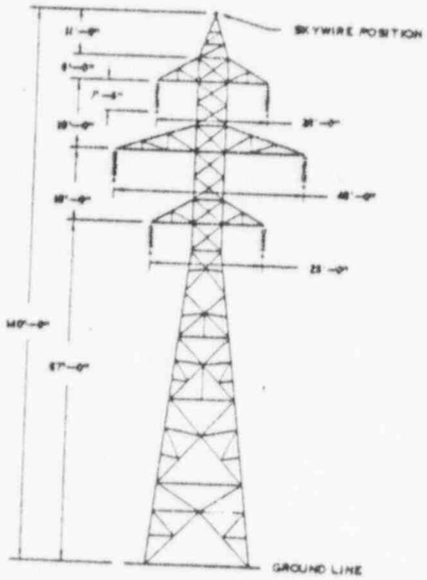

Fig. 9. Tower type of line *P*.

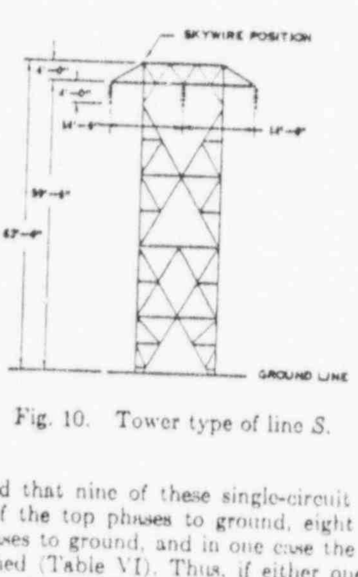

Fig. 10. Tower type of line *S*.

It was also noted that nine of these single-circuit tripouts (SCT) were from one of the top phases to ground, eight were from one of the center phases to ground, and in one case the phase involved was not established (Table VI). Thus, if either one of the bottom phases was involved in SCT at all it was not involved more than once. However, out of nine double-circuit tripouts (DCT) that occurred on this line during the same period, three tripouts involved both bottom phases.

The above findings suggested that the mechanisms initiating the single- and double-circuit tripouts on this line might not be the same. A reasonable explanation seemed to be that DCTs were initiated by backflashovers and SCT by shielding failures.

We were able to calculate the expected rate of shielding tripouts on this line, the tower type of which is shown in Fig. 9, using the methods which have been proposed in the literature. One of the

TABLE VI
LIGHTNING FAULTS ON ST. LAWRENCE TS–HINCHINBROOKE TS
230-kV DOUBLE-CIRCUIT TRANSMISSION LINE 1960–1967

Year	Line Length (miles)	Total Number of Faults	Number of DC Faults	Phase Involved in DC Faults*†	Phases Involved in Single-Circuit Faults*†
1960	100.25	2	0		W, W'
1961	100.25	1	1	R R'–W'	R, R', θ' ‡
1962	100.25	3	0		
1963	100.25	7	1	B B'	W, W, W, W, R', W'
1964	100.25	1	0		R'
1965	114.96§	5	4	W, B, B, R W', B', B', R'	W'
1966	114.96	5	2	R–W θ R'–W' θ'	R, R, R
1967	114.96	3	1	R R'–W'	R, R'
1960–1967		27	9		

* All faults are to ground.
† Primed phases are of circuit L21H and those not primed of circuit L20H.
‡ Phase involved not known.
§ Tap to Brockville TS added.

TABLE VII
CHARACTERISTICS OF LINES FOR WHICH SHIELDING TRIPOUT RATES HAVE BEEN CALCULATED

Line Designation	Number of Circuits	Voltage Rating (kV)	Line BIL	$\hat{H}$ (feet)	$\hat{V}$ (feet)	$\bar{\theta}$, (degrees)	Mile-Years of Reported Service Experience
P	2	230	1275	112	82	25	845
Q	1	500	1800	87	48	17	1380
R	1	115	675	65	36	25	1100
S	1	115	675	44	34	34, 67	500

methods tried was proposed in 1967 [4], and now has been expanded here. Its salient features are twofold: the length of the last step of lightning stroke is determined by the switching surge strength of long air-gaps, and stroke leaders are assumed to have angle distribution. It is assumed that the probability density of stroke leader angles orthogonally projected on a vertical plane, perpendicular to the direction of the transmission line, has a cosine distribution about a vertical line on such a plane. This latter parameter of lightning stroke has not been included previously in calculations of shielding tripouts. Instead, it has been customary to assume that all strokes proceed downward vertically.

The long and tedious mathematical computations, required to determine the exposure of line conductors to lightning strokes of various current magnitudes, were performed by a computer. The computer program provided the tripout rate on either single- or double-circuit lines.

The calculated value of SCT was 1.3 per 100 miles per year. The corresponding figure estimated from field data, assuming that all 18 single-circuit tripouts were because of shielding failures, was 1.6 and shows no conflict with the calculated value. Some SCT actually may have been caused by backflashovers, in which case there would be even better agreement between the above two figures. Plotting $\hat{H}$, $\bar{\theta}$, parameters of this line (designated in Table VI by P), in Fig. 6 a point is obtained that falls in the region of not effectively shielded lines.

Line Q in Table VII is a single-circuit 500-kV line with a horizontal phase configuration. Thus far it had two lightning tripouts (one of these involved the center phase) which constitutes 0.145 tripout per 100 miles per year. This tripout rate, according to the paper, qualifies this line as an effectively shielded line. The point obtained by plotting $\hat{H}$, $\bar{\theta}$, parameters of this line in Fig. 6 indicates that the line is indeed effectively shielded. In fact, it would be effectively shielded even if it had the BIL of 1600 kV instead of the actual BIL of 1800 kV. The computer calculations indicated no shielding tripouts for flat terrain.

The shielding tripout rate for line R in Table VII was estimated from the total lightning outages on this line and the flashover marks on the insulator strings observed during the helicopter patrol flights. It was observed that each of the outside phases of this line had 4.9 times as many insulator strings with flashover marks as the center phase had. The estimated value was 0.95 tripout per 100 miles per year which compares well with the calculated value of 0.90.

According to Fig. 6, the line with $\hat{H}$, $\bar{\theta}$, parameters corresponding to those of line R would be effectively shielded if it had a BIL of not less than 1300 kV. The actual BIL of this line, as shown in Table VI, is 675 kV.

From the above given and other similar applications, it was found that on lines with either one or two symmetrically located skywires, shielding failure rates calculated by this method compare favorably with those estimated from field data.

Next we tried this method on transmission lines with one skywire located asymmetrically (see Fig. 10 and Table VII). The calculated shielding tripout rates for such lines were found to be too high; considerably higher than the estimated value. The author's comments clarifying this point would be appreciated.

The field data obtained thus far from the Pathfinder project and reported by the authors have already elucidated a number of points concerning the shielding tripouts. It has demonstrated convincingly that on some transmission lines such tripouts may play an important role in determining the overall lightning performance. It is hoped that the authors will continue to make their excellent contribution in this field.

G. W. Brown and **E. R. Whitehead**: The authors wish to thank the discussers for their interesting and constructive comments.

Miss Chan presents a valuable tabulation of data on a variety of lines. We feel, however, that caution must be exercised in interpreting the apparent agreement with the Pathfinder results. The Pathfinders are located on 12 different lines with voltage levels from 115 kV to 345 kV, and with wide variations in shielding angle and terrain. Thus comparison of the overall results with specific lines suggests that caution be used. Miss Chan raises two specific questions. The strike distance is related to the stroke current by the empirical relation

$$r_s = K_{rs} I^{a}.$$

The following values have been given in or derived from the literature:

- r_s 7.1 $I^{0.75}$ in Brown and Whitehead
- r_s 6.7 $I^{0.80}$ Armstrong and Whitehead [4]
- r_s 3.3 $I^{0.78}$ derived from Golde's data as given by Chan
- r_s 10.6 $I^{0.31}$ derived from Wagner [2].

The values from Golde and Wagner yield critical height-shielding angle lines much below those given in Fig. 6. A possible explanation for this is that much lower current values, say 5–15 kA, are important in deriving critical lines for effective shielding of transmission lines, while the values cited by Miss Chan are much higher. Concerning Miss Chan's second question, the curves of Fig. 4 assume the line to be symmetrical. In the event of asymmetry, each side may be treated independently and the values of the curves divided by two.

Dr. Golde raises the very important question of the validity of the current probability distribution as used by the authors. Our own reservations are pointed out in the paper along with our tentative preference for a composite curve from the data of Baatz and Berger. The use of the so-called AIEE curve was dictated by a desire to facilitate comparison with other studies based on the same curve. Certainly improvement in our understanding of this relation (as well as the other constants and functions which make up our tentative calibration of the model) is needed. Regarding the question of the basis for the striking distance versus voltage relation, it is noted that (10a) is based on long front switching surges which Dr. Golde indicates as preferable.

Manuscript received August 7, 1968.

Dr. Golde suggests that the value for K_{sg} might perhaps be put at a value near unity, and a close examination of Fig. 6 will support this view. The value of $K_{sg} = 0.9$ was originally assigned to provide some protective margin against penetration of the mean striking distance surface by individual corona filaments when the model was used to predict *effective shielding*. Obviously, this practice should be reconsidered when the model is used to predict the results for *partially effective* shielding. Curves for $K_{sg} = 1.0$ are available.

The authors agree that (10h) is probably an oversimplification, but the alternatives do not yet appear justified in the presence of other basic uncertainties.

Dr. Golde directs our attention to the very intensive studies of CIGRE Study Committee 33 in endeavoring to determine the stroke density number from lightning-flash counter measurements. His pioneering work in this field has blossomed into most extensive studies throughout the world and extremely valuable data are becoming available. Proper interpretation, evaluation, and utilization of these data are of utmost importance to future numerical analysis of the lightning performance of EHV lines. Finally, Dr. Golde requests clarification of the fact that there are fewer than 27 points on the one-year average curve of Fig. 7. The explanation is that several single years had identical tripout rates and it is this rate that is grouped as one point. Unfortunately, the dashed line is still slightly in error, as the point at 10 specific tripouts was inadvertently omitted. The objective of the figure is, however, not impaired by this error.

The authors agree with Mr. Lishchyna that double-circuit tripouts are more likely to be associated with backflash events than with shielding failures. This is corroborated by Table I where it is seen that the double-circuit faults are invariably associated with high footing resistance or counterpoise. The authors are pleased that the agreement of the theory with Mr. Lishchyna's estimates of actual line failures is as good as he indicates for the symmetrical lines. Several comments are in order regarding the case which apparently did not agree with the method of [4]; namely, the single circuit with one asymmetrical ground wire.

Additional and poorly quantified influences become evident for very large shielding angles, say 50–90 degrees. Among these are: the shielding effects of the crossarm for steel construction or grounded insulator hangers for wood construction, effect of variations in length of corona filaments from the assumed mean striking radius, the poorly known current distribution curve between 0 and 10 kA, and the effect of nonlinear stroke resistance at these low currents. Fortunately, these perturbing influences do not appear to affect the principal relations for modern line configurations, though they may account in some measure for the scatter of points in data presentations such as Fig. 6. Mr. Lishchyna has kindly furnished the authors with additional data in private communications and his cooperation is much appreciated.

In general, the authors believe that the estimating curves for either $K_{sg} = 0.9$ or $K_{sg} = 1.0$ will yield results consistent with the performance classifications in Table III.